

THESIS / THÈSE

DOCTOR OF SCIENCES

Towards the Total Synthesis of Momilactones

Asymmetric Diels-Alder reactions of quinones and sulfinylquinones for the synthesis of terpenes

Jeanmart, Loic

Award date:
2021

Awarding institution:
University of Namur

[Link to publication](#)

General rights

Copyright and moral rights for the publications made accessible in the public portal are retained by the authors and/or other copyright owners and it is a condition of accessing publications that users recognise and abide by the legal requirements associated with these rights.

- Users may download and print one copy of any publication from the public portal for the purpose of private study or research.
- You may not further distribute the material or use it for any profit-making activity or commercial gain
- You may freely distribute the URL identifying the publication in the public portal ?

Take down policy

If you believe that this document breaches copyright please contact us providing details, and we will remove access to the work immediately and investigate your claim.



Towards the Total Synthesis of Momilactones

Asymmetric Diels-Alder reactions of quinones and sulfinylquinones for the synthesis of terpenes

A thesis submitted in fulfilment of the requirements for the degree of Doctor in Sciences

2021

Loïc Jeanmart

Laboratoire de Chimie Organique de Synthèse
Faculty of Sciences
University of Namur

Thesis supervisor: Pr. Steve Lanners (Université de Namur, Belgium)

Thesis jury:

- Pr. Johan Wouters (President, Université de Namur, Belgium)
- Pr. Stéphane Vincent (Université de Namur, Belgium)
- Dr. Gilles Hanquet (ECPM, Université de Strasbourg, France)
- Pr. M. Carmen Carreño (Universidad Autónoma de Madrid, Spain)
- Pr. Johan Winne (Universiteit Gent, Belgium)

“Chemistry is thought to be an arcane subject, one from which whole populations seems to have recoiled, and one that many think can be understood only by the monkishly initiated. It is thought to be abstract because all its explanations are in terms of scarcely imaginable atoms. But, in fact, once you accept that atoms are real and imaginable as they go about their daily lives, the theatre of chemical change becomes open to visualization.”
Reactions: The Private Life of Atoms, Peter Atkins

“Chemistry is like cooking, just don’t lick the spoon!”
meme found on 9GAG

*“In learning you will teach
And in teaching you will learn”*
Son of Man, Phil Collins

Université de Namur**Faculté des Sciences**

61 rue de Bruxelles, 5000 Namur, Belgique

Vers la synthèse totale des momilactones

Réactions de Diels-Alder asymétriques de quinones et sulfinylquinones pour la synthèse de terpènes

Loïc Jeanmart

Les momilactones A et B sont deux métabolites secondaires, isolés des balles de riz, qui participent aux mécanismes de défense de la plante de riz. Ce sont des diterpènes de la famille des pimaranes avec une γ -lactone 4,6-transannulaire et ont d'abord été identifiées comme composés antifongiques, antibactériens et inhibiteurs de croissance. Plus récemment, des études ont publié leurs activités anticancéreuses contre plusieurs lignées cellulaires sans pour autant réduire la viabilité des cellules saines. Elles présentent également une activité contre le diabète de type 2. Ces nombreuses activités biologiques en font de bons candidats en tant que potentiels agents médicamenteux.

Le but de ce projet était de proposer la première synthèse énantiosélective des momilactones en utilisant une réaction de Diels-Alder asymétrique, entre un diène oxygéné et une quinone, pour la construction des deux premiers cycles, suivie de la formation stéréosélective de la lactone transannulaire. La construction du troisième cycle est prévue par une annélation de type Tsuji-Trost d'une chaîne allylsilane sur une double liaison exocyclique.

Cette thèse présente d'abord le profil des pimaranes contenant le même motif γ -lactone 4,6-transannulaire. Elle se concentre ensuite sur les momilactones en présentant leurs activités biologiques, leur biosynthèse et l'unique synthèse totale racémique de la momilactone A. Un bref historique de la réaction de Diels-Alder et des caractéristiques qui ont rendu cette réaction si célèbre en synthèse totale est ensuite décrit. Certaines méthodes de réactions de Diels-Alder asymétriques sur les quinones et l'utilisation de sulfinylquinones chirales sont présentées plus en détails.

Après une description des voies de synthèse prévues pour la synthèse totale des momilactones, la deuxième partie de ce document présente la préparation et l'utilisation des précurseurs pour les réactions de Diels-Alder asymétriques prévues. Un chapitre est dédié à la préparation de six diènes oxygénés et, plus spécifiquement, au développement d'une nouvelle méthode de synthèse des 4-alkoxy- α -pyrones, par des cyclisations de β -cétocesters en milieu acide, qui nous a aussi menés à la découverte d'une nouvelle méthode de synthèse de thiométhylène-furanones.

Le chapitre suivant décrit la synthèse et l'étude des quinones et sulfinylquinones. Une analyse structurale, par diffraction aux rayons X et des méthodes théoriques, nous a permis de suggérer des ajouts aux modèles proposés précédemment pour expliquer la conformation préférentielle des sulfinylquinones et la stéréosélectivité de leurs cycloadditions. Par la suite, une étude de l'effet du solvant sur cette stéréosélectivité nous a conduit à la découverte du HFIP qui accélérerait grandement la réaction et donnait une excellente stéréosélectivité. Ces propriétés d'accélération ont aussi été démontrées avec d'autres quinones et différents diènes.

Enfin, le dernier chapitre de cette thèse présente les premiers essais de réactions de Diels-Alder asymétriques. Après avoir testé les différentes combinaisons de diènes et quinones, deux voies de synthèse potentielles sont ressorties. Elles nécessitent encore une optimisation mais sont prometteuses. L'échec d'un système catalytique nous a aussi mené à la conception d'une nouvelle quinone phtalide qui devrait fournir une voie de synthèse élégante pour les momilactones A et B.

Université de Namur

Faculté des Sciences

61 rue de Bruxelles, 5000 Namur, Belgium

Towards the Total Synthesis of Momilactones

Asymmetric Diels-Alder reactions of quinones and sulfinylquinones for the synthesis of terpenes

Loïc Jeanmart

Momilactones A and B are two secondary metabolites isolated from rice husks that participate in the defence mechanisms of the rice plant. They are pimarane diterpenes with a 4,6-transannular γ -lactone and have been first identified as antifungal, antibacterial compounds and growth inhibitors. More recently, studies reported that momilactones showed anticancer activities against several cell lines without decreasing the viability of healthy cells. They also exhibited activity against type 2 diabetes. Those numerous biological activities make them good candidates as potential medicinal agents.

The aim of this project was to propose the first enantioselective synthesis of momilactones using an asymmetric Diels-Alder reaction, between an oxygenated diene and a quinone, for the construction of the two first rings, followed by the stereoselective formation of the lactone. The formation of the third ring is planned *via* a Tsuji-Trost type annelation of an allylsilane chain on an exocyclic double bond.

This thesis first presents the profile of the pimarane diterpenes bearing the same 4,6-transannular γ -lactone pattern as the momilactones. It then focuses on momilactones by presenting their biological activities, their biosynthesis and the only racemic total synthesis of momilactone A that has been reported. Then, a brief historic of the Diels-Alder reaction and the main features that made this cycloaddition so famous in total synthesis is described. Some methods to carry out asymmetric Diels-Alder reactions on quinones and the use of chiral sulfinylquinones are extensively discussed.

After a description of the planned synthetic sequences for the total synthesis of momilactones, The second part of this document presents the preparation and the use of the different precursors for the planned asymmetric Diels-Alder reactions. A chapter is dedicated to the preparation of six oxygenated dienes and more specifically to the development of a new method for the synthesis of 4-alkoxy- α -pyrones, through the acid-promoted cyclisation of β -ketoesters, that also led us to the serendipitous discovery of a versatile method for the synthesis of thiomethylenefuranones.

The next chapter reports the synthesis and study of quinones and sulfinylquinones. A structural analysis of sulfinylquinones, using X-ray diffraction and computational methods, allowed us to suggest some complements to the models previously proposed to explain the preferential conformation of the sulfinylquinone and the stereoselectivity of their cycloadditions. Then, a study of the effect of the solvent on the stereoselectivity of the cycloadditions of sulfinylquinones led us to the discovery of HFIP that greatly accelerated the reaction and gave an excellent stereoselectivity. The accelerating properties of HFIP were also demonstrated with other quinones and different dienes.

Finally, the last chapter of this thesis depicts the first attempts of asymmetric Diels-Alder reactions between our oxygenated dienes and quinones. After testing the different combinations of dienes and quinones, two potential pathways stood out. They still need optimisation, but are most promising. One catalytic system that failed also led us to the design and preparation of a brand new phthalide quinone that should provide an elegant pathway for both momilactones A and B.

Acknowledgement

Je tiens tout d'abord à remercier le Prof. Johan Wouters d'avoir accepté de présider le jury de cette thèse de doctorat. Je remercie également le Prof. Stéphane Vincent, le Dr. Gilles Hanquet, le Prof. M. Carmen Carreño et le Prof. Johan Winne d'avoir fait partie de ce jury. Les discussions et les suggestions pour l'amélioration de ce manuscrit ont été plus qu'enrichissantes. Merci ! ¡Gracias! Dank u!

Je ne peux bien entendu pas continuer ces remerciements sans présenter toute ma gratitude au Prof. Steve Lanners de m'avoir accepté au sein du Laboratoire de Chimie Organique de Synthèse et sans qui ce projet n'aurait pas existé. Je me souviendrai toujours du jour où je suis entré dans son bureau, au moment du choix du mémoire, pour lui faire part de mon envie de faire de la chimie organique, ce à quoi il répondit : "c'est un excellent choix !" Je n'ai jamais douté de ce choix depuis. J'ai énormément appris sous sa tutelle et je pense que je resterai toujours impressionné par ses connaissances en chimie qui semblent sans fond. Mais travailler avec le Prof. Steve Lanners, c'est aussi partager des connaissances et des moments culinaires, musicaux et zythologiques. Je me souviendrai également des nombreuses anecdotes, que je pense d'ailleurs toutes connaître par cœur, qui nous ont souvent fait rire. Merci fir dès sechs Joer a fir alles.

Ce travail n'est pas que le fruit d'un travail personnel. De nombreuses personnes, sans forcément s'en rendre compte, ont contribué à la bonne conduite de ce projet. Je pense tout particulièrement aux techniciens et aux responsables des différents appareils nécessaires aux caractérisations des composés synthétisés lors de cette thèse. Je remercie Giuseppe Barbera pour la gestion de certains aspects techniques et pratiques de l'Unité de Chimie Organique, le Dr. Luca Fusaro pour l'analyse RMN, Bernadette Norberg et le Dr. Nikolay Tumanov pour l'excellent travail qu'ils ont réalisé concernant les nombreuses analyses cristallographiques de mes composés, mais également Marc Dieu et Xavier Maes pour les analyses HRMS. Je remercie aussi Xavier pour son aide précieuse pour l'utilisation d'autres appareils d'analyse.

Je remercie aussi le Prof. Laurence Miesch et le Prof. Philippe Geoffroy de m'avoir accueilli au Laboratoire de Synthèse Organique et Phytochimie à l'Institut Le Bel de Strasbourg pour les tests de réactions de Diels-Alder à haute pression.

Au bout de six ans de thèse, j'ai bien sûr rencontré énormément de personnes sans qui cette thèse n'aurait pas été pareille. Je ne pourrai malheureusement pas mentionner tout le monde et je m'excuse d'avance si votre nom ne se trouve pas dans les lignes qui suivent. Mais soyez assurés que je garde une pensée pour vous, que vous soyez proche ou loin.

Je fais un clin d'œil à Aurélie Plas, une des premières personnes au laboratoire avec qui je me suis tout de suite entendu, tout d'abord comme mentor et, par la suite, comme collègue et amie. Je n'oublie pas Eduard Dolušić, post-doc croate très singulier, dont les séances de dégustation de bière peu connues m'ont permis d'étendre ma connaissance du terroir belge, mais aussi Thanh Vy Hoàng qui avait su me mettre en confiance avec la chimie organique lorsque je n'étais qu'un étudiant.

Mais après eux sont arrivées de nouvelles générations, faisant de moi le “vieux” du laboratoire. Je les remercie fortement car, sans eux, l’ambiance du laboratoire n’aurait pas été ce qu’elle est. Du côté des collègues, je pense à François Simon. Bien qu’arrivé dans des circonstances peu joyeuses, il s’est tout de suite senti à l’aise et a su apporter un peu d’excentricité dans l’équipe. J’aimerais ensuite dire merci aux différents étudiants passés au sein du laboratoire : Kalina, Steffy, Pierre, Bastien, Loris, Mathilde, Oliver, Marie-Astrid et Amandine. Chacun a su apporter sa touche personnelle à l’ambiance avec sa personnalité, ses forces et ses faiblesses. Certains sont également devenus des collègues et de bons amis. Ça a été un grand plaisir de vous encadrer ou de vous conseiller, que ce soit de près ou de loin. J’espère vous avoir appris au moins autant que ce que j’ai appris de vous. Je dois particulièrement remercier Kalina, Bastien et Amandine d’avoir activement participé à mon projet de thèse. Votre travail a permis de grandement faire avancer le mien. Je vous souhaite à tous une belle continuation dans votre carrière.

J’aimerais faire un clin d’œil particulier à certains d’entre eux pour l’ambiance musicale du laboratoire, du Jerk à la kiffance (même si j’étais mitigé pour certaines chansons), en passant par des tentatives (parfois désespérées) d’agrandissement de la culture musicale qui nous font redécouvrir des grands classiques.

Je ne me serais également pas vu réaliser cette thèse sans avoir été assistant. Au-delà d’un moyen de financement, ce fut surtout une magnifique expérience qui m’a permis de découvrir ma passion pour l’enseignement. Je remercie toute l’équipe encadrante : les assistants, Sarah, Isabelle et, tout particulièrement, Diane avec qui les travaux pratiques de troisième année étaient, bien que très éprouvants, une période que j’attendais avec impatience. C’est avec nostalgie que je laisse la place à mon successeur qui, je l’espère, prendra autant de plaisir que moi à remplir cette tâche qu’est l’assistantat.

L’achèvement de cette thèse est aussi passé par de longues années d’études tout au long desquelles j’ai acquis des amis très chers. Merci pour les fous rires, les coups de gueule, les réconciliations, les délires et, surtout, le soutien nécessaire qui m’ont permis d’arriver jusqu’ici. Je pense notamment à Julien, Jean, Charlotte, Orian, Kim, Pierre, Sébastien, Nathalie, Lionel et Marie (même si j’ai dû survivre à certaines de ses tentatives d’assassinat culinaire). Je ne me serais pas vu passer tout ce temps à l’université sans vous. Je remercie également Olivia, Lucie, Mickael, Anthony et Riccardo. Ils sauront pourquoi.

Je remercie aussi tous les membres de l’UCO, anciens et actuels, dont certains sont devenus de bons amis également. J’ai réellement apprécié nos discussions, les bons moments et la découverte des cultures étrangères.

Merci à Véronique Alin de m’avoir donné le goût pour la chimie lors de mes études secondaires. Je ne suis pas certain que j’aurais suivi le même parcours sans sa passion pour cette magnifique science.

Remerciements spéciaux à Lionel pour ta patience, ton soutien et tes encouragements, même si tu as parfois une façon spéciale de les exprimer. Merci d’avoir été là.

Je réserve un remerciement tout particulier à ma maman qui a toujours su montrer de l'intérêt dans mon travail, même si cela lui était incompréhensible. Merci d'avoir cru en moi.

Enfin, si vous êtes arrivés à la fin de ces remerciements (peut-être un peu longs), merci chère lectrice et cher lecteur. J'espère que vous apprécierez la lecture de ce manuscrit.

List of abbreviations

$[\alpha]_D^{20}$	Specific optical rotation	DBU	1,8-Diazabicyclo(5.4.0)undec-7-ene
ABTS	2,2'-Azino-bis-(3-ethylbenzothiazoline-6-sulfonic acid)	DCC	<i>N,N'</i> -Dicyclohexylcarbodiimide
Ac	Acetyl	DDQ	2,3-Dichloro-5,6-dicyano-1,4-benzoquinone
ACF	Aberrant crypt foci	<i>de</i>	Diastereoisomeric excess
ADP	Adenosine diphosphate	DEA	<i>N,N</i> -Diethylacetamide
AIBN	Azobisisobutyronitrile	DEPT	Distortionless enhanced polarisation transfer
All	Allyl	DIBALH	Diisobutyl aluminium hydride
Alloc	Allyloxycarbonyl	DIPEA	Diisopropylethylamine
ANGPTL3	Angiopoietin-like-3	DMAP	<i>N,N</i> -Dimethyl-4-aminopyridine
Ar	Aryl	DMAPP	Diméthylallyl diphosphate
ATP	Adenosine triphosphate	DMDO	Dimethyldioxirane
BINOL	Binaphthol	DMF	<i>N,N</i> -Dimethylformamide
Bn	Benzyl	DMSO	Dimethyl sulfoxide
BHT	Butylated hydroxytoluene	DNA	Deoxyribonucleic acid
Boc	<i>tert</i> -butyloxycarbonyl	DPEPhos	Bis[(2-diphenylphosphino)phenyl] ether
BOx	Bisoxazoline	DPM	Diphosphomevalonate
BQ	<i>para</i> -benzoquinone	DPMD	Diphosphomevalonate decarboxylase
Bu	Butyl	DTBMP	2,6-Di- <i>tert</i> -butyl-4-methylpyridine
CAN	Cerium ammonium nitrate	DXP	1-Deoxy-D-xylulose-5-phosphate
Cat	Catalyst/catalysis	DXR	1-Deoxy-D-xylulose-5-phosphate reductoisomerase
CD	Circular dichroism	DXS	1-Deoxy-D-xylulose-5-phosphate synthase
CDI	1,1'-Carbonyldiimidazole	EDG	Electron donating group
CDP-ME	Cytidine diphosphomethylerythritol	<i>ee</i>	Enantiomeric excess
CDP-MEK	Cytidine diphosphomethylerythritol kinase	<i>ent</i>	Enantiomer
CDP-MES	Cytidine diphosphomethylerythritol synthase	Enz	Enzyme
chex	Cyclohexyl	EOE	Ethoxyethyl
Clm	Carbonylimidazole group	EOM	Ethoxymethyl
CMP	Cytidine monophosphate	eq.	Equivalent
CoA	Coenzyme A	ESI	Electron spray ionisation
cod	Cycloocta-1,5-diene	Et	Ethyl
Conv.	Conversion	EWG	Electron withdrawing group
COSY	Correlated spectroscopy	FMO	Frontier molecular orbital
Cp	Cyclopentadienyl	fod	6,6,7,7,8,8,8-Heptafluoro-2,2-dimethyl-3,5-octanedionate
CPP	Copalyl diphosphate	FPP	Farnesyl diphosphate
CSC	<i>cis-syn-cis</i>	FPPS	Farnesyl diphosphate synthase
ctDNA	Circulating tumor DNA	FT	Fourier Transform
CTP	Cytidine triphosphate	G3P	Glyceraldehyde-3-phosphate
CuTC	Copper(I) thiophene-2-carboxylate	GC	Gas chromatography
CYP	Cytochrome P450 oxidase	GGPP	Geranyl geranyl diphosphate
d	Day	GGPPS	Geranyl geranyl diphosphate synthase
DABCO	1,4-Diazabicyclo(2.2.2)octane	Glc	Glucopyranosyl
DAG	Diacetonideglucofuranosyl		
dba	Dibenzylideneacetone		

GPP	Geranyl diphosphate	MTPA	α -Methoxy- α -trifluoromethylphenyl-acetic acid
GPPS	Geranyl diphosphate synthase	M_w	Molar weight
HCA	Hexachloroacetone	NAD(P)	Nicotinamide adenine dinucleotide (phosphate)
Hex	Hexyl	NBA	<i>N</i> -Bromoacetamide
HFIP	1,1,1,3,3,3-Hexafluoroisopropanol	NMO	<i>N</i> -Methylmorpholine <i>N</i> -oxide
HMBC	Heteronuclear multiple bond correlation	NMR	Nuclear magnetic resonance
HMBDP	Hydroxymethylbutenyl diphosphate	n.O.e	Nuclear Overhauser effect
HMBDPR	Hydroxymethylbutenyl diphosphate reductase	NOESY	Nuclear Overhauser effect spectroscopy
HMBDPS	Hydroxymethylbutenyl diphosphate synthase	<i>o</i> Tol	<i>ortho</i> -tolyl
HMDS	Hexamethyldisilazane	<i>o/n</i>	Overnight
HMG	Hydroxymethylglutaryl	OP	Monophosphate
HMG-CoAS	Hydroxymethylglutaryl-CoA synthase	OPP	Disphosphate
HMGCS2	3-Hydroxy-3-methylglutarate-CoA synthase-2	ORD	Optical rotary dispersion
HMGR	Hydroxymethylglutaryl reductase	OsMAS	<i>Oryza sativa</i> momilactone A synthase
HMPA	Hexamethylphosphoramide	PCC	Pyridinium chlorochromate
HMQC	Heteronuclear multiple quantum coherence	PDC	Pyridinium dichromate
HRMS	High resolution mass spectrometry	PG	Protecting group
HOMO	Highest occupied molecular orbital	Ph	Phenyl
HPLC	High performance liquid chromatography	P_i	Inorganic phosphate
IC ₅₀	Half maximal inhibitory concentration	PIDA	Phenyliodonium diacetate
IDI	Isopentenyl diphosphate isomerase	PIFA	[Bis(trifluoroacetoxy)iodo]benzene
IPP	Isopentenyl diphosphate	PMB	<i>para</i> -Methoxybenzyl
<i>i</i> Pr	Isopropyl	PMP	<i>para</i> -Methoxyphenyl
IPr	1,3-Bis(2,6-diisopropylphenyl)imidazol-2-ylidene)	PMK	Phosphomevalonate kinase
IR	Infrared	PP _i	Inorganic diphosphate
L	Ligand	PPTS	Pyridinium <i>para</i> -toluenesulfonate
LDA	Lithium diisopropylamide	Pr	Propyl
LPL	Lipoprotein lipase	PTSA	<i>para</i> -Toluenesulfonic acid
LUMO	Lowest unoccupied molecular orbital	<i>p</i> Tol	<i>para</i> -Tolyl
M	Molar	Py	Pyridine
μ M	Micromolar	pybox	Pyridinyl-bis(oxazoline)
<i>m</i> CPBA	<i>meta</i> -chloroperbenzoic acid	quant.	Quantitative (yield)
Me	Methyl	RCM	Ring closing metathesis
MECDP	Methylerythritol cyclodiphosphate	R _f	Retardation factor
MECDPS	Methylerythritol cyclodiphosphate synthase	rt	Room temperature
MEP	Methylerythritol phosphate	SAR	Structure-activity relationship
MIC	Minimum inhibitory concentration	SET	Single electron transfer
min	Minute	SPhos	Dicyclohexyl(2',6'-dimethoxy[1,1'-biphenyl]-2-yl)phosphane
MK	Mevalonate kinase	SQS	Squalene synthase
MOM	Methoxymethyl	STAT5b	Signal transducer and activator of transcription 5B
m.p.	Melting point	TADA	Transannular Diels-Alder reaction
Ms	Methanesulfonyl	TBAF	Tetrabutylammonium fluoride
MS	Molecular sieve	TBME	<i>tert</i> -Butyl methyl ether
		TBS	<i>tert</i> -Butyldimethylsilyl
		<i>t</i> Bu	<i>tert</i> -Butyl
		Temp.	Temperature

TEMPO	(2,2,6,6-Tetramethylpiperidin-1-yl)oxyl
TES	Triethylsilyl
Tf	Trifluoromethanesulfonyl
TFA	Trifluoroacetic acid
TFP	Tri(2-furyl)phosphine
THF	Tetrahydrofuran
TIPS	Triisopropylsilyl
TLC	Thin layer chromatography
TMS	Trimethylsilyl
TOF	Time of flight
TPA	Tissue plasminogen activator
TPAP	Tetrapropylammonium perruthenate
TPP	Thiamine pyrophosphate
t_r	Time of retention
Ts	Toluenesulfonyl
TST	<i>trans-syn-trans</i>
TTC	<i>trans-trans-cis</i>
UV	Ultraviolet

Table of contents

I	Introduction	1
1	Pimarane diterpenes and momilactones	3
1.1	Terpenes and the isoprenoids family	5
1.2	The diterpene classes	8
1.3	The pimarane diterpenoids	10
1.3.1	Where to find them	10
1.3.2	Pimarane diterpenes with a 4,6-transannular γ -lactone	12
1.3.3	Total syntheses of myrocins C and G	22
1.4	Momilactones: secondary metabolites with extraordinary properties	25
1.4.1	Momilactones participating in the rice allelopathy and its defence mechanism	27
1.4.2	Momilactones A and B as new potential medicinal agents	28
1.4.3	Biosynthesis of momilactones A and B	30
1.4.4	First total synthesis of (\pm)-momilactone A	32
1.5	Conclusion	35
	References	37
2	Asymmetric Diels-Alder reactions on quinones	45
2.1	Origins of the Diels-Alder reaction	47
2.2	Features of the Diels-Alder reaction	50
2.2.1	Rates of the Diels-Alder reactions and frontier orbital interactions	50
2.2.2	Regioselectivity of the Diels-Alder reaction	52
2.2.3	Stereoselectivity of the Diels-Alder reaction	54
2.3	The asymmetric Diels-Alder reaction	57
2.3.1	Chiral auxiliaries	57
2.3.2	Asymmetric organocatalysis for Diels-Alder reactions	59
2.3.3	Lewis acid catalysed asymmetric Diels-Alder reactions	62
2.4	Catalytic asymmetric Diels-Alder reactions applied on quinones	63
2.5	Sulfinylquinones as chiral dienophiles	69
2.5.1	Synthesis of enantiomerically enriched sulfinylquinones	70
2.5.2	Double bond selectivity in Diels-Alder reactions with sulfinylquinones	72
2.5.3	Control of the facial diastereoselectivity	76
2.5.4	Applications of the asymmetric Diels-Alder reactions on the sulfinylquinones	80
2.6	Conclusion	88
	References	90
II	Results and discussion	97
3	Strategy and objectives	99
3.1	Retrosynthetic analysis of momilactones A and B	101

3.2	Synthetic plan for the total synthesis of momilactones	102
3.2.1	Choice of the quinonoid system	102
3.2.2	Choice of the diene	104
3.2.3	Formation of the third cycle	108
3.2.4	Specific route for the total synthesis of momilactone B	109
3.3	Additional objectives of this thesis	111
3.3.1	Synthesis of the starting materials	111
3.3.2	Formation of the third cycle	112
3.3.3	Study on the sulfinylquinones as dienophile in the Diels-Alder reaction	113
	References	114
4	Synthesis of the dienes	117
4.1	Synthesis of 3-trimethylsilyloxy-penta-1,3-diene 373a	119
4.2	Synthesis of 1,3-dialkoxy-penta-2,4-diene 373b	119
4.3	Synthesis of penta-2,4-dienoates 373c and 373d	120
4.3.1	Preparation of 6-vinyl-1,3-dioxin-4-one 373c	120
4.3.2	Preparation of 3-silyloxy-penta-2,4-dienoate 373d	121
4.4	Synthesis of α -pyrone 373e	122
4.4.1	Effenberger's synthesis	122
4.4.2	Metal-catalysed cyclisation of 3-oxopent-4-ynoates	123
4.4.3	Third strategy for the synthesis of pyrone 373e	130
4.5	Synthesis of a new diene by reduction of α -pyrone 373e	132
4.6	Conclusion	134
	References	136
5	Synthesis and study of quinones and sulfinylquinones	139
5.1	Synthesis of enantiomerically enriched sulfinylquinones	141
5.1.1	Preparation of non silylated sulfinylquinones	142
5.1.2	Preparation of silylated sulfinylquinone	144
5.2	Synthesis of quinones for the asymmetric catalyses	146
5.2.1	Preparation of the quinone for Corey's method	146
5.2.2	Preparation of the quinone for the Evans catalysis	147
5.3	Structural analysis of sulfinylquinones	148
5.3.1	Analysis of the X-ray structures of sulfinylquinones	148
5.3.2	Theoretical approach of the sulfoxide conformation	151
5.4	Reactivity study of quinones and sulfinylquinones	154
5.4.1	Effect of the solvent on the Diels-Alder reaction with sulfinylquinone 318a	154
5.4.2	The Diels-Alder reaction of 1,4-quinones in hexafluoroisopropanol	157
5.4.3	Diels-Alder reactions between sulfinylquinone 318a and different dienes	167
5.4.4	Limitations of the use of HFIP	170
5.5	Conclusion	170
	References	173

6	Diels-Alder reactions for the synthesis of momilactones	175
6.1	Sulfinylquinone pathway	177
6.1.1	Diels-Alder reaction with diene 373a	177
6.1.2	Diels-Alder reaction with pyrone 373e	179
6.1.3	Diels-Alder reaction with pentadienoates	182
6.1.4	Diels-Alder reactions with 1,3-dioxypenta-2,4-dienes	185
6.2	Corey's asymmetric catalysis pathway	186
6.2.1	Evaluation of the asymmetric catalysis with model dienes	187
6.2.2	Corey's catalysis for the synthesis of momilactones	188
6.3	Evans asymmetric catalysis pathway	190
6.3.1	Evaluation of the Evans catalysis with quinone 371a	190
6.3.2	Design and synthesis of a new quinone for the Evans catalysis	192
6.4	Conclusion	200
	References	202
7	Conclusion and outlook	205
7.1	Conclusion	207
7.1.1	Synthesis of dienes	207
7.1.2	Synthesis and use of 4-hydroxy-5-thiomethylenefuran-2-ones	207
7.1.3	Synthesis of quinones	208
7.1.4	Structural analysis of the sulfinylquinones	209
7.1.5	Reactivity study on sulfinylquinones and quinones	209
7.1.6	Diels-Alder reactions for the total synthesis of momilactones	211
7.2	Outlook	214
7.2.1	Synthesis of the silylated quinones	214
7.2.2	Computational study of the sulfinylquinones	216
7.2.3	Diels-Alder reactions for the synthesis of momilactones	217
7.2.4	Model study for the formation of the third cycle of momilactones	219
7.2.5	Total synthesis of momilactones	224
	References	225
III	Experimental section	227
8	Experimental	229
8.1	General methods	231
8.1.1	Reagents, solvents and handling of the reactions	231
8.1.2	Chromatography	232
8.1.3	Characterisation	233
8.2	Synthesis of the dienes	235
8.2.1	(<i>Z</i>)-Trimethyl(penta-1,3-dien-yloxy)silane (373a)	235
8.2.2	(<i>Z</i>)-1-Methoxy-4-(((3-methoxypenta-2,4-dien-1-yl)oxy)methyl)benzene (373b)	235
8.2.3	6-Ethenyl-2,2-dimethyl-2,4-dihydro-1,3-dioxin-4-one (373c)	240
8.2.4	<i>tert</i> -Butyl 3-((trimethylsilyl)oxy)penta-2,4-dienoate (373d)	242

8.2.5	4-Methoxy-3-methyl- α -pyrone (373e)	243
8.2.6	(<i>E</i>)-3-Methoxy-2-methylpenta-2,4-dien-1-ol (373f)	247
8.3	Synthesis of the 5-thiomethylenefuran-2-ones	248
8.3.1	Phenylthiomethylenefuranone 455a	248
8.3.2	Methylthiomethylenefuranone 455b	250
8.3.3	Butylthiomethylenefuranone 455c	253
8.3.4	(4-Methoxyphenyl)thiomethylenefuranone 455d	255
8.4	Synthesis of the sulfinylquinones	258
8.4.1	(<i>l</i>)-Menthyl (-)-(SS)- <i>para</i> -toluenesulfinate ((SS)- 292)	258
8.4.2	Sulfinylquinone 318a/SQ1	259
8.4.3	Sulfinylquinone 297/SQ2	266
8.4.4	Sulfinylquinone 307a/SQ4	268
8.4.5	Sulfinylquinone 488/SQ3	271
8.4.6	Silylated sulfinylquinone 318b	276
8.5	Synthesis of the quinones	284
8.5.1	Quinone 369a/Q3	284
8.5.2	Quinone 371a/Q8	286
8.5.3	Quinone Q2	287
8.5.4	Quinone Q4	288
8.5.5	Quinone Q5	288
8.5.6	Quinone Q7	290
8.5.7	Naphthoquinone Q9	291
8.5.8	Phthalide quinone 534	293
8.6	Diels-Alder reactions	304
8.6.1	Solvent study: expected cycloadducts and pyrolysed adducts	304
8.6.2	Solvent study: unexpected products	326
8.6.3	Diels-Alder reactions for the synthesis of momilactones	334
	References	339

Part I

Introduction

Chapter 1

Pimarane diterpenes and momilactones

1 Pimarane diterpenes and momilactones

Momilactones are natural substances of the pimarane diterpene family and bear a 4,6-transannular γ -lactone. The two first members of that family, momilactones A (1) and B (2), were isolated in 1973 from rice husks and participate in the defence mechanisms of the rice plant. They were first identified as antifungal, antibacterial compounds and growth inhibitors. More recently, they proved to possess anticancer activities against several cancer cell lines, but without decreasing the viability of healthy cells. They also showed to be active against type 2 diabetes. Given their numerous biological activities, making them good candidates as potential medicinal agents, the great interest shown in them is quite natural. Moreover, their peculiar structure makes them attractive to the chemist as a synthetic challenge.

Therefore, in this chapter, an overview of the diterpene family will be presented, including the biosynthesis of their common precursor, geranylgeranyl diphosphate, as well as the richness of the substructures of those natural compounds. We will then focus on the pimarane diterpenoids and use some examples to illustrate the natural sources from which this compounds can be isolated.

We will later focus on pimarane diterpenoids bearing a 4,6-transannular γ -lactone that is the general pattern of the momilactones, the natural compounds in which we take a great interest in this work. We will show the variety of those substructures and describe the natural sources of the compounds of that subfamily. We will also highlight the great interest that can be taken in those compounds by presenting the biological activities they possess and that can be very interesting for the human kind.

The final part of this chapter will provide more details on the momilactones and their origin, especially momilactones A and B. As said above, those two natural compounds play an important role in the protection of the rice plant, but also present a great interest as potential drug against human diseases. Thereby, a detailed description of their biological activities will be presented as well as their biosynthetic pathway, that is one of the best known for that family of compounds, and the first racemic total synthesis of momilactone A.

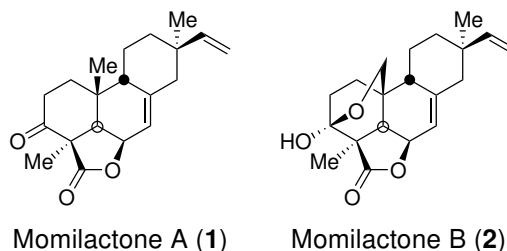
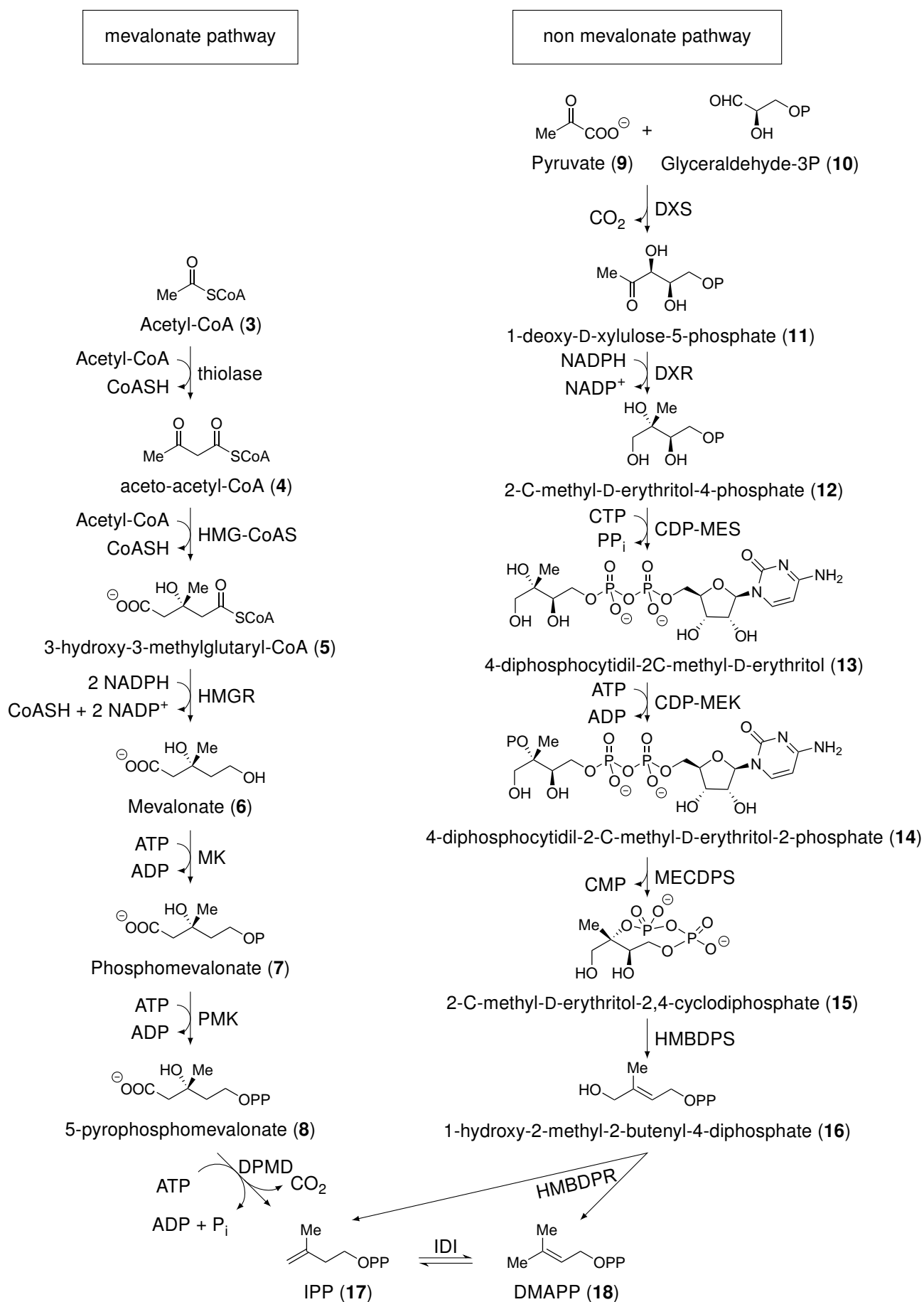


Figure 1.1: Structures of momilactones A and B.

1.1 Terpenes and the isoprenoids family

Plants, fungi and even marine organisms are seemingly an inexhaustible source of natural products with remarkable structural and biological diversity. Many of those natural compounds are part of the isoprenoid family and are constructed from the same five carbon atoms units: isopentenyl diphosphate (IPP, **17**) and its allylic isomer, dimethylallyl diphosphate (DMAPP, **18**). Oligomers of those two units, formed by head-to-tail union, undergo diverse biochemical transformations giving rise to a large library of natural substances (more than 30 000) ranging from vitamins to steroids or pigments.¹⁻³

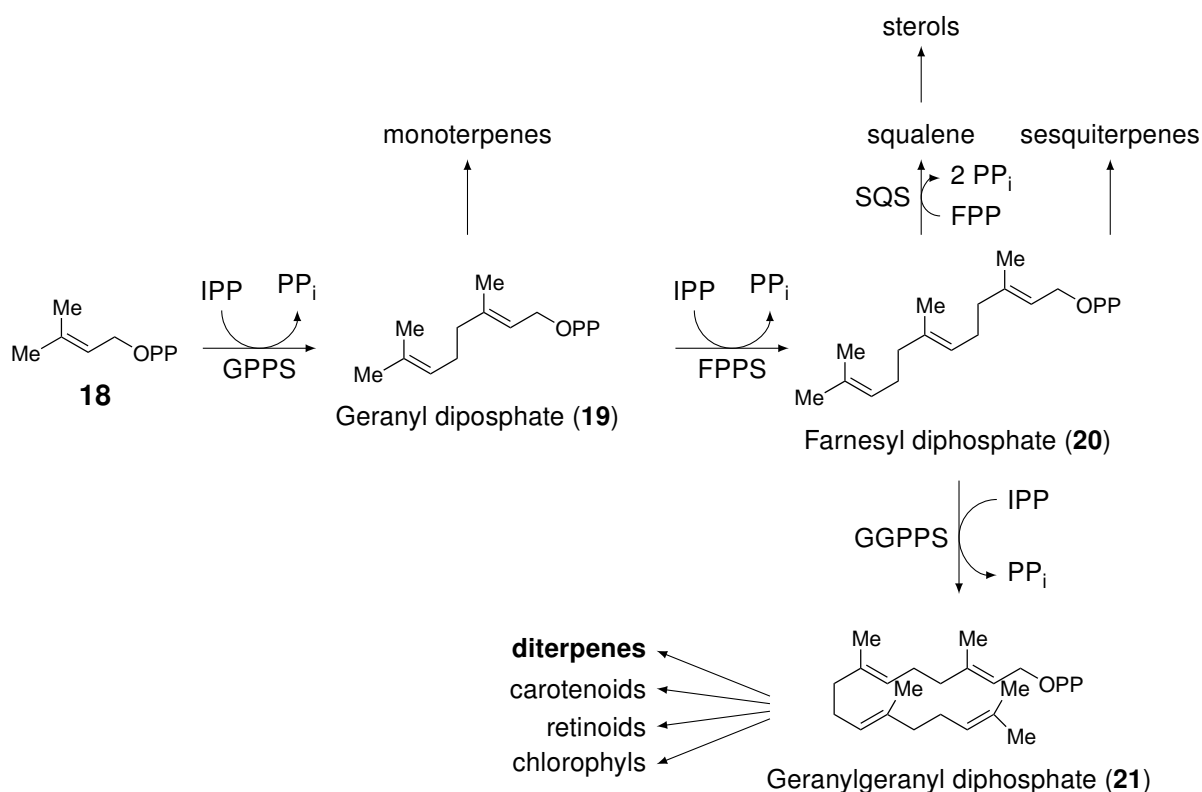
There are two known pathways for the biosynthesis of IPP. The first one that was discovered, and which was considered as the only one for decades, is the mevalonic pathway (Scheme 1.1).

Scheme 1.1: Diagram of both IPP biosynthesis pathways⁴⁻⁷.

This pathway starts with the condensation of three acetyl-CoA units, giving hydroxymethylglutaryl-CoA (HMG-CoA, **5**), which is then reduced into mevalonate (**6**). A double phosphorylation, performed by kinases, leads to 5-pyrophosphomevalonate (DPM, **8**). The latter then undergoes a decarboxylation and a dehydration, to give IPP (**17**).⁸

In the late eighties, ¹³C and ¹⁴C studies allowed to highlight the existence of a non-mevalonate IPP biosynthesis pathway (Scheme 1.1).^{9,10} This pathway, also called methylerythritol phosphate (MEP, **12**) pathway, starts with the condensation of pyruvate (**9**) and glyceraldehyde-3-phosphate (G3P, **10**), in presence of thiamine pyrophosphate (TPP), giving 1-deoxy-D-xylulose-5-phosphate (DXP, **11**). That intermediate is then reduced into 2-C-methyl-D-erythritol-4-phosphate (MEP, **12**). A molecule of cytidine triphosphate (CTP) is then introduced to form cytidine diphosphomethylerythritol (CDP-ME, **13**), which is then phosphorylated. A cyclisation reaction is then performed on intermediate **14**, with the elimination of cytidine monophosphate (CMP), giving methylerythritol cyclodiphosphate (MECDP, **15**). The latter is then reopened to give hydroxymethylbutenyl diphosphate (HMBDP, **16**), which is reduced into IPP (**17**) or DMAPP (**18**). IPP and DMAPP are in an equilibrium thanks to the action of the IPP isomerase (IDI).¹¹⁻¹³

Once those two units are synthesised, the oligomerisation process can be started (Scheme 1.2). In this process, an IPP unit and a DMAPP unit are condensed *via* a “head-to-tail” addition to give the first isoprenoid oligomer, geranyl diphosphate (GPP, **19**). The latter will serve as base unit for the biosynthesis of well known monoterpenes such as limonene, carvone, menthol, geraniol, and many others.^{14,15}



Scheme 1.2: Condensation of IPP (**17**) to give the first isoprenoid oligomers.^{3,5,7,14,16}

The sequence continues by addition of a third IPP unit to form farnesyl diphosphate (FPP, **20**), which can later lead to the biosynthesis of sesquiterpenes (e.g. parthenolide, artemisinin, and humulene).^{16,17} Along with the biosynthesis of sesquiterpenes, FPP (**20**) can also be dimerised into

squalene, through a “head-to-head” condensation, that can then lead to the synthesis of sterols.^{5,14} Finally, a fourth IPP unit can be added to form geranylgeranyl diphosphate (GGPP, **21**), that will be the base unit for the biosynthesis of chlorophylls, retinoids, and carotenoids.^{3,18} But most of all, GGPP can be transformed into diterpenes, the isoprenoid class that interests us in this work.

1.2 The diterpene classes

Due to its twenty carbon atom base unit, GGPP (**21**) can be transformed into many biologically active natural compounds, through complex chemo-, regio-, and stereoselective enzymatic processes.

In order to simplify the diterpene nomenclature, they have been classified according to the number of full carbon atom cycles formed with the diterpene chain. They are then further divided into subfamilies depending on the size of the cycles and the position of the remaining side chains. The main classes of diterpenes, based of the extended listing of Hanson over the last four decades,^{19–28} are represented in Figure 1.3, but many other structural types exist in nature. Taking into account the different stereochemical possibilities and the unclassified isomers, there are more than 120 types of diterpene structures.²⁹

The first group contains the acyclic diterpenes, also called the phytane (**24**) diterpenes. This family was named after phytol, the prenyl side chain of chlorophyll, from which phytane would be obtained after a series of reduction reactions.³⁰

As can be noticed in Figure 1.3, there is no subclass of monocyclic diterpenes, due to the fact very few examples have been found in nature. Although cembrane (**41**) could be classified as a monocyclic compound, it was rather defined as a macrocyclic one. Nevertheless, some examples can be cited, such as sauruchinenols A (**22a**) and B (**22b**), secondary metabolites extracted from the aerial parts of *Saururus chinensis*, a plant known as Asian lizard’s tail (Figure 1.2).³¹ Another example is jaspinquinol (**23**), a benzenoid monocyclic diterpene isolated from marine sponges *Suberea* sp. and *Jaspis splendens*.³²

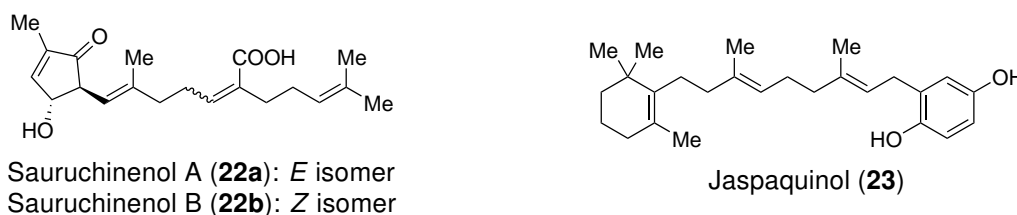
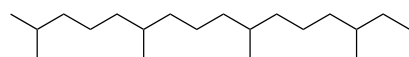
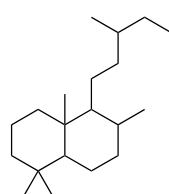


Figure 1.2: Structure of sauruchinenol A (**22a**) and B (**22b**), and jaspinquinol (**23**), three monocyclic diterpenoids.^{31,32}

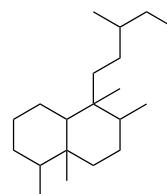
One of the constituents of the bicyclic diterpenoid group are labdanes (**25**). They are named after labdanum, a resin derived from the gum rockrose, from which several products of that family are extracted.^{33–35} This group is also composed of clerodanes (**26**), named after *Clerodendrum infortunatum*, a plant providing many very potent natural antifeedants.³⁶ There are also halimanans (**27**), that were initially called “rearranged labdanes”, but that were later renamed after the plant *Halimium viscosum*.^{37,38}

Acyclic diterpeneoids

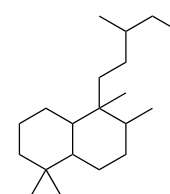
Phytane (24)

Bicyclic diterpenoids

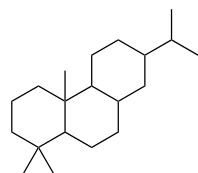
Labdane (25)



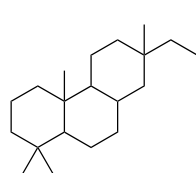
Clerodane (26)



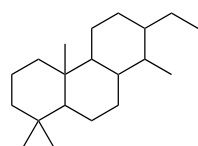
Halimane (27)

Tricyclic diterpenoids

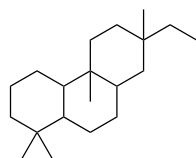
Abietane (28)



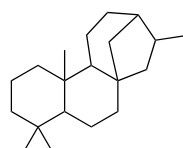
Pimarane (29)



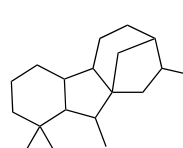
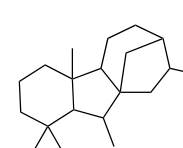
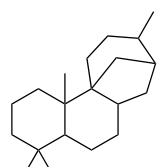
Cassane (30)



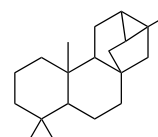
Rosane (31)

Tetracyclic diterpenoids

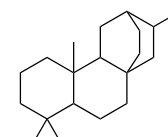
Kaurane (32)

C₁₉-Giberellane (33)C₂₀-Giberellane (34)

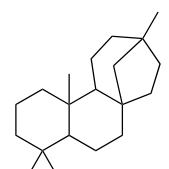
Aphidicolane (35)



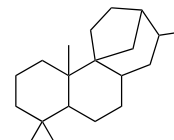
Trachylobane (36)



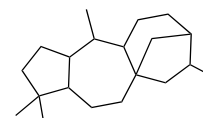
Atisane (37)



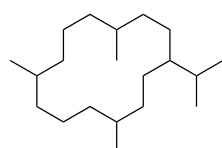
Beyerane (38)



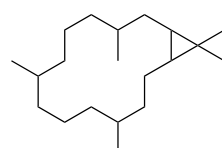
Stemarane (39)



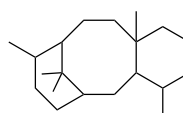
Grayanotoxin (40)

Macrocyclic diterpenoids

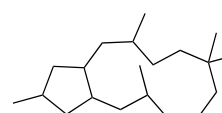
Cembrane (41)



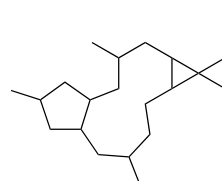
Casbane (42)



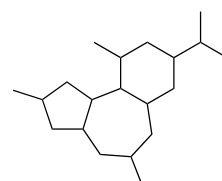
Taxane (43)



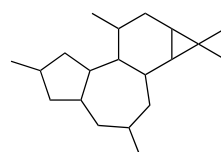
Jathropane (44)



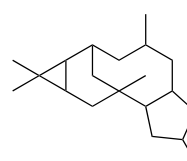
Lathyrane (45)



Daphnane (46)



Tigliane (47)



Ingenane (48)

Figure 1.3: Backbones of the main classes of diterpenoids organised by the number of cycles.^{19–28,41}

The next category of diterpenes are tricyclic compounds. This group is composed of abietanes (**28**), pimaranes (**29**), cassanes (**30**), and rosanes (**31**). The abietane subgroup takes its name from a series acidic compounds found in the distillation residue of pine resins (*Abies* is latin for pine).^{39,40} The cassane class was named after compounds isolated from plants of the *Caesalpinia* species. These tricyclic diterpenes often bear a furan ring or an α,β -butenolide.^{42,43} Most of the members of the rosane diterpenes, although very few examples are found in the literature, are isolated from the root bark of *Hugonia castaneifolia*, a medicinal plant found in the tropical areas of Africa, Madagascar and Mauritius.^{44,45}

The tetracyclic diterpenoid family is close to the tricyclic one, as their members possess three main carbon atoms rings, but with a carbon bridge on the third cycle. Eight recurring structural types have been identified in Hansons's work: kauranes (**32**), giberellanes (**33** and **34**), aphidicolanes (**35**), trachylobanes (**36**), atisanes (**37**), beyeranes (**38**), stemaranes (**39**), and grayanotoxins (**40**).¹⁹⁻²⁸ Among the members of that family, giberellins are the most abundant and are considered as phytohormones, necessary for the growth and development of the plants.^{46,47} The giberellins are also divided into two subgroups: a twenty carbon atom group and a nineteen carbon atom group, which have lost one carbon atom.⁴⁷

Diterpenoids containing at least one cycle of seven carbon atoms or more are listed in the macrocyclic diterpenoid family. They are especially composed of cembranes (**41**), casbanes (**42**), taxanes (**43**), jathrophanes (**44**), lathyrans (**45**), daphnanes (**46**), tiglianes (**47**), and ingenanes (**48**). Those compounds, besides the complexity of their macrocyclic structure, reveal various effects such as antitumor, cytotoxic, multidrug-resistance-reversing, antiviral properties, and anti-inflammatory activities.⁴⁸

1.3 The pimarane diterpenoids

1.3.1 Where to find them

The first occurrence of a pimarane diterpene we could find was pimaric acid⁴⁹ (**49**, Figure 1.4) that was isolated from the turpentine of the marine pine and whose name was created by contracting the latin name of that tree, *Pinus maritima*.⁵⁰ Since then, many other compounds entered that classification, such as *ent*-pimaradienes (**50a-f**) isolated from the air-dried tubers of *Viguiera arenaria*.^{51,52}

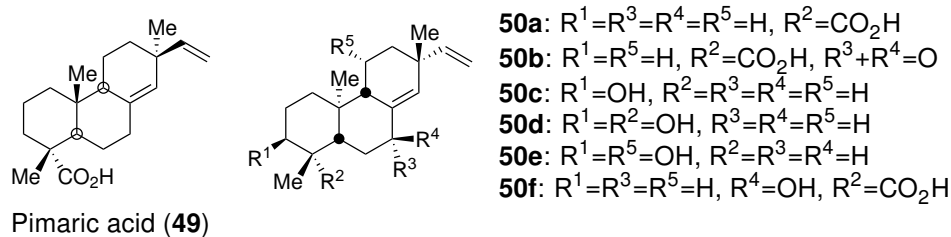


Figure 1.4: Structures of pimaric acid (**49**) and six *ent*-pimaradienes (**50a-f**).^{49,51,52}

It was shown that *ent*-8(14)15-pimaradiene-3 β -ol (**50c**) induced vascular relaxation, using standard muscle bath procedures with isolated aortic rings from male Wistar rats.⁵³ This property, which

is even more pronounced for pimaradienoic acid **50a**, was found to result from an inhibitory effect on the Ca^{2+} influx, which induces alterations of the smooth muscle cellular membrane.^{54,55}

Most pimarane diterpenes come from plants and fungi but are more rarely produced by marine organisms.^{56,57} Most importantly, they possess interesting biological activities along with potential applications in agriculture and medicine.^{58–60} In this section, a few examples of such pimarane diterpenes will be presented in order to highlight the large amount of sources and structural diversity.

Another provider of a large amount of pimarane diterpenes is *Oryza sativa*. The rice plants mostly produce those secondary metabolites as phytoalexin agents when they are infected with *Pyricularia oryzae*, a fungus being the causal agent of rice blast.⁶¹ One family of phytoalexins extracted from infected rice blast leaves are the oryzalexins A-D (**51a-d**, Figure 1.5).^{62,63} A few years later, Akatsuka *et al.* isolated oryzalexins E (**51e**) and F (**51f**) after UV-irradiation of rice leaves infected by *P. oryzae*.^{64,65} It was also evidenced, when tested against *P. oryzae* to evaluate its mode of action, that oryzalexin D (**51d**) caused membrane permeability, acting like a detergent.⁶⁶

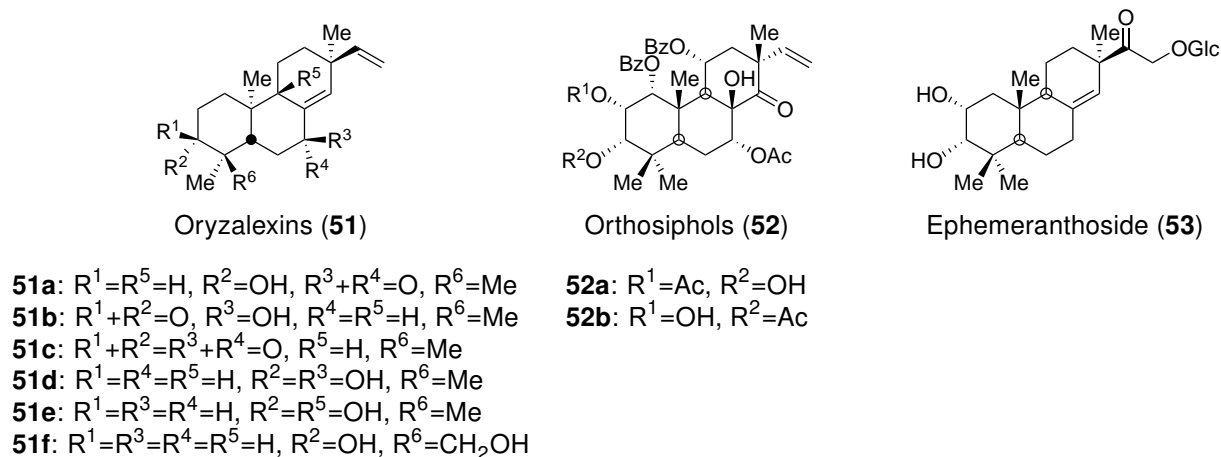


Figure 1.5: Structures of oryzalexins (**51**), orthosiphols (**52**), and ephemeranthoside (**53**), isolated from *O. sativa*, *O. stamineus*, and *E. lonchophylla*, respectively.^{62–65,67,68}

Another example pimarane diterpenes from plants are orthosiphols A (**52a**) and B (**52b**), both isolated from the dry leaves of *Orthosiphon stamineus*, a Southeast Asian plant, well-known for its diuretic and anti-inflammatory activity. It was shown that both compounds possess an anti-inflammatory activity against inflammation in mouse ears induced by TPA, a tumor promoter.⁶⁷

Another particularity observed in plants is their ability to produce metabolites with sugar fragments such as ephemeranthoside (**53**), a glycosylated pimarane diterpene, isolated from the stems of *Ephemerantha lonchophylla*, a plant used in traditional Chinese medicine.⁶⁸

Fungi are also contributors to the structural diversity of pimaranes and many of them were isolated from the liquid cultures of fungi belonging to the genus *Sphaeropsis* and *Diplodia*, causal agents of canker diseases of the Mediterranean cypress (*Cupressus sempervirens* L.).⁶⁹ Evidente *et al.*^{70,71} isolated sphaeropsidins A and B (**54a** and **54b**, Figure 1.6) from the fermentation of *Sphaeropsis sapinea* f. sp. *cupressi*, even though they had already been isolated from the fermentation of *Aspergillus chevalieri* two decades earlier,⁷² and confirmed the structure of **54a** by X-ray analysis.⁷³

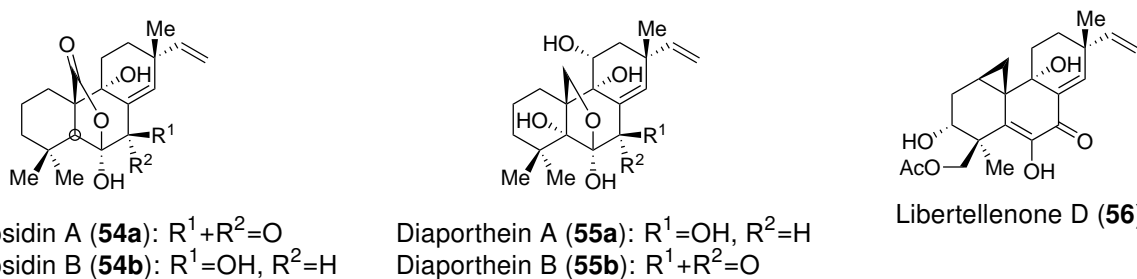


Figure 1.6: Structures of sphaeropsidins A (**54a**) and B (**54b**), diaportheins A (**55a**) and B (**55b**), and libertellenone D (**56**), isolated from *S. sapinea* f. sp. *cupressi*, *Diaporthe* sp. BCC 6140, and *Libertella* sp., respectively^{71,73–75}

In 2003, Kittakoop *et al.* isolated diaportheins A (**55a**) and B (**55b**), from the culture broth of the fungus *Diaporthe* sp. BCC 6140.⁷⁴ They showed **55b** has interesting biological activities, evidenced by the strong inhibition of the growth of *M. tuberculosis*.

Libertellenone D (**56**), along with three other derivatives, were biosynthesised by the marine-derived fungus *Libertella* sp. after addition of bacteria. It was also shown that **56** presented a strong cytotoxic activity against the HCT-116 human adenocarcinoma cell line ($IC_{50} = 0.76 \mu M$).⁷⁵

The last subgroup of pimarane-producers are marine organisms. As an example, *Aplysia dactylomela*, a sea hare, produces parguerol (**57**), a brominated pimarane diterpene. Analogues of parguerol also exhibit a cytotoxic activity *in vitro* against lymphocytic leukaemia (P388), supposedly due to the formation of an epoxyde on the bromohydrin moiety, which could later react with nucleophilic entities, such as glutathione or amino acid residues.⁷⁶



Figure 1.7: Structures of parguerol (**57**) and tedanol (**58**), two pimarane diterpenes isolated from *Aplysia dactylomela* and *Tedania ignis*, respectively.^{76,77}

Another brominated pimarane, tedanol (**58**), has been isolated from the Caribbean sponge *Tedania ignis*. Its structure also presents a sulfate group. The latter showed a potent anti-inflammatory activity at 1 mg kg^{-1} when assayed in a mouse model of inflammation.⁷⁷

1.3.2 Pimarane diterpenes with a 4,6-transannular γ -lactone

In the course of this thesis, a focus has been put on pimarane diterpene structures bearing a 4,6-transannular γ -lactone ring in a *cis* relation with respect to the C20 angular methyl group (Figure 1.8). Indeed, this pattern is the one observed in momilactones A (**1**) and B (**2**). An interest has also been taken into the 17-*nor*-pimarane equivalents, a pattern found in many of closely related compounds.⁷⁸ Momilactones will be further discussed in the next section, but a closer look will be taken at other natural products with a similar core structure.

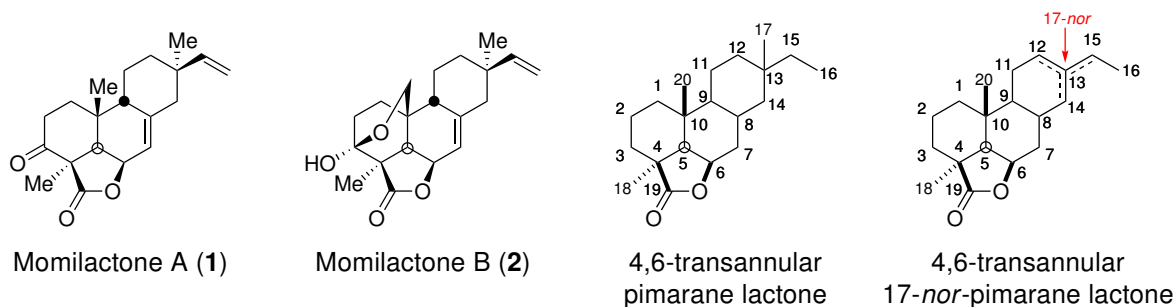


Figure 1.8: Structures of momilactones A (1) and B (2) and both patterns of 4,6-transannular pimarane and 17-*nor*-pimarane lactones.⁷⁸

The main providers of such pimarane diterpene lactones are the Icacinaceae, a family of flowering plants, composed of trees, shrubs, and lianas primarily found in the tropics (structures in Figure 1.9, names and sources in Table 1.1). The root decoctions of *Icacina claessensis* and *Icacina guessfeldtii* are used as anticonvulsant in popular medicine in the Democratic Republic of the Congo. Therefore, in order to identify the active principles of these plants, Vanhaelen *et al.* studied them and isolated icacinol (**59a**) from the ethanolic extract of the roots. They determined its structure using X-ray analysis. However only the relative configurations had been determined.⁷⁹

In 2014, Zhao *et al.* presented the isolation of a closely related diterpenoid, 17-hydroxyicacinol (**59b**), from the tubers of *Icacina trichanta*. They also restudied the structure of icacinol (**59a**) and determined its absolute configuration. By comparison of NMR analyses of **59b** with the latter, they observed very high similarities between both compounds and proposed a similar structure for both of them.⁸⁰ Among the bioactivities icacinol possesses, it was identified as a potential herbicidal agent, and a crop defence herbicide, as it highly reduced the germination rate and seedling growth of plants such as rice (*Oryza sativa*) and *Arabidopsis thaliana*.⁸¹

A few years before the isolation and identification of icacinol, different groups from the Université Libre de Bruxelles and the Université de Louvain isolated three diterpene-based alkaloids from the leaves of *Icacina guessfeldtii*.^{82,83} Using a series of reactivity experiments, coupled with analytical experiments and X-ray analysis, they could determine the structure of icacine (**60**) to be the one described in Figure 1.9.⁸² Two other alkaloids, icaceine (**61a**) and its de-*N*-methyl analogue **61b**, were correlated to icacine based on a set of several analytical and NMR experiments. Although Vanhaelen's group could resolve most of the structures, the absolute configurations of carbon atoms 13, 14, and 15 were not elucidated.⁸³ These three compounds are the very first examples — and, to the best of our knowledge, the only ones — of pimarane alkaloids.

In 2015 and 2016, the group of Zhao *et al.* described the identification and characterisation of thirteen new 17-*nor*-pimarane diterpenes (**62-69** and **71**) and two new pimarane diterpenes (**70** and **72**) called icacinlactones.⁸⁴⁻⁸⁸ They were isolated from the tubers of *Icacina trichanta*, another traditional herbal medicine used in Nigeria and other regions of western Africa to treat food poisoning, constipation, and malaria.⁸⁹ In their first paper, they elucidated the structures of icacinlactones A-G (**62a**, **63a** and **64-68**) by spectroscopic and HRMS techniques and determined the absolute configuration of icacinlactone B (**63a**) by X-ray crystallographic analysis. Due to the similarity of spectroscopic data, they assigned the same configurations on the other icacinlactones.⁸⁴

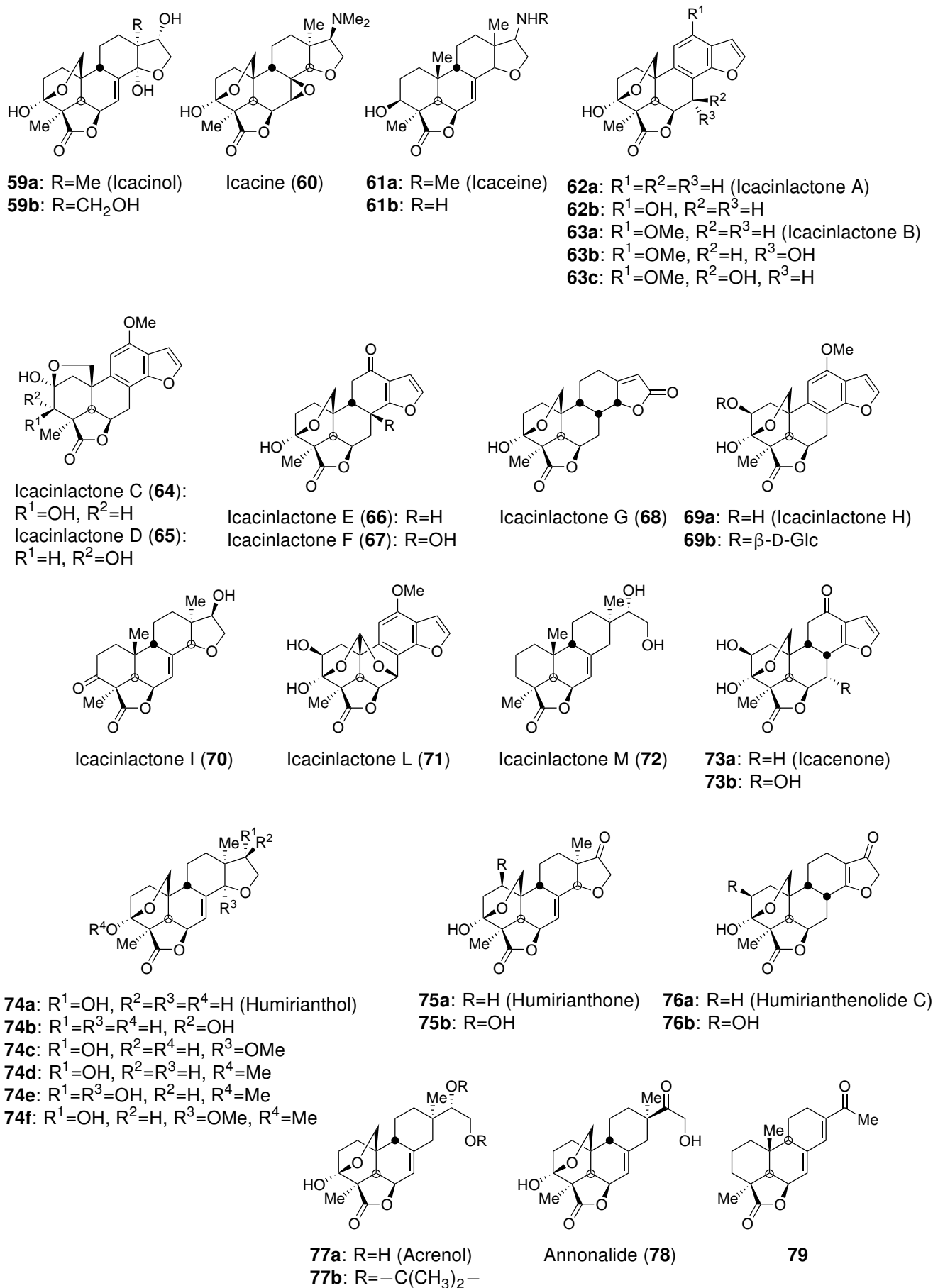


Figure 1.9: Structures of 4,6-transannular pimarane and 17-nor-pimarane lactones isolated from plants (*Icacina* sp., *Humirianthera* sp., *Annona coriacea*, *Juniperus chinensis*, and *Hypnum plumaeforme*).

In the course of the same year, the group published the isolation of icacinlactone H (**69a**), the eighth member of this family. Given the strong similarities in the spectroscopic analyses of **69a** and icacinlactone B **63a**, they could deduce that icacinlactone H (**69a**) had the same structure as **63a** but for the hydroxy group on the C2 position.⁸⁵ Unfortunately for the group, **69a** showed no antiviral activity when tested against HSV-1, HSV-2, and the Epstein-Barr virus, three herpes viruses.

A bit later, another set of icacinlactones have been extracted, including the 12-hydroxy analogue of icacinlactone A (**62b**), and the 7 α - and 7 β -hydroxy analogues of icacinlactone B (**63b** and **63c**). They also obtained icacinlactone I (**70**), which is the only member of the icacinlactone family that possesses the C17 carbon atom, and icacinlactone L (**71**), bearing a double bridged acetal moiety.^{86,87} Unsurprisingly, they could elucidate these structures by comparison with the already known icacinlactones and by detailed 2D NMR analysis.

Very recently, that group isolated the 2-*O*- β -D-glucopyranoside derivative of icacinlactone H (**69b**) and a brand new pimarane diterpene, icacinlactone M (**72**), from the tubers of *I. oliviformis*.⁸⁸

In 1985, the group of Vanhaelen isolated icacenone (**73a**) from *I. mannii*, another medicinal plant used for the treatment of fibrous tumours. Its structure was determined by X-ray analysis and comparison with icacinol (**59a**) and icacine (**60**) facilitated the interpretation of spectroscopic data.⁹⁰ Zhao's group also isolated it from *I. trichanta* along with its 7 α -hydroxy analogue (**73b**) whose structure was elucidated by comparison with the spectroscopic data of icacenone and a detailed analysis of 2D NMR spectroscopy.^{80,87}

Another major provider of pimarane diterpene lactones are the *Humirianthera* species, now re-grouped with the *Casimirella* species,⁹¹ belonging to the Icacinaceae as well. This plant is commonly used in the treatment of snakebites. One of the constituents isolated from *H. ampla* is humirianthol (**74a**), as well as its 15-*epi* isomer (**74b**).^{92,93} Elucidation of their structure was performed by standard spectroscopy analysis but was later confirmed, along with their absolute configurations, by the X-ray analysis of the 15-*O*-acetyl derivative of **74a**.⁹⁴

Although humirianthol was first discovered in *Humirianthera* species, hence the trivial name it was given, it was also isolated from *I. trichanta* and *I. oliviformis*, along with several analogues (**74c-f**) to which no new names have been given.^{80,86,88,95}

Closely related to humirianthol, two oxidised forms, humirianthone (**75a**) and its 1 β -hydroxy equivalent (**75b**), have been isolated from the same source. Its structure elucidation was really easy to perform as the spectroscopic data were almost identical but for the presence of a carbonyl group at the C15 position.⁹³

The last 17-*nor*-pimarane lactone isolated from a *Humirianthera* species is humirianthenolide C (**76a**), which was extracted from the tubers of *H. rupestris* and identified by Gottlieb *et al.*⁹⁶ Like humirianthol (**74a**), it was also isolated from *I. trichanta*, along with its 2 β -hydroxy analogue (**76b**).^{80,87}

Two other natural compounds isolated from icacenaceae as well are acenol (**77a**) and its oxidised analogue, annonalide (**78**). The first one to have been isolated is annonalide, which was extracted, not from an icacinacea, but from a fruit tree from Brazil, *Annona coriacea*, hence its taxonomic etymology.⁹⁷ As many of the previous examples, its structure was first elucidated by comparison of NMR data with other known pimarane diterpenes such as momilactones A (**1**) and B (**2**), but was later unambiguously confirmed by X-ray analysis.⁹⁸

Table 1.1: names and sources of 4,6-transannular pimarane and 17-*nor*-pimarane diterpene lactones isolated from plants and described in Figure 1.9.

names	sources
Icacinol (59a)	<i>I. claessensis</i> , ⁷⁹ <i>I. trichanta</i> , ^{80,81} <i>I. oliviformis</i> , ^{88,95} <i>H. ampla</i> ⁹³
17-Hydroxyicacinol (59b)	<i>I. trichanta</i> ⁸⁰
Icacine (60)	<i>I. guessfeldtii</i> ^{82,83}
Icaceine (61a)	<i>I. guessfeldtii</i> ⁸³
De- <i>N</i> -methylicaceine (61b)	<i>I. guessfeldtii</i> ⁸³
Icacinlactone A (62a)	<i>I. trichanta</i> , ⁸⁴ <i>I. oliviformis</i> ⁸⁸
12-Hydroxyicacinlactone A (62b)	<i>I. trichanta</i> , ⁸⁶ <i>I. oliviformis</i> ^{88,95}
Icacinlactone B (63a)	<i>I. trichanta</i> , ⁸⁴ <i>I. oliviformis</i> ⁸⁸
7 α -Hydroxyicacinlactone B (63b)	<i>I. trichanta</i> ⁸⁷
7 β -Hydroxyicacinlactone B (63c)	<i>I. trichanta</i> ⁸⁶
Icacinlactone C (64)	<i>I. trichanta</i> ⁸⁴
Icacinlactone D (65)	<i>I. trichanta</i> ⁸⁴
Icacinlactone E (66)	<i>I. trichanta</i> ⁸⁴
Icacinlactone F (67)	<i>I. trichanta</i> ⁸⁴
Icacinlactone G (68)	<i>I. trichanta</i> ⁸⁴
Icacinlactone H (69a)	<i>I. trichanta</i> , ⁸⁵ <i>I. oliviformis</i> ⁸⁸
Icacinlactone H 2- <i>O</i> - β -D-glucopyranoside (69b)	<i>I. oliviformis</i>
Icacinlactone I (70)	<i>I. trichanta</i> , ⁸⁶ <i>I. oliviformis</i> ⁹⁵
Icacinlactone L (71)	<i>I. trichanta</i> ⁸⁷
Icacinlactone M (72)	<i>I. oliviformis</i> ⁸⁸
Icacenone (73a)	<i>I. mannii</i> , ⁹⁰ <i>I. trichanta</i> ⁸⁰
7 α -hydroxyicacenone (73b)	<i>I. trichanta</i> ⁸⁷
Humirianthol (74a)	<i>H. ampla</i> , ^{92,93} <i>I. trichanta</i> , ⁸⁰ <i>I. oliviformis</i> ⁹⁵
(15 <i>R</i>)-Humirianthol (74b)	<i>H. ampla</i> ⁹³
14 α -Methoxyhumirianthol (74c)	<i>I. trichanta</i> , ⁸⁶ <i>I. oliviformis</i> ^{88,95}
3- <i>O</i> -Methylhumirianthol (74d)	<i>I. oliviformis</i> ⁹⁵
3- <i>O</i> -Methyl-14 α -hydroxymethylhumirianthol (74e)	<i>I. oliviformis</i> ⁹⁵
3- <i>O</i> -Methyl-14 α -methoxyhumirianthol (74f)	<i>I. oliviformis</i> ⁹⁵
Humirianthone (75a)	<i>H. ampla</i> ⁹³
1 β -Hydroxyhumirianthone (75b)	<i>H. ampla</i> ⁹³
Humirianthenolide C (76a)	<i>H. rupestris</i> , ⁹⁶ <i>I. trichanta</i> ⁸⁰
2 β -Hydroxyhumirianthenolide C (76b)	<i>I. trichanta</i> ⁸⁷
Acrenol (77a)	<i>H. ampla</i> , ^{92,93} <i>Hypnum plumaeforme</i> ⁹⁹
Acrenol acetonide (77b)	<i>I. oliviformis</i> ⁸⁸
Annonalide (78)	<i>Annona coriacea</i> , ^{97,98} <i>H. ampla</i> , ⁹³ <i>I. oliviformis</i> ⁸⁸
Compound 79	<i>Juniperus chinensis</i> ¹⁰⁰

Like other members of that family, annonalide (**78**) was also isolated with acrenol (**77a**) from icacinaceae such as *H. ampla* or *I. oliviformis*, although in the last case, acrenol was extracted under its acetone form (**77b**) as an artefact of the extraction.^{88,92,93} Although acrenol's structure was mostly elucidated by spectroscopic means, it was confirmed by X-ray analysis of its diacetyl derivative in 2003.¹⁰¹ Surprisingly, acrenol was also found in a completely different source, *Hypnum plumaeforme*, a moss which also provided other related compounds such as momilactones A (**1**) and B (**2**).⁹⁹

Finally, from plants, another 17-*nor*-pimarane diterpene lactone (**79**), which had not been given any name, was isolated from *Juniperus chinensis*, a common ornamental tree.¹⁰⁰ Besides its extraction and characterisation, this compound, to the best of our knowledge, was not studied further.

As expected for diterpenoids, a wide range of biological activities can be observed with such compounds. It is therefore quite logical that some of the groups cited here above tested some of those natural products against different cancer cell lines (Table 1.2).

Table 1.2: IC₅₀ (μM) values of the tested compounds against human cancer cell lines: ovarian cancer (A2780⁹³ and OVCAR3^{84,87,88}), melanoma (MDA-MB-435^{80,84,86-88}), breast cancer (MDA-MB-231^{84,87,88}), and colon cancer (HT-29⁸⁰).

Entry	Compounds	Cancer cell lines				
		A2780	OVCAR3	MDA-MB-435	MDA-MB-231	HT-29
1	59a	1.7	5.6	1.25	3.4	4.23
2	59b	—	—	5.61	—	18.27
3	67	—	10.50	6.16	8.94	—
4	73a	—	10.87	6.44	10.85	13.25
5	73b	—	7.53	2.91	7.60	—
6	74a	3.0	4.12	1.65	3.74	4.94
7	74b	2.2	—	—	—	—
8	74c	—	6.3	3.6	4.0	—
9	75a	6.1	—	—	—	—
10	76a	—	1.05	0.66	0.67	3.00
11	76b	—	3.23	1.48	2.85	—
12	77a	1.8	—	—	—	—
13	78	3.9	4.4	2.3	2.7	—

The group of Kingston *et al.* tested humirianthol (**74a**), 15*R*-humirianthol (**74b**), humirianthone (**75a**), acrenol (**77a**), and annonalide (**78**) against the A2780 human ovarian cancer cell line.⁹³ These compounds exhibited a rather good cytotoxic activity with IC₅₀ values below 6.1 μM, humirianthone being the most active one with 1.7 μM. They also demonstrated that humirianthone has a strong fungicidal activity against *Phytophthora infestans*, a phytopathogenic fungus, with an IC₅₀ value of 0.93 μM.

Throughout their work, the group of Zhao *et al.* tested several of the compounds cited here above against different human cancer cell lines, such as OVCAR3 ovarian cancer, MDA-MB-435 melanoma, MDA-MB-231 breast cancer, and HT-29 colon cancer cell lines.^{80,84,86-88}

They showed that against OVCAR3, all the tested compounds presented good cytotoxic activities below 10 μM (at the exception of icacinlactone F (**67**) and icacenone (**73a**)), with humirianthenolide C (**76a**) possessing the best activity with an IC_{50} of 1.05 μM .

Most of the compounds listed in Table 1.2 have also been tested against MDA-MB-435 human melanoma cells and showed good IC_{50} values. Similar tendencies have been observed when they were tested against MDA-MB-231 human breast cancer, but in both cases humirianthenolide C (**76a**) exhibited the best cytotoxic activity with 0.66 and 0.67 μM , respectively.

The last cancer cell line against whom some of the cited compounds were tested is the HT-29 human colon cancer cell line. In that case, icacicol (**59a**) and humirianthol (**74a**) showed good activity with IC_{50} values of 4.23 and 4.94 μM , respectively, but the best result was obtained with humirianthenolide C (**76a**) with 3.00 μM .

Although this group displayed significant interest as anticancer agent, the mode of action of these compounds has not been studied.

In 2018, the group of de Oliveira *et al.* further tested annonalide (**78**), along with semisynthetic derivatives, against other human cancer cell lines.¹⁰² It was tested against HL-60 leukemia, PC-3 prostate carcinoma, HepG2 hepatocellular carcinoma, SF-295 glioblastoma, and HCT-116 colon cancer with IC_{50} values of 2.1, 3.6, 5.7, 2.2, and 1.7 μM . It was therefore a good candidate as potential anticancer agent, although some of its derivatives exhibited even better cytotoxic activities.

They also evaluated the interaction of annonalide with ctDNA using spectroscopic techniques (molecular fluorescence and UV-visible spectroscopy), which confirmed the formation of a supramolecular complex. They also showed, *via* competition assays with fluorescent probes, that annonalide preferentially interacts through DNA intercalation.

Besides plants, fungi also provided many examples of 4,6-transannular pimarane γ -lactones (structures in Figure 1.10 and sources in Table 1.3), albeit less abundantly than in the former case.

The very first was described by Bodo *et al.* in 1987. They extracted hymatoxin A (**80a**) from *Hypoxylon mammatum*, a pathogenic fungus of Leuce poplars causing stem cankers.¹⁰³ Using standard spectroscopic techniques, they could determine its structure (with relative configurations), showing it bears a sulfate group, making hymatoxin A the first example of sulfate diterpene biosynthesised by a fungus.¹⁰⁴

Four years later, the group published the isolation of four new hymatoxins, including hymatoxins B (**81**) and E (**82**), which contains the same pattern of interest for this thesis.¹⁰⁵ They elucidated most of the structures using the same procedure, showing **81** has a sulfate group and a hydroxyl group at the C15 position, but whose relative configuration could not be determined. In the case of **82**, a hydroxyl group was present instead of a sulfate. The latter was also later extracted from a mutant strain *Tubercularia* sp. TF5, an endophytic fungal strain isolated from the medicinal plant *Taxus mairei*.^{106,107}

Hypoxylon mammatum also provided two α -D-mannopyranosyl related diterpenes, hymatoxins K (**83**) and L (**84**).¹⁰⁸ The first one was identified as the 16-mannopyranosyl equivalent of hymatoxin E (**82**) and the second one as possessing a completely new structure. Almost two decades later, they were also found in *Stilbohypoxyton elaeicola* YMJ173, a fungus belonging to the Xylariaceae.¹⁰⁹

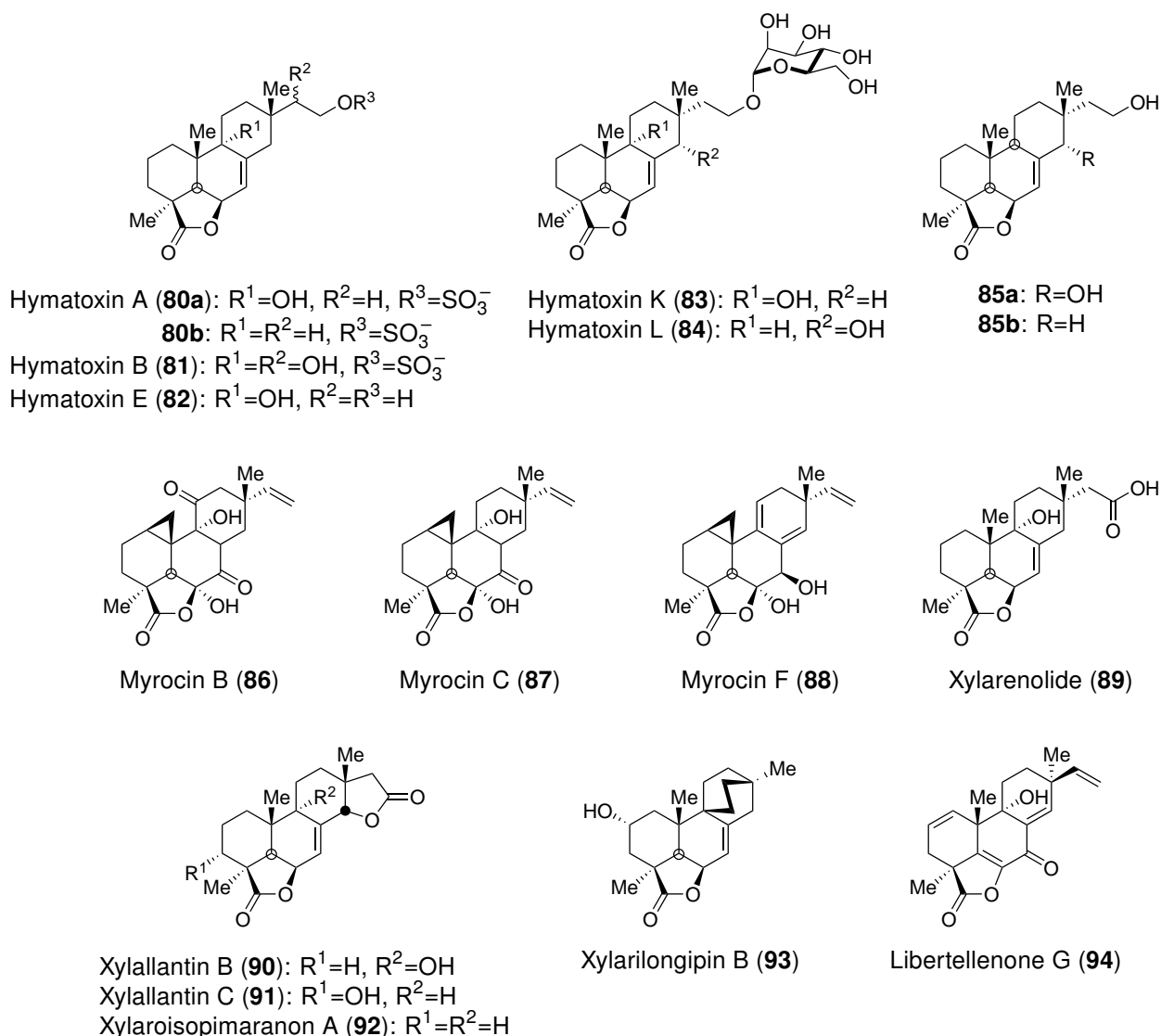


Figure 1.10: Structures of 4,6-transannular pimarane diterpene lactones isolated from fungi (*Xylaria* sp., *Hypoxylon mammatum*, *Tubercularia* sp., *Stilbohypoxylon elaeicola* YMJ173, *Myrothecium* sp., *Stilbella fimetaria*, *Xylaralyce* sp., and *Apiospora montagnei*).

From another member of the Xylariaceae, *Xylaria* sp. BCC 4584, hymatoxin E (**82**) was isolated along with a new related pimarane lactone (**85a**), which was given no name, but corresponds to hymatoxin L (**84**) without its mannopyranosyl moiety.¹¹⁰ The same compound **85a** was isolated from *Myrothecium inundatum*, an endolichenic fungus, by Liu *et al.*¹¹¹ Peculiarly, the group decided to name it hymatoxin L, although they present its structure without the sugar moiety, which is even more surprising as they claim having compared the NMR data of both **84** and **85a**. A second group isolated **85b** from *Xylaria longipes* HFG1018 and analysed and confirmed its structure by X-ray diffraction. By comparison with the NMR data described by the previous group, they noticed the high similarities between both structures and proposed a revision of that compound by removing the hydroxyl group on the C14 position. Although the described structure is even more different from the one described by Bodo *et al.*, they still named it hymatoxin L.¹¹²

In 2014, Wu *et al.* described the isolation of 9-deoxy-hymatoxin A (**80b**) from *Xylaria* sp. YM 311647, whose characterisation data were similar to hymatoxin A (**80a**) but for the alcohol group

Table 1.3: Names and sources of 4,6-transannular pimarane diterpene lactone isolated from fungi and described in Figure 1.10.

names	sources
Hymatoxin A (80a)	<i>Hypoxyton mammatum</i> ^{104,105}
9-deoxyhymatoxy A (80b)	<i>Xylaria</i> sp. YM 311647 ¹¹³
Hymatoxin B (81)	<i>Hypoxyton mammatum</i> ¹⁰⁵
Hymatoxin E (82)	<i>Tubercularia</i> sp. TF5, ^{106,107} <i>Xylaria</i> sp. BCC 5484, ¹¹⁰ <i>X. allantoidea</i> BCC 23163 ¹¹⁴
Hymatoxin K (83)	<i>Hypoxyton mammatum</i> , ¹⁰⁸ <i>Stilbohypoxylon elaeicola</i> YMJ173, ¹⁰⁹ <i>X. allantoidea</i> BCC 23163 ¹¹⁴
Hymatoxin L (84)	<i>Hypoxyton mammatum</i> , ¹⁰⁸ <i>Stilbohypoxylon elaeicola</i> YMJ173 ¹⁰⁹
Compound 85a	<i>Xylaria</i> sp. BCC 5484, ¹¹⁰ <i>M. inundatum</i> ¹¹¹
Compound 85b	<i>X. longipes</i> HFG1018 ¹¹²
Myrocine B (86)	<i>M. verrucaria</i> , ¹¹⁵ <i>Stilbella fimetaria</i> , ¹¹⁶ <i>Phomopsis</i> sp. S12 ¹¹⁷
Myrocine C (87)	<i>M. verrucaria</i> , ^{118,119} <i>Ganoderma applanatum</i> ¹²⁰
Myrocine F (88)	<i>Stilbella fimetaria</i> ¹²¹
Xylarenolide (89)	<i>Xylaria</i> sp. 101, ¹²² <i>X. allantoidea</i> BCC 23163 ¹¹⁴
Xylallantin B (90)	<i>X. allantoidea</i> BCC 23163 ¹¹⁴
Xylallantin C (91)	<i>X. allantoidea</i> BCC 23163 ¹¹⁴
Xylaroisopimarane A (92)	<i>Xylaralyce</i> sp. (HM-1) ¹²³
Xylarilongipin B (93)	<i>X. longipes</i> HFG1018 ¹¹²
libertellenone G (94)	<i>Apiospora montagnei</i> ¹²⁴

at C9.¹¹³ They studied the *in vitro* inhibitory activity of several compounds isolated from the same fungus, including **80b**, against different pathogenic fungi. Among the tested products, **80b** gave the best results against *C. albicans* YM 2005, *A. niger* YM 3029, *P. oryzae* YM 3051, *F. avenaceum* YM 3065, and *H. compactum* YM 3077 with MIC values of 16, 32, 16, 64, and 64 $\mu\text{g mL}^{-1}$, respectively.

A second class of pimarane lactones extracted from fungi are the myrocins. Nakyama *et al.* isolated two of those diterpenoids, myrocine B (**86**) and C (**87**), from *Myrothecium verrucaria* strain No. 55, a soil fungus.^{115,118} Using spectroscopic techniques, including 2D NMR experiments, they could identify the structures of both compounds, but only for their relative configurations. The structure of **87**, with relative configurations, was confirmed by X-ray analysis of its 6-*O*-acetyl derivative.¹²⁵

They tested both compounds against the Gram-positive bacterium *Bacillus subtilis* IFO 12210, the fungus *Aspergillus niger* IFO 4416, and the yeast *Candida albicans* which showed MIC values of 12.5, 50, and 25 $\mu\text{g mL}^{-1}$ for myrocine B (**86**) and 50, 100, and 50 $\mu\text{g mL}^{-1}$ for myrocine C (**87**). They also evaluated the therapeutic effect of those two compounds on mice injected with Ehrlich ascites carcinoma, which showed a prolongation rate (T/C) of 169% at a dose of 2.4 mg kg^{-1} for **86** and of 130% at a dose of 1.6 mg kg^{-1} for **87**. These results indicate that the presence of a ketone moiety at the C11 position seems to play an important role in the inhibitory activities. Both compounds, however, revealed to be ineffective against Gram-negative bacteria.

Myrocine B (**86**) was also identified from *Stilbella erythrocephala* (also known as *S. fimetaria*), a coprophilous fungus colonising individual rabbit pellets and using antifungal antibiosis metabolites as

a strategy for habitat conquest.¹¹⁶ Similarly to the work of Nakayama *et al.*, this paper presents the inhibitory activities of **86** against several bacteria and yeasts, which exhibited good MIC values.

Besides the sources cited here above, myrocins B (**86**) and C (**87**) has also been isolated from *Phomopsis* sp. and *Ganoderma applanatum*, respectively.^{117,120}

Finally, a third myrocin lactone, myrocin F (**88**), has been extracted from a marine-derived *Stilbella fimetaria* IBT 28361.¹²¹ They showed that **88** possesses a moderate cytotoxic activity against glioblastoma stem-like cells with a IC_{50} value of 40 μ M. It also possesses similar activity against A549 lung carcinoma, MCF7 breast carcinoma, SW480 colorectal adenocarcinoma, and DU145 prostate carcinoma cells with IC_{50} values between 20 and 50 μ M.

The next family of pimarane lactones from fungi was extracted from Xylariaceae, fungi commonly found on dead wood. From *Xylaria* sp. 101, the group of Shen *et al.* isolated and elucidated the structure of xylarenolide (**89**), which bears a carboxylic acid on the ethylene unit. Upon evaluation of the activity of the compounds extracted from that source against several bacteria but none of them had any effect.

Four years later, Isaka *et al.* found, from *X. allantoides* BCC 23163, two new diterpenes bearing the pattern described in Figure 1.8, xylallantins B (**90**) and C (**91**), as well as xylarenolide (**89**).¹¹⁴ It is noteworthy that those xylallantins look similar to the first compound but they possess a closed lactone ring instead of an open carboxylic acid moiety. This group tested all three products against different cancer cell lines, as well as *Plasmodium falciparum* K1 (malaria) and *Mycobacterium tuberculosis* H37Ra, but they exhibited no activity against them.

In 2019, Guo *et al.* isolated xylaroisopimaranin A (**92**) from *Xylaralyce* sp., an endophytic fungus, on the healthy leaves of *Distylium chinense*. After elucidation of its structure, they evaluated its cytotoxicity against Hep G2 cancer cells and its antimicrobial activity against plant-pathogenic *Erwinia carotovora* subsp. but no activity was evidenced. However, it exhibited an IC_{50} value of 10 μ mol mL^{-1} against the hatchability of brine shrimp.¹²³

One last compound of that family is xylarilongipin B (**93**), which is not a pimarane diterpene *per se* as it possesses a bicyclo[2.2.2]octane moiety.¹¹² However, its backbone does not correspond to any of the common tetracyclic diterpene families (Figure 1.3) and could correspond to a pimarane with its ethylene unit linked to the C9 position.

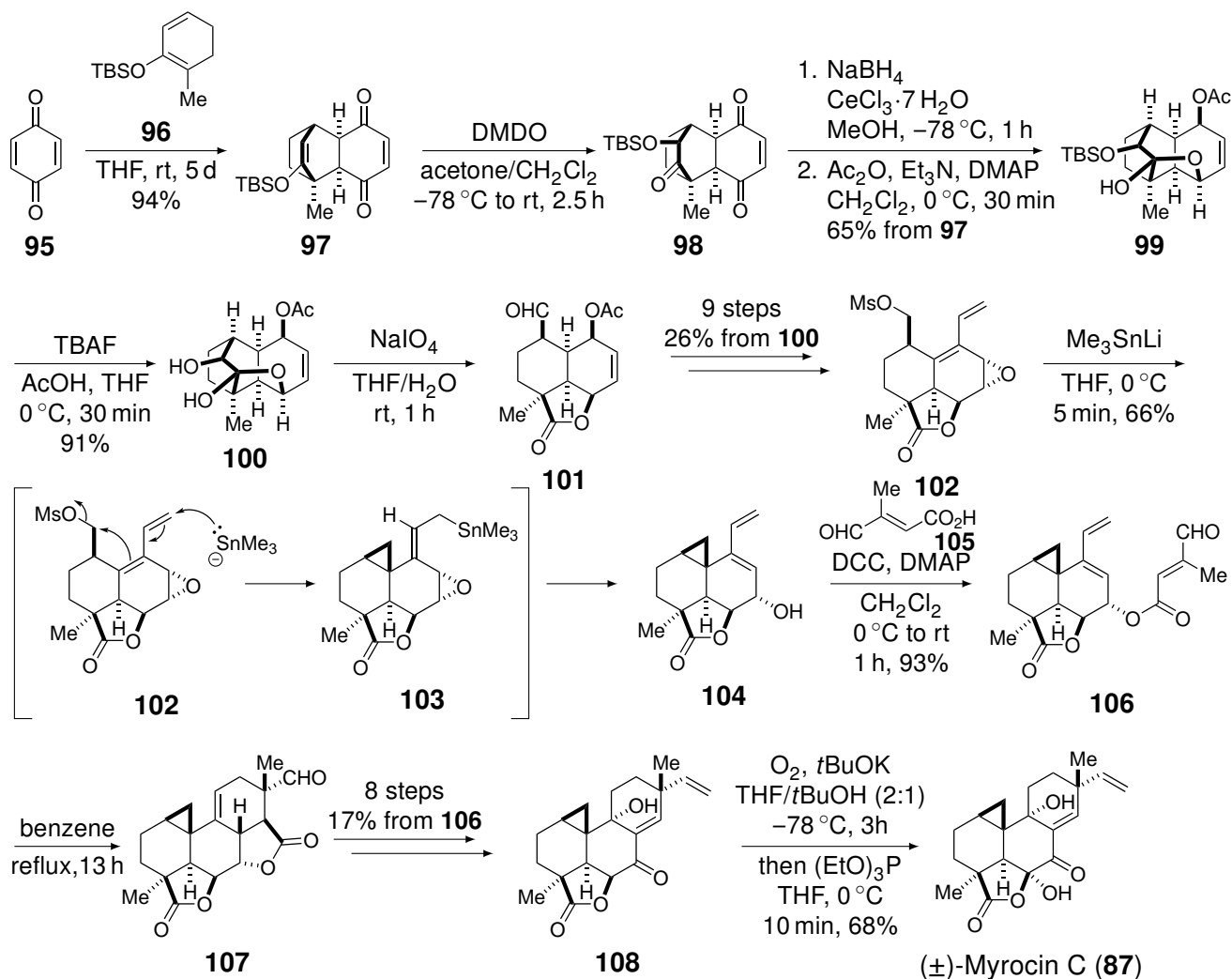
The last compound identified from a fungus which corresponds to the desired pattern, is libertellenone G (**94**), which was isolated from a lichen-associated fungus *Apiospora montagnei*.¹²⁴ As the carbon atom at the C6 position is involved in a double bond with the C5 carbon atom, only the C10 and C4 position keep stereogenic information, however the desired relative configuration of these two centers corresponds to the main pattern.

When this compound was tested against the L5178 murine lymphoma cell line, it gave one of the best results with an IC_{50} value of 2.6 μ M.

Despite the different results of bioactivities, no mode of action has been proposed by any of the cited groups for the molecules described in Figure 1.10.

1.3.3 Total syntheses of myrocins C and G

To the best of our knowledge, myrocin C (**87**) was the only example, among those presented in the previous section, that has been subjected to total synthesis. Danishefsky *et al.* published its racemic synthesis (Scheme 1.3) in 1992, followed by the fully detailed investigation of the best route in 1994.^{126,127}



Scheme 1.3: Total synthesis of myrocin C (**87**) by the group of Danishefsky *et al.* in 1992.^{126,127}

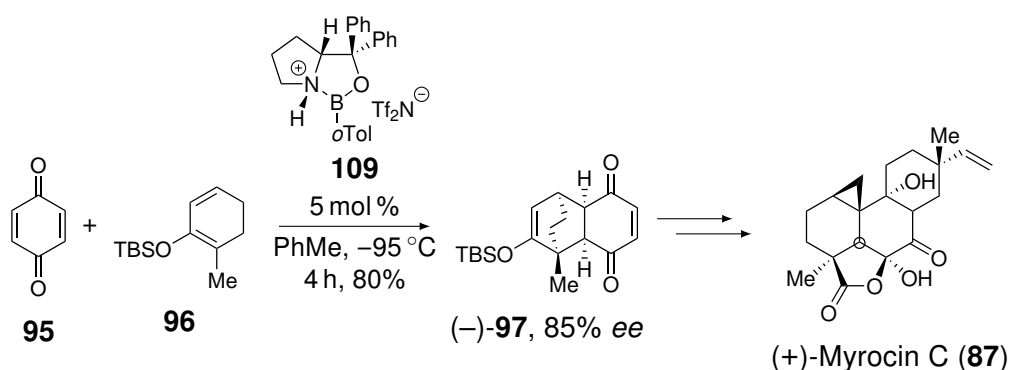
They started with a Diels-Alder reaction between benzoquinone (**95**) and the oxygenated diene **96** which gave adduct **97** in a very good yield, introducing three stereogenic centers with the desired relative configurations. DMDO oxidation of the enol ether gave intermediate **98** which, upon reduction in Luche's conditions, allowed the formation of a transannular lactol. The remaining allylic alcohol was later acetylated to give product **99** with a 65% yield over three steps. The TBS protecting group was then uneventfully removed with TBAF and the diol **100** underwent an oxidative cleavage to give the 4,6-transannular lactone ring.

Intermediate **101** was subjected to a series of transformations including the stereoselective epoxidation of the double bond, the conversion of the aldehyde into a mesylate group and the insertion of a conjugated vinyl moiety. The cyclopropane moiety was then formed by a nucleophilic addition of (trimethylstannyl)lithium on the vinyl group, followed by an intramolecular nucleophilic substitution of

the mesylate group. The stannane moiety was then eliminated, leading to the formation of a diene and the opening of the epoxyde, giving compound **104**.

The third cycle was stereoselectively obtained by tethering of butenoic acid **105**, followed by an intramolecular Diels-Alder reaction. The aldehyde was submitted to a Wittig olefination, the newly formed lactone was selectively cleaved and a series of oxidations, selectively gave 6-desoxymyrocin C (**108**) in nine steps and 17% global yield from intermediate **106**. Finally, the latter was hydroxylated through air oxidation, presumably passing through a peroxide later reduced by $(\text{EtO})_3\text{P}$, to give (\pm)-myrocin C (**87**) in 68% yield.

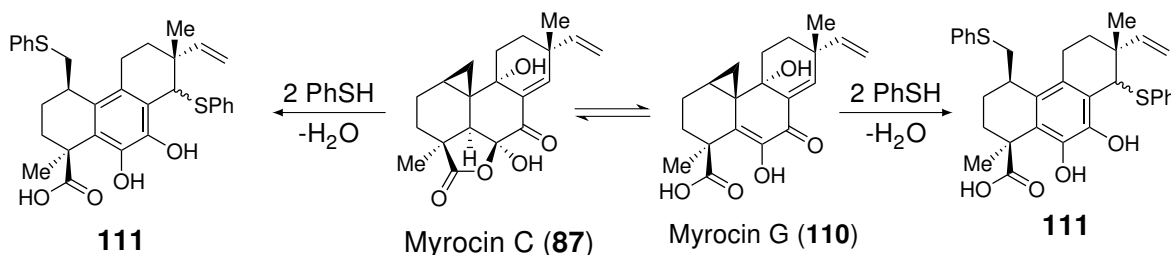
In 2004, Corey *et al.* proposed a way to carry out an enantioselective total synthesis of myrocin C (**87**), using an oxazaborolidinium salt as a chiral catalyst in the Diels-Alder reaction being the first step of the synthesis (Scheme 1.4).¹²⁸



Scheme 1.4: Asymmetric Diels-Alder reaction catalysed by a chiral oxazaborolidinium salt between benzoquinone (**95**) and diene **96** as starting step for the enantioselective total synthesis of myrocin C (**87**).¹²⁸

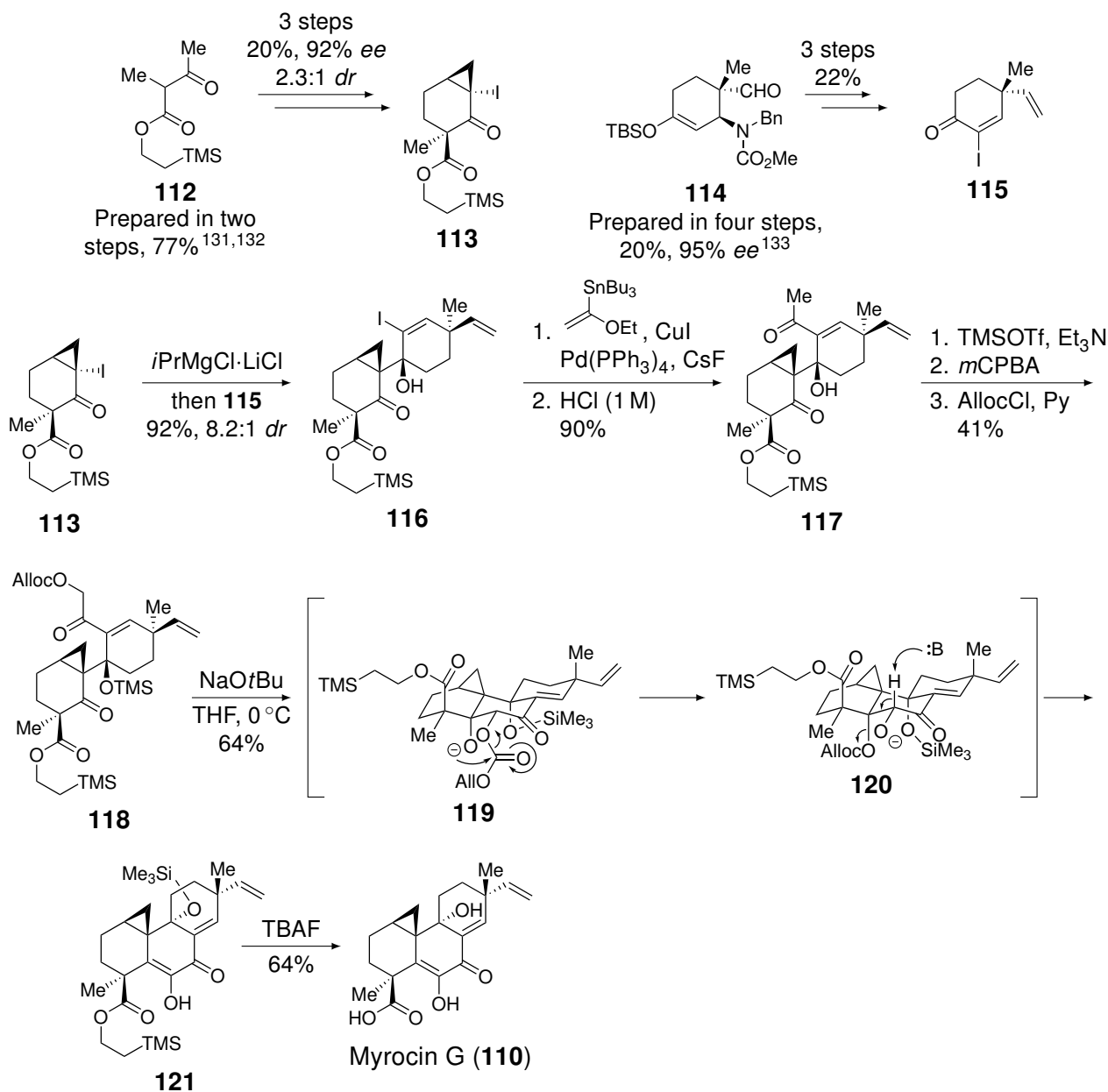
They run the reaction at -95°C for four hours in toluene, which gave the tricyclic dione **97** in 85% *ee* and 80% yield. Its enantiomeric purity was verified by reduction with LiAlH_4 of the dione to the corresponding diol (unacetylated version of **99**), conversion of the latter to its MTPA ester, and ^{19}F NMR analysis.

In Danishefsky's work, they reported that the treatment of myrocin C (**87**) with two equivalents of thiophenol led to bis(sulfide) **111** (Scheme 1.5).¹²⁹ This reactivity led them to speculate that the myrocins cross-link DNA by sequential nucleotide addition reactions. Given the similarities with myrocin B (**86**), whose active form is myrocin A, Herzon *et al.* suggested that the bioactivities of myrocin C (**87**) might actually be due to a hypothetical isomer, myrocin G (**110**).¹³⁰



Scheme 1.5: Structures of myrocins C (**87**) and G (**110**), and bis(sulfide) **111** resulting from the treatment of both myrocins by thiophenol.^{129,130}

In order to verify this hypothesis, they decided to develop the total synthesis of myrocin G (**110**) to obtain some material and compare its behaviour to the one of myrocin C (**87**). Contrariwise to Danishefsky's synthesis of myrocin C (**87**, Scheme 1.3), which was linear, Herzon *et al.* designed a convergent synthesis of myrocin G (**110**) from two key intermediates **113** and **115** (Scheme 1.6).



Scheme 1.6: Preparation of intermediates **115** and **113** and total synthesis of myrocin G (**110**) developed by Herzon *et al.*¹³⁰

They started that synthesis by preparing the intermediates **113** and **115**, that correspond to rings A and C respectively, both prepared in three steps from starting materials whose syntheses were already described (Scheme 1.6).^{131–133} Once those two precursors were prepared, they coupled them with an iodine magnesium exchange on **113**, followed by the addition of the intermediate organo-magnesium reagent on ketone **115**. They then performed a Stille coupling on iodide **116** using a methoxyvinyl stannane, followed by the acidic hydrolysis of the intermediate vinyl ether to reach ketone **117**. The synthesis continued with the protection of the tertiary alcohol, followed by a Rubottom oxidation on the ketone and conversion of the newly formed primary alcohol into an allyl carbonate.

After some investigation, they found out that the treatment of allyl carbonate **118** with NaOtBu in THF at 0 °C led to the formation of compound **121**, which correspond to a protected version of myrocin G (**110**). Mechanistic studies seemed to indicate that the latter is obtained *via* an aldol addition and intermediate **119** undergoes a carbonate migration, followed by a second order elimination.

Finally, deprotection of the carboxylic acid and the tertiary alcohol allowed them to obtain the desired myrocin G (**110**) which, after its treatment with thiophenol in the same conditions as described by Danishefsky,¹²⁹ led to the expected bis(sulfide) **111** (Scheme 1.5).

1.4 Momilactones: secondary metabolites with extraordinary properties

The very first description of momilactones was published by Kitahara *et al* in 1973.¹³⁴ They isolated two active components from the seed husk of *Oryza sativa* L., momilactones A (**1**) and B (**2**), which showed inhibition of the growth of the root of the rice plant at less than 100 ppm.

The structure of **1** (Figure 1.11) was unambiguously determined by X-ray analysis and its absolute configuration was determined by positive cotton curves of CD and ORD of **124**, isolated from the hydrolysate of momilactone A with aqueous KOH in hot dioxane. The structure of momilactone B (**2**) was determined by comparison of its spectral data with the ones of **1**. Given the similarities between both compounds, except for the presence of a lactol group instead of a ketone, the structure of **2**

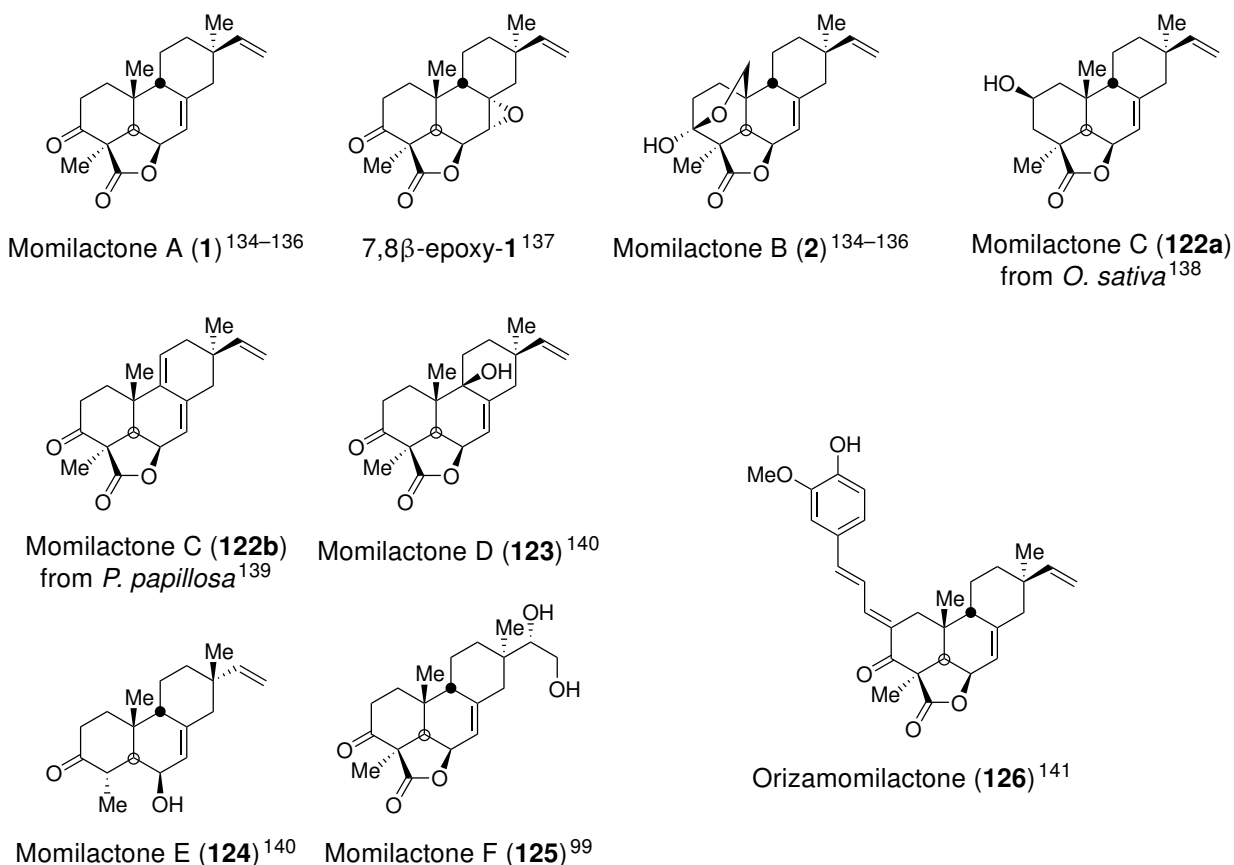


Figure 1.11: Structures of momilactones either isolated from *Oryza sativa*, *Hypnum plumaeforme*, *Plagiomnium acutum*, *Leucas urticifolia*, or *Pseudoleskeella papillosa*.

was assigned as described in Figure 1.11 and its absolute configuration was assumed due to the similarities with the ORD curves of **1**. They later confirmed the structures of **1** and **2** by a series of chemical transformations.¹⁴²

Momilactones A and B were further studied by several groups who isolated them, not only from the husk, but also from the coleoptiles¹⁴³, the straws¹⁴⁴, the root exudates¹⁴⁵, the rice seedlings¹⁴⁶ or even the rice environment at different levels throughout its life cycle.¹⁴⁷ Cartwright *et al.* also showed they could be produced in response to either infection by the blast fungus *Pyricularia oryzae* or by UV irradiation.^{148,149}

These two natural products have been found not only in rice, but also in two mosses, *Plagiomnium acutum* and *Hypnum plumaforme*.^{135,136} Similarly to the work of Cartwright *et al.*, another group showed it was possible to induce the production of both momilactone A and B by treatment of *H. plumaforme* with jasmonic acid, UV-irradiation, metals (CuCl₂ and FeCl₂) or cantharidin, a protein phosphatase inhibitor.¹⁵⁰

In 1976, the same group isolated a third minor component from the same plant, momilactone C (**122a**), whose structure was determined by X-ray analysis.¹³⁸ Peculiarly, the group of Lou *et al.* isolated two compounds from the moss *Pseudoleskeella papillosa*, momilactone A (**1**) and a second lactone diterpenoid **122b** with a very similar backbone.¹³⁹ They elucidated the structure of the latter by NMR experiments and optical rotation studies and named it momilactone C, even though its structure is different from the one previously described.

The 7,8 β -epoxy derivative of Momilactone A (7,8 β -epoxy-**1**) was described by Tahir *et al.* in 2008. They isolated it from *Leucas urtivilolia*, a wild Lamiacea herb found in Pakistan and north-west India and used in various medicinal applications, and elucidated its structure *via* X-ray analysis.¹³⁷

Two new momilactones, momilactone D (**123**) and E (**124**) were identified and their structure elucidated by Baek *et al.*¹⁴⁰ Even though momilactone E does not possess the lactone ring found in other momilactones, it was named as such. The latter was initially described by Kato *et al.* as a *nor* derivative coming from the treatment of momilactone A with aqueous KOH in hot dioxane,^{134,142} and its analogue oxidised at C6 was later identified as a degradation intermediate by Hasegawa *et al.*¹⁵¹.

The sixth member of momilactones, momilactone F (**125**), was isolated from the moss *Hypnum plumaforme* by Song *et al.*, along with **1** and **2**.⁹⁹ Its structure and absolute configuration were elucidated using NMR experiments and circular dichroism experiments.

The last compound extracted from *O. sativa*, and related to momilactones, was described by Tan *et al.* in 2018. After the study of the NMR analyses, they came to the conclusion that the structure bears the same structure as momilactone A (**1**), but for the presence of a phenyl allylidene unit on the C2 position. They then identified it as 2-[(*E*)-3-(4-hydroxy-3-methoxyphenyl)allylidene]momilactone A, but trivally named it orizamomilactone (**126**).¹⁴¹

1.4.1 Momilactones participating in the rice allelopathy and its defence mechanism

The particular interest in momilactones came from their role as agents participating in the defence of the rice plant *via* allelopathic properties.^a Many studies have been conducted on the different activities of the rice plant's allelochemicals onto its environment. One of those activities is their ability to inhibit the the growth of seedlings of diverse plants, but mostly invasive weeds. Indeed, it was shown that when it was co-cultivated with rice seedlings, the growth of other seedlings, such as barnyard grass (*Echinochloa crus-galli*)¹⁵² or the common water plantain (*Alisma plantago-aquatica*),¹⁵³ two of the most troublesome weeds in rice, was inhibited. They also performed the same study with the seedlings of alfalfa (*Medicago sativa*), cress (*Lepidium sativum*), and lettuce (*Lactuca sativa*) as model plants, and obtained the same observations.¹⁵⁴

The same studies correlated the production and release of momilactone B (**2**) to the growth inhibition depending on the rice cultivar. The higher was the growth inhibition, the higher was the concentration of momilactone B.^{152,153} The inducing factors of such allelopathy were also put under investigation. It has been demonstrated that the production of momilactones only starts when the rice plant is in the presence of barnyard grass, for example. The study showed that rice has the ability to recognise chemicals, released by the other plant, inducing the production of allelochemicals.¹⁵⁵

In order to show that momilactones, and more particularly momilactone B, was the most active allelochemical, the different compounds were tested individually on the seedlings of lettuce,^{156,157} barnyard grass,^{158,159} the common water plantain, and other weed seedlings as well.¹⁶⁰ They indeed showed that momilactones possess a high seedling growth inhibition activity on those plants. Moreover, momilactone B always had a higher activity than momilactone A.

The group of Kato-Noguchi *et al.* attempted to identify the mode of action of momilactones A and B using *Arabidopsis thaliana* as a model plant. They first observed, in addition to the growth inhibition, that the subject plant absorbed both momilactones through its roots.¹⁶¹ They later studied the protein expression on the same model plant when treated with momilactones. They observed a higher amount of cruciferin, a high molecular weight protein, in the plants treated with momilactones, indicating the tested compounds inhibited the breakdown of that protein.¹⁶² The breakdown of cruciferin is indeed essential for the growth of seedlings as it provides the initial source of nitrogen needed for the germination. Without its degradation, cell structures or components cannot develop. Momilactone B also inhibits the accumulation of enzymes needed for cell structures resulting in plant growth and development.¹⁶³

The second important, and main, activity of momilactones is their implication in the defence mechanism against the rice blast^b fungus, *Magnaporthe oryzae* (or *Pyricularia oryzae*). It was previously identified that the production of momilactones A (**1**) and B (**2**) was significantly higher when the rice plant was infected with the cited fungus.^{143,148} Many studies corroborated those results throughout the years (as examples, see Ohashi *et al.*¹⁶⁴, Kim *et al.*¹⁶⁵ or Ishihara *et al.*¹⁶⁶). This response mechanism in the rice plant and activation of the biosynthesis pathway of phytoalexins^c would be

^aSet of activating or inhibiting effects, direct or indirect, of one plant (including micro-organisms) on another by production and release of chemicals into the environment.

^bFungal disease of the aerial organs of the rice plant.

^cLow molecular weight anti-microbial chemicals only produced after infection of the organism.

induced by recognition of β -glucan fragments from the rice blast fungus.¹⁶⁷ It was also shown that depending on the rice cultivar the level of momilactones produced was different, inducing diverse levels of response to infection and, therefore, weaker or stronger protection against fungi.¹⁶⁸ In addition to that observation, it was determined that *M. oryzae* is able to metabolise those phytoalexins, leading to its detoxification as an effective solution to evade growth inhibition. It is then comprehensible that rice cultivars producing low levels of phytoalexins, such as momilactones, are more prone to infection, whereas rice types producing higher levels of those chemicals may more effectively protect themselves.¹⁵¹

It is noteworthy that they also showed a great *in vitro* inhibitory activity against other strains of fungi, such as *Botrytis cinerea*, *Fusarium solani*, *Colletotrichum gloeosporioides*, and *Fusarium oxysporum*.¹⁶⁹

Studies also showed that production and accumulation of momilactones in rice was induced by other factors such as infestation by herbivores,¹⁷⁰ UV-irradiation,¹⁷¹ or even drought and high levels of salinity.¹⁷² However, no evidence between those phytoalexins production and their implication in the rice defence against those stresses was found. Nevertheless, given their herbicidal and antifungal activity, these compounds possess a great potential as agricultural chemicals.⁷⁸

1.4.2 Momilactones A and B as new potential medicinal agents

Besides their important role in the rice plant's protection, momilactones A and B have also been tested against several pathogens and diseases afflicting humans.

In addition to the herbicidal and antifungal activity study of momilactones, Tawata *et al.* also evaluated their *in vitro* antibacterial activity against four bacteria strains: *Pseudomonas ovalis*, *Bacillus cereus*, *Bacillus pumilus*, and *Escherichia coli*. Although both momilactones showed good inhibitory activities against all four bacterial cultures, it was always lower than the one of ampicillin.¹⁶⁹

Without any surprises, both compounds have also been tested on cancer cell lines. In 2005, the *in vitro* study of Ahmad *et al.* showed that momilactones A and B exhibited IC_{50} values of 2.7 and 0.21 μ M against P388 murine leukemia cells, respectively.¹⁷³

Another study was led by Lee *et al.* in 2007.¹⁷⁴ In that work, a group of male rats was fed the methanolic extract of rice hulls and was then injected carcinogenic 1,2-dimethylhydrazine, a chemical inducing colonic aberrant crypt foci^d (ACF). It was observed that the frequency of ACF was 35% less with those rats than the ones that was fed a basal diet. More importantly, no sign of treatment-related adverse effects was observed in the clinical appearance of the animals, such as body or organ weight loss. They then identified the active agent to be momilactone B (**2**) and studied its *in vitro* activity against human colon cancer HT-29 and SW620 cell lines. The latter showed an IC_{50} value of less than 1 μ M.

Momilactone B was also efficient against human leukemic T cells (Jurkat cells) and murine mastocytoma p815 cells at less than 3 μ M.¹⁷⁵ The publication also presents that apoptosis of Jurkat cells was induced *via* the activation of caspase and induction of mitochondrial permeability.

^dClusters of abnormal tube-like glands in the lining of the colon and rectum, which are one of the earlier changes seen in the colon that may lead to cancer

In 2008, Yang *et al.* showed that momilactone B decreased the viability of human breast cancer T47D cells by $\pm 50\%$ at $50 \mu\text{M}$ under hypoxic conditions.¹⁷⁶ They suggested that apoptosis was induced through activation of caspase-3 and STAT5b (a transcription activator) protein pathways.

Momilactone B also reduced the cell viability by 50% in the case of B16 murine melanocytes for a concentration of $\pm 30 \mu\text{M}$. It represses tyrosinase enzyme activity and inhibits the protein kinase A signaling pathway, two processes involved in the melanin synthesis and, therefore, decreasing melanogenic expression.¹⁷⁷

The group of Yoo *et al.* wanted to determine the mode of action of momilactone B by studying its anticancer activity on cultured leukemia U937, against which it exhibited an IC_{50} of less than $1.5 \mu\text{g mL}^{-1}$.¹⁷⁸ They demonstrated that the compound of interest caused G1 cell cycle arrest and apoptosis in U937 cells through the induction of p21 expression, inhibition of cyclin-dependent and cyclin-associated kinase activities, and reduced phosphorylation of retinoblastoma protein, which may be related to anticancer activity.

Other than its antibacterial and anticancer activities momilactone B also inhibits ketosis, which is the accumulation of high levels of ketone bodies in the blood, resulting from the metabolism of fatty acids to provide energy when the body lacks glucose. It was shown, using *in vitro* assays on FL83B mouse hepatocyte cells, that **2** down-regulated the expression of angiopoietin-like-3 (ANGPTL3), which modulates lipoprotein metabolism by inhibiting lipoprotein lipase (LPL). The LPL enzyme was then up-regulated and could normally break down stored fat to produce triglyceride.

The second target studied in that work is 3-hydroxy-3-methylglutarate-CoA synthase-2 (HMGCS2), a mitochondrial enzyme that converts acetyl-CoA to ketone bodies. The results indicate that momilactone B suppresses the expression of HMGCS2 through the increased expression of STAT5b.¹⁷⁹

Two other biological properties of momilactones A and B have been evaluated by the group of Xuan *et al.* in 2019. The first one concerns the study of the skin ageing using chemical and biological assays.¹⁸⁰ When tested in ABTS (2,2'-azino-bis(3-ethylbenzothiazoline-6-sulfonic acid)) assays, momilactones A and B decolorised a solution of ABTS by 50% at concentrations of 2.838 and 1.283 mg mL^{-1} , respectively, which is rather high compared to tricetin (0.312 mg mL^{-1}), a well-known antioxidant and anti-skin-ageing flavonoid from rice, and BHT (0.080 mg mL^{-1}), the standard antioxidant. However, when both momilactones A and B were mixed in a 1:1 (v:v) ratio of prepared solution, this concentration lowered to 0.319 mg mL^{-1} , indicating a synergistic activity.

The second test was to evaluate the *in vitro* inhibition of elastase and tyrosinase, two key enzymes related to wrinkles and freckles. At a concentration of 2 mg mL^{-1} momilactones A and B inhibited the activity of pancreatic elastase by 30.9% and 18.5%, respectively, and the activity of tyrosinase by 37.6% and 12.6%, respectively. In that evaluation, momilactone A presented a much higher inhibition activity than tricetin at the same concentration (14% inhibition against elastase and 15.7% against tyrosinase). In this case, combination of both momilactones did not increase the inhibition of the enzymes significantly.

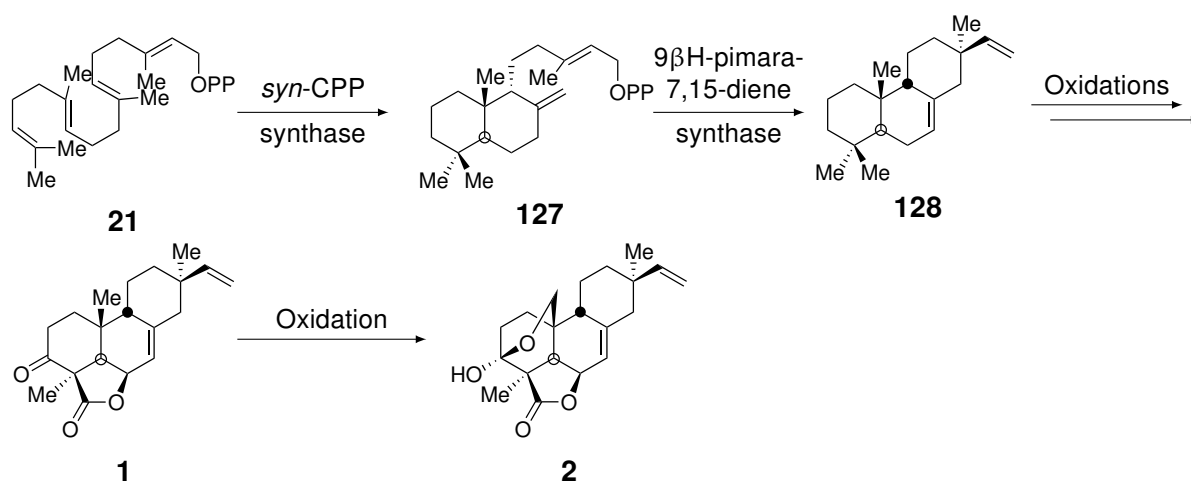
The second property studied by that group is their potential use as α -amylase and α -glucosidase inhibitors, two enzymes involved in type 2 diabetes.^{181,182} When tested against porcine pancreatic α -amylase, momilactones A and B exhibited IC_{50} values of 132.56 and $129.02 \mu\text{g mL}^{-1}$, respectively.

When the same test was made against α -glucosidase from *Saccharomyces cerevisiae*, they exhibited IC_{50} values of 991.95 and 612.03 $\mu\text{g mL}^{-1}$, respectively, which indicates a better inhibition activity than γ -oryzanol (1754.20 $\mu\text{g mL}^{-1}$), a well-known diabetes inhibitor.

Moreover, they also tested both compounds of interest against trypsin, an enzyme linked to both diabetes and obesity, and they found IC_{50} values of 921.55 $\mu\text{g mL}^{-1}$ for momilactone A and 884.03 $\mu\text{g mL}^{-1}$ for momilactone B.¹⁸²

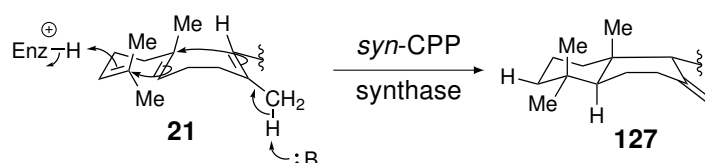
1.4.3 Biosynthesis of momilactones A and B

Many research groups have been working on the elucidation of the biosynthetic pathway of momilactones since the 1990s. In this section, only some representative work will be used in order to present their biosynthesis. As mentioned previously, momilactones are part of the diterpene family whose universal precursor is GGPP (**21**).



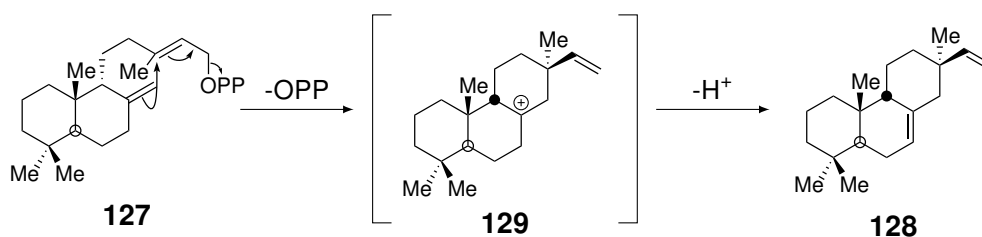
Scheme 1.7: Global biosynthetic pathway of both momilactones A (**1**) and B (**2**) via the bicyclisation of GGPP (**21**), followed by a series of oxidations.^{183–186}

As represented in the global overview of the biosynthesis (Scheme 1.7), the first step consists in the cyclisation of GGPP, initiated by the protonation of the terminal double bond, into *syn*-copalyl diphosphate (*syn*-CPP, **127**), forming the *trans*-decaline core.^{183–186} The represented configurations of *syn*-CPP are obtained thanks to the “chair-boat” conformation that GGPP adopts in the enzymatic pocket of the diterpene cyclase (Scheme 1.8). Other conformations (induced by different enzymes) allow to reach other intermediates leading to the biosynthesis of diverse secondary metabolites (for example, the “chair-chair” conformation forms the *ent*-CPP which leads to the biosynthesis of oryzalexins or phytocassanes).^{183,187}



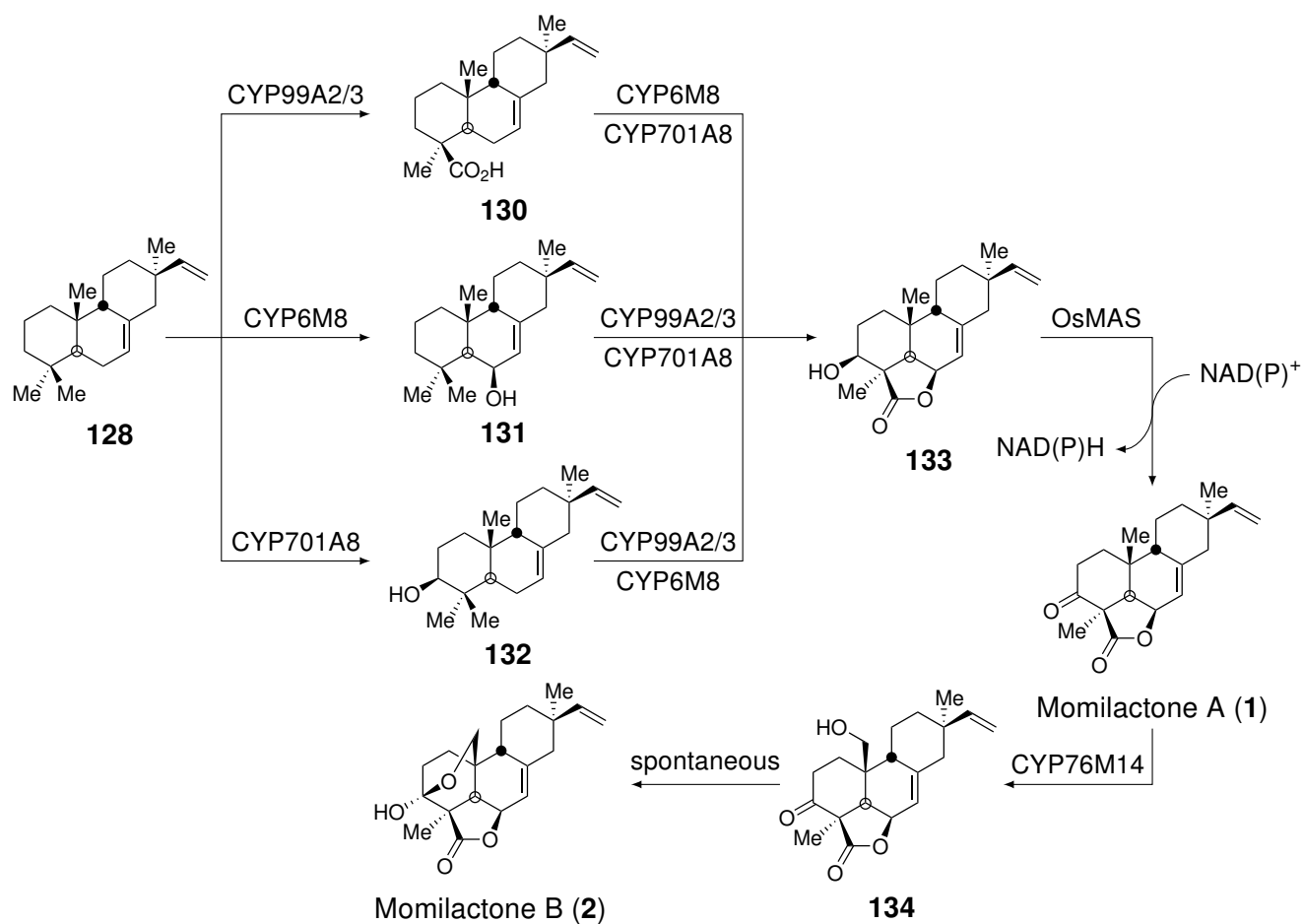
Scheme 1.8: Enzymatic mechanism of GGPP (**21**) cyclisation into *syn*-CPP (**127**).¹⁸⁷

The biosynthesis continues with the conjugate addition of the *exo*-cyclic double bond on remaining alkene along with the elimination of the pyrophosphate group, followed by first order elimination, forming the third cycle and the *endo*-cyclic double bond of the 9 β H-pimara-7,15-diene (**128**) as described in Scheme 1.9. That step is also catalysed by a diterpene cyclase.¹⁸⁷



Scheme 1.9: Enzymatic mechanism of the *syn*-CPP (**127**) cyclisation into 9 β H-pimara-7,15-diene (**128**).¹⁸⁷

Once pimaradiene **128**, the common precursor to several natural compounds, is synthesised, the latter undergoes a series of oxidation steps, on positions 3, 6 and 19 (Scheme 1.10), in order to reach momilactone A (**1**). These oxidations occur *via* a cluster of cytochrome P450 (CYP) oxidases. The oxidation of the C20 position happens through the action of CYP99A2 or CYP99A3 (both oxidases seemingly play the same role in the case of momilactones synthesis), leading to *syn*-pimara-7,15-dien-19-oic acid (**130**). This oxidation goes through the primary alcohol and the



Scheme 1.10: Oxidation steps in the biosynthesis of momilactones A (**1**) and B (**2**) from pimaradiene **128**.^{188–194}

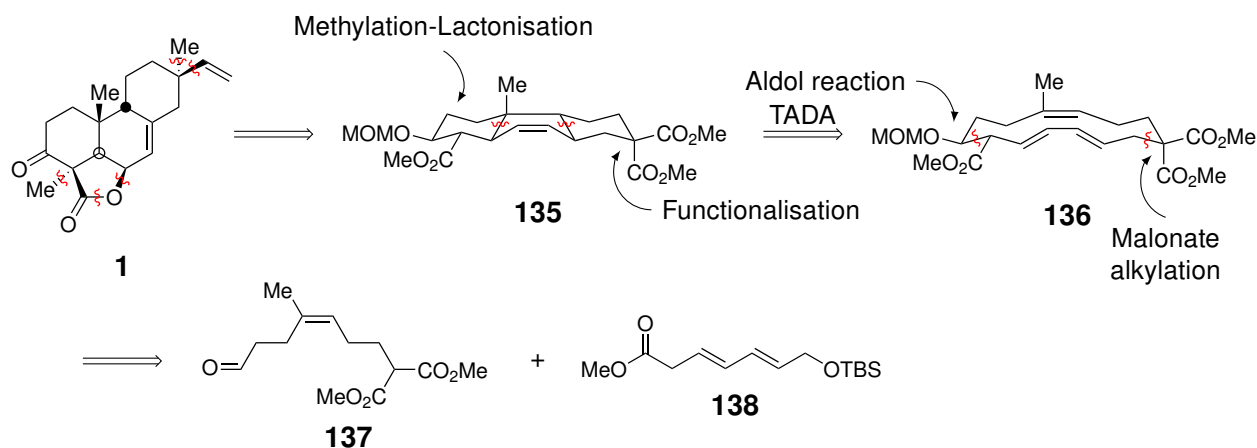
aldehyde, successively, before reaching the carboxylic acid.¹⁸⁸ In parallel the oxidations of positions 3 (**132**) and 6 (**131**) are obtained by CYP701A8 and CYP6M8, respectively. Results indicate that those three oxidations can occur in diverse orders.¹⁸⁹ All three oxidation paths lead to intermediate **133** which later undergoes the oxidation of the 6 β -hydroxy group into a ketone in order to obtain momilactone A (**1**). This transformation is performed by the *Oryza sativa* momilactone A synthase (OsMAS), a short-chain alcohol dehydrogenase/reductase, along with NAD(P)⁺ as co-factor.^{190–192}

Finally, momilactone B (**2**) is obtained by the oxidation of the C20 angular methyl group of momilactone A (**1**). Once again, a cytochrome P450 oxidase, CYP76M14, selectively converts the angular methyl group to an alcohol which spontaneously cyclises on the ketone to form the hemiacetal of momilactone B (**2**).^{193,194}

Remarkably, the results published by Sattely *et al.* earlier this year suggest that the oxidations on C19 and C6 are the first ones to occur (to form the lactone moiety). The intermediate is then either oxidised on the C3 position to obtain momilactone A (**1**), which is later oxidised to momilactone B (**2**), or it can first be oxidised on the C20 angular methyl group, and later be oxidised on the C3 position, directly leading to **2**.¹⁹⁴

1.4.4 First total synthesis of (\pm)-momilactone A

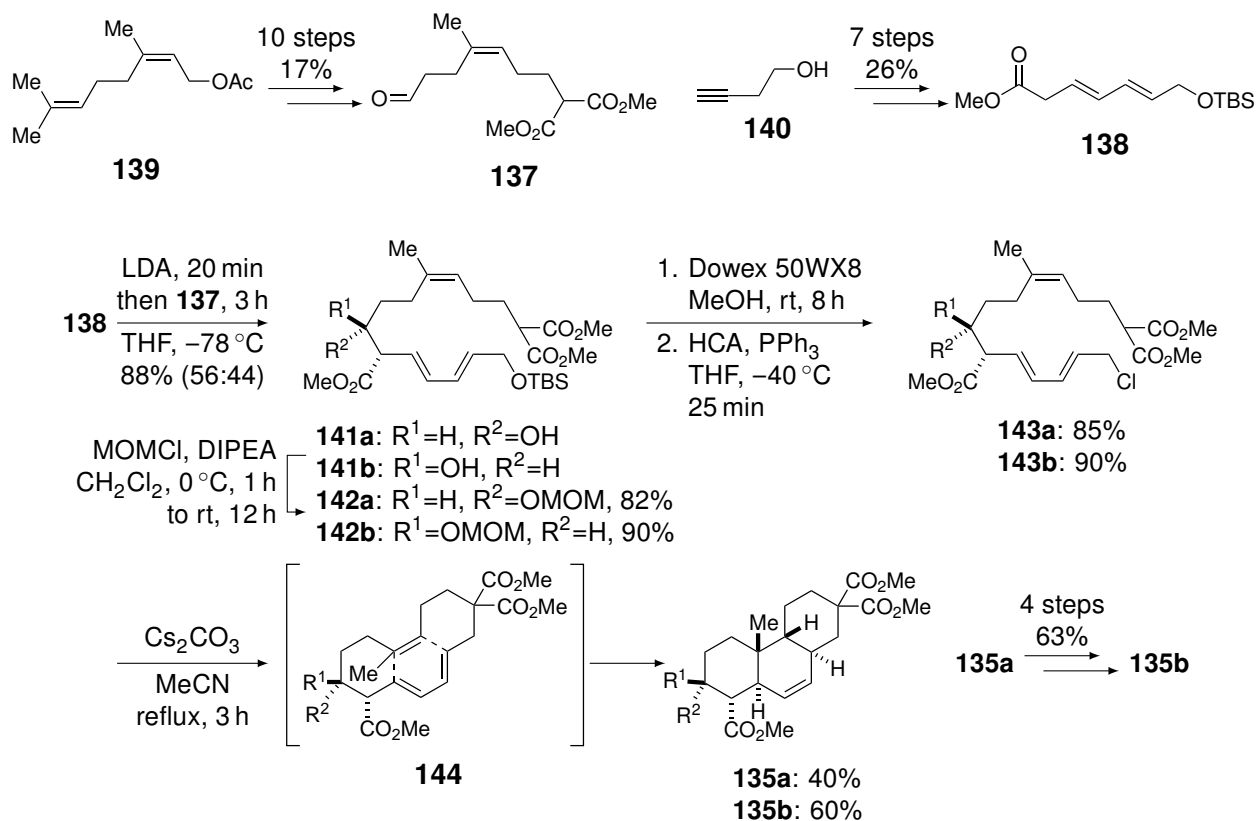
To the best of our knowledge, only one total synthesis of momilactone A (**1**), in its racemic form, has been published so far by Germain and Deslongchamps.^{195,196} In that total synthesis, the main strategy is the use of a transannular Diels-Alder (TADA) reaction on a 14-membered macrocycle having a *trans-trans-cis* olefin geometry, leading to the formation of the A.B.C [6.6.6] tricyclic pattern of **1** possessing a *trans-syn-trans* ring junction stereochemistry. This TADA reaction has indeed shown to be really efficient in total syntheses with a spectacular chemo-, regio- and diastereoselectivity.¹⁹⁷



Scheme 1.11: Retrosynthetic analysis of momilactone A (**1**) proposed by Germain and Deslongchamps.^{195,196}

In their retrosynthetic analysis (Scheme 1.11), they first disconnected the methyl group on the C3 position, opened the lactone ring, and transformed the methyl and vinyl groups on the C13 position into a malonate derivative, leading to cycloadduct **135**. They then identified the *trans-syn-trans* (TST) relation of the tricycle junctions and continued with the retro-transannular Diels-Alder deconnexion to reveal the macrocycle **136**, possessing a *trans-trans-cis* (TTC) olefin geometry. It was then disconnected *via* a malonate alkylation on the right part of the molecule and *via* an aldol reaction on the left part, leading to precursors **137** and **138**.

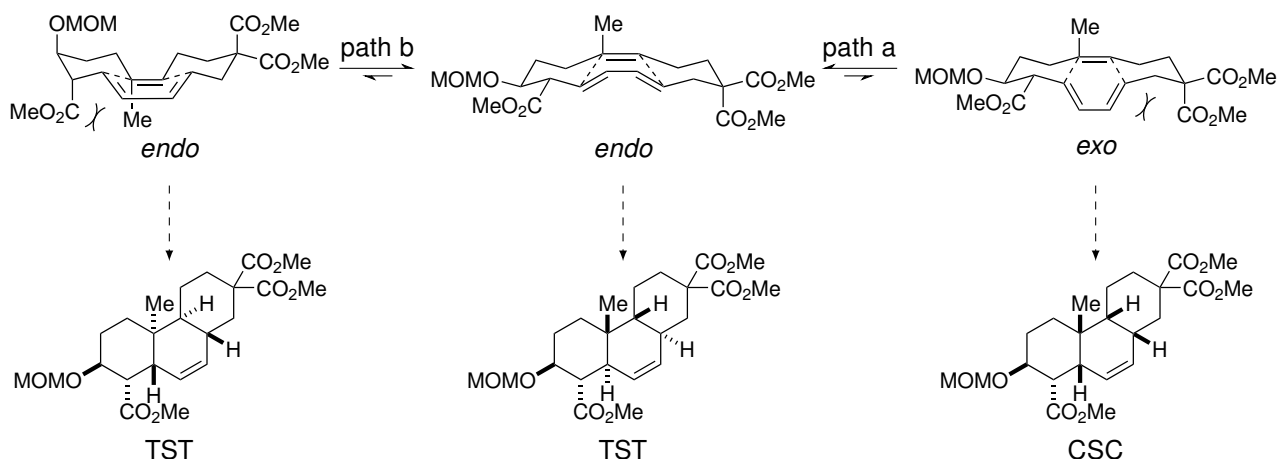
Both precursors **137** and **138** had to be synthesised, the first one in ten steps and 17% global yield from neryl acetate (**139**) and the second one in seven steps and 26% global yield from but-3-yn-1-ol (**140**) (Scheme 1.12). Once they were synthesised, they could engage those precursors into an aldol condensation which gave an almost equimolar mixture of *syn* and *anti* isomers of the β -hydroxyester **141**. The alcohol of both isomers was then uneventfully protected by a MOM group and the primary alcohol was efficiently deprotected and converted to a chloride.



Scheme 1.12: Formation of the 14-membered macrocycle and its TADA reaction in the total synthesis pathway of (\pm)-momilactone A ((\pm)-**1**) developed by Germain and Deslongchamps.^{195,196}

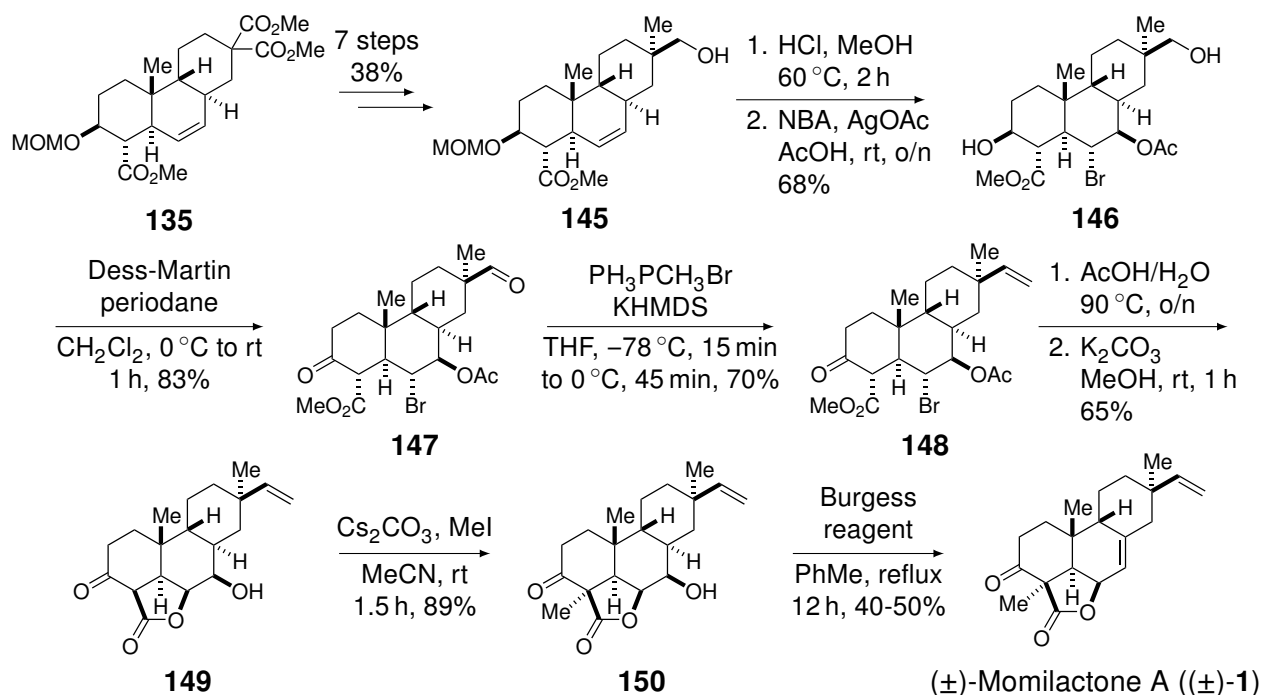
The next, and most important reaction of this sequence, was the one-pot macrocyclisation and subsequent TADA reaction. That step was performed in refluxing acetonitrile in the presence of Cs_2CO_3 as a base, giving the TST tricyclic cycloadduct in 40% and 60% yields for isomers **135a** and **135b**, respectively. The specific formation of the TST tricycle can be explained by the sterically favored *endo* transition state having a “chair-boat-chair” conformation as shown in Scheme 1.13.

The *exo* transition state suffers from steric interactions between the pseudoaxial ester group and one double bond of the diene (path a). Then, the macrocycle can adopt two interconvertible conformations, leading to a TST isomer (path b), with either the carboxymethyl and OMOM groups both in a pseudoaxial or pseudoequatorial orientation. In this case, the face selectivity is the result of the orientation of the C4-carbomethoxy group in a pseudoequatorial position. Indeed, the pseudoaxial orientation of this group leads to a steric interaction with the C10-methyl. The same conclusion can be reached for the specific formation of the *syn* isomer **135a**. In this case, the OMOM group occupied a pseudoaxial orientation in the transition state that further disfavored the formation of the *cis-syn-cis* (CSC) isomer.



Scheme 1.13: Model of the favoured approach in the TADA reaction for **144b** described in Scheme 1.12.^{195,196}

Once the TADA reaction took place, they could continue the synthesis of (\pm)-**1** (Scheme 1.14). But before pursuing the sequence, preliminary results showed that the selectivities obtained with isomer **135b** were better than with isomer **135a**. They then decided to convert the latter into **135b** by a four step sequence of alcohol deprotection, oxidation, stereoselective reduction, and MOM protection in a 63% global yield (Scheme 1.12).



Scheme 1.14: Next part of the total synthesis of (\pm)-momilactone A ((\pm)-**1**) developed by Germain and Deslongchamps.^{195,196}

The desired isomer was then submitted to a series of transformations in order to stereoselectively convert the malonate residue into a methyl group and a primary alcohol with the desired relative configuration (Scheme 1.14). The secondary alcohol of intermediate **145** was deprotected and the remaining olefin moiety was transformed into the bromoacetate **146**. The latter then underwent an

oxidation with the Dess-Martin periodane, followed by a Wittig olefination on the aldehyde **147** to give the alkene **148**.

Displacement of the bromide by the acetate group was accomplished in mixture of acetic acid and water at 90 °C. The formation of the lactone was then subsequently performed by methanolysis to yield compound **149**. The introduction of the methyl group on the C3 position was done using Cs₂CO₃ and MeI in refluxing acetonitrile to give hydroxymomilactone A (**150**) with a 89% yield. The structure and relative configuration of the latter were confirmed by X-ray analysis.

Finally, the last step of this synthesis consists in the elimination of the remaining alcohol. However, standard dehydration conditions did not work for this substrate, despite the ideal antiperiplanar alignment of the alcohol with the C8 hydrogen atom. In each case, they recovered the starting alcohol. Astonishingly, the use of the Burgess reagent allowed to overcome this issue, although the latter is more commonly employed in *syn*-eliminations.

In conclusion, Germain and Deslongchamps managed to synthesise momilactone A (**1**) in its racemic form in a 19 steps sequence from precursors **137** and **138** (the longest sequence being 29 steps from **137**) with a very high degree of chemo-, regio-, and stereoselectivity, except for the aldol condensation.

1.5 Conclusion

In the course of this chapter, we could highlight the enormous diversity of natural compounds that could be reached from one common precursor: isopentenyl diphosphate (**17**). Even by focusing our search of natural molecules on the pimaranes, one subgroup of the diterpene family that are built out of four IPP units, the amount of compounds remained quite important. Nevertheless, we could discuss the richness of structures by presenting the natural sources that provide those products, such as plants, fungi and marine organisms.

We continue the focus by getting closer to the structure of the natural compounds that interest us in this work: momilactones A (**1**) and B (**2**). We looked up for structures that are part of the pimarane diterpenoid family but that also bear a 4,6-transannular γ -lactone moiety. We broadened our search by taking into account the products whose C17 is missing (4,6-transannular 17-*nor*-pimarane lactone). In doing so, we found out around sixty structures, including the momilactone family. Based on what we found in the literature, those natural products are mainly isolated for plants ($\pm 2/3$) but also from fungi ($\pm 1/3$).

Some of those products have been tested against diverse diseases such as bacteria, fungi or cancers and have shown very interesting biological activities that could be of interest for the human health. However, no studies on the mode of action of those compounds have ever been done, to the best of our knowledge.

Among all the natural compounds bearing the studied pattern, we found only one example of total synthesis for myrocin C (**87**), in its racemic form, reported by Danishefsky *et al.* in 1992.¹²⁶ In 2004, Corey *et al.* proposed to perform that synthesis in an asymmetric manner by carrying out the first

step, a Diels-Alder reaction, using a chiral oxazaborolidinium salt.¹²⁸ They obtained the cycloadduct of that first step with a 85% *ee*. In 2018, Herzon *et al.* also proposed the total synthesis of myrocin G (**110**) which is suspected to be the putative form of myrocin C (**87**).¹³⁰

We then moved on to the presentation of the momilactone family. Nine natural products named momilactone have been found, albeit one of them is a 19-*nor*-pimarane diterpene whose lactone moiety is missing.

Among those compounds, it would seem that only momilactones A (**1**) and B (**2**) have been studied for their biological properties. The different groups could highlight the importance of those two phytoalexins for the defence mechanism of the rice plant, from which they are extracted, mainly against the rice blast fungus *P. oryzae* but also against the growth of seedlings in the environment of the rice plant.

But momilactones do not only represent an interest for the rice plant. Indeed, many studies have been carried out to demonstrate that both momilactones A and B could be potential medicinal agents against various diseases afflicting humans. They notably showed good inhibitory activities against four bacterial strains, albeit not as good as ampicillin.

More importantly, they exhibit very good activities as cytotoxic agents against different types of cancer. It was even shown that they could reduce the size of tumours injected in rats without inducing apparent side effects, such as body mass or hair loss. It would therefore make them very interesting anti-cancer agents. However, it was reported that, in most of the cases, momilactone B (**2**) exhibits a better activity than momilactone A (**1**).

It was also reported that they could act against ketosis, skin ageing or diabetes due to their inhibition of key enzymes in those diseases.

We could also present the biosynthesis of momilactone A (**1**) and B (**2**) that seems to be only one that is known for that family of compounds. Moreover, that biosynthesis is rather well-known as it has been studied by many groups since the early nineties. It was highlighted that the oxidation steps to reach both momilactones from a common intermediate, 9 β -*H*-pimara-7,15-diene (**128**), are performed by a series of cytochrome P450 oxidases gathered in a cluster of enzymes. Even though the different oxidations steps on the different positions of the common intermediate **128** are now known, their exact order is not completely sure yet.

Finally, we presented the only total synthesis of momilactone A (**1**) that has been carried out, in a racemic manner, by Germain and Deslongchamps.^{195,196} For that synthesis, they used a transannular-Diels-Alder reaction that exhibited extraordinary chemo-, regio- and diastereoselectivities.

It should be noticed that, despite the fact that momilactones, as well as other 4,6-transannular pimarane- γ -lactone, are known for several decades, only two total syntheses have been reported so far (and in a racemic manner). It is even more surprising given the extraordinary biological activities those compounds possess.

Given the synthetic challenge those natural products represent, we were even more motivated to work on this family of compounds and to develop a enantioselective synthesis for these pimarane diterpenes with a 4,6-transannular γ -lactone and, more specifically, momilactones A (**1**) and B (**2**).

References

- [1] Reveglia, P.; Cimmino, A.; Masi, M.; Nocera, P.; Berova, N.; Ellestad, G.; Evidente, A. Pimarane diterpenes: Natural source, stereochemical configuration, and biological activity. *Chirality* **2018**, *30*, 1115–1134.
- [2] Sacchettini, J. C.; Poulter, C. D. Creating Isoprenoid Diversity. *Science* **1997**, *277*, 1788–1789.
- [3] Fraser, P. D.; Bramley, P. M. The biosynthesis and nutritional uses of carotenoids. *Prog. Lipid Res.* **2004**, *43*, 228–265.
- [4] Eisenreich, W.; Bacher, A.; Arigoni, D.; Rohdich, F. Biosynthesis of isoprenoids via the non-mevalonate pathway. *Cell. Mol. Life Sci.* **2004**, *61*, 1401–1426.
- [5] Liu, Y.; Wang, H.; Ye, H.-C.; Li, G.-F. Advances in the Plants Isoprenoid Biosynthesis Pathway and Its Metabolic Engineering. *J. Integr. Plant Biol.* **2005**, *47*, 769–782.
- [6] Hemmerlin, A.; Harwood, J. L.; Bach, T. J. A *raison d'être* for two distinct pathways in the early steps of plant isoprenoid biosynthesis? *Prog. Lipid Res.* **2012**, *51*, 95–148.
- [7] Dewick, P. M. The Mevalonate and Methylerythritol Phosphate Pathways: Terpenoids and Steroids. In *Medicinal Natural Products: A biosynthesis Approach*, 3rd ed.; John Wiley & Sons, Ltd, 2009; Chapter 5, pp 187–310.
- [8] Lombard, J.; Moreira, D. Origins and Early Evolution of the Mevalonate Pathway of Isoprenoid Biosynthesis in the Three Domains of Life. *Mol. Biol. Evol.* **2011**, *28*, 87–99.
- [9] Rohmer, M.; Sutter, B.; Sahm, H. Bacterial Sterol Surrogates. Biosynthesis of the Side-chain of Bacteriohopanetetrol and of a Carbocyclic Pseudopentose from ¹³C-Labelled Glucose in *Zymomonas mobilis*. *J. Chem. Soc. Chem. Commun.* **1989**, 1471–1472.
- [10] Horbach, S.; Sahm, H.; Welle, R. Isoprenoid biosynthesis in bacteria: Two different pathways? *FEMS Microbiol. Lett.* **1993**, *111*, 135–140.
- [11] Rohmer, M.; Seemann, M.; Horbach, S.; Bringer-Meyer, S.; Sahm, H. Glyceraldehyde 3-Phosphate and Pyruvate as Precursors of Isoprenic Units in an Alternative Non-mevalonate Pathway for Terpenoid Biosynthesis. *J. Am. Chem. Soc.* **1996**, *118*, 2564–2566.
- [12] Schwender, J.; Seemann, M.; Lichtenthaler, H. K.; Rohmer, M. Biosynthesis of isoprenoids (carotenoids, sterols, prenyl side-chains of chlorophylls and plastoquinone) via a novel pyruvate/glyceraldehyde 3-phosphate non-mevalonate pathway in the green alga *Scenedesmus obliquus*. *Biochem. J.* **1996**, *316*, 73–80.
- [13] Sangari, F. J.; Pérez-Gil, J.; Carretero-Paulet, L.; García-Lobo, J. M.; Rodríguez-Concepción, M. A new family of enzymes catalyzing the first committed step of the methylerythritol 4-phosphate (MEP) pathway for isoprenoid biosynthesis in bacteria. *Proc. Natl. Acad. Sci.* **2010**, *107*, 14081–14086.
- [14] Holstein, S. A.; Hohl, R. J. Isoprenoids: Remarkable Diversity of Form and Function. *Lipids* **2004**, *39*, 293–309.
- [15] Grayson, D. H. Monoterpenoids. *Nat. Prod. Rep.* **1997**, *14*, 477–522.
- [16] Laskovics, F. M.; Poulter, C. D. Prenyltransferase: Determination of the Binding Mechanism and Individual Kinetic Constants for Farnesylpyrophosphate Synthetase by Rapid Quench and Isotope Partitioning Experiments. *Biochem.* **1981**, *20*, 1893–1901.
- [17] Fraga, B. M. Natural Sesquiterpenoids. *Nat. Prod. Rep.* **1993**, *10*, 397–419.
- [18] von Lintig, J. Metabolism of Carotenoids and Retinoids Related to Vision. *J. Biol. Chem.* **2012**, *287*, 1627–1634.
- [19] Hanson, J. R. Diterpenoids. *Nat. Prod. Rep.* **1987**, *4*, 399–413.
- [20] Hanson, J. R. Diterpenoids. *Nat. Prod. Rep.* **1988**, *5*, 211–227.
- [21] Hanson, J. R. Diterpenoids. *Nat. Prod. Rep.* **1992**, *9*, 1–16.
- [22] Hanson, J. R. Diterpenoids. *Nat. Prod. Rep.* **1995**, *12*, 207–218.
- [23] Hanson, J. R. Diterpenoids. *Nat. Prod. Rep.* **1996**, *13*, 59–71.
- [24] Hanson, J. R. Diterpenoids. *Nat. Prod. Rep.* **2000**, *17*, 165–174.
- [25] Hanson, J. R. Diterpenoids of terrestrial origin. *Nat. Prod. Rep.* **2011**, *28*, 1755–1772.
- [26] Hanson, J. R. Diterpenoids of terrestrial origin. *Nat. Prod. Rep.* **2012**, *29*, 890–898.
- [27] Hanson, J. R.; Nichols, T.; Mukrish, Y.; Bagley, M. C. Diterpenoids of terrestrial origin. *Nat. Prod. Rep.* **2019**, *36*, 1499–1512.
- [28] Eksi, G.; Kurbanoglu, S.; Erdem, S. A. Analysis of diterpenes and diterpenoids. In *Recent Advances in Natural Products Analysis*; Sanches Silva, A., Nabavi, S. F., Saeedi, M., Nabavi, S. M., Eds.; Elsevier, 2020; Chapter 9, pp 313–345.
- [29] Buckingham, J. *Dictionary of Natural Products on DVD*; CRC, 2007.
- [30] Didyk, B. M.; Simoneit, B. R. T.; Brassel, S. C.; Eglinton, G. Organic geochemical indicators of palaeoenvironmental conditions of sedimentation. *Nature* **1978**, *272*, 216–222.
- [31] Goa, X.; He, J.; Wu, X.-D.; Peng, L.-Y.; Shao, L.-D.; Li, Y.; Cheng, X.; Zhao, Q.-S. Sauruchinenols A and B, unprecedented monocyclic diterpenes with new carbon skeleton from the aerial parts of *Saururus*

- chinensis*. *Fitoterapia* **2017**, *116*, 116–120.
- [32] Demotie, A.; Fairlamb, I. J. S.; Lu, F.-J.; Shaw, N. J.; Spencer, P. A.; Southgate, J. Synthesis of jaspaquinol and effect on viability of normal and malignant bladder epithelial cell lines. *Bioorg. Med. Chem. Lett.* **2004**, *14*, 2883–2887.
- [33] Cocker, J. D.; Halsall, T. G.; Bowers, A. The Chemistry of Gum Labdanum. Part I. Some Acidic Constituents. *J. Chem. Soc.* **1956**, 4259–4262.
- [34] Cocker, J. D.; Halsall, T. G. The Chemistry of Gum Labdanum. Part II. The Structure of Labdanolic Acid. *J. Chem. Soc.* **1956**, 4262–4271.
- [35] Pal, M.; Mishra, T.; Kumar, A.; Tewari, S. K. Biological evaluation of terrestrial and marine plant originated labdane diterpenes (a review). *Pharm. Chem. J.* **2016**, *50*, 558–567.
- [36] Li, R.; Morris-Natschke, S. L.; Lee, K.-H. Clerodane diterpenes: sources, structures, and biological activities. *Nat. Prod. Rep.* **2018**, *33*, 1166–1226.
- [37] Urones, J. G.; de Pascual Teresa, J.; Sánchez Marco, I.; Díez Martín, D.; Martín Garrido, N.; Alfayate Guerra, R. Diterpenoids from *Halimum viscosium*. *Phytochemistry* **1987**, *26*, 1077–1079.
- [38] Martín Roncero, A.; Tobal, I. E.; Fernandez-Moro, R.; Díez, D.; Sánchez Marco, I. Halimane diterpenoids: sources, structures, nomenclature and biological activities. *Nat. Prod. Rep.* **2018**, *35*, 955–991.
- [39] San Feliciano, A.; Gordaliza, M.; Salinero, M. A.; Miguel del Corral, J. M. Abietane Acids: Sources, Biological Activities, and Therapeutic Uses. *Planta Med.* **1993**, *59*, 485–490.
- [40] González, M. A. Aromatic abietane diterpenoids: their biological activity and synthesis. *Nat. Prod. Rep.* **2015**, *32*, 684–704.
- [41] Devappa, R. K.; Makkar, H. P. S.; Becker, K. *Jatropha* Diterpenes: a Review. *J. Am. Oil Chem. Soc.* **2011**, *88*, 301–322.
- [42] Maurya, R.; Ravi, M.; Singh, S.; Yadav, P. P. A review on cassane and norcassane diterpenes and their pharmacological studies. *Fitoterapia* **2012**, *83*, 272–280.
- [43] Jing, W.; Zhang, X.-X.; Zhou, H.; Wang, Y.; Yang, M.; Long, L.; Gao, H. Naturally occurring cassane diterpenoids (CAs) of *Caesalpinia*: A systematic review of its biosynthesis, chemistry and pharmacology. *Fitoterapia* **2019**, *134*, 226–249.
- [44] Mdee, L. K.; Waibel, R.; Nkunya, M. H. H.; Jonker, S. A.; Hans, A. Rosane diterpenes and bisnorditerpenes from *Hugonia castaneifolia*. *Phytochemistry* **1998**, *49*, 1107–1113.
- [45] Baraza, L. D.; Joseph, C. C.; Munissi, J. J. E.; Nkunya, M. H. H.; Arnold, N.; Porzel, A.; Wessjohann, L. Antifungal rosane diterpenes and other constituents of *Hugonia castaneifolia*. *Phytochemistry* **2008**, *69*, 200–205.
- [46] Zi, J.; Mafu, S.; Peters, R. J. To Gibberellins and Beyond! Surveying the Evolution of (Di)Terpenoid Metabolism. *Annu. Rev. Plant Biol.* **2014**, *65*, 259–286.
- [47] Salazar-Cerezo, S.; Martínez-Montiel, N.; García-Sánchez, J.; Pérez-y Terrón, R.; Martínez-Contreras, R. D. Gibberellin biosynthesis and metabolism: A convergent route for plants, fungi and bacteria. *Microbiol. Res.* **2018**, *208*, 85–98.
- [48] Wang, J.-X.; Zheng, L.-L.; Zhou, X.-L. Lewis acid-mediated skeleton transformation of Euphorbia diterpenes: From lathyrane to euphoractane and myrsinane. *Fitoterapia* **2019**, *133*, 212–218.
- [49] Liebermann, C. Ueber Sylvlin- und Pimarsäure. *Ber. Dtsch. Chem. Ges.* **1884**, *17*, 1884–1887.
- [50] Senning, A. The naming of terpenes. In *The Etymology of Chemical Names*; 2019; Chapter 8.
- [51] Ansell, S. M.; Pegel, K. H.; Taylor, D. A. H. Diterenes from the Timber of 20 *Erythroxylum* Species. *Phytochemistry* **1993**, *32*, 953–959.
- [52] García, E. E.; Guerreiro, E.; Joseph-Nathan, P. Ent-Pimaradiene Diterpenes from *Gochnatia glutinosa*. *Phytochemistry* **1985**, *24*, 3059–3060.
- [53] Ambrósio, S. R.; Schorr, K.; Da Costa, F. B. Terpenoids of *Viguiera arenaria* (Asteraceae). *Biochem. Syst. Ecol.* **2004**, *32*, 221–224.
- [54] We, X.-D.; He, J.; Li, X.-Y.; Dong, L.-B.; Gong, X.; Song, L.-D.; Li, Y.; Peng, L.-Y.; Zhao, Q.-S. Diterpenoids from the Twigs and Leaves of *Fokienia hodginsii*. *J. Nat. Prod.* **2013**, *76*, 1032–1038.
- [55] Tirapelli, C. R.; Ambrósio, S. R.; Coutinho, S. T.; Oliveira, D. C.; Costa, F. B.; Oliveira, A. M. Pharmacological comparison of the vasorelaxant action displayed by keurenoic acid and pimaradienoic acid. *J. Pharm. Pharmacol.* **2005**, *57*, 997–1004.
- [56] Turner, W. B.; Aldridge, D. C. *Fungal Metabolites II*; Academic Press, 1983.
- [57] Osbourn, A. E.; Lanzotti, V. *Plant-Derived Natural Products*; Springer, 2009.
- [58] Cimmino, A.; Andolfi, A.; Evidente, A. Phytotoxic terpenes produced by phytopathogenic fungi and allelopathic plants. *Nat. Prod. Commun.* **2014**, *9*, 401–408.
- [59] Cimmino, A.; Masi, M.; Evidente, A. Fungal phytotoxins with potential herbicidal activity: chemical and biological characterization. *Nat. Prod. Rep.* **2015**, *32*, 1629–1653.
- [60] Evidente, A.; Kornienko, A.; Cimmino, A.; Andolfi, A.; Lefranc, F.; Mathieu, V.; Kiss, R. Fungal metabolites with anticancer activity. *Nat. Prod. Rep.* **2014**, *31*, 617–627.
- [61] Khan, M. A. I.; Ali, M. A.; Monsur, M. A.; Kawashi-Tanaka, A.; Hayashi, N.; Yanagihara, S.; Obara, M.;

- Mia, M. A. T.; Latif, M. A.; Fukuta, Y. Diversity and Distribution of Rice Blast (*Pyricularia oryzae* Cavara) Races in Bangladesh. *Plant Dis.* **2016**, *100*, 2025–2033.
- [62] Akatsuka, T.; Kodama, O.; Sekido, H.; Kono, Y.; Takeuchi, S. Novel phytoalexins (oryzalexins A, B and C) isolated from rice blast leaves infected with *Pyricularia oryzae*. Part II: structural studies of oryzalexins. *Agric. Biol. Chem.* **1985**, *49*, 1689–1701.
- [63] Sekido, H.; Endo, T.; Suga, R.; Kodama, O.; Akatsuka, T.; Kono, Y.; Takeuchi, S. Oryzalexin D (3,7-Dihydroxy-(+)-sandaracopimaradiene), a New Phytoalexin Isolated from Blast-infected Rice Leaves. *J. Pesticide Sci.* **1986**, *11*, 369–372.
- [64] Kato, H.; Osamu, K.; Akatsuka, T. Oryzalexin E, a diterpenephytoalexin from UV-irradiated rice leaves. *Phytochemistry* **1993**, *33*, 79–81.
- [65] Sediko, H.; Akatsuka, T. Oryzalexin F, a diterpenephytoalexin from UV-irradiated rice leaves. *Phytochemistry* **1994**, *36*, 299–301.
- [66] Sediko, H.; Akatsuka, T. Mode of action of oryzalexin D against *Pyricularia oryzae*. *Agric. Biol. Chem.* **1987**, *51*, 1967–1971.
- [67] Masuda, T.; Masuda, K.; Shiragami, S.; Jitoe, A.; Nakatani, N. Orthosiphol A and B, Novel Diterpenoids Inhibitors of TPA (12-*O*-tetradecanoylphorbol-13-acetate)-Induced Inflammation, from *Orthosiphon stamineus*. *Tetrahedron* **1992**, *48*, 6787–6792.
- [68] Tezuka, Y.; Hirano, H.; Kikuchi, T.; Xu, G.-J. Constituents of *Ephemerantha lonchophylla*; Isolation and Structure Elucidation of New Phenolic Compounds, Ephemeranthol-A, Ephemeranthol-B, and Ephemeranthoquinone, and of a New Diterpene Glucoside, Ephemeranthoside. *Chem. Pharm. Bull.* **1991**, *39*, 593–598.
- [69] Masi, M.; Maddau, L.; Linaldeddu, B. T.; Scanu, B.; Evidente, A.; Cimmino, A. Bioactive metabolites from pathogenic and endophytic fungi of forest trees. *Curr. Med. Chem.* **2018**, *25*, 208–252.
- [70] Evidente, A.; Sparapano, L.; Motta, A.; Giordano, F.; Fierro, O.; Frisullo, S. A phytotoxic pimarane diterpene of *Sphaeropsis sapina* f. sp. *cupressi*, the pathogen of canker disease of cypress. *Phytochemistry* **1996**, *42*, 1541–1546.
- [71] Evidente, A.; Sparapano, L.; Fiero, O.; Bruno, G.; Giordano, F.; Motta, A. Sphaeropsidins B and C, phytotoxic pimarane diterpenes from *Sphaeropsis sapinea* f. sp. *cupressi* and *Diplodia mutila*. *Phytochemistry* **1997**, *45*, 705–713.
- [72] Ellestad, G. A.; Kunstmann, M. P.; Mirando, P.; Morton, G. O. Structures of fungal diterpenes antibiotics LL-S491 β and $-\gamma$. *J. Am. Chem. Soc.* **1972**, *94*, 6206.
- [73] Masi, M.; Cimmino, A.; Maddau, L.; Kornienko, A.; Tuzi, A.; Evidente, A. Crystal structure and absolute configuration of sphaeropsidin A and its 6-*O*-*p*-bromobenzoate. *Tetrahedron Lett.* **2016**, *57*, 4592–4594.
- [74] Dettrakul, S.; Kittakoop, P.; Isaka, M.; Nopichai, S.; Chotika, S.; Tanticharoen, M.; Thebtaranonth, Y. Antimycobacterial Pimarane Diterpenes from the Fungus *Diaporthe* sp. *Bioorg. Med. Chem. Lett.* **2003**, *13*, 1253–1255.
- [75] Oh, D.-C.; Jensen, P. R.; Kauffman, C. A.; Fenical, W. Libertellenones A-D: Induction of cytotoxic diterpenoid biosynthesis by marine microbial competition. *Bioorg. Med. Chem.* **2005**, *13*, 5267–5273.
- [76] Schmitz, F. J.; Michaud, D. P.; Schmidt, P. G. Marine Natural Products: Parguerol, Deoxyparguerol, and Isoparguerol. New Brominated Diterpenes with Modified Pimarane Skeleton from the Sea Hare *Aplysia dactylomela*. *J. Am. Chem. Soc.* **1982**, *104*, 6415–6423.
- [77] Costantino, V.; Fattorusso, E.; Mangoni, A.; Perinu, C.; Cirino, G.; De Gruttola, L.; Roviezzo, F. Tedanol: A potent anti-inflammatory *ent*-pimarane diterpene from the Caribbean Sponge *Tedania ignis*. *Bioorg. Med. Chem.* **2009**, *17*, 7542–7547.
- [78] Zhao, M.; Cheng, J.; Guo, B.; Duan, J.; Che, C.-T. Momilactones and Related Diterpenoids as Potential Agricultural Chemicals. *J. Agric. Food Chem.* **2018**, *66*, 7859–7872.
- [79] On'Okoko, P.; Vanhaelen, M.; Vanhaelen-Fastré, R.; Declercq, J. P.; Van Meerssche, M. The Constitution of Icacinol, a New Diterpene with a Pimarane Skeleton from *Icacina claessensis*. *Tetrahedron* **1985**, *41*, 745–748.
- [80] Onakpa, M. M.; Zhao, M.; Gödecke, T.; Chen, W.-L.; Che, C.-T.; Santarsiero, B. D.; Swanson, S. M.; Asuzu, I. U. Cytotoxic (9 β H)-Pimarane and (9 β H)-17-Norpimarane Diterpenes from the Tuber of *Icacina trichanta*. *Chem. Biodivers.* **2014**, *11*, 1914–1922.
- [81] Zhao, M.; Guo, B.; Onakpa, M. M.; Wong, T.; Wakasa, K.; Che, C.; Warpeha, K. Activity of Icacinol from *Icacina trichanta* on Seedling Growth of *Oryza sativa* and *Arabidopsis thaliana*. *J. Nat. Prod.* **2017**, *80*, 3314–3318.
- [82] On'Okoko, P.; Hans, M.; Colau, B.; Hootelé, C.; Declercq, J. P.; Germain, G.; Van Meerssche, M. L'icacine, nouvel alcaloïde diterpenique de *Icacina gussfeldtii*. *Bull. Soc. Chim. Belg.* **1977**, *86*, 655–661.
- [83] On'Okoko, P.; Vanhaelen, M. Two New Diterpene-Based Alkaloids from *Icacina gussfeldtii*. *Phytochemistry* **1980**, *19*, 303–305.
- [84] Zhao, M.; Onakpa, M. M.; Chen, W.-L.; Santarsiero, B. D.; Swanson, S. M.; Burdette, J. E.; Asuzu, I. U.;

- Che, C.-T. 17-Norpimaranes and (9 β H)-17-Norpimaranes from the Tuber of *Icacina trichanta*. *J. Nat. Prod.* **2015**, *78*, 789–796.
- [85] Zhao, M.; Onakpa, M. M.; Santarsiero, B. D.; Huang, X.-J.; Zhang, X.-Q.; Chen, J.; Cheng, J.-J.; Longnecker, R.; Che, C.-T. Icacinlatone H and Icacintrichantholide from the Tuber of *Icacina trichanta*. *Org. Lett.* **2015**, *17*, 3834–3837.
- [86] Zhao, M.; Onakpa, M. M.; Santarsiero, B. D.; Chen, W.-L.; Szymulanska-Ramamurthy, K. M.; Swabson, S. M.; Burdette, J. E.; Che, C.-T. (9 β H)-Pimaranes and Derivatives from the Tuber of *Icacina trichanta*. *J. Nat. Prod.* **2015**, *78*, 2731–2737.
- [87] Guo, B.; Onakpa, M. M.; Huang, X.-J.; Santarsiero, B. D.; Chen, W.-L.; Zhao, M.; Zhang, X.-Q.; Swanson, S. M.; Burdette, J. E.; Che, C.-T. Di-nor- and 17-nor-pimaranes from *Icacina trichanta*. *J. Nat. Prod.* **2016**, *79*, 1815–1821.
- [88] Sun, M.; Guo, B.; Xu, M.; Zhao, M.; Onakpa, M. M.; Wu, Z.; Burdette, J. E.; Che, C.-T. (9 β H)- and 17-Nor-Pimaranes from *Icacina oliviformis*. *J. Nat. Prod.* **2021**. Not printed yet.
- [89] Asuzu, I. U.; Anukabar, I. I. The Effects of *Icacina trichanta* Tuber Extract on the Nervous System. *Phytother. Res.* **1995**, *9*, 21–25.
- [90] On'Okoko, P.; Vanhaelen, M.; Vanhaelen-Fastré, R.; Declercq, J. P.; Van Meerssche, M. Icacenone, a Furanoditerpene with a Pimarane Skeleton from *Icacina Mannii*. *Phytochemistry* **1985**, *24*, 2452–2453.
- [91] Howard, R. A. A revision of *Casimirella*, including *Humirianthera* (Icacenaceae). *Brittonia* **1992**, *44*, 166–172.
- [92] Graebner, I. B.; Mostardeiro, M. A.; Ethur, E. M.; Burrow, R. A.; Dessoy, E. C. S.; Morel, A. F. Diterpenoids from *Humirianthera ampla*. *Phytochemistry* **2000**, *53*, 955–959.
- [93] Adou, E.; Williams, R. B.; Schilling, J. K.; Malone, S.; Meyer, J.; Wisse, J. H.; Frederik, D.; Koese, D.; Werkhoven, M. C. M.; Snipes, C. E.; Werk, T. L.; Kingston, D. G. Cytotoxic diterpenoids from two lianas from the Suriname rainforest. *Bioorg. Med. Chem.* **2005**, *13*, 6009–6014.
- [94] Burrow, R. A.; Morel, A. F.; Graebner, I. B.; Farrar, D. H.; Lough, A. J. The acetyl derivative of humirianthol. *Acta Cryst.* **2003**, *E59*, o347–o349.
- [95] Zhou, J.; Wu, Z.; Guo, B.; Sun, M.; Onakpa, M. M.; Yao, G.; Zhao, M.; Che, C.-T. Modified diterpenoids from the tuber of *Icacina oliviformis* as protein tyrosine phosphatase 1B inhibitors. *Org. Chem. Front.* **2020**, *7*, 355–367.
- [96] Zoghbi, M. D. G. B.; Roque, N. F.; Gottlieb, H. E. Humirianthenolides, New Degraded Diterpenoids from *Humirianthera rupestris*. *Phytochemistry* **1981**, *20*, 1669–1673.
- [97] Mussini, P.; Orsini, F.; Pellizoni, F. The C-13 Configuration of Annonalide. *Tetrahedron Lett.* **1973**, *14*, 4849–4851.
- [98] Orsini, F.; Pellizoni, F. The Structure of Annonolide. *Tetrahedron Lett.* **1977**, *18*, 1085–1088.
- [99] Li, J.-L.; Chen, C.; Liu, D.; Gu, Y.-Q.; Duan-Mu, J.-X.; Chen, G.-T.; Song, Y. Bioactive Constituents from the Bryophyta *Hypnum plumaeforme*. *Chem. Biodiversity* **2020**, *17*, e2000552.
- [100] Fang, J.-M.; Lee, C.-K.; Cheng, Y.-S. Diterpenes from Leaves of *Juniperus chinensis*. *Phytochemistry* **1993**, *33*, 1169–1172.
- [101] Burrow, R. A.; Morel, A. F.; Graebner, I. B.; Lough, A. J.; Farrar, D. H. Absolute configuration of diacetylated acrenol as its chloroform solvate. *Acta Cryst.* **2003**, *E59*, o350–o352.
- [102] Marques, R. A.; Gomes, A. O. C. V.; de Brito, M. V.; dos Santos, A. L. P.; da Silva, G. S.; de Lima, L. B.; Nunes, F. M.; de Mattos, M. C.; de Oliveira, F. C. E.; do Ó Pessoa, C.; de Moraes, M. O.; de Fátima, n.; Franco, L. L.; de M. Silva, M.; de A. Dantas, M. D.; Santos, J. C. C.; Figueirido, I. M.; da Silva-Júnior, E. F.; de Aquino, T. M.; de Araújo-Júnior, J. X.; de Oliveira, M. C. F.; Gunatilaka, A. A. L. Annonalide and derivatives: Semisynthesis, cytotoxic activities and studies on interaction of annonalide with DNA. *J. Photochem. Photobiol., B* **2018**, *179*, 156–166.
- [103] Hubbes, M. New Facts on Host-Parasite Relationships in the Hypoxylon Canker of Aspen. *Can. J. Bot.* **1964**, *42*, 1498–1949.
- [104] Bodo, B.; Davoust, D.; Lecommandeur, D.; Rebuffat, S.; Genetet, I.; Pinon, J. Hymatoxin A, a Diterpene Sulfate Phytotoxin of *Hypoxylon mammatum*, Parasite of Aspen. *Tetrahedron Lett.* **1987**, *28*, 2355–2358.
- [105] Borgschulze, K.; Rebuffat, S.; Trowitzsch-Kienast, S.; Schomburg, D.; Pinon, J.; Bodo, B. Isolation and Structure Elucidation of Hymatoxins B - E and Other Phytotoxins from *Hypoxylon mammatum* Fungal Pathogen of Leuce Poplars. *Tetrahedron* **1991**, *47*, 8351–8360.
- [106] Wang, M.-z.; Liu, S.-s.; Li, Y.-Y.; Xu, R.; Lu, C.-H.; Shen, Y.-M. Protoplast Mutation and Genome Shuffling Induce the Endophytic Fungus *Tubercularia* sp. TF5 to Produce New Compounds. *Curr. Microbiol.* **2010**, *61*, 254–260.
- [107] Lu, V.-H.; Liu, S.-S.; Wang, J.-Y.; Wang, M.-Z.; Shen, Y.-M. Characterization of Eight New Secondary Metabolites from the Mutant Strain G-444 of *Tubercularia* sp. TF 5. *Helv. Chim. Acta* **2014**, *97*, 334–344.
- [108] Jossang, A.; Mbeminack, B.; Pinon, J.; Bodo, B. Hymatoxins K and L, Novel Phytotoxins from *Hypoxylon mammatum*, Fungal Pathogen of Aspens. *Nat. Prod. Lett.* **1995**, *6*, 37–42.
- [109] Wang, G.-J.; Liang, W.-L.; Ju, Y.-M.; Yang, W.-B.; Chang, Y.-W.; Lee, T.-H. Inhibitory Effects of Ter-

- penoids from the Fermented Broth of the Ascomycete *Stilbohypoxylon elaeicola* YMJ173 on Nitric Oxide Production in RAW264.7 Macrophages. *Chem. Biodivers.* **2012**, *9*, 131–138.
- [110] Isaka, M.; Srisanoh, U.; Sappan, M.; Kongthong, S.; Srikitikulchai, P. Eremophilane and eudsemene sesquiterpenoids and a pimarane diterpenoid from the wood-decay fungus *Xylaria* sp. BCC 5484. *Phytochem. Lett.* **2012**, *5*, 78–82.
- [111] Basnet, B. B.; Liu, L.; Chen, B.; Suleimen, Y. M.; Yu, H.; Guo, S.; Bao, L.; Ren, J.; Liu, H. Four New Cytotoxic Arborinane-Type Triterpenes from the Endolichenic Fungus *Myrothecium inundatum*. *Planta Med.* **2019**, *85*, 701–707.
- [112] Chen, H.-P.; Li, J.; Zhao, Z.-Z.; Li, X.; Liu, S.-L.; Wang, Q.-Y.; Liu, J.-K. Diterpenes with Bicyclo[2.2.2]octane Moieties from the Fungicolous Fungus *Xylaria longpipes* HFG1018. *Org. Biomol. Chem.* **2020**, *18*, 2410–2415.
- [113] Wu, S.-H.; He, J.; Li, X.-N.; Huang, R.; Song, F.; Chen, Y.-W.; Miao, C.-P. Guaiane sesquiterpenes and isopimarane diterpenes from an endophytic fungus *Xylaria* sp. *Phytochemistry* **2014**, *105*, 197–204.
- [114] Isaka, M.; Yangchum, A.; Supyhina, S.; Chanthaket, R.; Srikitikulchai, P. Isopimaranes and eremophilanes from the wood-decay fungus *Xylaria allantoidea* BCC 23163. *Phytochem. Lett.* **2014**, *8*, 59–64.
- [115] Hsu, Y.-H.; Nakagawa, M.; Hirota, A.; Shima, S.; Nakayama, M. Structure of Myrocin B, a New Diterpene Antibiotic Produced by *Myrothecium verrucaria*. *Agric. Biol. Chem.* **1988**, *52*, 1305–1307.
- [116] Lehr, N.-A.; Meffert, A.; Antelo, L.; Sterner, O.; Anke, H.; Weber, R. W. S. Antiamoebins, myrocin B and the basis of antifungal antibiosis in the coprophilous fungus *Stilbella erythrocephala* (syn. *S. fimetaria*). *FEMS Microbiol. Ecol.* **2006**, *55*, 105–112.
- [117] Wei, W.; Gao, J.; Shen, Y.; Chu, Y. L.; Xu, Q.; Tan, R. X. Immunosuppressive Diterpenes from *Phomopsis* sp. S12. *Eur. J. Org. Chem.* **2014**, 5728–2734.
- [118] Hsu, Y.-H.; Hirota, A.; Shima, S.; Nakagawa, M.; Nozaki, H.; Tada, T.; Nakayama, M. Structure of Myrocin C, a New Diterpene Antibiotic Produced by a Strain of *Myrothecium* sp. *Agric. Biol. Chem.* **1987**, *51*, 2455–3457.
- [119] Nakagawa, M.; Hsu, Y.-H.; Hirota, A.; Shima, S.; Nakayama, M. Myrocin C, a New Diterpene Antitumor Antibiotic from *Myrothecium verrucaria*. I. Taxonomy of the Producing Strain, Fermentation, Isolation and Biological Properties. *J. Antibiot.* **1989**, *42*, 218–222.
- [120] Elkhateeb, W. A.; Zaghlol, G. M.; El-Garawani, I. M.; Ahmed, E. F.; Rateb, E., Mostafa; Abdel Monem, A. E. *Ganoderma applanatum* secondary metabolites induced apoptosis through different pathways; *In vivo* and *in vitro* anticancer studies. *Biomed. Pharmacother.* **2018**, *101*, 264–277.
- [121] Kildgaard, S.; Subko, K.; Philips, E.; Goidts, V.; de la Cruz, M.; Díaz, C.; Gotfredsen, C. H.; Andersen, B.; Frisvad, J. C.; Nielsen, K. F.; Larsen, T. O. A dereplication and Bioguided Discovery Approach to Reveal New Compounds from a Marine-Derived Fungus *Stilbella fimetaria*. *Mar. Drugs* **2017**, *15*, 253/1–253/19.
- [122] Li, Y.-Y.; Hu, Z.-Y.; Lu, C.-H.; Shen, Y.-M. Four New Terpenoids from *Xylaria* sp. 101. *Helv. Chim. Acta* **2010**, *93*, 796–802.
- [123] Bao, S.-S.; Liu, H.-H.; Zhang, X.-Q.; Liu, C.-X.; Li, X.-C.; Guo, Z.-Y. Xylaroisopimarane A, a New Isopimarane Derivative from an Endophytic Fungus *Xylaralyce* sp. *Nat. Prod. Sci.* **2019**, *25*, 228–232.
- [124] Wang, H.; Umeokoli, E.; Eze, P.; Hering, C.; Janiak, C.; Müller, W. E. G.; Orfali, R. S.; Hartmann, R.; Dai, H.; Lin, W.; Liu, Z.; Porksch, P. Secondary metabolites of the lichen-associated fungus *Apiospora montagnei*. *Tetrahedron Lett.* **2017**, *58*, 1702–1705.
- [125] Hsu, Y.-H.; Hirota, A.; Shima, S.; Nakagawa, M.; Adachi, T.; Nozaki, H.; Nakayama, M. Myrocin C, a New Diterpene Antitumor Antibiotic from *Myrothecium verrucaria*. II. Physico-Chemical Properties and Structure Determination. *J. Antibiot.* **1989**, *42*, 223–229.
- [126] Chu-Moyer, M. Y.; Danishefsky, S. J. A Remarkable Cyclopropanation: The Total Synthesis of Myrocin C. *J. Am. Chem. Soc.* **1992**, *114*, 8333–8334.
- [127] Chu-Moyer, M.; Danishefsky, S. J.; Schule, G. K. Total Synthesis of (±)-Myrocin C. *J. Am. Chem. Soc.* **1994**, *116*, 11213–11228.
- [128] Hu, Q.-Y.; Zhou, G.; Corey, E. J. Application of Chiral Cationic Catalysts to Several Classical Syntheses of Racemic Natural Products Transforms Them into Highly Enantioselective Pathways. *J. Am. Chem. Soc.* **2004**, *126*, 13708–13713.
- [129] Chu-Moyer, M. Y.; Danishefsky, S. J. On the Mode of Action of Myrocin C: Evidence for a CC-1065 Connection. *Tetrahedron Lett.* **1993**, *34*, 3025–3028.
- [130] Economou, C.; Tomanik, M.; Herzon, S. B. Synthesis of Myrocin G, the Putative Active Form of the Myrocin Antitumor Antibiotics. *J. Am. Chem. Soc.* **2018**, *140*, 16058–16061.
- [131] Ueda, Y.; Roberge, G.; Vinet, V. A simple method of preparing trimethylsilyl- and *tert*-butyldimethylsilyl-enol ethers of α -diazoacetoacetates and their use in the synthesis of a chiral precursor to thienamycin analogs. *Can. J. Chem.* **1984**, *62*, 2936–2940.
- [132] Meng, Z.; Yu, H.; Li, L.; Tao, W.; Chen, H.; Wan, M.; Yang, P.; Edmonds, D. J.; Zhong, J.; Li, A. Total synthesis and antiviral activity of indolosesquiterpenoids from the xiamycin and oridamycin families. *Nat. Commun.* **2015**, *6*, 6069/1–6069/8.

- [133] Huang, Y.; Iwama, T.; Rawal, V. H. Highly Enantioselective Diels-Alder Reactions of 1-Amino-3-siloxydienes Catalyzed by Cr(III)-Salen Complexes. *J. Am. Chem. Soc.* **2000**, *122*, 7843–7844.
- [134] Kato, T.; Kabuto, C.; Sasaki, N.; Tsunagawa, M.; Aizawa, H.; Fujita, K.; Kato, Y.; Kitahara, Y. Momilactones, Growth Inhibitors from Rice, *Oryza sativa* L. *Tetrahedron Lett.* **1973**, *14*, 3861–3864.
- [135] Toyota, M.; Kimura, K.; Asakawa, Y. Occurrence of *ent*-Sesquiterpene in the Japanese Moss-*Plagiomnium acutum*: First Isolation and Identification of the *ent*-Sesqui- and Dolabellane-type Diterpenoids from the Musci. *Chem. Pharm. Bull.* **1998**, *46*, 1488–1489.
- [136] Nozaki, H.; Hayashi, K.-I.; Nishimura, N.; Kawaide, H.; Matsuo, A.; Takaoka, D. Momilactone A and B as Allelochemicals from Moss *Hypnum plumaeforme*: First Occurrence in Bryophytes. *Biosci. Biotechnol. Biochem.* **2007**, *71*, 3127–3130.
- [137] Habib, R. S.; Jamshaid, M.; Tahir, M. N.; Khan, T. J.; Khan, I. U. (4*R*,5*R*,6*S*,7*R*,8*S*,9*R*,10*S*,13*S*)-7,8β-Epoxymomilactone-A. *Acta Cryst.* **2008**, *E64*, o892.
- [138] Tsunakawa, M.; Ohba, A.; Sasaki, N.; Kabuto, C.; Kato, T.; Kitahara, Y.; Takahashi, N. Momilactone-C, a Minor Constituent of Growth Inhibitors in Rice Husk. *Chem. Lett.* **1976**, *5*, 1157–1158.
- [139] Liu, N.; Wang, S.; Lou, H. A new pimarane-type diterpenoid from moss *Pseudoleskeella papillosa* (Lindb.) Kindb. *Acta Pharm. Sin. B* **2012**, *2*, 256–259.
- [140] Cho, J.-G.; Cha, B.-J.; Lee, S. M.; Shrestha, S.; Jeong, R.-H.; Lee, D. S.; Kim, Y.-C.; Lee, D.-G.; Kang, H.-C.; Kim, J.; Baek, N.-I. Diterpenes from the Roots of *Oryza sativa* L. and Their Inhibition Activity on NO Production in LPS-Stimulated RAW264.7 Macrophages. *Chem. Biodiversity* **2015**, *12*, 1356–1364.
- [141] Zhang, Q.; Xu, Q.-L.; Xia, X.-M.; Dong, L.-M.; Luo, B.; Liu, W.-B.; Tan, J.-W. A new phenylpropane-pimarane heterodimer and a new *ent*-kaurene diterpene from the husks of *Oryza sativa*. *Phytochem. Lett.* **2018**, *24*, 120–124.
- [142] Kato, T.; Aizawa, H.; Tsunakawa, M.; Sasaki, N.; Kitahara, Y.; Takahashi, N. Chemical Transformation of the Diterpene Lactones Momilactones A and B. *J. Chem. Soc., Perkin Trans. 1* **1977**, 250–254.
- [143] Cartwright, D. W.; Langcake, P.; Pryce, R. J.; Leworthy, D. P.; Ride, J. P. Isolation and Characterization of Two Phytoalexins from Rice as Momilactones A and B. *Phytochemistry* **1981**, *20*, 535–537.
- [144] Lee, C. W.; Yoneyama, K.; Takeuchi, Y.; Konnai, M.; Tamogami, S.; Kodama, O. Momilactones A and B in Rice Straw Harvested at Different Growth Stages. *Biosci. Biotechnol. Biochem.* **1999**, *63*, 1318–1320.
- [145] Kato-Noguchi, H.; Ino, T.; Sata, N.; Yamamura, S. Isolation and identification of a potent allelopathic substance in rice root exudates. *Physiol. Plant.* **2002**, *115*, 401–405.
- [146] Kato-Noguchi, H.; Ino, T. Rice seedlings release momilactone B into the environment. *Phytochemistry* **2003**, *63*, 551–554.
- [147] Kato-Noguchi, H.; Ino, T.; Ichii, M. Changes in release level of momilactone B into the environment from rice throughout its life cycle. *Funct. Plant Biol.* **2003**, *30*, 995–997.
- [148] Cartwright, D.; Langcake, P.; Pryce, R. J.; Leworthy, D. P.; Ride, J. P. Chemical activation of host defence mechanism as a basis for crop protection. *Nature* **1977**, *267*, 511–513.
- [149] Langcake, P.; Cartwright, D.; Leworthy, D. P.; Pryce, R. J.; Ride, J. P. The dichlorocyclopropanes — Fungicides with an indirect mode of action? *Neth. J. Plant Pathol. (Suppl. 1)* **1977**, *83*, 153–155.
- [150] Kato-Noguchi, H.; Kobayashi, K. Jasmonic acid, protein phosphatase inhibitor, metals and UV-irradiation increased momilactone A and B concentrations in the moss *Hypnum plumaeforme*. *J. Plant Physiol.* **2009**, *166*, 1118–1122.
- [151] Imai, T.; Ohashi, Y.; Mitsuhashi, I.; Seo, S.; Toshima, H.; Hasegawa, M. Identification of a Degradation Intermediate of the Momilactone A Rice Phytoalexin by the Rice Blast Fungus. *Biosci. Biotechnol. Biochem.* **2012**, *76*, 414–416.
- [152] Kato-Noguchi, H. Barnyard grass-induced rice allelopathy an momilactone B. *J. Plant Physiol.* **2011**, *168*, 1016–1020.
- [153] Mennan, H.; Ngoujio, M.; Sahin, M.; Isik, D.; Altop, E. K. Quantification of momilactone B in rice hulls and the phytotoxic potential of rice extracts on the seed germination of *Alisma plantago-aquatica*. *Weed Biol. Manag.* **2012**, *12*, 29–39.
- [154] Kato-Noguchi, H.; Ino, T. Assessment of Allelopathic Potential of Root Exudate of Rice Seedlings. *Biol. Plant.* **2001**, *44*, 635–638.
- [155] Kato-Noguchi, H.; Ino, T. The chemical-mediated allelopathic interaction between rice and barnyard grass. *Plant Soil* **2013**, *370*, 267–275.
- [156] Takahashi, N.; Kato, T.; Tsunagawa, M.; Sasaki, N.; Kitahara, Y. Mechanism of Dormancy in Rice Seeds. II. New Growth Inhibitors, Momilactone-A and -B Isolated from the Hulls of Rice Seeds. *Jpn. J. Breed.* **1976**, *26*, 91–98.
- [157] Kato, T.; Tsunakawa, M.; Sasaki, N.; Aizawa, H.; Fujita, K.; Kitahara, Y.; Takahashi, N. Growth and Germination Inhibitors in Rice Husks. *Phytochemistry* **1977**, *16*, 45–48.
- [158] Kato-Noguchi, H. The chemical cross talk between rice and barnyard grass. *Plant Signaling Behav.* **2011**, *6*, 1207–1209.

- [159] Quan, N. V.; Xuan, T. D.; Tran, H.-D.; Thuy, N. T. D. Inhibitory Activities of Momilactones A, B, E, and 7-Ketostigmasterol Isolated from Rice Husk on Paddy and Invasive Weeds. *Plants* **2019**, *8*, 159/1–159/10.
- [160] Chung, I.-M.; Hahn, S.-J.; Ahmad, A. Confirmation of Potential Herbicidal Agents in Hulls of Rice, *Oryza sativa*. *J. Chem. Ecol.* **2005**, *31*, 1339–1352.
- [161] Kato-Noguchi, H.; Ota, K.; Kujime, H. Absorption of momilactone A and B by *Arabidopsis thaliana* L. and the growth inhibitory effects. *J. Plant Physiol.* **2012**, *169*, 1471–1476.
- [162] Kato-Noguchi, H.; Ota, K.; Kujime, H.; Ogawa, M. Effects of momilactone on the protein expression in *Arabidopsis* germination. *Weed Biol. Manag.* **2013**, *13*, 19–23.
- [163] Kato-Noguchi, H.; Kitajima, S. Momilactone Sensitive Proteins in *Arabidopsis thaliana*. *Nat. Prod. Commun.* **2015**, *10*, 729–732.
- [164] Hasegawa, M.; Mitsuhara, I.; Seo, S.; Imai, T.; Koga, J.; Okada, K.; Yamana, H.; Ohashi, Y. Phytoalexins Accumulation in the Interaction Between Rice and the Blast Fungus. *Mol. Plant-Microbe Interact.* **2010**, *23*, 1000–1011.
- [165] Wang, Y.; Kwon, S. J.; Wu, J.; Choi, J.; Lee, Y.-H.; Agrawal, G. K.; Tamogami, S.; Rakwal, R.; Park, S.-R.; Kim, B.-G.; Jung, K.-H.; Kang, K. Y.; Kim, S. G.; Kim, S. T. Transcriptome Analysis of Early Responsive Genes in Rice during *Magnaporthe oryzae* Infection. *Plant Pathol. J.* **2014**, *30*, 343–354.
- [166] Isahara, A.; Ando, K.; Yoshioka, A.; Murata, K.; Kokubo, Y.; Morimoto, N.; Ube, N.; Yabuta, Y.; Ueno, M.; Tebatashi, S.-I.; Ueno, K.; Osaki-Oka, K. Induction of defense response by extracts of spent mushroom substrates in rice. *J. Pestic. Sci.* **2019**, *44*, 89–96.
- [167] Yamaguchi, T.; Yamada, A.; Hing, N.; Ogawa, T.; Ishii, T.; Shibuya, N. Differences in the Recognition of Glucan Elicitor Signals between Rice and Soybean: β -Glucan Fragments from the Rice Blast Disease Fungus *Pyricularia oryzae* That Elicit Phytoalexin Biosynthesis in Suspension-Cultured Rice Cells. *The Plant Cell* **2000**, *12*, 817–826.
- [168] Dillon, V. D.; Overton, J.; Grayer, R. J.; Harbone, J. B. Differences in Phytoalexins Response Among Rice Cultivars of Different Resistance to Blast. *Phytochemistry* **1997**, *44*, 599–603.
- [169] Fukuta, M.; Xuan, T. D.; Deba, F.; Twata, S.; Khanh, T. D.; Chung, I. M. Comparative efficacies *in vitro* of antibacterial, fungicidal, antioxidant, and herbicidal activities of momilactones A and B. *J. Plant Interact.* **2007**, *2*, 245–251.
- [170] Kanno, H.; Hasegawa, M.; Kodama, O. Accumulation of salicylic acid, jasmonic acid and phytoalexins in rice, *Oryza sativa*, infested by the white-backed planthopper, *Sogatella furcifera* (Hemiptera: Delphacidae). *Appl. Entomol. Zool.* **2012**, *47*, 27–34.
- [171] Horie, K.; Inoue, Y.; Sakai, M.; Yao, Q.; Tanimoto, Y.; Koga, J.; Toshima, H.; Hasegawa, M. Identification of UV-Induced Diterpenes Including a New Diterpene Phytoalexin, Phytocassane F, from Rice Leaves by Complementary GC/MS and LC/MS Approaches. *J. Agric. Food Chem.* **2015**, *63*, 4050–4059.
- [172] Xuan, T. D.; Minh, T. N.; Anh, L. H.; Khanh, T. D. Allelopathic momilactones A and B are implied in rice drought and salinity tolerance, not weed resistance. *Agron. Sustain. Dev.* **2016**, *36*, 52/1–52/8.
- [173] Chung, I.-M.; Ali, M.; Hahn, S.-J.; Siddiqui, N. A.; Lim, Y. H.; Ahmad, A. Chemical Constituents from the Hulls of *Oryza sativa* with Cytotoxic activity. *Chem. Nat. Compd.* **2005**, *41*, 182–189.
- [174] Kim, S.-J.; Park, H.-R.; Park, E.; Lee, S.-C. Cytotoxic and Antitumor Activity of Momilactone B from Rice Hulls. *J. Agric. Food Chem.* **2007**, *55*, 1702–1706.
- [175] Lee, S. C.; Chung, I.-M.; Jin, Y. J.; Song, Y. S.; Seo, S. Y.; Park, B. S.; Cho, K. H.; Yoo, K. S.; Kim, T.-H.; Yee, S.-B.; Bae, Y.-S.; Yoo, Y. H. Momilactone B, an Allelochemical of Rice Hulls, Induces Apoptosis on Human Lymphoma Cells (Jurkat) in a Micromolar Concentration. *Nutr. Cancer* **2008**, *60*, 542–551.
- [176] Joung, Y.-H.; Lim, E.-J.; Kim, M.-S.; Lim, S. D.; Yoon, S.-Y.; Lim, Y. C.; Yoo, Y. B.; Ye, S.-K.; Park, T.; Chung, I.-M.; Bae, K.-Y.; Yang, Y. M. Enhancement of hypoxia-induced apoptosis of human breast cancer cells via STAT5b by momilactone B. *Int. J. Oncol.* **2008**, *33*, 477–484.
- [177] Lee, J. H.; Cho, B.; Jun, H.-J.; Seo, W.-D.; Kim, D.-W.; Cho, K.-J.; Lee, S.-J. Momilactone B inhibits protein kinase A signaling and reduces tyrosinase-related proteins 1 and 2 expression in melanocytes. *Biotechnol. Lett.* **2012**, *34*, 805–812.
- [178] Park, C.; Jeong, N. Y.; Kim, G.-Y.; Han, M. H.; Chung, I.-M.; Kim, W.-J.; Yoo, Y. H.; Choi, Y. H. Momilactone B induces apoptosis and G1 arrest of the cell cycle in human monocytic leukemia U937 cells through downregulation of pRB phosphorylation and induction of the cyclin-dependent kinase inhibitor p21^{Waf1/Cip1}. *Nutr. Cancer* **2008**, *60*, 542–551.
- [179] Kang, D. Y.; Nipin, S. P.; Darvin, P.; Joung, Y. H.; Byun, H. J.; Do, C. H.; Park, K. D.; Park, M. N.; Cho, K. H.; Yang, Y. M. Momilactone B Inhibits Ketosis *In Vitro* by Regulating the ANGPTL3-LPL Pathway and Inhibiting HMGCS2. *Int. J. Oncol.* **2008**, *33*, 477–484.
- [180] Quan, N. V.; Thien, D. D.; Khanh, T. D.; ; Tran, H.-D.; Xuan, T. D. Momilactones A, B, and Tricin in Rice Grain and By-Products are Potential Skin Aging Inhibitors. *Foods* **2019**, *8*, 602/1–602/12.
- [181] Quan, N. V.; Tran, H.-D.; Xuan, T. D.; Ahmad, A.; Dat, T. D.; Khanh, T. D.; Teschke, R. Momilactones A and B Are α -Amylase and α -Glucosidase Inhibitors. *Molecules* **2019**, *24*, 482/1–482/13.
- [182] Quan, N. V.; Xuan, T. D.; Tran, H.-D.; Ahmad, A.; Khanh, T. D.; Dat, T. D. Contribution of momilactones A

- and B to diabetes inhibitory potential of rice bran: Evidence from in vitro assays. *Saudi Pharm. J.* **2019**, *27*, 643–649.
- [183] Wilderman, P. R.; Xu, M.; Jin, Y.; Coates, R. M.; Peters, R. J. Identification of *Syn*-Pimara-7,15-Diene Synthase Reveals Functional Clustering of Terpene Synthases Involved in Rice Phytoalexin/Allelochemical Biosynthesis. *Plant Physiol.* **2004**, *135*, 2098–2105.
- [184] Tomoyasu, T.; Kagahara, T.; Okada, K.; Koga, J.; Hasegawa, M.; Mitsunashi, W.; Sassa, T.; Yamane, H. Diterpene Phytoalexins Are Biosynthesized in and Exuded from the Roots of Rice Seedlings. *Biosci. Biotechnol. Biochem.* **2008**, *72*, 562–567.
- [185] Yajima, A.; Toda, K.; Okada, K.; Yamane, H.; Yamamoto, M.; Hasegawa, M.; Katsuta, R.; Nukada, T. Stereocontrolled total synthesis of (\pm)-3 β -hydroxy-9 β -pimara-7,15-diene, a putative biosynthetic intermediate of momilactones. *Tetrahedron Lett.* **2011**, *52*, 3212–3215.
- [186] Yamane, H. Biosynthesis of Phytoalexins and Regulatory Mechanisms of It in Rice. *Biosci. Biotechnol. Biochem.* **2013**, *77*, 1141–1148.
- [187] Mohan, R. S.; Yee, N. K. N.; Coates, R. M.; Ren, Y.-Y.; Stamenkovic, P.; Mendez, I.; West, C. A. Further study on the diterpenes of *Aralia* spp. *Tetrahedron Lett.* **1969**, *21*, 1683–1686.
- [188] Wang, Q.; Hillwig, M. L.; Peters, R. J. CYP99A3: functional identification of diterpene oxidase from the momilactone biosynthetic gene cluster in rice. *Plant J.* **2011**, *65*, 87–95.
- [189] Kitaoka, N.; Wu, Y.; Xu, M.; Peters, R. J. Optimization of recombinant expression enables discovery of novel cytochrome P450 activity in rice diterpenoid biosynthesis. *Appl. Microbiol. Biotechnol.* **2015**, *99*, 7549–7558.
- [190] Atawong, A.; Hasegawa, M.; Kodama, O. Biosynthesis of Rice Phytoalexin: Enzymatic Conversion of 3 β -Hydroxy-9 β -pimara-7,15-dien-19,6 β -olide to Momilactone A. *Biosci. Biotechnol. Biochem.* **2002**, *66*, 566–570.
- [191] Kitaoka, N.; Wu, Y.; Zi, J.; Peters, R. J. Investigating inducible short-chain alcohol dehydrogenases/reductases clarifies rice oryzalexin biosynthesis. *Plant J.* **2016**, *88*, 271–279.
- [192] Miyamoto, K.; Fujita, M.; Shenton, M. R.; Akashi, S.; Sugawara, C.; Sakai, A.; Horie, K.; Hasegawa, M.; Kawaide, H.; Mitsunashi, W.; Nojiri, H.; Yamane, H.; Kurata, N.; Okada, K.; Toyomasu, T. Evolutionary trajectory of phytoalexin biosynthetic gene clusters in rice. *Plant J.* **2016**, *87*, 293–304.
- [193] Peters, R. J. Uncovering the complex metabolic network underlying diterpenoid phytoalexin biosynthesis in rice and other cereal crop plants. *Phytochemistry* **2006**, *67*, 2307–2317.
- [194] De La peña, R.; Sattely, E. S. Rerouting plant terpene biosynthesis enables momilactone pathway elucidation. *Nat. Chem. Biol.* **2021**, *17*, 205–212.
- [195] Germain, J.; Deslongchamps, P. Transannular Diels-Alder Approach to the Synthesis of Momilactone A. *Tetrahedron Lett.* **1999**, *40*, 4051–4054.
- [196] Germain, J.; Deslongchamps, P. Total Synthesis of (\pm)-Momilactone A. *J. Org. Chem.* **2002**, *67*, 5269–5278.
- [197] Marsault, E.; Toró, A.; Nowak, P.; Deslongchamps, P. The transannular Diels-Alder strategy: applications to total synthesis. *Tetrahedron* **2001**, *57*, 4243–4260.

Chapter 2

Asymmetric Diels-Alder reactions on quinones

2 Asymmetric Diels-Alder reactions on quinones

After taking an interest in the family of molecules that are at the centre of this thesis, the present chapter will cover a second aspect that is treated in this work: the Diels-Alder reaction.

First, a brief historical overview will be presented, from the publication of this [4+2] cycloaddition in 1928 to its increasing use that made it one of the most important reactions for the development of new strategies in total synthesis. We will also cover some of the controversies behind that reaction: were Otto Diels and Kurt Alder the true discoverers of that amazing pericyclic reaction?

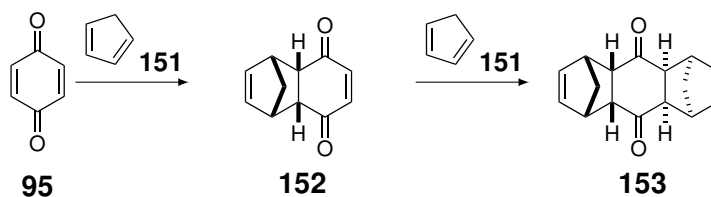
Claiming this reaction is one of the most important transformations in organic chemistry is far from an exaggeration. Indeed, over the years, its features have been extensively studied and make it possible, in most of the cases, to predict the outcome of those reactions. We will present those features and how the change of some of the parameters impact the rate, the chemo-, regio- and diastereoselectivities of the reactions.

Several methods have been developed in order to obtain enantioenriched cycloadducts. Some of those methods will be discussed in this document and concern, among other things, chiral auxiliaries, chiral organocatalysts or chiral Lewis acids. We will then continue this chapter with asymmetric Diels-Alder reactions specifically developed for quinones. The importance of such combination of quinone and asymmetric catalysis will be illustrated with some examples of enantioselective total syntheses of natural products.

The last part of this chapter will focus of the sulfoxide group as chiral auxiliary for the Diels-Alder reactions. More specifically, we will present a short review of what can be done when a quinone bears such sulfoxide group. After discussing the general pathway to synthesise such sulfinylquinones, we will present some of the works that describe the different parameters that allow the control of the stereoselectivities with those chiral quinones. Finally, some examples of enantioselective syntheses of natural compounds, as well as helicenes, using those compounds will be discussed.

2.1 Origins of the Diels-Alder reaction

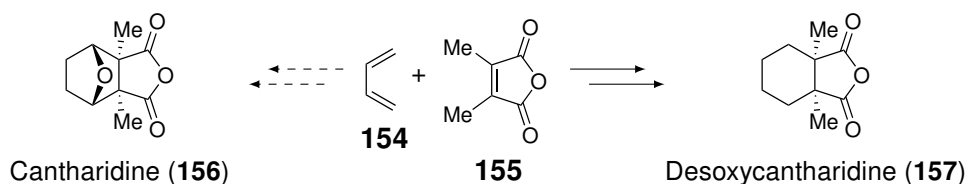
Nowadays, every chemist is aware of the [4+2] cycloaddition named after two German chemists, Otto Diels and Kurt Alder, after their seminal publication in 1928 describing the reaction between *para*-benzoquinone (**95**) and cyclopentadiene (**151**) (Scheme 2.1).¹ Not only did it open many possibilities in the field of organic synthesis, but it also allowed them to win the Nobel Prize in chemistry in 1950.²



Scheme 2.1: Reaction between benzoquinone (**95**) and cyclopentadiene (**151**) described by Otto Diels and Kurt Alder in 1928.¹

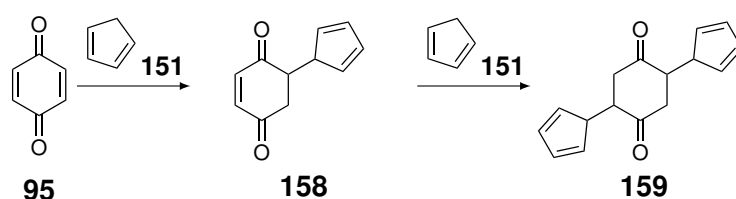
Interestingly, they were quite possessive about this new reaction they described and realised the great interest it could bring for the synthesis of natural molecules, mainly terpenes. Therefore, in order to discourage the scientific community to use “their” reaction for such purposes, they stated in their original publication: “*We explicitly reserve for ourselves the application of the reaction discovered by us to the solution of such problems.*”^a Ironically, they barely contributed to the synthesis of natural molecules using their discovery as they explored the inexhaustible richness of the mechanistic and stereochemical questions of the reaction. This could also in part be explained by the advent of World War II which completely disrupted academic research in Germany.

Astonishingly, until their Nobel Prize in 1950, no one published any work related to the use of the diene addition for the synthesis of natural compounds at the exception of the young Robert Burns Woodward. He indeed defied the implied prohibition by performing a failed attempt of a Diels-Alder strategy for the total synthesis of cantharidin (**156**), ending up in 6-deoxycantharidin (**157**) (Scheme 2.2).³ However, one year after they won their Nobel Prize, the chemical community came to ignore their claim of ownership of the reaction, and the use of that strategy for total synthesis took off.



Scheme 2.2: Synthesis of desoxycantharidine (**157**) by Robert Woodward, using a Diels-Alder strategy, in attempt to synthesise cantharidine (**156**).³

The Diels-Alder reaction had already been unknowingly observed by other researchers.⁴ The exactly same mono- and double addition of cyclopentadiene (**151**) on benzoquinone (**95**) had indeed already been discussed by Albrecht in 1906.⁵ In his description of the products, that he named cyclopentadienequinone (**158**) and dicyclopentadienequinone (**159**), he stated that cyclopentadiene binds itself on one of the double bonds of the quinone and that both double bonds of **151** are still present (Scheme 2.3). Unfortunately for him, as we all know, he misassigned the structure of the actual products.

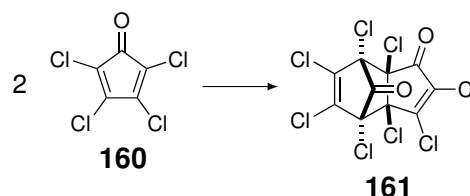


Scheme 2.3: Reaction between benzoquinone (**95**) and cyclopentadiene (**151**) as described by Walther Albrecht in 1906.⁵

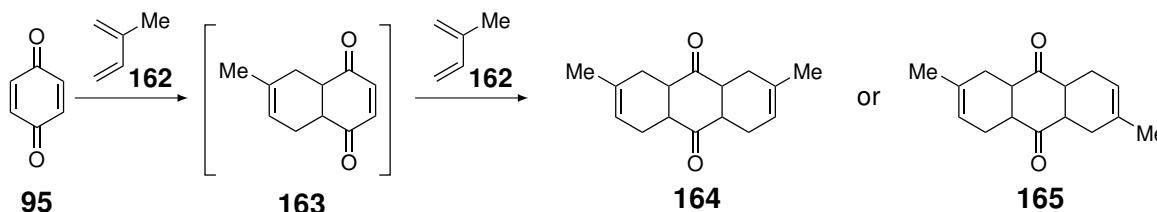
Six years later, Zincke had correctly found that tetrachloropentadienone (**160**) forms a dimer (Scheme 2.4), but he did not realise the generality of the process and missed the opportunity to further study the reaction.⁶

^aIn original version: “*Wir behalten uns die Anwendung der von uns gefundenen Reaktionen zur Lösung derartiger Probleme ausdrücklich vor.*”

One last example of missed opportunity is the reaction between benzoquinone (**95**) and isoprene (**162**) described by von Euler and Josephson in 1920 (Scheme 2.5).⁷ Based on their analysis, they proposed the structure to be **164** or **165**. Although they were very close to the correct elucidation of the cycloaddition reaction, they did not follow up on those remarkable results, most likely because von Euler, who later won the Nobel Prize in 1929, had been too busy with other projects.^{8,9}



Scheme 2.4: Dimerisation of tetrachloropentadienone (**160**).⁶



Scheme 2.5: Reaction between benzoquinone (**95**) and isoprene (**162**) described by von Euler and Josephson in 1920.⁷

Since then, the Diels-Alder reaction has been widely used in many synthetic strategies, including the total synthesis of natural products (see some examples in Figure 2.1).¹⁰ It ranges from steroids, to terpenes, passing by alkaloids and anthraquinones, or even the unnatural highly strained hydrocarbon cubane (**172**). Needless to say this represents only a tiny sample of what can be achieved with such an amazing reaction.

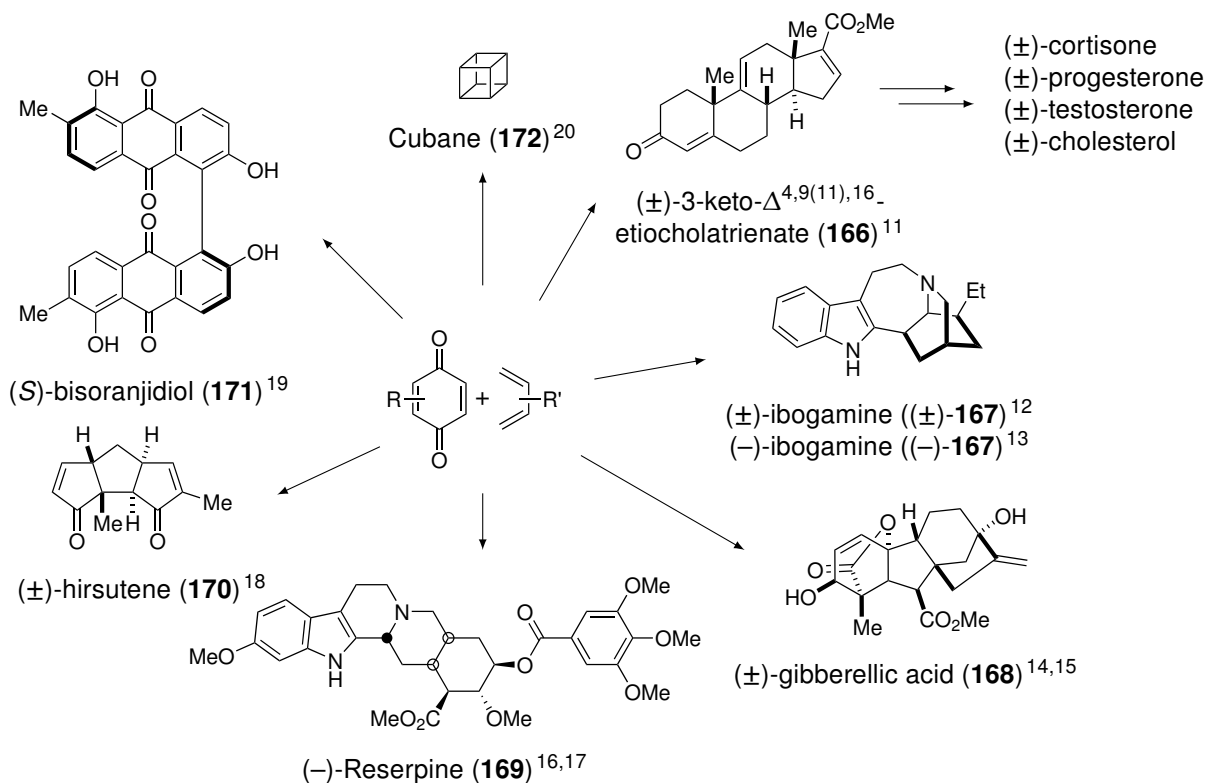


Figure 2.1: Examples of total syntheses carried out from diversely substituted quinones and dienes.¹⁰

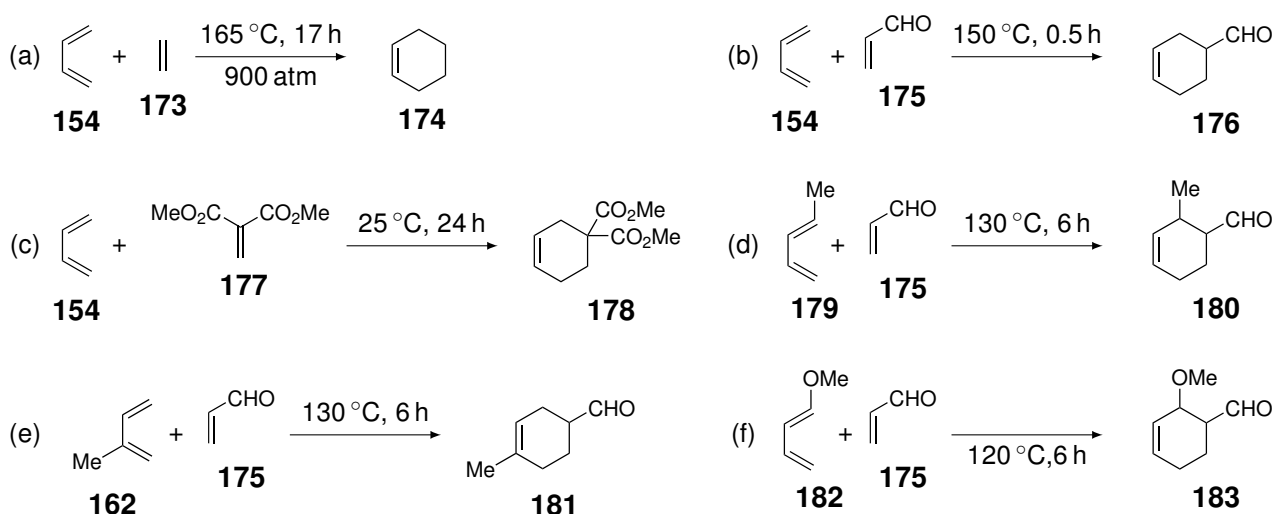
2.2 Features of the Diels-Alder reaction

The Diels-Alder reaction is a [4+2] cycloaddition between a conjugated (hetero)diene and a dienophile — that can be a double or triple bond between either two carbon atoms, a carbon atom and a heteroatom, or two heteroatoms — which is symmetry allowed in the ground state.²¹

The great interest in the Diels-Alder reaction mainly comes from its amazing properties. It is indeed a reaction that provides great control over the regio- and diastereoselectivity. This process is also diastereospecific which can prove useful in many cases. Depending on the substituents present on both diene and dienophile, the outcome of the reaction can be finely tuned.

2.2.1 Rates of the Diels-Alder reactions and frontier orbital interactions

Most Diels-Alder reactions are sluggish if no substituents are present on either the diene or the dienophile. As an example, the reaction between unsubstituted butadiene (**154**) and ethylene (**173**) (Scheme 2.6.a) takes 17 h at high temperatures (165 °C) and high pressure (900 atm).²² The addition of an electron withdrawing group (EWG) on the dienophile increases the reaction rates. For example, when ethylene (**173**) is replaced by acrolein (**175**) (Scheme 2.6.b), the reaction takes much less time (0.5 h) at lower temperatures (150 °C) and atmospheric pressure.²³ In the same vein, the presence of two EWG increases even more the rate of the reaction, as observed with methylenemalonate (**177**) that reacts at 25 °C (Scheme 2.6.c).²⁴



Scheme 2.6: Examples of Diels-Alder reactions with diverse dienes and alkenes to illustrate the effect of the substituents on the reaction rate.^{22–27}

On the other hand, the increase of the rate of the Diels-Alder reaction can be performed by the addition of an electron donating group (EDG) on position 1 or 2 of the diene. The reaction of acrolein (**175**) with piperylene (**179**) (Scheme 2.6.d) or isoprene (**162**) (Scheme 2.6.e), takes 20 °C less than the reaction with butadiene (Scheme 2.6.b).^{25,26} Unsurprisingly, this effect is even more pronounced with a stronger EDG, such as a methoxy group (**182**) (Scheme 2.6.f).

Given the fact that the Diels-Alder reaction is concerted, the acceleration of the reaction cannot be explained by the stabilisation of charges in a potential zwitterionic intermediate. The most rational explanation comes from the frontier orbitals theory, developed in 1952 by Kenichi Fukui and for which he won, together with Roald Hoffmann, the Nobel Prize in Chemistry in 1981.^{31,32}

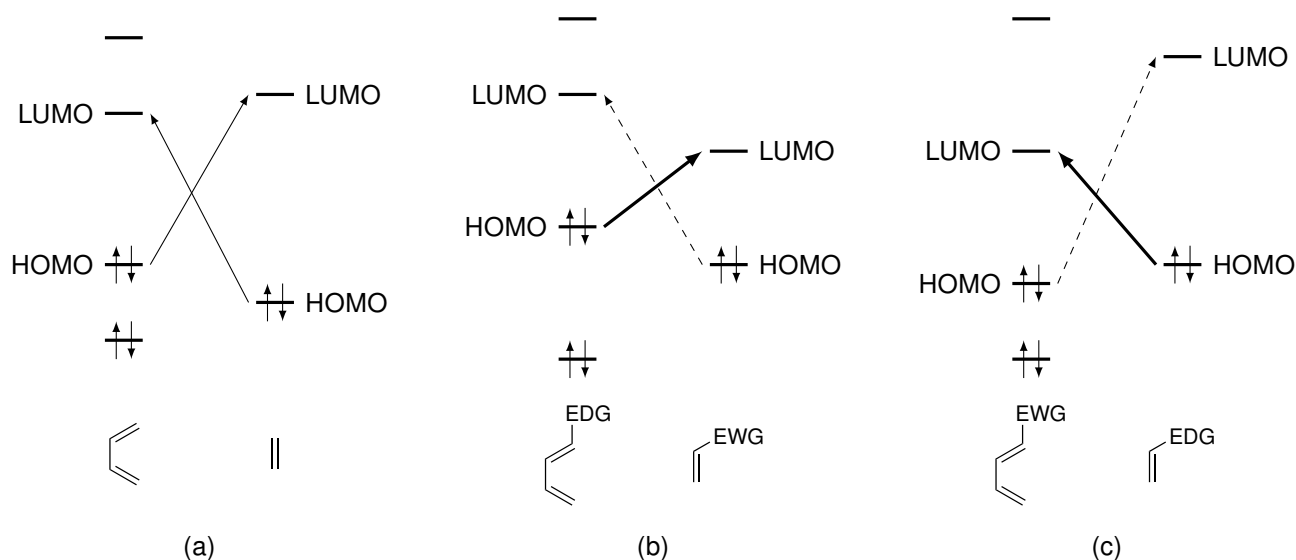
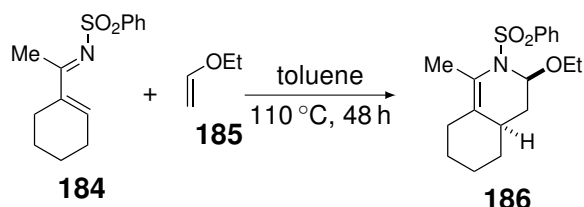


Figure 2.2: Frontier orbital interactions for Diels-Alder reaction for (a) butadiene with an unsubstituted dienophile; (b) an EDG-substituted butadiene with an EWG-substituted dienophile; (c) an EWG-substituted butadiene with an EDG-substituted dienophile.^{27–30}

As shown in Figure 2.2, in the Diels-Alder reaction with the unsubstituted butadiene (**154**) and ethylene (**173**) (Figure 2.2.a), the reaction occurs *via* the overlap of the HOMO orbital of the diene and the LUMO orbital of the dienophile as it corresponds to the smaller HOMO-LUMO gap. As this combination of orbitals corresponds to the “normal” situation, since no substituents are present on the reagents, it was named the normal electron demand Diels-Alder reaction.

As described in Scheme 2.6, unsubstituted diene and dienophile do not react rapidly and the addition of appropriate groups will help the reaction rate to increase. Indeed, the addition of an EWG on the dienophile lowers the energy of its LUMO orbital (Figure 2.2.b). Similarly, the presence of an EDG on the diene increases the energy of its HOMO orbital. Compared to the reaction between unsubstituted butadiene and ethylene (Figure 2.2.a), both effects participate in the reduction of the HOMO-LUMO gap, facilitating the overlap of the HOMO orbital of the diene and the LUMO orbital of the dienophile and, therefore, enhancing the rate of the reaction.^{28–30}

The inverse situation is possible as well, where the EWG is on the diene and the EDG is on the dienophile, leading to the inverse electron demand Diels-Alder reaction. An example, described by Boger *et al.*, involves ethyl vinyl ether (**185**) as an electron-rich dienophile and azadiene **184** as an electron-poor diene (Scheme 2.7).³³

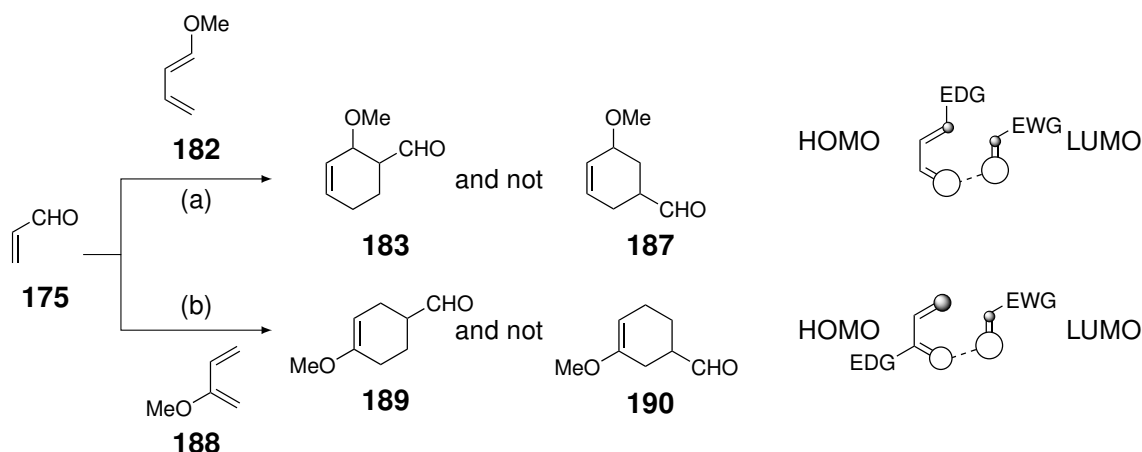


Scheme 2.7: Inverse electron demand Diels-Alder reaction between *N*-sulfonyl-1-aza-1,3-butadiene **184** and ethyl vinyl ether (**185**).³³

In that situation, the EWG on the diene lowers its LUMO orbital and the EDG on the dienophile increases the HOMO orbital of the latter (Figure 2.2.c). The gap is reduced as well, but the overlap occurs between the HOMO orbital of the dienophile and the LUMO orbital of the diene.

2.2.2 Regioselectivity of the Diels-Alder reaction

The question of regioselectivity in the Diels-Alder reaction concerns the orientation of the diene upon its addition on the dienophile. For example, the reaction between 1-methoxybutadiene (**182**) and acrolein (**175**) only gives the adduct in which the methoxy group and the aldehyde are in a 1,2-relation, also called the “*ortho*” adduct (Scheme 2.8.a).²⁷ On the other hand, the same reaction with 2-methoxybutadiene (**188**) only gives the “*para*” adduct (Scheme 2.8.b).³⁴

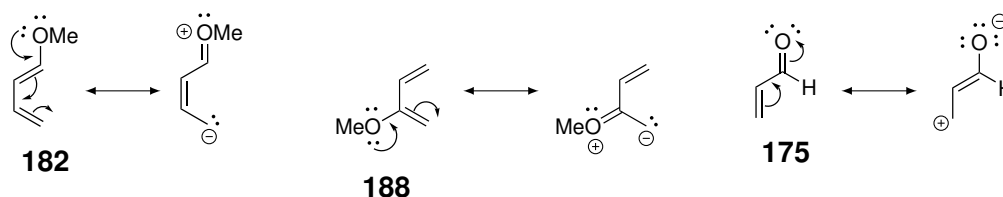


Scheme 2.8: Diels-Alder reactions between acrolein (**175**) and (a) 1-methoxybutadiene (**182**) or (b) 2-methoxybutadiene (**188**), regioselectivities thereof, and coefficients of the frontier orbitals of a butadiene substituted with an EDG on position 1 or 2, and EWG-substituted dienophile.^{27,34}

These observed results can be explained by the coefficients of the frontier orbitals. In these situations, the HOMO orbitals of the EDG-substituted diene will react with the LUMO orbital of the EWG-substituted dienophile as it leads to the smallest energy gap. Thereafter, the coefficients of the HOMO and LUMO orbitals must be calculated in order to determine which bonds are preferentially formed.^{28–30}

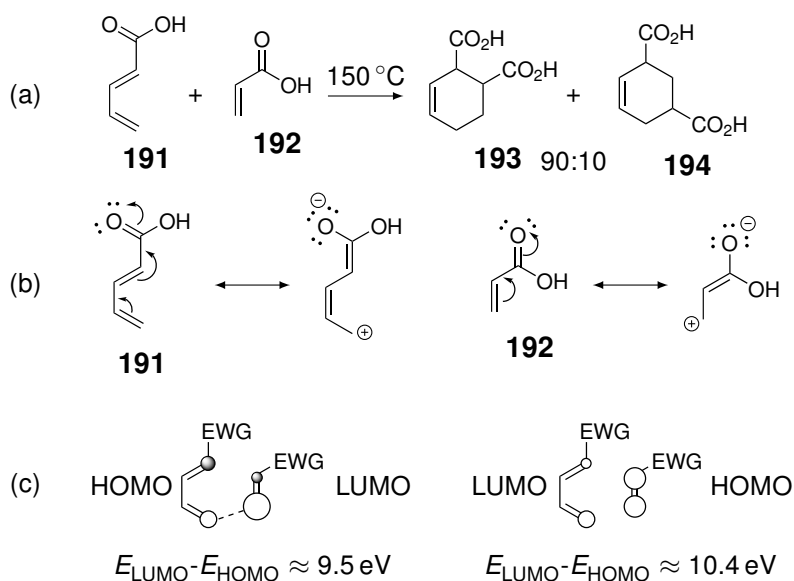
In these cases, the largest HOMO coefficients for 1- and 2-methoxybutadiene (EDG-substituted dienes) are on position 4 and 1, respectively, whereas the largest LUMO coefficient for acrolein (EWG-substituted dienophile) is on position 3. The regioselectivity can then be determined by pairing the largest HOMO and LUMO coefficients of both diene and dienophile.

However, one could be tempted to evaluate the regioselectivity based on the electron densities highlighted by the resonance forms of the reagents. Therefore, the drawing of such forms brings out a higher electron density on position 4 and 1 for 1- and 2-methoxybutadiene (**182** and **188**), respectively, and a lower electron density on position 3 for acrolein (**175**) (Scheme 2.9).



Scheme 2.9: Resonance forms of 1-methoxybutadiene (**182**), 2-methoxybutadiene (**188**), and acrolein (**175**).

Although it is a much simpler way to determine the regioselectivity, it does not make it possible to account for more complex examples, such as the reaction between butadienoic acid (**191**) and acrylic acid (**192**), both being EWG-substituted diene and dienophile (Scheme 2.10.a).³⁵



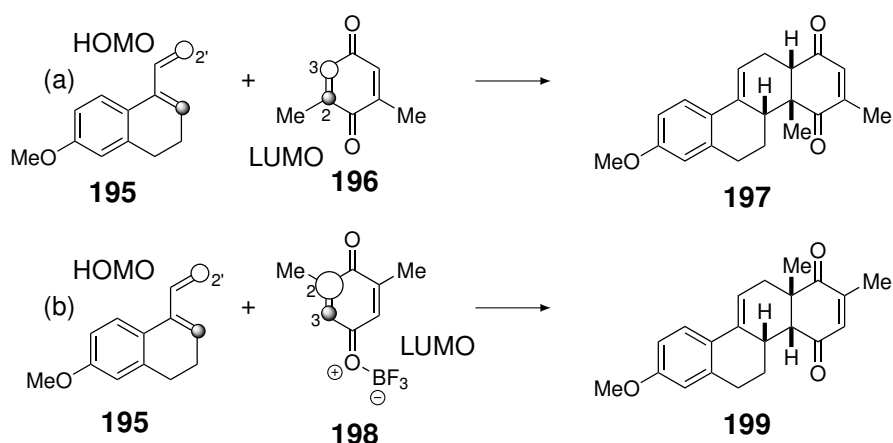
Scheme 2.10: Diels-Alder reaction between butadienoic acid (**191**) and acrylic acid (**192**), their resonance forms, and coefficients of the frontier orbitals thereof (HOMO-LUMO gap energies are approximated values).^{27,35}

As observed, the main product corresponds to the “*ortho*” adduct (**193**), along with a smaller amount of the “*meta*” adduct (**194**). If the resonance forms are used to determine the regioselectivity of that reaction, it shows that position 4 on the diene possesses a low electron density (Scheme 2.10.b). The latter should therefore not make any bond with the C3 position of acrylic acid, that also has a low electron density.

On the other hand, when the frontier orbitals are employed, it can be first determined that the smallest energy gap turns out to be between the HOMO orbital of the diene and the LUMO orbital of the dienophile. From this situation, it is found that butadiene bearing an EWG on position 1 has a slightly larger HOMO coefficient on the C4 position. The preferential pairing will then occur between the latter and the C3 position of acrylic acid (Scheme 2.10.c).

The FMO theory can also account for the observed regioselectivities in the case of polysubstituted dienes and dienophiles. In the course of their attempt to synthesise steroids, Dickinson *et al.* used the Diels-Alder reaction between diene **195** and 2,6-xyloquinone (**196**). Unfortunately, an adduct with a regioselectivity opposite to the desired one was obtained (Scheme 2.11).³⁶ Once again, it can be explained by the fact that the smallest energy gap exists between the HOMO of the diene and the LUMO of the dienophile and that, in such a situation, the HOMO coefficient of the diene is slightly higher on position 2' and the highest LUMO coefficient is on the C3 position of the quinone.

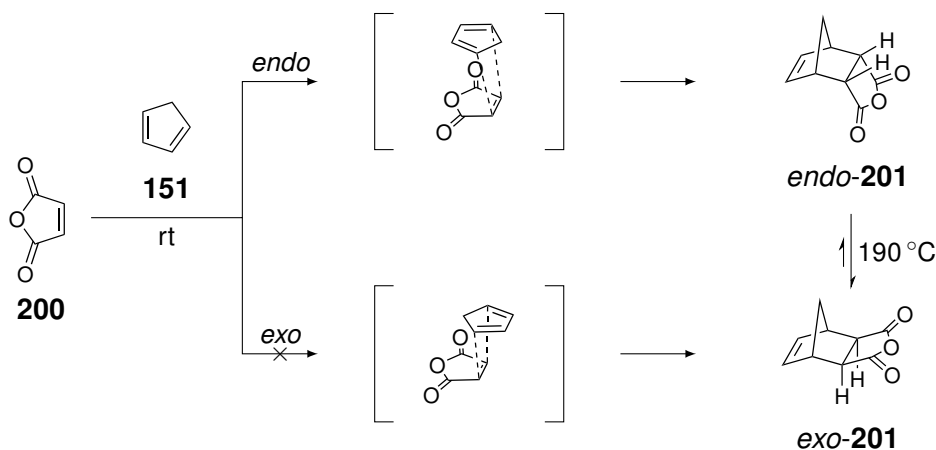
When the same group used BF_3 as Lewis acid in that reaction, the latter formed an adduct with the oxygen atom having the highest electron density. Consequently, it modified the coefficients of the LUMO orbital of the quinone, greatly increasing the LUMO coefficient on its C2 position, leading to the desired cycloadduct for the synthesis of steroids.³⁷



Scheme 2.11: Diels-Alder reaction between diene **195** and 2,6-xyloquinone (**196**) or the xyloquinone-BF₃ Lewis adduct **198**, and coefficients of the frontier orbital thereof.^{27,36,37}

2.2.3 Stereoselectivity of the Diels-Alder reaction

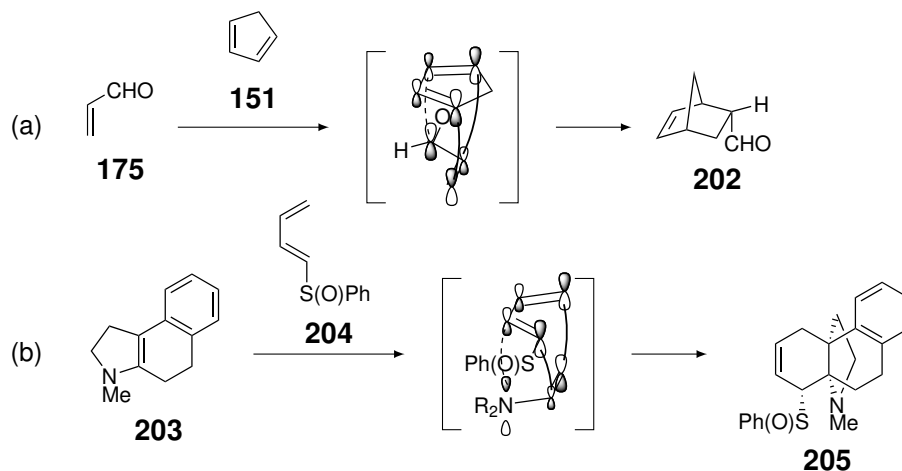
The third great feature of the Diels-Alder reaction is its stereoselectivity. Based on the outcome of different reactions, such as the addition of cyclopentadiene (**151**) on maleic anhydride (**200**) (Scheme 2.12), Alder stated that the favoured transition structure has the electron-withdrawing substituents in the more hindered environment, under the diene unit. This approach, which was called *endo*, seems to be the kinetically favoured one, but not the thermodynamically favoured one. Indeed, when cycloadduct *endo*-**201** was heated at 190 °C, it isomerised to the more stable cycloadduct *exo*-**201**, through a retro-cycloaddition and re-addition *via* the *exo* approach.³⁸



Scheme 2.12: Diels-Alder reaction between maleic anhydride (**200**) and cyclopentadiene (**151**), transition states of the *endo* and *exo* approaches, and the resulting cycloadducts *endo*-**201** and *exo*-**201**. Thermal isomerisation of the *endo* adduct into the *exo* adduct.³⁸

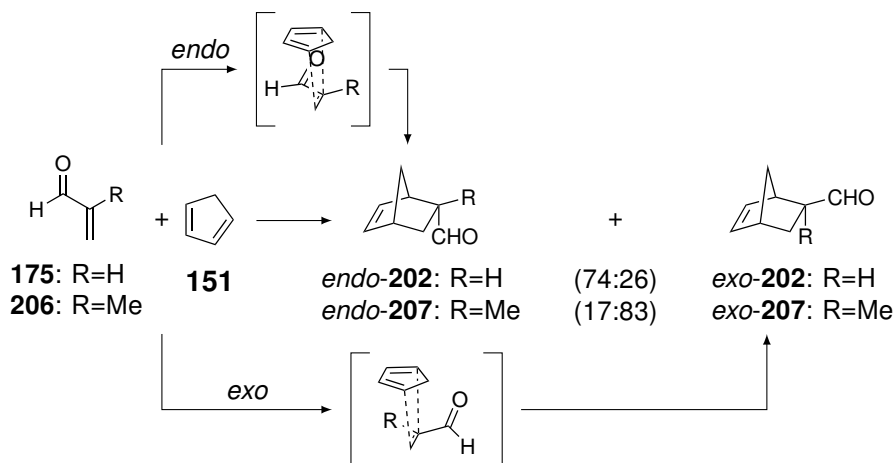
The usual explanation, behind the observation of the *endo* adducts as main products, is based on secondary orbital interactions. In the *endo* approach, the frontier orbitals show a potential overlap between lobes of the HOMO of the diene and the LUMO of the dienophile, which do not participate in the formation of new bonds, but whose coefficients have the same sign.³⁹ As an illustration, the *endo* approach of cyclopentadiene (**151**) and acrolein (**175**) exhibits primary orbital interactions (solid bold lines) that will lead to the new bond formation, and secondary orbital interactions (dashed line) between the carbon atom in position 2 of **151** and the carbonyl (Scheme 2.13.a).⁴⁰

Similarly, this model can also be applied to inverse electron demand Diels-Alder reactions (Scheme 2.13.b). In this case, secondary orbital interactions occur between the HOMO of the dienophile (**203**) and the LUMO of the diene (**204**). More precisely, those interactions occur between the nitrogen atom and the C2 carbon atom of the diene.⁴¹



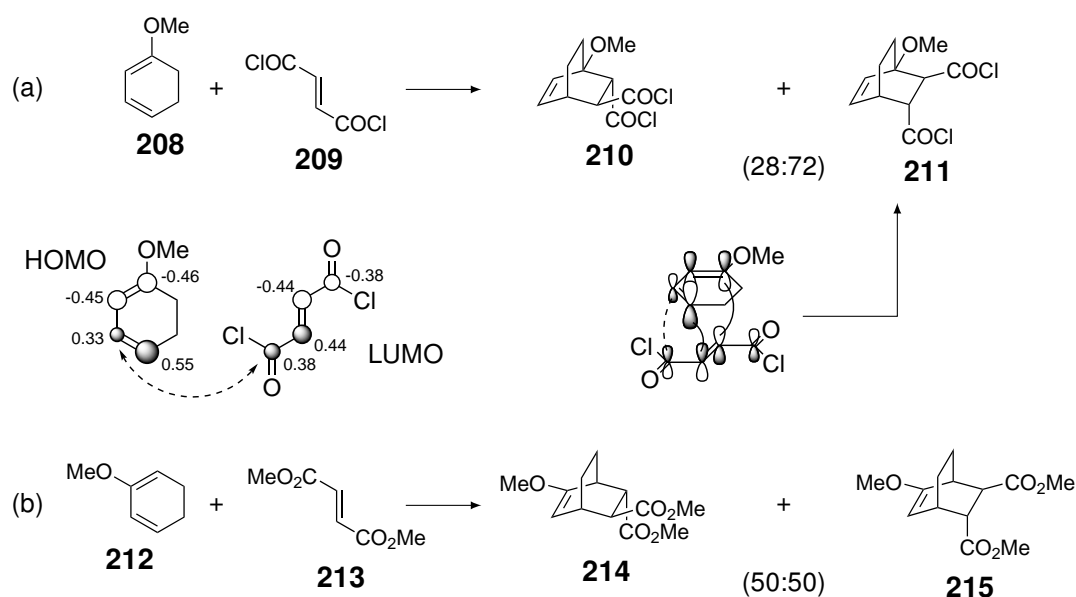
Scheme 2.13: Representation of the primary orbital interactions (solid bold lines) and of the secondary orbital interactions (dashed line) in the *endo* approach, and main product thereof, for: (a) normal demand Diels-Alder reaction between acrolein (**175**) and cyclopentadiene (**151**); (b) inverse electron demand Diels-Alder reaction between the sulfinyldiene **204** and the enamine **203**.^{27,39–41}

However, some counterexamples have also been described, casting doubt on the proposed model. As described here above, the reaction between acrolein (**175**) and cyclopentadiene (**151**) mainly gives the *endo* adduct according to the favourable secondary orbital interactions. Nevertheless, a small proportion of *exo* adduct is obtained (Scheme 2.14). On the other hand, when the same reaction is performed using methacrolein (**206**), the main adduct is not the one with the aldehyde in *endo* position, but the one with the methyl group in *endo* position.⁴⁰ This example puts the secondary orbital interactions in question, as the preference for the unexpected adduct is much higher than for the expected one.



Scheme 2.14: Diels-Alder reaction between cyclopentadiene (**151**) and acrolein (**175**) or methacrolein (**206**), and cycloadducts thereof.⁴⁰

Another set of examples are the reaction between 1-methoxycyclohexa-1,3-diene (**208**) and fumaroyl chloride (**209**) (Scheme 2.15.a) or the reaction between 2-methoxycyclohexa-1,3-diene (**212**) and methyl fumarate (**213**) (Scheme 2.15.b). In the former case, the main product is adduct **211**, which would come from an approach where the p orbital of the carbonyl has a favourable secondary overlap with the p orbital of the carbon atom on position 3 of the diene.⁴² Indeed, as illustrated in Scheme 2.15, the coefficient (determined with the Hückel method) on the carbonyl of fumaroyl chloride (**209**), in the LUMO orbital of the latter, is closer to the coefficient on the C3 position of **208**, in the HOMO orbital of the latter, than to the coefficient on the C2 position. Therefore, this better overlap leads to the most favourable secondary orbital interaction and to the kinetically favoured cycloadduct **211**.



Scheme 2.15: Diels-Alder reaction between: (a) 1-methoxycyclohexa-1,3-diene (**208**) and fumaroyl chloride (**209**), coefficients of the HOMO orbital of the diene and of the LUMO orbital of the dienophile, and representation of the primary orbital interactions (solid bold lines) and of the secondary orbital interactions (dashed line); (b) 2-methoxycyclohexa-1,3-diene (**212**) and methyl fumarate (**213**).^{42,43}

But in the second reaction, an equimolar amount of each adduct **214** and **215** is obtained.⁴³ This example implies that fumarate **213** does not approach the diene **212** with a preferential secondary orbital overlap and that the secondary orbital effects can be overridden.

Alongside those results, it was shown that the polarity of the solvent has a non negligible effect on the *endo:exo* ratios. The preference for the *endo* adduct in more polar solvents implies that electrostatic interactions might play a role in the preferential approach.^{44–46}

In the case of cyclopentadiene (**151**) reacting with acrolein (**175**), these electrostatic effects can be invoked, in the *exo* approach, by a repulsion between the methylene unit of cyclopentadiene, whose C-H bonds are slightly polarised towards the carbon atom, and the carbonyl group, whose bond is polarised towards the oxygen atom (Figure 2.3.a).⁴⁷ Similarly, when furan derivatives (**216**) are used with cyclopropanone derivatives (**217**) an attractive electrostatic interaction occurs between the oxygen atom and the carbonyl (Figure 2.3.b). In this specific case, the *exo* transition state leads to the cycloadduct which is the kinetically, as well as the thermodynamically favoured one.^{48,49}

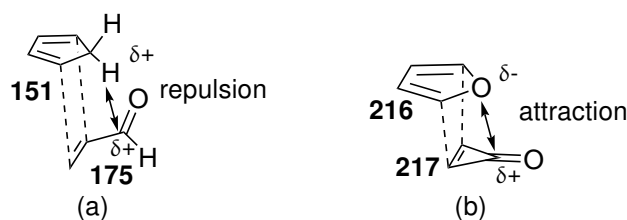


Figure 2.3: (a) Electrostatic repulsion between the carbonyl group of acrolein (**175**) and the hydrogen atoms of the methylene unit of cyclopentadiene (**151**).⁴⁷ (b) Electrostatic attraction between the carbonyl group of cyclopropanone (**217**) and the oxygen atom of furan (**216**).^{48,49}

In 2014, Fernández and Bickelhaupt performed computational studies on the Diels-Alder reaction between cyclopentadiene (**151**) and maleic anhydride (**200**) (Scheme 2.12) in order to determine the major contributors to the preferential *endo* approach of the reactants. This example was chosen as it exclusively gives the *endo* adduct and should therefore give a better insight in the stereoselectivity of the reaction.⁵⁰

In their calculation, they decomposed the potential energy surface into strain energy, associated with the structural deformation of the reactants, and the gain of energy due to the interactions between those two increasingly deformed reactants. They further decomposed the interaction component into electrostatic interactions, Pauli repulsion, primary and secondary orbital interactions, and dispersion forces.

Even though orbital interactions somewhat intervene in the stabilisation of the transition structures, they observed it has little to do with the preference between the *endo* or *exo* approach, as both of them showed similar stabilisation due to those effects. Instead, the selectivity seems to be mainly driven by steric factors as the activation strain was more destabilising for the *exo* approach than for the *endo* one. In this specific reaction, in the *exo* pathway, the methylene unit of cyclopentadiene (**151**) and the oxygen atom of maleic anhydride (**200**) suffer from an unfavourable steric arrangement in the transition state, leading to a more destabilising activation strain.

Comparatively, the use of butadiene does not lead to such unfavourable steric strain as the methylene unit is missing. This observation can be verified experimentally as the reaction between (deuterated) butadiene (**154**) and maleic anhydride (**200**) also gives a non negligible amount of *exo* adduct.⁵¹

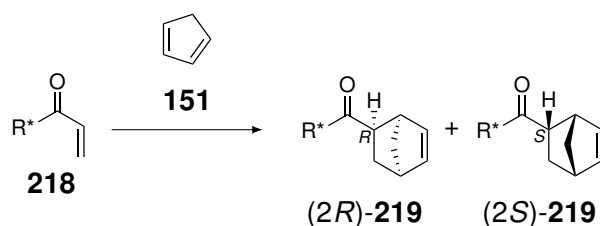
2.3 The asymmetric Diels-Alder reaction

Even though the Diels-Alder reaction already presents great features in terms of regio- and diastereoselectivity, one of the main remaining challenges is the formation of enantioenriched cycloadducts. Therefore, different types of strategies have been used throughout the years to answer this issue.

2.3.1 Chiral auxiliaries

One of those strategies consists in adding an enantiopure unit on one of the reactants, mostly derived from natural abundant compounds. Some of these examples are presented in Table 2.1.

Most of the examples found in the literature described those types of asymmetric Diels-Alder reactions with chiral auxiliaries added on the dienophile. Those chiral units are often derived from natural compounds, such as menthol (entries 1 and 2),^{54,55} camphorsulfonamide (entries 3 and 4),^{56,57} and

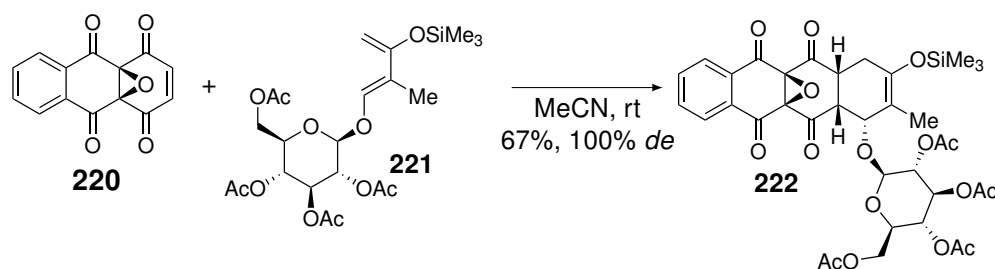
Table 2.1: Asymmetric Diels-Alder reactions of acrylate derivatives (**218**), functionalised with chiral auxiliaries, with cyclopentadiene **151**.^{52,53}

Entry	R*	Lewis Acid (eq.)	Solvent	Temp. (°C)	Major product	Yield (%)	endo (%)	de (%)
1 ⁵⁴		BF ₃ ·OEt ₂ (0.43)	CH ₂ Cl ₂	0	(2 <i>R</i>)- 219	74-81	95	74
2 ⁵⁵		TiCl ₄ (1.5)	CH ₂ Cl ₂	-20	(2 <i>R</i>)- 219	83	89	90
3 ⁵⁶		TiCl ₂ (O <i>i</i> Pr) ₂ (1.5)	CH ₂ Cl ₂	-20	(2 <i>R</i>)- 219	98	97	88
4 ⁵⁷		TiCl ₂ (O <i>i</i> Pr) ₂ (1.5)	CH ₂ Cl ₂	-20	(2 <i>R</i>)- 219	97	96	93
5 ⁵⁸		EtAlCl ₂ (1.5)	EtCl	-130	(2 <i>S</i>)- 219	84	99.5	95
6 ⁵⁹		TiCl ₄ (1)	CH ₂ Cl ₂	-10	(2 <i>R</i>)- 219	53	94	94
7 ⁵⁹		EtAlCl ₂ (1)	CH ₂ Cl ₂	0	(2 <i>S</i>)- 219	96	92	80
8 ⁶⁰		TiCl ₄ (2)	PhMe	-78	(2 <i>S</i>)- 219	71	>99	>99

champhorsultam (entry 5),⁵⁸ which are terpenes. They can also come from amino acids, such as proline (entry 6 and 7),⁵⁹ or sugars, such as arabinose (entry 8).⁶⁰

Depending on the auxiliary used, the facial selectivity can be improved. For example, adding a phenyl group on the isopropyl moiety of menthol significantly increases the diastereoisomeric excess (entries 1 and 2). The facial selectivity can also be inverted, going from (2*R*)-**219** (entries 1-4) to (2*S*)-**219** (entry 5). In some cases, with the same chiral auxiliary, the facial selectivity can be inverted by changing the Lewis acid used (entries 6 and 7).

Naturally, the addition of the chiral auxiliary can be done on the diene. As an illustration, Bourghli and Stoodley described cycloadditions between anthraquinones, such as **220**, and a glucosylated diene, such as **221** (Scheme 2.16).⁶¹ This example gave the diastereoisomer **222** exclusively.

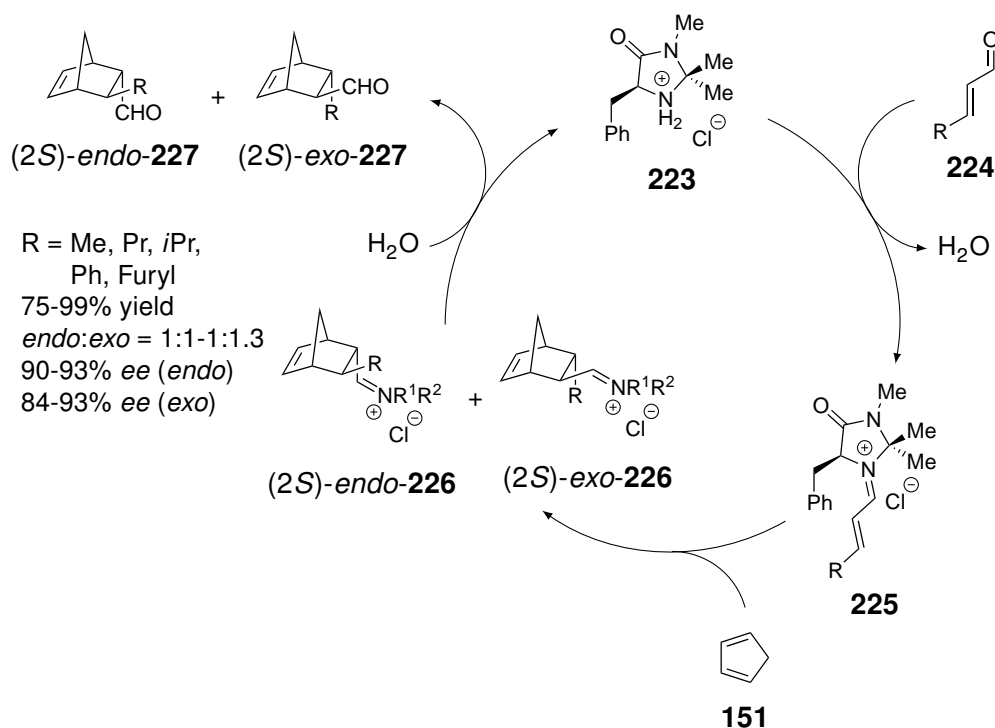


Scheme 2.16: Asymmetric Diels-Alder reaction between anthraquinone **220** and the glucosylated diene **221**.⁶¹

Obviously, many other types of chiral auxiliaries exist and can even be modified in order to increase, or even invert, the facial selectivities of these cycloadditions.^{52,53,62}

2.3.2 Asymmetric organocatalysis for Diels-Alder reactions

Another way to perform asymmetric Diels-Alder reactions is the use of organocatalysts.^{63,64} One of the most famous examples is the catalysis developed in 2000 by MacMillan, who is the first scientist to employ the term “organocatalysis”.⁶⁵ In that work, they used a chiral ammonium salt **223**, derived from (*S*)-phenylalanine, with enals **224** (Scheme 2.17). The combination of those two reagents forms an α,β -unsaturated iminium **225** that is more reactive but also chiral. Therefore, the diene, here cyclopentadiene (**151**), preferentially reacts on iminium **225** on the back face, as the front face is blocked by the benzyl group.



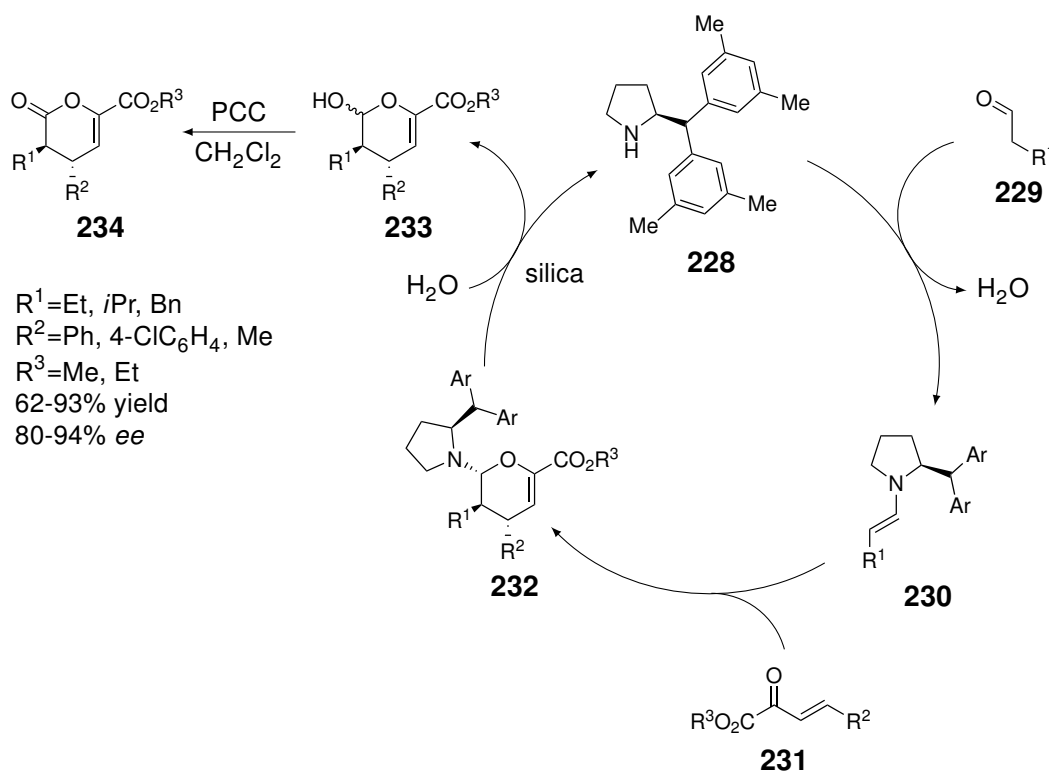
Scheme 2.17: Catalytic cycle of the catalysed asymmetric Diels-Alder reaction developed by MacMillan, using a chiral ammonium salt **223** as catalyst. The conditions are: **223** (5 mol %) in MeOH/H₂O (95/5 v/v, 1.0 M) at 23 °C.⁶⁵

The cycloaddition then leads to the formation of two adducts, (*2S*)-*endo*-**226** and (*2S*)-*exo*-**226**, followed by their hydrolysis to give the corresponding aldehyde version of the adducts, (*2S*)-*endo*-**227** and (*2S*)-*exo*-**227**. Even though the reaction has a low control on the *endo:exo* selectivity (equimolar amount in most of the examples with cyclopentadiene (**151**)), the enantiomeric excesses for both the *endo* and *exo* products were good to very good.

A second example of asymmetric organocatalysis is the use of chiral pyrrolidines with enolisable aldehydes, which form reactive enamine derivatives. This type of pyrrolidine-catalysed Diels-Alder reactions had already been reported by Boger in 1982,⁶⁶ but its asymmetric variation was developed and reported in 2003 by Jørgensen (Scheme 2.18).⁶⁷

The catalytic cycle starts with the formation of a chiral enamine **230**. This electron-rich dienophile undergoes a hetero-Diels-Alder reaction with the enone **231**. Hydrolysis of adduct **232** in presence of silica leads to the recovery of catalyst **228** and to lactol **233**, which was later oxidised into lactone **234**.

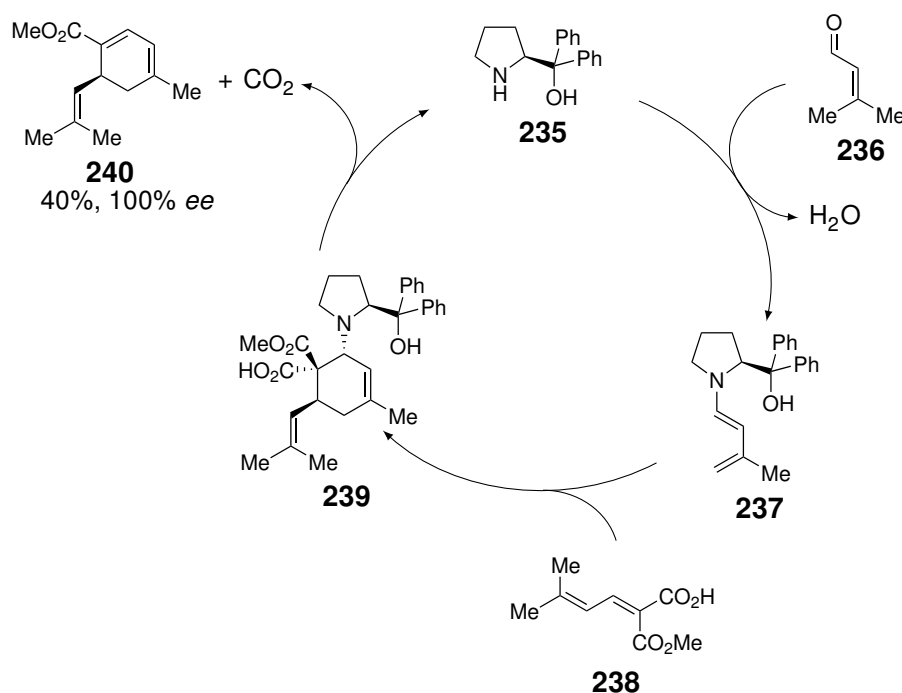
In their study, they determined that pyrrolidine **228** gave the best results with various aldehydes and enones. This reaction was proven efficient to reach good to excellent enantiomeric excesses.



Scheme 2.18: Catalytic cycle of the inverse electron demand hetero-Diels-Alder reaction developed by Jørgensen. The conditions used for the Diels-Alder part are (0.5 mmol scale): **228** (10 mol %), silica (50 mg), -15°C to rt, CH_2Cl_2 (0.5 mL). Yields and ee are given for product **234**.⁶⁷

Although the products obtained with that catalytic system correspond to Diels-Alder cycloadducts, the group of Jørgensen could not conclude whether these reactions are concerted or stepwise. A few years later, computational studies on similar processes would indicate that this type of catalysis goes through a stepwise mechanism (composed of consecutive Michael addition and Mannich-like reaction).^{68,69}

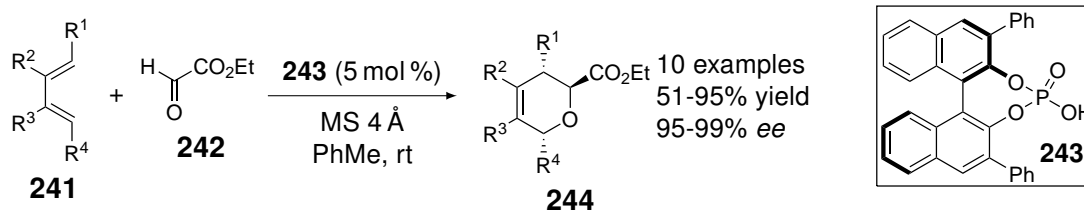
The version in which a chiral dienamine is formed also exists. The group of Serebryakov has published such a catalytic asymmetric Diels-Alder reaction in 1998 (Scheme 2.19).⁷⁰



Scheme 2.19: Catalytic cycle of the Diels-Alder reaction developed by Serebryakov. The conditions used for the Diels-Alder part are: **235** (10 mol %), 20 °C, 168 h in benzene. Yield and ee are given for product **240**.⁷⁰

In this pyrrolidine-catalysed cycloaddition, pyrrolidine **235** first reacts with the enal **236** to form the dienamine **237**. The latter reacts with compound **238** on its most reactive double bond. The formed adduct **239** later undergoes a β -*cis* elimination *via* a decarboxylation to recover the catalyst and to obtain cyclohexadiene **240**. Among their results, pyrrolidine **235** gave the best results in terms of enantiomeric excess, albeit the yield was lower with this example. They also determined that apolar solvents gave better results than polar and protic ones.

Another type of organocatalysis consists in the use of hydrogen bond donor and has proven to be efficient to accelerate many types of reaction, but also to carry out those reactions in an asymmetric manner.⁷¹ The Diels-Alder reactions are no exception to that rule as it has been illustrated by Terada *et al.*⁷² They used the chiral BINOL-phosphoric acid **243** to asymmetrically catalyse hetero-Diels-Alder reactions with excellent enantiomeric excesses (Scheme 2.20).



Scheme 2.20: Asymmetric hetero-Diels-Alder reaction, between dienes **241** and glyoxylate **242**, catalysed with the chiral BINOL-phosphoric acid **243**.⁷²

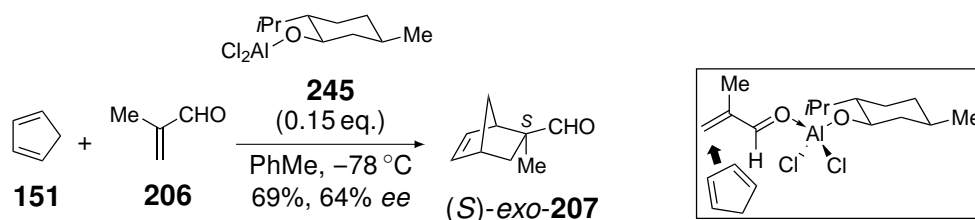
That example is not the only one and other groups also worked other types of such reactions, mostly hetero-Diels-Alder reactions, catalysed by chiral Brønsted acids.⁷³⁻⁷⁵

2.3.3 Lewis acid catalysed asymmetric Diels-Alder reactions

The third method, and probably the most used nowadays, is the use of chiral Lewis acids as catalysts. Diels-Alder reactions were the very first example of Lewis acid catalysed reactions and it was indeed shown that Lewis acids can increase the rate of the Diels-Alder reaction if the dienophile bears a carbonyl group.⁷⁶ It was later reported, *via* X-ray structures, that the oxygen atom of the carbonyl plays the role of a Lewis base and coordinates the Lewis acid, which lowers its LUMO orbital and, therefore, accelerates the reaction. The reactions can therefore be performed in milder conditions.^{77,78}

Besides the increase of reactivity, the use of chiral Lewis acids brings multiple advantages: a smaller amount of chiral precursor is required and the product is directly obtained. Such application of an asymmetric catalysis for the Diels-Alder reaction started in the late 1970's with the work of Koga *et al.* One of the reactions studied was the addition of cyclopentadiene (**151**) and methacrolein (**206**).⁷⁹ In order to induce some stereoselectivity in the reaction, they added 0.15 eq. of catalyst **245**, prepared from menthol and EtAlCl₂ (Scheme 2.21). As explained earlier, the major diastereoisomer is the one with the aldehyde group in *exo* position (Scheme 2.14), and an enantiomeric excess of 64% was reached.

As shown in the box in Scheme 2.21, the stereoselectivity would be explained by a coordination of the carbonyl to the aluminium with the methyl group pointing in the less hindered environment. The back face of methacrolein (**206**) is then hindered, and cyclopentadiene (**151**) will preferentially approach on the front face, in an *exo* orientation.



Scheme 2.21: Asymmetric Diels-Alder reaction between cyclopentadiene (**151**) and methacrolein (**206**) carried out using chiral catalyst **245**, prepared menthol as ligand and EtAlCl₂ as Lewis acid.⁷⁹

Since then, the development of chiral catalysts for the synthesis of enantioenriched cycloadducts took off.^{80–84} The Lewis acids used are numerous, such as boron, aluminium, iron, titanium, magnesium, copper, ruthenium, chromium, zirconium, samarium, gadolinium, or even ytterbium. The panel of ligands chosen for those reactions can be infinite, as modifying them with different substituents can allow a fine tuning of the reactions to reach the highest ee possible.

Nevertheless, reviewing of the literature reveals that some types of ligands stand out (Figure 2.4). They can be derived from natural terpenes, such as menthol or pinene, or amino acids, such as prolinol, oxazaborolidinium salts or oxazaborolidinones. Chelating ligands have also been developed such as diols, disulfonamides, diphosphanes, bisoxazolines, Schiff bases or binaphtols. Some groups also used metalloenzymes, containing a porphyrine as ligand for a metal core.⁸⁵

Since then, very good stereoselectivities can be achieved, allowing the application of this method as a powerful tool in many types of syntheses, including total synthesis. Indeed, the formation of enantiomerically enriched cycloadducts, with up to four controlled stereogenic centers, can alleviate synthetic issues encountered with other types of reactions.

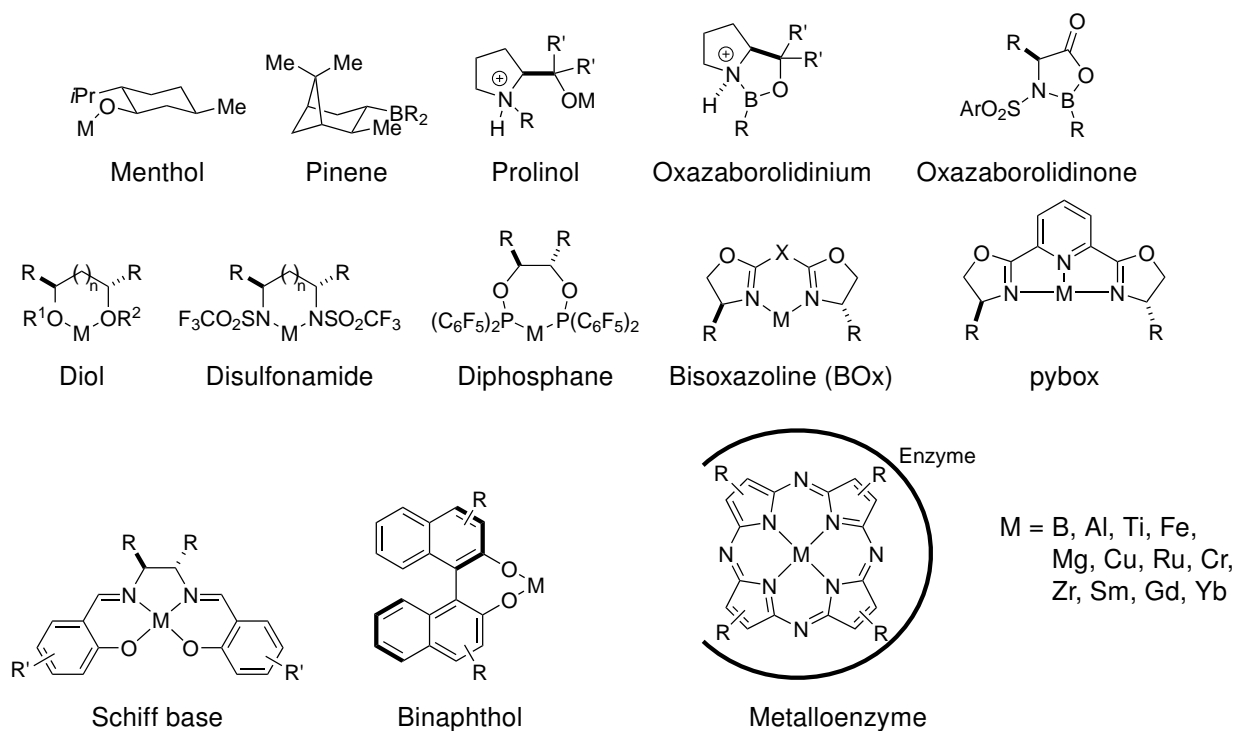
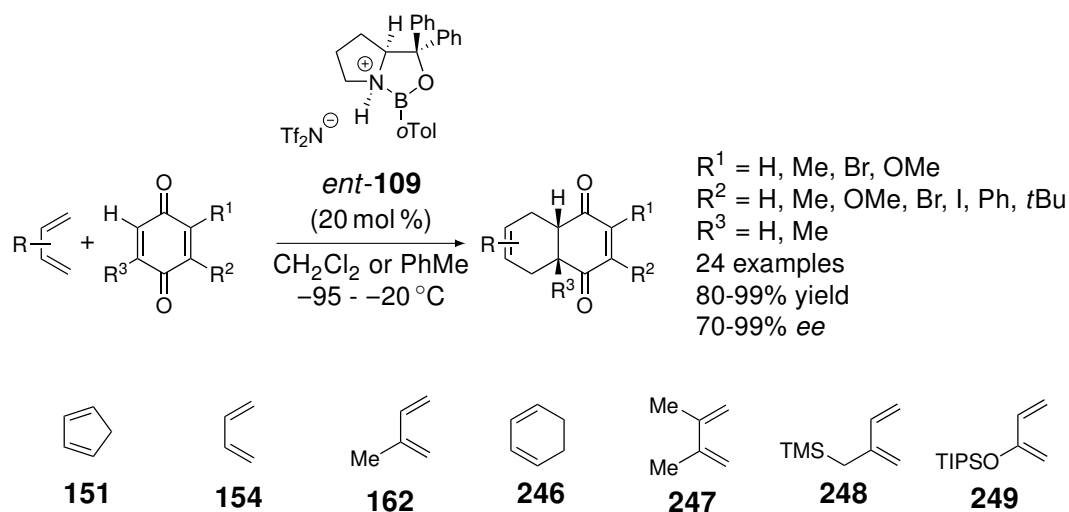


Figure 2.4: Examples of chiral catalysts used in asymmetric Diels-Alder reactions.^{80–85}

2.4 Catalytic asymmetric Diels-Alder reactions applied on quinones

In the course of this thesis, we took a particular interest in the asymmetric Diels-Alder reactions of quinones as it is one of the key steps for the total synthesis of momilactones, as it will be presented in Chapter 3. We report here some of the methods to perform such reactions in an asymmetric manner.

One of the main contributions to the catalytic asymmetric Diels-Alder reaction, with quinones as dienophiles, was reported by Corey's group (Scheme 2.22).^{86,87} In that work they use the oxazaborolidinium salt *ent*-**109** as catalyst with a variety of quinones and dienes. They obtained only *endo* adducts with moderate to excellent enantiomeric excesses.



Scheme 2.22: Asymmetric Diels-Alder reaction developed by Corey, using the oxazaborolidinium *ent*-**109** as chiral catalyst, between a quinone and diverse dienes (**151**, **154**, **162**, **246-249**).^{86,87}

In order to explain the facial selectivity observed with this catalysis, they proposed the model described in Figure 2.5. First, one of the carbonyl groups binds to the boron atom. Given the results obtained, it was postulated that the most electron-rich oxygen atom is the one to be involved in that bond. Then, a hydrogen bond, between a hydrogen atom in α position of the linked carbonyl group and the oxygen atom of the oxazaborolidinium salt, takes place. The back face is then blocked by one of the phenyl groups, and the diene arrives on the front face. In the case of 2-substituted dienes, the latter approaches the quinone with the preferential regioselectivity, described in Figure 2.5, in which the C1 position of the diene will make a new bond with the C5 position of the quinone.⁸⁶

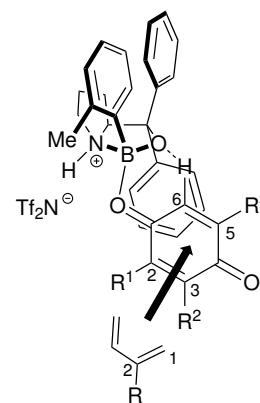
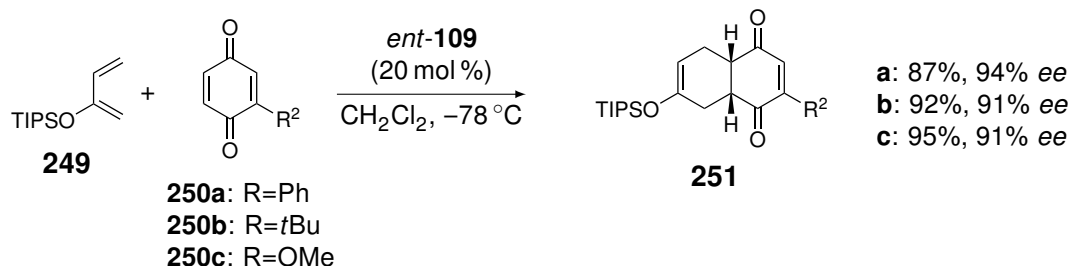


Figure 2.5: Model of the coordination of quinones to catalyst *ent*-109 for the asymmetric Diels-Alder reaction developed by Corey.⁸⁶

In their study, the group assessed the reactivity of mono-substituted quinones **250**. The cycloaddition occurred with an excellent enantioselectivity, with the preferential approach on the C5-C6 double bond and the expected regioselectivity (Figure 2.5). In those examples (Scheme 2.23), the hydrogen bond can occur with three different hydrogen atoms. Based on the structure of the resulting cycloadducts, they hypothesised that the quinone adopts an orientation in which the bulkiest group (R^2) is placed in the least hindered environment.⁸⁷



Scheme 2.23: Asymmetric Diels-Alder reactions between diene **249** and monosubstituted quinones **250** with *ent*-109 as chiral catalyst.⁸⁷

The only drawback presented in their work is the reaction of 2,5-dimethyl-1,4-benzoquinone (**252**) with unsymmetrical dienes **162** and **248**. Besides the good enantiomeric excesses observed for those examples, they encountered regioselectivity issues (Table 2.2).

They supposed, as those dienes are less electron-rich than diene **249**, their selectivity towards the C5-C6 double bond is lower. Therefore, even though quinone **252** would adopt the expected coordination to the catalyst, the dienes may react on the C2-C3 double bond as well with the new bond formed between the C1 position of the diene and the C3 of the quinone (Figure 2.6). Nevertheless, these latter still approach with an *endo* orientation on the front face of the quinone, leading to very good enantiomeric excesses.⁸⁶

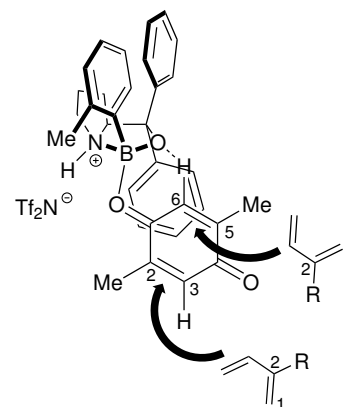
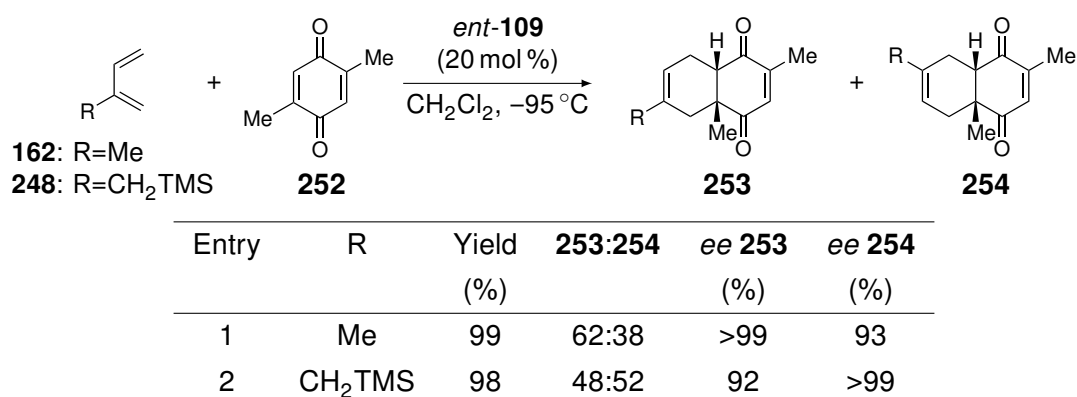
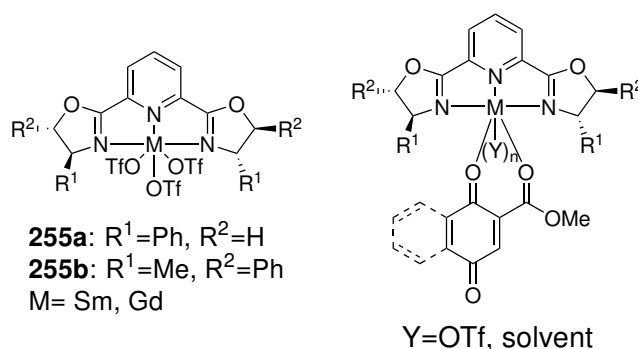


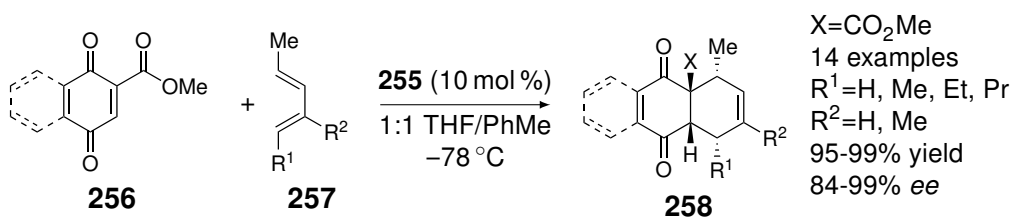
Figure 2.6: Model of the coordination of quinones **252** to catalyst *ent*-109 and the two possible approaches of dienes **162** and **248**.⁸⁶

Table 2.2: Asymmetric Diels-Alder reactions of dienes **162** or **248** with 2,5-dimethyl-1,4-benzoquinone (**252**), using *ent*-**109** a catalyst, and regioselectivity issues thereof.⁸⁶

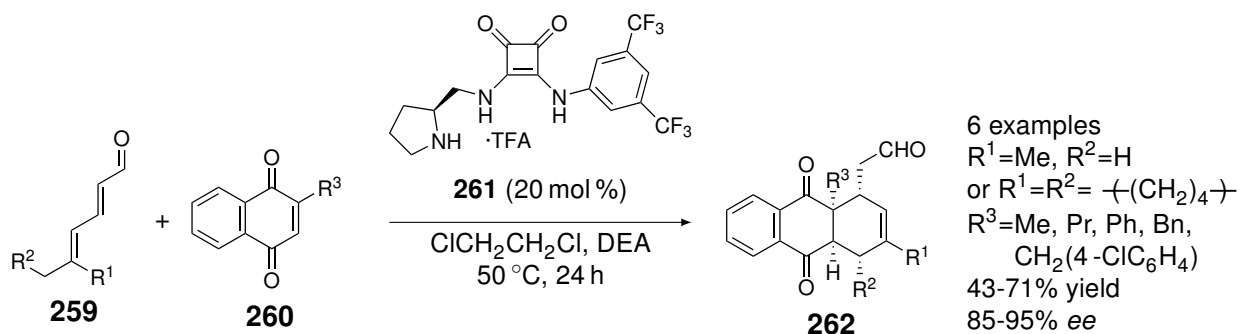
The same year, Evans' group published another method to perform asymmetric Diels-Alder reactions on 2-carboxylate-1,4-quinones **256**.⁸⁸ Their methodology focuses on the use of catalysts **255**, derived from pyridinyl-bis(oxazoline) (pybox) ligands and samarium or gadolinium triflates. The mode of coordination of the quinone consists in a chelation of the metal core between both carbonyl groups of the quinone and ester moieties (Figure 2.7). It was supposed that the third triflate anion might be replaced by one or several solvent molecules.

Figure 2.7: Structure of the catalyst **255**, derived from pyridinyl-bis(oxazoline) (pybox) ligands and samarium or gadolinium triflates, and structure of the coordination mode of quinones **256**.⁸⁸

They then assessed the efficiency of the catalysis by testing two benzoquinones and a naphthoquinone with five dienes substituted with aliphatic chains. They obtained good to excellent *ee* and determined that **255a** was the best catalyst for benzoquinones and **255b** was the best one for naphthoquinones. They also noticed that gadolinium triflate gave slightly better *ee* in some cases.⁸⁸

Scheme 2.24: Asymmetric Diels-Alder reactions between 2-benzoate-1,4-quinone (**256**) and diverse dienes, using catalyst **255**, derived from pyridinyl-bis(oxazoline) (pybox) ligands and samarium or gadolinium triflates.⁸⁸

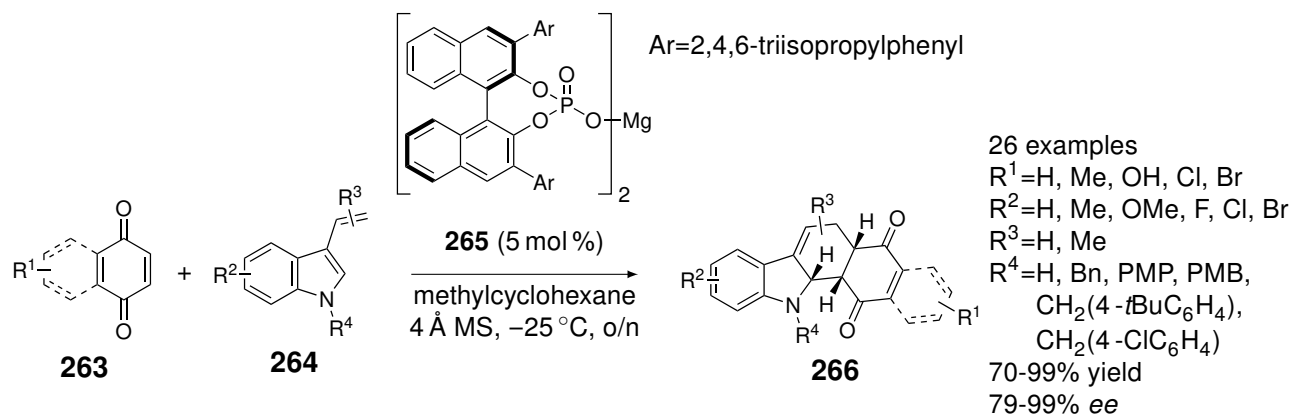
In 2013, Jørgensen *et al.* applied their enamine-mediated strategy (Scheme 2.18) on 1,4-naphthoquinone derivatives (Scheme 2.25).⁸⁹ In their study, they used a dienal, which was transformed into a trienamine *in situ* with catalyst **261**. In addition to the formation of a chiral enamine, the efficacy of the catalyst was reinforced thanks to the presence of a hydrogen bond donor moiety, facilitating the approach of the quinone on the desired face with an *exo* orientation. Even though the yields of the reaction were somewhat low, very good enantiomeric excesses were reached.



Scheme 2.25: Asymmetric Diels-Alder reaction, developed by Jørgensen *et al.*, using a trienamine, formed by reaction of catalyst **261** on dienal **259**, as diene and a naphthoquinone **260** as dienophile.⁸⁹

More recently, in 2019, Antilla *et al.* proposed an asymmetric catalysis for Diels-Alder reactions between quinones and naphthoquinones (**263**) and 3-vinylindoles (**264**), assisted by BINOL phosphate salt complexes.⁹⁰ That catalytic cycloaddition proved to be efficient for a wide range of quinones and vinylindoles with yields between 70 and 99% and *ee* between 79 and 99%. There were only a few exceptions with low *ee* of 5, 29 and 48%, one case where the conversion was very low, and one case where they encountered regioselectivity issues.

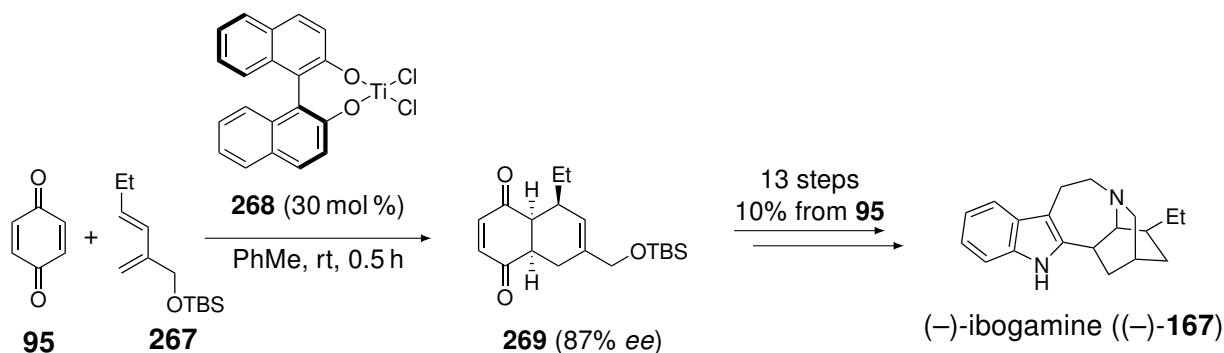
Using that strategy, the group tried to offer a global efficient synthetic pathway for the total synthesis of tetrahydrocarbazoles that can be found in Nature.



Scheme 2.26: Asymmetric Diels-Alder reaction between 1,4-quinones **263** and vinylindoles **264**, using BINOL phosphate complex **265** as chiral catalyst.⁹⁰

These few examples naturally represent a non-exhaustive part of what can be done on quinones in terms of cycloadditions. Although they are not the very first results of asymmetric catalytic Diels-Alder reaction on quinoid systems,⁹¹⁻⁹⁴ those works report some of the best *ees* achieved so far. Other catalytic systems have also been reported,⁹⁵⁻⁹⁷ including reactions on “masked” quinones.⁹⁸⁻¹⁰⁰

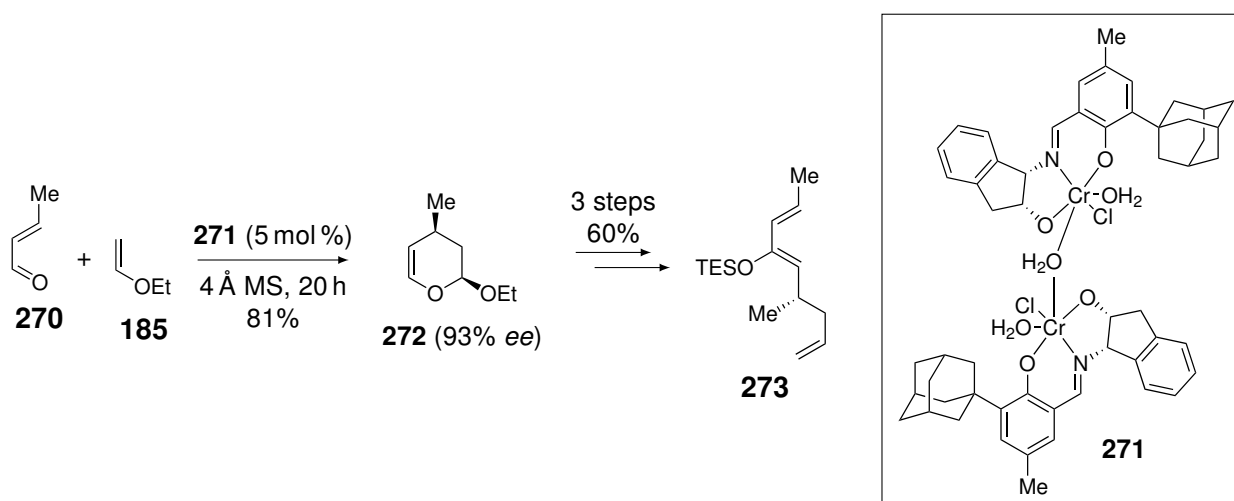
With the development of more complex systems for asymmetric Diels-Alder reactions, new applications in total synthesis can be envisaged. As an illustration, in 2000, White's group developed a new synthetic route for the synthesis of (–)-ibogamine ((–)-**167**).¹³ It started with a cycloaddition between benzoquinone (**95**) and diene **267**, asymmetrically catalysed by the BINOL complex **268**. They obtained the cycloadduct **269** with an enantiomeric excess of 87% (Scheme 2.27). Even though this *ee* is moderate, it remains an achievement as unsubstituted benzoquinone (**95**) possesses two double bonds that are equivalently reactive. A higher facial selectivity in those cases could then be thwarted by issues in the double bond selectivity. With an additional thirteen steps, they could finish the total synthesis of (–)-ibogamine with a 10% yield.



Scheme 2.27: Asymmetric total synthesis of (–)-ibogamine ((–)-**167**) from benzoquinone (**95**) and diene **267**, using BINOL catalyst **268** in the Diels-Alder step.¹³

Gaining in complexity, Jacobsen *et al.* proposed an enantioselective total synthesis of colombiasin A (**280**).¹⁰¹ They first performed attempts on different quinones and dienes to evaluate the efficiency of the catalyst they designed, the dimeric chromium complex **271**. Those tests gave adducts with yields between 62 and 92% and *ee* between 86 and 97%.¹⁰²

First, they had to synthesise the diene **273** that presents a stereogenic center (Scheme 2.28). Following the strategy they developed a few years earlier,^{103,104} they started their synthesis with an asymmetric hetero-Diels-Alder between crotonaldehyde (**270**) and ethyl vinyl ether (**185**), using catalyst **271**, obtaining dihydropyran **272** with a 93% *ee*. In three more steps, diene **273** was reached.



Scheme 2.28: Synthesis of diene **273**, starting from an asymmetric hetero-Diels-Alder between crotonaldehyde (**270**) and ethyl vinyl ether (**185**) using the dimeric chromium complex **271**.¹⁰¹

With the desired diene in hand, they could continue the synthesis with another asymmetric Diels-Alder reaction involving quinone **275** (Scheme 2.29). As the presence of a stereogenic center in the diene is not sufficient to induce a high stereoselectivity, they used the catalyst **274**, a monomeric version of the chromium complex. This reaction gave two products: the expected cycloadduct **276** and its isomer **277** with a 86% yield. Nevertheless, it was shown by other methods that a diastereomeric excess of 94% was reached, and both compounds gave the exact same products when engaged in the same reaction sequence.

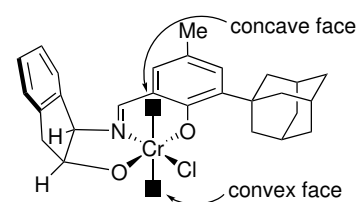
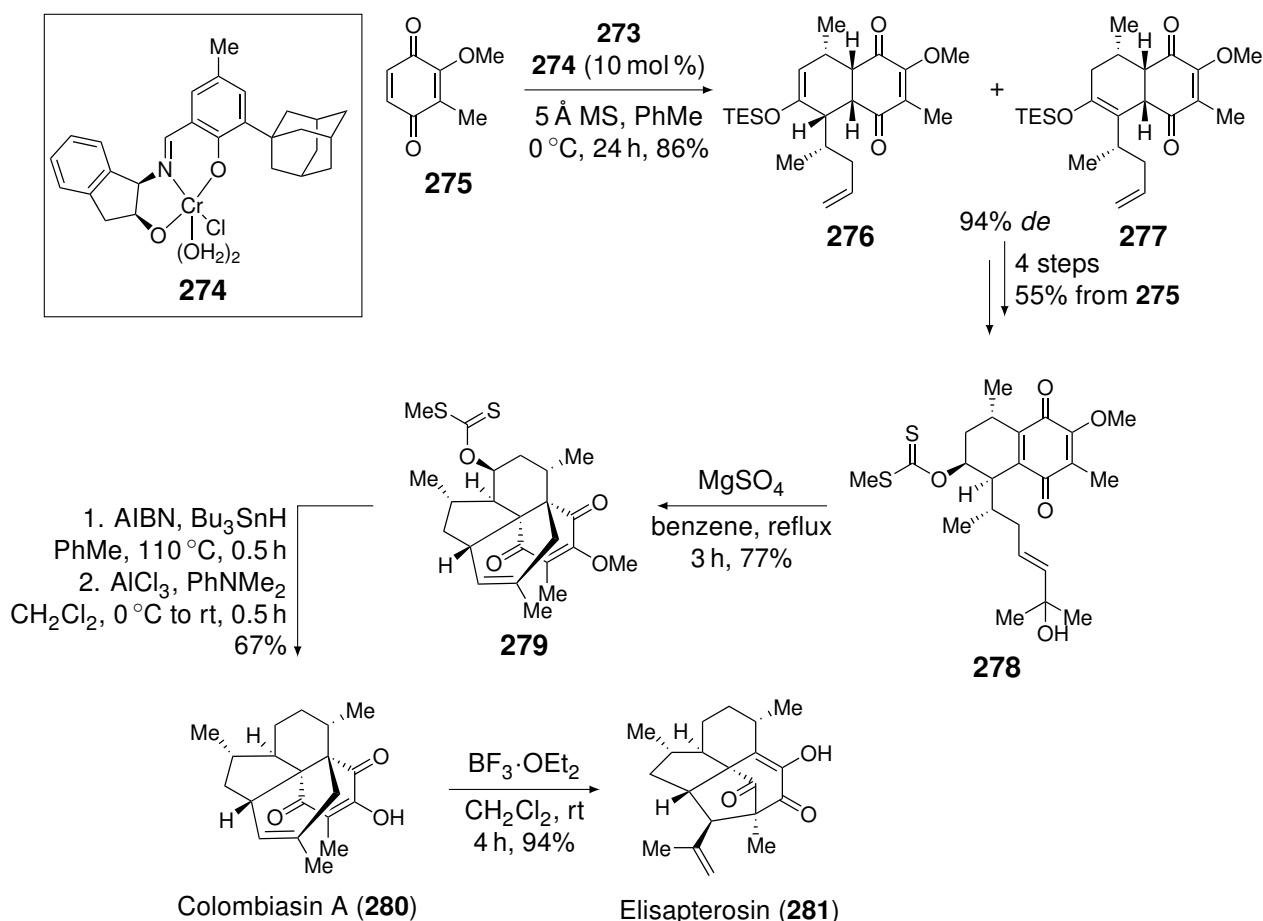


Figure 2.8: Representation of a 3D model of catalysts **271** or **274** and both possible approaches of a quinone.¹⁰²

The good stereoselectivity observed with those catalytic systems can be explained by an analysis of the structure of a monomeric unit of the catalyst (Figure 2.8). When water molecules are removed, it would appear, between both binding sites, that binding to the inner, concave face of the catalyst would be more consistent with the high enantioselectivities observed.¹⁰²



Scheme 2.29: Total synthesis of colombiasin A (**280**), starting with an asymmetric Diels-Alder reaction between diene **273** and quinone (**275**), and its conversion into elisapterosin B **281**.¹⁰¹

After four more reactions from **276** and **277**, intermediate **278** was obtained and dehydrated to form a diene *in situ*. The latter directly underwent an intramolecular Diels-Alder reaction to build the tetracyclic frame of colombiasin A (**280**). A Barton-McCombie deoxygenation, followed by a demethylation, led to the natural substance. With that sequence, Jacobsen's group accomplished the enantioselective total synthesis of Colombiasin A in 12 steps and 11.5% overall yield. The latter was

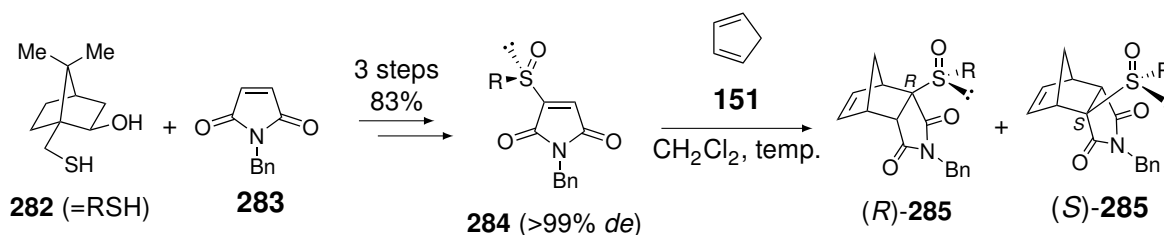
then efficiently converted into a second natural molecule, elisapterosin B (**281**), *via* a rearrangement catalysed by $\text{BF}_3 \cdot \text{OEt}_2$ in a very good 94% yield.¹⁰¹

2.5 Sulfinylquinones as chiral dienophiles

Over the last four decades, the chiral sulfinyl group has been widely used in stereoselective carbon-carbon or carbon-heteroatom bond forming reactions.^{105–111} More specifically, in our field of interest, it also proved to be a powerful chiral auxiliary for the Diels-Alder reactions.^{112,113}

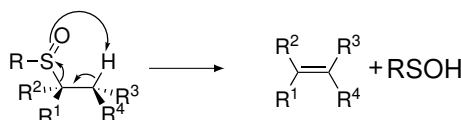
As an example, Shiro *et al.* reported, in 1991, the use of α -sulfinyl maleimides **284** as chiral dienophiles (Table 2.3).¹¹⁴ They tested the reaction with cyclopentadiene (**151**) at different temperatures with and without ZnCl_2 as Lewis acid. They first noticed that the temperature had little impact on the diastereoselectivity. They also highlighted that in the absence of a Lewis acid, the major adduct was (*S*)-**285**, but in the presence of ZnCl_2 , the selectivity is inverted towards (*R*)-**285** and is even better. They suggested that without catalyst, the preferential conformation of the sulfinyl moiety orientates the bulky group (*R*) on the front face, and forces the approach of the diene on the back face. On the other hand, when zinc is added to the reaction, a chelation of the metal by the sulfoxide group and the closest carbonyl of the maleimide can occur, changing the orientation of the *R* group towards the back face, forcing the approach of the diene on the top face.

Table 2.3: Diels-Alder reaction between cyclopentadiene (**151**) and α -sulfinyl maleimide **284**.¹¹⁴



Entry	Temp. (°C)	Lewis acid	Time (min)	Yield (%)	(<i>R</i>)- 285 :(<i>S</i>)- 285
1	40	—	5	>99	31:69
2	40	ZnCl_2	5	91	94:6
3	0	—	60	97	28:72
4	0	ZnCl_2	20	>99	97:3
5	-78	—	60	>99	36:64
6	-78	ZnCl_2	30	97	97:3

A particularity one should be aware of concerning the sulfinyl groups, is their ability to undergo a β -*syn* elimination when both sulfoxide group and a hydrogen atom are *syn*-periplanar (Scheme 2.30).¹¹⁵

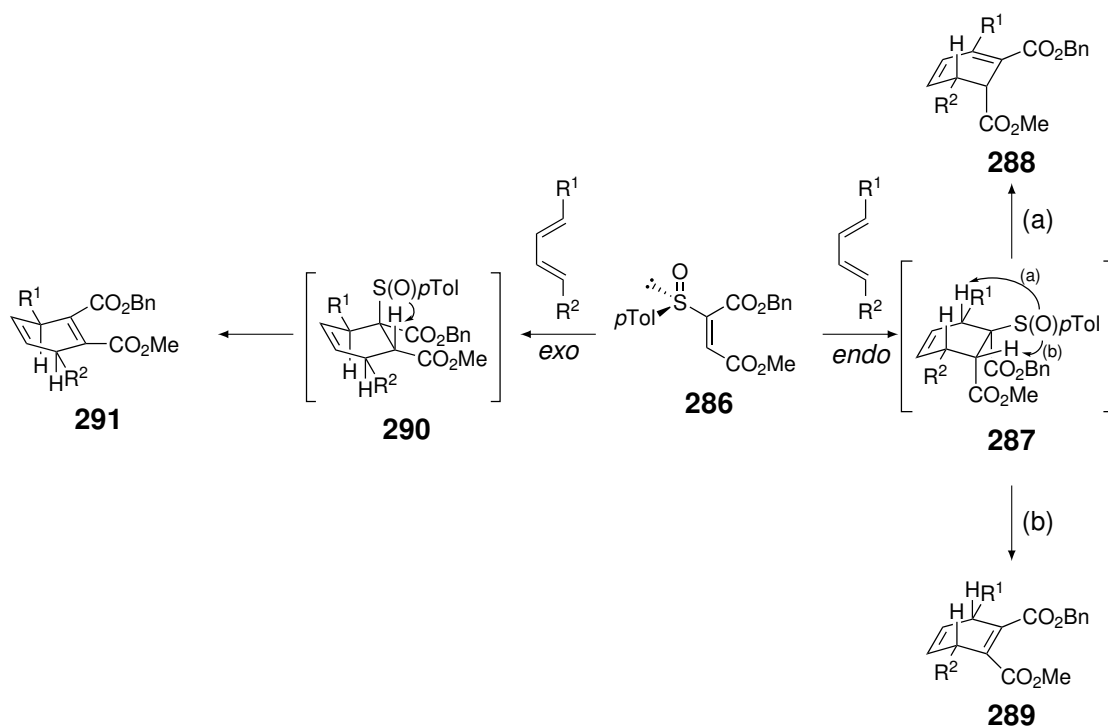


Scheme 2.30: β -*syn* elimination of the sulfinyl group.¹¹⁵

In 1994, García Ruano *et al.* described Diels-Alder reactions between diverse dienes and sulfinyl maleates (for example **286**), which could either take place *via* an *endo* or an *exo* approach (Scheme 2.31).¹¹⁶ However, the cycloadducts **287** and **290** were not stable, and the pyrolysis products were obtained after one to two days. Indeed, the orientation of the sulfoxide is propitious for the β -*syn* elimination described in Scheme 2.30.

In the case of the *endo* adduct **287** two pyrolysis products are reachable as two hydrogen atoms are in a *cis* orientation with respect to the sulfoxide, leading to cyclohexadienes **288** (pathway a) and **289** (pathway b). On the other hand, the *exo* adduct **290** only possesses one hydrogen atom in the adequate orientation and only one elimination product (**291**) was obtained.

In their communication, they reported that the reactions mainly underwent the *endo* route and that, on the whole, good enantiomeric excesses were reached, although mixtures of products **288** and **289** were obtained.



Scheme 2.31: Diels-Alder reactions between sulfinyl maleate **286** and diverse dienes, giving *endo* adduct **287**, that pyrolyses into **288** and **289**, or adduct **290**, that pyrolyses into **291**.¹¹⁶

2.5.1 Synthesis of enantiomerically enriched sulfinylquinones

As quinones, acting as dienophiles, seem to be important starting materials in the synthesis of many products, including natural ones, Carreño *et al.* wanted to synthesise chiral sulfinylquinones with high optical yields. For that purpose, they developed two different pathways, starting from bromodimethoxybenzene **293** (Scheme 2.32).¹¹⁷

The top pathway starts with the anodic oxidation (E) of **293** into its ketal form **294**, as described by Swenton *et al.*¹¹⁸ It later underwent a bromine lithium exchange, followed by a substitution on menthyl (-)-*S(S)*-*para*-toluenesulfinate (**292**, Figure 2.9). This chiral precu-

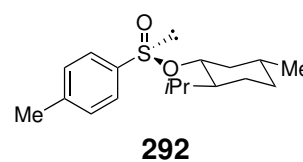
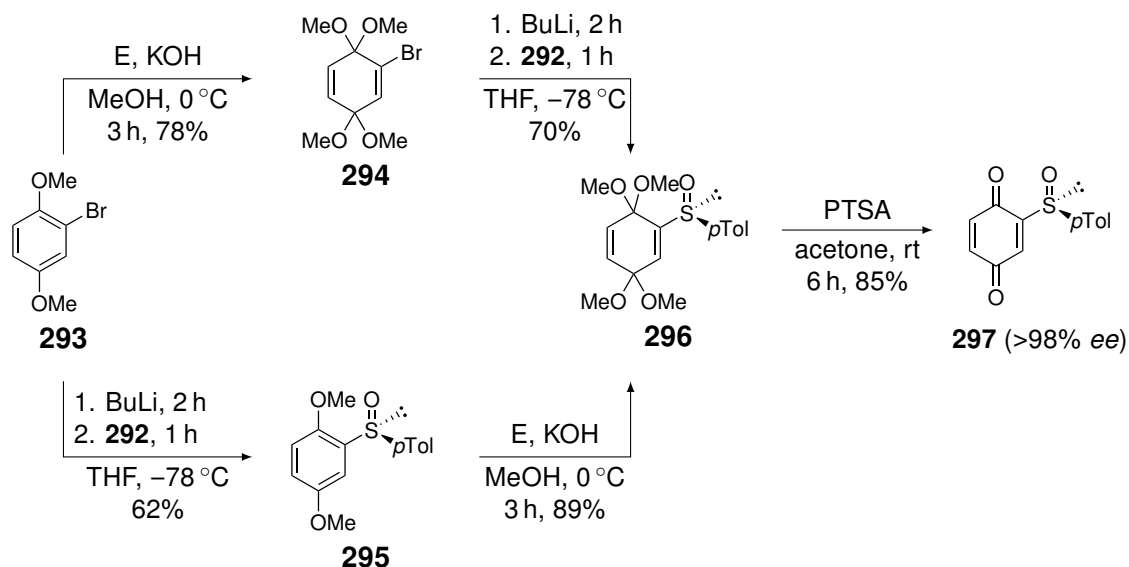


Figure 2.9: Structure of menthyl (-)-*S(S)*-*para*-toluenesulfinate (**292**).^{119–121}

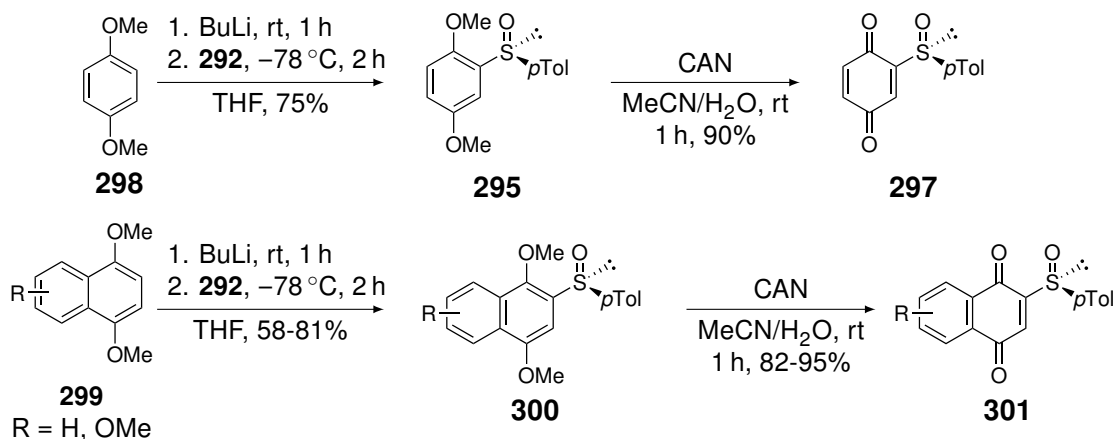
sor was prepared following the procedure of Andersen *et al.*,^{119,120} improved by the group of Solladié two decades later.¹²¹

The other pathway consists in inverting the synthetic steps, starting with the halogen metal exchange and the nucleophilic substitution, followed by the anodic oxidation. Both ways give approximately 55% overall yield. Finally, the sulfinyl ketal **296** is hydrolysed into the desired sulfinylquinone **297** that was obtained with an excellent enantiomeric excess.



Scheme 2.32: First synthesis of an enantiopure sulfinylquinone (**297**). E = electrochemical oxidation.¹¹⁷

Three years later, they improved their synthesis by performing an *ortho*-directed lithiation on 1,4-dimethoxybenzene (**298**), followed by the usual substitution on **292**, directly giving sulfoxide **295** (Scheme 2.33).¹²² The latter was then cleanly oxidised into its quinone form (**297**), using CAN instead of an electrochemical oxidation. This reagent does not oxidise the sulfinyl group, nor invert its absolute configuration. This route is one step shorter than the previous one (Scheme 2.32) and has a 68% overall yield.

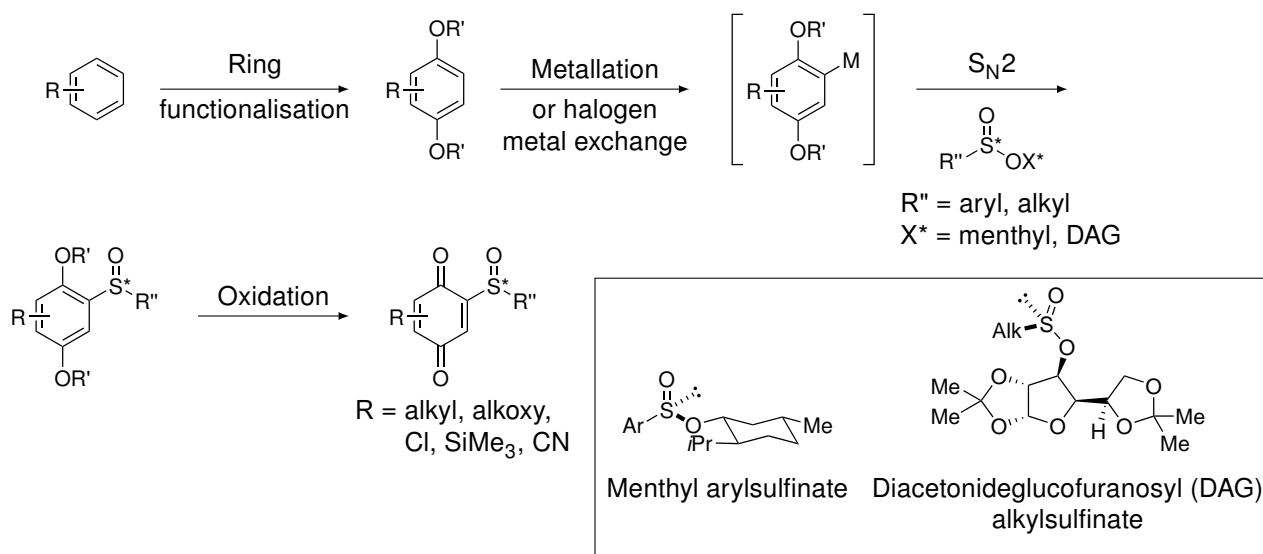


Scheme 2.33: Optimised synthesis of sulfinylquinone **297** and sulfinylnaphthoquinones **301**.¹²²

They then applied this strategy to the synthesis of various sulfinylnaphthoquinones (**301**) substituted with methoxy groups. They obtained three new examples of sulfinylquinone derivatives with moderate to very good yield in two steps with enantiomeric excesses above 95%.

Since then, many examples of sulfinylquinones and sulfinylnaphthoquinones have been synthesised with different types of substituents such as alkyl, alkoxy, chloride, silyl or nitrile groups.^{123–133} The main strategy to obtain such compounds is to start with the functionalisation of an aromatic ring. The latter, which contains a hydroquinone pattern, is converted into an organometallic compound either by metallation or halogen metal exchange, followed by a substitution on a sulfinate. Finally, the hydroquinone core is oxidised into a quinone, mostly with CAN or DDQ (Scheme 2.34).

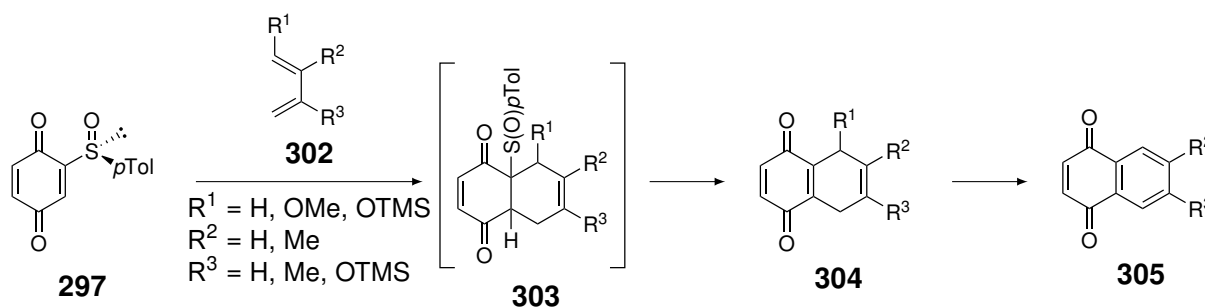
The nature of the sulfinyl group can also be modulated. The main chiral auxiliaries used are menthol and diacetonideglucofuranose (DAG) for arylsulfinyl and alkylsulfinyl groups, respectively. It is to be noticed that some of those sulfonates will lead to the *S* enantiomer, while others will lead to the *R* one.



Scheme 2.34: General route for the synthesis of enantiopure sulfinylquinones.

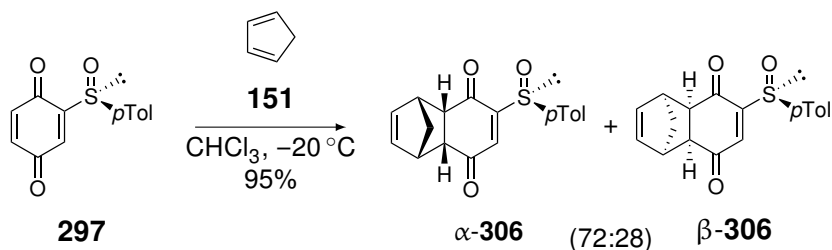
2.5.2 Double bond selectivity in Diels-Alder reactions with sulfinylquinones

With their enantiopure sulfinylquinone **297** in hand, Carreño's group assessed its reactivity in Diels-Alder reactions.¹¹⁷ They first started with acyclic dienes (**302**) (Scheme 2.35). As expected, they reacted on the sulfinyl-substituted double bond, as it is supposed to be the most electron poor, leading to the adducts **303**. However, those adducts were not detected as they pyrolysed rather quickly to the products **304**, that were themselves not isolable due to the further aromatisation to naphthoquinones **305**.



Scheme 2.35: Diels-Alder reactions between sulfinylquinone **297** and acyclic dienes **302** and products thereof.¹¹⁷

However, when the same reaction was performed with a cyclic diene, such as cyclopentadiene (**151**), it surprisingly occurred on the other double bond (Scheme 2.36). Nevertheless, as the adducts could not pyrolyse, the group was able to determine a facial selectivity with the preferential approach on the back face, leading to α -**306** as major adduct. They showed that the sulfinyl group was a good inducer of stereoselectivity, even though the diene did not react on the expected double bond.



Scheme 2.36: Diels-Alder reaction between sulfinylquinone **297** and cyclopentadiene (**151**), leading to cycloadducts α - and β -**306**.¹¹⁷

When the group used cyclohexadiene (**246**), they observed the same behaviour as for cyclopentadiene.¹³⁴ Given the unexpected results with cyclic dienes, the group proposed a model to explain such observations.¹³⁴ They postulated when cyclic dienes approach in an *endo* orientation on the sulfinyl double bond (Figure 2.10.a), a steric repulsion arises between the methylene unit (or the ethylene unit for cyclohexadiene) and the sulfinyl group, whether on the top or bottom face of the quinone. Therefore, the addition occurs on the other double bond, still with an *endo* approach (Figure 2.10.b), hence the unexpected cycloadducts.

On the other hand, when acyclic dienes are employed, such steric clash is no longer occurring, as the methylene or ethylene unit is missing. The reaction can therefore take place on the sulfinyl double bond, that is supposedly the most reactive one (Figure 2.10.c).

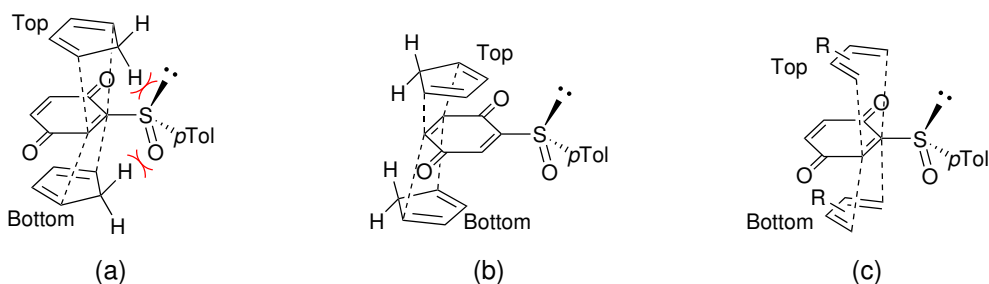


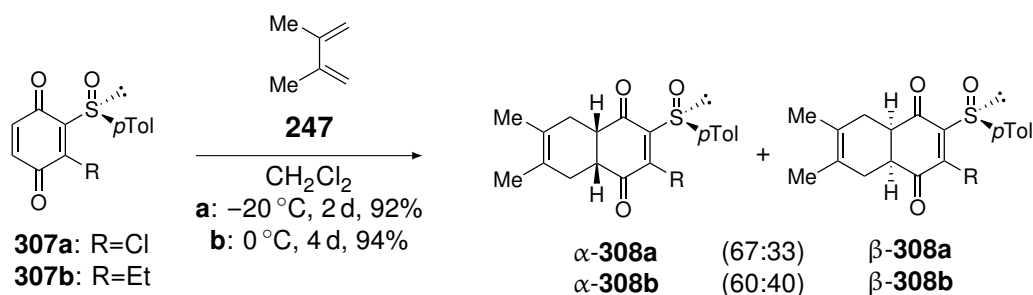
Figure 2.10: Proposed model for the explanation of the observed double bond selectivity with cyclic dienes (a and b) and acyclic ones (c).¹³⁴

In 2020, a group performed theoretical calculations on the cycloaddition between sulfinylquinone **297** and cyclopentadiene (**151**) and determined that the transition state with the lowest energy was indeed the approach on the bottom face in situation (b) described in Figure 2.10. They determined that this approach was stabilised by a CH- π interaction between the cyclopentadiene and the *para*-tolyl group.¹³⁵

As the goal of performing Diels-Alder reactions with sulfinylquinone **297** was to evaluate the facial diastereoselectivity of the cycloaddition on the sulfinyl-substituted double bond, Carreño's group

designed new sulfinylquinones with a substituent in C3 position. This way, the pyrolysis and aromatization processes observed with **297** (Scheme 2.36) should not take place.¹²³

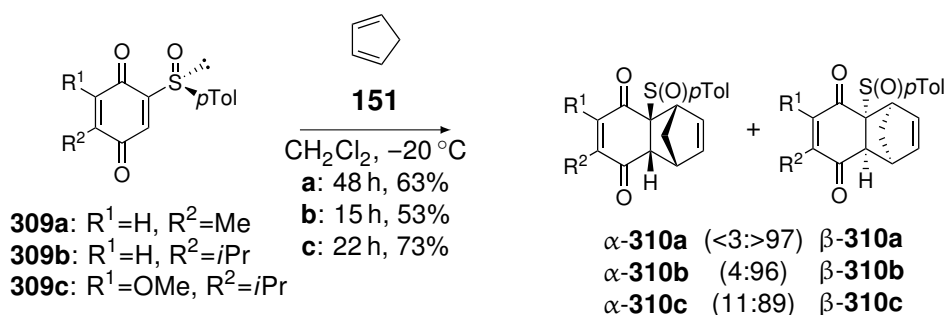
Unfortunately, the addition of a substituent on the C3 position made dimethylbutadiene (**247**) react on the C5-C6 double bond of quinones **307** (Scheme 2.37). They postulated that a group on the C3 position caused steric and/or electronic repulsions, which rendered the approach on that bond too difficult, even for acyclic dienes. Nonetheless, they could observe that some stereoselectivity was achieved as a slight preference was obtained for one of the diastereoisomers (determined on the basis of the selectivity observed for the reaction described in Scheme 2.36).



Scheme 2.37: Diels-Alder reaction between 3-substituted sulfinylquinones (**307**) and dimethylbutadiene (**247**), leading to cycloadducts α - and β -**308**.¹²³

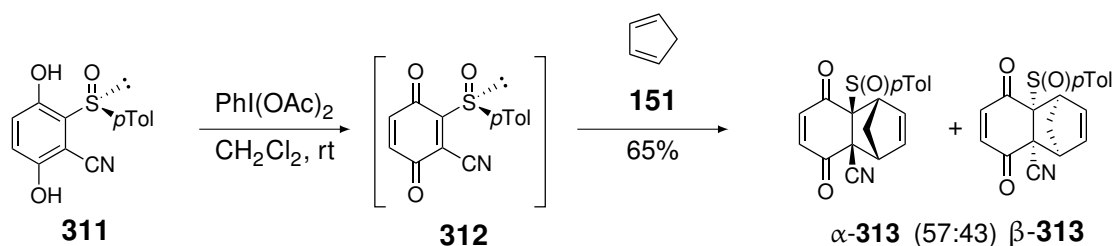
Since an unsubstituted sulfinylquinone (**297**) or 3-substituted ones leads to the addition of the diene on the C5-C6 double bond, a way to force the reaction on the C2-C3 double bond is to add bulky or electron donating groups on the C5 and/or C6 positions (Scheme 2.38).¹²⁵ Indeed, as observed by Carreño *et al.*, such substituted sulfinylquinones (**309**) led to the cycloaddition occurring on the sulfinyl-bearing double bond (adducts **310**).

In those examples, the preferential cycloadducts are the β -**310** ones, corresponding to the diene approaching on the front face with an *endo* orientation. The facial diastereoselectivities were much better on that double bond, as the reaction is happening closer to the sulfinyl moiety.



Scheme 2.38: Diels-Alder reactions between sulfinylquinones **309** and cyclopentadiene (**151**), leading to cycloadducts α - and β -**310**.¹²⁵

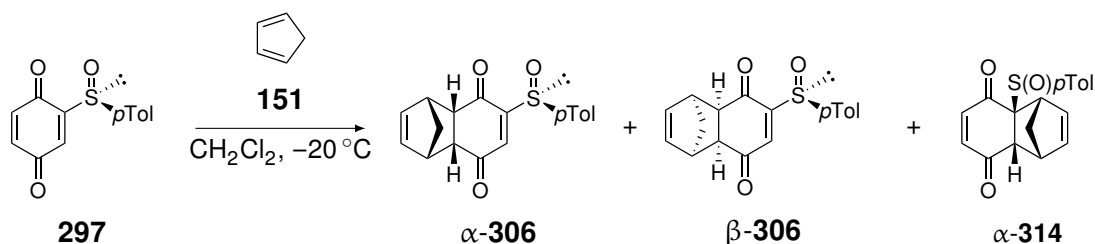
In the same vein, it would be possible to favour the addition on the C2-C3 double bond by the addition of an electron withdrawing group on the C3 position, such as a nitrile group, as performed by García Ruano's group in 2004 (Scheme 2.39).¹²⁹ Given that sulfinylquinone **312** was not stable, it was generated *in situ*, directly followed by the Diels-Alder reaction. As expected, the addition of the diene occurred on the quite reactive C2-C3 double bond, *via* an *endo* orientation of the diene, albeit with a poor facial diastereoselectivity.



Scheme 2.39: Diels-Alder reaction between 3-cyanosulfinylquinone **312** and cyclopentadiene (**151**), leading to adducts α - and β -**313**.¹²⁹

Another way to make an impact on the double bond selectivity is the use of Lewis acids. As already presented in Scheme 2.36, the reaction between the unsubstituted sulfinylquinone **297** and cyclopentadiene (**151**) leads to the addition on the C5-C6 double bond, with a preference for the adduct α -**306** (Table 2.4, entry 1).¹¹⁷ However, the use of different Lewis acids had an impact, not only on the facial diastereoselectivity, but also on the double bond selectivity.¹³⁴

Table 2.4: Diels-Alder reactions between sulfinylquinone **297** and cyclopentadiene (**151**) with or without Lewis acid as catalyst, and the resulting cycloadducts α -**306**, β -**306** or α -**314**.¹³⁴



Entry	Lewis acid (eq.)	Time (h)	Yield (%)	α - 306 : β - 306	α - 314
1	—	16	95%	71:29	—
2	$\text{BF}_3 \cdot \text{OEt}_2$ (5)	0.5	90%	10:90	—
3	Eu(fod)_3 (2)	0.5	80%	89:11	—
4	ZnBr_2 (2)	1	89%	26:38	36

When $\text{BF}_3 \cdot \text{OEt}_2$ was used (Table 2.4, entry 2), the reaction still occurred on the C5-C6 double bond, but the stereoselectivity was inverted towards the adduct β -**306**. On the other hand, the use of Eu(fod)_3 maintained the same facial selectivity as in the absence of Lewis acid, but with an increased preference for the α adduct (Table 2.4, entry 3). Finally, the use of zinc bromide as catalyst allowed to reach the adduct α -**314**, corresponding to the addition of the diene on the C2-C3 double bond, as initially expected for those reactions.

In an attempt to explain those observations, models have been developed (Figure 2.11). It has already been described that, in the absence of Lewis acid (Figure 2.10), the methylene unit of cyclopentadiene (**151**) and the sulfinyl group might repel each other due to a steric clash, leading to the preferential addition on the C5-C6 double bond. However, the link between the sulfoxide configuration and the stereoselectivity observed is unclear.¹¹⁷

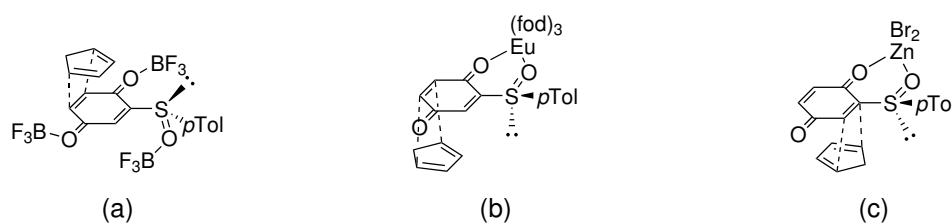


Figure 2.11: Proposed models for the preferential double bond selectivity of cyclopentadiene (**151**) on sulfinylquinone **297** with Lewis acids. (a) $\text{BF}_3 \cdot \text{OEt}_2$; (b) $\text{Eu}(\text{fod})_3$; (c) ZnBr_2 .¹³⁴

In the case of $\text{BF}_3 \cdot \text{OEt}_2$ (Figure 2.11.a), each oxygen atom individually coordinates a boron atom. The sulfoxide group would then be in an *s-cis* conformation due to too large steric and electrostatic repulsions between both BF_3 -coordinated oxygen atoms. Consequently, the *para*-tolyl group points towards the bottom face of the quinone plane, hindering it, and the diene preferentially approaches on the top face, leading to the adduct β -**306**.

When europium was used as catalyst, the coordination mode is different as it is able to form a chelate between the oxygen atom of the sulfoxide and the oxygen atom of the carbonyl. The sulfinyl group then adopts an *s-trans* conformation, orienting the *para*-tolyl group on the top face. Therefore, the diene goes on the bottom face, leading to the adduct α -**306**.

Similarly, zinc bromide is able to form a chelate, just as europium. However, zinc being a smaller atom, and the size and geometry of its ligands being less hindering, the chelate will be more planar, bringing the sulfoxide bond in the same plane as the quinone. The C2-C3 double bond should be more accessible, enabling the diene to approach on the latter, hence the non negligible proportion of adduct α -**314**. For the same reasons as for europium, the bulky *para*-tolyl group points towards the top face, forcing the reaction on the bottom one.

2.5.3 Control of the facial diastereoselectivity

Having a better understanding of the double bond selectivity, one can now focus on the facial diastereoselectivity observed in Diels-Alder reactions performed on sulfinylquinones. Although some of those selectivities have already been presented in the previous section, a deeper insight on that question will be developed below.

In the continuity of the work described in Table 2.4, the group of Carreño also studied the difference between cyclopentadiene (**151**) and 1,3-cyclohexadiene (**246**).¹³⁴ The stereoselectivities observed with **151** have received a hypothetical explanation based on the supposed conformation of the sulfinyl moiety, depending on the Lewis acid used (Table 2.5, entries 1-4).

Without any surprise, cyclohexadiene (**246**) presented a similar behaviour as **151** with α : β ratios almost identical (Table 2.5, entries 5-8). The only major difference is the absence of adduct resulting from the addition of diene **246** on the C2-C3 double bond. The ethylene unit must be bulkier than the methylene one to disfavour that cycloaddition, even when zinc bromide is used (Table 2.5, entry 8). Nonetheless, with both cyclopentadiene (**151**) and cyclohexadiene (**246**), a low facial selectivity is observed on the C5-C6 double bond.

Table 2.5: Diels-Alder reactions between sulfinylquinone **297** and cyclopentadiene (**151**) or 1,3-cyclohexadiene (**246**) with or without Lewis acid as catalyst.¹³⁴

Entry	Diene	Lewis acid (eq.)	Time (h)	Yield (%)	α - 306 : β - 306	α - 314	α - 315 : β - 315
1	151	—	16	95%	71:29	—	—
2	151	BF ₃ ·OEt ₂ (5)	0.5	90%	10:90	—	—
3	151	Eu(fod) ₃ (2)	0.5	80%	89:11	—	—
4	151	ZnBr ₂ (2)	1	89%	26:38	36	—
5	246	—	480	94%	—	—	83:17
6	246	BF ₃ ·OEt ₂ (5)	2	95%	—	—	9:91
7	246	Eu(fod) ₃ (2)	24	81%	—	—	90:10
8	246	ZnBr ₂ (2)	24	95%	—	—	46:54

In order to properly evaluate the stereoselectivity when the reaction takes place on the C2-C3 double bond, a similar assessment has been done on sulfinylquinone **309c** (Table 2.6).¹²⁵ When the reaction was run in the absence of Lewis acid, the main adduct is β -**310c** (entry 1). According to the model described in Figure 2.10.c, the sulfinyl moiety would adopt a preferential *s-cis* conformation, blocking the bottom face and forcing the approach on the top face, hence the preferred β adduct.

Table 2.6: Diels-Alder reactions between sulfinylquinone **309c** and cyclopentadiene (**151**) with and without Lewis acids, and their cycloadducts α - and β -**310c**.¹²⁵

Entry	Lewis acid (eq.)	Time (h)	Yield (%)	α : β
1	—	22	73	11:89
2	BF ₃ ·OEt ₂ (5)	1	50	69:31
3	ZnBr ₂ (3)	1	72%	>97:<3

In the case of BF₃·OEt₂ (entry 2), the β adduct remains the major one, but the facial selectivity is much lower than in the previous example. This could be explained by the coordination of each oxygen

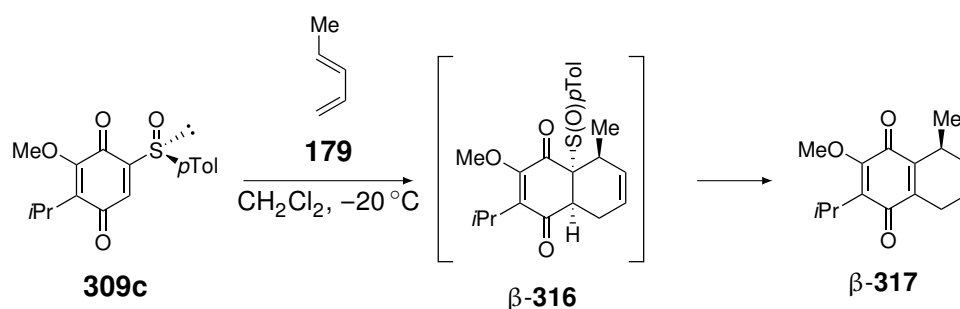
atom to boron, adding some hindrance to the sulfinylquinone and disfavoured a selective approach on only one face of the quinone part.

Finally, it was observed that zinc bromide almost totally inverted the diastereoselectivity. This can easily be explained by the model developed in Figure 2.11.c. The chelate formed by the zinc atom and both oxygen atoms of the sulfoxide and the carbonyl orientates the *para*-tolyl group towards the top face, forcing the diene to approach on the bottom face.

The same reaction has been performed with piperylene (**179**) to evaluate the stereoselectivity with acyclic dienes (Table 2.7).¹²⁵ In this case, the cycloadduct β -**316** was not stable and rapidly pyrolysed into β -**317**.

When the reaction was run in absence of Lewis acid or with $\text{BF}_3 \cdot \text{OEt}_2$, the expected β product is obtained in a high enantiomeric excess (entries 1 and 2), for the expected reasons discussed previously. However, the use of zinc bromide did not give an inversion of facial selectivity as observed with cyclopentadiene (Table 2.7, entry 3 vs. Table 2.6, entry 3).

Table 2.7: Diels-Alder reactions between sulfinylquinone **309c** and piperylene (**179**) with and without Lewis acid, and their product β -**317**.¹²⁵



Entry	Lewis acid (eq.)	Time (h)	Yield (%)	ee (%)
1	—	48	55	94
2	$\text{BF}_3 \cdot \text{OEt}_2$ (5)	0.8	80	84
3	ZnBr_2 (3)	0.5	79	92

Assuming zinc bromide is able to form a chelate with the sulfinylquinones (Figure 2.12.a), it should be in equilibrium with the non-chelated form (Figure 2.12.b). Somehow, the former should be less reactive than the latter in the case of piperylene (**179**). One possible explanation is the presence of the methyl group pointing in the direction of the chelated zinc, causing steric repulsion. Therefore, the more favourable approach would be the one in which zinc is coordinated to each oxygen atom individually, leading to the approach of **179** on the top face of the quinone moiety.

It was actually suggested, *via* computational methods, that the stereoselectivity observed in the case of ZnBr_2 -catalysed cycloadditions of sulfinylquinones was explained by the formation of a Zn_2Br_4 -sulfinylquinone complex.¹³⁶

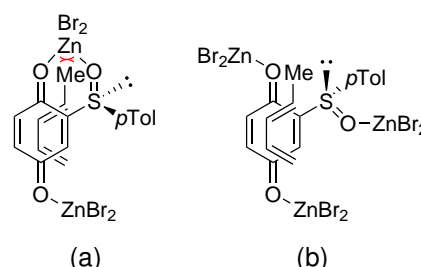
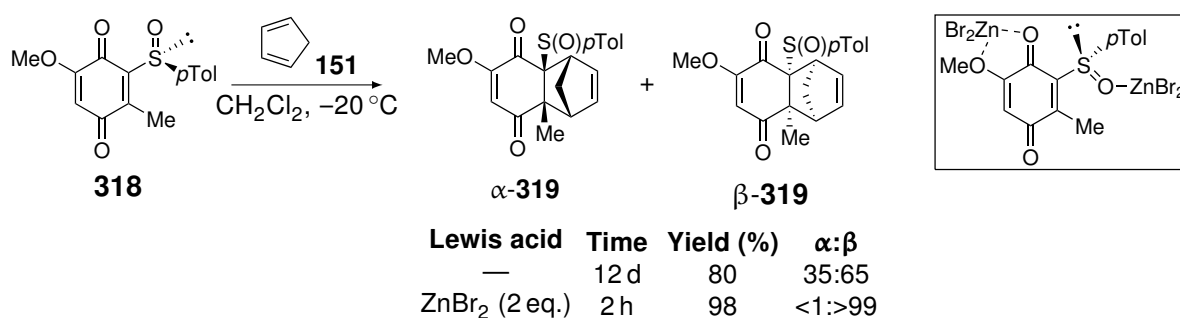


Figure 2.12: Model proposed for the retention of facial diastereoselectivity with piperylene (**179**) in the presence of zinc bromide as Lewis acid.¹²⁵

Another example presenting a retention of facial selectivity in the presence of ZnBr_2 was reported by Hanquet's group in 2006.¹³⁰ They assessed the stereoselectivities obtained between sulfinylquinone **318** and diverse dienes, including cyclopentadiene (**151**). As expected, given the results already reported by other publications, the reaction run under thermal conditions, in the absence of catalyst, gives β -**318** as major adduct (Scheme 2.40). However, the addition of zinc bromide, with the intention of forming a chelate and inverting the conformation of the sulfinyl group, did not give the adduct α -**318** as major product. It even had a much higher selection for the β adduct.

In order to explain that difference, it was proposed that the carbonyl group, usually forming a chelate with the sulfoxide group, will preferentially form a chelate with the methoxy group at C6 position. Consequently, the sulfinyl group would individually coordinate a zinc atom, maintaining it in an *s-cis* conformation. The bottom face would be blocked and the diene would preferentially approach on the top face, hence the excellent selectivity for the β adduct.



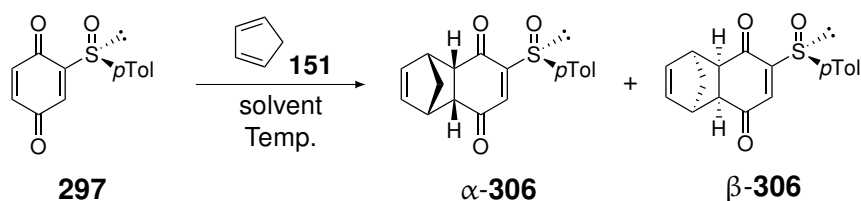
Scheme 2.40: Diels-Alder reactions between sulfinylquinone **318** and cyclopentadiene (**151**), with or without ZnBr_2 , and the proposed structure for the complex between sulfinylquinone **318** and zinc bromide.¹³⁰

Besides the evaluation of the use of Lewis acids, Carreño's group also studied the impact of the solvent on the facial selectivity of cyclopentadiene (**151**) on sulfinylquinone **297** (Table 2.8).¹³⁴ In the course of that study, the group used apolar, polar aprotic, and polar protic solvents, at low and higher temperature. It can be noticed that only the addition on the C5-C6 double bond was obtained and that the major adduct was α -**306** in every case. It was also highlighted that, in a given same solvent, the temperature had little impact on the stereoselectivity.

It can then be observed that reactions run in apolar solvents, such as benzene, gave low selectivities or no selectivity at all (entries 1-3). Increasing the polarity of the solvent increased the selectivity towards the α adduct, with better selectivities obtained in strongly polar solvents (entries 4-12).

The best selectivity was obtained in ethanol at $-20\text{ }^\circ\text{C}$ (entry 14). As the use of hydrogen bond donors seemed to increase the facial selectivity, the reaction has been tested in ethanol with the addition of water. However, although the reaction time significantly decreased, the stereoselectivity decreased as well (entries 15 and 16). It has also been directly tested in water as reaction solvent. It gave the lowest reaction time, but the selectivity was not as good as in ethanol (entry 17).

Those observations showed that Diels-Alder reactions are not insensitive to solvent effects, as already described for other systems.¹³⁷ The most remarkable example is the use of water, an unusual solvent for organic reactions, that actually proved to greatly accelerate the cycloaddition.¹³⁸⁻¹⁴⁰ These results showed that the choice of the solvent for the Diels-Alder reactions is of great importance in terms of rate and stereoselectivity, particularly in the case of sulfinylquinones. The phenomenon behind those results remains not well understood.

Table 2.8: Diels-Alder reactions between sulfinylquinone **297** and cyclopentadiene (**151**) in different solvents and at different temperatures.¹³⁴

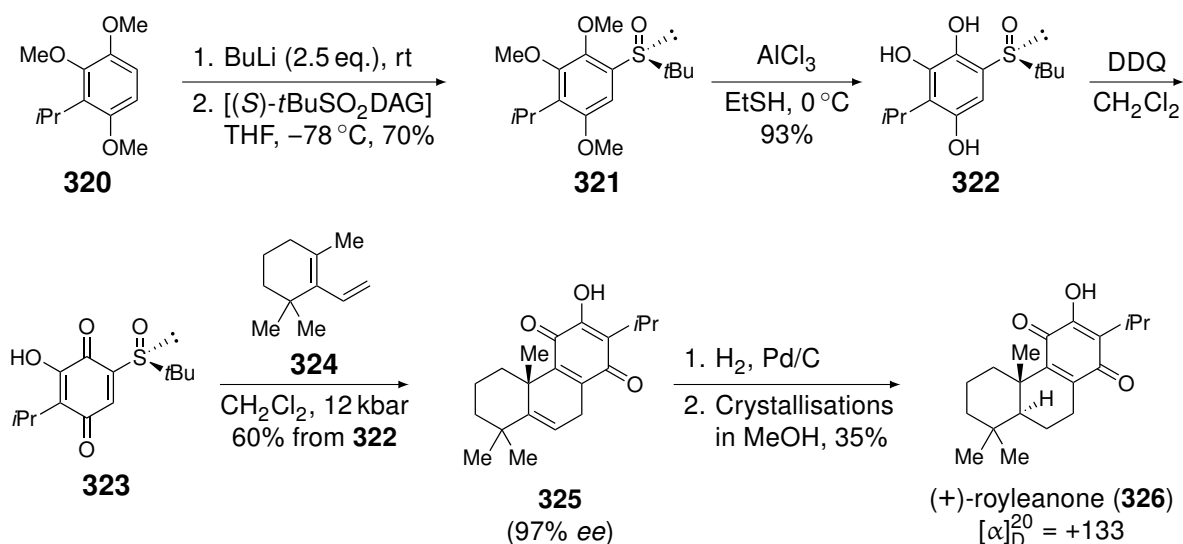
Entry	Solvent	Temp. (°C)	time (h)	Yield (%)	α : β
1	benzene	80	0.5	76	50:50
2	benzene	rt	2	81	57:43
3	benzene	5	2	85	60:40
4	THF	67	0.5	80	60:40
5	THF	rt	5	82	67:33
6	THF	-20	24	86	69:31
7	CH ₂ Cl ₂	rt	1	90	69:31
8	CH ₂ Cl ₂	-20	16	95	71:29
9	DMSO	-20	12	92	74:26
10	DMF	-20	10	91	75:25
11	acetone	-20	10	92	75:25
12	MeCN	-20	10	92	75:25
13	EtOH	0	1	91	80:20
14	EtOH	-20	6	95	86:14
15	EtOH:H ₂ O (19:1)	-20	1	90	81:19
16	EtOH:H ₂ O (9:1)	-20	1	92	78:22
17	H ₂ O	rt	0.5	91	70:30

The results presented above are not the only studies done on sulfinylquinones. It has been shown on several occasions that the choice of the solvent, the catalyst, the quinonoid system, or even the nature of the sulfinyl group, had a non negligible impact on the reactivity of the sulfinylquinone.^{126,131,141–144} Those parameters are to be taken into account to precisely control the double bond, regio- and stereoselectivity.

2.5.4 Applications of the asymmetric Diels-Alder reactions on the sulfinylquinones

Given the extraordinary features of the sulfinylquinones, they can be used as starting materials in many types of stereoselective processes. One of the first applications investigated by Carreño *et al.* was the synthesis of (+)-royleanone (**326**), an abietane diterpenoid isolated from the roots of *Inula royleana* D. C. by Edwards *et al.* in 1962.^{145,146}

They first started their synthesis with the preparation of sulfinylquinone **323** in three steps from **320**. They determined that a *tert*-butylsulfinyl group, prepared using the enantiomerically pure [(*S*)-*t*BuSO₂DAG],^{147,148} induced a better facial selection than its *para*-tolyl equivalent.



Scheme 2.41: Total synthesis of (+)-royleanone starting *via* an asymmetric Diels-Alder reaction between sulfanylquinone **323** and diene **324**.¹⁴⁶

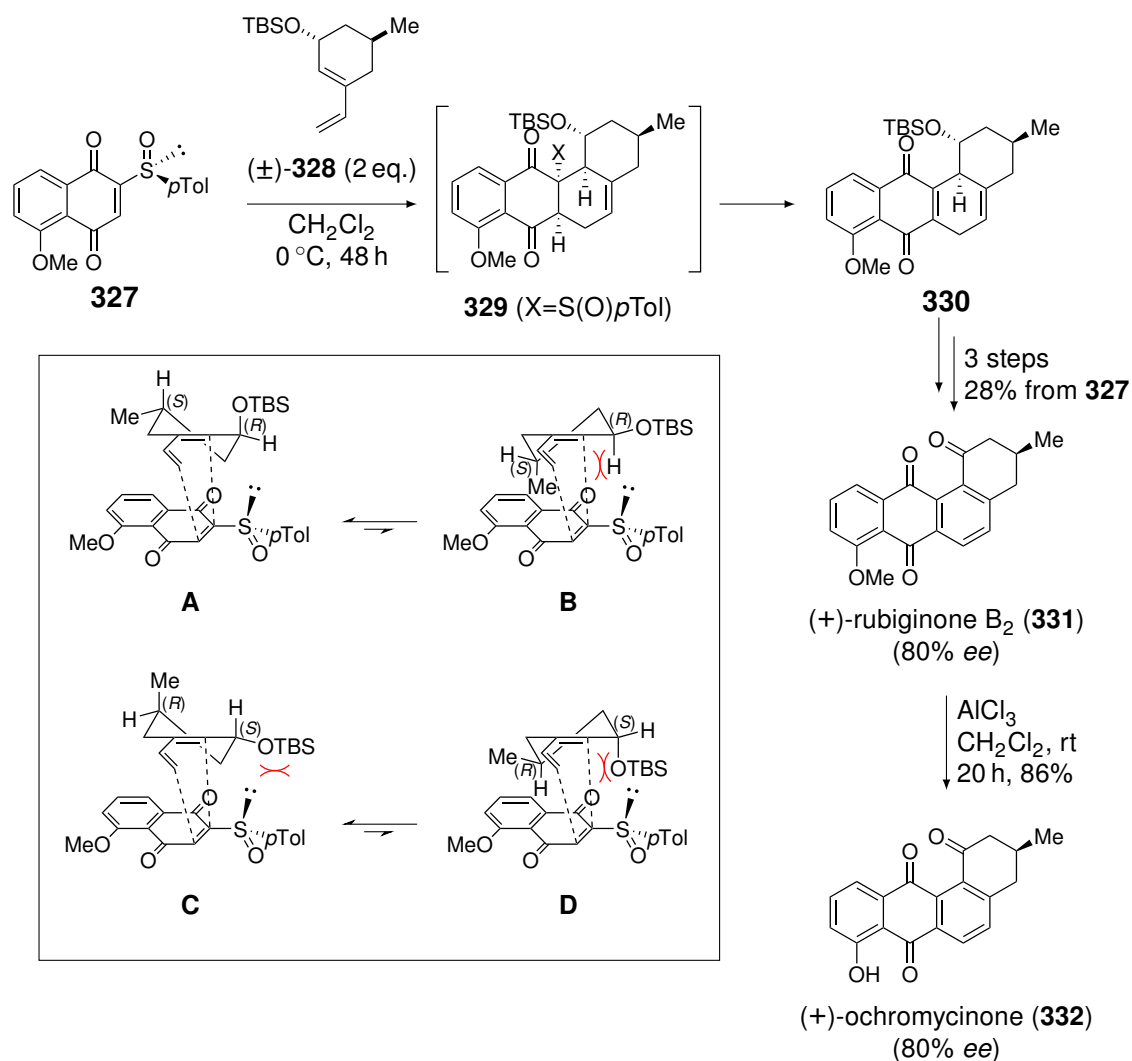
They then performed the Diels-Alder reaction with diene **324** at high pressure, giving the pyrolysed cycloadduct **325** with an excellent enantiomeric excess. Later on, hydrogenation of the latter gave a mixture of *cis* and *trans* isomers. The desired *cis* isomer was isolated by a series of three successive crystallisations in methanol to give pure (+)-royleanone with a 35% yield.

The same group published in the early 2000s several papers on the total synthesis of members of the angucyclinone family. For that purpose, they performed kinetic resolution studies, that they applied in their total synthesis.^{149–151}

The two first members of that family to have been synthesised using this kinetic resolution were (+)-rubiginone B₂ (**331**) and (+)-ochromycinone (**332**).¹⁵² For that purpose, they started with a Diels-Alder reaction between the enantiopure sulfynilnaphthoquinone **327** and a racemic mixture of diene **328** (Scheme 2.42). Even though the cycloadduct could not be isolated, due to the sulfoxide elimination, it was determined that the pyrolysed product **330** was obtained in an enantioenriched form. An additional three steps gave (+)-rubiginone B₂ (**331**) with 80% ee and in 28% overall yield from **327**. Demethylation of the phenolic unit of **331** led to (+)-ochromycinone (**332**) with 80% ee as well, and with 86% yield.

In order to explain the obtained product and, therefore, the selection of one of the enantiomers of diene **328**, a model has been proposed (in the box in Scheme 2.42). It was supposed that the sulfinyl group of **327** is in an *s-cis* conformation, orienting the reaction on the top face of the naphthoquinone moiety. Then, both enantiomers (*3R,5S*)-**328** (model **A** and **B**) and (*3S,5R*)-**328** (model **C** and **D**) are in an equilibrium between two half-chair conformations.

Transition states **B** and **D** have been discriminated based on the fact that the group in the allylic position (in this case, a hydrogen atom and an OTBS groups) must be staggered with respect to the forming bond, as suggested by Houk's work.^{153–156} Then, based on the major product obtained, the matched pair must correspond to transition state **A** with (*3R,5S*)-**328**. That selection might be due to a disfavoured steric repulsion between the TBS protected alcohol and the sulfinyl moiety in

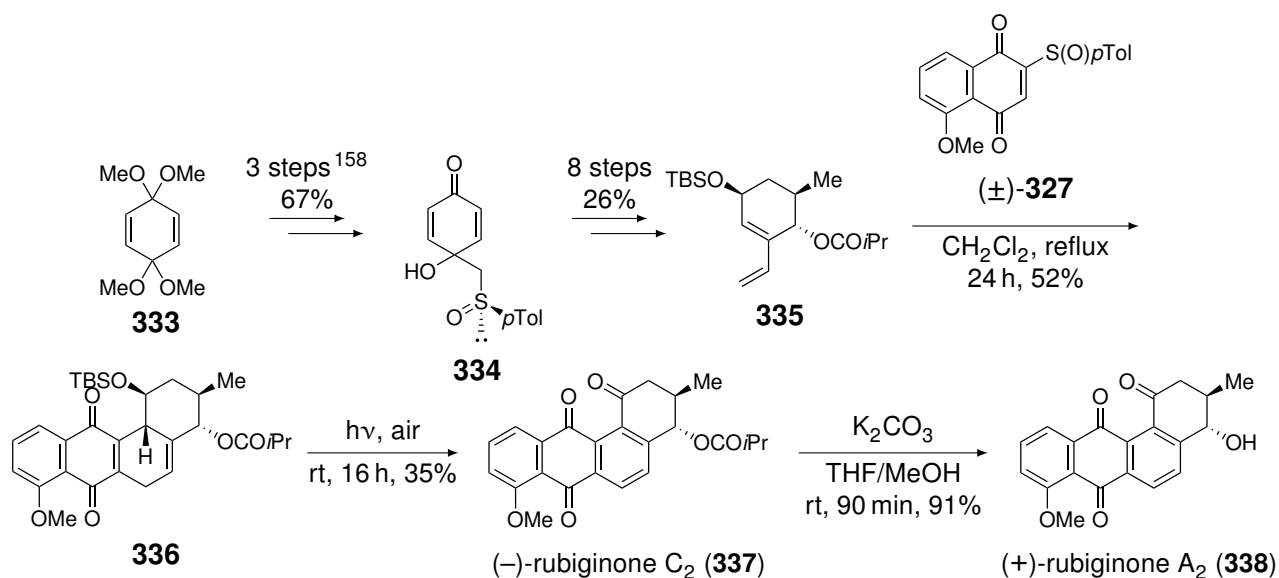


Scheme 2.42: Total synthesis of (+)-rubiginone B₂ (**331**) and (+)-ochromycinone (**332**), using a kinetic resolution process between sulfinylnaphthoquinone **327** and racemic diene **328**, and models of the transition states with both enantiomers of racemic diene **328**.¹⁵²

transition state **C**. The group indeed showed in their study that the increase of the protecting group size improved the stereoselectivity of the reaction.¹⁵⁰ Therefore, reaction of the diene (3*R*,5*S*)-**328** via transition state **A** would be the favourable pathway to selectively reach **330**.

In 2002, the same group used the same kinetic resolution principle for the synthesis of two other angucyclinone derivatives, rubiginones A₂ (**338**) and C₂ (**337**).¹⁵⁷ However, in that total synthesis, they used the diene **335** as the enantiopure partner and the sulfinylnaphthoquinone **327** as the racemic one (Scheme 2.43). The diene was stereoselectively prepared in eight steps from intermediate **334**, itself prepared in three steps from the diketal form of benzoquinone (**333**).¹⁵⁸

Based on the same principle used for their previous total synthesis (Scheme 2.42), one of the enantiomers of the sulfanylquinone **327** will form a matched pair with the enantiopure diene **335**, stereoselectively leading to the pyrolysed cycloadduct **336**. The product was then exposed to light and air to oxidise it into (–)-rubiginone C₂ (**337**). Finally, the hydrolysis of the latter gave (+)-rubiginone A₂ (**338**) in 91% yield. It was determined that both natural products were obtained over eleven steps with enantiomeric excesses above 95%, in a 4.8 and 4.4% overall yield from **334**.

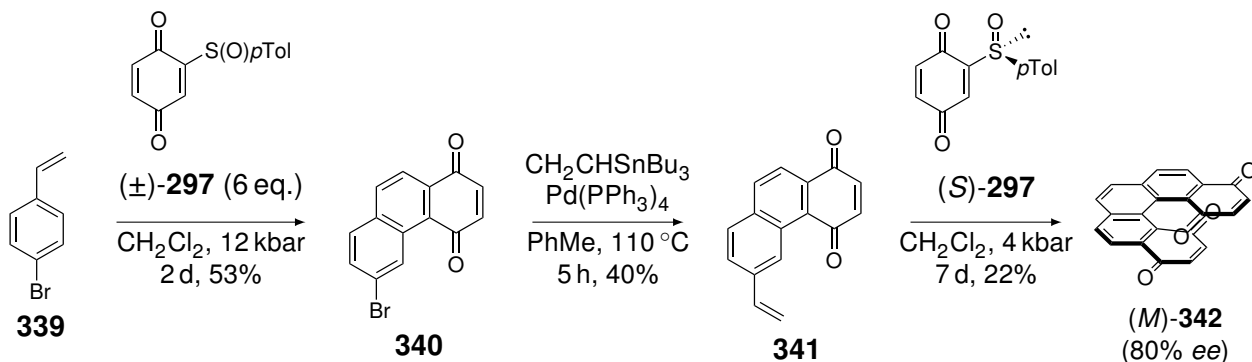


Scheme 2.43: Total synthesis of rubiginones A₂ (**338**) and C₂ (**337**), using a kinetic resolution process between the enantiopure diene **335** and the racemic sulfinylnaphthoquinone **327**.¹⁵⁷

Using the same process, Carreño *et al.* reported the synthesis of unnatural derivatives of the angucyclinone family with very good enantiomeric excesses.^{159,160} A few years later, Hanquet *et al.* employed the same strategy to develop a new route for the total synthesis of salvinorin A and its analogues.¹⁶¹

Another application developed by the group of Carreño, using enantiopure sulfanylquinone, is the synthesis of enantioenriched helical bisquinones.¹⁶² They are an important group of compounds that present extraordinary optical and electronic properties, closely related to their inherent chirality.^{163,164}

The first example of optically active helices prepared from sulfanylquinones starts with a Diels-Alder reaction between vinyl aryl bromide **339** and the racemic mixture of **297** (Scheme 2.44). The resulting cycloadduct directly pyrolysed to give quinone **340**. The bromine atom was then converted into a vinyl group. The intermediate **341** was later engaged in an asymmetric Diels-Alder reaction with the enantiopure sulfanylquinone (*S*)-**297** that gave, after pyrolysis of the cycloadduct, the helical bisquinone (*M*)-**342** with a 80% *ee*.



Scheme 2.44: Synthesis of an enantioenriched helical bisquinones (*M*)-**342**, based on an asymmetric Diels-Alder approach between a vinyl aryl quinone **341** and sulfanylquinone **297**.¹⁶²

To extend the results obtained, they performed the same type of reaction on divinyl naphthalene **344** (Scheme 2.45). They made the latter react with sulfinylquinone (*S*)-**297**. The double cycloadduct pyrolysed to give the helical bisquinone (*M*)-**345** with an excellent 88% *ee*, albeit with a rather low yield.

On the other hand, they also performed a mono-Diels-Alder reaction on 1-bromo-4-vinylnaphthalene (**343**) to obtain quinone **346**. The latter was reduced into a hydroquinone that was methylated (**347**), followed by the conversion of the bromine atom into a vinyl group (**348**). That intermediate then underwent a Diels-Alder reaction with (*S*)-**297**. This time, the major isomer obtained was the (*P*) helicene, with a 30% *ee*. They postulated that the presence of both methoxy groups somewhat destabilises the *endo* approach on the sulfinylquinone, due to steric and electrostatic repulsions, leading to a preferential *exo* approach on the opposite face (Figure 2.13). The pyrolysed cycloadduct (*P*)-**349** was then submitted to a CAN oxidation to yield the helicene bisquinone (*P*)-**345**, also with a 30% *ee*.

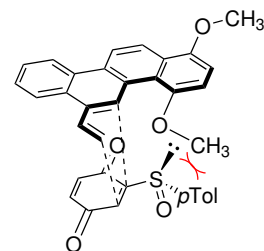
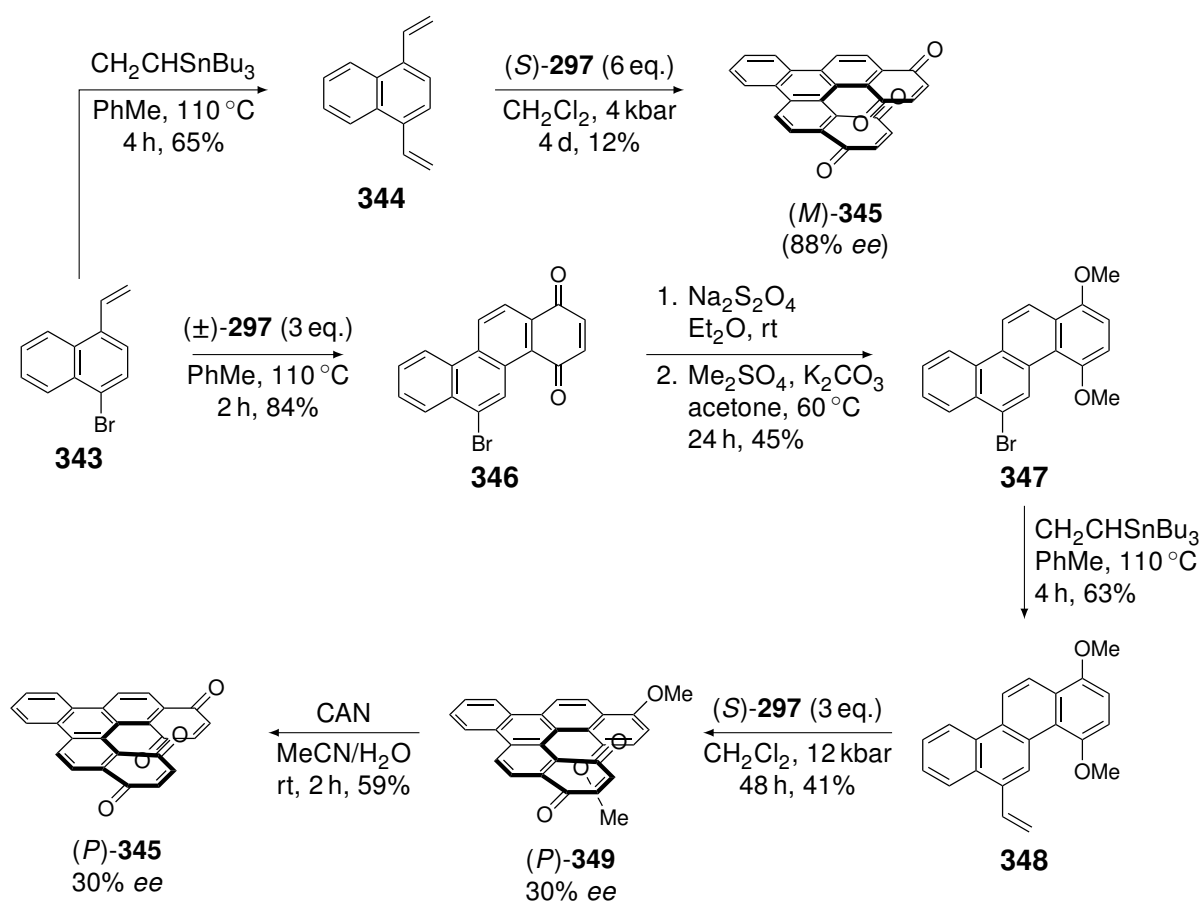


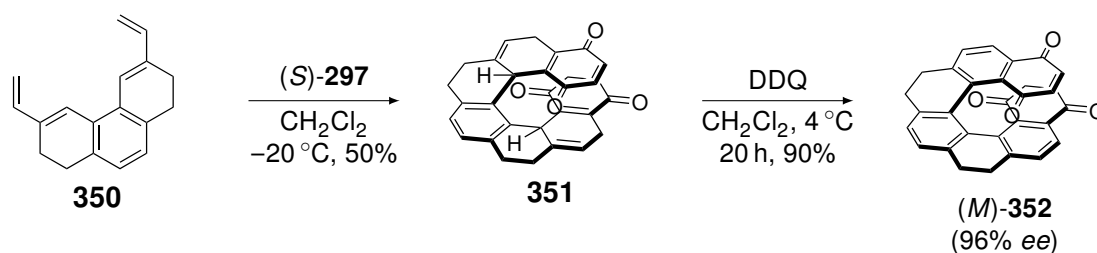
Figure 2.13: Proposed model on the steric and electrostatic repulsions between sulfinylquinone (*S*)-**297** and diene **348** to explain the preferred (*P*) adduct.¹⁶²



Scheme 2.45: Synthesis of both (*M*) and (*P*) isomers of the helical bisquinone **345**, using two divergent routes from aryl vinyl **343**.¹⁶²

With that type of strategy in hand, they later worked on larger helicenes. Therefore, in 2005, the group managed to synthesise [7]helicenebisquinones.¹⁶⁵ To that end, they performed a double Diels-Alder reaction between two equivalents of sulfinylquinone (*S*)-**297** and the *bis*-diene **350**. (Scheme

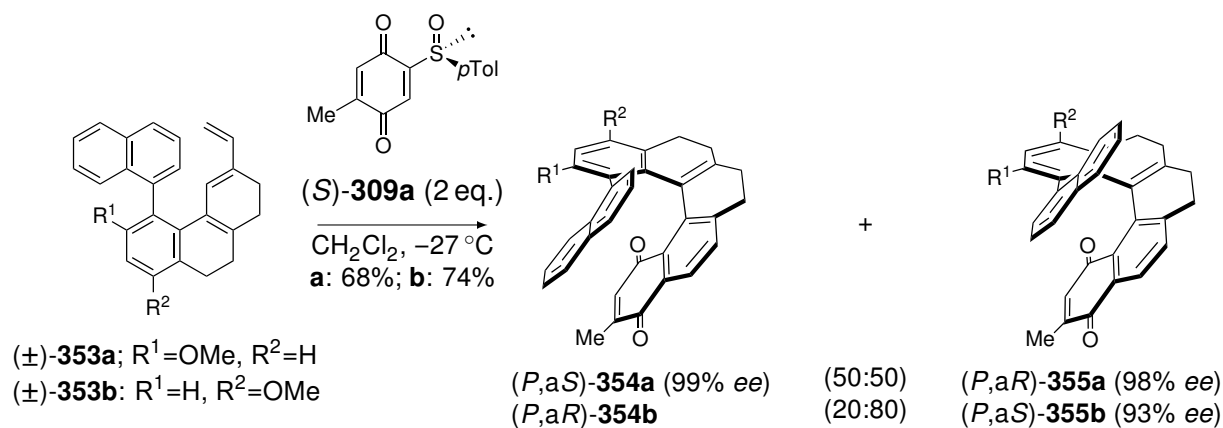
2.46). The resulting double cycloadduct was not isolated as it pyrolysed directly into bisquinone **351**. The latter was then oxidised with DDQ in order to rearomatise both resulting cyclohexadienes into product (*M*)-**352** with a 90% yield and a 96% *ee*. Alongside that helicenebisquinone, they also synthesised one example bearing an ethoxy group and one bearing a *tert*-butyldimethylsilyloxy group.



Scheme 2.46: Synthesis of the [7]helicenebisquinone (*M*)-**352** by a double Diels-Alder reaction between sulfanylquinone (*S*)-**297** and a *bis*-diene **350**.¹⁶⁵

In addition to those examples, the group reported the synthesis of a few more enantioenriched helicenequinones, with varying size, with saturated and unsaturated ring structures, and with bulky groups inducing helical chirality.^{166–171}

Later on, Carreño *et al.* took an interest in coupling optically active helicenes with other types of chirality. In 2009, they synthesised helicenequinones, with a labile chiral axis, by performing Diels-Alder reactions between (1-naphthyl)-substituted vinyl tetrahydrophenanthrenes (\pm)-**353**, in a racemic mixture of atropoisomers, and sulfanylquinone (*S*)-**297** (Scheme 2.47).¹⁷² With both substrates **353a** and **353b** (bearing a methoxy group on either position R^1 or R^2 , respectively), they stereoselectively obtained the *P* isomer of helicenequinones **354** and **355** with excellent enantiomeric excesses.

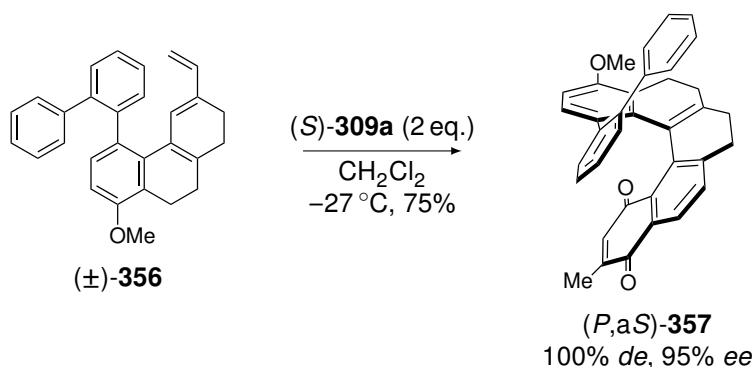


Scheme 2.47: Synthesis of (1-naphthyl)-substituted tetrahydro[5]helicene quinones **354** and **355**, using an asymmetric Diels-Alder reaction between diene (\pm)-**353** and sulfanylquinone (*S*)-**297**.¹⁷²

However, depending on the position of the methoxy group, both helicenes presented different ratios of atropoisomers. When the methoxy group is placed in position R^1 , a 50:50 ratio of isomers *aS* and *aR* are obtained. Indeed, as **353** is used in a racemic form and the methoxy group is in *ortho* position with respect to the chiral axis, the naphthyl group is not able to freely rotate around that axis. On the other hand, when the methoxy group is in R^2 , the *ortho* position is not hindered anymore and the naphthyl group can freely rotate. As postulated by the group and based on the X-ray structure of

the major isomer, (*P,aS*)-**355b**, the naphthyl group preferentially adopts the conformation illustrated in Scheme 2.47, presumably due to better π -stacking interactions with the naphthoquinone part of the helicene.

Similarly, they synthesised another compound with a biphenyl group instead of the naphthyl one (Scheme 2.48). As the previous example, they performed the cycloaddition of diene (\pm)-**356** on the same sulfinylquinone (*S*)-**309a**. In that case, they still selectively obtained the *P* helicene as well but with a total control of the axial chirality (100% of the *aS* isomer).



Scheme 2.48: Synthesis of (2-biphenyl)-substituted [5]helicene quinone (*P,aS*)-**357**, using an dynamic kinetic resolution system in a Diels-Alder reaction between diene (\pm)-**356** and (*S*)-**309a**.¹⁷²

A second type of helicene derivatives featuring a second element of chirality, studied by Carreño's group, are ferrocene helicene compounds.¹⁷³ Indeed, when ferrocenes bear two different substituents at positions 1 and 2, the loss of plane symmetry induces chirality, called planar chirality.¹⁷⁴

They first synthesised diene **359** in its racemic form in two steps from (\pm)-**358** (scheme in Table 2.9). Those dienes were then engaged in Diels-Alder reactions with sulfinylquinone (*S*)-**309a**. In order to verify the diastereoselectivity of the process, they first used two equivalents of sulfinylquinone, going from -78 °C to room temperature, leading to the formation of the pyrolysed cycloadduct (*pS,S,P*)-**360** as only diastereoisomer among the four possible ones, albeit with a low 55% *ee* (entry 1).

Then, 0.5 equivalent of sulfinylquinone was used (entry 2). In that case, product (*pS,S,P*)-**360** was isolated with a 34% yield and a 93% *ee* and the unreacted diene (*pR*)-**359** was recovered with 50% yield and a 63% *ee*. Those results indicates that sulfinylquinone (*S*)-**309a** forms a matched pair with diene (*pS*)-**359** (Figure 2.14).

The best result in terms of optical rotation for the recovered unreacted diene (*pR*)-**359** was obtained when 0.9 equivalent of quinone was used. Indeed, the greater amount of (*S*)-**309a** ensures that the totality of the diene (*pS*)-**359** is consumed. Even though only 28% of the unreacted diene was recovered, it possessed an excellent enantiomeric excess of 99% (entry 3).

Finally, the best results for the product (*pS,S,P*)-**360** were obtained with 0.5 equivalents of sulfinylquinone but, this time, the reaction was run at -10 °C (entry 4). The pyrolysed cycloadduct was isolated with a 45% yield and a remarkable 97% *ee*.

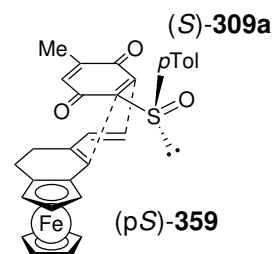
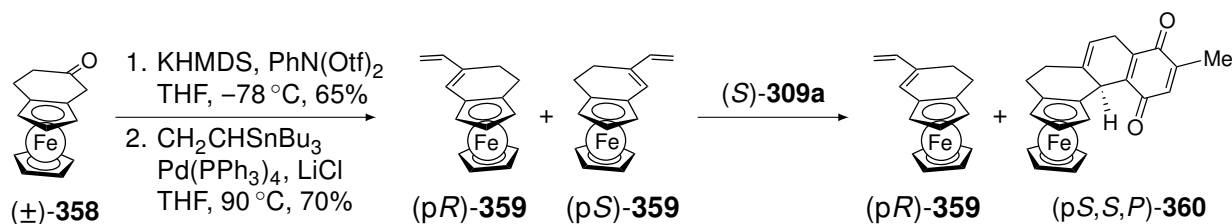
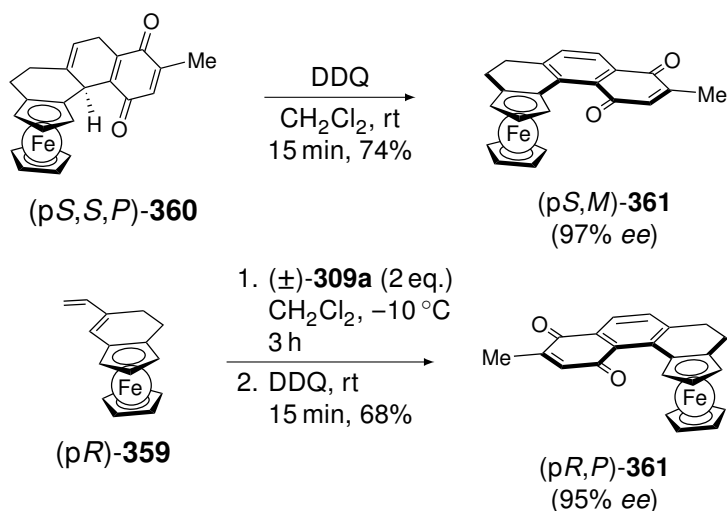


Figure 2.14: Matched pair for the double asymmetric induction between (*pS*)-**359** and (*S*)-**309a** en route to tetracyclic derivative (*pS,S,P*)-**360**.¹⁷³

Table 2.9: Kinetic process in the Diels-Alder reaction between the racemic mixture of diene **359** and sulfinylquinone (*S*)-**309a**.¹⁷³

Entry	Temp. (°C)	(<i>S</i>)- 309a (eq.)	(<i>pR</i>)- 359 (% yield/% ee)	(<i>pS,S,P</i>)- 360 (% yield/% ee)
1	-78 to rt	2	—	56/55
2	-78 to rt	0.5	50/63	34/93
3	-78 to rt	0.9	28/99	46/73
4	-10	0.5	32/47	45/97

Finally, the oxidation of the enantiomerically enriched product (*pS,S,P*)-**360** with DDQ led to the formation of the helical ferrocene (*pS,M*)-**361** with an excellent 97% ee (Scheme 2.49). The enantiomer of the latter could be reached as well by starting from the recovered diene (*pR*)-**359**. They made it react with two equivalents of racemic sulfinylquinone **309a**, to ensure the opposite matched pair, followed by the oxidation of the intermediate product. It was then possible to obtain the helical ferrocene (*pR,P*)-**361** with a 95% ee.

Scheme 2.49: Synthesis of enantiopure ferrocene[4]helicenequinones (*pS,M*)-**361** and (*pR,P*).¹⁷³

A few years later, the group did not stop at the compounds described above, but worked on the synthesis of more complex systems, with extraordinary optical and electronic properties, such as ferrocene helicene with a chiral sulfinyl group on the ferrocene unit or ferrocenes with two helicene units.^{175,176}

2.6 Conclusion

Throughout this chapter, one could realise that the use of the Diels-Alder reaction can reveal to be a powerful synthetic tool. That cycloaddition, described almost one century ago by two German chemists, indeed possesses extraordinary features that allow to determine and control the outcome of the reaction.

Despite the fact that Otto Diels and Kurt Alder were not exactly the first ones to have discovered the reaction, their tremendous amount of work on the understanding of that pericyclic reaction could bring some light on the way this transformation works. But many others took a close look in order to highlight the mechanistic aspects of that spectacular reaction and some aspects are still being studied today.

We discussed some of those features that include the rate of the reaction, its regioselectivity and its diastereoselectivity. It was highlighted that for all these three properties, the factor that has the main impact on the outcome of the reaction are the substituents present on both the diene and the dienophile. The impact of those substituents could be rationalised by the use of frontier molecular orbital theory developed by Fukui. On one hand, the use of that theory allows to determine the best HOMO-LUMO combination based on the smallest energy gap between the partners of the cycloaddition and how changing the substituents modify that gap. On the other hand, this theory also helps to explain the regioselectivity observed by using the coefficient of the orbitals and by pairing the orbitals with the closest coefficients.

The last feature, the diastereoselectivity of the reaction, has been first described as an *endo* approach of the diene and the dienophile, also called “*endo* rule” by Kurt Alder, based on the product obtained from the reaction between cyclopentadiene (**151**) and maleic anhydride (**200**). Once again, the FMO has been used to rationalise those results and secondary orbital interactions have been invoked to explain the outcome of the reactions. However, many counterexamples have been reported in the literature and indicate that steric and electrostatic repulsions have a non negligible influence on the stereoselectivity of the cycloaddition. More recently, the publication of computational studies suggested that the *endo* selectivity initially observed for cyclopentadiene (**151**) and maleic anhydride (**200**) would rather have a steric component and that the secondary orbital interactions actually have no or little impact on that stereoselectivity.

Several strategies have been developed in order to make this process asymmetric. One of them is to add a chiral auxiliary on one of the reagents, mostly on the dienophile. The use of such auxiliaries, prepared from readily available enantiopure natural substances, proved to efficiently obtain one of both possible cycloadducts, leading to very good stereoselectivities. However, this method requires two additional steps: one for the addition of the auxiliary and another for its removal.

The second way to perform asymmetric cycloadditions is to use chiral organocatalysts. One of the first examples, developed by MacMillan, uses a chiral ammonium derivative, prepared from an amino acid, that forms a chiral α,β -unsaturated iminium salt with enals. The dienophilicity of the latter is increased and it enantioselectively reacts with cyclopentadiene (**151**), albeit with a very low *endo/exo* selectivity. Similar processes have been later developed with enolisable aldehydes and enals to form reactive enamines and dienamines, respectively. In a more simple manner, the use of

chiral Brønsted acids also allows the Diels-Alder reaction to occur in an enantioselective manner with excellent enantiomeric excesses.

The third type of asymmetric Diels-Alder reaction uses chiral Lewis acids to favour one enantiomer over the other. Since the use of menthol as a chiral ligand for aluminium as Lewis acid, many types of chiral Lewis acid based catalysts have been developed and exhibited excellent stereoselectivities.

We then showed that some of the methods to carry out asymmetric Diels-Alder reactions have been specifically developed for quinone derivatives as dienophiles. A particular interest has been taken in those compounds as they are an important part of the work carried out in this thesis. Indeed, it was found out in the literature that those quinones are interesting starting materials for the synthesis of more complex structures, such as natural substances for example.

Among the presented methods, the use of chiral catalysts is the most described one, in particular the use of chiral Lewis acids. The different groups could reach very good enantioselectivities with a wide range of quinones and dienes. Some of them could also use their method to synthesise rather complex natural molecules with outstanding enantiomeric excesses.

The last part of this chapter focused on the use of sulfinylquinones as dienophiles. These compounds bear a sulfinyl group as chiral auxiliary and the first example of the preparation of such an enantiopure sulfinylquinone was described in 1989 by the group of M. Carmen Carreño. They have been extensively studied throughout the years and have proven to exhibit very good stereoselectivities and some light has been brought on their extraordinary reactivity.

The different works reported in the literature have shown that many parameters have an impact on the behaviour of those peculiar quinones. Indeed, the substituents on the quinone moiety, the solvent or the use of Lewis acids can drastically change the outcome of the reaction in terms of double bond selectivity or facial diastereoselectivity. Even the nature of the diene, such as going from cyclic to acyclic dienes, can have an impact on those outcomes.

Nevertheless, they also proved to be an excellent choice for the stereoselective synthesis of complex molecules, such as natural substances or enantioenriched helicene derivatives.

References

- [1] Diels, O.; Alder, K. Synthesen in der hydroaromatischen Reihe. I. Mitteilung: Anlagerungen von "Di-en"-kohlenwasserstoffen. *Liebigs Ann. Chem.* **1928**, *460*, 98–122.
- [2] Nobel Media AB 2021, The Nobel Prize in Chemistry 1950. NobelPrize.org. <https://www.nobelprize.org/prizes/chemistry/1950/summary/>, Accessed: 26 May 2021.
- [3] Woodward, R. B.; Lofffield, R. B. The Structure of Cantharidine and the Synthesis of Desoxycantharidine. *J. Am. Chem. Soc.* **1941**, *63*, 3167–3171.
- [4] Berson, J. A. Discoveries Missed, Discoveries Made: Creativity, Influence, and Fame in Chemistry. *Tetrahedron* **1992**, *48*, 3–17.
- [5] Albrecht, W. Additionsproducte von Cyklopentadien und Chinonen. *Liebigs Ann. Chem.* **1906**, *348*, 31–49.
- [6] Zincke, T.; Pfaffendorf, W. Über Tetrachlor-*o*-kresol und seine Umwandlung in Perchlorindon. *Liebigs Ann. Chem.* **1912**, *394*, 3–22.
- [7] von Euler, H.; Josephson, K. O. Über Kondensationen an Doppelbindungen. I.: über die Kondensation von Isopren mit Benzochinon. *Chem. Ber.* **1920**, *53*, 822–826.
- [8] Nobel Media AB 2021, The Nobel Prize in Chemistry 1929. NobelPrize.org. <https://www.nobelprize.org/prizes/chemistry/1929/summary/>, Accessed: 26 May 2021.
- [9] Franke, W. Zu Hans von Eulers 80. Geburtstag. *Naturwissenschaften* **1953**, *40*, 177–180.
- [10] Nawrat, C. C.; Moddy, C. J. Quinones as Dienophiles in the Diels-Alder Reaction: History and Applications in Total Synthesis. *Angew. Chem. Int. Ed.* **2014**, *53*, 2059–2077.
- [11] Woodward, R. B.; Sondheimer, F.; Taub, D.; Heusler, K.; McLamore, W. M. The Total Synthesis of Steroids. *J. Am. Chem. Soc.* **1952**, *74*, 4223–4251.
- [12] Sallay, S. I. Total Synthesis of *dl*-libogamine. *J. Am. Chem. Soc.* **1967**, *89*, 6762–6763.
- [13] White, J. D.; Choi, Y. Catalyzed Asymmetric Diels–Alder Reaction of Benzoquinone. Total Synthesis of (–)-libogamine. *Org. Lett.* **2000**, *2*, 2373–2376.
- [14] Corey, E. J.; Danheiser, R. L.; Chandrasekaran, S.; Keck, G. E.; Gopalan, B.; Larsen, S. D.; Patrice, S.; Gras, J.-L. Stereospecific Total Synthesis of Gibberellic Acid. A Key Tricyclic Intermediate. *J. Am. Chem. Soc.* **1978**, *100*, 8031–8034.
- [15] Corey, E. J.; Danheiser, R. L.; Chandrasekaran, S.; Keck, G. E.; Gopalan, B.; Larsen, S. D.; Patrice, S.; Gras, J.-L. Stereospecific Total Synthesis of Gibberellic Acid. *J. Am. Chem. Soc.* **1978**, *100*, 8034–8036.
- [16] Woodward, R. B.; Bader, F. E.; H, B.; Frey, A. J.; Kierstead, R. W. The Total Synthesis of Reserpin. *J. Am. Chem. Soc.* **1956**, *78*, 2023–2025.
- [17] Woodward, R. B.; Bader, F. E.; H, B.; Frey, A. J.; Kierstead, R. W. A simplified Route to a Key Intermediate in the Total Synthesis of Reserpin. *J. Am. Chem. Soc.* **1956**, *78*, 2657.
- [18] Mehta, G.; Reddy, A. V. Olefin Metathesis in Polycyclic Frames. A Total Synthesis of Hirsutene. *J. Chem. Soc. Chem. Commun.* **1981**, 756–757.
- [19] Podlesny, E. E.; Kozlowski, M. C. Enantioselective Total Synthesis of (S)-Bisoranjidiol, an Axially Chiral Bisanthraquinone. *Org. Lett.* **2012**, *14*, 1408–1411.
- [20] Barborak, J. C.; Watts, L.; Pettit, R. A Convenient Synthesis of the Cubane System. *J. Am. Chem. Soc.* **1966**, *88*, 1328–1329.
- [21] Woodward, R. B.; Hoffmann, R. The Conservation of Orbital Symmetry. *Angew. Chem. Int. Ed.* **1969**, *8*, 781–853.
- [22] Joshel, L. M.; Butz, L. W. The Synthesis of Condensed Ring Compounds. VII. The Successful Use of Ethylene in the Diels-Alder Reaction. *J. Am. Chem. Soc.* **1941**, *63*, 3350–3351.
- [23] Shortridge, R. W.; Craig, R. A.; Greenlee, K. W.; Derfer, J. M.; Boord, C. E. The Synthesis of Some Cyclopropane and Spirane Hydrocarbons. *J. Am. Chem. Soc.* **1948**, *70*, 946–949.
- [24] Bachman, G. B.; Tanner, H. A. Diethyl Methylmalonate. *J. Org. Chem.* **1939**, *4*, 493–501.
- [25] Petrov, A. A. The structure of the condensation product of piperylene with acrolein. *Zh. Obshch. Khim.* **1948**, *18*, 1125–1128.
- [26] Alder, K.; Vogt, W. Über den Aufbau von α -Terpineol durch Diensynthese. Zur Kenntnis der Diensynthese mit unsymmetrischen Addenden. *Liebigs Ann. Chem.* **1949**, *564*, 109–120.
- [27] Fleming, I. Thermal Pericyclic Reactions. In *Molecular Orbitals and Organic Chemical Reactions (Reference Edition)*, 1st ed.; John Wiley & Sons, Ltd, 2010; Chapter 6, pp 253–368.
- [28] Fleischhauer, J.; Asaad, A. N.; Schleker, W.; Scharf, H.-D. Zur Problematik der Einteilung von Diels-Alder-Reaktionen in "normale" und "inverse". *Liebigs Ann. Chem.* **1981**, 306–311.
- [29] Herndon, W. C. Theory of cycloaddition reactions. *Chem. Rev.* **1972**, *72*, 157–179.
- [30] Sustmann, R. Orbital energy control of cycloaddition reactivity. *Pure Appl. Chem.* **1975**, *40*, 569–593.
- [31] Fukui, K.; Yonezawa, T.; Shingu, H. A Molecular Orbital Theory of Reactivity in Aromatic Hydrocarbons. *J. Chem. Phys.* **1952**, *20*, 722–725.
- [32] Nobel Media AB 2021, The Nobel Prize in Chemistry 1981. NobelPrize.org. <https://www.nobelprize.org/>

- prizes/chemistry/1981/summary/, Accessed: 31 August 2021.
- [33] Boger, D. L.; Corbett, W. L.; Curran, T. T.; Kasper, A. M. Inverse Electron Demand Diels-Alder Reactions of *N*-Sulfonyl α,β -Unsaturated Imines: A General Approach to Implementation of the 4π Participation of 1-Aza-1,3-butadienes in Diels-Alder Reactions. *J. Am. Chem. Soc.* **1991**, *113*, 1713–1729.
- [34] Fiesselmann, H. Diensynthesen mit Oxyprenen. I. Mitteil.: Über 4-Methoxy, 4-Äthoxy- und 4-Methoxy-1-methyl- Δ^3 -tetrahydrobenzaldehyd. *Ber. Dtsch. Chem. Ges.* **1942**, *75*, 881–891.
- [35] Alder, K.; Schumacher, M.; Wolff, O. Über Diensynthesen mit unsymmetrischen Addenden Butadien-1-carbonsäure-(chlorid) und Acrylsäure-(chlorid). *Liebigs Ann. Chem.* **1949**, *564*, 79–96.
- [36] Dickinson, R. A.; R, K.; MacAlpine, G. A.; Stojanac, Z.; Valenta, Z. A Stereospecific Synthesis Of Ring A-aromatic Steroids. *Can. J. Chem.* **1972**, *50*, 2377–2380.
- [37] Stojanac, Z.; Dickinson, R. A.; Stojanac, N.; Woznov, R. J.; Valenta, Z. Catalyzed Orientation Reversals in Diels–Alder Reactions. *Can. J. Chem.* **1975**, *53*, 616–618.
- [38] Alder, K.; Stein, G. Über den sterischen Verlauf von Additions- und Substitutions-reaktionen. I. Zur Stereochemie der Dien-synthese. *Liebigs Ann. Chem.* **1934**, *514*, 1–33.
- [39] Ginsburg, D. Tetrahedron report number 149 : The role of secondary orbital interactions in control of organic reactions. *Tetrahedron* **1983**, *39*, 2095–2135.
- [40] Kobuke, Y.; Fueno, T.; Furukawa, J. The endo Selectivities of Some Methyl-Substituted Dienophiles in Diels-Alder Reactions with Cyclopentadiene. *J. Am. Chem. Soc.* **1970**, *92*, 6548–6553.
- [41] Evans, D. A.; Bryan, C. A.; Sims, C. L. The Complementarity of (4 + 2) Cycloaddition1 Reactions and [2,3] Sigmatropic Rearrangements in Synthesis. A New Synthesis of Functionalized Hasubanan Derivatives. *J. Am. Chem. Soc.* **1972**, *94*, 2891–2892.
- [42] Fleming, I.; Michael, J. P.; Overman, L. E.; Taylor, G. F. How important is secondary overlap in determining the regioselectivity of Diels-Alder reactions? *Tetrahedron Lett.* **1978**, 1313–1314.
- [43] Cruse, W. B. T.; Fleming, I.; Gallagher, P. T.; Kennard, O. The stereochemistry of the Diels-Alder reactions of fumaric acid derivatives. *J. Chem. Res., (S)* **1979**, 372–373.
- [44] Nakagawa, K.; Ishii, Y.; Ogawa, M. Beziehungen zwischen der Stereoselektivität zweier Diels—Alder-Reaktionen und den Molekularrefraktionen zahlreicher Lösungsmittel. *Tetrahedron* **1976**, *32*, 1427–1429.
- [45] Braun, R.; Schuster, F.; Sauer, J. (4+2)-Cycloadditionen in Micellen: Ein Vergleich des Produktspektrums und der Reaktionsgeschwindigkeit mit Reaktionen in Lösung. *Tetrahedron Lett.* **1986**, *27*, 1285–1288.
- [46] Cativiela, C.; García, J. I.; Gil, J.; Martínez, R. M.; Mayoral, J. A.; Salvatella, L.; Urieta, J. S.; Mainar, A. M.; Abraham, M. H. Solvent effects on Diels-Alder reactions. The use of aqueous mixtures of fluorinated alcohols and the study of reactions of acrylonitrile. *J. Chem. Soc. Perkin Trans. 2* **1997**, 653–660.
- [47] García, J. I.; Mayoral, J. A.; Salvatella, L. Do Secondary Orbital Interactions Really Exist? *Acc. Chem. Res.* **2000**, *33*, 658–664.
- [48] Jin, L.; Melaimi, M.; Kostenko, A.; Karni, M.; Apeloig, Y.; Moore, C. E.; Rheingold, A. L.; Guy, B. Isolation of cationic and neutral (allenylidene)(carbene) and bis(allenylidene)gold complexes. *Chem. Sci.* **2016**, *7*, 150–154.
- [49] Bachrach, S. M. Diels-Alder Reaction of Furan with Cyclopropanone. An ab Initio Study. *J. Org. Chem.* **1995**, *60*, 4395–4398.
- [50] Fernández, I.; Bickelhaupt, F. M. Origin of the “Endo Rule” in Diels-Alder Reaction. *J. Comput. Chem.* **2014**, *35*, 371–376.
- [51] Stephenson, L. M.; Smith, D. E.; Current, S. P. Endo Preference in the Diels-Alder Cycloaddition of Butadiene and Maleic Anhydride. *J. Org. Chem.* **1982**, *47*, 4170–4171.
- [52] Oppolzer, W. Asymmetrische Diels-Alder- und En-Reaktionen in der Organischen Synthese. *Angew. Chem.* **1984**, *96*, 840–854.
- [53] Whiting, A. Asymmetric Diels-Alder reactions. In *Advanced Asymmetric Synthesis*; Springer, Dordrecht, 1996; Chapter 7, pp 126–145.
- [54] Sauer, J.; Kredel, J. Asymmetrische Induktion bei Diels-Alder-Reaktionen. *Tetrahedron Lett.* **1966**, 6359–6364.
- [55] Oppolzer, W.; Kurth, M.; Reichlin, D.; Moffatt, F. A reinvestigation of asymmetric induction of Diels-Alder to chiral acrylates. *tetrahedron Lett.* **1981**, *22*, 2545–2548.
- [56] Oppolzer, W.; Chapuis, C.; Kelly, M. J. Practical Asymmetric Diels-Alder Additions to Camphor-10-sulfonic-Acid-Derived Acrylates. *Helv. Chim. Acta* **1983**, *66*, 2358–2361.
- [57] Oppolzer, W.; Chapuis, C.; Bernardinelli, G. Asymmetric Diels-Alder reactions: Facile preparation and structure of sulfonamido-isobornyl acrylates. *Tetrahedron Lett.* **1984**, *25*, 5885–5888.
- [58] Oppolzer, W.; Chapuis, C.; Bernardinelli, G. Camphor-Derived *N*-Acryloyl and *N*-Crotonoyl Sultams: Practical Activated Dienophiles in Asymmetric Diels-alder Reactions. Preliminary Communication. *Helv. Chim. Acta* **1984**, *67*, 1397–1401.
- [59] Waldmann, H. (*S*)-Proline Benzyl Ester as Chiral Auxiliary in Lewis Acid Catalyzed Asymmetric Diels-

- Alder Reactions. *J. Org. Chem.* **1988**, *53*, 6133–6136.
- [60] Nougier, R.; Gras, J.-L.; Giraud, B.; Virgili, A. Methyl 3,4-*O*-methylene- β -D-arabinoside as a new Chiral Template for the Asymmetric Diels-Alder Reaction. *Tetrahedron Lett.* **1991**, *32*, 5529–5530.
- [61] Bourghli, L. M. S.; Stoodley, R. J. Enantioselective synthesis of (+)-8-hydroxy-8-methylidarubicinone. *Bioorg. Med. Chem.* **2004**, *12*, 2863–2866.
- [62] Miller, J. P.; Stoodley, R. J. Studies directed towards anthracyclinone syntheses: The use of D-glucose as a chiral auxiliary in asymmetric Diels-Alder reactions. *J. Saudi Chem. Soc.* **2013**, *17*, 29–42.
- [63] Li, J.-L.; Liu, T.-Y.; Chen, Y.-C. Aminocatalytic Asymmetric Diels-Alder Reactions via HOMO Activation. *Acc. Chem. Res.* **2012**, *45*, 1491–1500.
- [64] Deepa,.; Singh, S. Recent Development of Recoverable MacMillan Catalyst in Asymmetric Organic Transformation. *Adv. Synth. Catal.* **2021**, *363*, 629–656.
- [65] Ahrendt, K. A.; Borths, C. J.; MacMillan, D. W. C. New Strategies for Organic Catalysis: The First Highly Enantioselective Organocatalytic Diels-Alder Reaction. *J. Am. Chem. Soc.* **2000**, *122*, 4243–4244.
- [66] Boger, D. L.; Panek, J. S.; Meier, M. M. Diels-Alder Reaction of Heterocyclic Azadiene. 2. Catalytic Diels-Alder Reaction of in situ Generated Enamines with 1,2,4-Triazines: General Pyridine Annulation. *J. Org. Chem.* **1982**, *47*, 895–897.
- [67] Jørgensen, K. A.; Juhl, K. The First Organocatalytic Enantioselective Inverse-Electron-Demand Hetero-Diels-Alder Reaction. *Angew. Chem. Int. Ed.* **2003**, *42*, 1498–1501.
- [68] Duarte, F. J. S.; Santos, A. G. Enantioselective Organocatalytic Intramolecular Diels-Alder Reactions: A Computational Study. *J. Org. Chem.* **2012**, *77*, 3252–3261.
- [69] Dieckmann, A.; Breugst, M.; Houk, K. N. Zwitterions and Unobserved Intermediates in Organocatalytic Diels-Alder Reactions of Linear and Cross-Conjugated Trienamines. *J. Am. Chem. Soc.* **2013**, *135*, 3237–3242.
- [70] Serebryakov, E. P.; Nigmatov, A. G.; Shcherbakov, M. A.; Struchkova, M. I. The effects of the nature of catalyst and of the solvent on the stereoselectivity in amine-catalyzed asymmetric synthesis of substituted cyclohexa-1,3-dienes from prenal and monoesters of ylidene malonic acids. *Russ. Chem. Bull.* **1998**, *47*, 82–90.
- [71] Parmar, D.; Sugiono, E.; Raja, S.; Rueping, M. Complete Field Guide to Asymmetric BINOL-Phosphate Derived Brønsted Acid and Metal Catalysis: History and Classification by Mode of Activation; Brønsted Acidity, Hydrogen Bonding, Ion Pairing, and Metal Phosphate. *Chem. Rev.* **2014**, *114*, 9047–9153.
- [72] Momiyama, N.; Tabuse, H.; Terada, M. Chiral Phosphoric Acid-Governed Anti-Diastereoselective and Enantioselective Hetero-Diels-Alder Reaction of Glyoxylate. *J. Am. Chem. Soc.* **2009**, *131*, 12882–12883.
- [73] Akiyama, T.; Morita, H.; Fuchibe, K. Chiral Brønsted Acid-Catalyzed Inverse Electron-Demand Aza Diels-Alder Reaction. *J. Am. Chem. Soc.* **2006**, *128*, 13070–13071.
- [74] Itoh, J.; Fuchibe, K.; Akiyama, T. Chiral Brønsted Acid Catalyzed Enantioselective Aza-Diels-Alder Reaction of Brassard's Diene with Imines. *Angew. Chem. Int. Ed.* **2006**, *45*, 4796–4798.
- [75] Akiyama, T.; Tamura, Y.; Itoh, J.; Morita, H.; Fuchibe, K. Enantioselective Aza-Diels-Alder Reaction Catalyzed by a Chiral Brønsted Acid: Effect of the Additive on the Enantioselectivity. *Synlett* **2006**, 0141–0143.
- [76] Yates, P.; Eaton, P. Acceleration of the Diels-Alder Reaction by Aluminium Chloride. *J. Am. Chem. Soc.* **1960**, *82*, 4436–4437.
- [77] Reetz, M. T.; Hüllmann, M.; Massa, W.; Rademacher, P.; Heymanns, P. Structure and Electronic Nature of the Benzaldehyde/Boron Trifluoride Adduct. *J. Am. Chem. Soc.* **1986**, *108*, 2405–2408.
- [78] Poll, T.; Metter, J. O.; Helmchen, G. Concerning the Mechanism of the Asymmetric Diels-Alder Reaction: First Crystal Structure Analysis of a Lewis Acid Complex of a Chiral Dienophile. *Angew. Chem. Int. Ed. Engl.* **1985**, *24*, 112–114.
- [79] Hashimoto, S.-I.; Komeshima, N.; Koga, K. Asymmetric Diels-Alder Reaction Catalysed by Chiral Alkoxyaluminium Dichloride. *J. Chem. Soc. Chem. Commun.* **1979**, 437–438.
- [80] Kagan, H. B.; Riant, O. Catalytic Asymmetric Diels-Alder Reactions. *Chem. Rev.* **1992**, *92*, 1007–1019.
- [81] Oh, T.; Reilly, M. Reagent-controlled asymmetric Diels-Alder reactions. A review. *Org. Prep. Proced. Int.* **1994**, *26*, 129–158.
- [82] Hayashi, Y. Catalytic Asymmetric Diels-Alder Reactions. In *Cycloaddition Reactions in Organic Synthesis*; Wiley-VCH Verlag GmbH, 2001; Chapter 1, pp 5–55.
- [83] Mamedov, E. G.; Klabunovskii, E. I. Asymmetric Diels-Alder Reaction of Cyclopentadiene in the Synthesis of Chiral Norbornene Derivatives. *Russ. J. Org. Chem.* **2008**, *44*, 1097–1120.
- [84] Vinogradov, M. G.; Turova, O. V.; Zlotin, S. G. Catalytic Asymmetric Aza-Diels-Alder Reaction: Pivotal Milestones and Recent Applications to Synthesis of Nitrogen-Containing Heterocycles. *Adv. Synth. Catal.* **2021**, *363*, 1466–1526.
- [85] Reetz, M. T. Artificial Metalloenzymes as Catalysts in Stereoselective Diels-Alder Reactions. *Chem. Rec.* **2012**, *12*, 391–406.

- [86] Ryu, D. H.; Corey, E. J. Triflimide Activation of a Chiral Oxazaborolidine Leads to a More General Catalytic System for Enantioselective Diels-Alder Addition. *J. Am. Chem. Soc.* **2003**, *125*, 6388–6390.
- [87] Ryu, D. H.; Zhou, G.; Corey, E. J. Enantioselective and Structure-Selective Diels-Alder Reactions of Unsymmetrical Quinones Catalyzed by a Chiral Oxazaborolidine Cation. Predictive Selection Rules. *J. Am. Chem. Soc.* **2004**, *126*, 4800–4802.
- [88] Evans, D. A.; Wu, J. Enantioselective Rare-Earth Catalyzed Quinone Diels-Alder Reactions. *J. Am. Chem. Soc.* **2003**, *125*, 10162–10163.
- [89] Albrecht, Ł.; Gómez, C. V.; Jacobsen, C. B.; Jørgensen, K. A. 1,4-Naphthoquinones in H-Bond-Directed Trienamine-Mediated Strategies. *Org. Lett.* **2013**, *15*, 3010–3013.
- [90] Bai, Y.; Yuan, J.; Hu, X.; Antilla, J. C. Catalytic Enantioselective Diels-Alder Reactions of Benzoquinones and Vinylindoles with Chiral Magnesium Phosphate Complexes. *Org. Lett.* **2019**, *21*, 4549–4553.
- [91] Mikami, K.; Terada, M.; Motoyama, Y.; Nakai, T. Chiral Titanium Complex-Catalyzed Diels-Alder Reaction: A Practical Route to Anthracycline Intermediates. *Tetrahedron: Asymmetry* **1991**, *2*, 643–646.
- [92] Mikami, K.; Motoyama, Y.; Terada, M. Asymmetric Catalysis of Diels-Alder Cycloadditions by an MS-Free Binaphthol-Titanium Complex: Dramatic Effect of MS, Linear vs Positive Nonlinear Relationship, and Synthetic Applications. *J. Am. Chem. Soc.* **1994**, *116*, 2812–2820.
- [93] Engler, T. A.; Letavic, M. A.; Takusagawa, F. Asymmetric Quinone-Based Diels-Alder Reactions. *Tetrahedron Lett.* **1992**, *33*, 6731–6734.
- [94] Engler, T. A.; Letavic, M. A.; Lynch, K. O.; Takusagawa, F. Formation and Isolation of Ebabtiomerically Pure Products in Quantity from Diels-Alder Reactions of 1,4-Benzoquinones. *J. Org. Chem.* **1994**, *59*, 1179–1183.
- [95] Payette, J. N.; Yamamoto, H. Regioselective and Asymmetric Diels-Alder Reaction of 1- and 2-Substituted Cyclopentadienes Catalyzed by a Brønsted Acid Activated Chiral Oxazaborolidine. *J. Am. Chem. Soc.* **2007**, *129*, 9536–9537.
- [96] Morimoto, K.; Le, T. P.; Manna, S. K.; Kiran, I. N. C.; Tanaka, S.; Kitamura, M. Water, an Essential Element for a Zn^{II}-Catalyzed Asymmetric Quinone Diels-Alder Reaction: Multi-Selective Construction of Highly Functionalized *cis*-Decalin. *Chem. Asian J.* **2019**, *14*, 3283–3290.
- [97] Varlet, T.; Gelis, C.; Retailleau, P.; Bernadat, G.; Neuville, L.; Masson, G. Enantioselective Redox-Divergent Chiral Phosphoric Acid Catalyzed Quinone Diels-Alder Reactions. *Angew. Chem. Int. Ed.* **2020**, *59*, 8491–8496.
- [98] Breuning, M.; Corey, E. J. Catalytic Enantioselective Diels-Alder Reactions of 1,4-Quinone Monoketals. *Org. Lett.* **2001**, *3*, 1559–1562.
- [99] Miyashita, K.; Imanishi, T. Syntheses of Natural Products Having an Epoxyquinone Structure. *Chem. Rev.* **2005**, *105*, 4515–4536.
- [100] Hashimoto, T.; Nakatsu, H.; Maruoka, K. Catalytic Asymmetric Diels-Alder Reaction of Quinone Imine Ketals: A Site-Divergent Approach. *Angew. Chem. Int. Ed.* **2015**, *54*, 4617–4621.
- [101] Boezio, A.; Jarvo, E. R.; Lawrence, B. M.; Jacobsen, E. N. Efficient Total Syntheses of (–)-Colombiasin A and (–)-Elisapterosin B: Application of the Cr-Catalyzed Asymmetric Quinone Diels-Alder Reaction. *Angew. Chem. Int. ed.* **2005**, *44*, 6046–6050.
- [102] Jarvo, E. R.; Lawrence, B. M.; Jacobsen, E. N. Highly Enantio- and Regioselective Quinone Diels-Alder Reactions Catalyzed by a Tridentate [(Schiff Base)Cr^{III}] Complex. *Angew. Chem. Int. ed.* **2005**, *44*, 6043–6046.
- [103] Gademann, K.; Chavez, D. E.; Jacobsen, E. N. Highly Enantioselective Inverse-Electron-Demand Hetero-Diels-Alder Reactions of α,β -Unsaturated Aldehydes. *Angew. Chem. Int. ed.* **2002**, *41*, 3059–3061.
- [104] Chavez, D. E.; Jacobsen, E. N. Catalyst-Controlled Inverse-Electron-Demand Hetero-Diels-Alder Reactions in the Enantio- and Diastereoselective Synthesis of Iridoid Natural Products. *Org. Lett.* **2003**, *5*, 2563–2565.
- [105] Solladié, G. Asymmetric Synthesis Using Nucleophilic Reagents Containing a Chiral Sulfoxide Group. *Synthesis* **1981**, 185–196.
- [106] Andersen, K. K. Stereochemistry, Conformation, and Chiroptical Properties of Sulfoxides. In *Sulphones and Sulphoxides*; John Wiley & Sons, Ltd, 1988; Chapter 3, pp 55–94.
- [107] Drabowicz, J.; Kielbasinski, P.; Mikołajczyk, M. Synthesis of Sulphoxides. In *Sulphones and Sulphoxides*; John Wiley & Sons, Ltd, 1988; Chapter 8, pp 233–378.
- [108] Posner, G. H. Asymmetric Synthesis Using α -Sulfinyl Carbanions and β -Unsaturated Sulfoxides. In *Sulphones and Sulphoxides*; John Wiley & Sons, Ltd, 1988; Chapter 16, pp 823–849.
- [109] Walker, A. J. Asymmetric Carbon-Carbon Bond Formation Using Sulfoxide Stabilised Carbanions. *Tetrahedron: Asymmetry* **1992**, *3*, 961–998.
- [110] Carreño, M. C. Applications of Sulfoxides to Asymmetric Synthesis of Biologically Active Compounds. *Chem. Rev.* **1995**, *95*, 1717–1760.
- [111] Hanquet, G.; Colobert, F.; Lanners, S.; Solladié, G. Recent developments in chiral non-racemic sulfinyl-

- group chemistry in asymmetric synthesis. *ARKIVOC* **2003**, 328–401.
- [112] Arai, Y.; Koizumi, T. Chiral Sulfinylethenes as Efficient Dienophiles for Asymmetric Diels-Alder Reactions. *Sulfur Rep.* **1993**, *15*, 41–65.
- [113] García Ruano, J. L.; Carretero, J. C.; Carreño, M. C.; M, M. C. L.; Urbano, A. The Sulfinyl group as a chiral inductor in asymmetric Diels-Alder reactions. *Pure & Appl. Chem.* **1996**, *68*, 925–930.
- [114] Arai, Y.; Matsui, M.; Koizumi, T.; Shiro, M. Powerful Dienophiles for Asymmetric Diels-Alder Reactions: α -(2-*exo*-Hydroxy-10-bornylsulfinyl)maleimides. *J. Org. Chem.* **1991**, *56*, 1983–1985.
- [115] Kingsbury, C. A.; Cram, D. J. Studies in Stereochemistry. XXXII. Mechanism of Elimination of Sulfoxides. *J. Am. Chem. Soc.* **1960**, *82*, 1810–1819.
- [116] Alonso, I.; Carretero, J. C.; García Ruano, J. L. Benzyl Methyl (*S*)-2-(*p*-Tolylsulfinyl)maleate, an Efficient Dienophile in Asymmetric Diels-Alder Reactions. *J. Org. Chem.* **1994**, *59*, 1499–1508.
- [117] Carreño, M. C.; García Ruano, J. L.; Urbano, A. Synthesis and asymmetric Diels-Alder reactions of (*S*)-2-*p*-tolylsulfinyl-1,4-benzoquinone. *Tetrahedron Lett.* **1989**, *30*, 4003–4006.
- [118] Manning, M. J.; Reynolds, P. W.; Swenton, J. S. Latent Quinone Carbanions via Anodic Oxidation of 2-Bromo-1,4-dimethoxybenzene. An “Umpolung” Reagent for Quinones. *J. Am. Chem. Soc.* **1976**, *98*, 5008–5009.
- [119] Andersen, K. K. Synthesis of (+)-ethyl *p*-tolyl sulfoxide from (–)-menthyl (–)-*p*-toluenesulfinate. *Tetrahedron Lett.* **1961**, *3*, 93–95.
- [120] Andersen, K. K.; Gaffield, W.; Papanikolaou, N. E.; Foley, J. W.; Perkins, R. I. Optically Active Sulfoxides. The Synthesis and Rotatory Dispersion of Some Diaryl Sulfoxides. *J. Am. Chem. Soc.* **1964**, *86*, 5637–5646.
- [121] Solladié, G.; Hutt, J.; Girardin, A. Improved Preparation of Optically Active Methyl *p*-Tolyl Sulfoxide. *Synthesis* **1987**, 173.
- [122] Carreño, M. C.; García Ruano, J. L.; Urbano, A. Synthesis of Optically Active *p*-Tolylsulfinylquinones. *Synthesis* **1992**, 651–653.
- [123] Carreño, M. C.; García Ruano, J. L.; Toledo, M. A.; Urbano, A. Synthesis and Diels-Alder reactions of (*S*)-3-Chloro and (*S*)-3-Ethyl-2-*p*-tolylsulfinyl-1,4-benzoquinones. *Tetrahedron Lett.* **1994**, *35*, 9759–9762.
- [124] Carreño, M. C.; García Ruano, J. L.; Toledo, M. A.; Urbano, A. *ortho*-Directed metallation in the regiocontrolled synthesis of enantiopure 2- and/or 3-substituted (*S*)-2-(*p*-tolylsulfinyl)-1,4-benzoquinones. *Tetrahedron: Asymmetry* **1997**, *8*, 913–921.
- [125] Carreño, M. C.; García Ruano, J. L.; Lafuente, C.; Toledo, M. A. Asymmetric Diels-Alder reactions of 5-substituted and 5,6-disubstituted (*S*)-2-(*p*-tolylsulfinyl)-1,4-benzoquinones with cyclopentadiene and *trans*-piperylene. *Tetrahedron: Asymmetry* **1999**, *10*, 1119–1128.
- [126] Carreño, J. L.; M Carmen and Gracia Ruano; Urbano, A.; Remor, C. Z.; Arroyo, Y. Diels-Alder Reactions with 2-(Arylsulfinyl)-1,4-benzoquinones: Effect of Aryl Substitution on Reactivity, Chemoselectivity, and π -Facial Diastereoselectivity. *J. Org. Chem.* **2000**, *65*, 453–458.
- [127] Noland, W. E.; Kedrowski, B. L. Quinone Approaches towards the Synthesis of Aflatoxin B₂. *Org. Lett.* **2000**, *2*, 2109–2111.
- [128] Chaplin, J. H.; Edwards, A. J.; Flynn, B. L. An enantioselective double Diels-Alder Approach to the tetracyclic framework of colombiasin A. *Org. Biomol. Chem.* **2003**, *1*, 1842–1844.
- [129] García Ruano, J. L.; Alemparte, C. Synthesis and Dienophilic Behavior of (*S*)-2-Cyano-3-(*p*-tolylsulfinyl)-1,4-benzoquinone. *J. Org. Chem.* **2004**, *69*, 1405–1408.
- [130] Lanfranchi, D. A.; Hanquet, G. Asymmetric Diels-Alder Reactions of a New Enantiomerically Pure Sulfinylquinone: A Straightforward Access to Functionalized Wieland-Miescher Ketone Analogues with (*R*) Absolute Configuration. *J. Org. Chem.* **2006**, *71*, 4854–4861.
- [131] de Sousa, A. L. F.; Cardoso Filho, J. E. P.; Wladislaw, B.; Marzorati, L.; Di Vitta, C. Studies on chemo- and diastereo-selectivity of the Diels-Alder reactions of sulfinyltoluquinones with cyclopentadiene. *Can. J. Chem.* **2009**, *87*, 1135–1143.
- [132] Evain-Bana, E.; Schiavo, L.; Bour, C.; Lanfranchi, D. A.; Berardozzi, S.; Ghirga, F.; Bagrel, D.; Botta, B.; Hanquet, G.; Mori, M. Synthesis, biological evaluation and molecular modeling studies on novel quinonoid inhibitors of CDC25 phosphatases. *J. Enz. Inhib. Med. Chem.* **2000**, *53*, 955–959.
- [133] Kahraman, D. C.; Hanquet, G.; Jeanmart, L.; Lanners, S.; Šramel, P.; Boháč, A.; Cetin-Atalay, R. Quinoides and VEGFR2 TKIs influence the fate of hepatocellular carcinoma and its cancer stem cells. *Med. Chem. Commun.* **2017**, *8*, 81–87.
- [134] Carreño, M. C.; García Ruano, J. L.; Toledo, M. A.; Urbano, A. Influence of the Sulfinyl Group on the Chemoselectivity and π -Facial Selectivity of Diels-Alder Reactions of (*S*)-2-(*p*-Tolylsulfinyl)-1,4-benzoquinone. *J. Org. Chem.* **1996**, *61*, 503–509.
- [135] Chow, K. H.; Gahan, L. R.; Krenske, E. H. Diels-Alder Reactions of Chiral Sulfinylquinones: From Sterically Directed to CH- π Directed Stereoselectivity. *Aust. J. Chem.* **2020**, *73*, 934–941.
- [136] Chow, K. H.; Krenske, E. H. Origins of stereoselectivity in uncatalyzed and ZnBr₂-catalyzed Diels-Alder

- reactions of a chiral sulfinylquinone. *Org. Biomol. Chem.* **2019**, *17*, 8756–8767.
- [137] Blokzijl, W.; Engberts, J. B. F. N. Initial-State and Transition-State Effects on Diels-Alder Reactions in Water and Mixed Aqueous Solvents. *J. Am. Chem. Soc.* **1992**, *114*, 5440–5442.
- [138] Rideout, D. C.; Breslow, R. Hydrophobic Acceleration of Diels-Alder reactions. *J. Am. Chem. Soc.* **1980**, *102*, 7816–7817.
- [139] Blokzijl, W.; Blandamer, M. J.; Engberts, J. B. F. N. Diels-Alder Reactions in Aqueous Solutions. Enforced Hydrophobic Interactions between Diene and Dienophile. *J. Am. Chem. Soc.* **1991**, *113*, 4241–4246.
- [140] Blake, J. F.; Jorgensen, W. L. Solvent Effect on a Diels-Alder Reaction from Computer Simulations. *J. Am. Chem. Soc.* **1991**, *113*, 7430–7432.
- [141] Carreño, M. C.; García Ruano, J. L.; Urbano, A. Asymmetric Diels-Alder Reactions of (S)-2-(p-Tolylsulfinyl)-1,4-naphthoquinones. *J. Org. Chem.* **1992**, *57*, 6870–6876.
- [142] Carreño, M. C.; García Ruano, J. L.; Urbano, A. Control of the Ring Selectivity in Diels-Alder Reactions of Naphthazarins mediated by Sulfur Functions. *Tetrahedron Lett.* **1994b**, *35*, 3789–3792.
- [143] Carreño, M. C.; García Ruano, J. L.; Urbano, A.; López-Solera, M. I. (SS)-2-(p-Tolylsulfinyl)norborneno-p-benzoquinones: A New Type of Facially Perturbed Enantiopure Quinones. *J. Org. Chem.* **1997**, *62*, 976–981.
- [144] Carreño, M. C.; García Ruano, J. L.; Remor, C. Z.; Urbano, A. Regio- and stereoselectivity in Diels-Alder reactions of 1,2-disubstituted dienes with enantiopure (SS)-(p-tolylsulfinyl)-1,4-benzoquinones. *Tetrahedron: Asymmetry* **2000**, *11*, 4279–4296.
- [145] Edwards, O. E.; Feniak, G.; Los, M. Diterpenoids quinones of *Inula royelana* D. C. *Can. J. Chem.* **1962**, *40*, 1540–1546.
- [146] Carreño, M. C.; García Ruano, J. L.; Toledo, M. A. Enantioselective Synthesis of (+)-Royleanone from Sulfinyl Quinones. *Chem. Eur. J.* **2000**, *6*, 288–291.
- [147] Fernández, I.; Khiar, N.; Alcludia, F. Asymmetric Synthesis of Alkane- and Arenesulfinates of Diacetone-D-glucose (DAG): An Improved and General Route to Both Enantiomerically Pure Sulfoxides. *J. Org. Chem.* **1992**, *57*, 6789–6796.
- [148] Khiar, N.; Fernández, I.; Alcludia, F. Asymmetric synthesis of optically pure *tert*-butyl sulfoxides using the “DAG methodology”. *Tetrahedron Lett.* **1994**, *35*, 5719–5722.
- [149] Carreño, M. C.; Urbano, A.; Fischer, J. Enantioselective Diels-Alder Approach to Angucyclinones from (S)-2-(p-Tolylsulfinyl)-1,4-naphthoquinone and Substituted Racemic Vinylcyclohexenes. *Angew. Chem. Int. Ed. Engl.* **1997**, *36*, 1621–1623.
- [150] Carreño, M. C.; Urbano, A.; Di Vitta, C. Enantioselective Diels-Alder Cycloadditions with (SS)-2-(p-Tolylsulfinyl)-1,4-naphthoquinone: Efficient Kinetic Resolution of Chiral Racemic Vinylcyclohexenes. *J. Org. Chem.* **1998**, *63*, 8320–8330.
- [151] Carreño, M. C.; García-Cerrada, S.; Urbano, A.; Di Vitta, C. Studies of Diastereoselectivity in Diels-Alder Reactions of Enantiopure (SS)-2-(p-Tolylsulfinyl)-1,4-naphthoquinone and Chiral Racemic Acyclic Dienes. *J. Org. Chem.* **2000**, *65*, 4355–4363.
- [152] Carreño, M. C.; Urbano, A.; Di Vitta, C. Short and efficient enantioselective total synthesis of angucyclinone type antibiotics (+)-rubiginone B₂ and (+)-ochromycinone. *Chem. Commun.* **1999**, 817–818.
- [153] Caramella, P.; Rondan, N. G.; Paddon-Row, M. N.; Houk, K. N. Origin of π -Facial Stereoselectivity in Additions to π -Bonds: Generality of the Anti-Periplanar Effect. *J. Am. Chem. Soc.* **1981**, *103*, 2439–2440.
- [154] Rondan, N. G.; Paddon-Row, M. N.; Caramella, P.; Mareda, J.; Mueller, P. H.; Houk, K. N. Origin of Huisgen’s Factor “x”: Staggering of Allylic Bonds Promotes Anomalously Rapid Exo Attack on Norbornenes. *J. Am. Chem. Soc.* **1982**, *104*, 4974–4976.
- [155] Paddon-Row, M. N.; Rondan, N. G.; Houk, K. N. Staggered Models for Asymmetric Induction: Attack Trajectories and Conformations of Allylic Bonds from ab Initio Transition Structures of Addition Reactions. *J. Am. Chem. Soc.* **1982**, *104*, 7162–7166.
- [156] Houk, K. N.; Moses, S. R.; Wu, Y.-D.; Rondan, N. G.; Jäger, V.; Schohe, R.; Fronczek, f. R. Stereoselective Nitrile Oxide Cycloadditions to Chiral Allyl Ethers and Alcohols. The “Inside Alkoxy” Effect. *J. Am. Chem. Soc.* **1984**, *106*, 3880–3882.
- [157] Carreño, M. C.; Ribagorda, M.; Somoza, I.; Urbano, A. Enantioselective Total Synthesis of Angucyclinone-Type Antibiotics Rubiginones A₂ and C₂. *Angew. Chem. Int. Ed.* **2002**, *41*, 2755–2757.
- [158] Carreño, M. C.; Pérez González, M.; Houk, K. N. π -Facial Diastereoselection in Diels-Alder Reactions of (R)-4-[(p-Tolylsulfinyl)methyl]quinols. *J. Org. Chem.* **1997**, *62*, 9128–9137.
- [159] Carreño, M. C.; Urbano, A.; Di Vitta, C. Enantioselective Diels-Alder Approach to C-3-Oxygenated Angucyclinones from (SS)-2-(p-Tolylsulfinyl)-1,4-naphthoquinone. *Chem. Eur. J.* **2000**, *6*, 906–913.
- [160] Carreño, M. C.; Ribagorda, M.; Somoza, I.; Urbano, A. Asymmetric Synthesis of Rubiginones A₂ and C₂ and Their 11-Methoxy Regioisomers. *Chem. Eur. J.* **2007**, *13*, 879–890.
- [161] Lanfranchi, D. A.; Bour, C.; Hanquet, G. Enantioselective Access to Key Intermediates for Salvinorin A and Analogues. *Eur. J. Org. Chem.* **2011**, 2818–2826.

- [162] Carreño, M. C.; Hernández-Sánchez, R.; Mahugo, J.; Urbano, A. Enantioselective Approach to Both Enantiomers of Helical Bisquinones. *J. Org. Chem.* **1999**, *64*, 1387–1390.
- [163] Grimme, S.; Harren, J.; Sobanski, A.; Vögtle, F. Structure/Chiroptics Relationships of Planar Chiral and Helical Molecules. *Eur. J. Org. Chem.* **1998**, 1491–1509.
- [164] Katz, T. J. Syntheses of Functionalized and Aggregating Helical Conjugated Molecules. *Angew. Chem. Int. Ed.* **2000**, *39*, 1921–1923.
- [165] Carreño, M. C.; González-López, M.; Urbano, A. Efficient asymmetric synthesis of [7]helicene bisquinones. *Chem. Commun.* **2005**, 611–613.
- [166] Carreño, M. C.; García-Cerrada, S.; Sanz-Cuesta, M. J.; Urbano, A. First asymmetric synthesis of dihydrobenzo[*c*]phenanthrene-1,4-quinones with helical chirality. *Chem. Commun.* **2001**, 1452–1453.
- [167] Carreño, M. C.; García-Cerrada, S.; Urbano, A. Divergent enantioselective of (*P*)- and (*M*)-dihydro[5]helicenequinones from a common tetrahydroaromatic precursor. *Chem. Commun.* **2002**, 1412–1413.
- [168] Carreño, M. C.; García-Cerrada, S.; Urbano, A. Enantiopure Dihydro-[5]-helicenequinones via Diels-Alder Reactions of Vinyl Dihydrophenanthrenes and (*SS*)-2-(*p*-Tolylsulfinyl)-1,4-benzoquinone. *J. Am. Chem. Soc.* **2001**, *123*, 7929–7930.
- [169] Carreño, M. C.; García-Cerrada, S.; Urbano, A. From Central to Helical Chirality: Synthesis of *P* and *M* Enantiomers of [5]Helicenequinones and Bisquinones from (*SS*)-2-(*p*-Tolylsulfinyl)-1,4-benzoquinone. *Chem. Eur. J.* **2003**, *9*, 4118–4131.
- [170] Carreño, M. C.; García-Cerrada, S.; Sanz-Cuesta, M. J.; Urbano, A. Influence of Diene Substitution on Diels-Alder Reactions between Vinyl Dihydronaphthalenes and (*SS*)-2-(*p*-Tolylsulfinyl)-1,4-benzoquinone. *J. Org. Chem.* **2003**, *68*, 4315–4321.
- [171] Carreño, M. C.; Enríquez, I.; García-Cerrada, S.; Sanz-Cuesta, M. J.; Urbano, A.; Maseras, F.; Nonell-Canals, A. Towards Configurationally Stable [4]Helicenes: Enantioselective Synthesis of 12-Substituted 7,8-Dihydro[4]helicene Quinones. *Chem. Eur. J.* **2008**, *14*, 603–620.
- [172] Latorre, A.; Urbano, A.; Carreño, M. C. Dynamic kinetic resolution in the asymmetric synthesis of atropisomeric biaryl[4] and [5]helicene quinones. *Chem. Commun.* **2009**, 6652–6654.
- [173] Latorre, A.; Urbano, A.; Carreño, M. C. Synthesis and chiroptical properties of ferrocene-[4]-helicenequinones: kinetic resolution of a planar-chiral diene. *Chem. Commun.* **2011**, *47*, 6652–6654.
- [174] Atkinson, R. C. J.; Gibson, V. C.; Long, N. J. The syntheses and catalytic applications of unsymmetrical ferrocene ligands. *Chem. Soc. Rev.* **2004**, *33*, 313–328.
- [175] del Hoyo, A. M.; Latorre, A.; Díaz, R.; Urbano, A.; Carreño, M. C. Enantiopure Helical Ferrocene-Triazole-Quinone Triads: Synthesis and Properties. *Adv. Synth. Catal.* **2015**, *357*, 1154–1160.
- [176] del Hoyo, A. M.; Urbano, A.; Carreño, M. C. Enantioselective Synthesis of Four Stereoisomers of Sulfinyl Ferrocenyl Quinones with Central, Planar, and Helical Chirality. *Org. Lett.* **2016**, *18*, 20–23.

Part II

Results and discussion

Chapter 3

Strategy and objectives

3 Strategy and objectives

Despite the fact that momilactones A (**1**) and B (**2**) have been known since the early 1970s,¹ only one total synthesis of racemic momilactone A has been reported (*cf.* Chapter 1, section 1.4.4).² Therefore, the goal of this thesis is to propose a new, and enantioselective, route towards both momilactones.

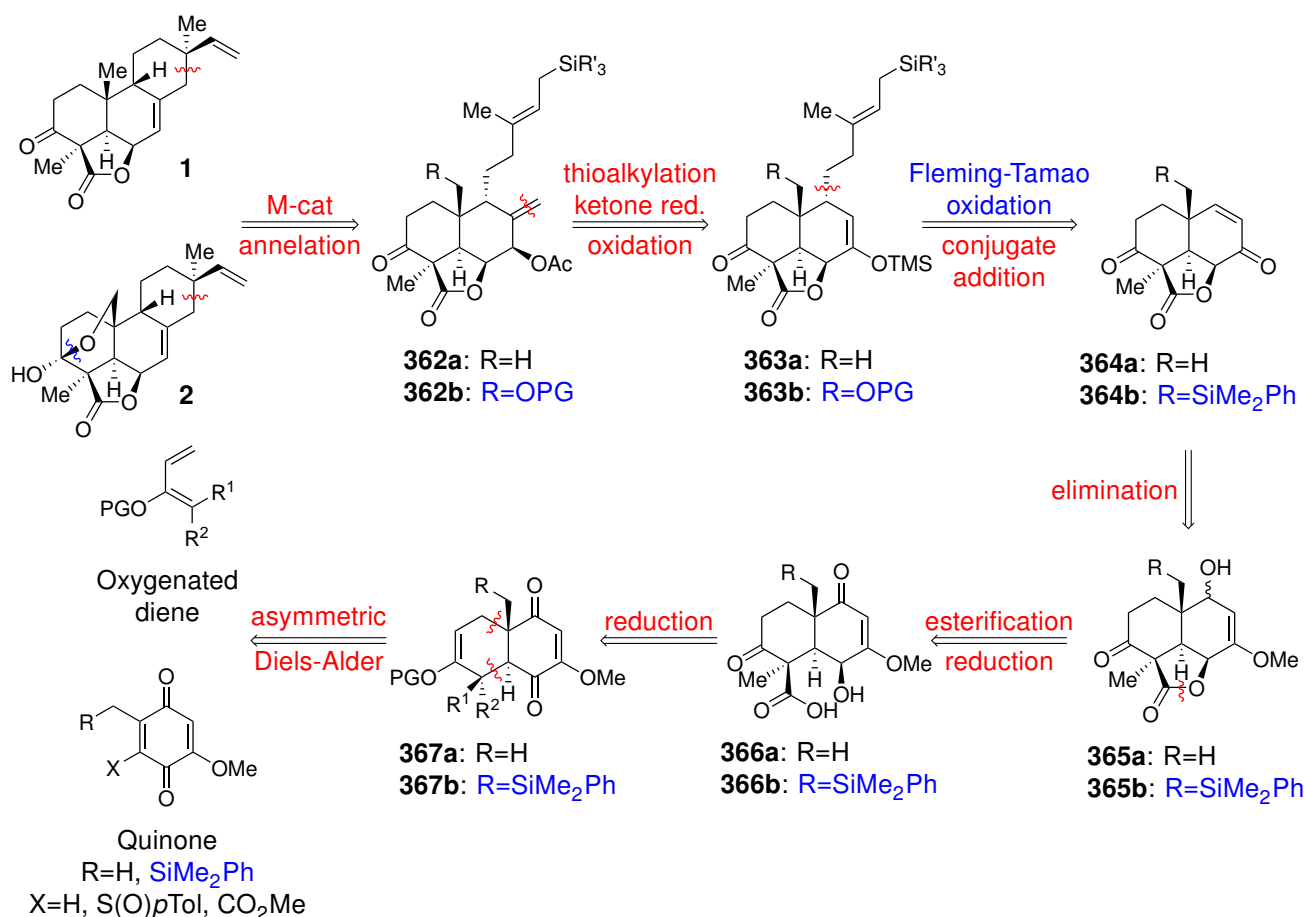
First, a retrosynthetic analysis will be established in order to highlight the main strategic transformations, followed by a more detailed description of the planned synthetic steps.

However, as in most of the total syntheses, it is preferable not to directly dive in. Therefore, a series of methodology studies will be proposed in order to evaluate the key steps of the synthetic pathway described below.

3.1 Retrosynthetic analysis of momilactones A and B

In order to develop the total synthesis of momilactones A (**1**) and B (**2**), the retrosynthetic analysis, presented in Scheme 3.1, presents the main transformations, leading to two precursors, an oxygenated diene and an adequately substituted quinone.

The first disconnection consists in the opening of the third cycle. The latter will be formed using a metal-catalysed cyclisation that is closely related to Bäckvall's intramolecular additions.³ This Tsuji-



Scheme 3.1: Retrosynthetic analysis of momilactones A (**1**) and B (**2**) to an oxygenated diene and a quinone as precursors. The retrosynthetic steps specific to momilactone B (**2**) are highlighted in blue.

Trost type reaction occurs on an exocyclic double bond, previously introduced *via* thioalkylation of intermediate **363**, and uses an allylsilane group, introduced *via* a conjugate addition on enone **364**, as nucleophile. It should be noticed that in the case of momilactone B, the alcohol needed for the formation of the lactol moiety is obtained using a Fleming-Tamao oxidation on the corresponding silane.⁴⁻⁷ This step is the only one differing between both momilactones.

Enone **364** is obtained by the elimination of the alcohol in intermediate **365**. That alcohol and the lactone ring of intermediate **365** come from the reduction of the conjugated ketone of intermediate **366** and from the intramolecular condensation between the carboxylic acid and the alcohol of intermediate **366**, respectively. Transformation of the alcohol of **366** into a carbonyl and changing the enone into an enol ether highlights the Diels-Alder cycloadduct between an oxygenated diene and a quinone.

3.2 Synthetic plan for the total synthesis of momilactones

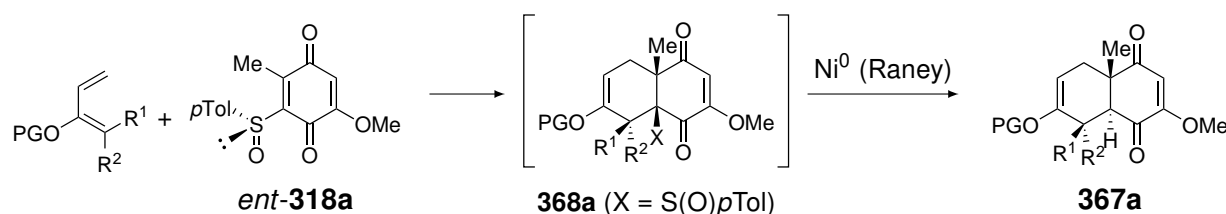
As described in Scheme 3.1, the total synthesis of momilactones should start with an asymmetric Diels-Alder reaction between an oxygenated diene and a quinone. In order to selectively form the two first hydrocarbon rings of the natural compounds, as well as the lactone ring, several quinonoid systems, combined with different dienes, can be used.

3.2.1 Choice of the quinonoid system

The first type of strategy that will be investigated in this work is the use of a sulfinylquinone. In order to reach the cycloadduct with the desired absolute configuration, and given the observed facial diastereoselectivities obtained with such systems (*cf.* Chapter 2), sulfinylquinone *ent*-**318a** would be a suitable candidate (Scheme 3.2). Its synthesis would be the same as that described by Hanquet *et al.*, except for the chiral precursor that would be prepared from *d*-menthol instead of *l*-menthol.⁸

The first step of the sequence proposed in Scheme 3.2 is the asymmetric Diels-Alder reaction of an oxygenated diene and sulfinylquinone *ent*-**318a**. What may seem surprising in this cycloaddition is the regioselectivity with respect to the diene. But, as already reported with sulfinylquinone **318a**, the presence of a methyl group next to the sulfoxide led to the same unusual regioselectivity with 3-trimethylsilyloxy-penta-1,3-diene (PG = TMS, R¹ = H, R² = Me).⁸ It was suggested that a steric clash between both methyl groups disfavoured the expected regioselectivity. We expect the same behaviour for other dienes bearing a substituent in R².

Once the Diels-Alder reaction is done, the intermediate cycloadduct **368a** will be treated with Raney nickel to reduce the carbon-sulfur bond. This reagent is indeed one of the most used for this transformation.⁹⁻¹⁴ However, attention must be paid to the stability of such an adduct. The



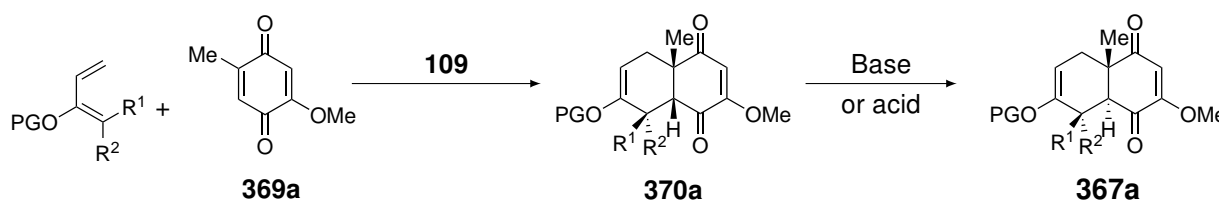
Scheme 3.2: Diels-Alder reaction between an oxygenated diene and sulfinylquinone *ent*-**318a**, followed by the desulfinylation of cycloadduct **368a** into the corresponding *trans*-decalin **367a**.

promptitude of sulfoxides to undergo an elimination reaction when a hydrogen atom is placed in *syn* orientation, sometimes even at low temperatures, might complicate the use of this strategy.

Nevertheless, if the reduction of the carbon-sulfur bond is successful, the *trans*-decalin **367a** would be obtained with the desired absolute configurations. Indeed, due to the presence of the carbonyl group next to the sulfoxide, an inversion of the configuration is expected during the reduction step as it will form the most stable decalin.

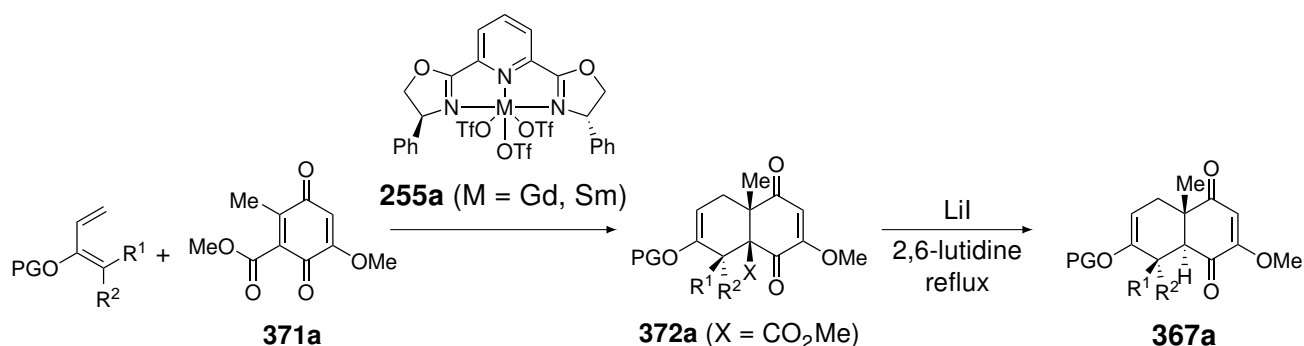
In the event the strategy *via* the sulfinylquinone does not give satisfactory results, it is envisaged to turn towards asymmetric catalysis. The first one to be tested will be Corey's catalysis, using an oxazaborolidinium salt as chiral catalyst.^{15,16} In that reaction (Scheme 3.3), the diene will undergo the cycloaddition with quinone **369a** in the presence of catalyst **109**. Similarly to what was discussed in the previous strategy, the unusual regioselectivity is likely to take place as well.

The resulting cycloadduct, the *cis*-decalin **370a**, will be converted into its *trans* isomer **367a** by the action of a base, such as MeONa,¹⁷ or in an acidic medium, such as silica gel in ethyl acetate.¹⁸



Scheme 3.3: Diels-Alder reaction between an oxygenated diene and quinone **369a** using Corey's asymmetric catalysis, followed by the isomerisation of cycloadduct **370a** into the corresponding *trans*-decalin **367a**.

The second asymmetric catalytic system that could be used for the desired cycloaddition is the one described by Evans (Scheme 3.4).¹⁹ In this case, quinone **371a** will be used in the presence of catalyst **255a**, once again with the unusual regioselectivity. The cycloadduct **372a** can then undergo a modified version of the Krapcho dealkoxycarbonylation, using lithium iodide in refluxing 2,6-lutidine. This method has already been used with success in other total syntheses.^{20,21}



Scheme 3.4: Diels-Alder reaction between an oxygenated diene and quinone **371a** using Evans' asymmetric catalysis, followed by the decarboxylation of cycloadduct **372a** into the corresponding *trans*-decalin **367a**.

Based on the same first key step, being an asymmetric Diels-Alder reaction between a quinone and an oxygenated diene, three potential pathways could be used to reach a common intermediate

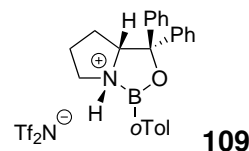


Figure 3.1: Structure of oxazaborolidinium salt **109**.

367a. One of them employs a chiral sulfinylquinone that will be prepared according to an already described synthesis of the opposite enantiomer.⁸ The other two use an asymmetric catalysis, one developed by Corey and the other by Evans. In those cases, the syntheses of both quinones **369a** and **371a** first have to be designed and optimised.

In any case, in all three of the strategies proposed here, the evaluation of the reactions should be done in order to determine which of them gives the best results in terms of yield, as well as in terms of regio- and stereoselectivity.

3.2.2 Choice of the diene

Based on the retrosynthetic analysis that has been proposed (Scheme 3.1), the diene can be varied as well. For that purpose, five oxygenated dienes are proposed for the asymmetric Diels-Alder reaction (Figure 3.2).

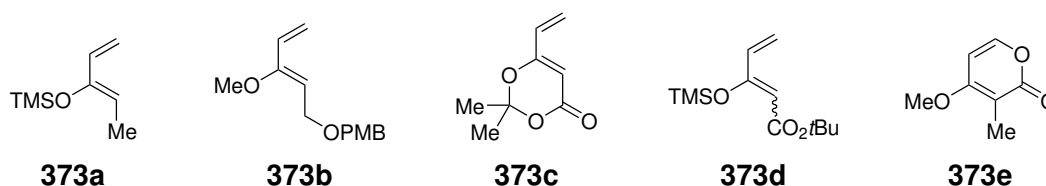
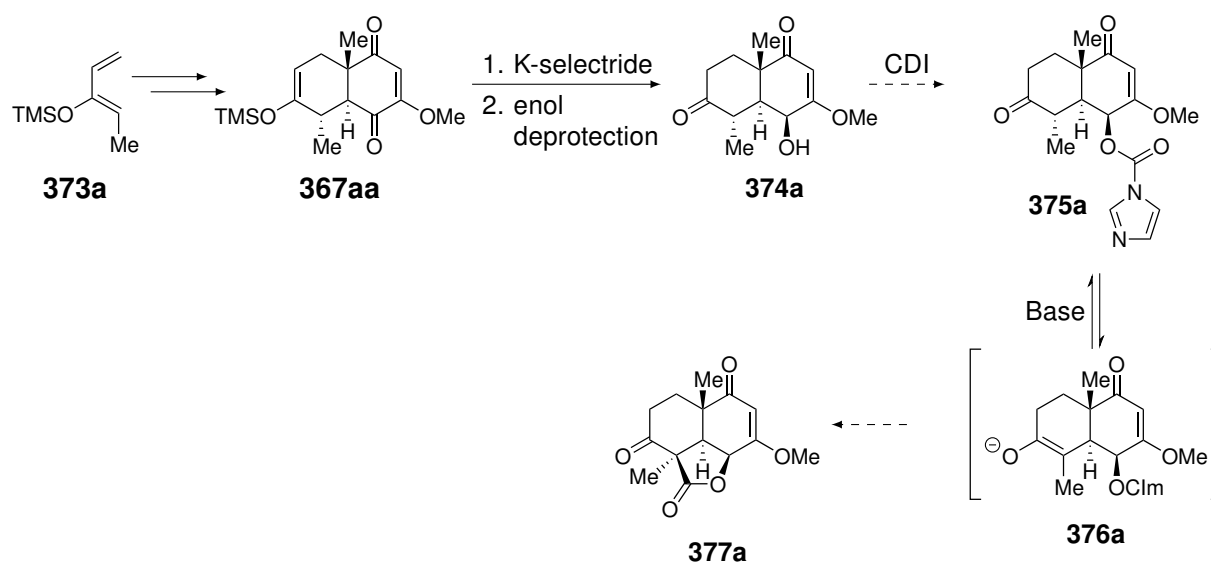


Figure 3.2: Structures of the five oxygenated dienes proposed as starting materials for the total synthesis of momilactones.

The first diene that is potentially envisaged, for this total synthesis, is diene **373a**. Its synthesis has already been described by several groups^{22–24} and its use in cycloadditions has been studied, notably with sulfinylquinone **318a**.⁸ However, this diene does not possess an oxidised carbon atom on position 1 of the diene, but a methyl group. Therefore, the subsequent insertion of an oxidised carbon must be taken into account in the design of the synthesis.



Scheme 3.5: Planned reaction sequence to get to the intermediate **377a** from diene **373a** engaged in an asymmetric Diels-Alder reaction.

After the cycloaddition and conversion of the cycloadduct into the *trans*-decalin **367aa**, the strategy will continue with the reduction of the ketone of the latter with K-selectride and the enol deprotection (Scheme 3.5). The next important transformation will be the insertion of the oxidised carbon atom that will serve for the formation of the transannular lactone ring. Unfortunately, such an insertion cannot be carried out using a simple nucleophilic attack of a cyclic enolate, formed from **374a**, on an electrophile. Indeed, as described by Stork, the alkylation of such enolates in a *trans*-decalin system should normally occur in axial orientation (Figure 3.3).²⁵ However, when an angular methyl group is present, the axial position is too hindered and the nucleophilic attack preferentially occurs in equatorial orientation. Thus, in order to overcome this issue, the oxidised carbon would be tethered on the secondary alcohol *via* the use of carbonyldiimidazole (CDI). Next, Intermediate **375a** will be treated with a base to form a cyclic enolate **376a**. As the electrophilic oxidised carbon is positioned on the top face of the *trans*-decalin, the nucleophilic attack has no choice but to occur in equatorial position, leading to intermediate **377a**.

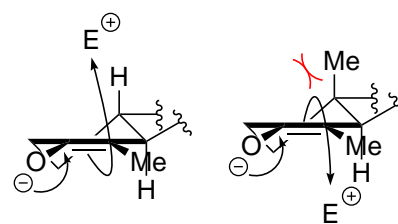
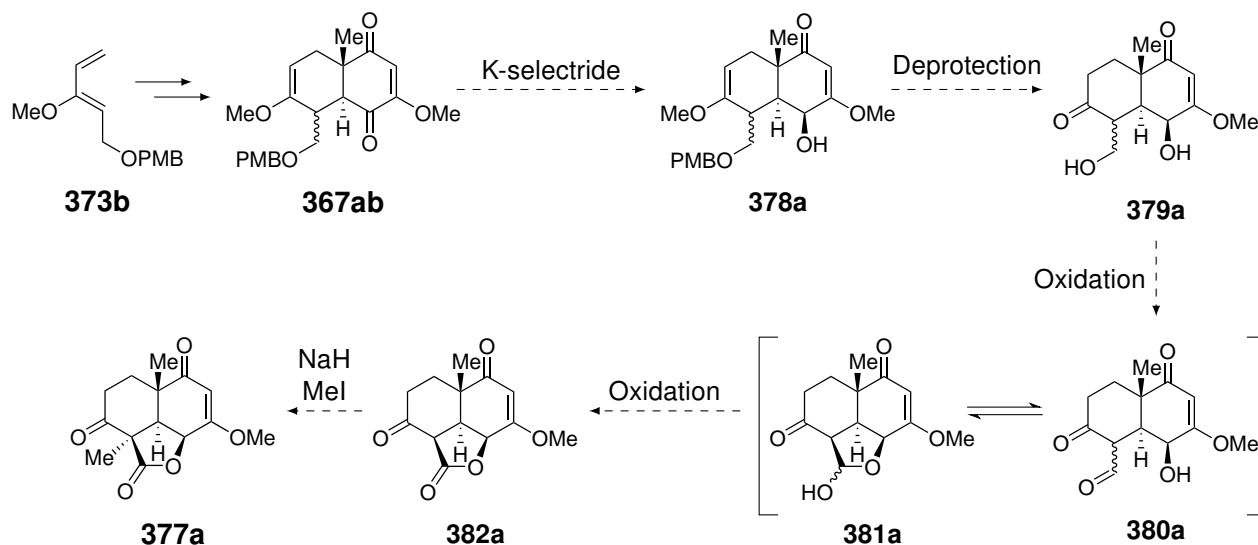


Figure 3.3: Nucleophilic attack of a cyclic enolate in a *trans*-decalin system without (left) and with (right) an angular methyl group.²⁵

The next diene (**373b**), designed as potential starting material for this total synthesis, possesses an oxidised carbon atom on position 1. To the best of our knowledge, that diene is not described in the literature and its synthesis will need to be designed and optimised.

After the Diels-Alder reaction and the transformation of the adduct into the *trans*-decalin **367ab**, the latter will undergo a selective reduction of the carbonyl next to the methoxy group to give intermediate **378a** (Scheme 3.6).

Then, the primary alcohol and the enol will be deprotected to reach intermediate **379a** that will undergo oxidation. Using the right conditions, the oxidation of the primary alcohol and the formation of the lactone can be done in one-pot. Indeed, the primary alcohol will first be oxidised into an aldehyde



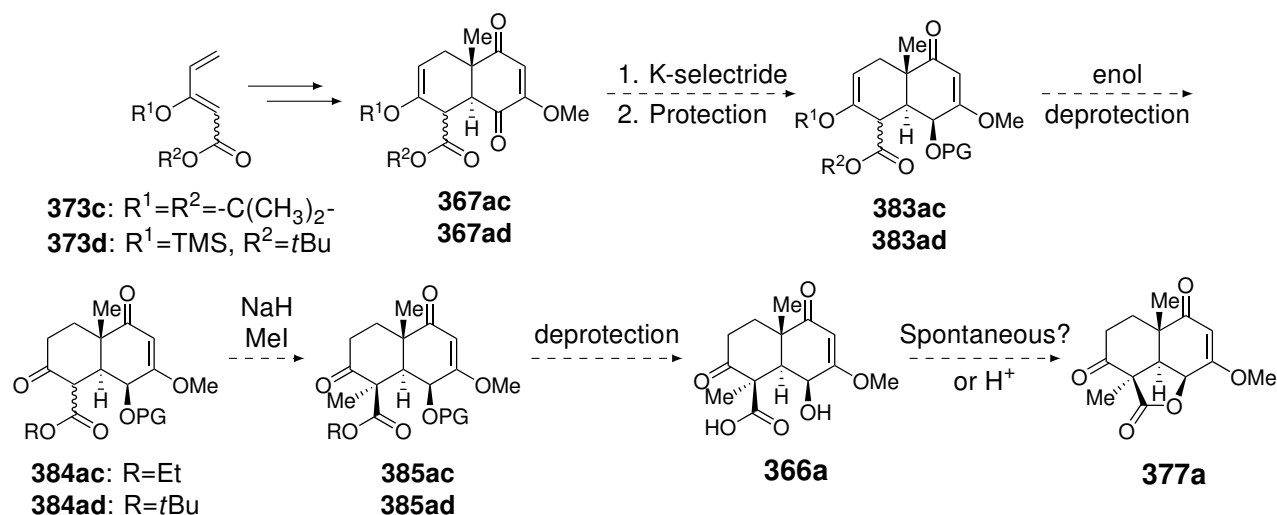
Scheme 3.6: Planned reaction sequence to get to the intermediate **377a** from diene **373b** engaged in an asymmetric Diels-Alder reaction.

(**380a**) that is in equilibrium with its lactol form (**381a**). The reaction will continue with the oxidation of the latter into the lactone **382a**. Given the facts that the aldehyde intermediate **380a** is able to epimerise, and that the secondary alcohol is oriented on the top face, the formation of the hemiketal **381a**, and subsequently the lactone **382a**, will take place on the top face. In order to perform such transformation, one can either use pyridinium dichromate (PDC),²⁶ phenyliodonium diacetate (PIDA) with a catalytic amount of (2,2,6,6-tetramethylpiperidin-1-yl)oxyl (TEMPO)²⁷ or *N*-methylmorpholine *N*-oxide (NMO) with a catalytic amount of tetrapropylammonium perruthenate (TPAP).²⁸

Finally, the insertion of the missing methyl group will be performed. In this case, the insertion of that methyl should easily be done on the opposite face to the angular methyl group, as described in the model developed by Stork (Figure 3.3). Using diene **373b**, we should remove the selectivity issue that is expected with diene **373a** and the oxidised carbon atom needed for the lactone should selectively and easily be oriented on the same face as the angular methyl group.

The next type of diene proposed for the synthesis are 3-oxypentadienoates **373c** and **373d**. Similarly to diene **373b**, both those dienes contain the oxidised carbon atom but at a higher oxidation state. Therefore, the oxidation step needed for the previous diene will not be necessary with these two. However, we also take the risk of lowering the reactivity of the dienes as they are conjugated to a carbonyl group.

The preparation of diene **373c** was reported by Gebauer and Blechert in 2006, but they did not use it in a Diels-Alder reaction.²⁹ On the other hand, diene **373d** has been described by Dickschat and co-workers and was effectively used in a Diels-Alder reaction.³⁰

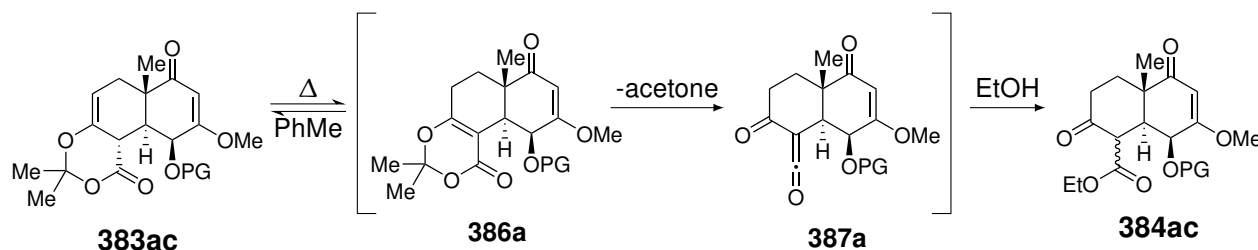


Scheme 3.7: Planned reaction sequence to get to intermediate **377a** from dienes **373c** or **373d** engaged in an asymmetric Diels-Alder reaction.

Those two dienes will follow a similar pathway (Scheme 3.7). After the cycloaddition and the series of transformations leading to *trans*-decalin **367ac** or **367ad**, one of the ketones will be selectively reduced with K-selectride. The resulting alcohol will then be protected. From intermediates **383ac** and **383ad**, the goal will be to reveal a β -ketoester in order to perform the methylation step (Scheme 3.8). The deprotection of compound **383ac** can be done by treating the latter with ethanol in refluxing toluene, as described by Suzuki *et al.*³¹ Firstly, an isomerisation of the double bond has to occur,

followed by a cycloreversion that will release one molecule of acetone and reveal a ketene. The ketene moiety will then react with ethanol to form the corresponding ester in **384ac**.

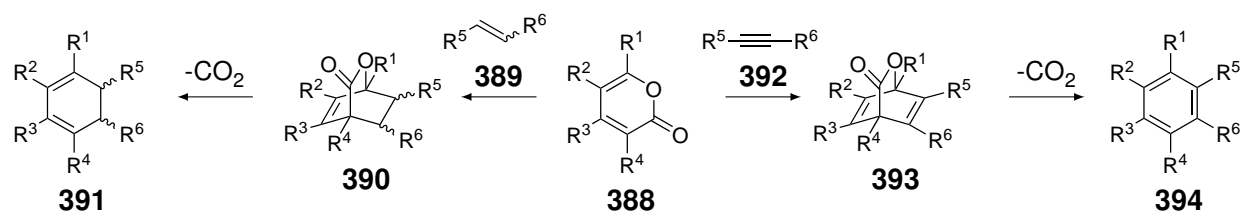
On the other hand, the deprotection of enol **383ad** is more straightforward as a standard treatment with TBAF should easily give the desired β -ketoester **384ad**.



Scheme 3.8: Synthetic plan for the deprotection of the enol ethers **383ac** into the β -ketoesters **384ac**.

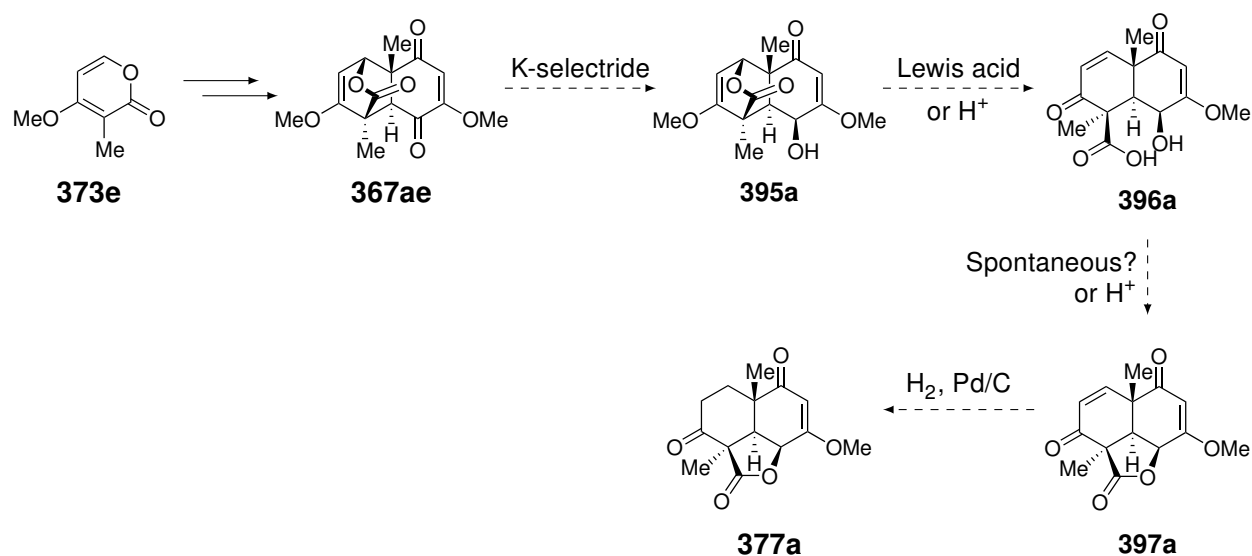
Then, the deprotonation with sodium hydride should selectively occur between both carbonyl groups of the β -ketoester, followed by the addition of iodomethane. That methylation, similarly to the sequence with diene **373b** should occur on the opposite face to the angular methyl group, orienting the ester on the same face as that angular methyl. Once the addition of the methyl group is done, deprotection of both the carboxylate and the alcohol will be done and their condensation, which should be spontaneous or in acidic medium, will lead to the common intermediate **377a**

The last diene proposed for this total synthesis is the α -pyrone **373e**. The preparation of this reactant has already been described by Effenberger *et al.* in 1985.³² The same group reported its use as diene in Diels-Alder reactions with maleic anhydride (**200**) two years later.³³ However, Diels-Alder reactions with α -pyrones are known since the early 1960s³⁴ and have already been used in many total syntheses.³⁵ They indeed possess a strategic interest as they are able to form cyclohexadienes, or even polysubstituted benzenes if reacted with alkynes, upon decarboxylation *via* a retro-Diels-Alder reaction (Scheme 3.9).



Scheme 3.9: Diels-Alder reaction between an α -pyrone (**388**) and an alkene (**389**) or an alkyne (**392**), leading to cycloadducts **390** and **393**, respectively, that can decarboxylate to cyclohexadiene **391** and benzene **394**, respectively.

The main difference between pyrone **373e** and all the previous dienes is the presence of both the methyl group and the oxidised carbon atom at the desired oxidation state. If the Diels-Alder reaction of this pyrone undergoes the expected *endo* selectivity, the oxidised carbon atom will be oriented on the same face as the angular methyl group and the other methyl group will be oriented on the opposite face, in one single step. Should this diene work with one of the three quinonoid system, the number of steps will be greatly reduced and the stereoselectivity issues will be avoided. These prospects make **373e** the most desirable of the five dienes.

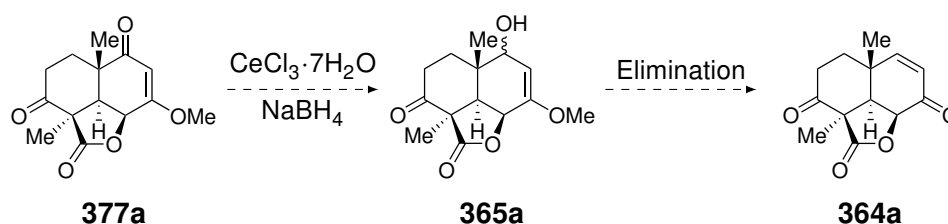


Scheme 3.10: Planned reaction sequence to get to intermediate **377a** from pyrone **373e** engaged in an asymmetric Diels-Alder reaction.

After the Diels-Alder reaction and a series of transformations, leading to the *trans*-decalin **367ae**, the selective reduction will be performed with K-selectride (Scheme 3.10). The lactone will then be opened with an acidic catalysis. Once the lactone ring is opened, the condensation between the carboxylic acid and the alcohol will occur in acidic media, but could also be spontaneous (given their proximity). The synthesis will continue with the palladium-catalysed hydrogenation of the enone **397a** into the corresponding ketone **377a**.

3.2.3 Formation of the third cycle

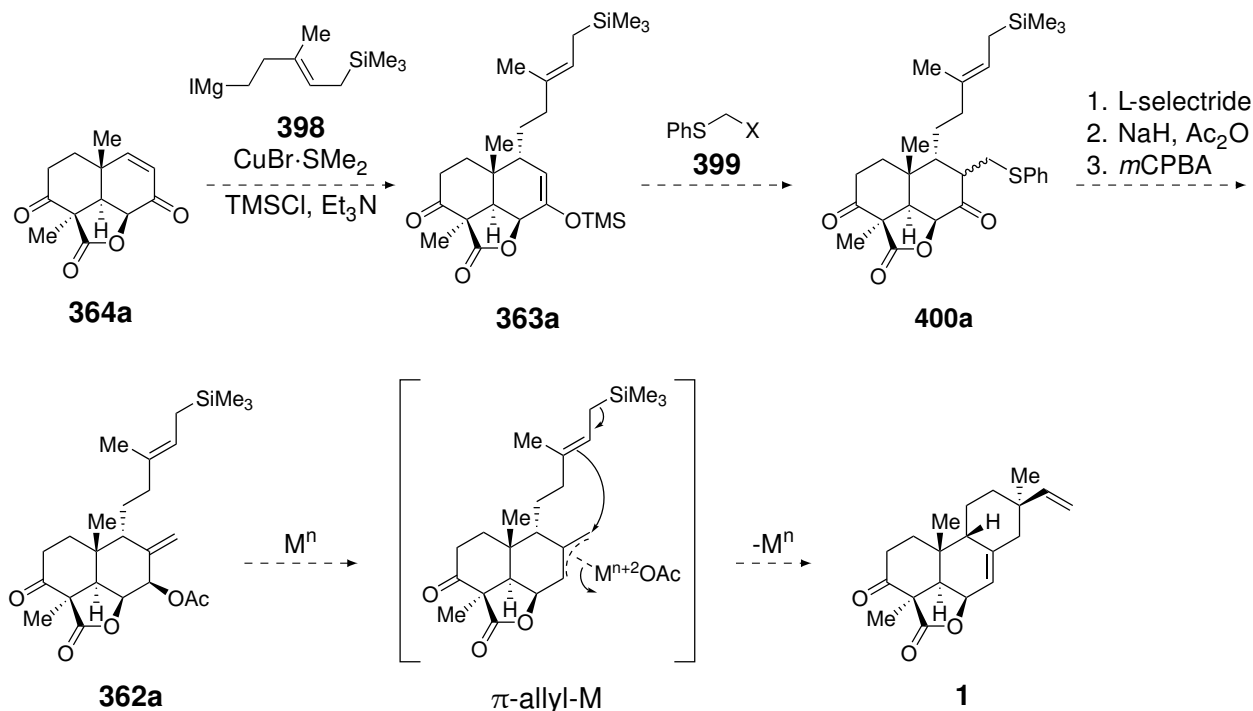
The next part of the synthesis will focus on the preparation of an enone in order to insert an allylsilane chain *via* a 1,4-addition. Intermediate **377a** will undergo a selective reduction of one of its ketones using Luche's conditions (Scheme 3.11). The resulting alcohol **365a** will then be eliminated to obtain the enone **364a** on which the allylsilane chain will be added.



Scheme 3.11: Preparation of intermediate **364a** from intermediate **377a**.

The next steps from enone **364a** involve a new strategy which will need a methodological development (Scheme 3.12). The stereocontrolled conjugate addition of the allylsilane fragment **398** on enone **364a** will form the corresponding enolate, converted into enol ether **363a**. As α -methylene-cyclohexanone derivatives are unstable, since they can dimerise *via* a hetero-Diels-Alder reaction,^{36–38} the α -methylene unit will be masked using an appropriate sulfide derivative (**400a**) introduced by the alkylation of the enolsilane **363a**. Before the revelation of the exocyclic double bond, the ketone will be

regioselectively reduced and the corresponding alcohol acetylated. Finally, oxidizing the sulfide into the sulfoxide followed by the elimination of the sulfenic acid will lead to the α -methylene unit (**362a**).



Scheme 3.12: Synthetic plan from the enone **364a** to momilactone A (**1**).

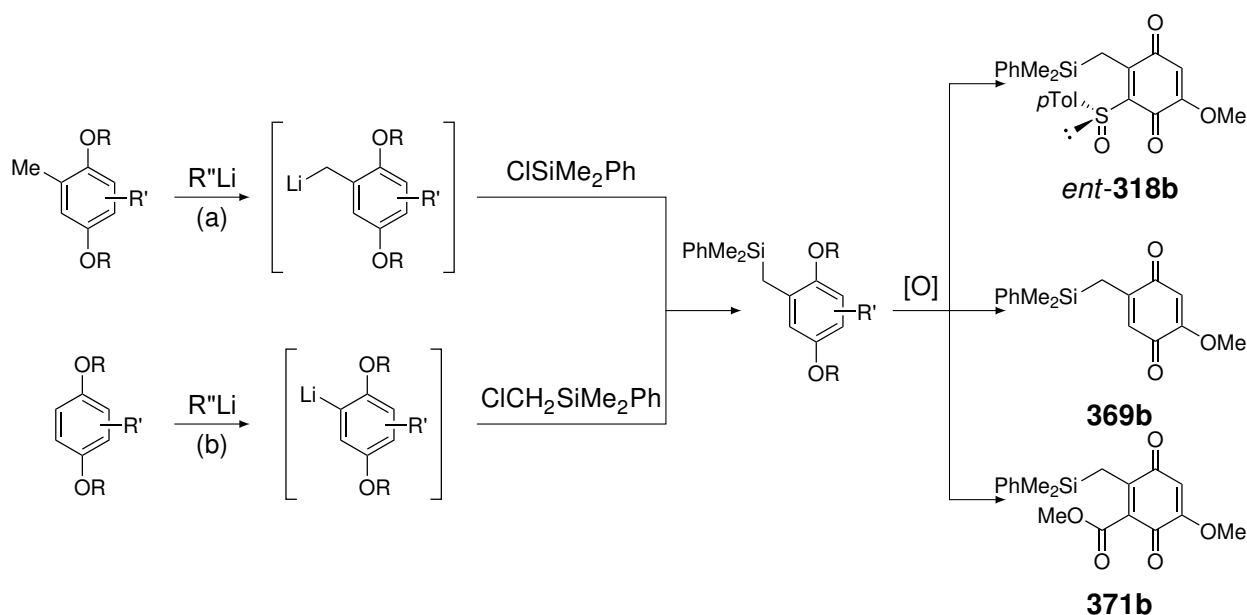
The final step in the synthetic plan towards momilactone A (**1**) is the formation of the third cycle. This cyclisation will be done by the addition of the allyl silane moiety on a π -allyl-metal complex. A similar intermolecular addition of a nucleophile onto a π -allyl-metal complex has already been described by Carreira *et al.*, using iridium as metal.^{39–41} However, that transformation, similar to a Tsuji-Trost reaction,^{42,43} has never been described intramolecularly. Nevertheless, allylsilanes have already been studied in intramolecular 1,4-additions on conjugated dienes, in order to perform carbocyclisations.³

3.2.4 Specific route for the total synthesis of momilactone B

As described in the retrosynthetic analysis (Scheme 3.1), the additional oxygen atom present on the angular methyl in momilactone B (**2**) will be inserted in the structure through a Fleming-Tamao oxidation of a dimethylphenylsilyl group.^{4–7}

But first, those silylated quinones (Scheme 3.13) must be prepared by metallation on the benzylic position, followed by the nucleophilic addition of the formed carbanion on ClSiMe₂Ph (pathway a). Another way to reach the same quinones would be to start from a benzene derivative without the methyl group, to regioselectively metallate the aromatic core, and to add (chloromethyl)dimethylphenylsilane as electrophile (pathway b).

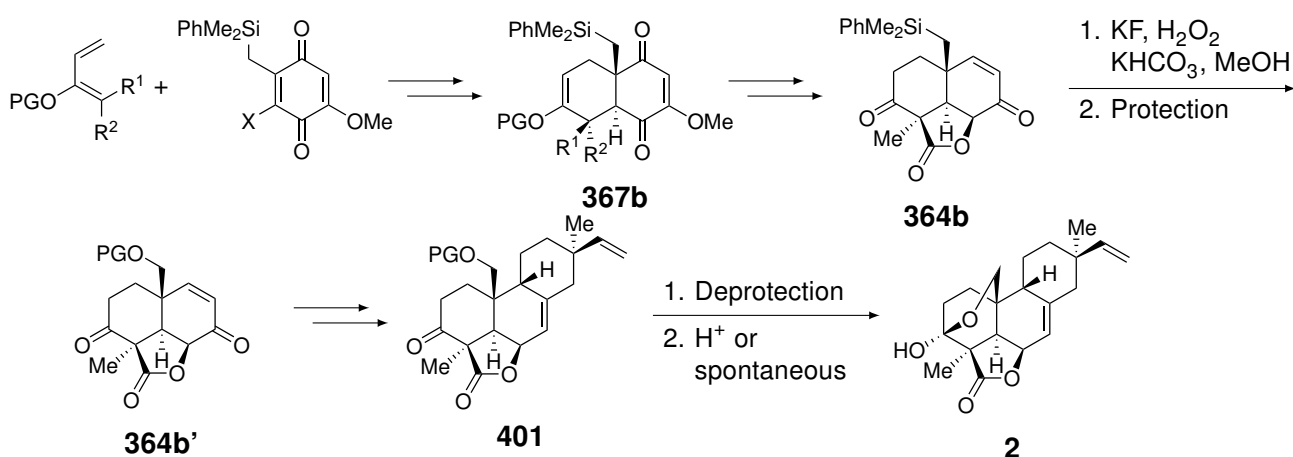
The silylated hydroquinone derivative will then be converted into the corresponding quinone by oxidation. The choice of the silylated quinone will depend on the best pathway, which will be determined during the total synthesis of momilactone A (**1**).



Scheme 3.13: Structure of the three silylated quinones that could be used for the total synthesis of momilactone B, following one of the three strategies developed in Schemes 3.2, 3.3, and 3.4.

Once the desired silylated quinone is synthesised, the same reaction sequence as for momilactone A (**1**) can be used (Scheme 3.14). It will start with a Diels-Alder reaction with the most appropriate oxygenated diene, as it will be determined during the total synthesis of **1**. Then, a series of transformations will lead to the *trans*-decalin **367b**.

From that intermediate, the same reactions should give compound **364b**. The silyl moiety of the latter will be converted into an alcohol using the Fleming-Tamao oxidation, followed by a protection step. The sequence can go on to reach the precursor **401**. The primary alcohol can be deprotected and will cyclise on the ketone to form the lactol moiety of momilactone B (**2**). That last transformation will be done under acidic catalysis or might even be spontaneous.



Scheme 3.14: Synthetic steps towards the total synthesis of momilactone B (**2**) from an oxygenated diene and a silylated quinone.

In conclusion, different strategic plans have been proposed, including three potential asymmetric Diels-Alder reactions, on three different quinones, as first key step, that could be used to reach a *trans*-decalin **367**. Subsequently, five different dienes have been proposed with different synthetic

plans depending on the diene. Therefore, several combinations of quinones and dienes must be tested in order to determine the best pathway to reach a common intermediate **377**.

Then, from intermediate **377**, a few more steps should lead to the desired natural products. The enone **364** will be prepared in order to insert an allylsilane chain into the structure. After a few transformations that will introduce an exocyclic double bond, a metal catalysis would allow the formation of the third cycle *via* the addition of the allylsilane chain onto that double bond, giving the momilactones.

The only difference in the synthetic pathways of momilactone B (**2**) is the presence of a substituted angular methyl group. At the beginning of the synthesis of **2**, that substituent will be the dimethylphenylsilyl group, that corresponds to a hidden hydroxyl group. Such a group is to be inserted during the synthesis of the quinone and will be converted into a hydroxyl group right before the 1,4-addition of the allylsilane chain.

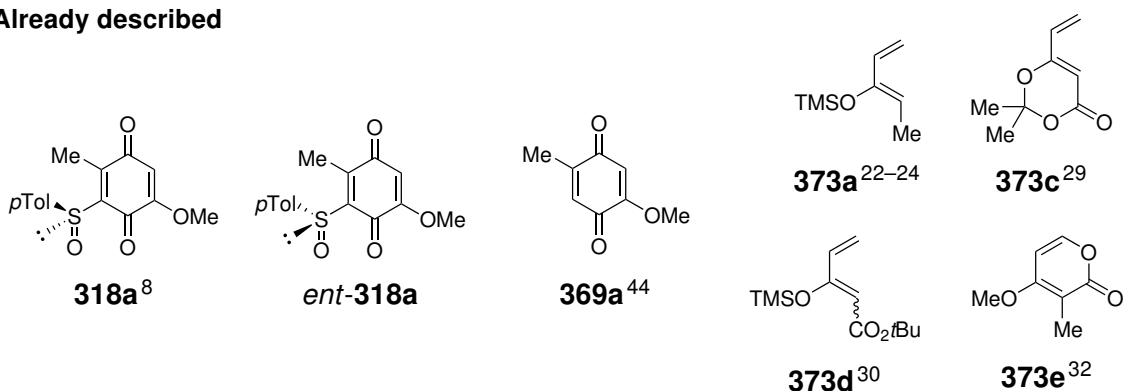
3.3 Additional objectives of this thesis

Besides the ultimate goal that is the total synthesis of both momilactones A (**1**) and B (**2**), several intermediate studies are planned in the course of this thesis. These objectives concern the syntheses of the starting materials that are not described yet, as well as the development and optimisation of the key step reactions through model studies. More specifically, the study of the Diels-Alder reactions with sulfinylquinones will be analysed in depth at different levels.

3.3.1 Synthesis of the starting materials

The first objective will consist in the synthesis of the different quinones and dienes previously presented (Figure 3.4). As explained, some of them have already been synthesised by other groups.

Already described



Starting materials whose synthesis must be developed

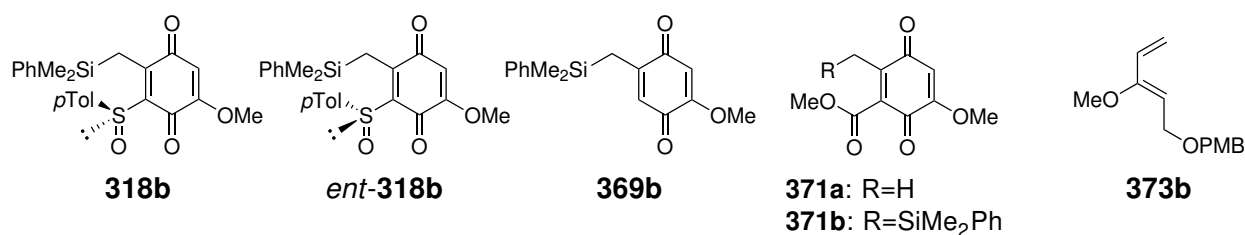


Figure 3.4: Structures of the quinones and dienes proposed for the different pathways developed for the total synthesis of momilactones A (**1**) and B (**2**).

As presented above, sulfinylquinone **318a** was already prepared, using *l*-menthol as chiral auxiliary.⁸ In the synthetic plan that has been developed earlier, and based on the stereoselectivities reported in the literature (*cf.* Chapter 2), its enantiomer *ent*-**318a**, prepared from *d*-menthol, should be used. Among the other quinones, the synthesis of **369a** has also been described.⁴⁴

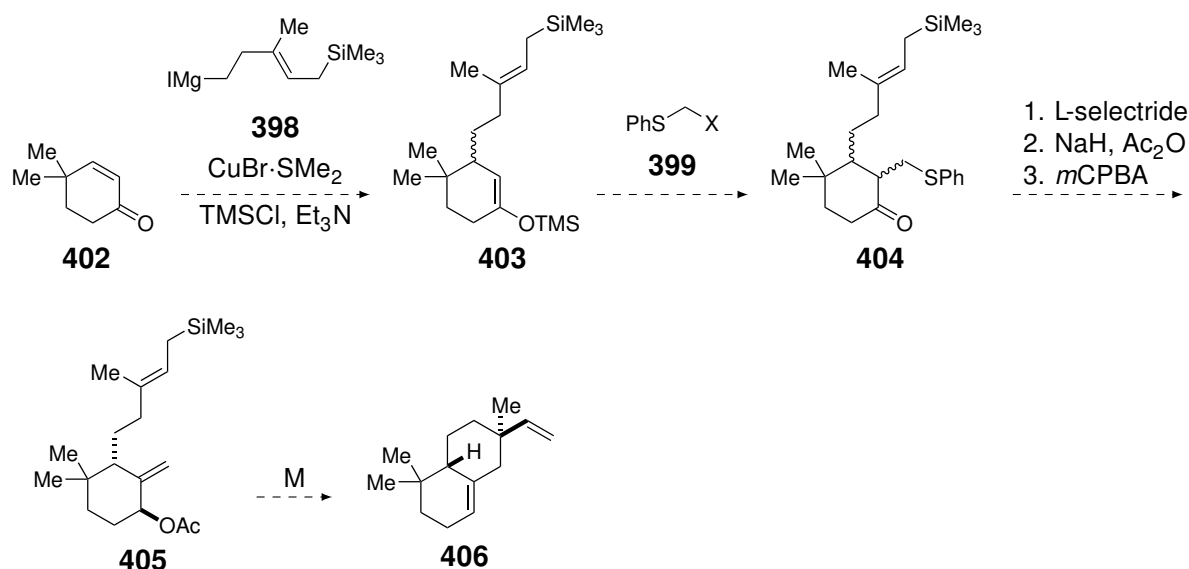
On the other hand, quinone **371a** and the silylated version of all of the quinones have never been described so far. Concerning the silylated quinones, only few examples of them are described in the literature, and none bearing a (dimethylphenylsilyl)methyl group. Therefore, their synthesis will need optimisation.

On the diene part, four out of the five chosen dienes have already been described. The only one that will need to be developed and optimised is diene **373b**.

Once all the desired quinones and dienes are obtained, the different possible combinations for the Diels-Alder reactions must be tested, and the most promising pathways must be optimised.

3.3.2 Formation of the third cycle

Once the Diels-Alder reaction and the next steps are optimised, the next key step of this strategy is the formation of the third cycle of momilactones. In order to evaluate the feasibility and the efficiency of that sequence (Scheme 3.12), a model study will be performed on the commercially available 4,4-dimethylcyclohex-2-en-1-one (**402**) that mimics the cyclohexenone part of intermediate **364**. Moreover, the diastereoselectivity of the cyclisation will be evaluated.



Scheme 3.15: Model study for the insertion of the allylsilane chain and the palladium catalysed cyclisation, using cyclohexenone **402** as model for the cyclohexenone part of intermediate **364**.

However, before performing the insertion of the allylsilane chain, another alkyl chain, such as a butyl group, may be used. This way, the reactions can be studied up to intermediate **405**. Indeed, as the synthesis of the organomagnesium reagent **398** must be developed and optimised as well, it would be laborious to directly develop the sequence described in Scheme 3.15 with the desired allylsilane moiety.

3.3.3 Study on the sulfinylquinones as dienophile in the Diels-Alder reaction

Although the Diels-Alder reaction of sulfinylquinones had already been thoroughly studied, mostly by Carreño and co-workers, the models proposed to explain the obtained stereoselectivities are solely based on the products of those reactions. Based on that work, the phenomena behind the results of those reactions are not yet fully understood, even though a good overview has already been reached (*cf.* Chapter 2). Therefore, the evaluation of the reactivity and the stereoselectivities of these sulfinylquinones will be further studied from different points of view.

Firstly, a structural analysis will be attempted. For that purpose, various sulfinylquinones will be synthesised and submitted to crystallisation. If the formation of suitable crystals is successful, their analysis by X-ray diffraction will be possible. This way, information on the sulfoxide conformation at the solid state will be collected. Although that structural analysis would not be fully representative of the situation in solution, those results would already give a better understanding on the preferential sulfoxide conformation.

Then, in addition to the X-ray analysis of those sulfinylquinones, computational methods will be employed to add another level of understanding on the preferential conformation of those compounds. That theoretical study will determine the impact of the substituents on more complex sulfinylquinones than the ones that could be easily synthesised. Moreover, simulations of Diels-Alder reactions with those quinones could be done to calculate the potential energy curves of the different approaches of the dienes on the quinone core.

Finally, complementary reactivity studies will be performed on sulfinylquinone **318a** with the evaluation of the impact of the solvent on the reaction rate and the facial diastereoselectivity. Those tests are similar to the ones reported by Carreño in 1996.⁴⁵ However, the group worked on the unsubstituted sulfinylquinone **297** that underwent a cycloaddition on its C5-C6 double bond. In the case of sulfinylquinone **318a**, the reaction is expected on the C2-C3 double bond. This way, it will be possible to evaluate the impact of the solvent on the double bond that is the closest to the sulfinyl moiety. Different model dienes will also be tested on sulfinylquinone **318a** in order to determine which substituents, on the diene, are compatible in that specific case.

Investigating the sulfinylquinones from these three points of view, we hope to be able to make a more detailed and comprehensive model to explain the stereo-outcome of these reactions when the cycloaddition occurs on the C2-C3 double bond.

References

- [1] Kato, T.; Kabuto, C.; Sasaki, N.; Tsunagawa, M.; Aizawa, H.; Fujita, K.; Kato, Y.; Kitahara, Y. Momilactones, Growth Inhibitors from Rice, *Oryza sativa* L. *Tetrahedron Lett.* **1973**, *14*, 3861–3864.
- [2] Germain, J.; Deslongchamps, P. Total Synthesis of (±)-Momilactone A. *J. Org. Chem.* **2002**, *67*, 5269–5278.
- [3] Castaño, A. M.; Persson, B. A.; Bäckvall, J.-E. Allylsilanes as Carbon Nucleophiles in the Palladium-Catalyzed 1,4-Oxidation of Conjugated Dienes. *Chem. Eur. J.* **1997**, *3*, 482–490.
- [4] Tamao, K.; Ishida, N.; Kumada, M. (Diisopropoxymethylsilyl)methyl Grignard Reagent: A New, Practically Useful Nucleophilic Hydroxymethylating Agent. *J. Org. Chem.* **1983**, *48*, 2120–2122.
- [5] Fleming, I.; Henning, R.; Plaut, H. The Phenyltrimethylsilyl Group as a Masked Form of the Hydroxy Group. *J. Chem. Soc., Chem. Commun.* **1984**, 29–31.
- [6] Fleming, I.; Henning, R.; Parker, D. C.; Plaut, H.; Sanderson, P. E. J. The Phenyltrimethylsilyl Group as a Masked Hydroxy Group. *J. Chem. Soc., Perkin Trans. 1* **1995**, 317–337.
- [7] Jones, G. R.; Landais, Y. The Oxidation of the Carbon-Silicon Bond. *Tetrahedron* **1996**, *52*, 7599–7662.
- [8] Lanfranchi, D. A.; Hanquet, G. Asymmetric Diels-Alder Reactions of a New Enantiomerically Pure Sulfinylquinone: A Straightforward Access to Functionalized Wieland-Miescher Ketone Analogues with (*R*) Absolute Configuration. *J. Org. Chem.* **2006**, *71*, 4854–4861.
- [9] Kondo, K.; Negishi, A.; Matsui, K.; Tunemoto, D. A New Approach to the Stereospecific Total Synthesis of Racemic *Cecropia* Juvenile Hormone. *J. Chem. Soc., Chem. Commun.* **1972**, 1311–1312.
- [10] Boekelheide, V.; Anderson, P. H.; Hylton, T. A. Transformation of sulfide linkages to carbon-carbon double bonds. Syntheses of [2.2]metaparacyclophane-1,9-dienes. *J. Am. Chem. Soc.* **1974**, *96*, 1558–1564.
- [11] Tsuchihashi, G.-I.; Mitamura, S.; Ogura, K. Asymmetric synthesis using α,β -unsaturated sulfoxides. Creation of both (*R*)- and (*S*)-asymmetric centers from a single chiral origin. *Tetrahedron Lett.* **1976**, 855–858.
- [12] Solladié, G.; Greck, C.; Demailly, G.; Solladié-Cavallo, A. Reduction of β -ketosulfoxides: a highly efficient asymmetric synthesis of both enantiomers of methyl carbinols from the corresponding esters. *Tetrahedron Lett.* **1982**, *23*, 5047–5050.
- [13] Caubère, P.; Coutrot, P. Reduction of Sulfur–Carbon Bonds and of Other Heteroatoms Bonded to Tetrahedral Carbon. In *Comprehensive Organic Synthesis*; Trost, B. M., Fleming, I., Eds.; Pergamon: Oxford, 1991; pp 835–870.
- [14] Nishide, K.; Shigeta, Y.; Obata, K.; Inoue, T.; Node, M. Reductive Desulfurization Using the Raney Nickel - Sodium Hypophosphite Combination System without Racemization of a Secondary Alcohol. *Tetrahedron Lett.* **1996**, *37*, 2271–2274.
- [15] Ryu, D. H.; Corey, E. J. Triflimide Activation of a Chiral Oxazaborolidine Leads to a More General Catalytic System for Enantioselective Diels-Alder Addition. *J. Am. Chem. Soc.* **2003**, *125*, 6388–6390.
- [16] Hu, Q.-Y.; Zhou, G.; Corey, E. J. Application of Chiral Cationic Catalysts to Several Classical Syntheses of Racemic Natural Products Transforms Them into Highly Enantioselective Pathways. *J. Am. Chem. Soc.* **2004**, *126*, 13708–13713.
- [17] Bold, G.; Chao, S.; Bhide, R.; Wu, S.-H.; Patel, D. V.; Sih, C. J. A chiral bicyclic intermediate for the synthesis of forskolin. *Tetrahedron Lett.* **1987**, *28*, 1973–1976.
- [18] Anglea, T. A.; Pinder, A. R. Total Synthesis of (+)-Balanitol and of (+)-Selin-4-(15)-ene-1 β ,11-diol. *Tetrahedron* **1987**, *43*, 5537–5543.
- [19] Evans, D. A.; Wu, J. Enantioselective Rare-Earth Catalyzed Quinone Diels-Alder Reactions. *J. Am. Chem. Soc.* **2003**, *125*, 10162–10163.
- [20] Hayakawa, I.; Asuma, Y.; Ohyoshi, T.; Aoki, K.; Kigoshi, H. Synthetic study on 13-oxyingenol: construction of the fullcarbon framework. *Tetrahedron Lett.* **2007**, *48*, 6221–6224.
- [21] Pronin, S. V.; Shenvi, R. A. Synthesis of a Potent Antimalarial Amphilectene. *J. Am. Chem. Soc.* **2012**, *134*, 19604–19606.
- [22] Danishefsky, S. J.; Yan, C. F. A useful divinyl ketone equivalent. *Synth. Comm.* **1978**, *8*, 211–218.
- [23] Ackland, D. J.; Pinhey, J. T. The Chemistry of Aryl-lead(IV) Tricarboxylates. Reaction with Vinylogous β -Keto Esters. *J. Chem. Soc., Perkin Trans. 1* **1987**, 2689–2694.
- [24] Cazeau, P.; Duboudin, F.; Moulines, F.; Babot, O.; Dunogues, J. A new practical synthesis aldehydes and ketones. II. From α,β -unsaturated aldehydes and ketones. *Tetrahedron* **1987**, *43*, 2089–2100.
- [25] Stork, G.; Rosen, P.; Goldman, N.; Coombs, R. V.; Tsuji, J. Alkylation and Carbonation of Ketones by Trapping the Enolates from the Reduction of α,β -Unsaturated Ketones. *J. Am. Chem. Soc.* **1965**, *87*, 275–286.
- [26] Nakashima, K.; Kawano, H.; Kumano, M.; Kodama, H.; Kameoka, M.; Yamamoto, A.; Mizutani, R.; Sono, M.; Tori, M. What is the absolute configuration of (+)-crispatanolide isolated from *Makinoa crispata* (liverwort)? *Tetrahedron Lett.* **2015**, *56*, 4912–4915.
- [27] Lee, J.-H.; Cho, C.-G. H-Bonding Mediated Asymmetric Intramolecular Diels–Alder Reaction in the Formal Synthesis of (+)-Aplykurodinone-1. *Org. Lett.* **2018**, *20*, 7312–7316.

- [28] Liu, W.; Wang, B. Synthesis of (\pm)-Merrilactone A by a Desymmetrization Strategy. *Chem. Eur. J.* **2018**, *24*, 16511–16515.
- [29] Gebauer, J.; Blechert, S. Synthesis of γ,δ -Unsaturated- β -keto Lactones via Sequential Cross Metathesis-Lactonization: A Facile Entry to Macrolide Antibiotic (–)-A26771B. *J. Org. Chem.* **2006**, *71*, 2021–2025.
- [30] Rabe, P.; Klapschinski, T. A.; Brock, N. L.; Citron, C. A.; D'Alvise, P.; Gram, L.; Dickschat, J. S. Synthesis and bioactivity of analogues of the marine antibiotic tropodithietic acid. *Beilstein J. Org. Chem.* **2014**, *10*, 1796–1801.
- [31] Aoki, Y.; Mochizuki, Y.; Yoshinari, T.; Ohmori, K.; Suzuki, K. Expedient Modular Assembly of Multisubstituted Cyclohexanes via Dioxanone-Diene. *Chem. Lett.* **2011**, *40*, 1192–1194.
- [32] Effenberger, F.; Ziegler, T.; Schönwälder, K.-H. Enoether, XVI. Synthese von 4-Hydroxy-2H-pyran-2-onen. *Chem. Ber.* **1985**, *118*, 741–752.
- [33] Effenberger, F.; Ziegler, T. Diels-Alder-Reaktionen mit 2H-Pyran-2-onen: Reaktivität und Selektivität. *Chem. Ber.* **1987**, *120*, 1339–1346.
- [34] Märkl, G. Diensynthesen mit chlorierten α -Pyronen. *Chem. Ber.* **1963**, *96*, 1441–1445.
- [35] Cai, Q. The [4+2] Cycloaddition of 2-Pyrone in Total Synthesis. *Chin. J. Chem.* **2019**, *37*, 946–976.
- [36] Harde, C.; Bohlmann, F. Synthesis of 3 α -hydroxy-5 β ,10 β -epoxychilolide, an isolabdane derivative from *Chiliotrichium rosmarinifolium*. *Tetrahedron* **1988**, *44*, 81–90.
- [37] Nicolaides, D. N.; Adamopoulos, S. G.; Hatzigrigoriou, E. J.; Litinas, K. E. Synthesis and Study of 10-(4-Methoxybenzylidene)-9(10H)-phenanthrone, a Stable *ortho*-Quinone Methanide. *J. Antibiot.* **1989**, *42*, 218–222.
- [38] Zhu, H.; Meng, X.; Zhang, Y.; Chen, G.; Cao, Z.; Sun, X.; You, J. Chemoselective α -Methylenation of Aromatic Ketones Using the NaAuCl₄/Selectfluor/DMSO System. *J. Org. Chem.* **2017**, *82*, 12059–12065.
- [39] Schafroth, M. A.; Sarlah, D.; Krautwald, S.; Carreira, E. M. Iridium-Catalyzed Enantioselective Polyene Cyclization. *J. Am. Chem. Soc.* **2015**, *134*, 20276–20278.
- [40] Schafroth, M. A.; Rummelt, S. M.; Sarlah, D.; Carreira, E. M. Enantioselective Iridium-Catalyzed Allylic Cyclizations. *Org. Lett.* **2017**, *19*, 3235–3238.
- [41] Rössler, S. L.; Petrone, D. A.; Carreira, E. M. Iridium-Catalyzed Asymmetric Synthesis of Functionally Rich Molecules Enabled by (Phosphoramidite,Olefin) Ligands. *Acc. Chem. Res.* **2019**, *52*, 2657–2672.
- [42] Tsuji, J.; Takahashi, H.; Morikawa, M. Organic synthesis by means of noble metal compounds. XVII. Reaction of π -allylpalladium chloride with nucleophiles. *Tetrahedron Lett.* **1965**, 4387–4388.
- [43] Trost, B. M.; Fullerton, T. J. New Synthetic Reactions. Allylic Alkylation. *J. Am. Chem. Soc.* **1973**, *95*, 292–294.
- [44] McDonald, J. W.; Miller, J. E.; Kim, M.; Velu, S. E. An expedient synthesis of murrayaquinone A via a novel oxidative free radical reaction. *Tetrahedron Lett.* **2018**, *59*, 550–553.
- [45] Carreño, M. C.; García Ruano, J. L.; Toledo, M. A.; Urbano, A. Influence of the Sulfinyl Group on the Chemoselectivity and π -Facial Selectivity of Diels-Alder Reactions of (S)-2-(p-Tolylsulfinyl)-1,4-benzoquinone. *J. Org. Chem.* **1996**, *61*, 503–509.

Chapter 4

Synthesis of the dienes

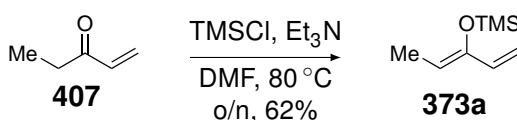
4 Synthesis of the dienes

As explained in the previous chapter, two partners are needed for the Diels-Alder reaction, a quinone and an oxygenated diene. As the desired dienes are not commercially available, work must be put into their synthesis. Their preparations are presented below.

Among the five dienes proposed for the total synthesis of momilactones, four were already reported in the literature. Nevertheless, they still need to be synthesised and the efficiency of the published protocols must be verified to validate the synthesis and the use of those dienes. Moreover, as the synthesis of diene **373b** has never been described, it will need to be designed and optimised.

4.1 Synthesis of 3-trimethylsilyloxy-penta-1,3-diene **373a**

As presented in the strategic plan, the first proposed diene, 3-trimethylsilyloxy-penta-1,3-diene (**373a**), has already been studied by several groups in Diels-Alder reactions. Several syntheses of the latter have also been reported, but the one published by Ackland and Pinhey was chosen as it gave one of the best yields.¹



Scheme 4.1: Synthesis of diene **373a**, using the method reported by Ackland and Pinhey.¹

This diene, in its *Z* configuration, is easily prepared in one step from ethyl vinyl ketone (**407**) by treatment of the latter with Et₃N and TMSCl in DMF (Scheme 4.1).

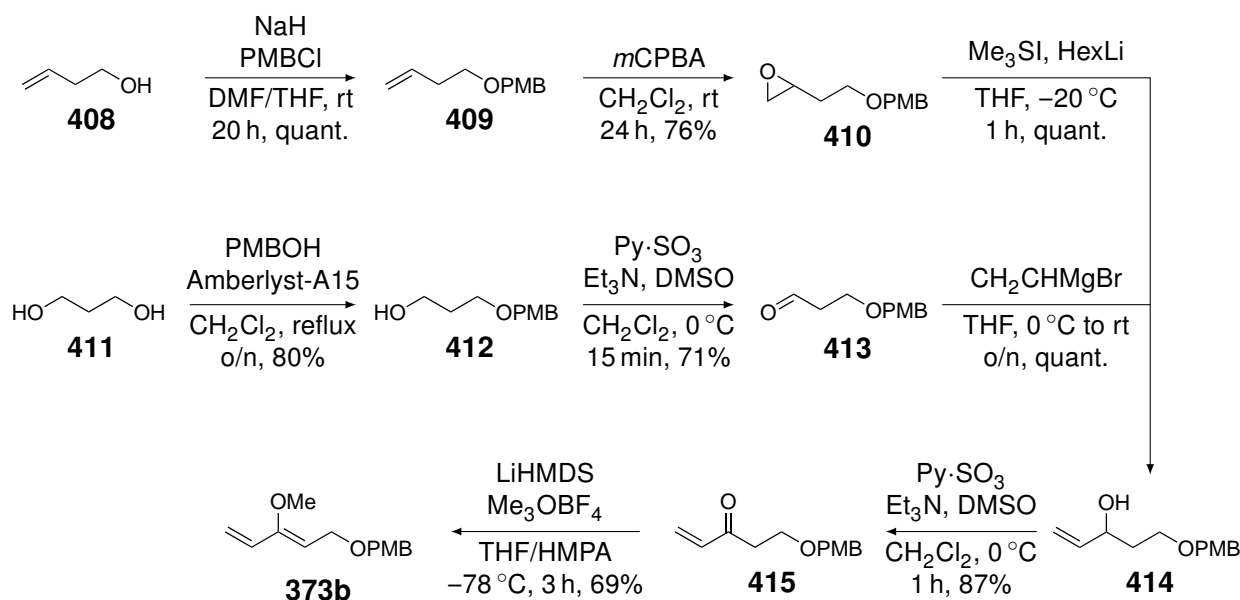
4.2 Synthesis of 1,3-dialkoxy-penta-2,4-diene **373b**

The second diene that has been designed in this project is a 1,3-dialkoxy-penta-2,4-diene **373b**. To the best of our knowledge, it has never been described and its synthesis must be developed and optimised. For that purpose, two pathways have been tried in parallel, one starting from but-3-en-1-ol (**408**) and one from propan-1,3-diol (**411**), that will converge to the same goal (Scheme 4.2).

The first pathway, from butenol **408**, starts with the protection of the alcohol with PMBCl to give intermediate **409**² and the alkene is then converted into an epoxide (**410**) with the help of *m*CPBA.³ The latter is opened by a sulfur ylide to form an allylic alcohol **414**.⁴

On the other side of the synthesis, the same intermediate **414** can be reached, starting with a monoprotection of propanediol **411** with PMBOH in acidic conditions,⁵ and the remaining alcohol of **412** is oxidised into an aldehyde (**413**) using the Parikh-Doering oxidation.⁶ That aldehyde was then converted into the same allylic alcohol **414**, as obtained in the first sequence, by the nucleophilic addition of vinylmagnesium bromide.⁷

Although both pathways were quite efficient, the first one, starting from butenol **408**, gave the best results to obtain the common intermediate **414**. The synthesis continued with the transformation of **414** into enone **415**, using once again the Parikh-Doering oxidation. The use of the same conditions as for the oxidation of **412** proved to be quite efficient as well.



Scheme 4.2: Synthetic pathways for diene **373b**, one starting from but-3-en-1-ol (**408**) and one starting from propane-1,3-diol (**411**).

The final step for the synthesis of the desired diene **373b** is the formation of the enol ether. Ideally, the diene should be synthesised in its *Z* configuration. Indeed, the *E* isomer would highly disfavour the *s-cis* conformation required for the Diels-Alder reaction. Therefore, the conditions used were inspired from the work of Xie and Saunders who developed a method for the selective synthesis of *Z* silyl enol ethers.⁸ However, a more robust enol ether is desired in our case and we decided to orientate the synthesis towards a methyl enol ether. For that purpose, Me_3OBF_4 has been chosen as electrophile as it should be more selective for the *O*-alkylation^{9,10} than alkyl halides or dialkyl sulfates, that would rather lead to the *C*-alkylation.^{11–13}

We scrupulously followed the procedure of Saunders and diene **373b** was obtained with a 69% yield. The configuration of the diene was then verified *via* n.O.e analyses (Figure 4.1), which indicated a correlation between both vinylic protons, as well as a correlation between the allylic methylene and the methyl group of the enol ether. We were confident that the *Z* isomer was obtained as those correlations are consistent with that isomer.

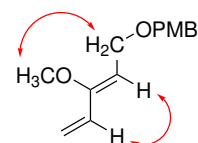


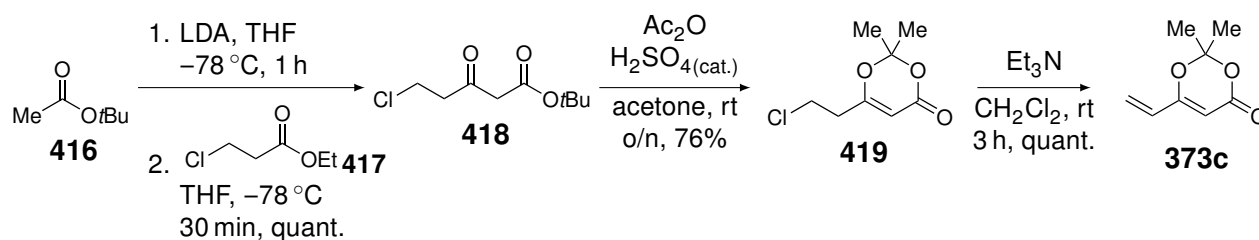
Figure 4.1: n.O.e correlations for diene **373b**.

4.3 Synthesis of penta-2,4-dienoates **373c** and **373d**

The next two dienes to be tested in the Diels-Alder reaction, as described in the previous chapter, are dienes **373c** and **373d** that are two penta-2,4-dienoates.

4.3.1 Preparation of 6-vinyl-1,3-dioxin-4-one **373c**

For this third diene, the first intermediate, 5-chloro-3-oxopentanoate **418**, was prepared according to a procedure described by the group of Ohta *et al.* (Scheme 4.3).¹⁴ It consisted in a Claisen condensation between *tert*-butyl acetate (**416**) and the 3-chloropropanoate **417**. This reaction was really efficient as chloropentanoate **418** was obtained with a quantitative yield and did not require any purifications.

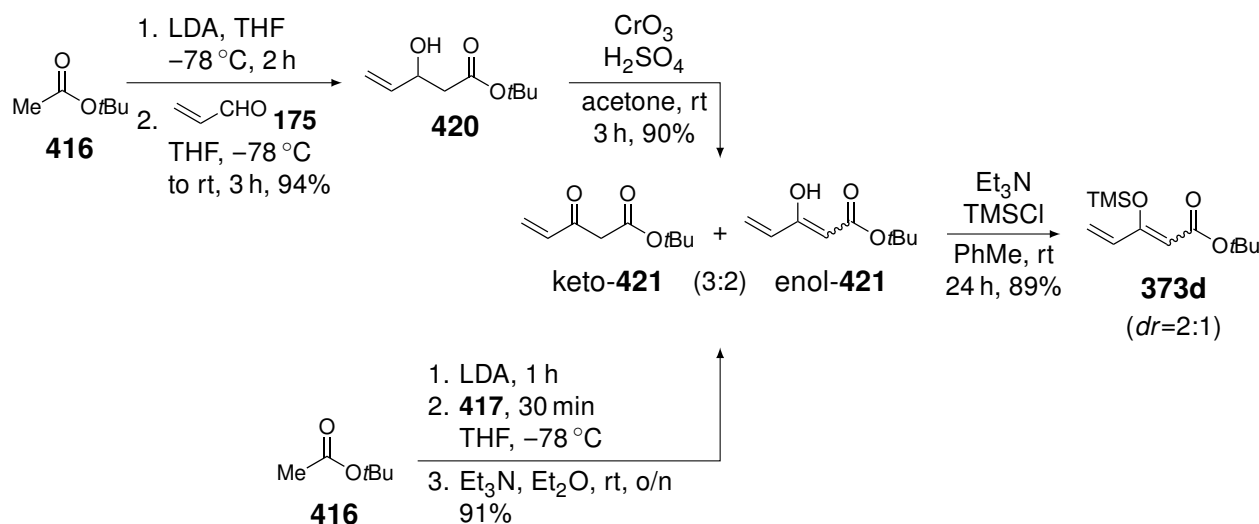


Scheme 4.3: Synthetic pathway used to reach diene **373c** according to described procedures.^{14,15}

The next step was the formation of the acetonide **419** that was described by Blechert *et al.*¹⁵ This reaction was performed using acetic anhydride and a catalytic amount of sulfuric acid in acetone. Intermediate **419** was uneventfully isolated with a 76% yield. Finally, the elimination of the chlorine atom quantitatively afforded the desired diene **373c**.

4.3.2 Preparation of 3-silyloxy-penta-2,4-dienoate **373d**

The diene **373d** was reported by the group of Dickschat *et al.* (Scheme 4.4)¹⁶ In their work, they synthesised the latter starting with an aldol condensation between *tert*-butyl acetate and acrolein (**175**). They then oxidised the β -aldol into the 3-oxopent-4-enoate **421** with chromium(VI) oxide. In this thesis, the route described by Ohta *et al.* was chosen as it starts with the same reaction as for the synthesis of diene **373c** (Scheme 4.3).¹⁴ The difference here is that the chloropentanoate **418** is not isolated and is directly engaged in an elimination reaction, after the work up of the Claisen condensation, giving the pentenoate **421** with a good yield (a 3:2 mixture of the keto and enol forms was observed by NMR in CDCl₃).



Scheme 4.4: Synthetic sequence for the synthesis of diene **373d**. The pathway from acrolein (**175**) was reported by Dickschat *et al.*,¹⁶ while the pathway used in this thesis, for the synthesis of **421** started from chloropentanoate **417** as described by Ohta *et al.*¹⁴

The last step of this synthesis was the formation of the silyl enol ether using Et₃N and TMSCl. Initially, this reaction was described in benzene as solvent, but performing it in toluene gave the same product with a similar yield. As described by Dickschat's group, the diene was isolated in a 2:1 mixture of both *E* and *Z* isomers (the assignment of the major and minor isomers was not done).

4.4 Synthesis of α -pyrone **373e**

As presented in Chapter 3, the fifth, and peculiar, diene **373e**, an α -pyrone, was also chosen as it is the most interesting one, and probably the most ambitious one, for the total synthesis. Indeed, if this diene proves to be efficient in the Diels-Alder reaction, it would allow the insertion of the oxidised carbon atom, needed for the 4,6-transannular γ -lactone of the natural compounds, on the same face as the angular methyl group (Scheme 3.10).

To the best of our knowledge, the synthesis of that specific pyrone has only been described by the group of Effenberger. It was also used as a diene in a Diels-Alder reaction with maleic anhydride two years later.^{17,18}

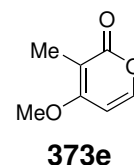
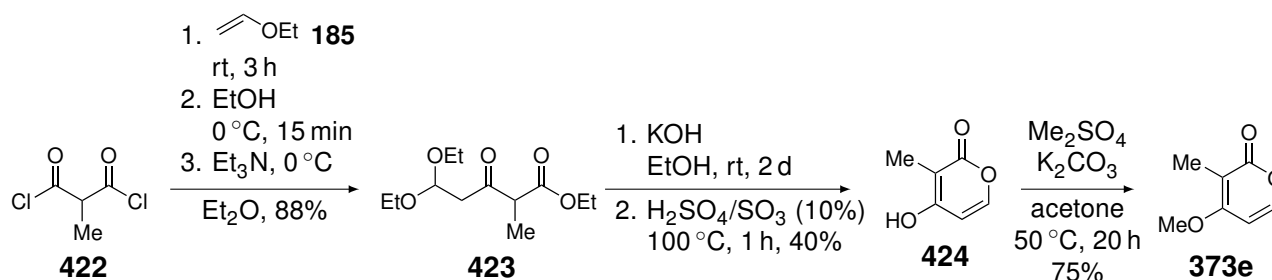


Figure 4.2: Structure of pyrone **373e**.

4.4.1 Effenberger's synthesis

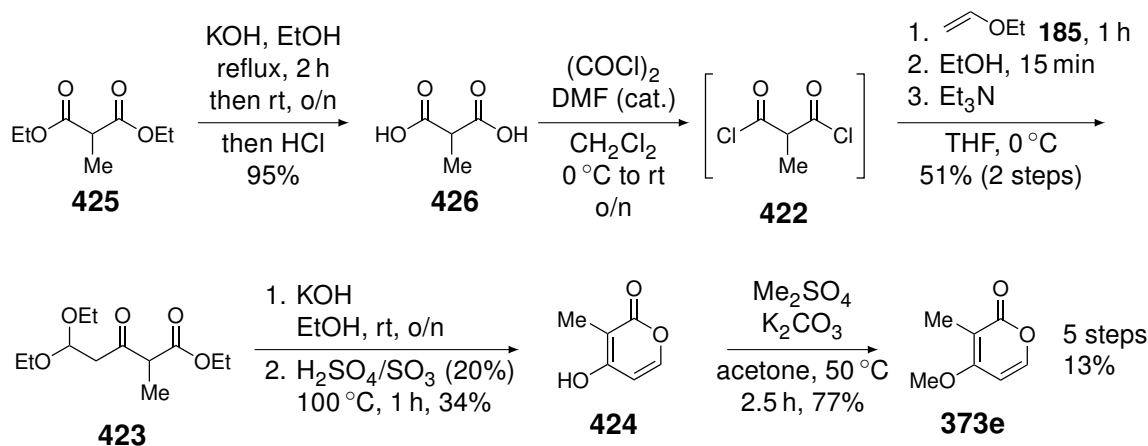
The synthetic route reported by Effenberger *et al.* started with 2-methylmalonyl chloride (**422**) which was treated by ethyl vinyl ether (**185**) at room temperature in diethyl ether (Scheme 4.5).¹⁷ Ethanol was then added to the solution at 0 °C, followed by the quench of the reaction with triethylamine, to give the oxopentanoate **423** with a 88% yield. The latter was then submitted to a basic hydrolysis for two days. The solvent was removed and the intermediate carboxylate was treated with fuming sulfuric acid (10% SO₃) at 100 °C to yield hydroxypyronone **424**. Finally, methylation of the hydroxy group gave pyrone **373e** with a 75% yield.¹⁸



Scheme 4.5: Synthetic pathway of α -pyrone **373e** as reported by Effenberger *et al.*^{17,18}

As that synthesis seemed to be quite efficient, we tried to reproduce it. Unfortunately, none of the standard chemical suppliers used in our laboratory provided malonyl chloride **422**. Therefore, that reagent needed to be synthesised as well.

The new synthesis started with the saponification of diethyl 2-methylmalonate (**425**) using potassium hydroxide in ethanol (Scheme 4.6) as reported by Ng and McMorris.¹⁹ The same article also presented the transformation of diacid **426** into its diacyl chloride equivalent **422** using thionyl chloride, in toluene, as a chlorinating agent. However, it was preferred to replace thionyl chloride by oxalyl chloride with a catalytic amount of DMF, in dichloromethane, as proposed by Körner and Hiersemann on a similar substrate.²⁰ Indeed, in the first conditions, diacyl chloride **422** needed to be distilled at very low pressures as the temperature could not go over 45 °C. In the second conditions, removal of dichloromethane and the excess of oxalyl chloride could be performed at room temperature with a rotary evaporator. This way, malonyl chloride **422** could be used in the next step without any further purification.



Scheme 4.6: Synthetic pathway for α -pyrone **373e** performed in our group.

Diacyl chloride **422** was then engaged in the same reaction as described by Effenberger. However, it was observed that better yields were obtained if all the steps of the reaction, including the addition of ethyl vinyl ether (**185**), were performed at 0 °C. Another issue that was not anticipated in that reaction was the low purity of the oxopentanoate **423** in the crude mixture, as the group depicted the product as pure without any purification. The only way to gain some purity for this compound was to use flash chromatography on demetallated²¹ and neutralised²² silica gel (otherwise, more than 70% of the product was lost during the chromatography). Nevertheless, the purification remained complex as a lot of side products were present. It was suspected that those undesired products came from the difficulty to differentiate both acid chlorides of malonyl **422**. But, given the problems encountered, it was still possible to isolate oxopentanoate **423** with a 51% yield from diacid **426**.

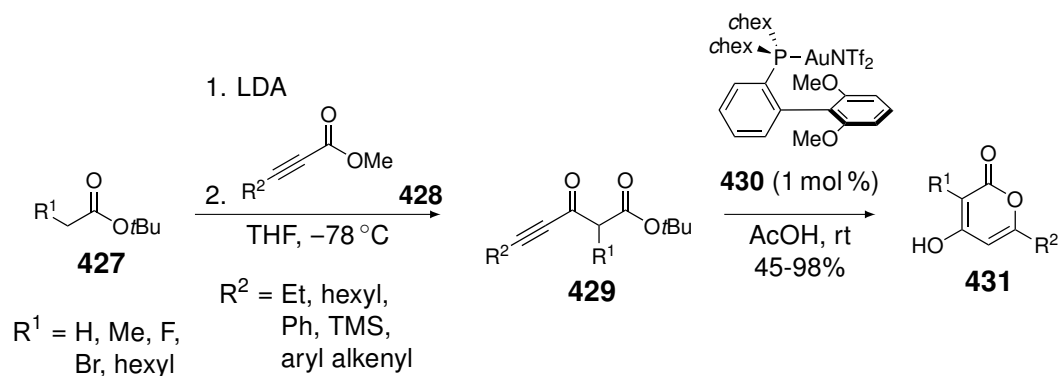
Finally, the two last steps were performed as described by Effenberger. Pentanoate **423** was hydrolysed with KOH, but one night instead of two days, and the resulting carboxylate was treated with fuming sulfuring acid (with 20% SO₃ instead of 10%), giving hydroxypyrone **424** with a 34% yield. The latter was then methylated using dimethyl sulfate and potassium carbonate to give the desired methoxypyrone **373e** with a 77% yield.

Even though the yields were similar to the ones reported by Effenberger *et al.*, the sequence was a bit long and the overall yield (13%) rather low for such a small molecule. Therefore, it was decided to try and find a more suitable pathway with a lower amount of steps and a higher overall yield.

4.4.2 Metal-catalysed cyclisation of 3-oxopent-4-ynoates

Among the publications reporting the synthesis of 4-hydroxypyrone derivatives, the group of Fürstner *et al.* presented a general method based on a gold-catalysed cyclisation of 3-oxopent-4-ynoates **429** (Scheme 4.7).^{23,24}

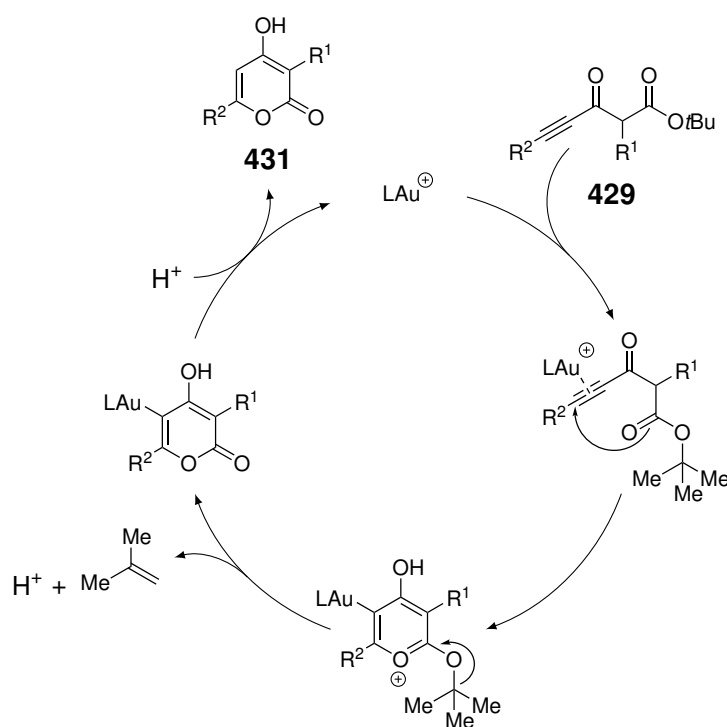
In their study, they worked on substrates, either commercially available or prepared by a Claisen condensation of esters **427** and alkynoates **428**, bearing various types of substituents such as alkyl groups and halides for ester **427** (R¹) and alkyl, phenyl, TMS or an aryl alkenyl group for alkynoate **428** (R²).



Scheme 4.7: Synthesis of 4-hydroxy-2-pyrones **431** via a gold-catalysed cyclisation of 3-oxopent-4-ynoates **429**.²³

The group determined the best catalyst was the SPhos-AuNTf₂ complex **430** and the reaction was conducted with 1 mol % of the catalyst in acetic acid as solvent. Among the tested substrates, most of them gave 4-hydroxy-2-pyrones **431** with very good to excellent yields (82-98%). The only counter-example was the one bearing the TMS group on the alkyne (45%), which is not surprising given the sensitivity of the silyl groups towards acidic media.

Alongside their results, they proposed a plausible catalytic cycle for the reaction (Scheme 4.8). It starts with the coordination of the gold catalyst by the triple bond, which increases the electrophilicity of the latter. Then, the ester group attacks the triple bond to form the cycle in a 6-*endo*-dig manner. The pyrone pattern is later obtained by elimination of the *tert*-butyl group and proto-deauration.



Scheme 4.8: Proposed catalytic cycle for the gold-catalysed cyclisation of 3-oxopent-4-ynoates **429** into 4-hydroxy-2-pyrones **431**.²³

Given the good results of that new cyclisation for the synthesis of 4-hydroxy-2-pyrones, they applied their new strategy to the synthesis of Neurymenolide A (**432**), a macrolide isolated from a red alga of the Fiji, containing the hydroxypyronone pattern (Figure 4.3).

In 2014, the same strategy, using a gold catalysis, was applied by Lee *et al.* for the synthesis of (+)-violapyrone C (**433**) and violapyrone I (**434**)²⁵ and by Liu *et al.* for the synthesis of wailupemycin G (**435**).²⁶ More recently, Yang and co-workers also used that gold-catalysed cyclisation to synthesise various 4-*O*-glycosylated 2-pyrones **436** with moderate to good yields.²⁷

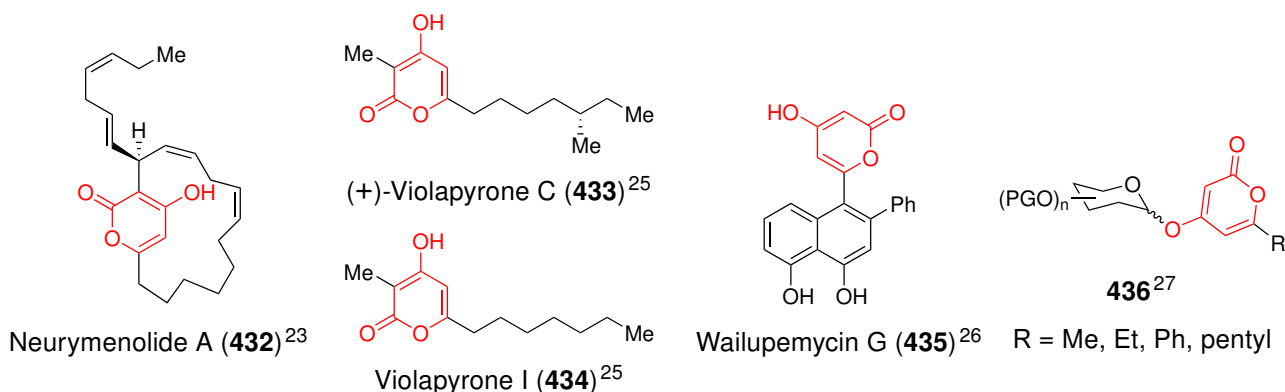
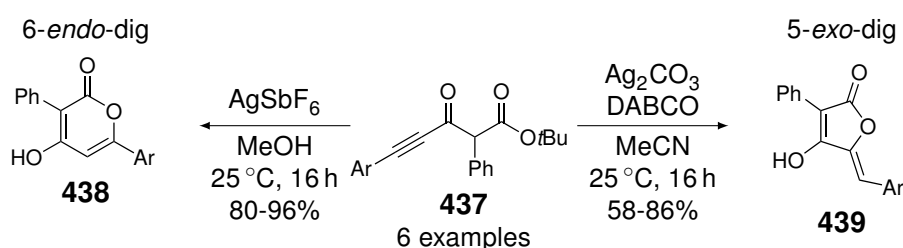


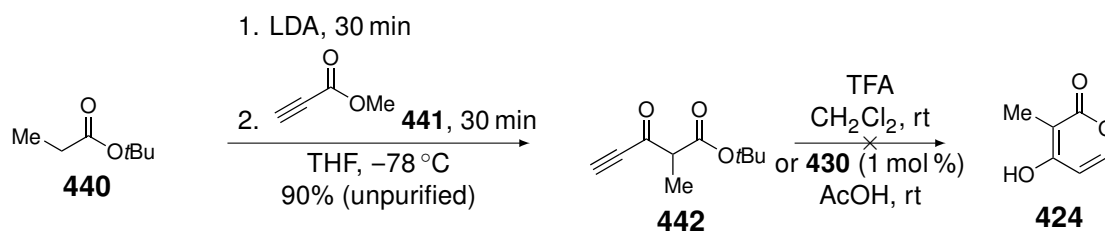
Figure 4.3: Structures of four natural compounds (**432-435**) and sugar derivatives **436** containing the 4-hydroxy-2-pyrone pattern (highlighted in red) synthesised by a gold-catalysed cyclisation of a 3-oxopent-4-ynoate derivative.

Similarly, another group performed the same type of cyclisation using silver catalysts on 3-oxopent-4-ynoate bearing aryl substituents (Scheme 4.9).²⁸ On one hand, they could reach 4-hydroxy-2-pyrones **438**, corresponding to a 6-*endo*-dig cyclisation, by using AgSbF_6 in methanol with good to excellent yields. On the other hand, when they switched the catalytic system to silver carbonate in acetonitrile, in the presence of DABCO as a base, they obtained the 4-hydroxy-2-furanones **439**, predominantly under the *Z* isomer form.



Scheme 4.9: Silver-catalysed cyclisation of 3-oxopent-4-ynoates **437** into the corresponding 4-hydroxy-2-pyrones **438** or 4-hydroxyfuran-2-ones **439**.²⁸

Given those promising results reported in the literature, we decided to carry out the same type of reaction to the desired pyrone **373e**. For that specific compound, a hydrogen atom is needed on the alkyne. Therefore, methyl propiolate (**441**) should be used (Scheme 4.10). The sequence first starts with the Claisen condensation between *tert*-butyl propionate (**440**) and methyl propiolate (**441**). The 3-oxopent-4-ynoate **442** was obtained uneventfully with a 90% yield. Unfortunately, any attempt to purify that intermediate turned out to be unsuccessful. Even a simple filtration over silica gel led to the complete degradation of the compound. Nevertheless, its purity was sufficient to be engaged in the next reaction as such.

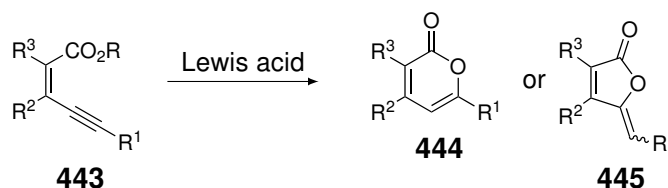


Scheme 4.10: Synthetic sequence for hydroxypyrrone **424**, using the gold catalysis strategy on oxopentynoate **442**.

We first tried to perform the cyclisation using trifluoroacetic acid (TFA) in dichloromethane. Indeed, besides the use of Lewis acids, increasing the electrophilicity of an alkyne should also work with the use of Brønsted acids.²⁹ The concentration of TFA was gradually increased but the only reaction observed was the partial loss of the *tert*-butyl group. The reaction was finally attempted with TFA as solvent but, in those conditions, a complex mixture was obtained.

The next attempt was to use the gold catalyst **430** in acetic acid but, unfortunately, even in the optimal conditions described by Fürstner,²³ the formation of the desired hydroxypyrrone **424** was not observed.

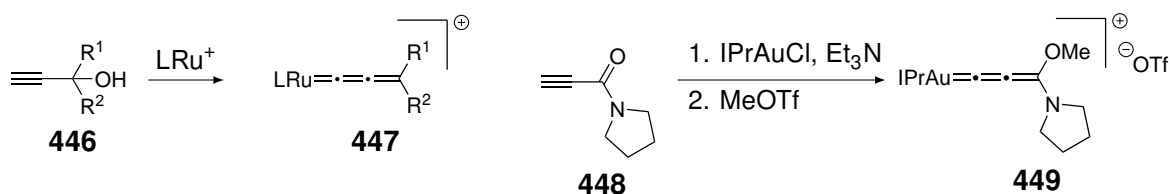
Indeed, none of the groups previously cited presented the synthesis of such 4-hydroxy-2-pyrone with terminal alkyne moiety. By looking up in the literature, such Lewis acid catalysed cyclisations were already described on pent-2-en-4-ynoic acids (**443**), leading to either the 2-pyrones **444** or the 2-furanones **445** (Scheme 4.11). The first example was described in 1964 by the group of Serratosa³⁰ and several groups reported the same type of synthesis throughout the years.^{31–36} However, none of the reported syntheses of 2-pyrones, *via* that method, used terminal alkyne derivatives, and the only examples of pent-2-en-4-ynoic acids with a terminal alkyne led to the 2-furanone derivatives **445**.^{37,38} It was then supposed that the lack of substitution on the alkyne must play a role in the lack of reactivity of oxopentynoate **442**.



Scheme 4.11: Synthesis of 2-pyrones **444**, and their 2-furanone isomer **445**, *via* the cyclisation of pent-2-en-4-ynoic acids **443**.

A hypothesis for that lack of reactivity would be the possible formation of an allenylidene gold complex. Indeed, in 1992 Trost and Flygare suggested the formation of such a complex as an intermediate in the ruthenium catalysed coupling of prop-2-yn-1-ols (being a terminal alkyne) with allylic alcohols (Scheme 4.12).³⁹ A few years later, Fürstner employed that phenomenon to develop new cationic ruthenium allenylidene complexes as precatalyst for ring closing metathesis.^{40,41}

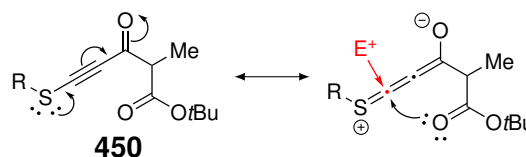
More recently, another group reported the first preparation of a stable gold-allenylidene complex **449** (Scheme 4.12).⁴² They obtained that complex by treating IPrAuCl with propiolamide **448** under basic conditions. The intermediate gold-acetylide was then treated with MeOTf to give the stable gold-allenylidene complex **449**.



Scheme 4.12: Formation of metal allenylidene complexes: from ruthenium and propynol derivatives **446** (left)^{39–41} and from gold and propiolamide **448** (right).⁴²

The formation of such a complex, that occurs with terminal alkynes, might be possible in our case and might explain the lack of reactivity of **442**. Given those metal-allenylidene complexes appeared to be stable, it might quench the expected reactivity in our case (Scheme 4.10), even though we had no evidence for the formation of such a complex.

Despite the lack of success of the catalysed cyclisation of oxopentynoate **442**, it was decided not to give up on that strategy. As the absence of substitution on the alkyne does not allow the reaction to occur, the addition of a substituent, that would be easily removed afterwards, might solve this issue. To that purpose, the use sulfides has been envisaged.



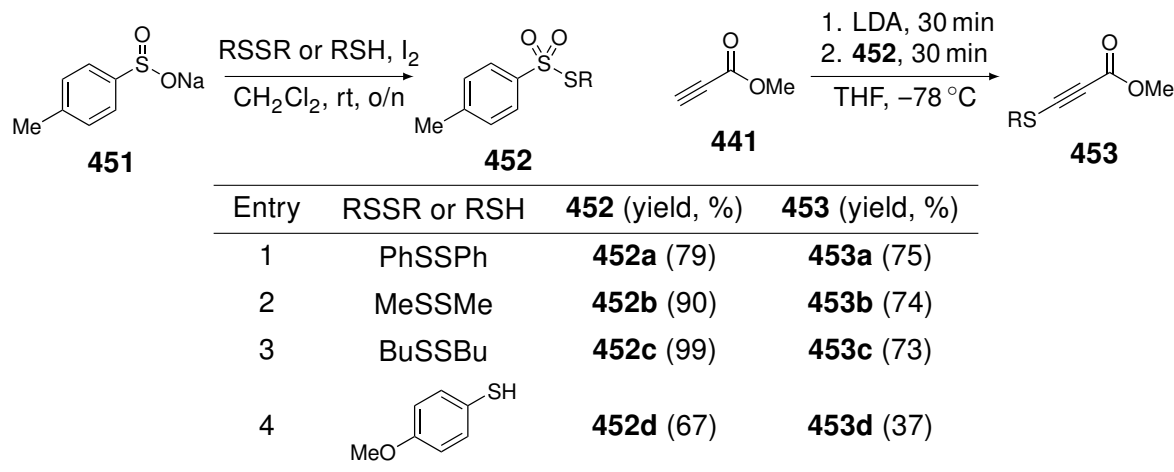
Scheme 4.13: Resonance form of 3-oxo-5-thiopent-4-ynoates **450** highlighting the increased electrophilicity on the C5 position.

The use of such sulfide substituents has several advantages. They should be easily inserted onto the alkyne as multiple forms of electrophilic sulfide derivatives are available or can be prepared in very few steps. The removal of the sulfide groups at the end of the pyrone synthesis, using Raney nickel, should also be feasible without any issue. Moreover, its electron donating property should also help the reaction to occur as it should increase the electrophilicity of the triple bond on the C5 position of the oxopentynoate **450** (as highlighted in the resonance form in Scheme 4.13).

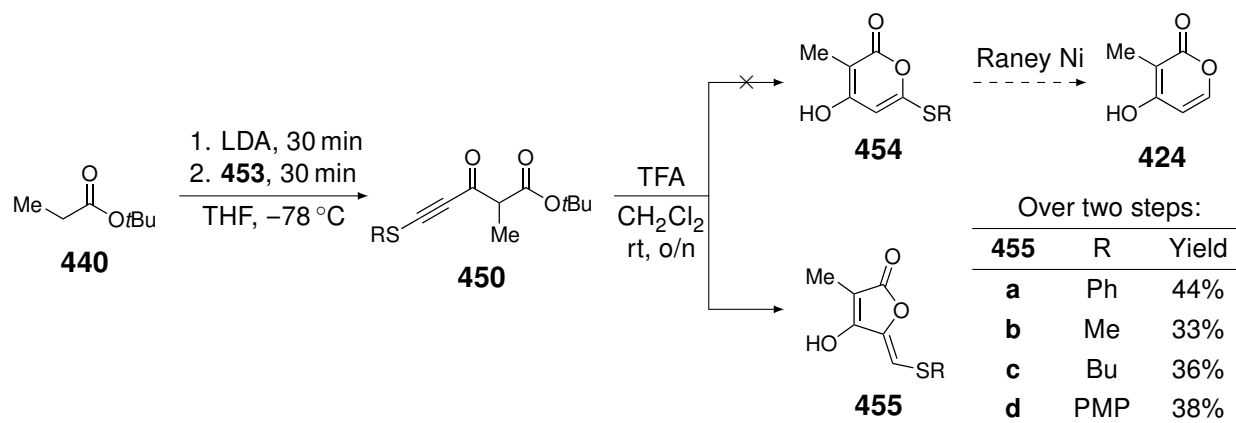
In order to prepare such 3-oxo-5-thiopentynoates (**450**), diverse electrophilic sulfide derivatives, namely thiosulfonates (**452**), were chosen as they are easily prepared in one step from sodium *para*-tolylsulfinate (**451**) and disulfides (Table 4.1), as reported by Fujiki *et al.*⁴³ Moreover, both those reagents were already available in the laboratory.

The reactions were easily carried out by mixing sulfinate **451**, the corresponding disulfide and iodine. Diphenyl, dimethyl, and dibutyl disulfide led to the synthesis of the thiosulfonates **452** with good to excellent yields (entries 1-3). In the last case (entry 4), however, the disulfide derivative was not available and its thiophenol equivalent was used. Similarly to the previous examples, the same conditions were employed. Indeed, the use of iodine will first generate the corresponding disulfide *in situ*.⁴⁴ The reaction will directly continue to the formation of thiosulfinate **452d** with a good yield.

After the preparation of the electrophilic sulfides, they could be used to insert the sulfide group on propiolate **441**. The sulfonylation was carried out following a slightly modified procedure described by Minkata *et al.*⁴⁵ It consisted in deprotonating propiolate **441** with LDA, followed by the nucleophilic substitution on thiosulfonates **452**. From that reaction, 3-thiopropiolates **453a-c** were obtained with good yields (entries 1-3). On the other hand, the use of thiosulfonate **452d** (entry 4), gave the desired 3-thiopropiolate **453d** but with a more moderate yield.

Table 4.1: Preparation of thiosulfonates **452** and their use as electrophiles to synthesise 3-thiopropiolates **453**.

Then, the synthesis could continue with the Claisen condensation between 3-thiopropiolates **453** and propionate **440** (Scheme 4.14). Those condensations were performed with the same procedure that was applied with propiolate **441** (Scheme 4.10). Similarly to 3-oxopentynoate **442**, any attempt to purify the 3-oxo-5-thiopentynoates **450** resulted in their complete degradation, even with the use of demetallated and neutralised silica gel. Therefore, after treatment of the reaction mixture and evaporation of the solvent, the crude product was directly engaged in the next step.

Scheme 4.14: Planned sequence for the synthesis of hydroxypyrene **424** from 3-thiopropiolates **453** and yields of the obtained 4-hydroxy-5-thiomethylenefuran-2-ones **455** via that sequence.

As described earlier, it was first tried to perform the cyclisation using a Brønsted acid, such as TFA, as it should already be able to increase the electrophilicity of the alkyne. Interestingly enough, using such conditions led to the formation of a clear precipitate that could simply be filtered off to afford a pure product with moderate yields between 33 and 44%.

Initially, the first example was done with the phenylthio group and it was thought the desired 4-hydroxy-5-phenylthio-2-pyrone **454a** had been obtained. Indeed, the chemical shifts in the ^1H NMR spectrum were consistent with that structure. Nevertheless, the compound was easily crystallised and was submitted to an X-ray analysis for structure confirmation (Figure 4.4). Unfortunately, it turned out the structure of the isolated compound was not the expected pyrone **454a**, that would have come from a 6-*endo*-dig cyclisation, but its 5-methylene-2-furanone isomer **455a**, that came from a 5-*exo*-dig cyclisation.

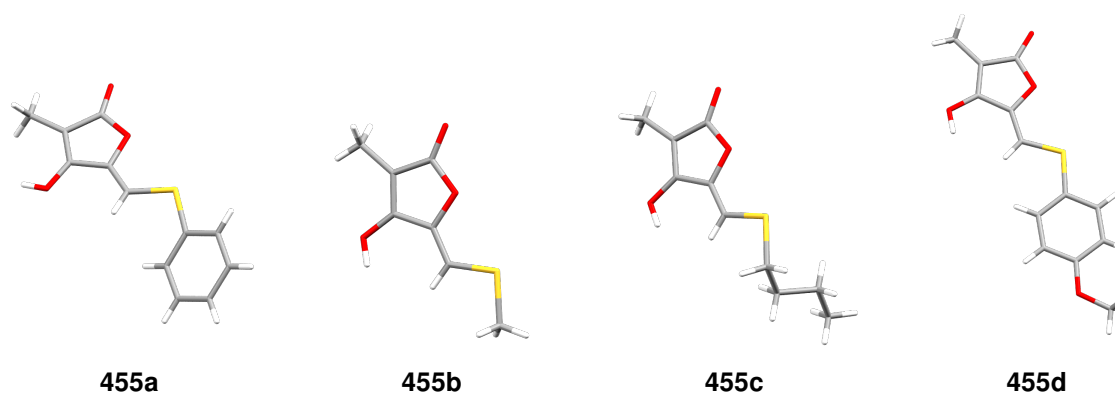


Figure 4.4: X-ray structures of the four 4-hydroxy-5-thiomethylenefuran-2-ones **455** obtained with the reaction sequence described in Scheme 4.14.

Given those results, it was supposed that the presence of the phenyl group, to which the sulfur atom is conjugated, decreased its electron donating contribution towards the alkyne and would therefore lower its ability to increase the electrophilicity of the latter. It was then imagined that replacing the phenyl group with an alkyl group, such as a methyl or a butyl group, could help the sulfur atom to increase its electron donating effect towards the alkyne. Nonetheless, the analogous furanones **455b** and **455c** were obtained as well, as proven by their X-ray structures (Figure 4.4). A last attempt was done by using the *para*-methoxyphenyl group which should highly increase the electron donating effect of the sulfur atom but, once again, the 5-*exo*-dig cyclisation occurred.

Despite the fact that the desired pyrones **454** were not obtained, it is to be noticed that all four of the synthesised 4-hydroxy-5-thiomethylene-2-furanones possess a *Z* configuration for the alkene, as revealed by their X-ray structures.

Given that modifying the substituent on the sulfur atom had no effect on the regioselectivity of the cyclisation, the electronic properties of the alkyne must have little effect. It is most likely that the conformation of the reagent has the highest impact as it is the case for the Baldwin rules. In 2011, Alabugin *et al.* revised and extended those rules for the cyclisation of an anionic nucleophile on an alkyne.⁴⁶ They reported that the activation energy barrier of the 6-*endo*-dig cyclisation is much higher than for the 5-*exo*-dig pathway. This difference in energy is mostly due to a shorter distance of the nucleophilic oxygen atom to the internal carbon atom of the alkyne.

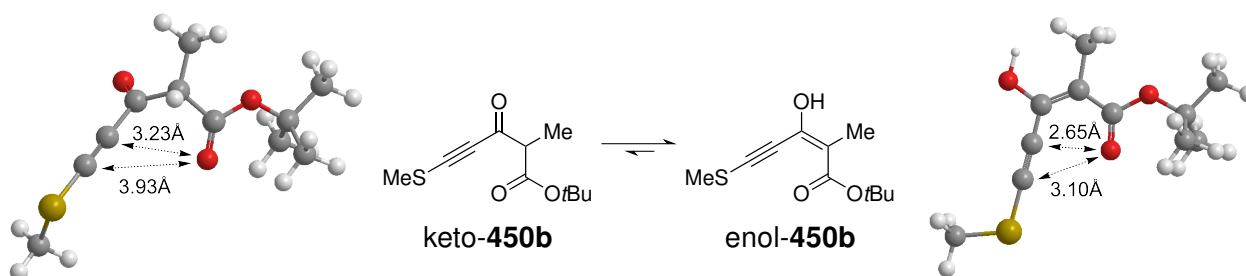


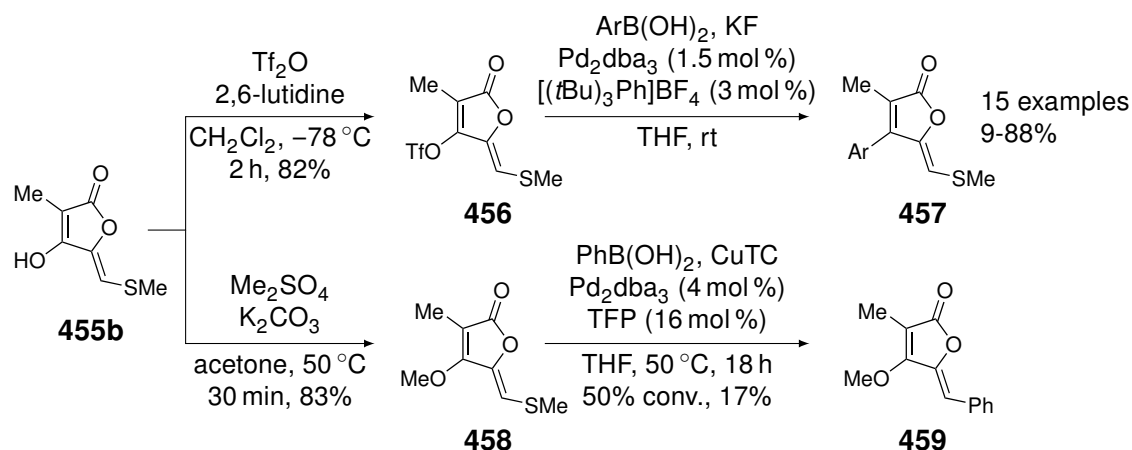
Figure 4.5: Keto-enol equilibrium of methylthiooxopentynoate **450b** and modelled structures of its ketone and enol forms with the distances between the oxygen atom of the ester and both carbon atoms of the alkyne.

Indeed, when both ketone and enol forms of the 5-methylthio-3-oxopent-4-ynoate **450b** were modelled and their conformation was optimised, using the MM2 energy-minimisation of the Chem3D software, it was highlighted in both forms that the oxygen atom of the ester group was closer to the internal carbon atom of the alkyne than to the external one. Although it was determined using a simple optimisation rather than an advanced calculation method, it could already give a good idea of the difference in distance in each case.

In order to favour the 6-*endo*-dig cyclisation, the gold or silver catalysis, as described by the different groups presented earlier, should be used. The regioselectivity observed with those cases could be explained by the formation of a gold complex leading to the most stabilised carbocation, as suggested by Fürstner.⁴⁷ In the case of our 5-methylthio-3-oxopent-4-ynoates **450**, such a carbocation, stabilised by gold, would be on the C5 position. However, it was decided not to use a gold- or silver-catalysed reaction as the presence of the sulfur atom might poison the catalysts. We therefore preferred to change our strategy.

Nevertheless, the synthesised 3-oxo-5-thiomethylene-2-furanones **455** seem to be interesting compounds with a rather exotic pattern, and only a few examples are reported in the literature.^{48–56} Therefore, it would be interesting to study them further.

A master student in our lab did this by converting the furanone **455b** into the corresponding triflate **456**.⁵⁷ He then performed Suzuki coupling reactions⁵⁸ with different arylboronic acids, and he obtained fifteen examples of aryl derivatives **457** with yields ranging from very low to very good. On the other hand, he also methylated **455b** and tried to optimise Liebeskind-Srogl coupling reactions (coupling reactions with thioethers as leaving groups) on **458** with phenylboronic acid.⁵⁹ Unfortunately, in this last case, the student could only reach a maximum conversion of 50% and isolate the phenylmethylene-furanone **459** with a 17% yield.



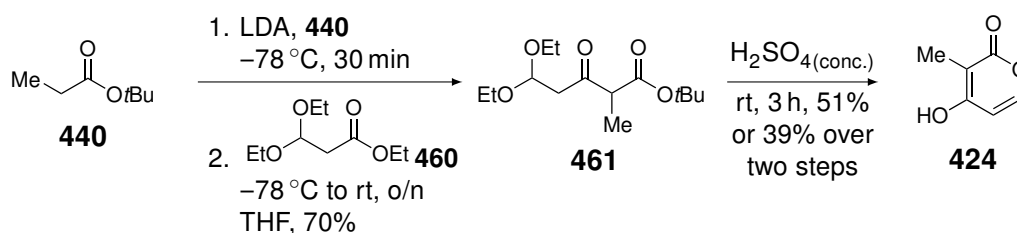
Scheme 4.15: Synthetic pathways of triflate **456** and methoxy **458**, both prepared from **455b**, Suzuki coupling reactions of triflate **456** with arylboronic acids⁵⁸ (top) and the Liebeskind-Srogl coupling reaction⁵⁹ of **458** with phenylboronic acid (bottom).⁵⁷

4.4.3 Third strategy for the synthesis of pyrone **373e**

Our initial strategy provided pyrone **373e** with a rather long sequence (Scheme 4.6), for a such a small molecule, and a low overall yield, probably due to the need to differentiate both carbonyl groups of the malonyl reagent, even though it was described as successful by Effenberger *et al.* (Scheme 4.5).¹⁷

The second strategy, reported by Fürtsner *et al.* for the synthesis of 4-hydroxypyrrone (Scheme 4.7),²³ was quite promising but did not work with an unsubstituted alkyne (Scheme 4.10). The addition of a sulfide group on the alkyne, that was easy to insert and should have been easy to remove, led to the undesired 5-*exo*-dig cyclisation.

However both strategies presented advantages. The first one, using a dialkoxyoxopentanoate, such as **423**, avoided the regioselectivity issues in the cyclisation and only led to the formation of the six-membered cycle. The second one, using a Claisen condensation to form the precursor of the cyclisation, avoided the differentiation issue. Therefore, a step backwards was taken to rethink the synthesis of the desired **373e**. For our third strategy, we thought to use a Claisen condensation between *tert*-butyl propionate (**440**) and an ester already bearing the acetal group such as **460** (Scheme 4.16).



Scheme 4.16: Third strategy for the synthesis of hydroxypyrrone **424**, using a Claisen condensation between propionate **440** and 3,3-diethoxypropionate **460**, followed by the cyclisation in sulfuric acid.

We found that the best conditions were to start the Claisen condensation at low temperatures and to slowly warm the mixture up to room temperature overnight. Indeed, keeping the reaction at low temperature led to an incomplete conversion of the starting materials and warming it up too quickly led to the formation of undesired side products. But applying those conditions gave the desired β -ketoester **461** with a 70% yield. However, to achieve such a yield, demetallated and neutralised silica gel had to be used during purification to avoid a drop in yield.

Then, the cyclisation reaction to reach hydroxypyrrone **424** was first attempted using TFA at different concentrations, and also as solvent, but the only product obtained was the partial removal of the *tert*-butyl group. We then decided to use concentrated sulfuric acid, as used by Effenberger in its synthesis.¹⁷ Those conditions gave the best results as **424** was obtained with a 51% yield. The main advantage of the use of a *tert*-butyl ester is its deprotection in acidic media, whereas the ethyl ester needed a basic hydrolysis first.

It is worth noting that oxopentanoate **461** may also be directly engaged in the cyclisation step without any further purification. In doing so, a 39% yield over two steps was achieved. This would correspond to the overall yield reported by Effenberger for the synthesis of hydroxypyrrone **424** (Scheme 4.5), but with a sequence one step shorter as the basic hydrolysis of the ester group is no longer necessary. Moreover, compared to the sequence that had to be used in our case (Scheme 4.6), this one is three steps shorter and the overall yield was more than doubled. Even more interestingly, no chromatography was needed as **424** was obtained pure using a simple trituration in dichloromethane.

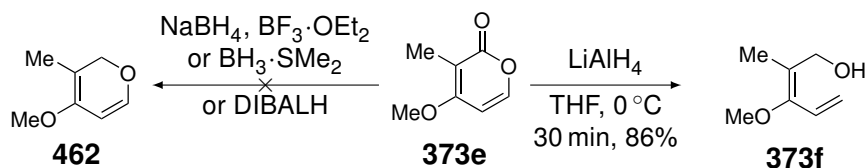
Consequently, it was possible to develop a shorter and more efficient synthesis sequence for 4-hydroxypyrrones that gave an analytical sample. In order to validate the efficiency of that method, it could be applied to other substrates with various substituents in order to enlarge the scope of that strategy.

In the meantime, it was possible to achieve a multigram scale synthesis of 4-methoxypyrene **373e**, after the methylation of hydroxypyrene **424** following the procedure described in Scheme 4.5, to study the Diels-Alder reaction with sulfinylquinone **318a**.

4.5 Synthesis of a new diene by reduction of α -pyrone **373e**

In the course of this thesis, it was also attempted to reduce pyrone **373e** into its pyran derivative **462**. Indeed, given the aromaticity of pyrone **373e**, a lower reactivity in a Diels-Alder reaction was expected. Therefore, pyrone **373e** was submitted to reduction reactions (Scheme 4.17).

The first reducing agent that was tested was sodium borohydride in combination with $\text{BF}_3 \cdot \text{OEt}_2$. However, this method was described on benzochromenone and not on pyrones.^{60,61} Unfortunately, no reaction occurred with that reagent. A similar reagent, $\text{BH}_3 \cdot \text{SMe}_2$, has been attempted as it was used for the desired transformation on coumarins and benzochromenones,^{62,63} but it did not work on our pyrone **373e**. It was then decided to increase the strength of the reducing agent by using DIBALH, which was used to perform a similar transformation on pyranonaphthyl or benzochromenone.^{64,65} But, again, it was never described on pyrones and was still not strong enough to reduce pyrone **373e** into the desired pyran **462**.



Scheme 4.17: Reduction of α -pyrone **373e**, leading to the new diene **373f**.

Finally, LiAlH_4 , that was described on coumarins and iscoumarins,^{66,67} was employed and, in that case, a reaction occurred. However, the product obtained was not the desired pyran **462** but its opened form **373f**. To the best of our knowledge, that compound had never been described and it was decided to include it in the list of the dienes to be tested in Diels-Alder reactions. However, before using that diene, its configuration had to be determined. Similarly to diene **373b**, an n.O.e analysis was performed.

This analysis showed correlations between the allylic methylene and one vinylic proton, between the vinylic methyl group and the methoxy group, and between the methoxy group and one of the terminal vinylic protons. Those correlations indicated the *E* isomer had been obtained, corresponding to a retention of the double bond configuration with respect to that in the pyrone **373e**. Moreover, the n.O.e response for those signals was quite intense, indicating that the conformation presented in Figure 4.6 must be the most favoured one.

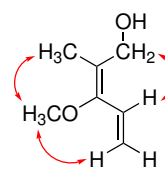
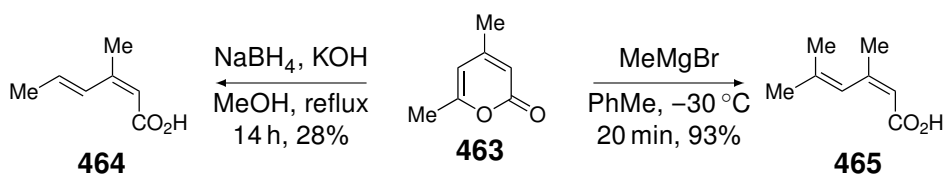


Figure 4.6: n.O.e correlations for diene **373f**.

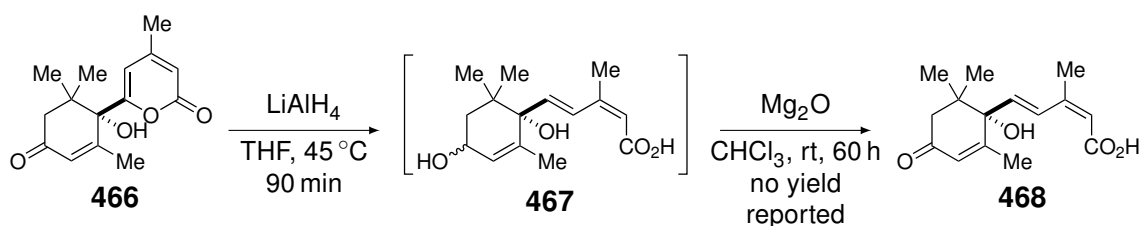
By looking up in the literature, it was found out that this kind of opening of 2-pyrones is not so unexpected. Indeed, in 1995, Mestres *et al.* reported the treatment of pyrone **463** with NaBH_4 in basic conditions.⁶⁸ It led to the formation of the hexanedienoic acid **464** that has retained the configurations

for both double bonds. Two decades later, Fürstner *et al.* published the addition of a nucleophile, methylmagnesium bromide, on the same pyrone **463** and obtained a similar hexanedienoic acid **465** that also had retained the *Z* configuration for one of the double bonds.⁶⁹



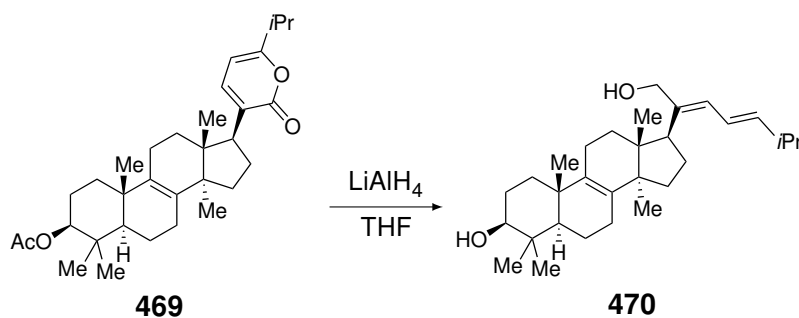
Scheme 4.18: Nucleophilic 1,4-additions on pyrone **463**, followed by its opening, either by a reducing agent, such as NaBH_4 ,⁶⁸ or by methylmagnesium bromide.⁶⁹

Very few examples of pyrones reacting with LiAlH_4 were found. Nevertheless, Cornforth *et al.* published, in 1992, the synthesis of (\pm)-abscisic acid (**468**) using that reductant on the pyrone derivative **466** at the end of the sequence (Scheme 4.19).⁷⁰ Similarly to the reduction reported in Scheme 4.18, a dienoic acid **467** was obtained. As the enone was also reduced in the same process, the resulting alcohol was oxidised in order to reach the desired natural product **468**, albeit no yield was reported.



Scheme 4.19: Synthesis of (\pm)-abscisic acid (**468**) by reduction of compound **466**, followed by the subsequent oxidation of the allylic alcohol.⁷⁰

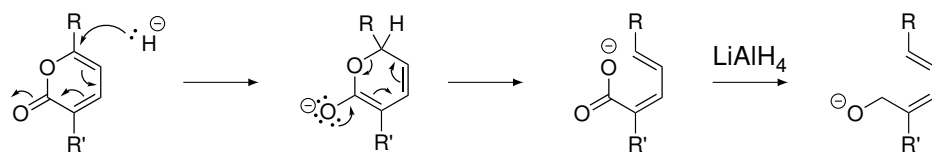
Although the use of LiAlH_4 opened the pyrone core in that last example, the carboxylic acid group was left untouched, as described for the majority of reactions leading to such opening of pyrones, whether a reduction or a nucleophilic addition. To the best of our knowledge, only one example of reduction of an α -pyrone to a pentadienol derivative was described by Rosenthal and co-workers in 1962 (Scheme 4.20).⁷¹ Even though their example is more complex than ours, the process seems to be equivalent and they were not expecting it either.



Scheme 4.20: Reduction of the pyrone core of compound **469** into the pentadienol equivalent **470**.⁷¹

Nevertheless, the group proposed a mechanism that would explain the isolated product (Scheme 4.21). It would start with the nucleophilic addition of a hydride ion on the δ -carbon atom of the pyrone

as it exhibits a rather strong electrophilicity. The intermediate dienolate would then be opened to form a dienolate. From there, the reaction continues further with the reduction of the carboxylate into the corresponding alkoxide.



Scheme 4.21: Proposed mechanism for the reductive opening of an α -pyrone, followed by the subsequent reduction of the carboxylate into an alkoxide.⁷¹

Given the fact that no examples of α -pyrone reduction to the corresponding pyran were found, it is unlikely that such transformation could be done with a classical reducing agent, although it appears to be working on benzo- and dibenzopyranone derivatives such as coumarins or benzochromenone.

Nevertheless, this new diene **373f** is not without interest as it bears the desired functional groups, including the oxidised carbon that will serve to introduce the lactone moiety, with the proper configuration to obtain a cycloadduct with the desired relative configurations for the total synthesis of momilactones.

4.6 Conclusion

For this part of the project, the syntheses of five dienes were initially planned and we succeeded in synthesising all five of them. Among those dienes, **373a** (Scheme 4.1),¹ **373c** (Scheme 4.3)¹⁵ and **373d** (Scheme 4.4)¹⁶ were already described and we were able to reproduce their synthesis, even though a slight modification was done in the case of diene **373d**.

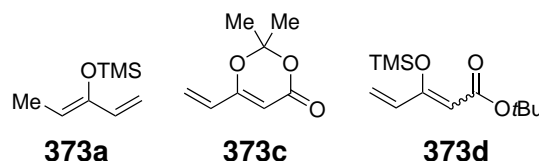


Figure 4.7: Structures of dienes **373a**, **373c** and **373d**.

We also managed the synthesis of diene **373b** (Scheme 4.2) that, to the best of our knowledge, had never been described. We developed a synthesis from two different starting materials that both gave the desired diene **373b** in five steps and with good overall yields (45% from butenol **408** and 34% from propanediol **411**). More importantly, we succeeded in forming the *Z* enol ether selectively.

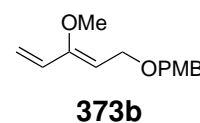


Figure 4.8: Structure of diene **373b**.

The fifth diene whose synthesis was planned was pyrone **373e**. Its preparation was already described by Effenberger *et al.* (Scheme 4.5)^{17,18} but we could not reproduce their synthesis as efficiently as them (Scheme 4.6).

We tried a second strategy, based on the work of Fürstner.²³ We efficiently prepared the 3-oxopent-4-ynoate **442**, prepared *via* a Claisen condensation between *tert*-butyl propionate (**440**) and methyl propiolate (**441**), but the cyclisation did not work either with TFA nor the gold catalysis (Scheme 4.10). As the absence of substituent on the alkyne seemed to be the cause for the lack

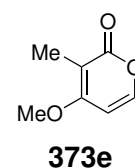


Figure 4.9: Structure of pyrone **373e**.

of reaction, we decided to functionalise the alkyne with a sulfide group that should be easy to insert and remove, as well as increase the electrophilicity of the alkyne.

We prepared four 3-thiopropiolate derivatives **453** (Table 4.1) that were engaged in the Claisen condensation with propionate **440**. We could not isolate the intermediate β -ketoesters **450** and we directly engaged them in the cyclisation step with TFA (Scheme 4.14). Although a cyclisation occurred for all four examples, the products obtained were 5-thiomethylenefuran-2-ones **455**, coming from a 5-*exo*-dig cyclisation, and not the desired pyrones **454**. We did not try the gold catalysis as the presence of a sulfide group is likely to poison the catalyst.

We then used a third strategy by performing a Claisen condensation between *tert*-butyl propionate (**440**) and ethyl 3,3-diethoxypropanoate (**460**) (Scheme 4.16). The intermediate β -ketoester **461** was efficiently obtained and treating the latter with concentrated sulfuric acid gave the desired hydroxypyronone **424** with 39% over two steps. Moreover, the new method we developed for the synthesis of 4-hydroxypyrones did not require any purification but a simple trituration in dichloromethane. We could therefore prepare the 4-methoxypyronone **373e** on a multi-gram scale.

Finally, by serendipity, we obtained a new diene **373f** by reduction of pyrone **373e** with LiAlH_4 (Scheme 4.17). Initially, we wanted to obtain pyran **462**, with a milder reductant, but only LiAlH_4 could reduce pyrone **373e** into diene **373f**, with an *E* configuration. Surprisingly, this transformation is not so common as only one group reported the opening of a pyrone with a nucleophilic hydride, followed by the reduction of the carbonyl to the alcohol.⁷¹ We have thus prepared a new diene that was not described in the literature and we will test the latter in the tests of asymmetric Diels-Alder reactions.

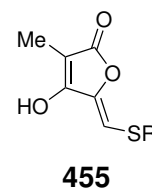


Figure 4.10: Structure of thiomethylenefuranones **455**.

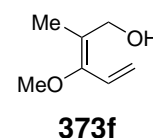


Figure 4.11: Structure of diene **373f**.

References

- [1] Ackland, D. J.; Pinhey, J. T. The Chemistry of Aryl-lead(IV) Tricarboxylates. Reaction with Vinylogous β -Keto Esters. *J. Chem. Soc., Perkin Trans. 1* **1987**, 2689–2694.
- [2] Schrof, R.; Altmann, K.-H. Studies toward the Total Synthesis of the Marine Macrolide Salarin C. *Org. Lett.* **2018**, *20*, 7679–7683.
- [3] Gupta, P.; Kumar, P. An Efficient Total Synthesis of Decastrictine D. *Eur. J. Org. Chem.* **2008**, 1195–1202.
- [4] Sudina, P. R.; Motati, D. R.; Seema, A. Stereocontrolled Total Synthesis of Nonenolide. *J. Nat. Prod.* **2018**, *81*, 1399–1404.
- [5] Padhi, B.; Reddy, D. S.; Mohapatra, D. K. Gold-catalyzed diastereoselective synthesis of 2,6-*trans*-disubstituted tetrahydropyran derivatives: application for the synthesis of the C1–C13 fragment of bis-tramide A and B. *RSC Adv.* **2015**, *5*, 96758–96768.
- [6] Hayashi, Y.; Yamaguchi, H.; Toyoshima, M.; Okado, K.; Toyo, T.; Shoji, M. Formal Total Synthesis of Fostriecin by 1,4-Asymmetric Induction with an Alkyne–Cobalt Complex. *Chem. Eur. J.* **2010**, *16*, 10150–10159.
- [7] Matsubara, R.; Jamison, T. F. Nickel-Catalyzed Allylic Substitution of Simple Alkenes. *J. Am. Chem. Soc.* **2010**, *132*, 6880–6881.
- [8] Xie, L.; Saunderson, W. H., Jr. Unusual induced isotope effects in the reaction of 2-pentanone with dialkylamide bases. Evidence on the nature of the reactive base species. *J. Am. Chem. Soc.* **1991**, *113*, 3123–3130.
- [9] Stahl, I.; Seapy, D. G. Trimethyloxonium Tetrafluoroborate. In *Encyclopedia of Reagents for Organic Synthesis*; American Cancer Society, 2008.
- [10] Perst, H.; Seapy, D. G. Triethyloxonium Tetrafluoroborate. In *Encyclopedia of Reagents for Organic Synthesis*; American Cancer Society, 2008.
- [11] Heiszwolf, G. J.; Kloosterziel, H. Alkylation of Enolate Anions. Formation of Enol Ethers. *Recl. Trav. Chim. Pays-Bas* **1970**, *89*, 1153–1169.
- [12] Rizzardo, E. 1,3-Diethoxy-1,3-diene from β -Diketone. *J. Chem. Soc., Chem. Commun.* **1975**, 644.
- [13] Solladié, G.; Maugein, N.; Morreno, I.; Almario, A.; Carreño, M. C.; García-Ruano, J. L. Synthesis of Enantiomerically Pure 4-Substituted (1*Z*,3*E*)-1[(*R*)-*p*-Tolylsulfanyl]-2-*t*-Butyldimethylsilyloxy-1,3-Butadienes. *Tetrahedron Lett.* **1992**, *33*, 4561–4562.
- [14] Ohta, S.; Shimabayashi, A.; Hatano, S.; Okamoto, M. Preparation of *t*-Butyl 3-Oxopent-4-enoate and its Use as a Nazarov Reagent. *Synthesis* **1983**, 715–716.
- [15] Gebauer, J.; Blechert, S. Synthesis of γ,δ -Unsaturated- β -keto Lactones via Sequential Cross Metathesis-Lactonization: A Facile Entry to Macrolide Antibiotic (–)-A26771B. *J. Org. Chem.* **2006**, *71*, 2021–2025.
- [16] Rabe, P.; Klapschinski, T. A.; Brock, N. L.; Citron, C. A.; D'Alvise, P.; Gram, L.; Dickschat, J. S. Synthesis and bioactivity of analogues of the marine antibiotic tropodithietic acid. *Beilstein J. Org. Chem.* **2014**, *10*, 1796–1801.
- [17] Effenberger, F.; Ziegler, T.; Schönwälder, K.-H. Enoether, XVI. Synthese von 4-Hydroxy-2H-pyran-2-onen. *Chem. Ber.* **1985**, *118*, 741–752.
- [18] Effenberger, F.; Ziegler, T. Diels-Alder-Reaktionen mit 2H-Pyran-2-onen: Reaktivität und Selektivität. *Chem. Ber.* **1987**, *120*, 1339–1346.
- [19] Ng, K.-M. E.; McMorris, T. C. An efficient synthesis of pterosin C and other pterosins. *Can. J. Chem.* **1984**, *62*, 1945–1953.
- [20] Körner, M.; Hiersemann, M. Enantioselective Synthesis of the C8–C20 Segment of Curvicolide C. *Org. Lett.* **2007**, *9*, 4979–4982.
- [21] Hubbard, J. S.; Harris, T. M. Condensations at the 6 Position of the Methyl Ester and the Dimethylamide of 3,5-Dioxohexanoic Acid via 2,4,6-Tri-anions. *J. Org. Chem.* **1981**, *46*, 2566–2570.
- [22] Pirrung, M. C. Purification of products. In *The Synthetic organic chemist's companion*; John Wiley & Sons, Inc., 2007; Chapter 13, pp 131–139.
- [23] Chładaj, W.; Corbet, M.; Fürstner, A. Total Synthesis of Neurymenolide A Based on a Gold-Catalyzed Synthesis of 4-Hydroxy-2-pyrones. *Angew. Chem. Int. Ed.* **2012**, *51*, 6929–6933.
- [24] Preindl, J.; Jouvin, K.; Laurich, D.; Seidel, G.; Fürstner, A. Gold- and Silver-Catalyzed Synthesis of Pyrones and Pyridine Derivatives: Mechanistic and Synthetic Aspects. *Chem. Eur. J.* **2016**, *22*, 237–247.
- [25] Lee, J. S.; Shin, J.; Shin, H. J.; Lee, H.-S.; Lee, Y.-J.; Lee, H.-S.; Won, H. Total Synthesis and Configurational Validation of (+)-Violapyrone C. *Eur. J. Chem. Org.* **2014**, 4472–4476.
- [26] Chen, Y.; Wang, L.; Sun, N.; Xie, X.; Zhou, X.; Chen, H.; Li, Y.; Liu, Y. Gold(I)-Catalyzed Furan-yne Cyclizations Involving 1,2-Rearrangement: Efficient Synthesis of Functionalized 1-Naphthols and Its Application to the Synthesis of Wailupemycin G. *Chem. Eur. J.* **2014**, *20*, 12015–12019.
- [27] Liu, R.; Li, X.; Li, X.; Wang, J.; Yang, Y. Gold(I)-Catalyzed Intermolecular Rearrangement Reaction of Glycosyl Alkynoic β -Ketoesters for the Synthesis of 4-*O*-Glycosylated 2-Pyrones. *J. Org. Chem.* **2019**,

- 84, 14141–14150.
- [28] Hermann, D.; Brückner, R. Silver-Catalyzed *tert*-Butyl 3-Oxopent-4-ynoate π -Cyclizations: Controlling the Ring Size—Hydroxypyronone or Pulvinone Formation—by Counterion and Additive Optimization. *Org. Lett.* **2018**, *20*, 7455–7460.
- [29] Yamamoto, Y.; Gridnev, I. D.; Patil, N. T.; Jin, T. Alkyne activation with Brønsted acids, iodine, or gold complexes, and its fate leading to synthetic application. *Chem. Commun.* **2009**, 5075–5087.
- [30] Belil, C.; Pascual, J.; Serratos, F. Intramolecular cyclization of alkylpropargylidenemalononic acids. Catalytic and directing effect of silver ion. *Tetrahedron* **1964**, *20*, 2701–2708.
- [31] Bellina, F.; Biagetti, M.; Carpita, A.; Rossi, R. A novel route to 6-substituted and 5,6-disubstituted 2-pyrones. *Tetrahedron Lett.* **2001**, *42*, 2859–2863.
- [32] Anastasia, L.; Xu, C.; Negishi, E.-i. Catalytic and selective conversion of (*Z*)-2-en-4-ynoic acids to either 2*H*-pyran-2-ones in the presence of ZnBr₂ or (*Z*)-5-alkylidenefuran-2(5*H*)-ones in the presence of Ag₂CO₃. *Tetrahedron Lett.* **2002**, *43*, 5673–5676.
- [33] Faizi, D. J.; Issaian, A.; Davis, A. J.; Blum, S. A. Catalyst-Free Synthesis of Borylated Lactones from Esters Via Electrophilic Oxyboration. *J. Am. Chem. Soc.* **2016**, *138*, 2126–2129.
- [34] Pathare, R. S.; Sharma, S.; Gopal, K.; Sawant, D. M.; Pardasani, R. T. Palladium-catalyzed convenient one-pot synthesis of multi-substituted 2-pyrones via transesterification and alkenylation of enynoates. *Tetrahedron Lett.* **2017**, *58*, 1387–1389.
- [35] Qiu, S.-Q.; Ahmad, T.; Xu, Y.-H.; Loh, T.-P. Palladium-Catalyzed Cascade Intramolecular Cyclization and Allylation of Enynoates with Allylic Alcohols. *J. Org. Chem.* **2019**, *84*, 6729–6736.
- [36] Yata, T.; Kita, Y.; Nishimoto, Y.; Yasuda, M. Regioselective Synthesis of 5-Metalated 2-Pyrones by Intramolecular Oxymetalation of Carbonyl-ene-yne Compounds Using Indium Trihalide. *J. Org. Chem.* **2019**, *84*, 14330–14341.
- [37] Yao, T.; Larock, R. C. Synthesis of Isocoumarins and α -Pyrones via Electrophilic Cyclization. *J. Org. Chem.* **2003**, *68*, 5936–5942.
- [38] Yoshikawa, T.; Shindo, M. Stereoselective Synthesis of (*E*)-2-En-4-ynoic Acids with Ynolates: Catalytic Conversion to Tetrionic Acids and 2-Pyrones. *Org. Lett.* **2009**, *11*, 5378–5381.
- [39] Trost, B. M.; Flygare, J. A. A Novel Ru-Catalyzed Tandem Cyclization-Reconstitutive Addition of Propargyl Alcohols with Allyl Alcohols. *J. Am. Chem. Soc.* **1992**, *114*, 5476–5477.
- [40] Fürstner, A.; Picquet, M.; Bruneau, C.; Dixneuf, P. H. Cationic ruthenium allenylidene complexes as a new class of performing catalysts for ring closing metathesis. *Chem. Commun.* **1998**, 1315–1316.
- [41] Fürstner, A.; Liebl, M.; Lehmann, C. W.; Picquet, M.; Kunz, R.; Bruneau, C.; Touchard, D.; Dixneuf, P. H. Cationic Ruthenium Allenylidene Complexes as Catalysts for Ring Closing Olefin Metathesis. *Chem. Eur. J.* **2000**, *6*, 1847–1857.
- [42] Hansmann, M. M.; Rominger, F.; Hashmi, A. S. K. Gold–allenylidenes – an experimental and theoretical study. *Chem. Sci.* **2013**, *4*, 1552–1559.
- [43] Fujiki, K.; Tanifuji, N.; Sasaki, Y.; Yokoyama, T. New and Facile Synthesis of Thiosulfonates from Sulfinate/Disulfide/I₂ System. *Synthesis* **2002**, 343–348.
- [44] Zeynizadeh, B. Oxidative coupling of thiols to disulfides with iodine in wet acetonitrile. *J. Chem. Res.* **2002**, 564–566.
- [45] Okumura, S.; Takeda, Y.; Kiyokawa, K.; Minakata, S. Hypervalent Iodine(III)-Induced Oxidative [4+2] Annulation of *o*-Phenylenediamines and Electron-Deficient Alkynes: Direct Synthesis of Quinoxalines from Alkyne Substrates under Metal-Free Conditions. *Chem. Commun.* **2013**, *49*, 9266–9268.
- [46] Alabugin, I. V.; Gilmore, K.; Manoharan, M. Rules for Anionic and Radical Ring Closure of Alkynes. *J. Am. Chem. Soc.* **2011**, *133*, 12608–12623.
- [47] Fürstner, A.; Morency, L. On the Nature of the Reactive Intermediates in Gold-Catalyzed Cycloisomerization Reactions. *Angew. Chem. Int. Ed.* **2008**, *47*, 5030–5033.
- [48] Weinstock, J.; Blank, J. E.; Oh, H.-J.; Sutton, B. M. A Regiospecific Synthesis of Substituted Vulpinic Acids. *J. Org. Chem.* **1979**, *44*, 673–676.
- [49] Babidge, P. J.; Massy-Westropp, R. A. The Synthesis of 5-Alkylidenefuran-2(5*H*)-ones. *Aust. J. Chem.* **1981**, *34*, 1745–1756.
- [50] Bouillon, J.-P.; Kikelj, V.; Tinant, B.; Harakat, D.; Portella, C. Synthesis of New Trifluoromethylated Furans, Dihydrofurans and Butenolides Starting from γ -Ketothioesters and Diisopropylamine. *Synthesis* **2006**, 1050–1056.
- [51] Bouillon, J.-P.; Shermolovich, Y.; Mykhaylychenko, S.; Haralat, D.; Tinant, B. Synthesis of new 3-(2,2,2-trifluoroethyl)-5-hydroxy-5-(phenylsulfanyl- or phenylsulfonyl-methyl)-1,5-dihydropyrrol-2-ones starting from α,β -unsaturated γ -lactones and primary amines. *J. Fluorine Chem.* **2007**, *128*, 931–937.
- [52] Mykhaylychenko, S.; Harakat, D.; Dupas, G.; Shermolovich, Y. G.; Bouillon, J.-P. Synthesis of (2,2,2-trifluoroethyl) substituted pyridazin-3(2*H*)-ones and 1,5-dihydropyrrol-2-ones from α,β -unsaturated γ -lactones and hydrazines. *J. Fluorine Chem.* **2009**, *130*, 418–427.
- [53] Kanishchev, O. S.; Lavoignat, A.; Picot, S.; Médebielle, M.; Bouillon, J.-P. New route to the 5-(arylthio-

and heteroarylthio)methylene)-3-(2,2,2-trifluoroethyl)-furan-2(5*H*)-ones—Key intermediates in the synthesis of 4-aminoquinoline γ -lactams as potent antimalarial compounds. *Bioorg. Med. Chem. Lett.* **2013**, *23*, 6167–6171.

- [54] Cornut, D.; Lemoine, h.; Kanishchev, O.; Okada, E.; Albrieux, F.; Beavogui, A. H.; Bienvenu, A.-L.; Picot, S.; Bouillon, J.-P.; Médebielle, M. Incorporation of a 3-(2,2,2-Trifluoroethyl)- γ -hydroxy- γ -lactam Motif in the Side Chain of 4-Aminoquinolines. Syntheses and Antimalarial Activities. *J. Med. Chem.* **2013**, *56*, 73–83.
- [55] Benneche, T.; Chamgordani, E. J.; Scheie, A. A. Reaction of (*Z*)-5-(bromomethylene)thiophen-2(5*H*)-one with some nucleophiles in search for new biofilm inhibitors. *Synthetic Commun.* **2013**, *43*, 431–437.
- [56] Huang, Y.-Q.; Huang, X.-Z.; Huang, P.-Q. Synthesis of 5-(1-Alkoxyalkylidene)tetronates by Direct Condensation Reactions of Tetronates with Thionolactones and Thionoesters. *J. Org. Chem.* **2021**, *86*, 2359–2368.
- [57] Deneffe, B. Étude de la réactivité du 4-hydroxy-5-thiométhylènebuténolide dans des réactions de couplages organométalliques. M.Sc. thesis, Université de Namur, Belgium, 2021.
- [58] Miyaura, N.; Suzuki, A. Palladium-Catalyzed Cross-Coupling Reactions of Organoboron Compounds. *Chem. Rev.* **1995**, *95*, 2457–2483.
- [59] Liebeskind, L. S.; Srogl, J. Heteroaromatic Thioether–Boronic Acid Cross-Coupling under Neutral Reaction Conditions. *Org. Lett.* **2002**, *4*, 979–981.
- [60] Sun, W.; Cama, L. D.; Birzin, E. T.; Warriar, S.; Locco, L.; Mosley, R.; Hammond, M. L.; Rohrer, S. P. 6*H*-Benzo[*c*]chromen-6-one derivatives as selective ER β agonists. *Bioorg. Med. Chem. Lett.* **2006**, *16*, 1468–1472.
- [61] Dai, J.-J.; Wu, W.-T.; Wu, Y.-D.; Zhang, W.-M.; Gong, Y.; He, X.-P.; Zhang, X.-Q.; Xu, H.-J. Silver-Catalyzed C(sp²)–H Functionalization/C–O Cyclization Reaction at Room Temperature. *J. Org. Chem.* **2015**, *80*, 911–919.
- [62] Verma, P.; Singh, S.; Dikshit, D. K.; Ray, S. Smooth Conversion of 3,4-Diarylcoumarins and 3,4,5-Triaryl-2(5*H*)-furanones to 2*H*-Chromene and 2,5-Dihydrofuran Derivatives with Dimethyl Sulfide-Borane Complex. *Synthesis* **1988**, 68–70.
- [63] Pandey, J.; Jha, A. K.; Hajela, K. Synthesis and biological activities of some new dibenzopyranones and dibenzopyrans: search for potential oestrogen receptor agonists and antagonists. *Bioorg. Med. Chem.* **2004**, *12*, 2239–2249.
- [64] Zhi, L.; Ringgerberg, J. D.; Edwards, J. P.; Tegley, C. M.; West, S. J.; Pio, B.; Motamedi, M.; Jones, T. K.; Marschke, K. B.; Mais, D. E.; Schrader, W. T. Development of Progesterone Receptor Antagonists from 1,2-Dihydrochromeno[3,4-*f*]quinoline Agonist Pharmacophore. *Bioorg. Med. Chem. Lett.* **2003**, *13*, 2075–2078.
- [65] Wadsworth, A. D.; Sperry, J.; Brimble, M. A. Synthesis of the Pyranonaphthoquinones Dehydroherbarin, (+)-Astropaquinone B and (+)-Astropaquinone C en Route to Ascomycones A and B. *Synthesis* **2010**, 2604–2608.
- [66] Bury, P. S.; Christiansen, L. B.; Jacobsen, P.; Jørgensen, A. S.; Kanstrup, A.; Nærum, L.; Bain, S.; Fledelius, C.; Gissel, B.; Hansen, B. S.; Korsgaard, N.; Thorpe, S. M.; Wasserman, K. Synthesis and Pharmacological Evaluation of Novel *cis*-3,4-Diaryl-hydroxychromanes as High Affinity Partial Agonists for the Estrogen Receptor. *Bioorg. Med. Chem.* **2002**, *10*, 125–145.
- [67] De Angelis, M.; Stossi, F.; Waibel, M.; Katzenellenbogen, B. S.; Katzenellenbogen, J. A. Isocoumarins as estrogen receptor beta selective ligands: Isomers of isoflavone phytoestrogens and their metabolites. *Bioorg. Med. Chem.* **2005**, *13*, 6529–6542.
- [68] Aurell, M. J.; Ceita, L.; Mestres, R.; Parra, M.; Tortajada, A. Trienediolates of Hexadienoic Acids in Synthesis. Addition to Unsaturated Ketones. A Convergent Approach to the Synthesis of Retinoic Acids. *Tetrahedron* **1995**, *51*, 3915–3928.
- [69] Sun, C.-L.; Fürstner, A. Formal Ring-Opening/Cross-Coupling Reactions of 2-Pyrones: Iron-Catalyzed Entry into Stereodefined Dienyl Carboxylates. *Angew. Chem. Int. Ed.* **2013**, *52*, 13071–13075.
- [70] Cornforth, J.; Hawes, J. E.; Mallaby, R. A Stereospecific Synthesis of (\pm)-Abscisic Acid. *Aust. J. Chem.* **1992**, *45*, 179–185.
- [71] Rosenthal, D.; Fried, J.; Grabowich, P.; Sabo, E. F. Transformation of eburicoic acid. Side chain degradation to pregnane derivatives. *J. Am. Chem. Soc.* **1962**, *84*, 877–879.

Chapter 5
Synthesis and study of
quinones and
sulfinylquinones

5 Synthesis and study of quinones and sulfinylquinones

This chapter will present the studies performed on quinones and sulfinylquinones that will be used in diverse Diels-Alder reactions. With these studies, we hoped to get a better understanding of the cycloadditions with those particular dienophiles. By searching the scope and limitations of the first key step of the developed sequence for the total synthesis of momilactones (*cf.* Chapter 3), we planned to determine which diene is the most appropriate. If necessary, a new diene might even be designed based on the results obtained from such attempts.

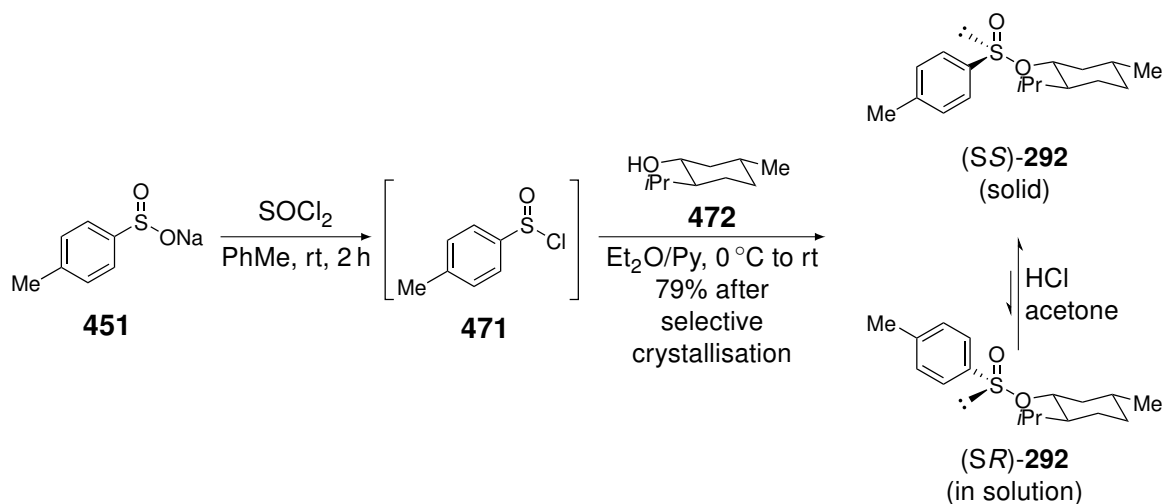
First, the synthesis of the desired quinones and sulfinylquinones will be presented. We will not limit ourselves to the ones described for the total synthesis, but also others whose structure might be of interest for the different reactions that will be performed.

Then, we will focus on sulfinylquinones and study them from a structural point of view. As explained in Chapter 3, to the best of our knowledge, no X-ray structure of such compounds has been described yet. Therefore, several sulfinylquinones were synthesised in order to propose a correlation between the conformation of the sulfinyl moiety at the solid state to the observed stereoselectivities when they are engaged in a Diels-Alder reaction. The analysis of the X-ray structures will also be coupled to a computational study to afford a deeper understanding of the preferred conformations.

Finally, reactivity studies were undertaken by changing different parameters. On one hand, the effect of the solvent on the reaction rates, and the stereoselectivities in the case of the sulfinylquinones, was investigated as previously done by Carreño *et al.*¹ On the other hand, the impact of the nature of the (sulfinyl)quinones and dienes will be evaluated.

5.1 Synthesis of enantiomerically enriched sulfinylquinones

As presented in Chapter 2, the main methodology for the preparation of sulfinylquinones consists in the addition of a chiral sulfoxide on a functionalised aromatic core through a S_N2 process. The sulfoxide originates from a sulfinate, itself stereoselectively prepared from a chiral auxiliary.



Scheme 5.1: Synthesis of the menthyl (-)-(S)-*para*-toluenesulfinate ((SS)-292).²⁻⁴

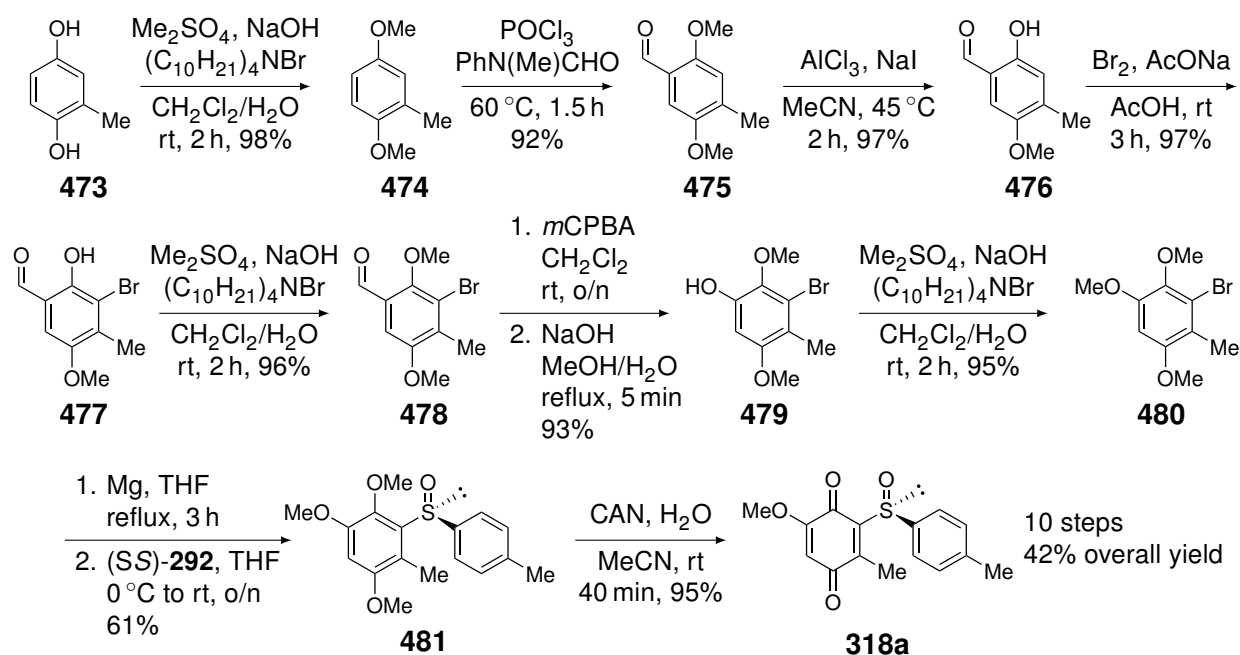
As described earlier, the most used chiral auxiliary for the preparation of such stereochemically defined sulfonates is (–)-menthol (**472**). As described by Andersen *et al.*, sodium *para*-toluenesulfinate (**451**) is first converted into the corresponding sulfinylchloride **471** with the use of SOCl_2 (Scheme 5.1).^{2,3} The chloride **471** is directly engaged in the next step to react with (–)-menthol (**472**). However, as chloride **471** is racemic, the menthyl sulfinate **292** will be obtained as a mixture of diastereoisomers. Fortunately, Solladié *et al.* optimised this process by recrystallisation in acetone using hydrochloric acid to epimerise the sulfur center.⁴ As (SS)-**292** crystallises, whereas its epimer (SR)-**292** remains in solution, the equilibrium is shifted towards the formation of (SS)-**292**. In doing so, the yield of that reaction can go up to 80% of the SS isomer.

5.1.1 Preparation of non silylated sulfinylquinones

As described in Chapter 3, two sets of sulfinylquinones (and quinones) are planned depending on whether momilactone A (**1**) or B (**2**) is desired. In the case of the former, the series without the silyl group are to be used. More specifically, sulfinylquinone *ent*-**318a** should be used in order to reach the proper enantiomer of **1**. However, in order to synthesise that sulfinylquinone, the enantiomer of (SS)-**292**, itself prepared from (+)-menthol (*ent*-**472**), must be used. As (–)-menthol (**472**) is more abundant and cheaper than its enantiomer, it was decided to first study the synthesis of momilactones on the opposite enantiomeric series.

Therefore, we will first focus on the synthesis of sulfinylquinone **318a** that has already been described by Lanfranchi and Hanquet and starts from methylhydroquinone **473** (Scheme 5.2).⁵

The first step consists in the protection of both phenols with dimethyl sulfate. The protected hydroquinone **474** then undergoes a Vilsmeier-Haack formylation to introduce an aldehyde (that will later serve for the introduction of a third oxygen atom on the aromatic ring). The selective deprotection of **475** reveals the phenol **476** which activates the *ortho* position to selectively introduce a bromine

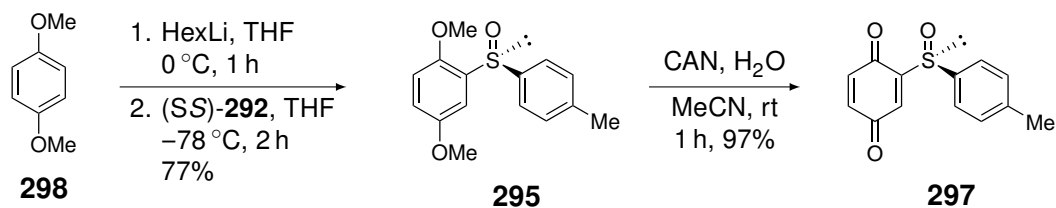


Scheme 5.2: Synthetic pathway of sulfinylquinone **318a** carried out following the procedures described by Lanfranchi and Hanquet.⁵

atom to obtain bromide **477**. After reprotection of the phenol group, a Dakin rearrangement of **478**, followed by the hydrolysis of the corresponding formate, gave phenol **479** that was later methylated to give intermediate **480**. The latter was treated with magnesium to form a Grignard reagent that reacted with sulfinate (SS)-**292** to introduce the sulfoxide group. The hydroquinone **481** was then oxidised into the desired quinone **318a**. This sequence is quite long (ten steps), but only the formation of the sulfoxide has a yield below 90%. Therefore, it was possible to obtain **318a** with 42% overall yield, which is quite good for such a long synthesis. In addition to the excellent overall yield, no chromatography was needed to purify the different intermediates of the sequence.

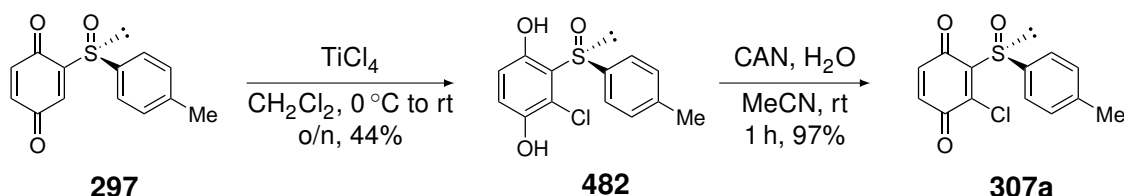
As explained earlier, sulfinylquinone **318a** is not the only one in which we are interested. In order to make a more complete structural and reactivity study, other sulfinylquinones, bearing other substituents, will be used to propose a model to explain the sulfoxide conformation and the stereoselectivities with those quinones when they are engaged in Diels-Alder reactions.

The second sulfinylquinone that was chosen is the one without any substituents and that was the first example described in 1989 by Carreño's group.⁶ However, we chose to use the synthetic sequence described in 1992, starting from 1,4-dimethoxybenzene (**298**) as presented in Scheme 5.3.⁷ The latter undergoes an *ortho* lithiation (in our case, we used hexyllithium instead of butyllithium) to insert the sulfoxide using sulfinate (SS)-**292**, followed by an oxidation to reach quinone **297**.



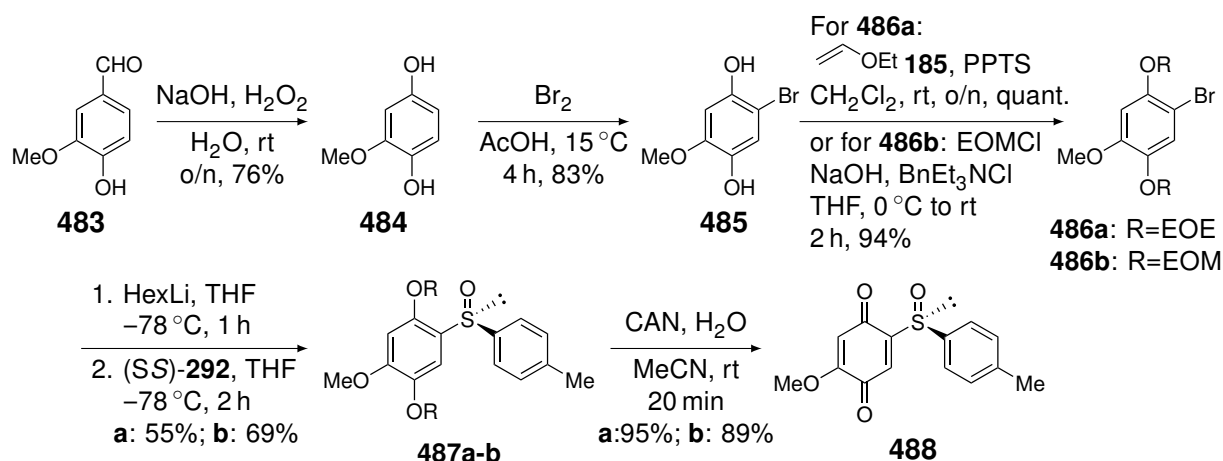
Scheme 5.3: Synthetic pathway for sulfinylquinone **297** as described by Carreño *et al.*⁷

From **297**, a second sulfinylquinone can easily be reached. As reported in 1994 by the same group, a chlorine atom can be inserted next to the sulfoxide (Scheme 5.4).⁸ For that purpose, sulfinylquinone **297** is treated with TiCl_4 in dichloromethane. The group described that reaction with an 82% yield, but no precise procedure was described in the corresponding paper and we were able to reach 44% at best. Nevertheless, it gave us enough material for our study.



Scheme 5.4: Synthetic pathway for sulfinylquinone **307a** as described by Carreño *et al.*⁸

Finally, it was decided to synthesise a fourth sulfinylquinone that, to the best of our knowledge, was not described yet. We wanted to assess the effect of the position of the methoxy group on the quinone core. In the case of sulfinylquinone **318a**, the methoxy group is on position 6. It was thought to synthesise another one with the methoxy group on position 5.

Scheme 5.5: Synthetic pathway for sulfinylquinone **488**.

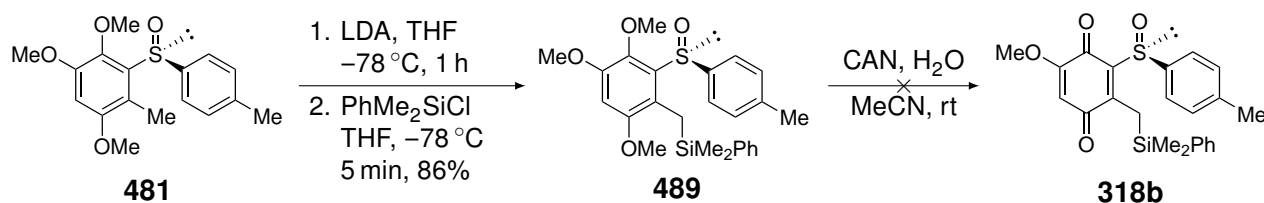
The synthesis of that new sulfinylquinone **488** starts with a Dakin oxidation of vanillin (**483**), directly following a procedure reported by Ferreira *et al.* in 1995 (Scheme 5.5).⁹ This hydroquinone **484** is then brominated, following the procedure of Keana and co-workers,¹⁰ to obtain aryl bromide **485**. Both phenol groups must be then protected. However, methoxy groups cannot be used in this case. Indeed, as reported by Carreño's group, it would seem that the CAN oxidation does not work to convert sulfinyltrimethoxybenzene into the corresponding quinone in the absence of a methyl group, as opposed to sulfinylquinone **318a**.^{11,12} Therefore, a more labile protecting group must be employed. Two of them have been tested: the ethoxyethyl (EOE) group, introduced using ethyl vinyl ether (**185**),¹³ and the ethoxymethyl (EOM) group, introduced using the corresponding chloride.¹⁴ Both protected derivatives **486a** and **486b** were then engaged in the bromine-lithium exchange to undergo the nucleophilic substitution on (SS)-**292** to insert the sulfoxide group. Both versions of the sulfoxide intermediate **487** were then oxidised using CAN to give the desired new sulfinylquinone **488**.

Both protecting groups gave similar overall yields, albeit the EOM pathway was slightly better. However, from a practical point of view, the EOM series was much easier to handle and intermediates **486b** and **487b** were much more stable than their EOE counterparts (for example, **487a** was fully degraded in one day, even when it was conserved in the fridge, under inert atmosphere, and with a small amount of K_2CO_3). Moreover, from the analytical point of view, the EOM series was easier to analyse. Indeed, each EOE protecting group adds a stereogenic centre in the structure, leading to a mixture of four diastereoisomers for **487a**, leading to rather complex spectra that could not allow us to be completely confident in the purity of the product.

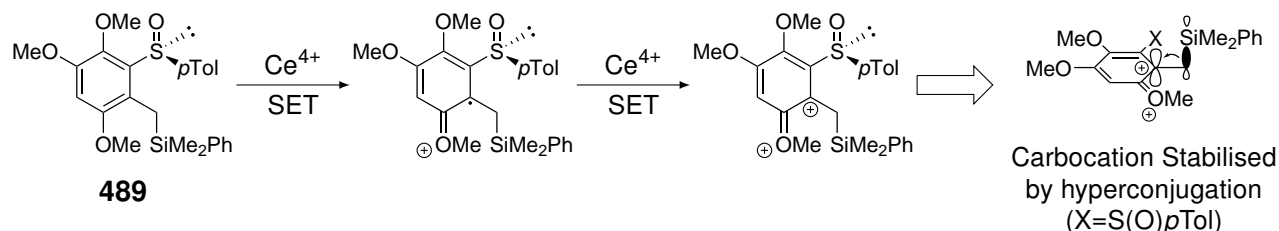
5.1.2 Preparation of silylated sulfinylquinone

As described in Chapter 3, in order to synthesise momilactone B (**2**), according to our plan (Scheme 3.14), a silylated version of sulfinylquinone *ent*-**318a** must be synthesised. For the same reasons explained here above, we first started on the opposite enantiomeric series and attempted to synthesise **318b**.

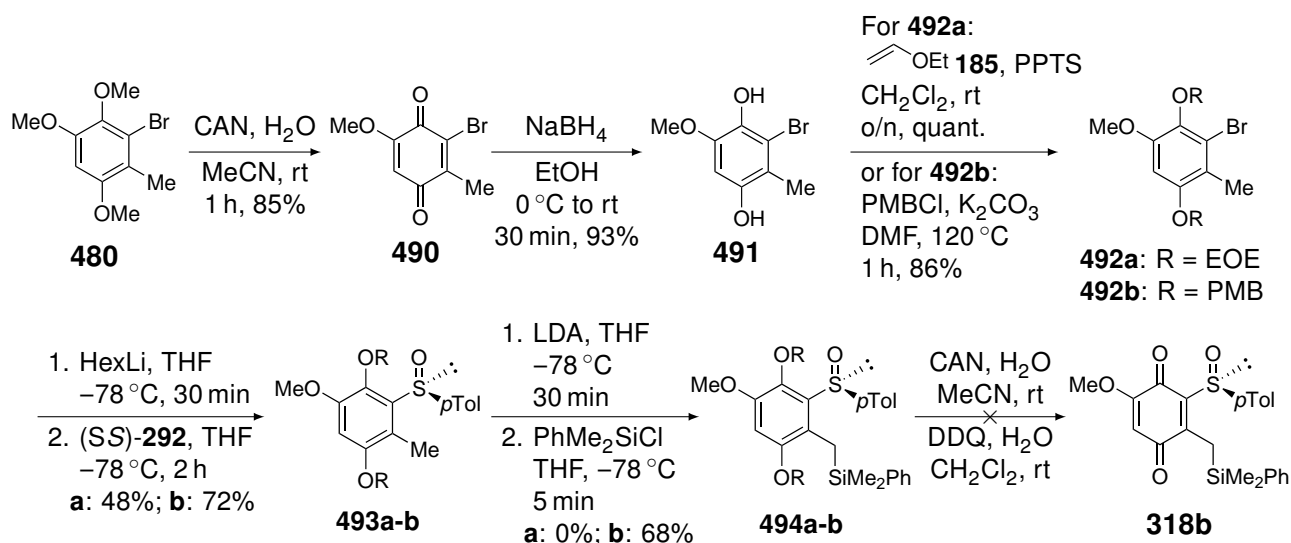
In order to synthesise this sulfinylquinone, we decided to start from sulfoxide **481** and to use the general procedure for lateral functionalisation reported by García Ruano *et al.*^{15,16} As described in Scheme 5.6, we have been able to perform the lateral lithiation and to insert the silyl group on the benzylic methyl group with a very good 87% yield.

Scheme 5.6: First plan for the synthesis of sulfinylquinone **318b**.

We then tried to oxidise **489** into the desired quinone, using CAN as previously done for the other sulfinylquinones. Unfortunately, it did not work and a complex mixture was obtained. We supposed that the presence of the silane moiety in *ortho* position of a methoxy group could cause some issues. Indeed, during this process, there is a carbocation intermediate on the aromatic core that could be stabilised by the silane group on the β position, hence a series of degradations (Scheme 5.7).

Scheme 5.7: Proposed mechanism and explanation for the degradation of sulfoxide **489** during its oxidation.

Therefore, as a solution, it was thought to replace the methoxy groups by more labile protecting groups that could more easily be removed, such as EOE or PMB (Scheme 5.8). Rather than designing a completely new synthetic pathway, we thought of a way to selectively remove the two methoxy groups we wanted to replace. We then tried to simply oxidise the aryl bromide **480** with CAN. Luckily enough, it gave the corresponding *para*-benzoquinone **490** selectively. Reducing that quinone with NaBH₄ gave back the unprotected hydroquinone.

Scheme 5.8: Second sequence for the synthesis of sulfinylquinone **318b**.

From hydroquinone **491**, we then have the possibility to add the chosen protecting groups. The ethoxyethyl group was added, using the same method as described in Scheme 5.5. On the other hand, the PMB groups were added, using PMBCl and K₂CO₃ in DMF at 120 °C. Both those protections have proven to be efficient. Afterwards, the insertion of the sulfoxide is achieved *via* a bromine lithium exchange, followed by the nucleophilic substitution on sulfinate (SS)-**292**. In the case of the EOE group, the desired sulfoxide **493a** was obtained with a moderate yield of 48%, whereas the reaction on substrate **492b** (PMB groups) gave sulfoxide **493b** with a good yield of 72%. The lower yield for **493a** can be explained by stability issues of the protecting groups, just as observed during the synthesis of sulfinylquinone **488** (Scheme 5.5).

Then, the insertion of the silyl group was performed using the same method attempted on **481** (Scheme 5.6). It worked with a good yield (68%) for the PMB protected hydroquinone **493b**. However, in the case of the EOE protected hydroquinone **493a**, the TLC monitoring indicated the consumption of the latter, but the NMR analysis showed the silylation did not take place and deprotected **493a** was found in traces in the spectrum along complex mixtures of unidentified products.

Finally, sulfoxide **494b** was submitted to the CAN oxidation but, similarly to **489**, a complex mixture of unidentified products was obtained. Therefore, we switched the oxidant to DDQ. Indeed, that oxidant should be able to first remove the PMB protecting groups and, then, oxidise the deprotected hydroquinone in one pot. Unfortunately, no reaction occurred at all, not even the deprotection of the phenols.

The synthesis of quinones bearing a silylmethyl group does not seem easy to carry out. Indeed, so far, only two publications reported the oxidation of a hydroquinone derivative, bearing such silylmethyl group, to the corresponding quinone. In both cases, the hydroxy groups were not protected and the oxidation was done using silver(I) oxide¹⁷ or PIDA.¹⁸

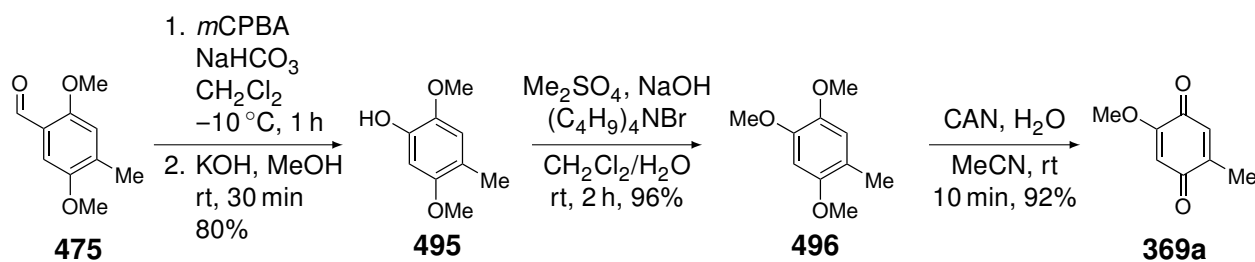
We could have decided to find a way to cleanly deprotect the PMB groups, or to redesign the synthesis with another protecting group that could be easily removed, to reach such unprotected hydroquinones. However, given the appearing difficulties to synthesise such silylated quinones, it has been decided that sulfinylquinone **318b** was not a priority and that it would be wiser to first focus on the total synthesis of momilactone A (**1**).

5.2 Synthesis of quinones for the asymmetric catalyses

As explained in Chapter 3, in the event the sulfinylquinone would not prove to be efficient, the main strategy will be rerouted to catalytic asymmetric Diels-Alder reactions. Two methods have been chosen for that purpose: Corey's oxazaborolidinium salt catalysis^{19,20} and Evans' pybox catalysis.²¹

5.2.1 Preparation of the quinone for Corey's method

The first catalyst to be tested is the oxazaborolidinium salt *ent*-**109** employed by Corey.^{19,20} But first, quinone **369a**, that should correspond to the type of substrates used by Corey, had to be prepared. Therefore, a short synthetic pathway, described in Scheme 5.9, was designed from compound **475** that was already in our hands as it is an intermediate in the synthesis of sulfinylquinone **318a** (Scheme 5.2).

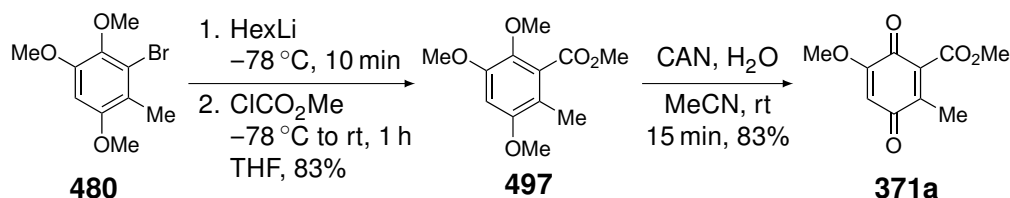
Scheme 5.9: Synthetic pathway for quinone **369a**.

The first step is a Dakin oxidation, similar to the one used in Scheme 5.2. However, as this transformation was already described on that specific benzaldehyde **475**, it was decided to use that slightly different procedure.²² Then, methylation of the obtained phenol **495** was done, using the standard procedure employed in other syntheses described above. Finally, the oxidation of the hydroquinone derivative **496** was uneventfully carried out using the usual CAN oxidation.

It is to be noticed that the synthesis of this quinone was already described several times in the literature, but not with the sequence we present here. However, with that pathway, containing reactions already used in other synthesis reported in this thesis, we efficiently reached the desired quinone **369** that will be tested with Corey's catalytic system.

5.2.2 Preparation of the quinone for the Evans catalysis

The second catalytic system that will be tried is the samarium or gadolinium complex **255a**, using a pybox ligand, developed by Evans' group.²¹ Once again, the design of a quinone matching the general pattern of the substrates used by that group must be done. In this case, an ester group must be present on the quinone. Just as for quinone **369a**, we did not need to go very far to design that synthesis. Indeed, we took aryl bromide **480**, from the synthetic pathway for sulfinylquinone **318a** (Scheme 5.2), and we engaged it in a bromine lithium exchange, followed by the nucleophilic substitution of methyl chloroformate (Scheme 5.10), following a described procedure.²³ The obtained benzoate **497** was then oxidised, once again with CAN, and it gave the desired ester substituted quinone **371a**.

Scheme 5.10: Synthetic pathway for quinone **371a**.

As opposed to **369a**, quinone **371a** has never been described. Therefore, its behaviour in Diels-Alder reactions is unknown and needs to be assessed. It will first be reacted with simple dienes in order to evaluate its reactivity. Then, it will undergo the Evans asymmetric catalysis to determine if this quinone can be used in the context of the total synthesis of momilactones.

5.3 Structural analysis of sulfinylquinones

As discussed earlier, the reactivity of sulfinylquinones has already been extensively studied, mainly by the group of Carreño. But, the exact explanation of the facial diastereoselectivity observed with those compounds, when they are engaged in Diels-Alder reactions, is not yet well understood. However, based on the products obtained, hypotheses have been emitted concerning those stereoselectivities.²⁴ As represented in Figure 5.1, the sulfoxide can adopt two conformations called *s-trans* and *s-cis* with respect to the double bond of the quinone part. It was supposed that in the *s-trans* conformation, an electrostatic repulsion arises between both oxygen atoms of the sulfoxide and the carbonyl. Therefore, that conformation is destabilised, inducing the rotation of the sulfinyl moiety towards the *s-cis* conformation. In that situation, the sulfoxide can place itself in the same plane as the quinone, ensuring the conjugation with the double bond and minimising the electrostatic repulsions.

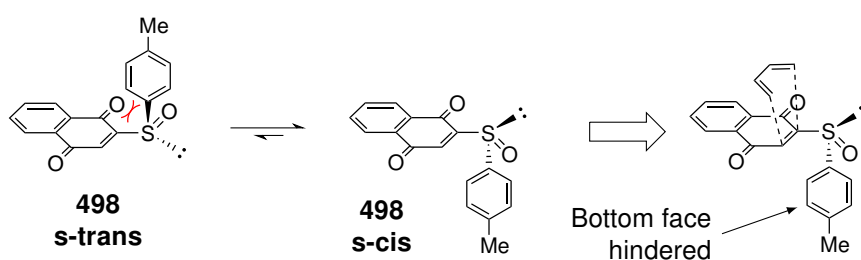


Figure 5.1: Proposed model for the preferential conformation of the sulfinyl moiety in sulfinyl naphthoquinone **498** and for the preferential approach of a diene.²⁴

From that conformation, as observed in the cycloadducts with that sulfinylquinone, the preferential approach of the diene would be on the top face of the quinone (if one looks at the structures as represented in Figure 5.1). This approach would be explained by the hindrance of the bottom face caused by the *para*-tolyl group oriented on that side of the quinone. Therefore, the diene has no choice but to arrive on the top face.

Although this model seems to work well to explain the products obtained, it is based only on the outcomes of the cycloadditions. Therefore, we are going to try to bring some new perspectives on the stereoselectivities reached with the sulfinylquinones.

5.3.1 Analysis of the X-ray structures of sulfinylquinones

One of the ways to study the sulfinylquinones from a structural point of view is to achieve their crystallisation, as well as obtaining crystals with a sufficient quality, in order to submit them to an X-ray analysis. Indeed, to the best of our knowledge, no example of such X-ray structure of a sulfinylquinone has ever been reported, even though the recrystallisation of some sulfinylquinones has already been described.

Among the four sulfinylquinones we have prepared, the recrystallisation method for **318a** and **297** was described. In the first case, boiling methanol was used⁵ and, in the second case, boiling diethyl ether.⁷ We then reused the same conditions but by slowly decreasing the temperature after the total dissolution of the compound, in order to obtain the biggest crystals possible, even if it meant losing some material. Fortunately, the crystals obtained in both cases had a high enough quality to be analysed by X-ray diffraction (Figure 5.2).

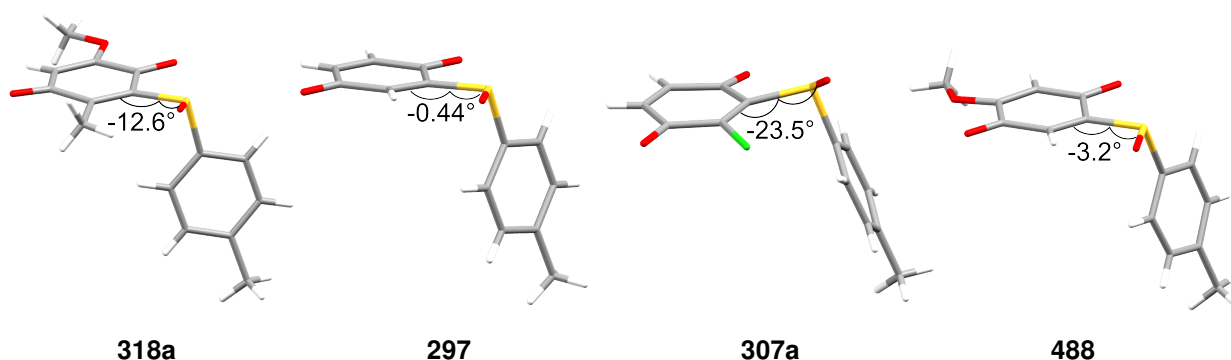


Figure 5.2: X-ray structures of sulfanylquinones **318a**, **297**, **307a**, and **488** and dihedral angle between the quinone plane and the sulfoxide.

However, for sulfanylquinones **307a** and **488**, the recrystallisation conditions had to be found. We determined that the best crystals were obtained in a boiling mixture of pentane and toluene for **307a**, and in boiling ethanol for **488**.

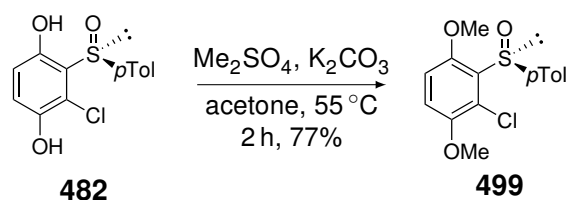
As it can be seen, in all four of the sulfanylquinones, the preferential conformation of the sulfoxide is the *s-cis* one, as hypothesised by Carreño. However, it can be seen that the dihedral angle between the sulfoxide and the quinone plane varies depending on the substituents. In the case of sulfanylquinone **318a**, the sulfoxide adopts an angle of -12.6° . When we moved to the unsubstituted sulfanylquinone **297**, that angle lowers to -0.44° , indicating that the torsion of the sulfoxide in the first case might be due to the steric hindrance of the methyl group.

However, when a chlorine atom is added next to the sulfinyl moiety on the quinone, that same angle goes up to -23.5° . As chlorine is a rather small atom (compared to a methyl group), it is most likely that the repulsion of the sulfoxide should be due to electrostatic interactions.

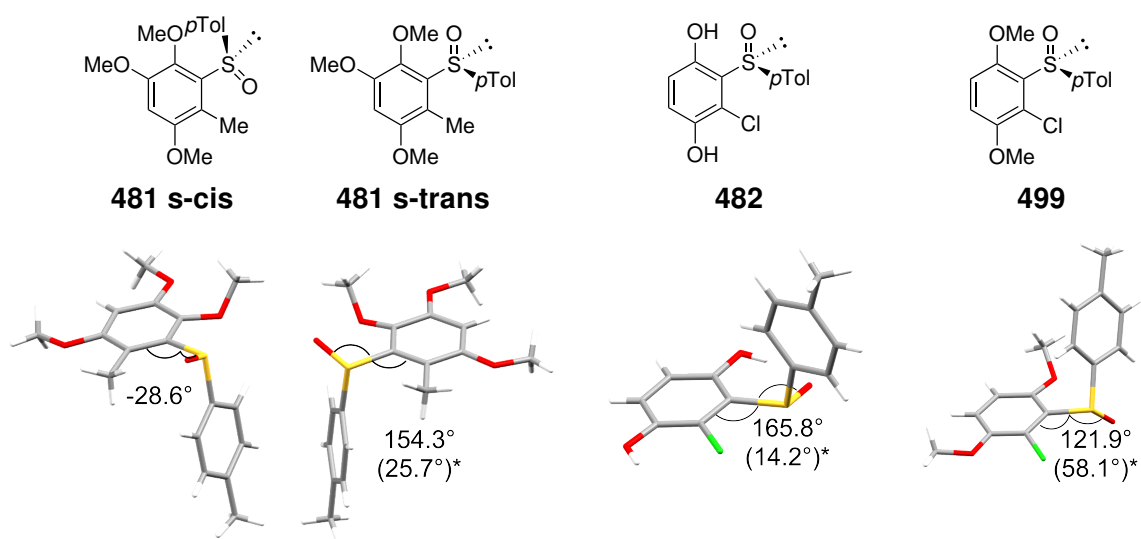
Finally, the fourth sulfanylquinone **488** had been synthesised in order to see if the position of the methoxy group on the opposite double bond, compared to the position of the methoxy group in **318a**, might play a role in the preferential conformation of the sulfoxide. But, given the dihedral angle of -3.2° observed for that sulfanylquinone, it seems that the position of the methoxy group on the opposite double bond has no or little effect on the preferential orientation of the sulfoxide.

So far, we can conclude that the groups on the opposite double bond to the one bearing the sulfinyl moiety do not directly influence the preferred conformation of the sulfoxide. We can also assert that the carbonyl and the group next to the sulfinyl moiety have an effect on that same conformation (mainly *via* electrostatic repulsions, but also steric ones).

We decided to take that structural analysis a bit further by doing the same analysis on hydroquinone derivatives. For that purpose, we crystallised compound **481** (from the synthesis of sulfanylquinone **318a**, Scheme 5.2). We also had the opportunity to obtain the non alkylated hydroquinone **482**. In order to be able to compare the latter with its alkylated version, we methylated it with dimethyl sulfate (Scheme 5.11). It was then possible to try and crystallise both **482** and **499**.

Scheme 5.11: Methylation of hydroquinone **482**.

All three hydroquinones were successfully crystallised and submitted to X-ray diffraction, which provided the structures presented in Figure 5.3. The first surprising result was obtained with the hydroquinone derivative **481** that is present in both *s*-cis and *s*-trans conformations inside the same unit cell. Compared to the result obtained with the corresponding quinone **318a** (Figure 5.2), the simple fact to go from a carbonyl to an ether group seems to be enough to reduce the electrostatic repulsion between both oxygen atoms. This observation actually makes sense as the electron density on the oxygen atom of the ether group is lower than for the carbonyl. It would also seem that the repulsion caused by the methyl group (which might be steric and/or electrostatic) is similar to the one caused by the methoxy group as both conformations are present with similar dihedral angles for the sulfoxide group (28.6° for the *s*-cis conformation and 25.7° for the *s*-trans one).

Figure 5.3: X-ray structures of hydroquinone derivatives **481**, **482**, and **499** and dihedral angles between the sulfoxide and the hydroquinone plane. *Deviation angle from the hydroquinone plane.

In the case of the hydroquinone **482**, it can be seen that the preferred conformation is the *s*-trans one. Indeed, not only does the chlorine atom destabilise the *s*-cis conformation, by causing an important electrostatic repulsion on the sulfoxide group as observed in the X-ray structure of **307a** (Figure 5.2), but the presence of the free phenol group allows an intramolecular hydrogen bond. This bond must greatly stabilise the *s*-trans conformation as indicated by the deviation angle (14.2°). When methyl groups are added on those phenols, the hydrogen bond in **499** is no longer possible and the sulfoxide is repelled with an angle of 58.1° out the hydroquinone plane, in the *s*-trans conformation. The repulsion of the chlorine atom must be too important in this example to allow the sulfoxide to adopt the *s*-cis conformation.

The additional study on those three hydroquinones corroborates the observations done on the sulfinylquinones (Figure 5.2). The preferential conformation, *s*-cis or *s*-trans, is highly dependent on the groups next to the sulfoxide moiety and is most likely due to the electrostatic repulsion caused by those substituents.

However, those observations were made in the solid state. Although these structures are consistent with the proposed hypothesis, it does not prove the *s*-cis conformation remains the favoured one in solution nor justify the selectivities observed for Diels-Alder reactions with these sulfinylquinones. It is most likely that the interactions with the solvent and other sets of parameters must be taken into account.

5.3.2 Theoretical approach of the sulfoxide conformation

To complete the model, geometry optimisations on both *s*-cis and *s*-trans conformations of the sulfoxide have been run. First, analyses on sulfinylquinones bearing different substituents (general structure **500** in Figure 5.4) have been made to compare the effect of each of them on the preferential conformation. The dihedral angles between the sulfoxide and the quinone plane (concerned atoms circled in blue on the represented structure in Figure 5.4) for both *s*-cis and *s*-trans conformation and the energy difference between those two conformers have been listed in Table 5.1.

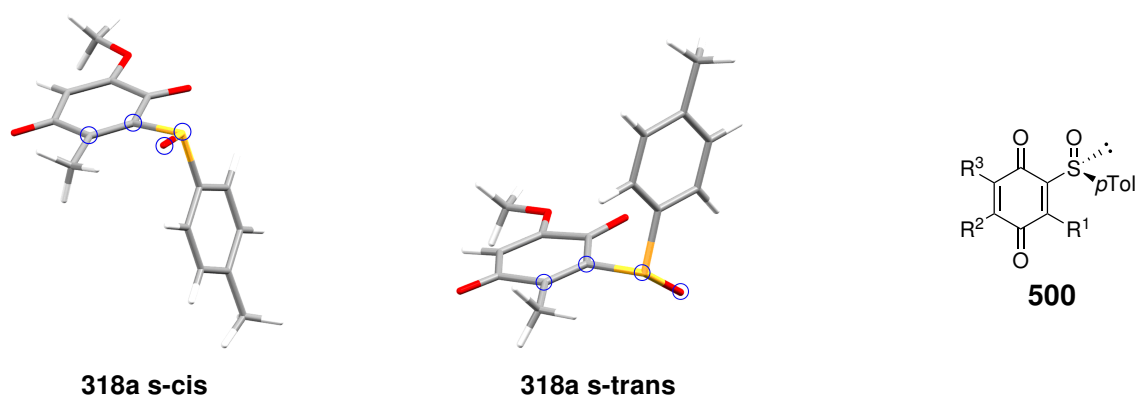


Figure 5.4: Optimised geometries for *s*-cis and *s*-trans conformations (illustrated here with the sulfinylquinone **318a**) and general structure for the studied sulfinylquinones (**500**). The atoms of the concerned dihedral angles (Table 5.1) are circled in blue.

It can be directly noticed that the calculated dihedral angles for **318a**, **297**, **307a**, and **488** are close to the one in the crystal structure. It indicates that the results obtained from the calculation are consistent with the observed ones (for the conformations). Then, whatever the substituents are, the angles for the *s*-trans conformation do not vary a lot (between 45° and 60°). We can conclude that only the oxygen of the carbonyl group influences the orientation of the sulfoxide group in the *s*-trans conformation. Moreover, the negative ΔE indicates that the *s*-cis conformer is the more stable one in each case.

When the methyl group in R¹ is removed (**500a**) it can be observed that the angle decreases from 17° from the quinone plane to 2° and that the energy difference almost doubles. A similar result is obtained when the methoxy group is absent (**297**). The R³ substituent does not seem crucial for the preferential conformation. On the other hand, if the size of the R¹ substituent is increased, such as an isopropyl group (**500b**), the sulfoxide moves further from the quinone plane (32°) even if the stabilisation energy is similar to **318a**.

Table 5.1: Dihedral angles (atoms circled in blue in Figure 5.4) and energy difference between the s-cis and s-trans conformations of different sulfinylquinones in vacuum at 25 °C. Level of theory: M06-2X/6-31+G(d,p).

Quinone	Substituents			Dihedral angle (°)		$E_{\text{cis}} - E_{\text{trans}}$ (kcal mol ⁻¹)
	R ¹	R ²	R ³	s-cis	s-trans	
318a	Me	H	OMe	-17 (-13) ^[a]	129 (51) ^[b]	-2.91
500a	H	H	OMe	2.0	128 (52) ^[b]	-5.62
297	H	H	H	3.0 (-0.44) ^[a]	128 (52) ^[b]	-5.99
500b	<i>i</i> Pr	H	OMe	-32	129 (51) ^[b]	-3.13
488	H	OMe	H	1.5 (-3.2) ^[a]	128 (52) ^[b]	-6.51
500c	NH ₂	H	OMe	-14.3	119 (61) ^[b]	-9.19
500d	SiH ₃	H	OMe	0.9	135 (45) ^[b]	-5.30
318b	CH ₂ SiMe ₂ Ph	H	OMe	-20	124 (56) ^[b]	-2.08
500e	F	H	H	-16	130 (50) ^[b]	-0.81
307a	Cl	H	H	-21 (-23) ^[a]	135 (45) ^[b]	-0.77
500f	CN	H	H	-9.1	138 (42) ^[b]	-2.06

[a] Dihedral angles from the crystal structures. [b] Deviation angle from the quinone plane.

In the case of the sulfinylquinone **488**, where the methoxy group is in position R² instead of R³, a similar angle to **500a** is obtained but the stabilisation energy is almost 1 kcal mol⁻¹ greater. This higher value could be explained by an increase of the electronic density on the oxygen of the carbonyl group due to the electrodonating properties of the methoxy group conjugated to the carbonyl group, increasing the electrostatic repulsion. In the case of **500a**, the methoxy group is indeed not conjugated to the upper carbonyl group and does not influence its electronic density.

In the case of **500c**, we observe a greater angle (14 °) than the previous cases but a much greater stabilisation energy. This stabilisation should most likely be due to an intramolecular hydrogen bond between the sulfoxide and the amine group. The higher angle could be caused by the conformation the sulfoxide has to adopt to make such a hydrogen bond. When the amine is replaced by a silane group (**500d**), a similar phenomenon is observed. The angle gets closer to the quinone plane (almost in the same plane) and the s-cis conformation comes with a great stability. In this case, the silicon atom could play the role of a Lewis acid and the oxygen of the sulfoxide the role of the Lewis base. The calculations have also been made on the sulfinylquinone **318b** and, even though the R¹ group is rather bulky, the angle only goes up to 20 ° out of plane. This should probably be due to the same Lewis pair interaction, getting the sulfoxide closer to the plane.

As explained earlier, we wanted to observe the effect of an electronegative atom on the "ortho" position to see if the repulsion observed in the s-cis conformation was due to a steric or an electrostatic repulsion. Calculations have then been made with a fluorine and a chlorine atom. As expected, the dihedral angle is high (16 ° for fluorine and 21 ° for chlorine) even though those atoms do not occupy a large volume. The stabilisation energy also gets smaller. The electrostatic repulsion would then be the key to explain the higher repulsion of the sulfoxide in the s-trans conformation.

In the last case (where R¹ is a nitrile group), we could have expected a high angle and a low stabilisation energy due to the electrostatic repulsion of the nitrogen atom. But as shown in Table 5.1, those two values are quite reasonable. Once again, an interaction with the electrophilic carbon atom of the nitrile group could explain that the conformation of the sulfoxide does not deviate too far from the quinone plane and that the energy does not decrease a lot.

As we suggested, the effect of the solvent should also play a role in the observed selectivities in asymmetric Diels-Alder reactions. The relative stability of both conformations for sulfinylquinone **318a** have been studied using an implicit solvation and are listed in Table 5.2.

Table 5.2: Energy and free ΔG difference between both s-cis and s-trans conformations of sulfinylquinone **318a**, and ratios therefore, in different solvents (implicit solvation) at 25 °C. Level of theory: M06-2X/6-31+G(d,p).

Solvent	ϵ_r	$E_{\text{cis}} - E_{\text{trans}}$ (kcal mol ⁻¹)	ΔG (kcal mol ⁻¹)	s-cis/s-trans
Vacuum	1	-2.91	-2.36	98/2
Hexane	1.9	-2.12	-1.02	85/15
Benzene	2.3	-1.90	—	—
CHCl ₃	4.8	-1.16	—	—
CH ₂ Cl ₂	8.9	-0.70	0.16	43/57
DMSO	47	-0.20	0.41	33/67
H ₂ O	80	-0.05	0.23	40/60

The first observation that can be made, based on the results presented in Table 5.2, is that the more polar the solvent becomes, the lower the ΔE between the s-cis and s-trans conformations gets. It can also be noticed that the ΔG tends to increase with the polarity of the solvent and even becomes positive for dichloromethane, indicating the s-trans conformation is favoured over the s-cis one.

Even though one can argue, in the case of DMSO and water, that the implicit solvation does not allow to take into account the solvent-solute interactions and, therefore, discredits the results for those two solvents, the case of dichloromethane raises questions. Indeed, no strong interactions are expected between molecules of dichloromethane and sulfinylquinone **318a** and the use of an implicit solvation in that case might be sufficient to model the solvent. Therefore, the values obtained for that solvent, indicating a slight preference for the s-trans conformation, may be reliable.

However, it was experimentally proven that the Diels-Alder reaction of sulfinylquinone **318a** mainly led to the adduct corresponding to the approach of the diene on the top face of the quinone,⁵ which would correspond to the situation in which the sulfoxide is in the s-cis conformation, according to the proposed model (Figure 5.1).²⁴

The contradiction between those theoretical and experimental results may indicate that the preferred conformation of the sulfoxide in solution is not directly correlated to the facial diastereoselectivity of the Diels-Alder reaction of sulfinylquinones, although the importance of the sulfoxide conformation is undeniable. A reasonable explanation would be a high enough difference in reactivity between the s-cis and s-trans conformation. As shown in Table 5.1, the deviation angle of the sulfoxide from the quinone plane ranges from 0.9 to 21 ° in the s-cis conformation and from 45 to 61 ° in the s-trans one. Thereby, even in the most unfavourable situation (sulfinylquinone **307a**), the sulfoxide is always closer to the quinone plane in the s-cis conformation. As a consequence, the conjugation between the double bond and the sulfoxide should be much better in the s-cis conformation, which makes that conformation more reactive than the s-trans one, even if the s-trans conformer is more favoured in more polar solvents.

Moreover, it was calculated that, in vacuum and at 0 °C, the energy barrier for the rotation of the sulfoxide has a value of 6.5 kcal mol⁻¹. That value is not excessively high and the sulfoxide group can freely rotate. Therefore, the equilibration may be fast enough in a range of temperature close to room temperature.

In addition to our calculations made in 2016, a group published in 2019 theoretical calculations to explain the stereoselectivity observed for the Diels-Alder reaction of sulfinylquinones.²⁵ They showed that the preferential approach of a diene occurred on the top face of the *s*-cis conformer of a modelled sulfinylquinone. More interestingly, they also showed that even the minor α adduct was obtained by the approach of the diene on the bottom face of the *s*-cis conformer as well. These results corroborate our conclusion saying the *s*-cis conformer must be the most reactive one.

In order to complete this theoretical study on sulfinylquinone **318a** and propose a more accurate model, calculation of the transition state energies, for the Diels-Alder reaction of our sulfinylquinone, should be performed on both *s*-cis and *s*-trans conformers. In the cases of strongly polar solvents, such as DMSO, or even protic ones, such as water, explicit solvation will be necessary, for both calculations of the preferential conformation of the sulfoxide and the transition state energies, as the solvent-solute interactions cannot be disregarded.

5.4 Reactivity study of quinones and sulfinylquinones

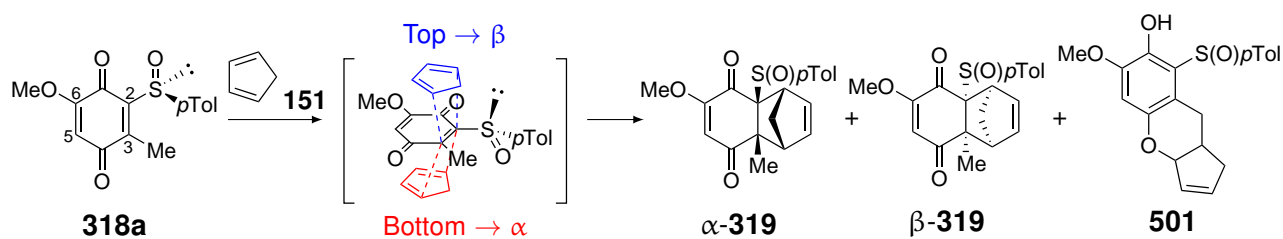
In order to complete our evaluation on the stereoselectivities obtained with sulfinylquinone **318a** and with sulfinylquinones in general, those compounds will be engaged in diverse Diels-Alder reactions. This way, we have the intention to complete the models described before, as well as the ones presented in this thesis.

5.4.1 Effect of the solvent on the Diels-Alder reaction with sulfinylquinone **318a**

The first study that has been done is the study of the effect of the solvent on the facial diastereoselectivity of sulfinylquinone **318a** with cyclopentadiene (**151**). That work has been done in our lab by a master student.²⁶ As already explained, a similar study has been performed by Carreño *et al.* on sulfinylquinone **297** (Table 2.8).¹ However, the Diels-Alder reaction occurred on the C5-C6 double bond, whereas, in our case, the reaction takes place on the C2-C3 double bond.

When the reaction is run in apolar solvents such as benzene or chloroform (Table 5.3, entries 1 and 2), the major adduct obtained is the one resulting from the top approach of the diene, as expected by the different models proposed. It can be seen that when the polarity slightly increases, the selectivity for β -**319** slightly decreases. Interestingly enough, when the reaction was run in cyclopentadiene (**151**) as solvent (entry 3), the reaction rate was much higher, surely due to the high concentration of diene. Moreover, the stereoselectivity towards the β -adduct was also higher, even though its polarity is similar to benzene. Therefore, this selectivity cannot only be explained by the polarity of the solvent, but most likely by solvent-solute interactions.

When polar aprotic solvents were used (entries 4, 6 and 8), a different pair of unexpected products was obtained. After a deeper analysis of the products, it appeared to be a mixture of diastereoisomers and we proposed the structure **501**. Unfortunately, we could not separate those diastereoisomers and we have not been able to assign the absolute nor the relative configurations yet. As proposed in Scheme 5.12, this compounds could come from a hetero-Diels-Alder reaction between a tautomer of sulfinylquinone **318a**, playing the role of the diene, and cyclopentadiene, playing the role of the dienophile. Although this reactivity is not the same as the standard Diels-Alder reaction, it seemed to possess a rather good stereoselectivity in DMF and DMSO.

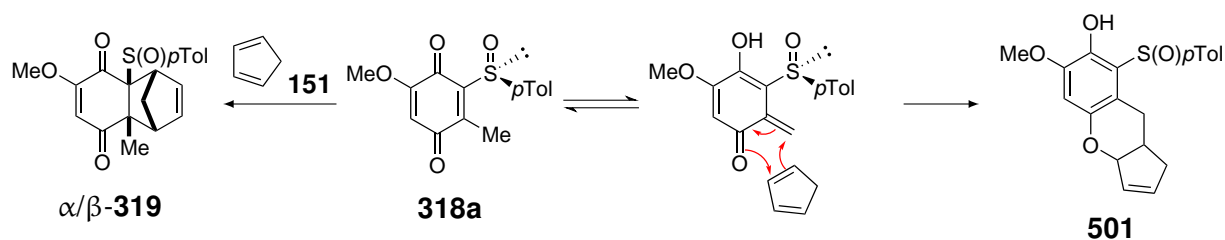
Table 5.3: Times, ratios and yields of the different products obtained for the reaction between sulfinylquinone **318a** and two equivalents of cyclopentadiene (**151**) in different solvents at room temperature.²⁶

Entry	Solvent	Time	Conv. ^[a] (%)	α - 319 : β - 319 ^[b]	501a : 501b ^[b]	Isolated yield (%)
1	C ₆ D ₆	10 d	80	21:79	—	n.d.
2	CHCl ₃	5 d	quant.	32:68	—	74
3	neat ^[c]	24 h	quant.	17:83	—	91
4	THF	18 h	quant.	—	50:50	47
5	Acetone	5 d	quant.	22:56	16:6	89
6	DMF	26 h	quant.	—	28:72	82
7	MeCN	5 d	quant.	30:70	—	70
8	DMSO	10 h	quant.	—	19:81	46
9	AcOH	2 h	quant.	64:36	—	75
10	HFIP	35 min	quant.	88:12	—	66
11	CH ₂ Cl ₂ /HFIP (1 eq.)	3 d	quant.	69:31	—	96
12	EtOH	3 d	quant.	42:58	—	85
13	H ₂ O	5 d	quant.	93:7	—	86
14	EtOH/H ₂ O (9/1)	4 d	quant.	56:44	—	n.d.

n.d. = non determined yield. [a] Based on the ¹H ratio of the remaining sulfinylquinone **318a** and the products in the crude mixture. [b] Based on the ¹H NMR ratio of the products in the crude mixture. [c] Reaction directly run in cyclopentadiene (**151**) as solvent, corresponding to 34 eq. of diene **151**.

In acetonitrile (entry 7), on the other hand, the partners underwent a standard Diels-Alder reaction with a similar selectivity for the β adduct as in benzene or chloroform. Acetone gave a mixture of all four possible adducts with a slight preference for the standard Diels-Alder reaction and a good selectivity for the β -adduct.

We tried to observe the presence of the tautomer of sulfinylquinone **318a** *via* NMR in deuterated DMSO but we did not succeed. It was concluded that the concentration of that species was rather low but, for some reasons, much more reactive in THF, DMF and DMSO. It is also possible that this hetero-Diels-Alder reaction might be asynchronous or even ionic.

Scheme 5.12: Pathways for a Diels-Alder or a hetero-Diels-Alder reaction between sulfinylquinone **318a** and cyclopentadiene (**151**).

The third part of this study (entries 9-14) used protic solvents. The interest of those tests was to determine the influence of the hydrogen bond on the selectivity of the reaction. We suggested that two types of interactions could be possible when hydrogen bond donors were present. As illustrated in Figure 5.5, a hydrogen bond donor can either form a six membered ring where both oxygen atoms of the carbonyl and the sulfoxide act as acceptors or make hydrogen bonds with each oxygen atom individually. In the first arrangement, the sulfoxide is blocked in *s-trans* conformation and the *para*-tolyl group hinders the top face. In the second case, due to steric hindrance, the sulfoxide is blocked in *s-cis* conformation and the *para*-tolyl hinders the bottom face. The preference for one or the other arrangement should probably be linked to the strength of the donor.

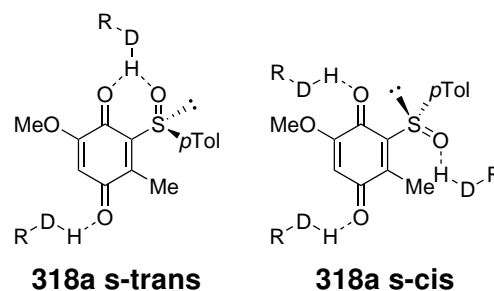


Figure 5.5: Possible interactions between protic solvents and sulfanylquinone **318a**. D = hydrogen bond donor.

First of all, it can be noticed that most of the reactions run in those solvents gave a preference for the α adduct (bottom approach). It can be supposed that the arrangement with the six membered ring (leading to the *s-trans* conformation) is, in most of the cases, the favoured one.

The reaction has been run in acetic acid (entry 9) and gave a slight preference for the α adduct. As explained earlier, the formation of the six membered system is likely to depend on the strength of the donor. In this case, acetic acid is a good donor but also a good acceptor. It is well known that acetic acid dimerises to be both donor and acceptor which probably decreases its donor strength towards the sulfanylquinone.

One astonishing solvent that was used is HFIP (entry 10). Indeed, the reaction time in this solvent was very short compared to the other reaction times (35 min instead of a few hours to a few days). In that solvent, the observed selectivity was also quite high towards the α adduct. This can be explained by the fact that HFIP is a very good hydrogen bond donor and a poor acceptor. It is then expected to form the six membered arrangement rather than the other one. Its hydrogen bond donor strength can also be highlighted when it is used as one equivalent in dichloromethane (entry 11). An inversion of facial selectivity is observed compared to reactions run in aprotic solvents. It is therefore not necessary to work in pure HFIP to benefit from its properties.

As for Carreño's work, ethanol, water and a mix of the two have been tested as solvents (entries 12-14). The reaction in ethanol did not give a good selectivity (with a slight preference for the β adduct). This solvent is indeed a less good donor than acetic acid or HFIP, leading to a mixture of both possible arrangements. We expected that water would give a similar result (as they possess similar pKa values) but, surprisingly, the best diastereoselectivity was observed in the latter. This can be explained by the fact that both sulfanylquinone **318a** and cyclopentadiene (**151**) are not soluble in water and will have a tendency to aggregate. The interactions between the solvent and the solutes happen then at the interface between both phases. In order to make a hydrogen bond with **318a**, a water molecule needs to break favourable interactions with the rest of the solvent. It will afterwards make a less favourable interaction with an organic molecule. To minimise the loss of favourable interactions, the six membered arrangement should be the favoured one as it uses one less molecule of hydrogen bond donor. The sulfoxide will then preferentially be oriented in an *s-trans* conformation,

leading to the α adduct as the major one. When a mixture 9/1 of ethanol and water is used as solvent, the selectivity goes towards the α adduct but remains low. The presence of water might increase the amount of cyclic arrangement but the ethanol being the main solvent, its counter effect is not strong enough to get a high facial selectivity.

5.4.2 The Diels-Alder reaction of 1,4-quinones in hexafluoroisopropanol

Given the outstanding results of the cycloaddition between sulfinylquinone **318a** and cyclopentadiene (**151**) in hexafluoroisopropanol (HFIP), we wanted to study further the use of that solvent for the Diels-Alder reaction of 1,4-quinones. It was found that HFIP has already been used in a wide range of reactions since it is a strong hydrogen bond donor, but a weak acceptor and nucleophile. It has been shown to accelerate a variety of transformations,^{27–33} and was shown to be an excellent solvent to promote [4+2] cycloadditions.^{33–35} However, to the best of our knowledge, only few examples of such Diels-Alder reactions of quinones in that solvent were reported.^{36,37} In those examples, *endo* selectivities were exclusively obtained, in addition to very high regioselectivities.

In order to assess the scope and limitations of the use of HFIP as solvent for the [4+2] cycloaddition reactions with 1,4-quinones, different substituted quinones have been employed. As presented in Figure 5.6, eight benzoquinones (**Q1-8**), two naphthoquinones (**Q9** and **Q10**), as well as the four sulfinylquinones that have been prepared (**SQ1-4**) have been chosen to compare the reactions run in HFIP to the ones run in dichloromethane. Among those quinones, different properties, due to the substituents, have been targeted such as hindrance, electron donation, and electron withdrawal.

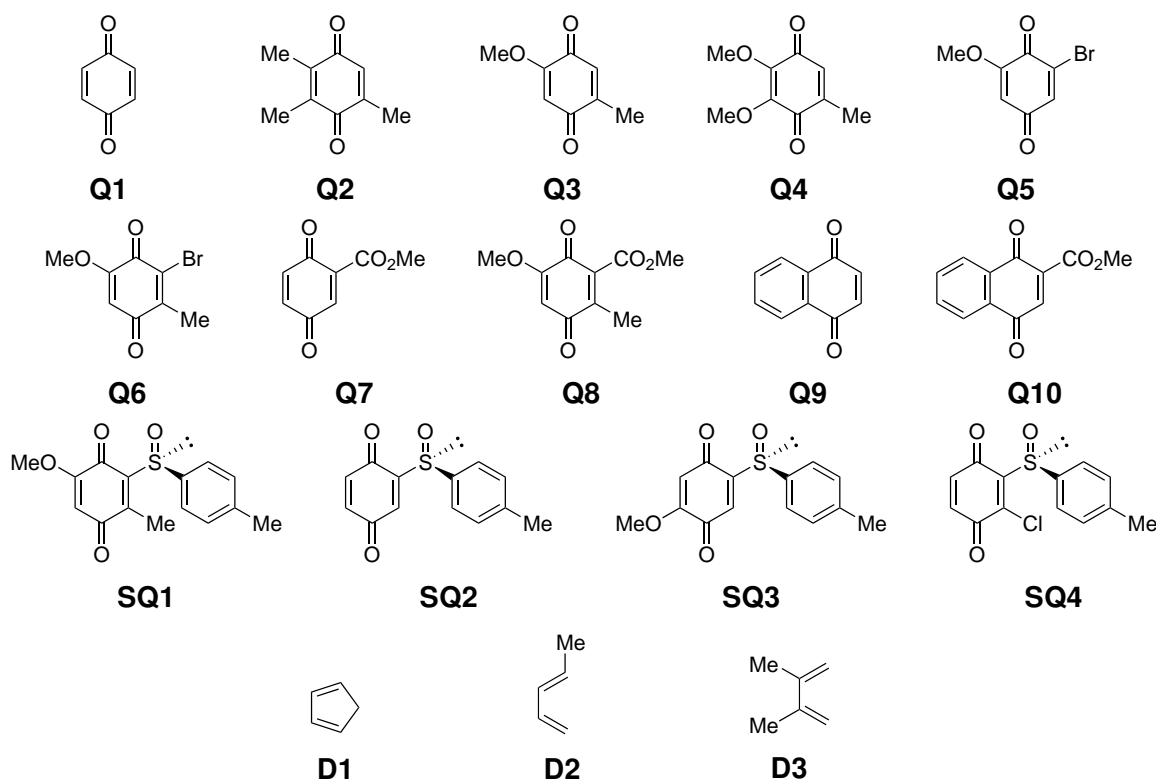


Figure 5.6: Structures of the quinones (**Q1-10**), sulfinylquinones (**SQ1-4**), and dienes (**D1-3**) used in this study, and their new labelling specific to this section. Quinones **Q1** and **Q9** are commercially available. The syntheses of quinones **Q2**, **Q4**, **Q5**, **Q7**, and **Q10** are described in the experimental section.

Moreover, the question of facial dastereoselectivity will be studied in the case of the sulfinylquinones (**SQ1-4**). As partners for those quinones, three model dienes have been selected: cyclopentadiene (**D1**), piperylene (**D2**) and 2,3-dimethylbutadiene (**D3**).^a In order to have reproducible results, we decided to run the reaction at room temperature in both dichloromethane and HFIP at similar concentrations. It has also been decided to stop the reaction after fifteen days maximum.

The first set of reactions have been done with benzoquinones **Q1-8** and are presented in Table 5.4. On first glance, it can be noted that all the reactions run in HFIP were much faster than the ones run in dichloromethane (from days to hours or even minutes in some cases). For example, the reaction of benzoquinone **Q1** (entries 1-6) took 30 min with cyclopentadiene (**D1**) and a few days with acyclic dienes **D2** and **D3** when it was done in dichloromethane. But when it was performed in HFIP, the reaction time dropped to less than one minute^b for dienes **D1** and **D2** and barely five minutes with diene **D3**, which is impressive due to the low reactivity of the latter. This acceleration of the reaction rate can be explained by the strong hydrogen bonds between the solvent and the carbonyl groups of the quinone, which cause an effect similar to a Lewis acid. It therefore lowers the LUMO orbital of the quinone and highly increases its reactivity towards the cycloaddition.

Without any surprise, the substituents on the quinone substrates greatly influence their reactivity. Indeed, when we moved to a rather hindered quinone, such as **Q2** (entries 7-12), the conversions in dichloromethane were rather low (entries 7 and 9) after fifteen days, or no reaction occurred at all (entry 11). However, when the solvent was replaced by HFIP, full conversion was reached within a few hours with all three dienes (entries 8, 10, and 12). Similar observations have been made with quinones **Q3** and **Q4** (entries 13-24) that bear methoxy groups, that are both hindering and electron donating groups. Besides the reaction with cyclopentadiene, in dichloromethane, low conversion or no conversion at all were obtained. Using HFIP, on the other hand, led to the full conversion of the quinones within a very reasonable amount of time.

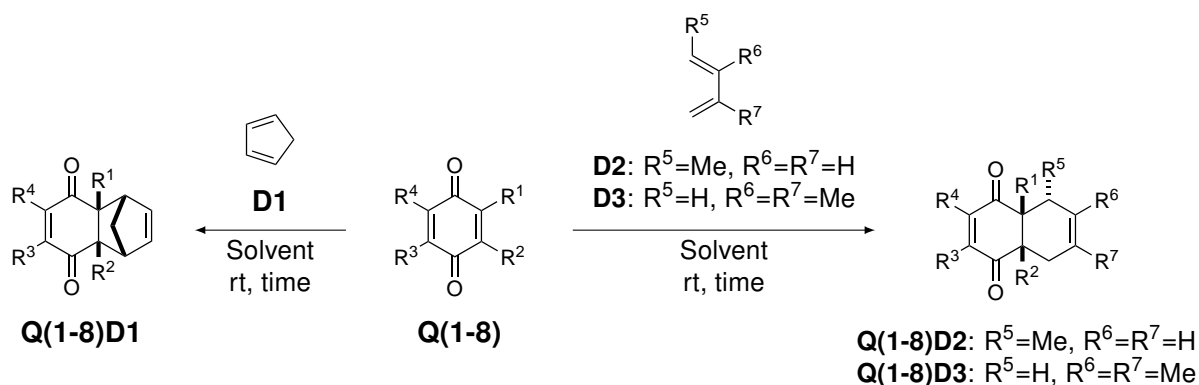
The reaction of quinone **Q5** with diene **D1** (entries 25 and 26) worked uneventfully, whether in dichloromethane or HFIP. However, when that quinone was reacted with acyclic dienes **D2** and **D3**, unexpected products were obtained. They will be presented later in Table 5.7.

In the case of quinone **Q6** (entries 27-32), the most reactive double bond bears a bromine atom and a methyl group, making the latter very hindered. When that quinone was engaged in a Diels-Alder reaction with dienes **D1** and **D3**, no reaction took place and a very low conversion was reached with diene **D2**. The use of HFIP could solve this reactivity issue with **D1** and **D2**. However, even the use of that solvent did not allow to go over 55% conversion with diene **D3**, which is not surprising given that both partners are very hindered reagents.

We then moved forward to quinone **Q7** that bears an electron withdrawing group (entries 33-38). That quinone being quite reactive, the rate of the cycloadditions were high, even in dichloromethane. As an illustration, the reaction of **Q7** with cyclopentadiene (**D1**) was over within less than one minute

^aAs it can be noticed, the labelling of the reagents and the products have been changed in order to simplify the reading of the results in this section. This new labelling is specific to this section and will not be used in other parts of this document. The letter code **Q** was given to quinones and naphthoquinones, **SQ** to sulfinylquinones and **D** to dienes. The label of the expected cycloadducts is built by combining the labels of the quinone and the diene (for example, quinone **Q1** reacting with **D1** will give the expected cycloadduct **Q1D1**). In the case of the Diels-Alder reactions of the sulfinylquinones, the letter code **P** was added to the label for pyrolysed cycloadducts.

^bExperimentally, one can visually observe that the reaction is instantly over as the quinone solution directly discolours upon the addition of the diene.

Table 5.4: Reaction times, products, conversions, and yields for the Diels-Alder reactions between quinones **Q1-8** and dienes **D1-3** in dichloromethane and HFIP at room temperature.

Entry	Quinone	R ¹	R ²	R ³	R ⁴	Diene (eq.)	Solvent	Time	Product	Conv. ^[a] (%)	Isolated yield (%)
1	Q1					D1 (2)	CH ₂ Cl ₂	30 min	Q1D1	quant.	94
2	Q1					D1 (1)	HFIP	<1 min	Q1D1	quant.	>98
3	Q1					D2 (2)	CH ₂ Cl ₂	6 d	Q1D2	quant.	92
4	Q1	H	H	H	H	D2 (2)	HFIP	<1 min	Q1D2	quant.	97
5	Q1					D3 (2)	CH ₂ Cl ₂	8 d	Q1D3	quant.	80
6	Q1					D3 (2)	HFIP	5 min	Q1D3	quant.	96
7	Q2					D1 (2)	CH ₂ Cl ₂	>15 d	Q2D1	68	60
8	Q2					D1 (2)	HFIP	2 h	Q2D1	quant.	>98
9	Q2	H	Me	Me	Me	D2 (2)	CH ₂ Cl ₂	>15 d	Q2D2	40	31
10	Q2	H	Me	Me	Me	D2 (2)	HFIP	31 h	Q2D2	quant.	>98
11	Q2					D3 (2)	CH ₂ Cl ₂	>15 d	—	0	—
12	Q2					D3 (2)	HFIP	24 h	Q2D3	quant.	70
13	Q3					D1 (2)	CH ₂ Cl ₂	15 d	Q3D1	quant.	>98
14	Q3					D1 (2)	HFIP	2 h	Q3D1	quant.	93%
15	Q3	H	Me	H	OMe	D2 (2)	CH ₂ Cl ₂	>15 d	—	0	—
16	Q3	H	Me	H	OMe	D2 (2)	HFIP	28 h	Q3D2	quant.	81%
17	Q3					D3 (2)	CH ₂ Cl ₂	>15 d	—	0	—
18	Q3					D3 (2)	HFIP	36 h	Q3D3	quant.	97%
19	Q4					D1 (2)	CH ₂ Cl ₂	10 d	Q4D1	quant.	98
20	Q4					D1 (2)	HFIP	1 h	Q4D1	quant.	>98
21	Q4	H	Me	OMe	OMe	D2 (2)	CH ₂ Cl ₂	>15 d	Q4D2	35	23
22	Q4	H	Me	OMe	OMe	D2 (2)	HFIP	19 h	Q4D2	quant.	95
23	Q4					D3 (2)	CH ₂ Cl ₂	>15 d	—	0	—
24	Q4					D3 (2)	HFIP	24 h	Q4D3	quant.	70
25	Q5	Br	H	H	OMe	D1 (2)	CH ₂ Cl ₂	2 h	Q5D1	quant.	>98
26	Q5	Br	H	H	OMe	D1 (2)	HFIP	<1 min	Q5D1	quant.	>98
27	Q6					D1 (2)	CH ₂ Cl ₂	>15 d	—	0	—
28	Q6					D1 (2)	HFIP	22 h	Q6D1	quant.	>98
29	Q6	Br	Me	H	OMe	D2 (2)	CH ₂ Cl ₂	>15 d	Q6D2	13	—
30	Q6	Br	Me	H	OMe	D2 (2)	HFIP	20 h	Q6D2	quant.	>98
31	Q6					D3 (2)	CH ₂ Cl ₂	>15 d	—	0	—
32	Q6					D3 (2)	HFIP	>15 d	Q6D3	55	36
33	Q7					D1 (2)	CH ₂ Cl ₂	<1 min	Q7D1	quant.	88
34	Q7					D1 (2)	HFIP	<1 min	Q7D1	quant.	92
35	Q7	CO ₂ Me	H	H	H	D2 (2)	CH ₂ Cl ₂	1 h	Q7D2	quant.	>98
36	Q7	CO ₂ Me	H	H	H	D2 (2)	HFIP	<1 min	Q7D2	quant.	>98
37	Q7					D3 (2)	CH ₂ Cl ₂	100 min	Q7D3	quant.	>98
38	Q7					D3 (2)	HFIP	<1 min	Q7D3	quant.	98
39	Q8					D1 (2)	CH ₂ Cl ₂	15 d	Q8D1	quant.	85
40	Q8	CO ₂ Me	Me	H	OMe	D1 (2)	HFIP	7 h	Q8D1	quant.	82
41	Q8	CO ₂ Me	Me	H	OMe	D2 (2)	HFIP	8 h	Q8D2	quant.	79
42	Q8					D2 (2)	HFIP	14 h	Q8D3	quant.	82

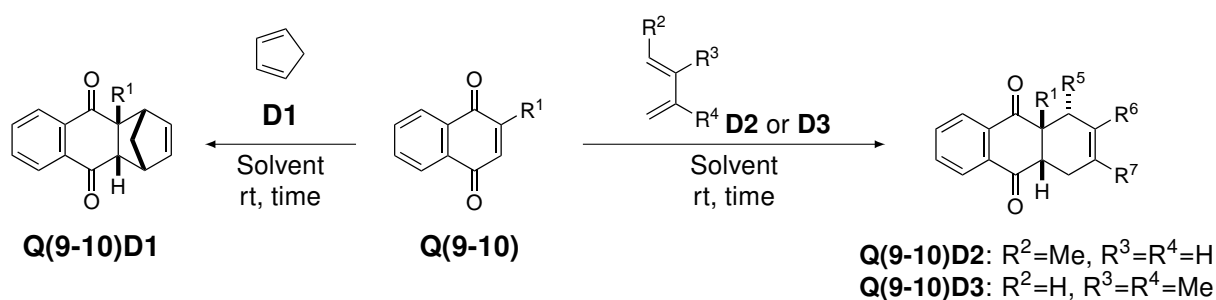
[a] Based on the ¹H NMR ratio of the starting material and the products in the crude mixture.

in dichloromethane. It took a bit longer for dienes **D2** and **D3**, but it was still a very reasonable amount of time. In HFIP, the reactions with all three of the dienes were almost instantly over.

The last benzoquinone that was tested, **Q8**, is the one planned for the total synthesis of momilactones *via* the Evans catalysis (Scheme 5.10). This example is a bit particular as it bears an electron donating group (OMe) on one of the double bond and an electron withdrawing group (CO₂Me) on the other. Nonetheless, the Diels-Alder reactions were expected on the double bond that bears the ester group as it is supposed to be the most electron poor one. When the reaction with cyclopentadiene (**D1**) was run in dichloromethane (entry 39), it took fifteen days for the reaction to be complete. We were a bit astonished as both **D1** and **Q8** should be quite reactive. The second astonishment came when the reactions were performed with **D2** and **D3**. Indeed, not only did they not reach completion, but the standard cycloadducts were not the products obtained. As for quinone **Q5**, those unexpected products are presented in Table 5.7. However, when the same reactions were done in HFIP (entries 40-42), not only were they much faster (only a few hours), but they also gave the expected cycloadducts for dienes **D2** and **D3**. As it will be evidenced later at the end of this section, these two examples are the only ones that led to a different double bond selectivity depending on whether the reaction is run in dichloromethane or HFIP.

The next category of substrates studied are naphthoquinones **Q9** and **Q10** (Table 5.5). These two examples gave similar tendencies, albeit their reactions were slower than their benzoquinones counterparts, if **Q9** and **Q10** are compared to **Q1** and **Q7**, respectively.

Table 5.5: Reaction times, products, conversions, and yields for the Diels-Alder reactions between naphthoquinones **Q9-10** and dienes **D1-3** in dichloromethane and HFIP at room temperature.



Entry	Quinone	R ¹	Diene (eq.)	Solvent	Time	Product	Conv. ^[a] (%)	Isolated yield (%)
1	Q9		D1 (2)	CH ₂ Cl ₂	3 h	Q9D1	quant.	93
2	Q9		D1 (2)	HFIP	<1 min	Q9D1	quant.	>98
3	Q9	H	D2 (2)	CH ₂ Cl ₂	14 d	Q9D2	quant.	>98
4	Q9	H	D2 (2)	HFIP	30 min	Q9D2	quant.	>98
5	Q9		D3 (2)	CH ₂ Cl ₂	>15 d	Q9D3	68	59
6	Q9		D3 (2)	HFIP	40 min	Q9D3	quant.	95
7	Q10		D1 (2)	CH ₂ Cl ₂	10 min	Q10D1	quant.	95
8	Q10		D1 (2)	HFIP	<1 min	Q10D1	quant.	97
9	Q10	CO ₂ Me	D2 (2)	CH ₂ Cl ₂	6 h	Q10D2	quant.	>98
10	Q10	CO ₂ Me	D2 (2)	HFIP	<1 min	Q10D2	quant.	>98
11	Q10		D3 (2)	CH ₂ Cl ₂	18 h	Q10D3	quant.	>98
12	Q10		D3 (2)	HFIP	<1 min	Q10D3	quant.	>98

[a] Based on the ¹H NMR ratio of the starting material and the products in the crude mixture.

In the case of **Q9** (entries 1-6), it took several days for the reaction with **D2** to be complete, and completion was not reached after fifteen days with **D3**. However, replacing dichloromethane by HFIP lowered that reaction rate to 40 min at maximum.

As expected for a dienophile bearing an electron withdrawing group, **Q10** was more reactive and, in less than one day, all three reactions were complete in dichloromethane (entries 7, 9, and 11). Nevertheless, the use of HFIP made those reactions instantly complete (entries 8, 10, and 12).

In the case of sulfinylquinones **SQ1-4**, many products can be obtained compared to the other quinones. Indeed, as described in the scheme of Table 5.6, the possible cycloadducts can be obtained as mixtures of diastereoisomers. As presented in the scheme of Table 5.3, the diene can either approach on the top face of the quinone, leading to the β adduct, or on the bottom face, leading to the α adduct. In addition, the sulfoxide group can undergo a β -*syn* elimination and provide pyrolysis products. Therefore, the cycloadducts resulting from the reaction with **D1** may pyrolyse into product **SQ(1-3)D1P** if the R^1 substituent is a hydrogen atom. Similarly, the adducts obtained with **D2** and **D3** may pyrolyse following two paths, leading to the corresponding products **P1** or **P2**. Typically for that pyrolysis, the *para*-toluenesulfenic acid is not recovered as such, but rather as a thiosulfinate **502**, that comes from the condensation of two molecules of sulfenic acid.

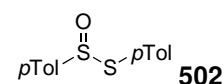
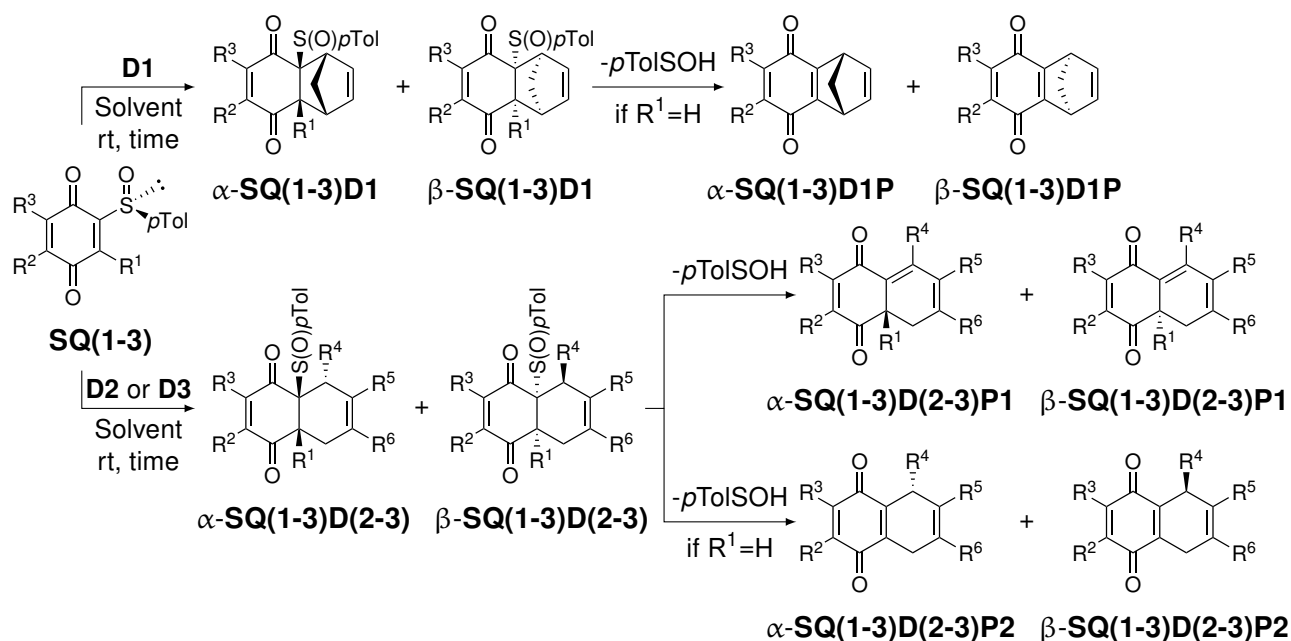


Figure 5.7: Structure of thiosulfinate **502**.

The relationship between the structure of those sulfinylquinones and their reactivity is less obvious as they possess a rather bulky electron withdrawing group. The main factor in those cases seems to be steric hindrance, as less substituted sulfinylquinones (**Q2-4**) react rapidly (less than 24 h), while **SQ1** needs days to achieve complete conversion in dichloromethane. The reactivity of **SQ1** and **SQ2** in dichloromethane was already known^{5,6,8} and we compared those results to the ones in HFIP. As can already be seen, **SQ4** did not react following any of the expected pathways described in the scheme of Table 5.6. Its products will be discussed later in Table 5.7.

For the cycloadditions involving quinones **SQ1** and **SQ2**, in dichloromethane (entries 1, 3, 5 and 7), the β -adduct (either followed by pyrolysis or not) was the major one for all three dienes, when the latter reacted on the expected double bond, as already explained by diverse models.^{5,24} When the solvent was replaced by HFIP, with cyclopentadiene (**D1**), the selectivity was inverted towards the α adduct (entry 2), as already described above. Surprisingly, acyclic dienes (**D2** and **D3**) did not show the same inversion of facial diastereoselectivity (entries 4 and 8). Instead, the same selectivity as in dichloromethane was observed. Such observations had already been made by Carreño's group (and has already been presented in Chapter 2, Table 2.7) by studying the reaction of diverse sulfinylquinones with cyclopentadiene (**D1**) and piperylene (**D2**) in the presence of Lewis acids.³⁸ When they used a chelating Lewis acid (ZnBr_2), favouring the *s-trans* conformation and the approach of the diene on the opposite face of the quinone, an inversion of facial selectivity was observed compared to the reaction without catalyst or with a non-chelating Lewis acid ($\text{BF}_3 \cdot \text{OEt}_2$). However, with acyclic dienes, such as piperylene, the stereoselectivity remained unchanged whether a chelating or non-chelating Lewis acids were used. In order to rationalise those different behaviours, they postulated a significant difference in the transition states energy between cyclic and acyclic dienes, leading to the selection of one face or the other in the presence of chelating Lewis acids.

Table 5.6: Reaction times, products, selectivities and yields for the Diels-Alder reactions between sulfinylquinones **SQ1-3** and dienes **D1-3** in dichloromethane and HFIP at room temperature.

Entry	Quinone	R ¹	R ²	R ³	Diene (eq.)	Solvent	Time	Products	α : β ratio	Isolated yield (%)
1	SQ1				D1 (2)	CH ₂ Cl ₂	5 d	SQ1D1	36:65	93
2	SQ1				D1 (2)	HFIP	35 min	SQ1D1	88:12	66
3 ⁵	SQ1				D2 (2)	CH ₂ Cl ₂	10 d	SQ1D2P1	<2:98<	90
4	SQ1	Me	H	OMe	D2 (2)	HFIP	2 h	SQ1D2P1	<5:95< ^[a]	79
5 ⁵	SQ1				D3 (2)	CH ₂ Cl ₂	12 d	α - SQ1D3P1 + β - SQ1D3	10:90	81
6	SQ1				D3 (2)	HFIP	24 h	α - SQ1D3P1 + β - SQ1D3	12:88 ^[b]	81
7 ³⁸	SQ2	H	H	H	D2 (1)	CH ₂ Cl ₂	20 h	SQ2D2P2	<3:97<	71
8	SQ2	H	H	H	D2 (1)	HFIP	5 min	—	—	— ^[c]
9	SQ3				D1 (2)	CH ₂ Cl ₂	20 min	SQ3D1P	<5:95< ^[a,d]	36
10	SQ3	H	OMe	H	D1 (2)	HFIP	<1 min	SQ3D1P	>95:5> ^[a,d]	46
11	SQ3				D2 (2)	CH ₂ Cl ₂	16 h	SQ3D2P2	α << β ^[d,e]	59
12	SQ3				D2 (2)	HFIP	3 min	SQ3D2P2	α < β ^[d,e]	63

[a] Based on the ¹H NMR ratio of the non-pyrolysed adducts in the crude mixture. [b] Based on the ¹H NMR of the pyrolysed α -adduct and the non-pyrolysed β -adduct in the crude mixture. [c] No product could be isolated, although the presence of thiosulfinate in the crude mixture suggests the formation of cycloadducts followed by pyrolysis. [d] Assignment of the structure based on the selectivity for **SQ1**. [e] The exact selectivity could not be determined.

Despite the presence of thiosulfinate **502** in the crude mixture, suggesting the formation of a cycloadduct followed by pyrolysis, we were not able to isolate nor identify any Diels-Alder adduct from the reaction between quinone **SQ2** and diene **D2**, neither in HFIP nor by reproducing Carreño's procedure (entries 7 and 8),³⁸ and therefore could not assess the effect of the solvent in this particular case.

Finally, we tested quinone **SQ3** that has never been described in Diels-Alder reactions so far. When it was reacted with diene **D1** (entries 9 and 10), we obtained, after chromatography, the pyrolysed product **SQ3D1P**, both in dichloromethane and HFIP. Nevertheless, the reaction being quite fast in both solvents, we were able to analyse the cycloadducts by ¹H NMR before they pyrolysed.

Each one of them possessed a different spectrum with the presence of only one diastereoisomer, leading us to the conclusion that we may have obtained both α and β adducts individually depending on the solvent we used. The opposite optical rotations for each sample after pyrolysis confirmed that hypothesis. We suspected that, as for quinone **SQ1**, the product formed in dichloromethane is β -**SQ3D1P** and the one obtained in HFIP is α -**SQ3D1P**, corresponding to an inversion of selectivity, as observed for quinone **SQ1** with cyclopentadiene.

When the same quinone was reacted with diene **D2** (entries 11 and 12), the cycloadduct **SQ3D2** could not be observed, probably due to a rather fast pyrolysis, and we isolated **SQ3D2P2** as product of that reaction. Although we did not assess the stereoselectivity obtained from both reactions, we measured the specific optical rotations of both samples; $+100.9^\circ$ for the product obtained in dichloromethane and $+85.1^\circ$ for the one obtained in HFIP. We assumed, for the same reasons as described earlier, that the major adduct obtained in dichloromethane was the β isomer (possessing a positive optical rotation). The relatively high positive optical rotation measured for the HFIP sample would indicate that, although the selectivity was slightly decreased, the β adduct remained the major one, just as observed with quinone **SQ1**.

Even though the involvement of strong hydrogen bonds is consistent with the spectacular acceleration of the reactions, its influence on the diastereoselectivity of the Diels-Alder reactions with sulfinylquinones remains unclear.

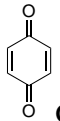
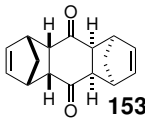
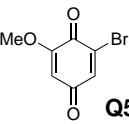
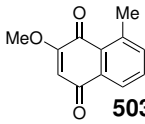
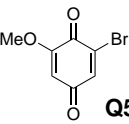
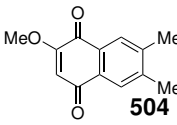
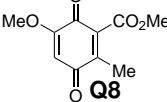
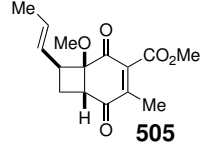
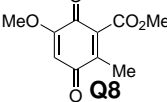
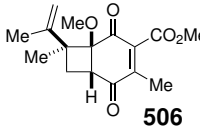
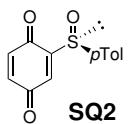
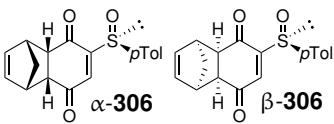
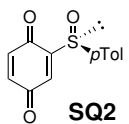
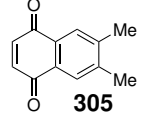
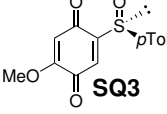
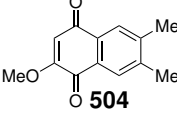
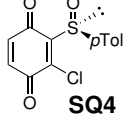
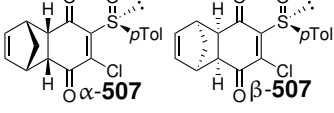
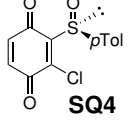
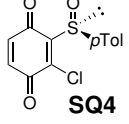
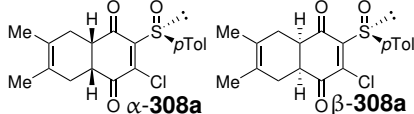
As mentioned earlier in this section, some of the reactions did not give any of the expected cycloadducts, or pyrolysed adducts in the case of the sulfinylquinones. Therefore, we gathered those unexpected products in Table 5.7 and will attempt to provide an explanation of their formation.

As it can be seen in Table 5.4 for benzoquinone **Q1**, only one equivalent of cyclopentadiene (**D1**) has been used for the reaction in HFIP (entry 2). Indeed, if a second equivalent of diene was added to the mixture, it was not possible to obtain adduct **Q1D1** because a second cycloaddition quickly occurred (Table 5.7, entry 1). Therefore, the double cycloadduct **153**, with a *trans* relation between both cyclopentadiene units, was obtained in forty minutes, whereas it took thirty minutes in dichloromethane to reach the mono-cycloadduct **Q1D1** (Table 5.4, entry 1).

The second quinone that gave unexpected products is **Q5** when it reacted with acyclic dienes **D2** and **D3** (entries 2-5). Even though the reaction was much faster in HFIP than in dichloromethane, we were not able to isolate the cycloadducts. Any attempt to dry the crude mixture led to the degradation of the adducts. We identified them as being naphthoquinone derivatives coming from the elimination of the bromide, followed by an oxidative aromatisation. In order to obtain those products more cleanly, we treated the cycloadducts with Et_3N to control the elimination process (HFIP was removed and replaced by dichloromethane for that step). We were then able to isolate naphthoquinones **503** and **504** in acceptable yields.

As described for quinone **Q8**, its reactions with acyclic dienes **D2** and **D3** gave different products in dichloromethane and HFIP. Although the reactions with those dienes gave the expected adducts in HFIP (Table 5.4, entries 41 and 42), they did not react on the expected double bond in dichloro-

Table 5.7: Reaction times, products, conversions, selectivities and yields for the Diels-Alder reactions that did not lead to the standard cycloadducts and pyrolysis products, in dichloromethane and HFIP at room temperature.

Entry	Quinone	Diene (eq.)	Solvent	Time	Products	Conv. ^[a] (%)	Ratio ^[b]	Isolated yield (%)
1		D1 (2)	HFIP	40 min		quant.	—	93
2 ^[c]		D2 (2)	CH ₂ Cl ₂	24 h		quant.	—	74
3 ^[c]		D2 (2)	HFIP	3 min		quant.	—	71
4 ^[c]		D3 (2)	CH ₂ Cl ₂	42 h		quant.	—	75
5 ^[c]		D3 (2)	HFIP	10 min		quant.	—	72
6 ^[d,e]		D2 (2)	CH ₂ Cl ₂	>15 d		54	—	50
7 ^[d,e]		D3 (2)	CH ₂ Cl ₂	>15 d		30	—	24
8 ^[d]			D1 (1)	CH ₂ Cl ₂	1 h		quant.	68:32 ^[f]
9 ^[d]	D1 (1)		HFIP	<1 min	quant.		77:23 ^[f]	78
10 ^[g]		D3 (1)	CH ₂ Cl ₂	20 h		quant.	—	11
11 ^[g]		D3 (1)	HFIP	5 min		quant.	—	15
12 ^[g]		D3 (2)	CH ₂ Cl ₂	22 h		quant.	—	53
13 ^[g]		D3 (2)	HFIP	3 min		quant.	—	56
14 ^[d]		D1 (1)	CH ₂ Cl ₂	1 h		quant.	55:45 ^[f]	75
15 ^[d]		D1 (1)	HFIP	<1 min		quant.	77:23 ^[f]	72
16		D2 (1)	CH ₂ Cl ₂	20 h	Complex mixture	quant.	—	—
17		D2 (1)	HFIP	10 min		Complex mixture	quant.	—
18 ^[d]		D3 (2)	CH ₂ Cl ₂	20 h		quant.	79:21 ^[f]	90
19 ^[d]		D3 (2)	HFIP	10 min		quant.	39:61 ^[f]	82

[a] Based on the ¹H NMR ratio of the starting material and the products in the crude mixture. [b] Based on the ¹H NMR ratio of the products in the crude mixture. [c] After the formation of the cycloadduct, the latter was treated with two equivalents of Et₃N overnight at room temperature in dichloromethane. [d] Reaction on the less reactive double bond of the quinone. [e] [2+2]-cycloaddition. [f] Assignment of the structure as proposed in Carreño's work.⁸ [g] Pyrolysis of the cycloadduct followed by an oxidative aromatisation.

methane. Even more than that, they also provided products that were not Diels-Alder adducts. Through ^1H - ^{13}C correlation NMR experiments, we determined the structure to be the result of a [2+2]-cycloaddition of the diene on the more electron rich double bond of the quinone. The relative configurations were determined by a series of n.O.e experiments (Figure 5.8).

Even though this quinone presents a strong electron withdrawing group, and should behave like **Q7** or **Q10**, it also presents a methoxy group and a methyl group, that both disfavour the standard Diels-Alder reaction by electron donation and steric hindrance, respectively. As can be seen in its X-ray structure (Figure 5.9), the ester group of **Q8** is twisted out of the quinone plane by 54.0° , probably due to an electrostatic repulsion between both oxygen atoms of the quinone carbonyl and the ester group, as well as steric hindrance caused by the methyl group, in analogy to what was discussed previously for sulfinylquinones.

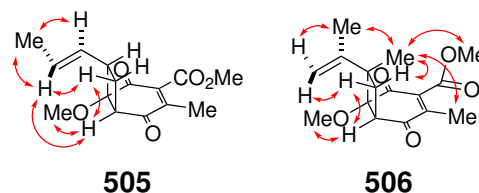


Figure 5.8: Tridimensional representation of products **505** and **506** and n.O.e correlations.

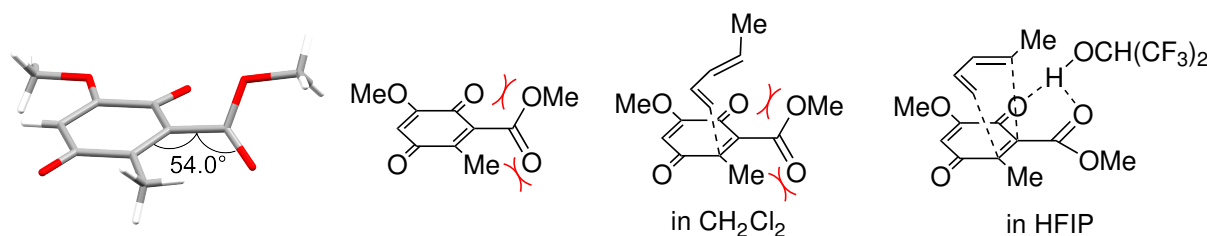
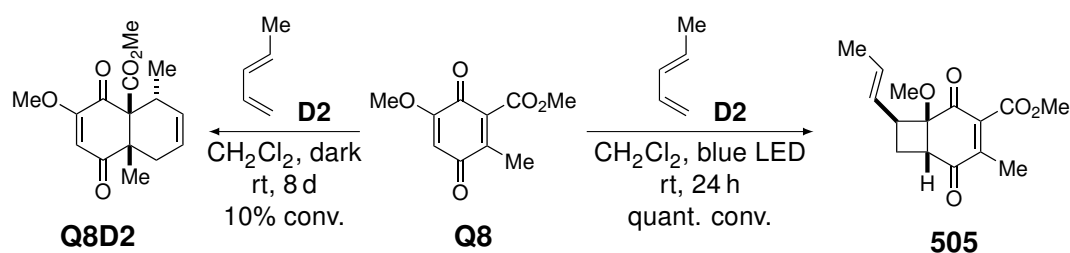


Figure 5.9: X-ray structure of quinone **Q8**, torsion angle between the ester group and the quinone plane, and representation of the supposed approaches of an acyclic diene in dichloromethane and in HFIP.

Assuming the conformation in an apolar aprotic solvent (such as dichloromethane) is similar to the one in the solid state, the out-of-plane conformation of the ester reduces its electron withdrawing effect, decreasing the reactivity of the double bond in a Diels-Alder reaction. We also supposed that, being almost perpendicular to the quinone plane, the ester group, combined with the methyl group, causes a significant steric hindrance, disfavoring the approach on the double bond (Figure 5.9). However, as can be seen in Table 5.4, the expected Diels-Alder reaction with cyclopentadiene (entry 39) took place, albeit very slowly. We supposed that the forced *s-cis* conformation of **D1** increases its reactivity enough to compensate the steric hindrance.

Due to the strong hydrogen bond donation of HFIP, the ester group could be brought back into the quinone plane (as shown in Figure 5.9), increasing its electron withdrawing effect and decreasing its steric hindrance, thereby increasing the reactivity of the quinone double bond. Indeed, reactions with dienes **D2** and **D3** in HFIP gave the expected cycloadducts and the reactions of all three dienes **D1-3** were complete within hours (Table 5.4, entries 40-42).

In order to verify if the unexpected [2+2]-cycloaddition is a photochemical pericyclic or a stepwise ionic process, we decided to perform the reaction between quinone **Q8** and diene **D2** in two different conditions: one in the dark and one under blue LED light. The choice of this light source was made on the basis of the λ_{max} of quinone **Q8**, which gave a value of 367 nm (near UV) in dichloromethane.



Scheme 5.13: Reactions between quinone **Q8** and diene **D2** in absence of light and under blue LED.

On one hand, the reaction run in absence of light did not give **505** and, after eight days, it was determined that a small amount (10% conversion) of the cycloadduct **Q8D2** was obtained (Scheme 5.13). On the other hand, the use of blue light led to the quantitative conversion of quinone **Q8** into the [2+2] cycloadduct **505** (the isolated yield has not been determined) within only 24 h.

Given these results, we could assume that the reaction occurs *via* a slow photoinduced [2+2] process and that quinone **Q8** is capable of being photochemically excited by artificial and/or sun light present in the laboratory, albeit in only a small proportion. Moreover, it also means that the [2+2]-cycloaddition in this particular case is faster than the Diels-Alder reaction. This difference between the reaction rates might be explained by the conformation of the ester group, which disfavours the approach of the diene on the ester-substituted double bond.

A similar phenomenon as for quinone **Q5** was observed with sulfinylquinone **SQ2** and diene **D3** (Table 5.7, entries 10 and 11). As described by Carreño's group,⁶ after the formation of the cycloadduct, the latter undergoes a pyrolysis, followed by aromatisation. Unfortunately, the cycloadduct could not be observed and the stereoselectivity could not be determined as an achiral product (**305**) was formed. Given the low yields, this product may not be the major one, but no others were isolated.

The same observation was made for quinone **SQ3** reacting with diene **D3** (entries 12 and 13). After the cycloaddition, the pyrolysis process most probably occurred on the ring junction, followed by an oxidative aromatisation leading to compound **504** in moderate yields.

Another unusual observation was made with quinone **SQ1** reacting with diene **D1** (entries 8 and 9) and quinone **SQ4** reacting with dienes **D1** and **D3** (entries 14, 15, 18 and 19). Against all odds, the Diels-Alder reaction occurred on the more electron rich double bond. This phenomenon was already described in Carreño's work who studied the effect of different parameters on the selectivity of those reactions.^{6,8} In the case of quinone **SQ2**, they observed a preference for the α adduct that was reinforced when the reaction occurred in protic solvents. As expected, when the reaction was run in HFIP, not only the reaction rate, but also the selectivity towards the α product, increased.

In the case of the reaction of sulfinylquinone **SQ4** with cyclopentadiene (**D1**), a similar reactivity was observed towards the α adduct and reinforced in HFIP (based on the structural assignment proposed by Carreño⁸). When the same quinone was reacted with diene **D3**, one diastereoisomer stood out and was assigned as the α adduct in Carreño's work, in agreement with the stereoselectivities observed so far for those particular examples.⁸ But when the reaction was run in HFIP, an inversion of selectivity, supposedly towards the β adduct, occurred. These last results confirmed that the stere-

oselectivities observed for sulfinylquinones are far from trivial. Even though the models proposed up to now seem to give rational explanations for the observed selectivity in aprotic solvents, the ones proposed for reactions in protic solvents do not apply to every examples presented in this work.

Finally, the reaction between quinone **SQ4** and diene **D2** (entries 16 and 17) was rapidly finished in both dichloromethane and HFIP, but complex mixtures of isomers were obtained and we were not able to isolate the different constituents nor identify them.

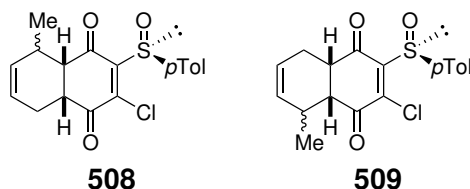


Figure 5.10: Proposed structures of the products obtained from the Diels-Alder reaction between quinone **SQ4** and diene **D2**.

We suggested that the reaction occurred on the least hindered double bond (as for dienes **D1** and **D3** reacting with **SQ4**), as the ^1H NMR of the crude mixture showed the disappearance of the vinylic protons of sulfinylquinone **SQ4** around 6.8 ppm. We also supposed that two regioisomers (**508** and **509**, Figure 5.10) were formed as the regioselectivity on that double bond is poorly controlled. This was supported by the observation of the mass of the expected cycloadducts by HRMS in the crude mixtures (HRMS (ESI+) for $[\text{M}+\text{H}]^+$ calc.: 349.0660, found: 349.0656).

5.4.3 Diels-Alder reactions between sulfinylquinone **318a** and different dienes

In the course of her master thesis and in addition to the study of the effect of the solvent on the diastereoselectivity obtained in the Diels-Alder reaction of sulfinylquinone **318a** with cyclopentadiene (**151**), Kalina Mambourg also studied the cycloaddition reactions of that sulfinylquinone with other dienes (Figure 5.11).²⁶ Besides the three dienes used so far (cyclopentadiene (**151**), piperylene (**179**), and dimethylbutadiene (**247**)), she also used isoprene (**162**), cyclohexa-1,3-diene (**246**), 2,4-hexadiene (**510**), hexa-2,4-dien-1-ol (**511**), 2-trimethylsilyloxybutadiene (**512**), Danishefsky's diene **513**, furan (**514**), and hydroxymethylfuran (**515**).

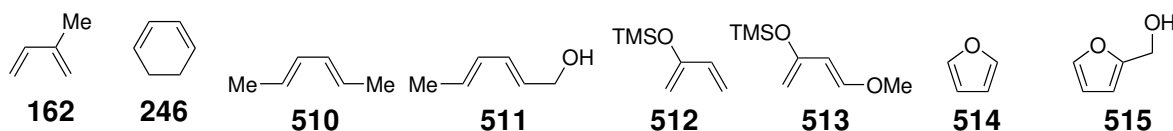
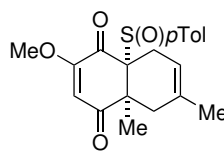
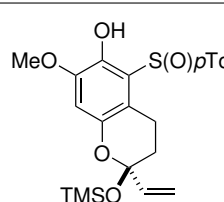
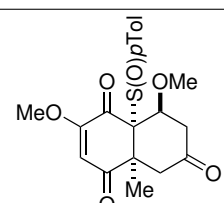


Figure 5.11: Structures of the different dienes used for the Diels-Alder reaction with sulfinylquinone **318a**, in dichloromethane or HFIP as solvent.

The aim of these choices was to have a wide range of dienes with different properties. This way, we could have a larger idea of the type of dienes that might be used or not with sulfinylquinones **318a**. It was also planned to compare the reactions of those dienes with **318a** in both dichloromethane and HFIP (Table 5.8).

Table 5.8: Reaction conditions, yields, and adducts corresponding to the Diels-Alder reaction between sulfinyl-quinone **318a** and different dienes at room temperature in dichloromethane or HFIP.²⁶

Entry	Diene	Solvent	Time	Adduct	Isolated yield (%)
1	162	CH ₂ Cl ₂	—	—	n.r.
2	162	HFIP	27 h	 516	57
3	246	CH ₂ Cl ₂	—	—	n.r.
4	246	HFIP	—	—	n.r.
5	510	CH ₂ Cl ₂	—	—	n.r.
6	510	HFIP	—	—	n.r.
7	511	CH ₂ Cl ₂	—	—	n.r.
8	511	HFIP	—	—	n.r.
9	512	CH ₂ Cl ₂	18 d	 517 (71:29)	42
10	512	HFIP	—	—	deg.
11	513	CH ₂ Cl ₂	4 h	 518	96%
12	513	HFIP	—	—	deg.
13	514	CH ₂ Cl ₂	—	—	n.r.
14	514	HFIP	—	—	n.r.
15	515	CH ₂ Cl ₂	—	—	n.r.
16	515	HFIP	—	—	n.r.

n.r. = no reaction. deg. = degradation of the diene.

When isoprene (**162**) was used as diene (entries 1 and 2), no reaction took place in dichloromethane. However, as already shown several times in this chapter, when dichloromethane was replaced by HFIP a solvent, the reaction was finished within 27 h. Although only one isomer of cycloadduct **516** seemed to have been obtained, the absolute configurations have not been determined. Nevertheless, given the stereoselectivities obtained when acyclic dienes are used in a Diels-Alder reaction with **318a**, it was supposed that the β adduct was the one isolated.

The next diene that has been tested is cyclohexadiene **246**. Surprisingly, no reaction occurred neither in dichloromethane nor in HFIP. It was somewhat surprising that this diene gave no reactions as, being in a forced s-cis conformation, it should possess a similar reactivity to cyclopentadiene (**151**). In order to explain that lack of reactivity with diene **246**, the approach of both cyclic dienes **151** and **246** have been compared

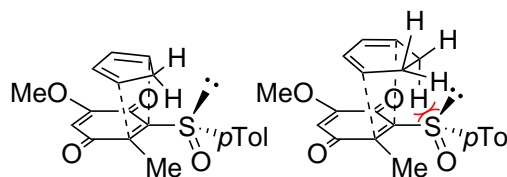


Figure 5.12: Approaches of cyclopentadiene (**151**, left) and cyclohexadiene (**246**, right) on sulfinylquinone **318a**.²⁶

(Figure 5.12). In the case of the cyclopentadiene (**151**), the hydrogen atoms of the methylene unit can manage to fit between the methyl and sulfoxide groups that are present on the reactive double bond of the quinone. On the other hand, when the same reaction is attempted with cyclohexadiene (**246**), the conformation of the ethylene unit forces one hydrogen atom to be pointed towards the double bond, causing a steric clash with either the methyl or the sulfoxide groups. Although this model is only based on conformational conceptions of the dienes, it might give a reasonable explanation to the total absence of reactivity with cyclohexadiene (**246**).

The same lack of reactivity has been observed with dienes **510** and **511** (entries 5-8). These examples were more straightforward to explain. Indeed, the reactive double bond of sulfinylquinone **318a** being a tetrasubstituted dienophile, and therefore a very hindered one, it is not surprising that it cannot react with 1,4-disubstituted dienes, even with an optimal (*E,E*) configuration.

This master student then continued with dienes containing enol ethers. The first one, diene **512**, gave a product that was not a Diels-Alder cycloadduct. It was determined that, in dichloromethane (entry 9), a hetero-Diels-Alder reaction occurred (on a tautomer of sulfinylquinone **318a**), as already observed with cyclopentadiene in certain conditions (Table 5.3). That product **517** was obtained in a 71:29 ratio of two diastereoisomers, albeit the absolute configuration of the ketal center was not determined for either isomer. When HFIP was used as solvent for the same reaction (entry 10), no reaction occurred due to the degradation of the silyl enol ether. Indeed, HFIP being quite acidic for an alcohol ($pK_a = 9.3$), it is likely that this solvent may be able to cleave silyl enol ethers.

In the case of the reaction with Danishefsky's diene **513** in dichloromethane (entry 11), the [4+2] cycloaddition occurred and was over in four hours. However, the adduct was not stable and the silyl enol ether was cleaved upon purification *via* chromatography on silica gel and product **518** was isolated with a very good yield. Similarly to diene **512**, the reaction in HFIP (entry 12) gave no adduct as the solvent cleaved the silyl enol ether of the diene.

The last substrates that have been tested by that master student were furan (**514**, entries 13 and 14) and hydroxymethylfuran (**515**, entries 15 and 16). Furan derivatives have already been used as diene in Diels-Alder reactions with benzoquinones but they were often very electron rich ones or the reaction was done under high pressure.³⁹⁻⁴⁴ It was hoped that the use of HFIP might increase sufficiently the reactivity of the sulfinylquinone to be able to perform such cycloadditions with furans. Unfortunately, no reaction occurred at all, whether in dichloromethane or HFIP. Even if HFIP proved to be a very good solvent to accelerate the [4+2] cycloadditions with quinones and sulfinylquinones, it did not increase the reactivity of **318a** high enough to make it react with a poorly reactive diene such as furan derivatives.

5.4.4 Limitations of the use of HFIP

Although HFIP showed attractive properties in Diels-Alder reactions with quinones, its use cannot be extended to all dienes. The main limitation comes from its relatively high acidity. We tried to use oxygenated dienes, such as 2-trimethylsilyloxybutadiene (**512**) or Danishefsky's diene (**513**), but the only reaction occurring was the cleavage of the silyl enol ether group, leading to the ketone. However, this side reaction does not represent a major drawback, since both dienes were quite reactive, even in dichloromethane. It was not presented in the results but we also observed that, at temperatures of and above 30 °C, a clear precipitate was forming with dimethylbutadiene (**247/D3**) but no Diels-Alder reaction was occurring. We suspected a polymerisation of the diene, once again, because of the acidity of the solvent.

The sensitivity of the reagents to acidic media should be then taken into account before attempting to use HFIP as solvent.

5.5 Conclusion

In the course of the study on sulfinylquinones, we have first been able to synthesise four sulfinylquinones: three that were already known (**318a**,⁵ **297**,⁶ and **307a**⁸, Scheme 5.2, 5.3 and 5.4) and one brand new sulfinylquinone (**488**, Scheme 5.5). We also attempted to synthesise the silylated version of sulfinylquinone **318a** (Schemes 5.6 and 5.8), that would allow us to study the synthetic pathway towards momilactone B (**2**). We were able to reach the sulfoxide precursor of that quinone, whose hydroquinone core was protected with diverse groups but, unfortunately, none of them gave the desired quinone **318b** when they were engaged in the oxidation step, either with CAN or DDQ. We highlighted that obtaining such a silylated sulfinylquinone is not straightforward. As found in the literature, it is likely that the hydroquinone must be deprotected prior to oxidation. Therefore, we will have to find the adequate conditions for the clean removal of the PMB, or find a protecting group that is robust enough to withstand the insertions of the sulfoxide and the silyl group, but that can also be smoothly removed without degrading the hydroquinone precursor.

In addition to the synthesis of the sulfinylquinones, the preparation of two quinones of interest for the total synthesis of momilactones have been developed. The first one, quinone **369** (Scheme 5.9), has been designed to match the general pattern of the quinones used by Corey in his catalysed asymmetric Diels-Alder reactions.^{19,20} We efficiently obtained that quinone in four steps from one of the intermediate of the synthesis of **318a**.

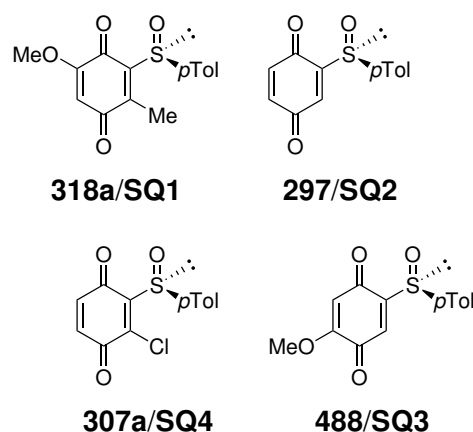


Figure 5.13: Structures of the four sulfinylquinones synthesised and studied in this work.

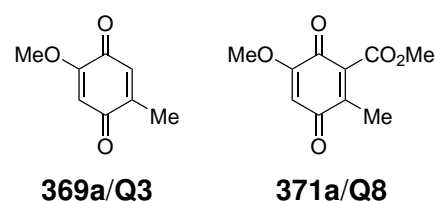


Figure 5.14: Structure of the quinones for Corey and Evans's catalytic systems.

The second quinone of interest has to correspond to the substrates studied by Evans, in his own version of asymmetric Diels-Alder reactions, that contain an ester group.²¹ Therefore, a route from another intermediate of the synthesis of **318a** has been designed to obtain quinone **371a** in a two step sequence with very good yields (Scheme 5.10).

We then took an interest in studying the preferential conformation of the sulfoxide of sulfinylquinones by X-ray analysis and computational calculations. The X-ray structures of all four sulfinylquinones showed the *s-cis* conformation for the sulfoxide in the solid state (Figure 5.2), as expected by the model proposed by Carreño (Figure 5.1).²⁴ We highlighted that only the substituent next to the sulfoxide impacted the deviation angle of the latter from the quinone plane and that the substituents on the other double bond had no or little effect on that angle (Table 5.1). That hypothesis was comforted with the theoretical study of other sulfinylquinones that indicated that bulky substituents or electronegative atoms repelled the sulfoxide from the quinone plane, but also decreased the energy difference between the *s-cis* and *s-trans* conformations.

An implicit solvation was then used to evaluate the impact of the solvent polarity on the preferred conformation of sulfinylquinone **318a** (Table 5.2). We noticed that the data for dichloromethane, that indicated a slight preference for the *s-trans* conformation, were not in agreement with experimental results, if one considers the preferred conformation of the sulfoxide is directly linked to the stereoselectivity of the Diels-Alder reactions of quinone **318a**. However, the use of implicit solvation for dichloromethane might be sufficient to model that solvent, as there should be no strong solvent-solute interactions, and the almost 1:1 ratio of both conformations could not be discredited right away. We concluded that, even if both conformations are present in an almost equimolar amount, the *s-cis* conformation must be more reactive than the *s-trans* one, hence the preference for the addition of the diene on the top face of the quinone.

To complete that theoretical study, the transition state energies of the Diels-Alder reaction of sulfinylquinones must be calculated. In doing so, we will be able to propose a complete model of the approach of dienes onto the sulfinylquinones.

The next part of this work consisted in a reactivity study of quinones and sulfinylquinones. A master student in our group studied the effect of the solvent in the Diels-Alder reaction with sulfinylquinone **318a** and cyclopentadiene (**151**) was performed (Table 5.3), similarly to the study reported by Carreño (Table 2.8).¹ The difference in this work is that the reaction occurred on the double bond bearing the sulfinyl group, whereas it occurred on the opposite double bond in Carreño's work.

It was observed that in apolar solvents, adduct β -**319** was the major one, whereas polar protic solvents led to a preference for α -**319**, with the exception of ethanol. The use of apolar aprotic solvents, however, surprisingly gave a mixture of diastereoisomers of **501**, that came from a hetero-Diels-Alder reaction between a tautomer of **318a** and cyclopentadiene (**151**). The only exceptions to that last case were acetonitrile, that led to the standard cycloaddition with a preference for the β adduct, and acetone, that gave all four possible products with a preference for β -**319**.

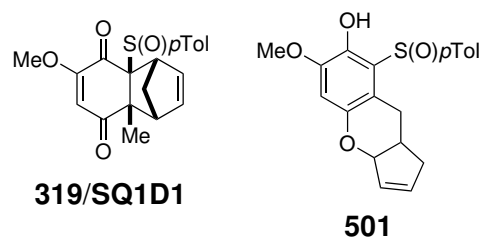


Figure 5.15: Structures of cycloadduct **319** and product **501**.

From those results, we highlighted that cyclopentadiene, as solvent, gave the best selectivity for the β adduct within a reasonable amount of time and water gave the best selectivity towards the α adduct with a reaction time of five days. But the most impressive solvent was HFIP as it gave a very good selectivity for the α adduct within a very short amount of time (only 35 min).

Given the amazing results obtained with HFIP, in terms of rate and stereoselectivity, we decided to study the Diels-Alder reaction of diverse quinones and sulfinylquinones in that solvent (Tables 5.4 to 5.7). We showed that the reaction time for those cycloadditions could be greatly reduced and we even were able to reach full conversion of the quinone with example where no or very low conversion was reached in dichloromethane. There was only one example, between two very hindered partners, that never reached full conversion, even in HFIP.

Moreover, there was two examples that gave us totally unexpected products, in dichloromethane, coming from a [2+2]-cycloaddition on the supposedly least reactive double bond of the quinone. But when the reaction was run in HFIP, not only the reaction was much faster, but it also led to the standard [4+2] cycloaddition on the expected double bond.

The same comparison between dichloromethane and HFIP was also done for the Diels-Alder reaction of sulfinylquinones. It was shown that, when the reaction occurred on the double bond bearing the sulfinyl group, an inversion of selectivity was observed with cyclic diene **151/D1** (preference for the β adduct in dichloromethane and for the α adduct in HFIP). However, acyclic dienes **179/D2** and **247/D3** led to the same preference for the β adduct whether the reaction was done in dichloromethane or HFIP. In the example of dienes reacting on the opposite double bond to the one bearing the sulfoxide group, the α adduct is the major in dichloromethane. This preference was reinforced in HFIP, except for the reaction of dimethylbutadiene (**247/D3**) with sulfinylquinones **307a/SQ4** that seemed to show a preference for the β adduct in HFIP.

Finally, the comparison between dichloromethane and HFIP was also investigated for the Diels-Alder reaction of sulfinylquinone **318a** with diverse dienes (Table 5.8). Despite the potency of HFIP to greatly increase the reaction rate of cycloadditions with quinones, it cannot outweigh the steric clash of two partners that are too hindered to react together (such as 1,4-disubstituted dienes and tetrasubstituted dienophiles) or not reactive enough (such as furan derivatives).

In conclusion, we showed that HFIP could be a good choice of a solvent to accelerate the Diels-Alder reaction of quinones and that it could help some cycloadditions to take place when there is no or low conversions in dichloromethane. We also highlighted that the use of this solvent led to very good stereoselectivities for the Diels-Alder reactions of sulfinylquinones with a preference for the α adducts with cyclic dienes and for the β adduct with acyclic ones. We finally determined that this solvent had some limitations and could not be used with reagents sensitive to acidic media, such as diene bearing a silyl enol ether, although it did not represent a major setback as those dienes were reactive enough in dichloromethane.

References

- [1] Carreño, M. C.; García Ruano, J. L.; Toledo, M. A.; Urbano, A. Influence of the Sulfinyl Group on the Chemoselectivity and π -Facial Selectivity of Diels-Alder Reactions of (*S*)-2-(*p*-Tolylsulfinyl)-1,4-benzoquinone. *J. Org. Chem.* **1996**, *61*, 503–509.
- [2] Andersen, K. K. Synthesis of (+)-ethyl *p*-tolyl sulfoxide from (–)-menthyl (–)-*p*-toluenesulfinate. *Tetrahedron Lett.* **1961**, *3*, 93–95.
- [3] Andersen, K. K.; Gaffield, W.; Papanikolaou, N. E.; Foley, J. W.; Perkins, R. I. Optically Active Sulfoxides. The Synthesis and Rotatory Dispersion of Some Diaryl Sulfoxides. *J. Am. Chem. Soc.* **1964**, *86*, 5637–5646.
- [4] Solladié, G.; Hutt, J.; Girardin, A. Improved Preparation of Optically Active Methyl *p*-Tolyl Sulfoxide. *Synthesis* **1987**, 173.
- [5] Lanfranchi, D. A.; Hanquet, G. Asymmetric Diels-Alder Reactions of a New Enantiomerically Pure Sulfinylquinone: A Straightforward Access to Functionalized Wieland-Miescher Ketone Analogues with (*R*) Absolute Configuration. *J. Org. Chem.* **2006**, *71*, 4854–4861.
- [6] Carreño, M. C.; García Ruano, J. L.; Urbano, A. Synthesis and asymmetric Diels-Alder reactions of (*S*)-2-*p*-tolylsulfinyl-1,4-benzoquinone. *Tetrahedron Lett.* **1989**, *30*, 4003–4006.
- [7] Carreño, M. C.; García Ruano, J. L.; Urbano, A. Synthesis of Optically Active *p*-Tolylsulfinylquinones. *Synthesis* **1992**, 651–653.
- [8] Carreño, M. C.; García Ruano, J. L.; Toledo, M. A.; Urbano, A. Synthesis and Diels-Alder reactions of (*S*)-3-Chloro and (*S*)-3-Ethyl-2-*p*-tolylsulfinyl-1,4-benzoquinones. *Tetrahedron Lett.* **1994**, *35*, 9759–9762.
- [9] Ferreira, A. J.; Nel, J. W.; Brandt, E. V.; Bezuidenhout, B. C. B.; Ferreira, D. Oligomeric isoflavonoids. Part 3. Daljanelins A–D, the first pterocarpan- and isoflavanoid-neoflavanoid analogues. *J. Chem. Soc., Perkin Trans. 1* **1995**, 1049–1056.
- [10] Guzikowski, A. P.; Cai, S. X.; Espitia, S. A.; Hawkinson, J. E.; Huettner, J. E.; Nogales, D. F.; Tran, M.; Woodward, R. M.; Weber, E.; Keana, J. F. W. Analogs of 3-Hydroxy-1*H*-1-benzazepine-2,5-dione: Structure-Activity Relationship at *N*-Methyl-D-aspartate Receptor Glycine Sites. *J. Med. Chem.* **1996**, *39*, 4643–4653.
- [11] Carreño, M. C.; García Ruano, J. L.; Toledo, M. A.; Urbano, A. *ortho*-Directed metallation in the regiocontrolled synthesis of enantiopure 2- and/or 3-substituted (*S*)-2-(*p*-tolylsulfinyl)-1,4-benzoquinones. *Tetrahedron: Asymmetry* **1997**, *8*, 913–921.
- [12] Carreño, M. C.; García Ruano, J. L.; Toledo, M. A. Enantioselective Synthesis of (+)-Royleanone from Sulfinyl Quinones. *Chem. Eur. J.* **2000**, *6*, 288–291.
- [13] Noland, W. E.; Kedrowski, B. L. Quinone Approaches towards the Synthesis of Aflatoxin B₂. *Org. Lett.* **2000**, *2*, 2109–2111.
- [14] Crisp, G. T.; Bubner, T. P. Preparation of Stereically Constrained Arylalkyne Oligomers. *Tetrahedron* **1997**, *53*, 11899–11912.
- [15] García Ruano, J. L.; Alemán, J.; Aranda, M. T.; Arévalo, M. J.; Padwa, A. Highly Stereoselective Vinylogous Pummerer Rearrangement. *Phosphorus, Sulfur Silicon Relat. Elem.* **2005**, *180*, 1497–1498.
- [16] García Ruano, J. L.; Alemán, J.; Aranda, M. T.; Arévalo, M. J.; Padwa, A. Highly Stereoselective Vinylogous Pummerer Reaction Mediated by Me₃SiX. *Org. Lett.* **2005**, *7*, 19–22.
- [17] Taing, M.; Moore, H. W. *o*-Quinone Methides from 4-Allelylcyclobutenones: Synthesis and Chemistry. *J. Org. Chem.* **1996**, *61*, 329–340.
- [18] Feldman, K. S.; Selfridge, B. R. Exploration of Braverman reaction chemistry. Synthesis of tricyclic dihydrothiophene dioxide derivatives from bispropargyl sulfones. *Heterocycles* **2010**, *81*, 117–143.
- [19] Ryu, D. H.; Corey, E. J. Triflimide Activation of a Chiral Oxazaborolidine Leads to a More General Catalytic System for Enantioselective Diels-Alder Addition. *J. Am. Chem. Soc.* **2003**, *125*, 6388–6390.
- [20] Ryu, D. H.; Zhou, G.; Corey, E. J. Enantioselective and Structure-Selective Diels-Alder Reactions of Unsymmetrical Quinones Catalyzed by a Chiral Oxazaborolidine Cation. Predictive Selection Rules. *J. Am. Chem. Soc.* **2004**, *126*, 4800–4802.
- [21] Evans, D. A.; Wu, J. Enantioselective Rare-Earth Catalyzed Quinone Diels-Alder Reactions. *J. Am. Chem. Soc.* **2003**, *125*, 10162–10163.
- [22] Miyawaki, A.; Kikuchi, D.; Niki, M.; Manabe, Y.; Kanematsu, M.; Yokoe, H.; Yoshida, M.; Shishido, K. Total Synthesis of Natural Enantiomers of Heliespirones A and C *via* the Diastereoselective Intramolecular Hosomi-Sakurai Reaction. *J. Org. Chem.* **2012**, *77*, 8231–8243.
- [23] Roush, W. R.; Madar, D. J.; Coffey, D. S. Synthesis of highly functionalized naphthoate precursors to damavaricin D — Observation of kinetically stable benzocyclohexadienones in the bromination reactions of highly functionalized β -naphthol derivatives. *J. Can. Chem.* **2001**, *79*, 1711–1726.
- [24] Carreño, M. C.; García Ruano, J. L.; Urbano, A. Asymmetric Diels-Alder Reactions of (*S*)-2-(*p*-Tolylsulfinyl)-1,4-naphthoquinones. *J. Org. Chem.* **1992**, *57*, 6870–6876.
- [25] Chow, K. H.; Krenske, E. H. Origins of stereoselectivity in uncatalyzed and ZnBr₂-catalyzed Diels-Alder

- reactions of a chiral sulfinylquinone. *Org. Biomol. Chem.* **2019**, *17*, 8756–8767.
- [26] Mambourg, K. Étude de la réaction de Diels-Alder utilisant une sulfinylquinone chirale comme diénophile et développement d'un modèle expliquant la stéréosélectivité. M.Sc. thesis, Université de Namur, Belgium, 2018.
- [27] Bégué, J.-P.; Bonnet-Delpon, D.; Crousse, B. Fluorinated Alcohols: A New Medium for Selective and Clean Reaction. *Synlett* **2004**, 18–29.
- [28] Vuluga, D.; Legros, J.; Crousse, B.; Slawin, A. M. Z.; Laurence, C.; Nicolet, P.; Bonnet-Delpon, D. Influence of the Structure of Polyfluorinated Alcohols on Brønsted Acidity/Hydrogen-Bond Donor Ability and Consequences on the Promoter Effect. *J. Org. Chem.* **2011**, *76*, 1126–1133.
- [29] Shuklov, I. A.; Dubrovina, N. V.; Börner, A. Fluorinated Alcohols as Solvents, Cosolvents and Additives in Homogeneous Catalysis. *Synthesis* **2007**, 2925–2943.
- [30] Heydari, A.; Khaksar, S.; Tajbakhsh, M. 1,1,1,3,3,3-Hexafluoroisopropanol: A Recyclable Organocatalyst for *N*-Boc Protection of Amines. *Synthesis* **2008**, 3126–3130.
- [31] Choy, J.; Jaime-Figueroa, S.; Lara-Jaime, T. A novel practical cleavage of *tert*-butyl esters and carbonates using fluorinated alcohols. *Tetrahedron Lett.* **2010**, *51*, 2244–2246.
- [32] Khaksar, S.; Heydari, A.; Tajbakhsh, M.; Vahdat, S. M. Lewis acid catalyst free synthesis of benzimidazoles and formamidines in 1,1,1,3,3,3-hexafluoro-2-propanol. *J. Fluor. Chem.* **2010**, *131*, 1377–1381.
- [33] Dohi, T.; Yamaoka, N.; Kita, Y. Fluoroalcohols: versatile solvents in hypervalent iodine chemistry and syntheses of diaryliodonium(III) salts. *Tetrahedron* **2010**, *66*, 5775–5785.
- [34] Cativiela, C.; García, J. L.; Mayoral, J. A.; Royo, A. J.; Salvatella, L. Fluorinated Alcohols as Solvents for Diels-Alder Reactions of Chiral Acrylates. *Tetrahedron: Asymmetry* **1993**, *4*, 1613–1618.
- [35] Bolm, C.; Martin, M.; Simic, O.; Verrucci, M. *C*₂-Symmetric Bissulfoximines as Ligands in Copper-Catalyzed Enantioselective Diels–Alder Reactions. *Org. Lett.* **2003**, *5*, 427–429.
- [36] Mubofu, E. B.; Engberts, J. B. F. N. Specific acid catalysis and Lewis acid catalysis of Diels-Alder reactions in aqueous media. *J. Phys. Org. Chem.* **2004**, *71*, 180–186.
- [37] Tzouma, E.; Mavridis, I.; Vidali, V.; Pitsinos, E. Diels–Alder reaction between 1,3,3-trisubstituted-2-vinylcyclohexenes and quinones under exceptionally mild conditions: a concise entry to the cassane-type furanoditerpenoid skeleton. *Tetrahedron Lett.* **2016**, *57*, 3643–3647.
- [38] Carreño, M. C.; García Ruano, J. L.; Lafuente, C.; Toledo, M. A. Asymmetric Diels-Alder reactions of 5-substituted and 5,6-disubstituted (*S*)-2-(*p*-tolylsulfinyl)1,4-benzoquinones with cyclopentadiene and *trans*-piperylene. *Tetrahedron: Asymmetry* **1999**, *10*, 1119–1128.
- [39] Hofmann, A. A.; Wyrsh-Walraf, I.; Iten, P. X.; Eugster, C. H. Cycloadditionen von 3,4-Dimethoxyfuran an Benzoquinone. *Helv. Chim. Acta* **1979**, *62*, 2211–2217.
- [40] Jurczak, J.; Koźluk, T.; Tkacz, M.; Eugster, C. H. Cycloaddition of 3,4-Dimethoxyfuran with 1,4-Benzoquinones under High Pressure. *Helv. Chim. Acta* **1983**, *66*, 218–221.
- [41] Jurczak, J.; Koźluk, T.; Filipek, S.; Eugster, C. H. [2+4]-Cycloadditions under High Pressure: First Realization of a Diels-Alder Addition of Furan with Simple 1,4-Benzoquinones. *Helv. Chim. Acta* **1983**, *66*, 222–225.
- [42] Jurczak, J.; Kawczyński, A. L.; Koźluk, T. Stability of Cycloadducts Obtained by High-Pressure Diels-Alder Reaction between 3,4-Dimethoxyfuran and 1,4-Benzoquinones: Kinetic Studies of Retro-Diels-Alder Reaction. *J. Org. Chem.* **1985**, *50*, 1106–1107.
- [43] Constantino, M. G.; Beatriz, A.; José da Silva, G. V.; Zukerman-Schpector, J. Synthetic studies on the Diels-Alder adduct from 3,4-dimethoxyfuran and benzoquinone. *Synth. Commun.* **2001**, *31*, 3329–3336.
- [44] Reddy, P. P.; Lavekar, A. G.; Babu, K. S.; Rao, R. R.; Shashidar, J.; Shashikiran, G.; Rao, J. M. Synthesis, cytotoxic activity and structure-activity relationships of hedychenone analogues. *Bioorg. Med. Chem. Lett.* **2010**, *20*, 2525–2528.

Chapter 6

Diels-Alder reactions for the synthesis of momilactones

6 Diels-Alder reactions for the synthesis of momilactones

Now that the synthesis of the different proposed quinones and dienes have been carried out, as well as the study of the behaviour of the sulfinylquinones in the Diels-Alder reaction, we can focus on the first steps of the total synthesis of momilactones.

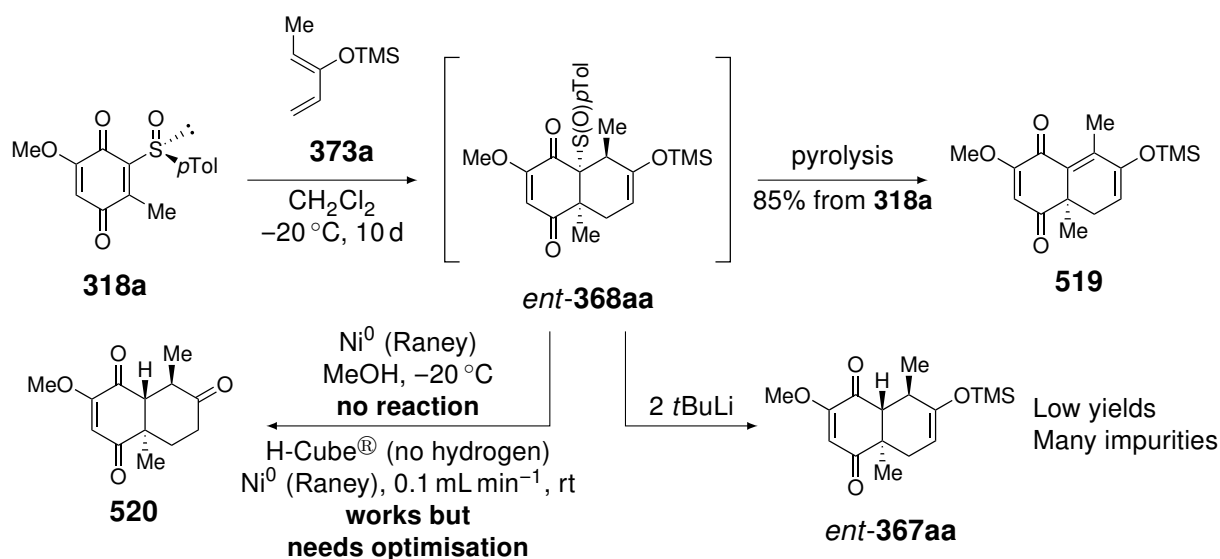
In the present chapter, we will report the results obtained for different combinations of quinones and dienes. We will also try to give some rationalisation of the outcomes of the reactions performed, as well as some ideas for improvement.

6.1 Sulfinylquinone pathway

As discussed in Chapter 3, the first strategy that will be attempted is the one using sulfinylquinone **318a**. As a reminder, according to the results reported in the literature for that sulfinylquinone,¹ *ent*-**318a** should be used in order to reach the desired enantiomer of momilactone A (**1**) (Chapter 3, Scheme 3.2). However, as already explained, we decided to develop the synthesis on the other enantiomeric series.

6.1.1 Diels-Alder reaction with diene **373a**

The Diels-Alder reaction between sulfinylquinone **318a** and diene **373a**, the simplest of all the dienes proposed in Chapter 3, is known to work (Scheme 6.1).¹ Indeed, the combination of this diene and this dienophile worked very well (full conversion of the reagents after ten days in dichloromethane at $-20\text{ }^{\circ}\text{C}$). However, the isolation of adduct *ent*-**368aa** was not possible due to the rapid pyrolysis leading to product **519**.



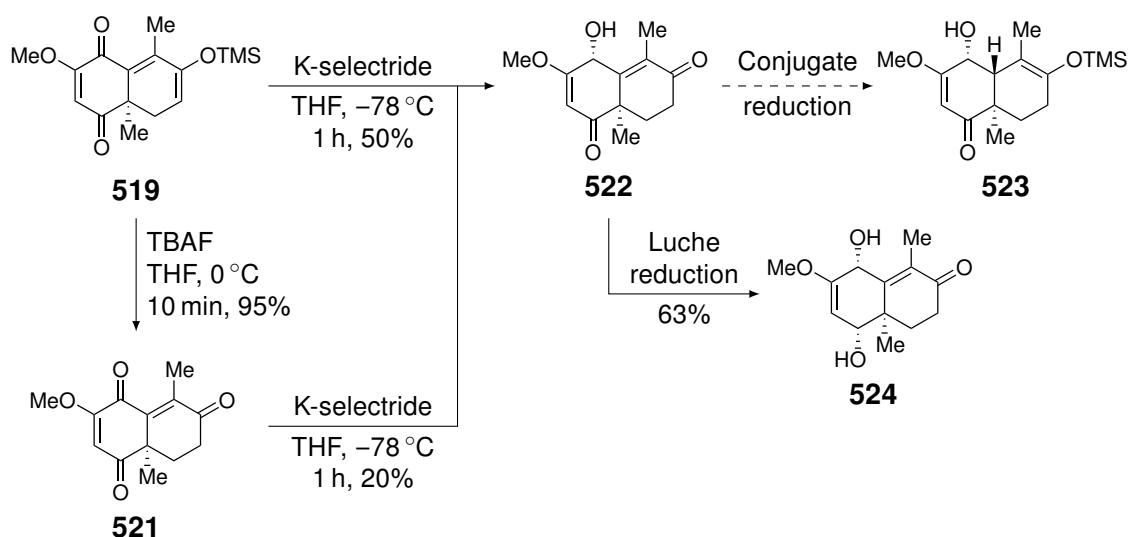
Scheme 6.1: Diels-Alder reaction between sulfinylquinone **318a** and diene **373a**, pyrolysis of adduct *ent*-**368aa** into product **519** and attempts of desulfenylation of *ent*-**368aa**.^{1,2}

In the course of the total synthesis of momilactones, conditions should be found in order to desulfenylate the adduct **368aa**, using Raney nickel for example, before the pyrolysis takes place.

This procedure might be tricky given that the desulfinylation of *ent*-**368aa** with Raney Nickel does not work at low temperatures, whereas the sulfoxide undergoes the β -*syn* elimination at temperature above 0 °C as it has been highlighted by a master's student in our group.² Yet, it was possible to perform that desulfinylation, directly on the crude mixture of *ent*-**368aa** with an H-Cube[®] system (continuous flow chemistry), that also led to the cleavage of the silyl enol ether, albeit with low yields for product **520**.

Another way to remove the sulfoxide moiety that has been tried during the same internship was to use *tert*-butyllithium. In that case, *ent*-**367aa** has been obtained but in low yields and in a complex mixture of unidentified side products.

Another potential way to get closer to the desired intermediate *ent*-**367aa** would be to do a series of controlled reductions on **519**. For this purpose, the same student studied different reduction routes of the latter (Scheme 6.2).² She first studied the use of K-selectride on both **519** and its desilylated derivative **521**. In the case of the former, the reduction occurred, with a moderate yield, on the carbonyl group next to the methoxy group, but also came with the deprotection of the enol ether. When the same reaction was applied to **521**, it led to the same product **522**, albeit with a lower yield than in the previous case.



Scheme 6.2: Study on the reduction reactions of **519** and its derivatives.²

From that intermediate **522**, it could be envisaged to perform a conjugate reduction, such as the Birch reduction conditions, and to trap the intermediate enolate with TMSCl to obtain **523**. However, it is rather difficult to selectively reduce that double bond, and it would probably lead to a mixture of several reduction products.³

As a proof of concept, it has been attempted to carry out the Luche reduction on intermediate **522**. That reaction has proven to selectively reduce the most electron rich carbonyl group, leading to diol **524** in moderate yields.

Even though some work has been done on the cycloaddition between sulfinylquinone **318a** and diene **373a** and the reduction of the different derivatives of the resulting cycloadduct, that pathway is not the most attractive among the ones presented in Chapter 3. Indeed, it was highlighted that the desulfinylation of cycloadduct *ent*-**368aa**, or the selective reductions of **519**, was difficult to carry out.

More importantly, in the pathway developed from those two partners (Scheme 3.5), we foresaw potential issues linked to the stereoselective insertion of the oxidised carbon atom that would serve for the formation of the transannular lactone (Chapter 3, pages 104 and 105).

Therefore, the strategy using diene **373a** will be kept as last resort as it appears to come with several issues, already encountered or foreseen.

6.1.2 Diels-Alder reaction with pyrone **373e**

Instead of using diene **373a**, it was decided to start the trials of this first key step with the most ambitious diene: α -pyrone **373e**. Indeed, as explained in Chapter 3 (Scheme 3.10), if the Diels-Alder reaction occurs with an *endo* selectivity, it should give us the cycloadduct with the desired relative configurations, the carbonyl group would directly be present on the structure and given the quaternary carbon atom next to the sulfinyl moiety, the latter cannot undergo a β -*syn* elimination. The desulfinylation reaction should, therefore, be carried out without any issue.

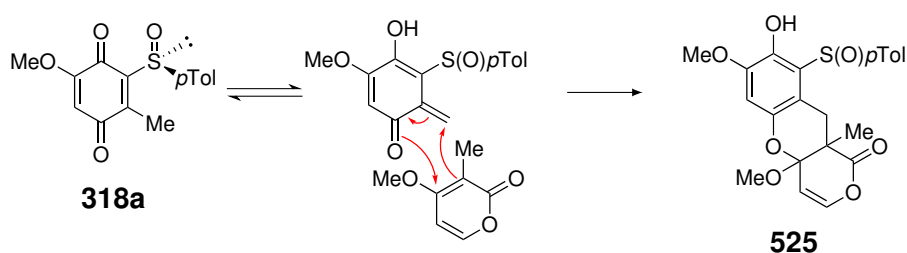
Therefore, the first test was done by mixing sulfinylquinone **318a** and pyrone **373e** in deuterated chloroform at room temperature in order to monitor the reaction by ^1H NMR (Table 6.1, entry 1). As no reaction occurred in those conditions, we decided to heat up the reaction to the reflux of the solvent (entry 2). In those conditions, conversion of the reagent was complete after three days and two products, seemingly a pair of diastereoisomers, were obtained in a 1:2 ratio. We later performed a scale up in non deuterated chloroform to obtain enough material for a full characterisation (entry 3). The mass spectrometry of both isolated isomers gave values corresponding to the sum of both partners, indicating the addition of one reagent to the other without any loss of atoms or groups. However, the ^1H NMR of both products were not quite matching the expected spectrum for cycloadduct **368ae**. Indeed, after deeper NMR analyses, using ^1H - ^{13}C correlation techniques, we proposed the structure **525** as product of that reaction.

Table 6.1: Conditions, ratio and yields for the reaction between sulfinylquinone **318a** and pyrone **373e**.

Entry	Solvent	Lewis acid	Temp.	Time	368ae	525a:525b ^[a]	Yield (%)
1	CDCl_3	—	rt	—	—	—	n.r.
2	CDCl_3	—	reflux	—	—	1:2	n.d.
3	CHCl_3	—	reflux	3 d	—	1:2	62
4	C_6D_6	—	reflux	2 d	—	1:3	n.d.
5	CH_2Cl_2	ZnBr_2 (2 eq.)	reflux	—	—	—	n.r.
6	HFIP	—	rt	—	—	—	n.r.
7	HFIP	—	reflux	—	—	—	n.r.

[a] Based on the ^1H NMR ratio of the products in the crude mixture. n.r. = no reactions.
n.d. = yield not determined

This product would come from a hetero-Diels-Alder reaction between a tautomer of sulfinylquinone **318a** and pyrone **373a** (Scheme 6.3). This unexpected reaction is similar to what was obtained in certain conditions for the reaction of **318a** and cyclopentadiene (**151**), as presented in Chapter 5 (Table 5.3). We tried to determine the relative and absolute configurations of both diastereoisomers of **525** with n.O.e experiments but could not come to any conclusion based on these analyses. We also attempted to crystallise each isomer but we could not obtain any crystal of good enough quality for an X-ray diffraction analysis.



Scheme 6.3: Proposed pathway for the formation of product **525** via a hetero-Diels-Alder of a tautomer of sulfinylquinone **318a**.

When the same reaction was attempted in refluxing deuterated benzene (entry 4), the same product **525** was obtained, albeit with a 1:3 ratio. We hoped that the use of a less polar solvent could help to avoid the formation of the tautomer intermediate but it still led to the same outcome.

An attempt to increase the reaction rate, as well as the selectivity for the standard Diels-Alder reaction, was performed by using zinc bromide (entry 5). The use of this catalyst indeed showed to accelerate the cycloadditions with sulfinylquinone **318a** as well as others.^{1,4,5} Unfortunately, no reaction occurred, even in refluxing dichloromethane. In addition to that lack of reactivity, when a ¹H NMR of the reaction medium was done, the peaks corresponding to pyrone **373e** were shorter and broader than in the absence of zinc bromide (Figure 6.2). It was therefore suggested that the α -pyrone **373e** is a better Lewis base than sulfinylquinone **318a**. This might be due to a high electron density on the oxygen atom of the carbonyl. If one takes a look at the resonance form of that compound, it is possible to delocalise the lone pair of the endocyclic oxygen atom onto the exocyclic one and, therefore, increase the electron density on the latter. Consequently, the reactivity of the pyrone is even more reduced.

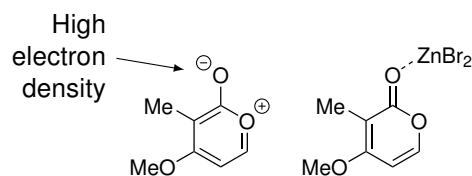


Figure 6.1: Resonance form of pyrone **373e** and its proposed coordination mode to ZnBr₂.

The next experiment that was tested to make **318a** and **373e** react together in a Diels-Alder reaction was to use HFIP as solvent (Table 6.1, entry 6) as it proved to be good solvent to increase the rate of the cycloadditions (Chapter 5, section 5.4.2). Disappointingly, no reaction was observed at all, even when the solvent was set to reflux (entry 7). If our previous assumption with zinc bromide is correct, pyrone **373e** being the strongest Lewis base, the latter strongly interacts with HFIP and its reactivity is greatly reduced.

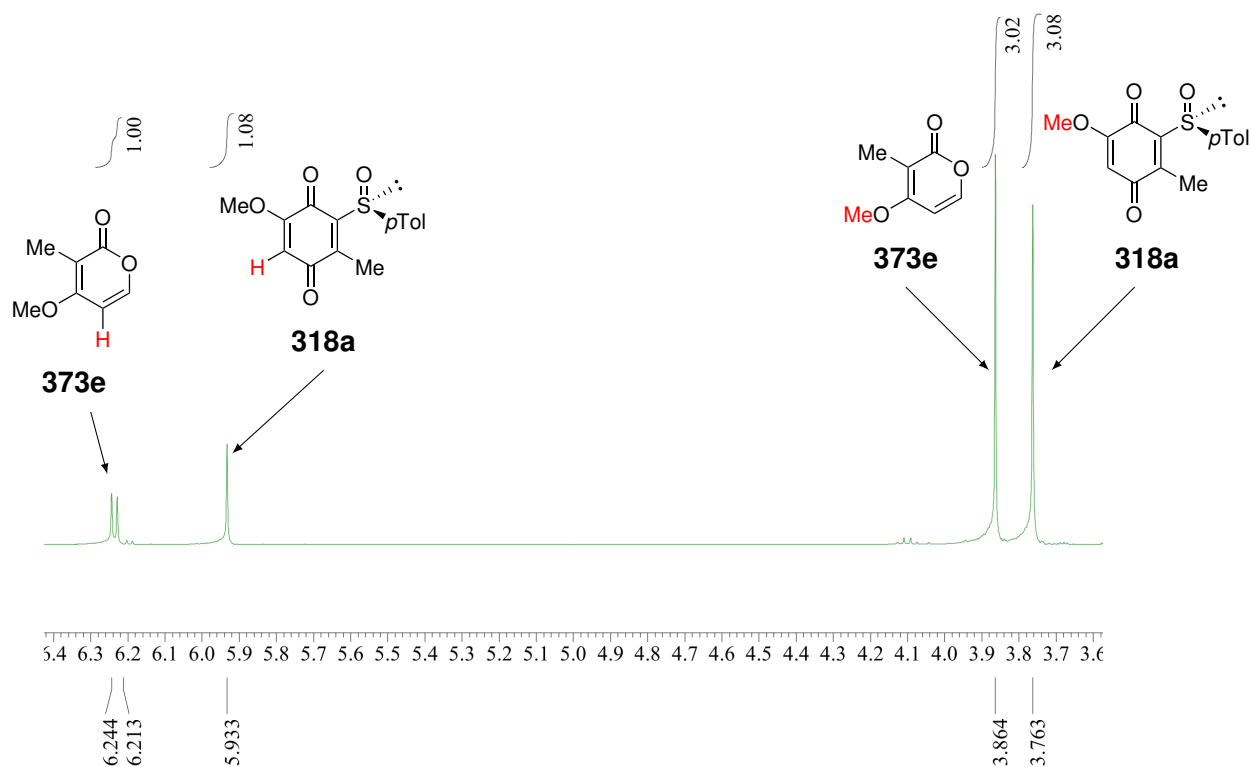
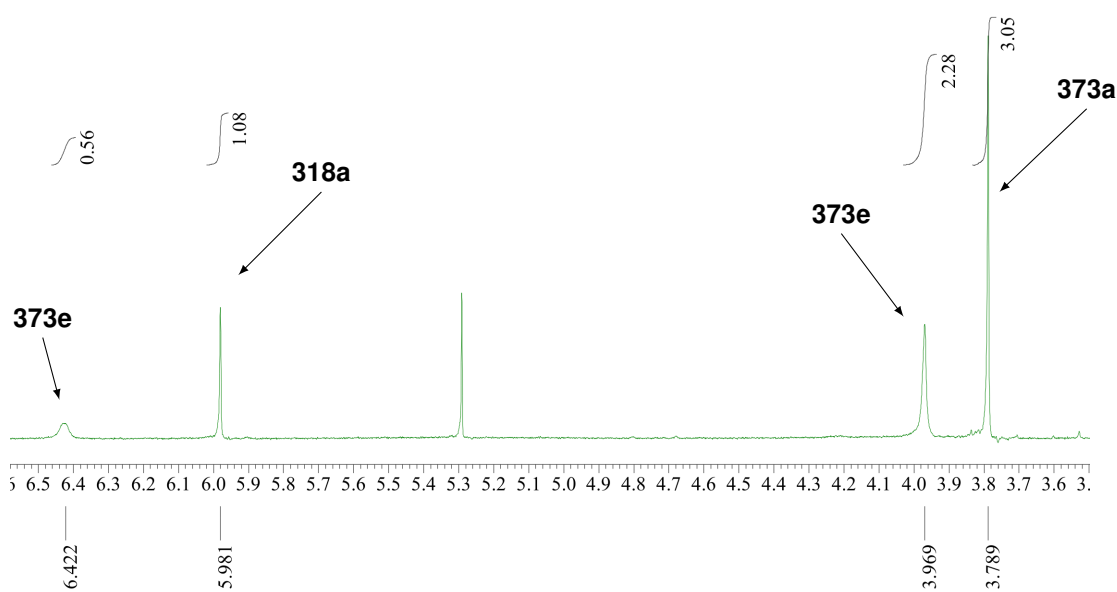
(a) Without ZnBr_2 (b) With ZnBr_2

Figure 6.2: ^1H NMR spectra of the reaction media containing sulfinylquinone **318a** and pyrone **373e** (a) in absence of zinc bromide and (b) with zinc bromide (in the window between 6.5 and 3.0 ppm).

In the course of this thesis, we also had the opportunity to try Diels-Alder reactions with sulfinylquinone **318a** under high pressure in the Laboratoire de Synthèse organique et Phytochimie at the Institut Le Bel in Strasbourg. It was indeed shown throughout the years that high pressure could increase the rate of Diels-Alder reactions.^{6–10}



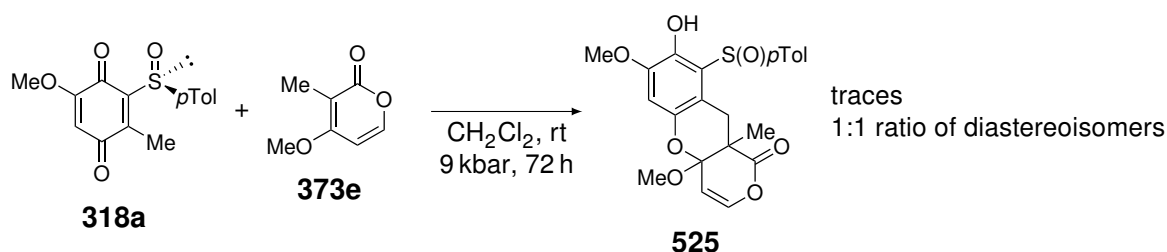
(a) High pressure reactor

(b) Vial for the high pressure reactor

Figure 6.3: High pressure reactor and vial used for the high pressure reactions.

From a practical point of view, those high pressure reactions are carried out by preparing the reaction mixture in a dedicated vial (Figure 6.3.b) and by inserting the latter in a steel cylinder with a wall with a thickness of 5 cm. The cylinder is then filled up with a fluid (petroleum ether in this case) and placed inside the enclosure of the reactor (Figure 6.3.a). The pressure build-up is done with a mechanical piston that compresses the fluid inside the cylinder and allows to reach a pressure of 9 kbar (with this device).

Given the interest of high pressure for Diels-Alder reactions, we tried to use that technique for the reaction between sulfinylquinone **318a** and pyrone **373e** (Scheme 6.4). Unfortunately, that last method was not very effective and we could only get product **525** in traces.

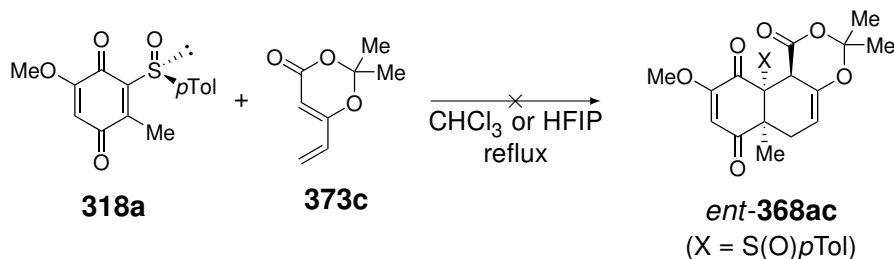
Scheme 6.4: Conditions for the high pressure reaction between sulfinylquinone **318a** and pyrone **373e**.

In spite of all the methods that have been tested to make the Diels-Alder reaction work between those two partners, we could never obtain the desired cycloadduct. Therefore, we came to the conclusion that pyrone **373e** could not be a suitable diene for our total synthesis because of its unexpected reactivity and we decided to move on to other dienes.

6.1.3 Diels-Alder reaction with pentadienoates

Given that pyrone **373e** did not give the desired product, we had to change the diene. Therefore, the next diene that has been tested is **373c**, which should be a reasonable compromise between reactivity and structure of the reagent. As explained in Chapter 3 (Scheme 3.7), the absence of the methyl group is not a major drawback as it should be easily inserted later in the synthesis and the oxidised carbon atom needed for the lactone is still present.

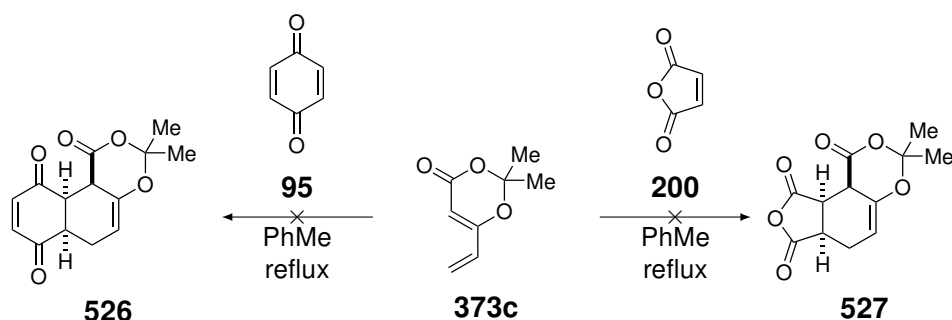
We first tried to make it react with sulfinylquinone **318a** in chloroform (Scheme 6.5). As no reaction was occurring at room temperature, the solvent was set to reflux but it did not help to make the reaction work. We then tried to use HFIP as solvent, but the same absence of reaction was observed whether at room temperature or at reflux of the solvent.



Scheme 6.5: Attempt of Diels-Alder reactions between sulfinylquinone **318a** and diene **373c**.

This vinyldioxinone **373c**, whose synthesis was reported by Blechert *et al.*,¹¹ has never been described, to the best of our knowledge, as a diene in a cycloaddition. We were thereby wondering if that reagent was actually reactive enough to undergo a Diels-Alder reaction.

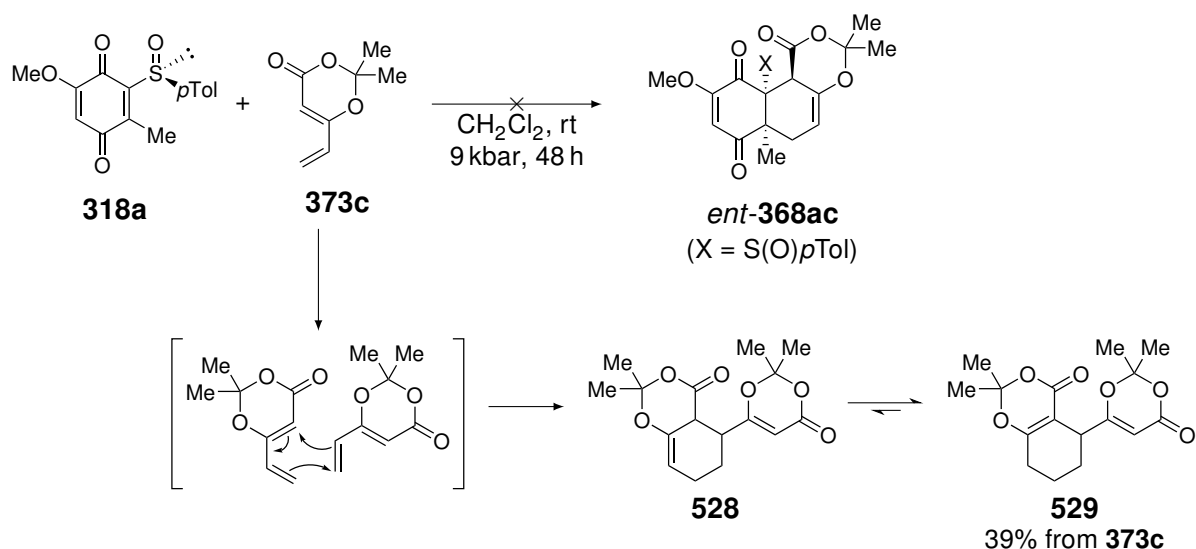
In the aim to verify its ability to react as a diene, we attempted Diels-Alder reaction with simpler, and more reactive, dienophile, such as *para*-benzoquinone (**95**) and maleic anhydride (**200**) (Scheme 6.6). However, neither of these two reactions worked, even in refluxing toluene for several days.



Scheme 6.6: Attempts of Diels-Alder reactions of diene **373c** with *para*-benzoquinone (**95**) and maleic anhydride (**200**) in refluxing toluene.

It was suspected that **373c** was too electron poor due to the carbonyl group conjugated to the diene part. Moreover, the presence of the *gem*-dimethyl group might also be a source of an important steric hindrance as both methyl groups point out of the diene plane.

Nevertheless, in the course of the tests of the high pressure Diels-Alder reactions, we also tried the reaction between diene **373c** and sulfinylquinone **318a** (Scheme 6.7). At first, we thought that the cycloaddition took place as a new spot appeared on the TLC analysis. But, after purification of the crude mixture to isolate that new product, the ¹H NMR did not correspond to the expected cycloadduct at all. The ¹H and ¹³C NMR seemed to indicate the presence of two dioxinone units (two *gem*-dimethyl units, two esters). Therefore, it would appear that a dimer of **373c** has been formed. The most likely pathway for such a dimerisation passes through a Diels-Alder reaction between two units of diene **373c**, giving the adduct **528** (bottom part of Scheme 6.7).

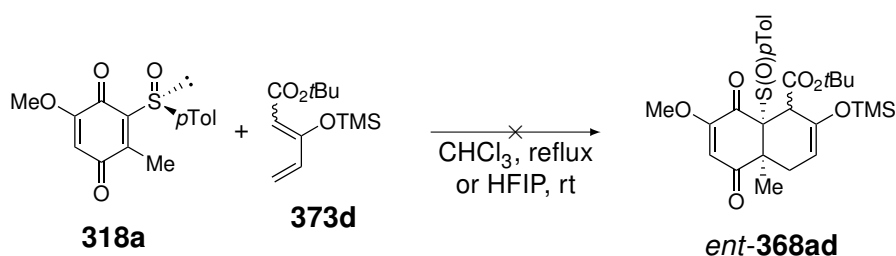


Scheme 6.7: Attempt of Diels-Alder reactions between sulfanylquinone **318a** and diene **373c** under high pressure and product **529** coming from the dimerisation of **373c**.

Yet, that product still did not match the NMR spectra. Indeed, the DEPT analysis indicated the presence of one tertiary carbon atom and three secondary ones in the aliphatic area, as well as only one vinylic proton, whereas **528** contains two sets of each of these signals. In order to match the obtained NMR spectra, we proposed an isomerisation of adduct **528** into product **529** by moving the double bond of the cyclohexene, which allows the conjugation of the double bond with the carbonyl group. Not only the new structure matched the ^1H and ^{13}C NMR spectra, but it was also in agreement with the ^1H - ^{13}C correlation experiments. If the structure we proposed corresponds to the product that was actually isolated, the latter was obtained with a 39% yield from diene **373c**.

We then tried the Diels-Alder reaction with pentadienoate **373d** that, opposed to **373c**, has already been described as a diene in a cycloaddition.¹² Similarly to the two previous dienes, we started doing the reaction in refluxing chloroform but, once again, no reaction occurred.

We also tried the reaction in HFIP, but as described in Chapter 5, the acidity led to the degradation of the diene by cleavage of the silyl enol ether group, even at room temperature.



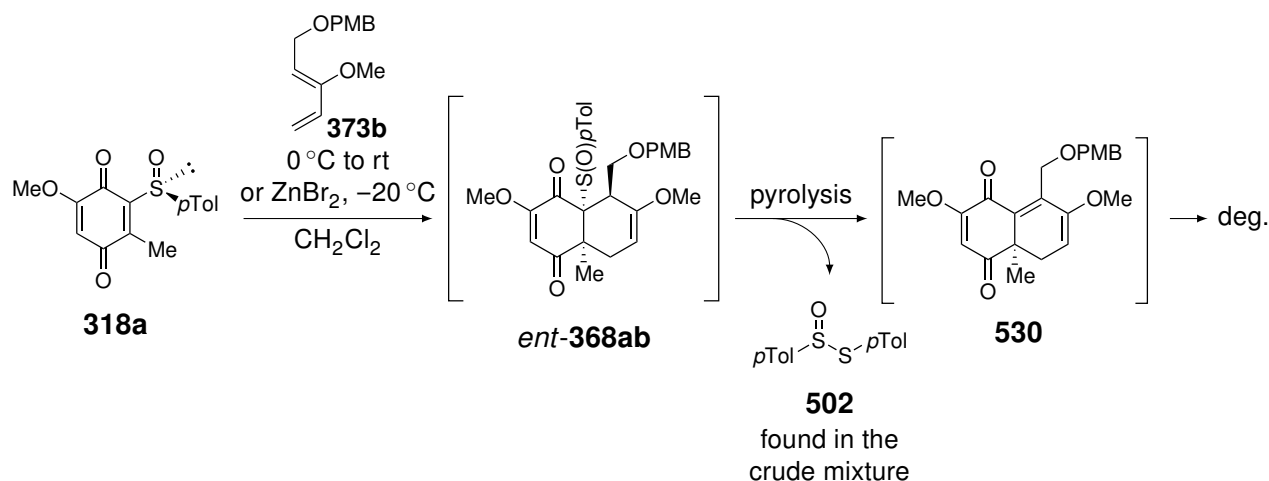
Scheme 6.8: Attempt of Diels-Alder reactions between sulfanylquinone **318a** and diene **373d**.

As neither of these two pentadienoates gave the expected outcome for the Diels-Alder reaction with sulfanylquinone **318a**, it was concluded that the presence of an EWG on the diene lowered the reactivity of the diene towards the cycloaddition too much.

By looking up in the literature we indeed found no example of Diels-Alder reactions of sulfinylquinones with a diene bearing an EWG conjugated to the double bonds. It should therefore be wiser to use a diene without the carbonyl group and to form it or insert it later in the synthesis.

6.1.4 Diels-Alder reactions with 1,3-dioxypenta-2,4-dienes

As explained here above, the presence of an EWG on the diene seems to reduce too much its reactivity to make it react in a Diels-Alder reaction with sulfinylquinone **318a**. Therefore, diene **373b**, that possesses the closest pattern to the pentadienoates **373c** and **373d** but for the carbonyl group, has been tested (Scheme 6.9).



Scheme 6.9: Attempt of Diels-Alder reactions between sulfinylquinone **318a** and diene **373b** (deg. = degradation).

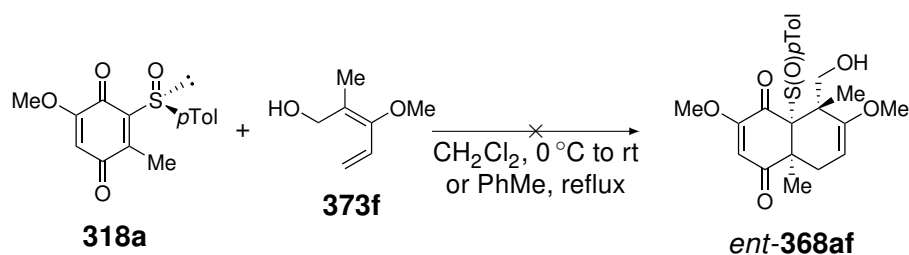
As diene **373b** should be more reactive than the previous ones, we started the reaction at 0 °C in dichloromethane and slowly warmed up the reaction mixture to room temperature. In that case, the TLC monitoring indicated the full conversion of sulfinylquinone **318a** after a few hours but multiple new spots also appeared. The analysis of the crude mixture showed a complex mixture of unidentified products and we were not able to isolate any compounds of interest.

Nevertheless, we identified thiosulfinate **502** in the crude mixture. The presence of the latter would indicate that the cycloaddition took place, but also that adduct **368ab** quickly pyrolysed. Unfortunately, for some reasons, the pyrolysed adduct **530** seemed to be unstable and to quickly degrade as well.

We attempted to perform the reaction at lower temperature (-20 °C) with zinc bromide as catalyst. In those conditions, the reaction was also over within a few hours, but the same outcome was obtained and no product of interest could be isolated.

The second diene of this category, diene **373f**, has also been tested in the Diels-Alder reaction with **318a**. In term of structure, that diene has a small advantage over diene **373b** as it bears a methyl group that will not need to be inserted later in the synthesis. Moreover, diene **373f** has the same configuration as pyrone **373e** and, thereby, should also lead to the cycloadduct with the desired relative configurations of both methyl groups and the hydroxymethyl group, if the *endo* selectivity is observed.

As for diene **373b**, we first tried the reaction in dichloromethane but no reaction occurred, whether at 0 °C or at room temperature (Scheme 6.10).



Scheme 6.10: Attempt of Diels-Alder reactions between sulfanylquinone **318a** and diene **373f**.

As this diene seems to be less reactive than the previous one, we replaced the solvent with toluene and set it to reflux. Unfortunately, it did not help the reaction to take place and the degradation of the diene was even observed.

We suspected that this particular diene might be too hindered to be able to react with sulfanylquinones **318a**. Moreover, as indicated by the n.O.e analysis of diene **373f**, it would seem that the *s-trans* conformation (Figure 6.4) is the major one as no n.O.e correlation that would correspond to the *s-cis* conformation could be observed, even in small amounts. It would therefore seem unlikely that this diene would be able to undergo a cycloaddition with a tetrasubstituted dienophile such as sulfanylquinone **318a**. Even its ability to react as a diene in a cycloaddition might be questioned as the *s-trans* conformation seems to be highly favoured over the *s-cis* one.

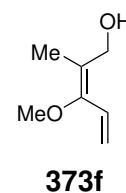


Figure 6.4: Preferential conformation of **373f**.

6.2 Corey's asymmetric catalysis pathway

Since none of the dienes **373b-f** gave any desired outcome in the Diels-Alder reactions with sulfanylquinone **318a** and that the route with diene **373a** is to be kept as last resort, it was decided to move on to the second strategy proposed in Chapter 3: the catalytic asymmetric Diels-Alder reactions.

In those reactions, the cycloadducts obtained do not suffer the issue of uncontrolled pyrolysis as it was the case with sulfanylquinone **318a**, but other methods must be put in place to convert the *cis*-decalin obtained after the cycloaddition into the corresponding *trans*-decalin.

The first asymmetric catalysis that has been attempted was the use of the chiral oxazaborolidinium salt as employed by Corey's group.^{13,14} For that purpose, and as described in Chapter 3 (Scheme 3.3), quinone **369a** has been chosen to carry out that catalytic asymmetric Diels-Alder reaction in the context of the total synthesis of momilactones.

Based on Corey's work, catalyst **109**, prepared from the enantiopure (*R*)-(-)- α,α -diphenyl-2-pyrrolidinemethanol, should give us the cycloadduct with the desired absolute configurations. However, we cannot be totally sure this selectivity will be the one obtained with quinone **369a**. Therefore, we decided to use the same catalyst *ent*-**109** employed in their asymmetric Diels-Alder reactions. Besides, this enantiomer of the catalyst is prepared from (*S*)-(-)- α,α -diphenyl-2-pyrrolidinemethanol which is slightly cheaper than its *R* isomer.

In the case of quinone **369a**, two coordination modes are possible according to the model proposed by Corey (Figure 6.5). The latter can either bind to the catalyst with the carbonyl in position 1

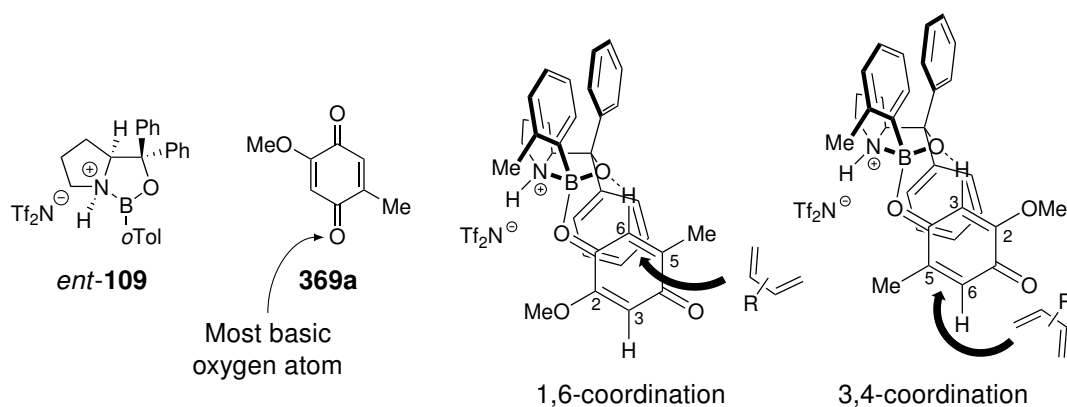


Figure 6.5: Structures of the oxazaborolidinium salt *ent*-**109** and quinone **369a**, and both their possible mode of coordination.

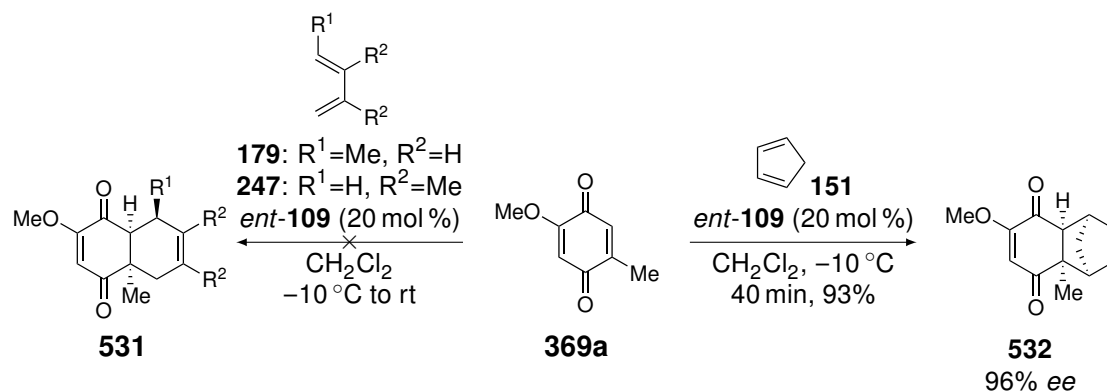
and the hydrogen in position 6 or with the carbonyl in position 4 and the hydrogen atom in position 3. As the most basic oxygen atom preferentially binds the boron atom, the second situation should be the most probable. Nevertheless, both modes of coordination should lead to the same adduct as the C5-C6 double bond should remain the most reactive one.

But, as said earlier, we cannot be totally sure the model proposed by Corey will correspond to our quinone. Indeed, in the quinones tested by the group, none of them bore two different groups in position 2 and 5. Therefore, the regio- and stereoselectivity must be evaluated.

6.2.1 Evaluation of the asymmetric catalysis with model dienes

Before trying the asymmetric cycloaddition with the oxygenated dienes proposed in this thesis, we wanted to assess the reaction with more simple dienes (Scheme 6.11). The conditions described by Corey have been applied to our quinone, except for the temperature that was set to $-10\text{ }^{\circ}\text{C}$.

When the reaction was tried with piperylene (**179**) or dimethylbutadiene (**247**), we observed no conversion of the reagents even when the reaction mixture was warm up to room temperature for several hours. This lack of reactivity in presence of catalysts *ent*-**109** was a bit surprising, especially since **247** was tested by Corey's group and worked uneventfully. But, we indeed observed that both



Scheme 6.11: Asymmetric Diels-Alder reaction between quinone **369a** and model dienes, using *ent*-**109** as catalyst. The configurations of products **531** are based on the products reported by Corey *et al.*^{13,14} and the configurations of **532** were confirmed by its X-ray structure (Figure 6.6).

dienes did not react at all with quinone **369a** in dichloromethane at room temperature (Chapter 5, Table 5.4). The Diels-Alder reaction of these partners must be too disfavoured, even in presence of the catalyst, to form any cycloadduct.

On the other hand, when cyclopentadiene (**151**) was used as diene, the same conditions led to full conversion of the quinone in forty minutes and the product was isolated with a 93% yield and a 96% *ee*. In addition to this excellent reactivity and enantioselectivity, the X-ray structure of that product (Figure 6.6) showed that the enantioenriched cycloadduct **532** was obtained *via* the same facial selectivity as reported by Corey.^{13,14} This example showed that the use of catalyst *ent*-**109** could really increase the reactivity of quinone **369a**. Indeed, the same reaction run in dichloromethane without any catalyst took fifteen days at room temperature (Chapter 5, Table 5.4, **Q3** and **D1** that gives **Q3D1**). More importantly, this reaction proved to provide an excellent enantioselectivity which will be of great interest for the total synthesis of momilactones.

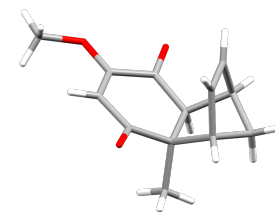


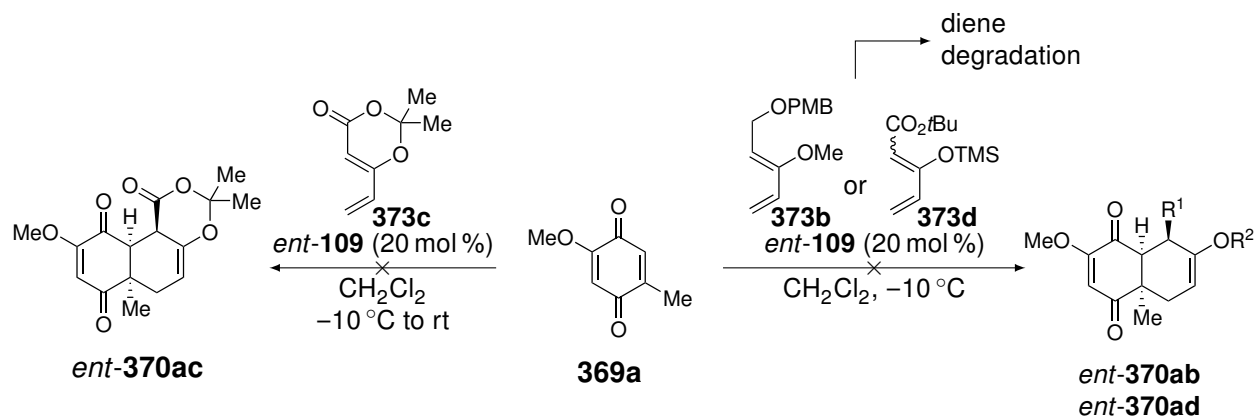
Figure 6.6: X-ray structure of the enantiomerically enriched cycloadduct **532**.

However, given that only the reaction with cyclopentadiene (**151**) seemed to work, we supposed that a rather reactive diene is still needed for the cycloaddition to occur.

6.2.2 Corey's catalysis for the synthesis of momilactones

Now that we have established that the catalytic asymmetric Diels-Alder reaction could work with quinone **369a**, we decided to move on to the oxygenated dienes chosen for the total synthesis of momilactones. Pyrone **373e** was not tested in this part of the work, since, as discussed earlier in this chapter, we suspected the pyrone to be a better Lewis base than the quinone.

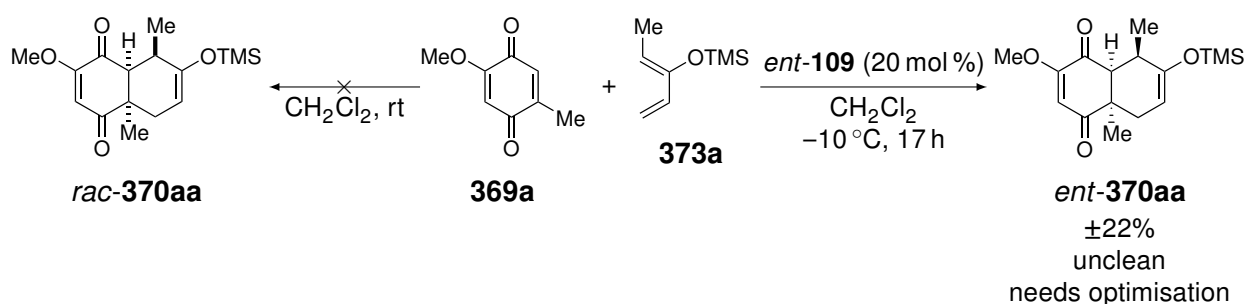
We tested the asymmetric Diels-Alder reaction, using Corey's catalyst, between quinone **369a** and dienes **373b-d** (Scheme 6.12). Unfortunately, none of those three dienes led to the cycloadducts *ent*-**370b-d**. In the case of diene **373c** no reaction occurred at all, even after warming the reaction mixture up to room temperature. This lack of reactivity was not really surprising as we suspected that diene not to be reactive enough due to the presence of the conjugated carbonyl group, as well as the *gem*-dimethyl group that likely causes an important steric hindrance.



Scheme 6.12: Attempts of asymmetric Diels-Alder reaction between quinone **369a** and dienes **373b-d**, using *ent*-**109** as catalyst. The absolute configurations of the products are based on the products reported by Corey *et al.*^{13,14}

In the case of dienes **373b** and **373d**, another issue arose. After a few hours at low temperature, not only no reaction had occurred, but the diene disappeared from the reaction medium, as indicated by the TLC monitoring. It would seem the conditions used for Corey's catalysis are acidic enough to cleave enol ethers. As the corresponding enones were not found in the crude mixture, we also suspected that the latter underwent side reactions that led to their consumption. We were somewhat disappointed by that outcome as Corey reported the use of a diene containing a silyl enol ether group. Yet, the silyl group used in Corey's work was a TIPS that is more robust than a TMS or a methyl group, which might explain the degradation of our dienes.

As deduced from the test with the model diene (Scheme 6.11), in the case of quinone **369a**, a more reactive diene is probably needed for the reaction to work. Therefore, diene **373a**, that is the most reactive one among the chosen oxygenated diene for the synthesis of momilactones, has been tested (Scheme 6.13).



Scheme 6.13: Diels-Alder reaction between quinone **369a** and diene **373a** with and without catalyst **109**. The absolute configurations of *ent*-**370aa** were based on the product reported by Corey *et al.*^{13,14}

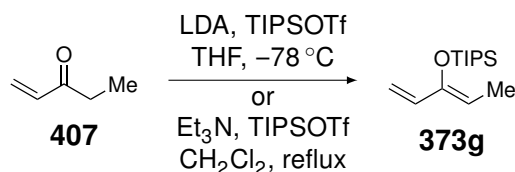
In order to assess the efficacy of the catalytic system with that diene, the reaction was first carried out in dichloromethane at room temperature in absence of the catalyst. In those conditions, the partners did not react together, even after several days.

We then used the conditions previously employed with the other dienes. After 17 h at -10°C , quinone **369a** was fully consumed. The ^1H NMR analysis of the crude mixture indicated the formation of a major product that would correspond to cycloadduct *ent*-**370aa**, albeit the latter was not very clean. Indeed, as explained above, we suspect the catalyst to be acidic enough to cleave enol ether but, this diene reacting faster, it was possible to observe a cycloadduct in this case, even if it was not clean. Unfortunately, when we attempted to purify the crude mixture to isolate the cycloadduct, it came out even less clean, even with the use of demetallated and neutralised silica gel.

As we could not isolate a pure sample of the cycloadduct, we did not determine its enantiomeric excess. Nevertheless, the reaction seemed to work as indicated by the NMR spectrum which corresponded to the expected cycloadduct. Therefore, if the pathway using diene **373a** turns out to be the best solution for the total synthesis of momilactones, the asymmetric cycloaddition between **369a** and **373a** must be optimised and the enantioselectivity must be determined.

One potential solution to improve this process would be to directly engaged cycloadduct *ent*-**370aa** in the next steps of the synthesis. In doing so, we could find an intermediate stable enough to be isolated in a pure form and to determine its *ee*. A second way would be to change the silyl group

to a TIPS, that should be more robust than the TMS. The preparation of such a diene (**373g**) might be done using TIPSOTf with LDA in THF at $-78\text{ }^{\circ}\text{C}$ ¹⁵ or with Et_3N in refluxing dichloromethane (Scheme 6.14).¹⁶



Scheme 6.14: Proposed synthetic pathway for 3-triisopropoxy-penta-1,3-diene (**373g**) based on reported procedures.^{15,16}

If we manage to improve the outcome of this asymmetric Diels-Alder reaction with 3-silyloxy-penta-1,3-dienes and if the enantioselectivity of the process is high enough to be used for the total synthesis of momilactones, this sequence is more interesting than the sulfinylquinone pathway. Indeed, contrarily to the quinone bearing the sulfinyl moiety, no undesired side reaction should occur with adduct *ent*-**370aa**. The handling of the latter should then be easier.

Yet, for the same reasons described in the previous section, the use of that type of diene later leads to potential issues concerning the selective insertion of the oxidised carbon atom. We therefore moved on to the next pathway proposed in Chapter 3 but kept Corey's catalytic asymmetric Diels-Alder reaction between quinone **369a** and dienes **373a** or **373g** in mind as a potential route.

6.3 Evans asymmetric catalysis pathway

The second catalytic system, that was planned to carry out the asymmetric Diels-Alder reaction for the synthesis of momilactones, is the one developed by Evans.¹⁷ That process uses a pybox complex **255a**, with samarium or gadolinium as Lewis acid, on quinones bearing an ester group. For the synthesis of momilactones, quinone **371a** has been designed and successfully synthesised (as presented in Chapter 5, Scheme 5.10).

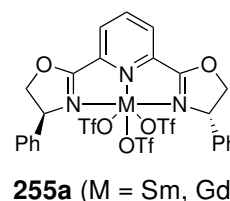


Figure 6.7: Structure of Evans's catalyst.

6.3.1 Evaluation of the Evans catalysis with quinone **371a**

As a reminder, the Diels-Alder reaction of quinone **371a** (**Q8** in Chapter 5) has already been studied in dichloromethane and HFIP and is summarised in Scheme 6.15. It was observed that in dichloromethane, the product obtained for the reaction with piperylene (**179**, **D2** in Chapter 5) was not the expected cycloadduct *rac*-**533** (**Q8D2** in Chapter 5), but product **505**. As we suggested, due to the out-of-plane conformation of the ester observed in its X-ray structure (Figure 6.8), the addition on the ester-bearing double bond is disfavoured and the reaction rather occurs on the other double bond through a (2+2) cycloaddition. But, in HFIP, that is a very strong hydrogen bond donor, the latter would be able to bring the ester back in the quinone plane and the standard cycloaddition can take place.

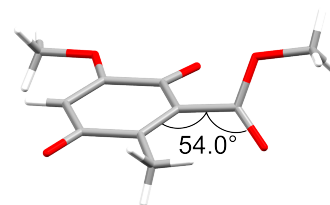
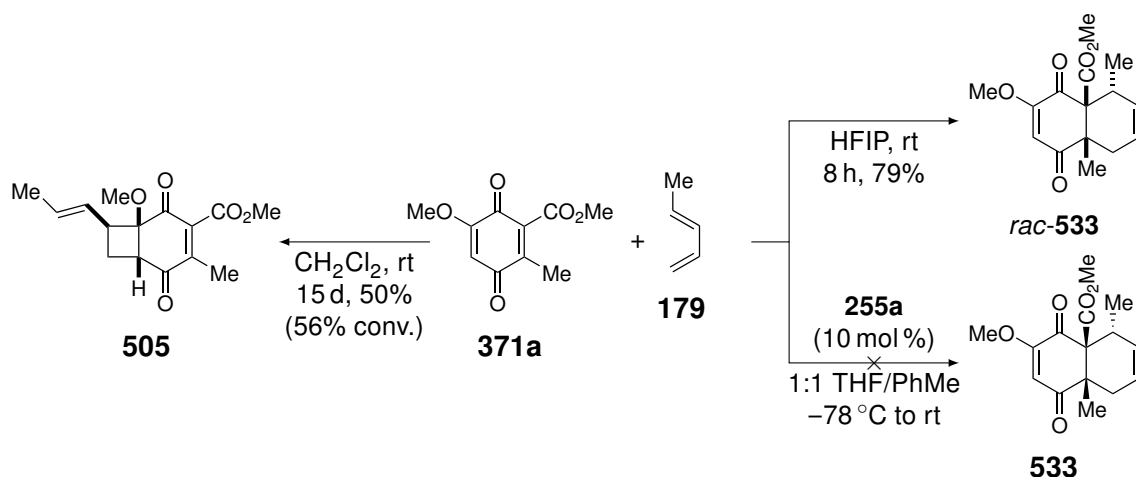


Figure 6.8: X-ray structure of **371a** and dihedral angle between the ester and the quinone plane.



Scheme 6.15: Reactions between quinone **371a** and piperylene (**179**), as presented in Chapter 5 (Tables 5.4 and 5.7), and attempt of the asymmetric Diels-Alder reaction with catalyst **255a**. The absolute configurations of **533** were proposed based on the products reported by Evans *et al.*¹⁷

Similarly to Corey's catalysis, we decided to first evaluate the efficacy of the Evans catalysis for quinone **371a** with a model diene. In order to make a comparison with Evans's work, we tested piperylene (**179**) that was also used in that study.

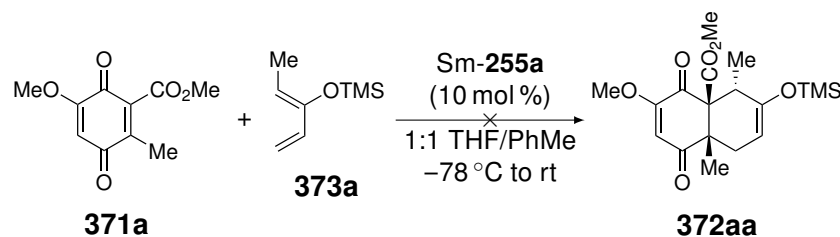
In spite of the unexpected reactivity of quinone **371a** in dichloromethane in absence of catalyst (Scheme 6.15), we were still expecting the Evans catalysis to work on that quinone. As the use of HFIP could help the standard cycloaddition to take place, supposedly thanks to the strong hydrogen bond donation that could bring the ester back in the quinone plane, we thought that a Lewis acid could do the same. Unfortunately, the reaction of quinone **371a** and piperylene (**179**) run in the conditions described by Evans gave no product at all, whether samarium or gadolinium were used as Lewis acid. We even let the reaction warm up to room temperature but, even after several hours, the quinone remained unconsumed.

Given the preferred conformation of **371a** observed in its X-ray structure, which might be the same in apolar solvents, it might be possible that only strongly coordinating species, such as a strong hydrogen bond donor like HFIP, can switch the reactivity of that quinone towards the expected [4+2] cycloaddition. In the case of catalyst **255a**, we supposed that neither samarium nor gadolinium may be a strong enough Lewis acid to force the ester group to be in the same plane as the quinone part. On one hand, the Lewis acid might not succeed in binding both oxygen atoms of the ester and the carbonyl. On the other hand, the metal might manage the binding of both oxygen atoms, but the geometry of the quinone-metal complex maintains the ester group out of the quinone plane, which still blocks the reaction on the ester-substituted double bond.

By looking up in Evans's work,¹⁷ we realised that none of the quinones used, or at least described, bore a substituent next to the ester group. Therefore, Evans's group may not have encountered the drawback of the unfavourable ester conformation we had in our case, and we therefore had no way of making comparisons with similar quinones.

In a last attempt to see if that reaction could work, we decided to use diene **373a** as it is allegedly the most reactive of the oxygenated dienes we had. We then engaged quinone **371a** with diene **373a** in the conditions described by Evans with Sm-**255a** as catalyst (Scheme 6.16). Unfortunately, as

observed with piperylene (**179**, Scheme 6.15), no reaction occurred, even when the reaction mixture was warmed up at room temperature.



Scheme 6.16: Attempt of the catalysed asymmetric Diels-Alder reaction between quinone **371a** and diene **373a** using catalyst Sm-**255a**. The absolute configurations of **372aa** were based on the products reported by Evans.¹⁷

Despite the lack of reactivity in the Evans catalysed asymmetric Diels-Alder reaction with quinone **371a**, we did not give up on that method as synthetic tool for the total synthesis of momilactones. As the main issue with our quinone seems to be the out-of-plane conformation of the ester group, we considered modifying the quinone substrate to alleviate this conformational drawback as we will discuss in the next section.

6.3.2 Design and synthesis of a new quinone for the Evans catalysis

Design of quinone **534**

As said above, we suspected that the conformation of the ester group in quinone **371a** might be the cause of the lack of reaction when it is engaged in a cycloaddition in the Evans conditions. Therefore, in order to use that catalytic system, we thought of modifying the quinone substrate and to find a way to lock the ester in the quinone plane. The simplest solution that came to our mind would be to tether the ester to the benzylic methyl group, giving quinone **534** derived from a phthalide (Figure 6.9).

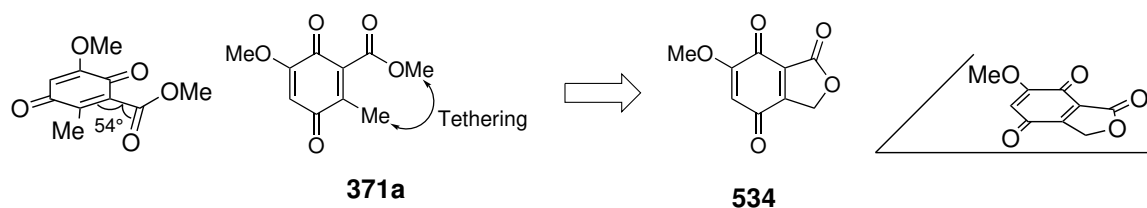


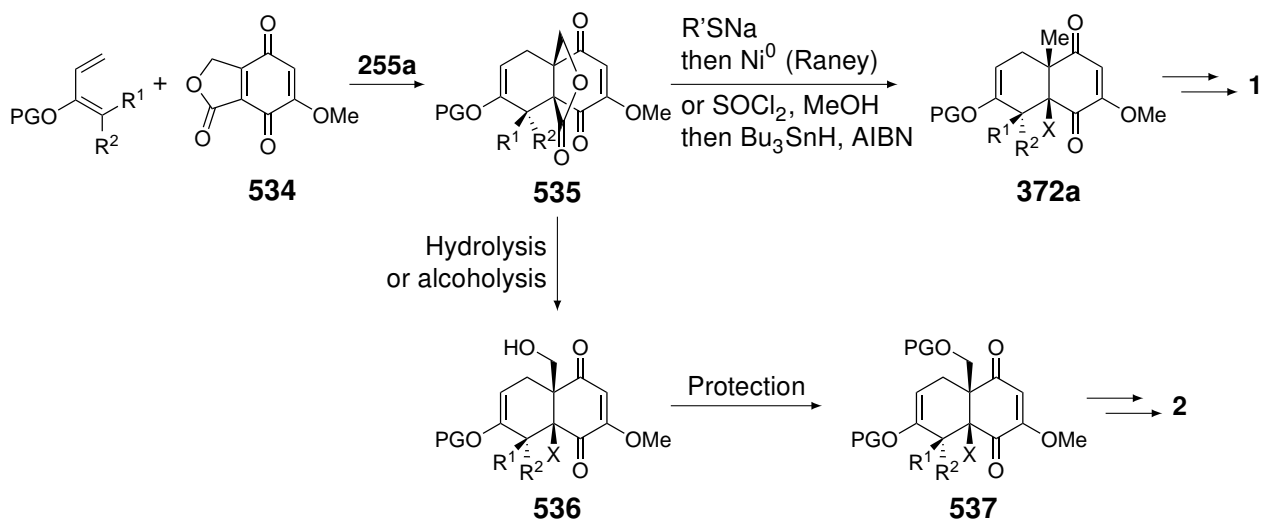
Figure 6.9: Design of a new quinone **534** by tethering of the ester and the benzylic methyl group of quinone **371a** and tridimensional representation of both quinones.

This phthalide quinone **534** should solve the conformational issue of **371a**. Indeed, the γ -lactone ring has no choice but to be in the same plane as the quinone core. Thereby, the carbonyl group is also in the same plane and is conjugated to the double bond, which will significantly increase its reactivity. Another important advantage is the orientation of the carbonyl groups of the quinone and the lactone in the same direction. They are thereby adequately positioned to strongly chelate a Lewis acid. This quinone should therefore be an excellent substrate for the Evans catalysis.

Quinone **534** for the synthesis of momilactones

Now that we have designed a new quinonoid system for the total synthesis of momilactones, the reaction sequence initially planned using quinone **371a** (Chapter 3, Scheme 3.4) must be revised.

As discussed for the other quinonoid systems presented in Chapter 3 (Schemes 3.2 to 3.4), the Diels-Alder reaction of dienes with an oxygenated group on position 2 and substituents on position 1 (R^1 and/or R^2) is most likely to give the opposite regioselectivity to the one expected for such dienes as observed, for example, for the reaction of diene **373a** with sulfinylquinone **318a**.¹ It was suggested that the presence of the methyl group next to the EWG caused a steric clash with the methyl group on position 1 of the diene. In the case of quinone **534**, we expect the same inversion of regioselectivity as presented in Scheme 6.17.



Scheme 6.17: Planned reaction sequence for the total synthesis of momilactones A (**1**) and B (**2**) from the asymmetric Diels-Alder reaction of quinone **534** using Evans catalytic system. X = CO₂R.

After the Diels-Alder reaction between one of the chosen oxygenated diene and phthalide quinone **534**, the next step will be the opening of the lactone ring. On one hand, to reach momilactone A (**1**), we need to fall back on an intermediate similar to **372a** that possesses the angular methyl group and the carboxylate.

One way to open the lactone ring to obtain such a pattern could be the use of a sulfide (Scheme 6.17).^{18,19} Then, the newly formed carbon-sulfur bond will be reduced with Raney nickel to reach **372a** under its carboxylic acid form.

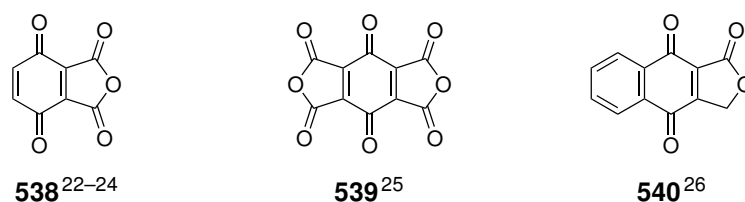
A second way to carry out the same transformation is the use of SOCl₂ in methanol.²⁰ The lactone ring will be opened and give, on one side, a carboxylic acid that will be converted into a methyl ester and, on the other side, a chloromethyl group. The latter will be reduced to the corresponding methyl group with Bu₃SnH and AIBN. Then, the decarboxylation will be performed to obtain the *trans*-decalin **367a** and the rest of the synthetic pathway will be the same as developed in Chapter 3 (Scheme 3.4).

Interestingly, one important advantage of using the newly designed quinone **534**, is that momilactone B (**2**) can also be reached without having to insert the dimethylphenylsilyl group first. Indeed, from adduct **535**, hydrolysis or alcoholysis of the lactone will lead to the carboxylic acid (or ester group), on one side and to the hydroxymethyl group on the other side (**536**). The primary alcohol will

then be protected to give intermediate **537**. The rest of the synthetic pathway will be the same as described in Chapter 3 but, instead of the silane group initially planned for the synthesis of momilactone B (**2**), we directly have the oxygenated angular methyl group which, therefore, should also shorten the sequence.

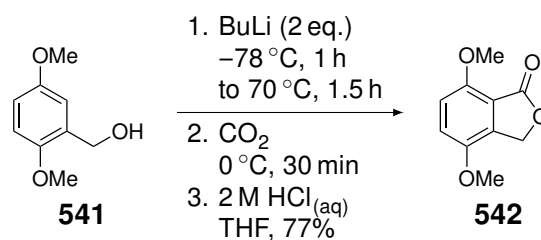
Development of the synthesis of phthalide quinone **534**

The development of the synthesis of phthalide quinone **534** is currently the subject of a master thesis in our group.²¹ By looking up in the literature, no example of syntheses of a compound with the same pattern (even without the methoxy group) could be found. The closest structures we could find are quinones **538**, **539**, and **540**.^{22–26} Among those three compounds, only **538** has been studied in Diels-Alder reactions.^{22,23}



Scheme 6.18: Structures of reported quinones with the closest pattern to the desired phthalide quinone **534**.

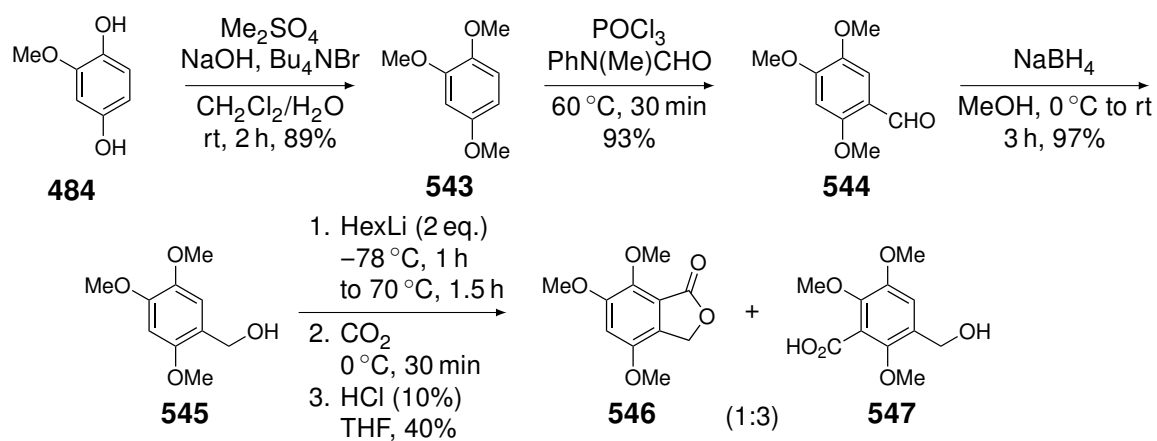
Therefore, the synthesis of the desired quinone must be fully developed and optimised. The simplest way to do so would be to manage the synthesis of the corresponding hydroquinone (protected or not) and to oxidise it. In 2017, Parsons *et al.* reported the synthesis of the 4,7-dimethoxyphthalide **542** (Scheme 6.19).²⁷ In that synthesis, they performed an *ortho*-lithiation on compound **541**, followed by the addition of carbon dioxide and the lactonisation with hydrochloric acid.



Scheme 6.19: Synthesis of dimethoxyphthalide **542** from **541** reported by Parsons *et al.*²⁷

Although they managed the synthesis of dimethoxyphthalide **542**, they did not need to convert the latter into a quinone for the rest of their work. But, as the reported phthalide is very close to the one we need for our synthesis, we decided to use their procedure to form the lactone ring. However, in our case, a third methoxy group is needed on the aromatic ring.

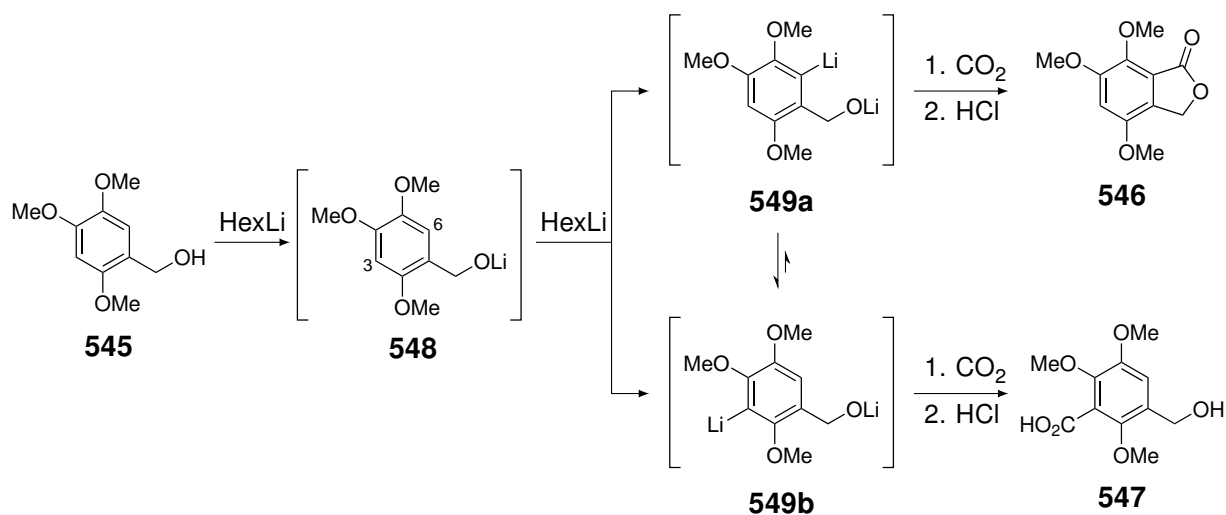
In the course of her master thesis, Amandine Traina proposed a four step sequence from methoxyhydroquinone **484** to reach trimethoxyphthalide **546** (Scheme 6.20). She first methylated hydroquinone **484** with dimethyl sulfate and then performed a Vilsmeier-Haack formylation to reach benzaldehyde **544**. Those two steps were similar to those used for the synthesis of sulfinylquinone **318a** (Chapter 5, Scheme 5.2). The aldehyde is then reduced with NaBH₄ into the corresponding alcohol **545**. So far, the three first steps have been carried out uneventfully with very good yields.



Scheme 6.20: First investigated pathway for the synthesis of trimethoxyphthalide **546** from methoxy hydroquinone **484**.²¹

The next step consists in the insertion of the oxidised carbon atom to form the lactone ring. For that transformation, the same conditions as Parsons *et al.* (Scheme 6.19) have been employed (except for the use of hexyllithium instead of butyllithium). After treatment of the reaction, a mixture of two products was obtained. After purification of the crude mixture, the first compound that has been identified was the desired phthalide **546**. But the second product, the benzoic acid **547**, was obtained in majority (1:3 ratio in favour of **547**).

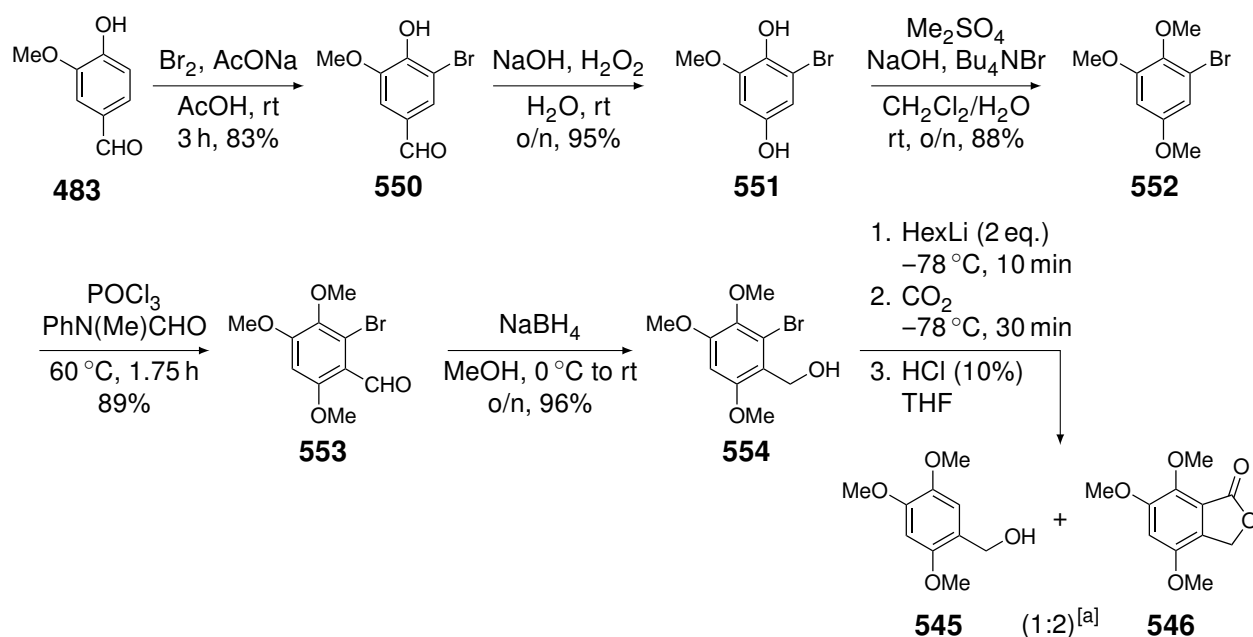
The formation of **547** was not expected as Parsons *et al.* described only the formation of the phthalide **542**. But in our case, a third methoxy group is present on the aromatic ring. After the first equivalent of hexyllithium deprotonates the alcohol into alkoxide **548**, both position 3 and 6 can undergo the *ortho*-lithiation. As methoxy groups are better *ortho*-directing groups than alkoxides, two methoxy groups will more effectively direct the lithiation (on position 3) than one methoxy group and one alkoxide (on position 6).²⁸ As a consequence, benzoic acid **547** is obtained as the major product.



Scheme 6.21: Both pathways for the *ortho*-lithiation of compound **545**.^{21,28}

To overcome that regioselectivity issue, she proposed to add a bromine atom on position 6. In doing so, the bromine-lithium exchange should occur on position 6 and, if the temperature is kept low and the addition of CO₂ is quickly done, phthalide **546** should be the only product obtained.

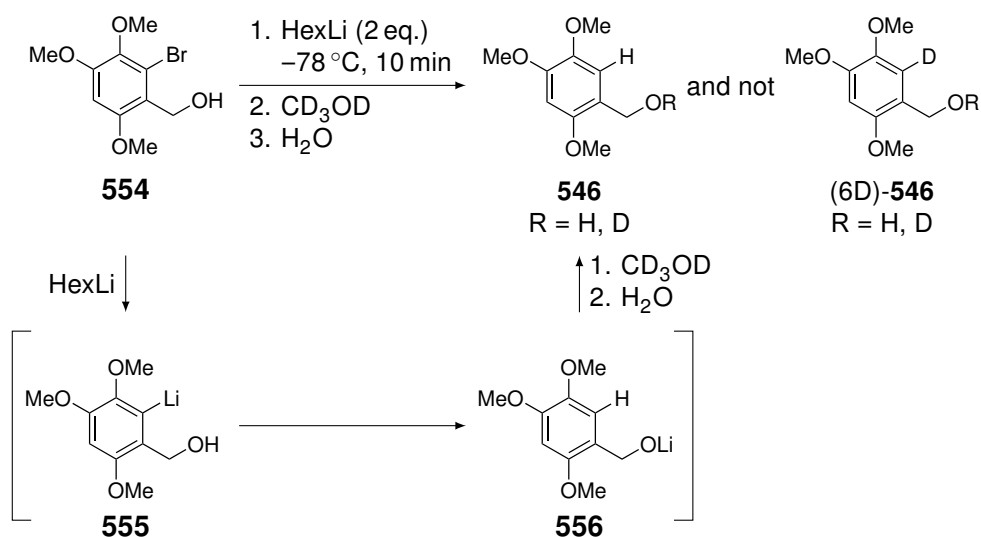
In order to insert the bromine atom in the synthesis, the bromination reaction of vanillin (**483**) is carried out (Scheme 6.22), following the same procedure than the one used in the synthesis of sulfinylquinone **318a** (Chapter 5, Scheme 5.2). The brominated vanillin **550** then underwent a Dakin oxidation as described by Cross and Zamitt.²⁹ The three next steps (the methylation of the phenols, the Vilsmeier-Haack formylation and the reduction of the aldehyde) are the same as in the first route towards phthalide **546** (Scheme 6.20). The intermediate **554** was then engaged in the bromine-lithium exchange, followed by the addition of carbon dioxide. After treatment of that reaction with hydrochloric acid, two products were once again obtained. In this case, the major one was the desired trimethoxyphthalide **546**, together with the debromination product **545** (1:2 ratio in favour of **546**). Even though the major product was the desired **546**, the master student did not succeed in separating them.



Scheme 6.22: Second investigated pathway for the synthesis of trimethoxyphthalide **546** from vanillin (**483**). [a] The yield of the last step has not been determined and the ratio of the products was based on their ratio in the ¹H NMR spectrum of the crude mixture.²¹

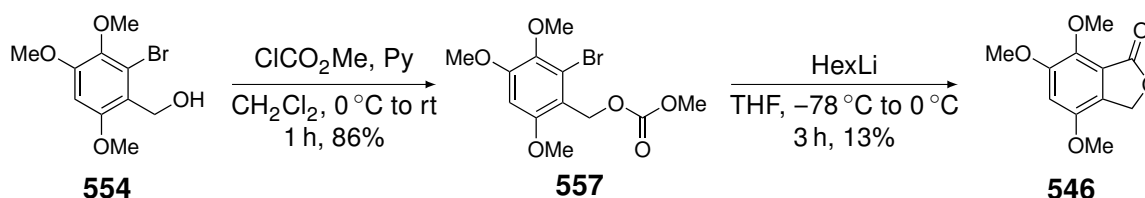
In the attempt to understand the reason the debromination of **554** occurred during that last step, and determine where the proton came from, she treated **554** with two equivalents of hexyllithium, followed by the addition of deuterated methanol (Scheme 6.23). After that treatment, the product obtained did not bear a deuterium on position 6, but a hydrogen atom.

The hypothesis behind that observation would be that the bromine-lithium exchange is faster than the deprotonation of the alcohol, which is then followed by the intramolecular deprotonation of the alcohol by the newly formed organolithium. In 1990, the group of Narasimhan suggested that such phenomenon was occurring with a (hydroxymethyl)quinoline,³⁰ even though it was questioned by Gallagher and Beak.³¹ Nevertheless, other examples highlighted that the halogen-lithium exchange could actually be faster than the deprotonation of an acidic hydrogen.^{32,33} A similar process has also been reported by Okamura and Theobald in 1990 in which they showed that the sulfoxide-lithium exchange of vinyl sulfoxides was faster than the deprotonation of an alcohol.³⁴



Scheme 6.23: Treatment of bromide **554** with two equivalents of hexyllithium and deuterated methanol in order to determine the reasons for the debromination process of the last reaction described in Scheme 6.22.²¹

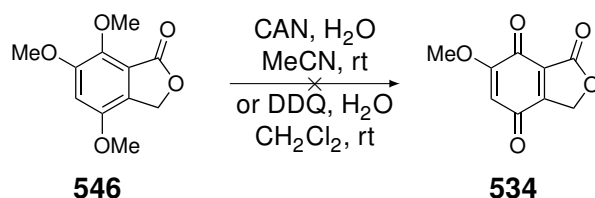
As the separation of the desired phthalide **546** and the debrominated product **545** could not be achieved, a new tactic to introduce the carbonyl group has been proposed in that master thesis. Instead of using carbon dioxide as an external source of the oxidised carbon atom, the student first inserted the carbonyl by forming a carbonate with the use of methyl chloroformate (Scheme 6.24). A subsequent bromine-lithium exchange followed by the intramolecular cyclisation of the organolithium on the carbonate gave the desired phthalide **546** as sole product. However, she performed that reaction only once and a low yield was obtained. Nevertheless, she proved that quinone **546** could selectively be synthesised and optimisation of the reaction should lead to better yields.



Scheme 6.24: Formation of the trimethoxyphthalide **546** by insertion of a carbonate on intermediate **554** and intramolecular cyclisation after the bromine-lithium exchange of **557**.²¹

Now that a potential pathway has been found for the synthesis of the phthalide **546**, the next step was the oxidation of the latter into the corresponding quinone **534**. For that purpose, the usual reagent used for the oxidation of hydroquinone, CAN, has been first tested (Scheme 6.25). Unfortunately, it gave a complex mixture of unidentified products. She then tried DDQ but, in that case, no reaction took place.

This behaviour is similar to the one encountered during the synthesis of the silylated sulfinylquinone **318b** (Chapter 5, Scheme 5.6). It would seem that the presence of a conjugated EWG on the aromatic core and a heteroatom on the benzylic position leads to the degradation of the compound when the CAN oxidation is employed and to no reaction at all with DDQ.



Scheme 6.25: Attempts of oxidation of phthalide **546** into quinone **534**.²¹

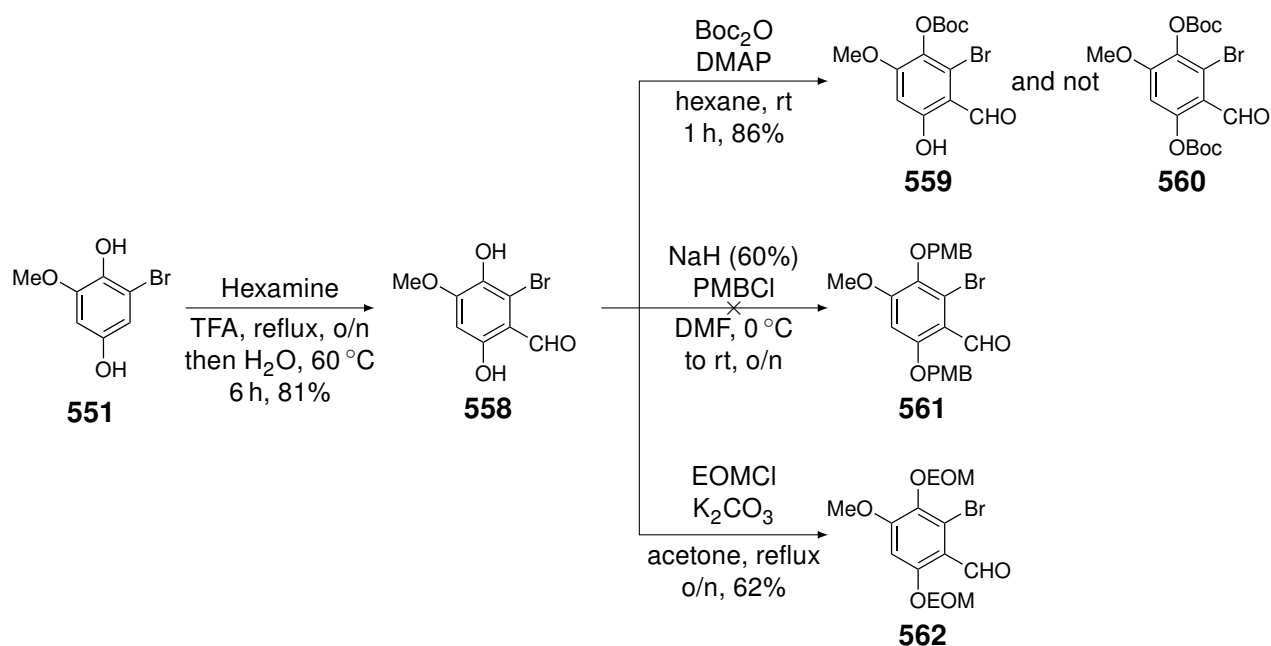
Therefore, the student proposed to replace the methyl group protecting the hydroquinone with more labile groups that can be more easily removed during or before the oxidation step.

It was determined that the best stage to introduce those protecting groups was right before the reduction of the aldehyde. In that new synthetic pathway, the formylation reaction had to be carried out on the unprotected hydroquinone **551**. The student attempted to use the standard Vilsmeier-Haack formylation with DMF and POCl_3 but it did not work. She then determined that the Duff formylation was the best way to obtain benzaldehyde **558** (Scheme 6.26).

Later on, she first tried to protect the phenols with Boc groups, that should easily be removed in acidic conditions. However, when she performed the reaction, only one of the phenols was protected, giving **559** and not **560**. It was determined by n.O.e experiments that the Boc was added on the phenol next to the methoxy group (as a correlation was observed between those two groups).

The second protecting group that was tested is PMB. Advantageously, the use of DDQ can remove the PMB groups and oxidise the hydroquinone into the quinone in one single step. Unfortunately, the attempt to protect **558** with those groups did not work.

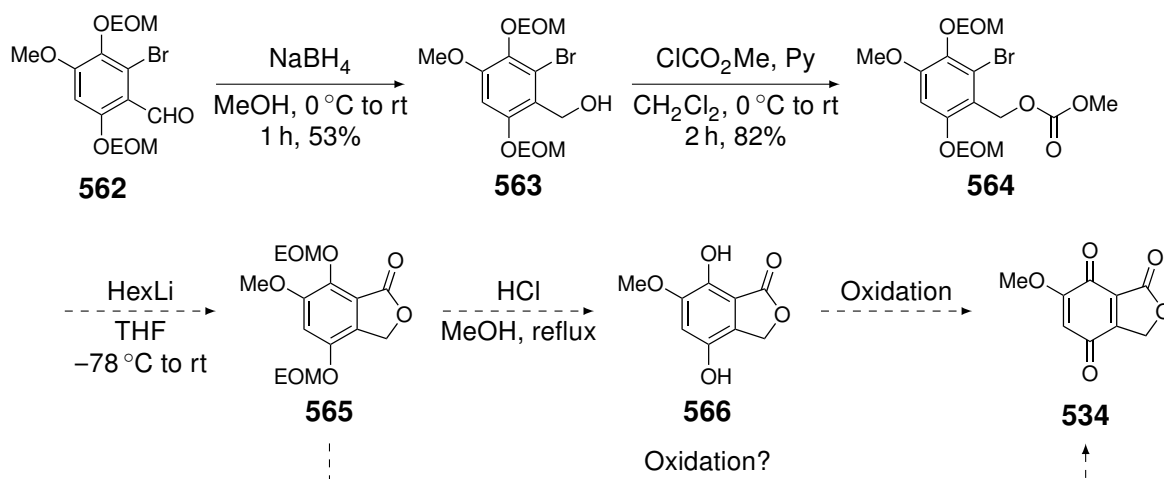
Finally, the protection of both phenols was possible with EOM groups. This protecting group has already been successfully used in the synthesis of sulfinylquinone **488** (Chapter 5, Scheme 5.5).



Scheme 6.26: Synthetic pathways for the preparation of hydroquinones derivatives with different protecting groups.²¹

Given EOM is more labile than a methoxy group, it might be removed during the oxidation step. In the event the oxidation does not directly work on the protected hydroquinone, removal of the EOM groups can be performed using acidic conditions.

The rest of the synthesis was carried out similarly to the one described in Schemes 6.22 and 6.24. The reduction of the benzaldehyde was done with a moderate yield of 53%, but the student performed this reaction only once and she will most certainly do it again to optimise the conditions. On the other hand, the formation of the carbonate was carried out with a good 82% yield.



Scheme 6.27: New synthetic pathway proposed for the synthesis of phthalide quinone **534**, using EOM as protecting group for the phenols.²¹

So far, the master student arrived at the formation of carbonate **564** and she will soon pursue the development and optimisation of this new synthetic pathway. From **564**, the formation of the lactone ring will be carried out with the use of hexyllithium. Then, the direct oxidation from the EOM-protected hydroquinone **565** will be tested with CAN and DDQ. In the event those oxidations do not succeed in providing the phthalide quinone **534**, the phenol will be first deprotected to give hydroquinone **566**. The latter will be submitted to diverse oxidising agents including CAN and DDQ, but also other such as PIDA, PIFA or silver(I) oxide.

Diels-Alder reaction with quinone **534**

Once this newly designed phthalide quinone **534** is synthesised, its reactivity in Diels-Alder reaction will be assessed. First, model dienes, such as the one used for the study presented in Chapter 5 (Figure 5.6) will be used with quinone **534** in dichloromethane, but also in HFIP in order to complete the study.

Then various catalyst will also be employed to evaluate their impact on the cycloaddition of **534** with those model dienes. We will start with achiral catalysts and then Evans's catalyst **255a** to assess if this new quinone is an adequate substrate for that asymmetric catalysis.

If the use of this quinone with simple dienes gives promising results, we will move on to the use of the oxygenated dienes and determine which one(s) can be used with Evans's asymmetric catalysis and, subsequently, as precursor for the total synthesis of momilactones.

6.4 Conclusion

So far, we have shown that sulfinylquinone **318a** could react with simple oxygenated dienes such as **373a**. It was also highlighted that the selective reduction of the carbon-sulfur bond to reach the desired *trans*-decalin *ent*-**367aa** was not easy to carry out, but could be done using a H-Cube[®] system (continuous flow chemistry) (Scheme 6.1).² Yet, this strategy still needs optimisation. It was also demonstrated that the carbonyl groups of the pyrolysed adduct **519** could be selectively reduced (Scheme 6.2).

When we tested the Diels-Alder reaction between sulfinylquinone **318a** with α -pyrone **373e**, the only product obtained (**525**) corresponded to a hetero-Diels-Alder reaction between a tautomer of quinone **318a**, acting as the diene, and pyrone **373a**, acting as the dienophile (Scheme 6.3).

We later showed that the use of less reactive dienes such as **373c** (Scheme 6.5) and **373d** (Scheme 6.8), that bear an EWG, or **373f** (Scheme 6.10), that is quite hindered, could not react with sulfinylquinone **318a** due to that lack of reactivity. On the other hand, the use of diene **373b** seemed to form a cycloadduct followed by the pyrolysis of the sulfinyl moiety, as indicated by the presence of thiosulfinate **502**. But the pyrolysed cycloadduct **530** was rapidly degraded (Scheme 6.9).

These results therefore indicated that only simple oxygenated dienes, such as **373a**, would be suitable precursors, with sulfinylquinone **318a** as dienophile, for the total synthesis of momilactone A (**1**). It was also demonstrated that the reduction steps planned for the total synthesis of momilactones (Chapter 3, section 3.2.2 and Scheme 3.11) are feasible.

The next part of this work was to test Corey's asymmetric catalysis as potential synthetic tool for the synthesis of momilactones. We first tested that reaction with the designed quinone **369a** and simple dienes and showed that only the most reactive one, cyclopentadiene (**151**), was able to undergo the catalysed asymmetric cycloaddition (Scheme 6.11). That example also led to the formation of a cycloadduct with an excellent enantioselectivity and the structure and absolute configurations were confirmed by X-ray diffraction.

The same process was tested with dienes **373b-d** but they either were not reactive enough or degraded (Scheme 6.12). We indeed suspected that Corey's catalyst might be acidic enough to cleave the enol ether moiety, which might also lead to further side reactions and the degradation of the dienes.

Nevertheless, we could make the reaction work with the simpler (and smaller) oxygenated diene **373a** and the NMR analysis of the crude product was consistent with the expected adduct (Scheme 6.13). Unfortunately, we could not isolate a pure sample nor determine the enantiomeric excess of the formed cycloadduct. Yet, this reaction still deserves our attention and could be optimised.

We therefore showed that quinone **369a** was able to undergo enantioselective Diels-Alder reactions with Corey's catalyst. Similarly to sulfinylquinone **318a**, it appeared that, for that catalytic system, only small and reactive oxygenated dienes would be suitable as precursor for the total synthesis of momilactones.

Finally, we moved on to Evans asymmetric catalysis. We observed that with quinone **371a**, specifically designed for this catalysis, no reaction took place whether with piperylene (**179**, Scheme 6.15), a diene used in Evans work,¹⁷ or the more reactive oxygenated diene **373a** (Scheme 6.16).

We suggested that the out-of-plane conformation of the ester, as observed in its X-ray structure (Figure 6.8), might be the cause of this lack of reactivity. As Evans did not present any examples of quinone substrates bearing a substituent next to the ester, we could not compare our results with reported ones and could not propose another hypothesis. We therefore came to the conclusion that the conformational issue of quinone **371a** could not allow the latter to be a suitable quinone substrate for the Evans catalytic system and that its use as precursor for the total synthesis of momilactones was compromised.

Therefore, a new phthalide quinone **534** was designed in order to overcome the conformational issue. A master student in our group worked on the development of the synthesis of this quinone **534** and highlighted that the preparation of the hydroquinone precursor, trimethoxyphthalide **546**, was not straightforward (Schemes 6.20 and 6.22). Nevertheless, she managed to develop a seven step sequence to reach the trimethoxyphthalide **546** precursor (Schemes 6.22 and 6.24). However, the oxidation of that compound did not work with either CAN or DDQ (Scheme 6.25).

Therefore, she developed a new synthetic pathway with the use of EOM instead of methyl groups for the protection of the hydroquinone (Schemes 6.26 and 6.27). So far, she could reach the carbonate **564**, precursor to the phthalide **565**, without any issues.

In order to determine if that route is suitable for the synthesis of this new phthalide quinone **534**, a few more steps are needed. Once this quinone is synthesised, its reactivity in Diels-Alder reactions must be assessed with different systems.

References

- [1] Lanfranchi, D. A.; Hanquet, G. Asymmetric Diels-Alder Reactions of a New Enantiomerically Pure Sulfinylquinone: A Straightforward Access to Functionalized Wieland-Miescher Ketone Analogues with (*R*) Absolute Configuration. *J. Org. Chem.* **2006**, *71*, 4854–4861.
- [2] Colas, L. Contribution à la synthèse totale de la momilactone A. Master internship at the Laboratoire de Chimie Organique de Synthèse, Faculté Universitaire Notre-Dame de la Paix, Namur, Belgium, 2010.
- [3] Lanfranchi, D. A. Vers la synthèse totale de la salvinorine A et d'analogues structuraux. Ph.D. thesis, Université Louis Pasteur, Strasbourg, France, 2006.
- [4] Carreño, M. C.; García Ruano, J. L.; Toledo, M. A.; Urbano, A. Influence of the Sulfinyl Group on the Chemoselectivity and π -Facial Selectivity of Diels-Alder Reactions of (*S*)-2-(*p*-Tolylsulfinyl)-1,4-benzoquinone. *J. Org. Chem.* **1996**, *61*, 503–509.
- [5] Carreño, M. C.; García Ruano, J. L.; Lafuente, C.; Toledo, M. A. Asymmetric Diels-Alder reactions of 5-substituted and 5,6-disubstituted (*S*)-2-(*p*-tolylsulfinyl)1,4-benzoquinones with cyclopentadiene and *trans*-piperylene. *Tetrahedron: Asymmetry* **1999**, *10*, 1119–1128.
- [6] Jones, W. H.; Mangold, D.; Plieninger, H. Diensynthese Unter Hohem Druck. *Tetrahedron* **1962**, *18*, 267–272.
- [7] Minuti, L.; Taticchi, A.; Marrocchi, A.; Broggi, A.; Gacs-Baitz, E. High pressure Diels–Alder reactions of (+)-nopadiene with cycloalkenones. *Tetrahedron: Asymmetry* **2004**, *15*, 1187–1192.
- [8] Minuti, L.; Temperini, A.; Ballerini, E. High-Pressure-Promoted Diels–Alder Approach to Biaryls: Application to the Synthesis of the Cannabinols Family. *J. Org. Chem.* **2012**, *77*, 7923–7931.
- [9] Pandey, S. K.; Orellana, A.; Greene, A. E.; Poisson, J.-F. High-Pressure Diels–Alder Approach to Natural Kainic Acid. *Org. Lett.* **2006**, *8*, 5665–5668.
- [10] Kiselev, V. D. High-Pressure Influence on the Rate of Diels–Alder Cycloaddition Reactions of Maleic Anhydride with Some Dienes. *Int. J. Chem. Kinet.* **2013**, *45*, 613–622.
- [11] Gebauer, J.; Blechert, S. Synthesis of γ,δ -Unsaturated- β -keto Lactones via Sequential Cross Metathesis-Lactonization: A Facile Entry to Macrolide Antibiotic (–)-A26771B. *J. Org. Chem.* **2006**, *71*, 2021–2025.
- [12] Rabe, P.; Klapschinski, T. A.; Brock, N. L.; Citron, C. A.; D'Alvise, P.; Gram, L.; Dickschat, J. S. Synthesis and bioactivity of analogues of the marine antibiotic tropodithietic acid. *Beilstein J. Org. Chem.* **2014**, *10*, 1796–1801.
- [13] Ryu, D. H.; Corey, E. J. Triflimide Activation of a Chiral Oxazaborolidine Leads to a More General Catalytic System for Enantioselective Diels-Alder Addition. *J. Am. Chem. Soc.* **2003**, *125*, 6388–6390.
- [14] Hu, Q.-Y.; Zhou, G.; Corey, E. J. Application of Chiral Cationic Catalysts to Several Classical Syntheses of Racemic Natural Products Transforms Them into Highly Enantioselective Pathways. *J. Am. Chem. Soc.* **2004**, *126*, 13708–13713.
- [15] Nakashima, D.; Yamamoto, H. Design of Chiral *N*-Triflyl Phosphoramidate as a Strong Chiral Brønsted Acid and Its Application to Asymmetric Diels-Alder Reaction. *J. Am. Chem. Soc.* **2006**, *128*, 9626–9627.
- [16] Sow, B.; Bellavance, G.; Barabé, F.; Barriault, L. One-pot Diels–Alder cycloaddition/gold(I)-catalyzed 6-*endo*-dig cyclization for the synthesis of the complex bicyclo[3.3.1]alkenone framework. *Beilstein J. Org. Chem.* **2011**, *7*, 1007–1013.
- [17] Evans, D. A.; Wu, J. Enantioselective Rare-Earth Catalyzed Quinone Diels-Alder Reactions. *J. Am. Chem. Soc.* **2003**, *125*, 10162–10163.
- [18] Kelly, T. R.; Dali, H. M.; Tsang, W.-G. Lithium thiomethoxide: a convenient mercaptide reagent. *Tetrahedron Lett.* **1977**, 3859–3860.
- [19] Levine, J. A.; Ferrendelli, J. A.; Covey, D. F. Alkyl-Substituted Thiolo-, Thiono-, and Dithio- γ -butyrolactones: New Classes of Convulsant and Anticonvulsant Agents. *J. Med. Chem.* **1986**, *29*, 1996–1999.
- [20] Sarkar, S.; Ghosh, S. Carbon-Carbon Bond Cleavage via Carbon Centred Radical in Strained Tricyclo[5.2.1.0^{2,6}]decenes. A Facile Route to Bridged Eight Membered Rings Related to Taxanes. *Tetrahedron* **1994**, *50*, 921–930.
- [21] Traina, A. Catalytic asymmetric Diels-Alder reaction of a phthalide quinone. M.Sc. thesis, Université de Namur, Belgium, 2021–2022.
- [22] Morita, S.; Fukushima, S.; Kanematsu, K. *p*-Benzoquinone-2,3-dicarboxylic anhydride as highly reactive and versatile electron-accepting dienophile. *Tetrahedron Lett.* **1979**, 2151–2154.
- [23] Kanematsu, K.; Morita, S.; Fukushima, S.; Ōsawa, E. Reagent Design and Study of *p*-Benzoquinone Derivatives as Highly Reactive Electron-Attracting Dienophiles. A Promising Class of Reagents (Synthons) for Cycloaddition. *J. Am. Chem. Soc.* **1981**, *103*, 5211–5215.
- [24] Potman, R. P.; van Kleef, F. J.; Scheeren, H. W. Tailor-Made Butadienes for the Site-Selective Cycloaddition with Quinizarinquinone and Other Unsymmetrically Substituted Quinones. *J. Org. Chem.* **1985**, *50*, 1955–1959.
- [25] Hammond, P. R. 3,6-Dioxocyclohexa-1,4-diene-1,2,4,5-tetracarboxylic Acid Dianhydride, a Strong Elec-

- tron Acceptor. *J. Chem. Soc. C* **1971**, 1521–1523.
- [26] Kraus, G. A.; Sugimoto, H. An annelation route to quinones. *Tetrahedron Lett.* **1978**, 2263–2266.
- [27] Parsons, P. J.; Jones, R., Daniel; Walsh, L. J.; Allen, L. A. T.; Onwubiko, A.; Preece, L.; Board, J.; White, A. J. P. An Approach to the Core of Lactonamycin. *Org. Lett.* **2017**, *19*, 2533–2535.
- [28] Clayden, J. Regioselective Synthesis of Organolithiums by Deprotonation. In *Organolithiums: Selectivity for Synthesis*; Clayden, J., Ed.; Tetrahedron Organic Chemistry Series; Elsevier, 2002; Vol. 23; Chapter 2, pp 9–109.
- [29] Cross, B. E.; Zamitt, L. J. Pigments of *Gnomonia erythrostoma* — IV. The synthesis of 5,8-dibenzyloxy-3-hydroxy-6-methoxy-1,4-naphthoquinone. *Tetrahedron* **1976**, 1587–1590.
- [30] Narasinhani, N. S.; Sunder, N. M.; Ammanamanchi, R.; Bonde, B. D. Evidence in Favor of Lithium-Halogen Exchange Being Faster Than Lithium-Acidic Hydrogen (Deuterium) Exchange. *J. Am. Chem. Soc.* **1990**, *112*, 4431–4435.
- [31] Gallagher, D. J.; Beak, P. Is Halogen-Lithium Exchange Intramolecularly Competitive with Removal of an Acidic Hydrogen? Reinvestigation of a Recent Claim. *J. Am. Chem. Soc.* **1991**, *113*, 7984–7987.
- [32] Lamrani, M.; Hamasaki, R.; Yamamoto, Y. Is the halogen-metal exchange faster than deprotonation in the reaction of *ortho*-carbonyl aryl bromide with butyllithium? *Tetrahedron Lett.* **2000**, *41*, 2499–2501.
- [33] Clayden, J. Regioselective Synthesis of Organolithium by X-Li Exchange. In *Organolithiums: Selectivity for Synthesis*; Clayden, J., Ed.; Tetrahedron Organic Chemistry Series; Elsevier, 2002; Vol. 23; Chapter 3, pp 111–147.
- [34] Theobald, P. G.; Okamura, W. H. Stereospecific Reductive Desulfurization of Vinyl Sulfoxides with *tert*-Butyllithium and an Internal Proton Source. *J. Org. Chem.* **1990**, *55*, 741–750.

Chapter 7

Conclusion and outlook

7 Conclusion and outlook

The main goal of this thesis was to find the most suitable pathway for the enantioselective synthesis of momilactones A (**1**) and B (**2**), two pimarane diterpenes from the rice plant *Oriza sativa*, using an asymmetric Diels-Alder reaction as key step of the synthesis. Many interesting results were obtained but we also encountered some setbacks. We will below present the achievements of this work, but also propose some improvements of the syntheses carried out as well as new ideas for the development of the project.

7.1 Conclusion

7.1.1 Synthesis of dienes

One of the partners planned for the Diels-Alder reaction was an oxygenated diene. Initially, five dienes (**373a-e**, Figure 7.1), with increasing structural complexity, were chosen as potential precursors for the total synthesis and we succeeded in synthesising all of them. Dienes **373a**,¹ **373c**,² and **373d**³ were already described and their syntheses were uneventfully reproduced.

The preparation of pyrone **373e**, the most interesting diene for the total synthesis of momilactones, was already reported by Effenberger *et al.*^{4,5} but we could not entirely reproduce their synthesis. Therefore, we developed a new efficient synthetic pathway for the preparation of such 4-alkoxypyrones that gave us pyrone **373e** in three steps and 30% overall yield from *tert*-butyl propionate (**440**) and ethyl 3,3-diethoxypropanoate (**460**) (Scheme 4.16).

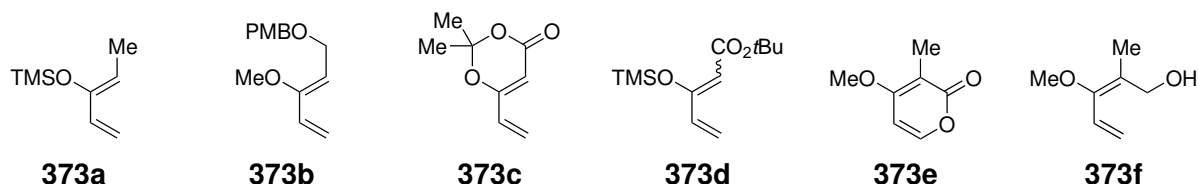


Figure 7.1: Structures of the six dienes **373a-f** that have been synthesised.

The synthesis of diene **373b**, on the other hand, had never been described. Nevertheless, we managed to stereoselectively synthesise the latter in five steps and 46% overall yield from but-3-en-1-ol (**408**) (Scheme 4.2).

Finally, in the attempt to reduce pyrone **373e** into the corresponding pyran (**462**), we serendipitously obtained the peculiar diene **373f** in 86% yield.

7.1.2 Synthesis and use of 4-hydroxy-5-thiomethylenefuran-2-ones

One of the most surprising results was the unexpected synthesis of 4-hydroxy-5-thiomethylenefuran-2-ones **455** with a *Z* configuration (four examples). These products were obtained during one of the attempts to synthesise 4-hydroxy- α -pyrones (**454**). Nevertheless, this type of exotic pattern is barely present in the literature and we therefore have developed a new and versatile synthetic method to reach such products.

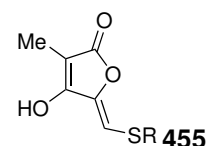


Figure 7.2: Structure of thiomethylenefuranones **455**.

Moreover, a master student also showed it was possible to perform Suzuki couplings on the triflate derivative of **455b** (R = Me) to reach new thiomethylenefuranone compounds with various aryl substituents (15 examples).⁶

7.1.3 Synthesis of quinones

In addition to the synthesis of oxygenated dienes, three quinones (**318a**, **369a** and **371a**, Figure 7.3) were chosen for the total synthesis of momilactones and three other sulfinylquinones (**297**, **307a** and **488**) were designed for the structural study of such chiral quinones. Similarly to the dienes, we managed to synthesise all of them. The syntheses of sulfinylquinones **318a**,^{7,8} **297**⁹ and **307a**¹⁰ were uneventfully reproduced.

The preparation of quinone **369a** was reported several times but we proposed a new synthetic pathway and the latter was synthesised in five steps and 64% overall yield from methylhydroquinone **473** (Scheme 5.9).

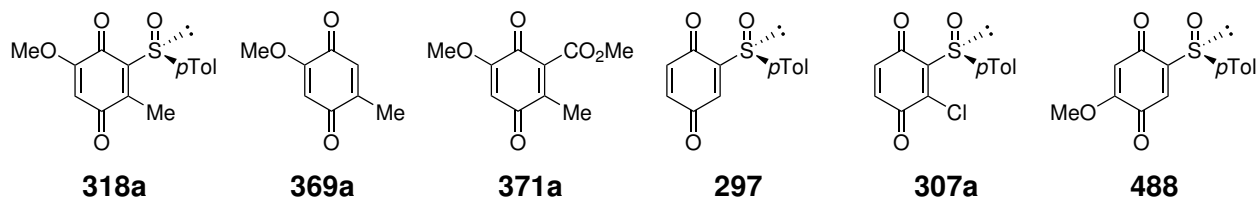
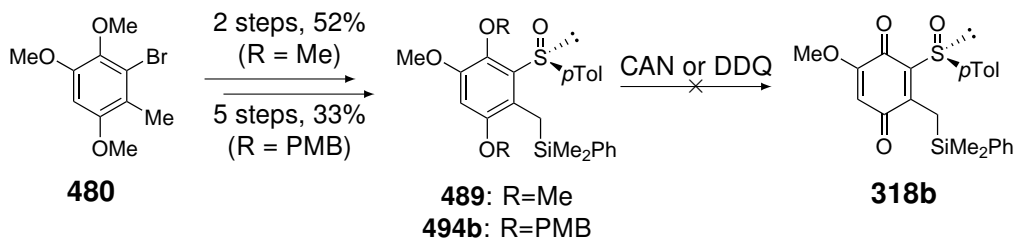


Figure 7.3: Structures of the quinones and sulfinylquinones that have been synthesised.

We also achieved the syntheses of two new quinones: quinone **371a**, that was prepared in ten steps and 50% overall yield from methylhydroquinone **473** (Scheme 5.10), and sulfinylquinone **488**, that was prepared in five steps and 36% overall yield from vanillin (**483**) (Scheme 5.5).

We then tried the synthesis of the silylated sulfinylquinone **318b** (Scheme 7.1) that was intended to serve for the total synthesis of momilactone B (**2**). We efficiently introduced the dimethylphenylsilyl group on the benzylic position of the aryl sulfoxide **481** (Scheme 5.6), but the oxidation of **489** did not work.

We then proposed a second synthetic pathway with other protecting groups for the hydroquinone part (Scheme 5.8) and we were able to obtain the PMB-protected aryl sulfoxide **494b**. Unfortunately, we did not manage to oxidise the latter either.



Scheme 7.1: Attempts for the synthesis of the silylated sulfinylquinone **318b**.

As we gave the priority to the development of the synthesis of momilactone A, we decided to leave the synthesis of the silylated sulfinylquinone **318b** aside.

7.1.4 Structural analysis of the sulfinylquinones

The next objective of this project was to obtain crystals of the synthesised sulfinylquinones in order to analyse them by X-ray diffraction and observe the conformation of the sulfoxide in the solid state. For all four sulfinylquinones (Figure 7.3), we succeeded in finding the best conditions to make suitable crystals and they could all be analysed by X-ray diffraction (Figure 5.2). To the best of our knowledge, we were the first ones to obtain X-ray structures of sulfinylquinones.

We observed that all the sulfinylquinones adopted the *s-cis* conformation (Figure 7.4), which was consistent with the proposed model that was solely based on the obtained cycloadduct.¹¹ It was also determined that the torsion angle between the sulfoxide and the quinone plane was more important when a bulky group (a methyl group compared to a hydrogen atom) or an electronegative atom (such as a chlorine atom) was present next to the sulfinyl moiety. It also seemed that the substituents on the double bond opposite to the one bearing the sulfoxide had no or little effect on the preferred conformation.

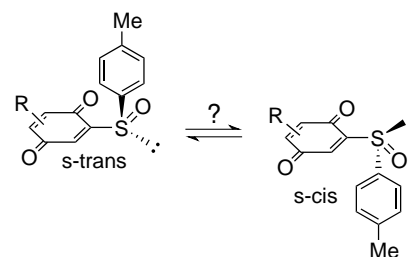


Figure 7.4: Representation of the *s-cis* and *s-trans* conformations of the sulfinylquinones.

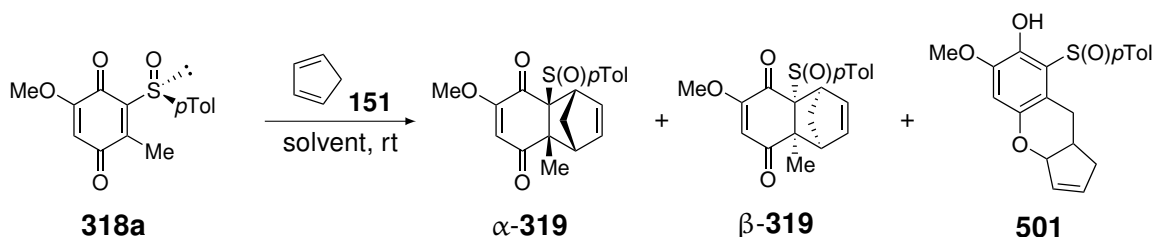
The analysis of the X-ray structures was completed with a computational analysis of differently substituted sulfinylquinones. It was indeed highlighted that the *s-cis* conformation was more stable than the *s-trans* one (in the gas phase). Those calculations also comforted the hypothesis that the substituent next to the sulfinyl moiety had the most important impact on the dihedral angle of the sulfoxide and, subsequently, its relative stability (compared to the *s-trans* conformation).

Another theoretical study on the preferential conformation of sulfinylquinone **318a** was also carried out to compare the effect of the polarity of the solvent, using an implicit solvation. It indicated that increasing the polarity decreased the preference for the *s-cis* conformation in favour of the *s-trans* one. We found out that the calculated *s-cis/s-trans* ratio in dichloromethane (almost 1/1) was not in agreement with the diastereoselectivities experimentally observed when the reactions were run in that solvent (majority of adducts coming from the reaction on the *s-cis* conformer, according to the proposed model). We therefore came to the conclusion that, even though a similar amount of *s-cis* and *s-trans* conformers are present in solution, the *s-cis* conformation must be more reactive than the *s-trans* one, hence the preference for products coming from the reaction with the *s-cis* conformer. It is therefore undeniable that the conformation of the sulfoxide plays an important role in the facial diastereoselectivity of the cycloaddition of sulfinylquinones, but that selectivity is not directly correlated to the preferential conformation in solution.

However, in the case of strongly polar or protic solvents, that implicit solvation did not allow to take into account the solvent-solute interactions that are known to be important, especially in the case of the Diels-Alder reaction.

7.1.5 Reactivity study on sulfinylquinones and quinones

After the structural study of the sulfinylquinones, we moved on to the evaluation of their reactivity. A master student in our group studied the impact of the solvent on the facial diastereoselectivity of the cycloaddition of sulfinylquinone **318a** with cyclopentadiene (**151**) (Scheme 7.2 and Table 5.3).¹²



Scheme 7.2: Diels-Alder reaction between sulfinylquinone **318a** and cyclopentadiene (**151**) in different solvents at room temperature.¹²

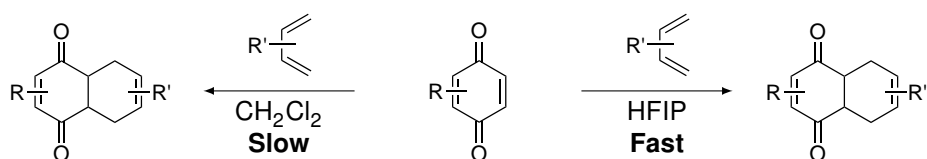
She first observed that the use of apolar solvents led to the β adduct in majority, which was consistent with the models proposed. When the polarity of the solvent increased, the selectivity for β -**319** slightly decreased.

On the other hand, the use of protic solvent inverted the selectivity towards the α adduct, most likely due to the formation of a hydrogen bond between the oxygen atoms of the sulfoxide and the carbonyl group that stabilises the s-trans conformation. The stronger the hydrogen bond donor was, the higher the selectivity for α -**319** was.

The most unexpected results were obtained in polar aprotic solvents. A new product **501**, coming from a hetero-Diels-Alder reaction between a tautomer of sulfinylquinone **318a** and cyclopentadiene (**151**), was obtained as a mixture of diastereoisomers. Similarly to the standard cycloaddition, the increase of the polarity of the solvent increased the preference for one of the diastereoisomers.

From those tests, three solvents remarkably stood out. Cyclopentadiene (**151**), directly used as a solvent, gave the best selectivity for the β adduct (α : β 17:83). On the contrary, water gave the best selectivity towards the α adduct (α : β 93:7). The solvent that really captured our attention was HFIP that, not only gave a very good selectivity for α -**319** (α : β 88:12), but also decreased the reaction time from several days to only 35 min.

Given the extraordinary accelerating effect of HFIP for the cycloadditions of quinones, we compared the Diels-Alder reactions run in dichloromethane and in HFIP for fourteen quinonoid systems with three model dienes (which made 42 combinations to be compared in both dichloromethane and HFIP). We observed that the use HFIP drastically increased the reaction rate in all the examples. This solvent could even help some reactions to proceed until completion when there was no or low conversions in dichloromethane.



Scheme 7.3: Comparison of the Diels-Alder reaction of quinones in dichloromethane and HFIP

In the case of the sulfinylquinones, when the reaction occurred on the sulfinyl-substituted double bond, the selectivity was always in favour of the β adduct in dichloromethane. When the same

reactions were run in HFIP, the selectivity switched towards the α adduct with cyclopentadiene (**151**), but remained in favour of the β adduct with acyclic dienes. When the reaction occurred on the double bond opposite to the sulfonyl-substituted one, the main adduct was the α one in dichloromethane and the preference for the α adduct was increased even more in HFIP.

All the examples gave the same double bond selectivity in both dichloromethane and HFIP, at the exception of quinone **371a** (or **Q8**) with piperylene (**179**) and dimethylbutadiene (**247**). In dichloromethane, an unexpected [2+2]-cycloaddition occurred on the most electron rich double bond. We suggested the out-of-plane conformation of the ester group hindered the double bond to which it was bonded, hence the reaction on the other double bond. But when HFIP was employed, the standard [4+2] cycloaddition took place on the most electron poor double bond. We hypothesised that HFIP could make a hydrogen bond with both oxygen atoms of the ester and the carbonyl of the quinone, which brought the ester back into the quinone plane.

The same master student, who studied the effect of the solvent on the Diels-Alder reaction between sulfinylquinone **318a** and cyclopentadiene (**151**), also studied the reaction of that sulfinylquinone with different dienes in both dichloromethane and HFIP.¹² She highlighted that too hindered or poorly reactive dienes (like furans) did not react with **318a**, even in HFIP. She also observed that dienes sensitive to acidic medium, such as silyl enol ethers, were degraded in HFIP. Those last results did not constitute a major drawback as those dienes are already reactive enough in dichloromethane.

7.1.6 Diels-Alder reactions for the total synthesis of momilactones

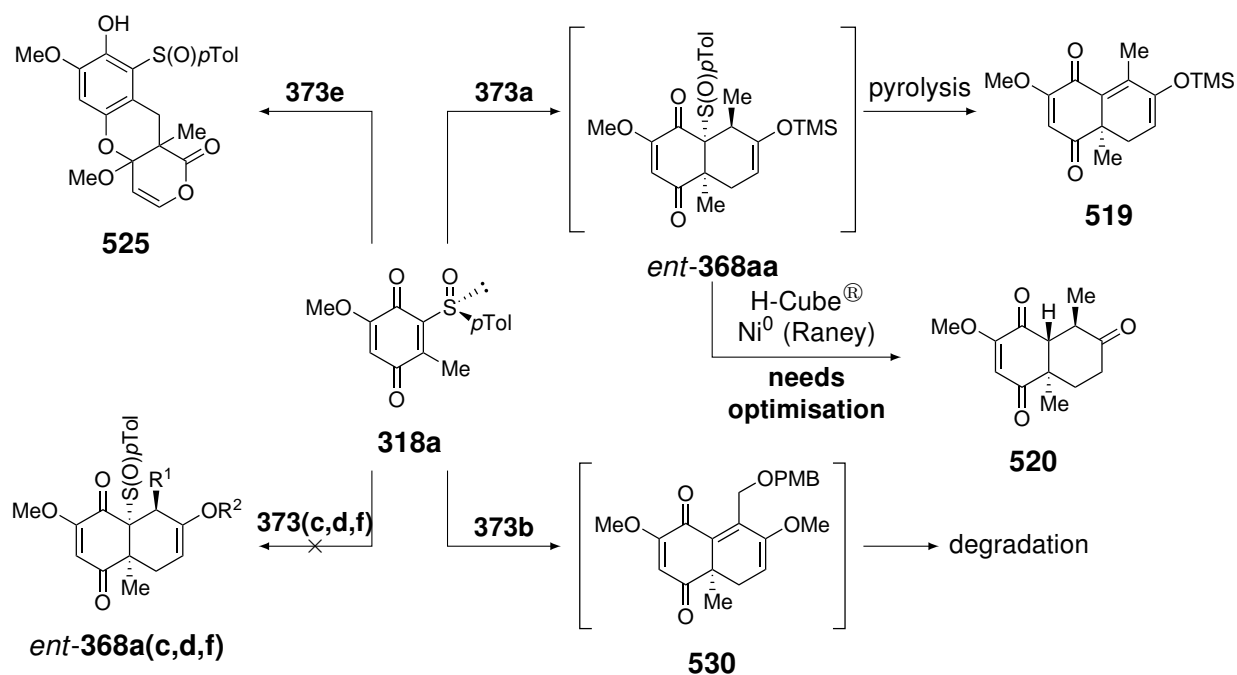
The last part presented in this work concerned the Diels-Alder reactions with the oxygenated dienes **373a-f** (Figure 7.1) for the synthesis of momilactones. The first quinonoid system used was the sulfinylquinone **318a** (Scheme 7.4).

The reaction of **318a** with diene **373a** was already known and led to a rapid pyrolysis of the adduct *ent*-**368aa**, which rendered the isolation of the latter difficult.^{7,8} Nevertheless, it was found out that the use of a H-Cube[®] system (continuous flow chemistry) with Raney nickel, directly on the crude mixture, allowed the carbon-sulfur bond reduction, giving triketone **520**.¹³ Even though this system worked, optimisations are still required. It was also demonstrated, on the pyrolysed adduct **519**, that it was possible to selectively reduce one carbonyl group over the other.

We then tried the reaction with α -pyrone **373e**. We observed that no reaction occurred in mild conditions and that it was necessary to heat up the reaction mixture to reflux of the solvent to obtain a product. In those conditions, we did not obtain the expected adduct, but product **525** coming from the hetero-Diels-Alder of the tautomer of sulfinylquinone **318a** and pyrone **373e**. We also highlighted that the use of other conditions (HFIP, ZnBr₂ or high pressure) gave no reaction at all.

In the case of diene **373b**, we observed the full conversion of sulfinylquinone **318a**, but we were not able to isolate any products of interest. Even though the presence of thiosulfinate **502** in the crude mixture indicated the formation of the pyrolysed adduct **530**, the latter underwent a rapid degradation.

Finally, the reactions of dienes **373c**, **373d** and **373f** never took place with sulfinylquinone **318a** due to a too low reactivity caused by the presence of an EWG or a too important steric hindrance.



Scheme 7.4: Outcomes of the Diels-Alder reactions of sulfanylquinone **318a** with dienes **373a-f**.

The next quinonoid system used was quinone **369a** with Corey's chiral catalyst *ent*-**109** (Scheme 7.5).^{14,15} When this system was used with cyclopentadiene (**151**), we obtained cycloadduct **532** with a good yield and an excellent enantioselectivity for the expected enantiomer (based on the products described in Corey's work).

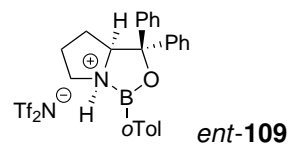
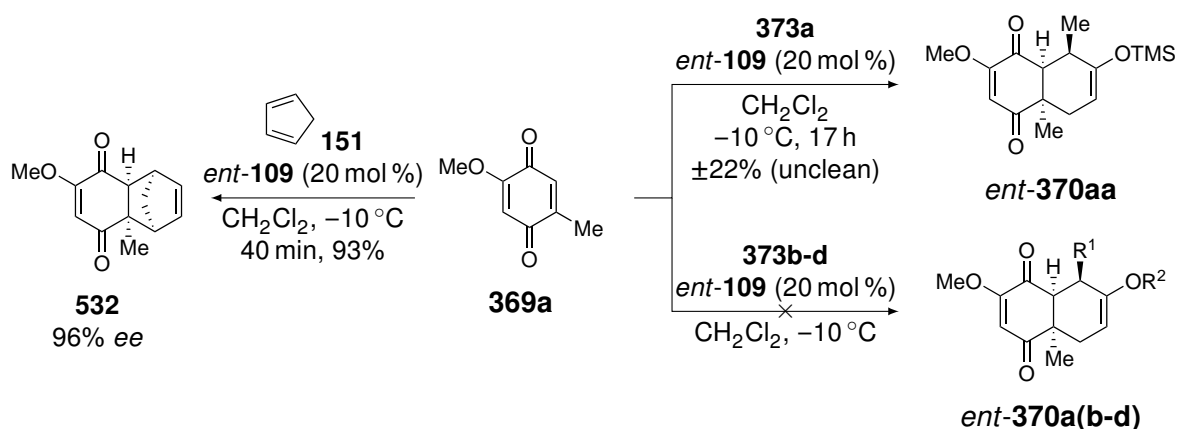


Figure 7.5: Structure of oxazaborolidinium salt *ent*-**109**.

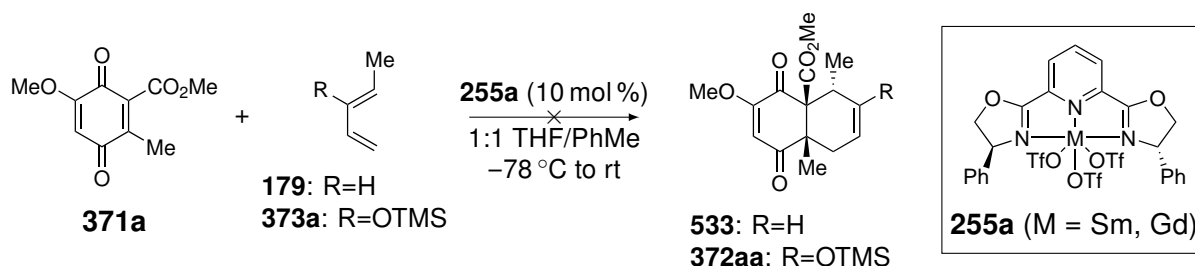
When the reaction was carried out with the oxygenated diene **373a**, a cycloadduct corresponding to *ent*-**370aa**, based on the ¹H NMR spectrum of the crude mixture, was obtained. However, when we attempted to purify the product, the latter degraded. We were therefore not able to determine the enantiomeric excess of the cycloadduct.

We carried out the same procedure with dienes **373b-d** but no reactions took place. We even observed the degradation of dienes **373b** and **373d**, possibly through the cleavage of the enol ether.



Scheme 7.5: Outcomes of Corey's asymmetric catalysis for the Diels-Alder reactions of quinone **369a** with cyclopentadiene (**151**) and oxygenated dienes **373a-d**.

We then tested Evans's asymmetric catalysis¹⁶ on quinone **371a** with piperylene (**179**) and diene **373a** but neither of those reactions worked (Scheme 7.6).

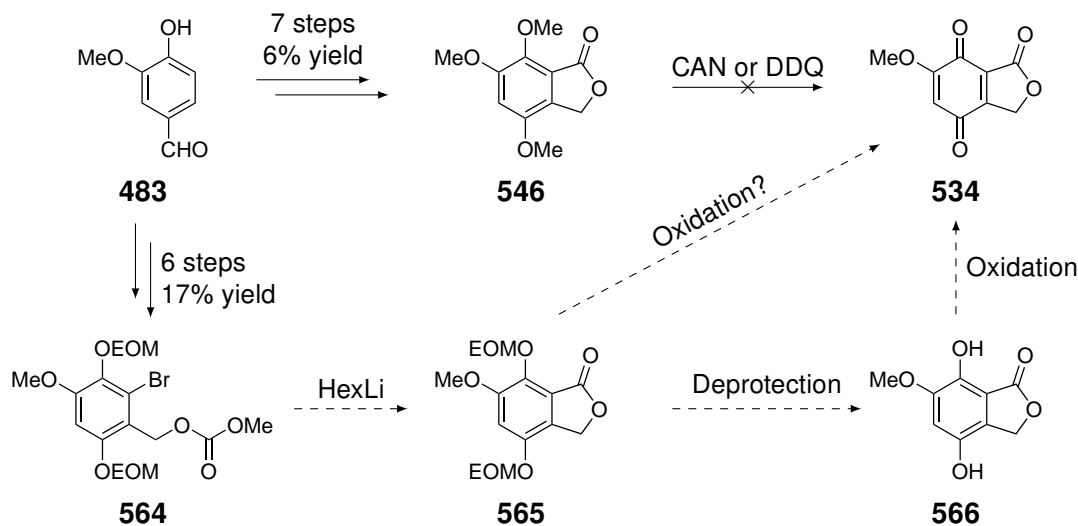


Scheme 7.6: Outcomes of Evans asymmetric catalysis for the Diels-Alder reactions of quinone **371a** with piperylene (**179**) and diene **373a**.

As we thought the conformation of the ester group was the cause of the lack of reactivity of quinone **371a**, we designed the new quinone **534** that should alleviate that issue. A master student in our group is currently working on the synthesis of that quinone.¹⁷

So far, she succeeded in synthesising the trimethoxyphthalide precursor **546** in seven steps and 6% overall yield (some steps still require optimisation) from vanillin (**483**) but the oxidation step did not work whether with CAN or DDQ (Scheme 7.7).

She then proposed a new pathway with EOM as protecting groups, instead of methoxy ones, and she managed to synthesise **564** in six steps and 17% overall yield from vanillin (**483**). The next steps of the synthesis of phthalide quinone **534** are still under study.



Scheme 7.7: Synthetic pathways for the synthesis of phthalide quinone **534**.¹⁷

What have we learned?

We developed new synthetic pathways and methods for the preparation of various compounds (dienes, quinones and sulfinylquinones), some of them by serendipity (thiomethylenefuranones), whose structures were rather complex or exotic. We also showed that, for some of these products, their syntheses were not straightforward and improvements, or development of new tactics, were needed.

We also completed the models to explain the preferential conformation of the sulfinylquinones, as well as the diastereoselectivity of the Diels-Alder reactions of the latter. X-ray and computational analyses showed that the *s-cis* conformation was the preferred one, even though its relative stability, compared to the *s-trans* one, was highly dependent on the substituent next to the sulfoxide. The comparison of experimental and theoretical results indicated that the stereoselectivity of the cycloaddition of sulfinylquinones was more likely to depend on the most reactive conformation of those quinones rather than on the ratio of the two conformers. Nonetheless, additional computational studies, notably the calculation of the transition state energies of those cycloadditions, will allow us to propose an even more accurate model for the approach of the dienes on the sulfinylquinones.

In the course of the reactivity study of quinones and sulfinylquinones, we highlighted that HFIP was a potent solvent to promote and greatly increase the rate of the Diels-Alder reaction of quinones, even in cases that did not work in dichloromethane. This solvent was also able to give a good, and sometimes inverted, stereoselectivity with sulfinylquinones. We also observed a change in reactivity for one substrate in that solvent, compared to the reaction in dichloromethane.

Finally, the first attempts on the asymmetric Diels-Alder reactions for the total synthesis of momilactones showed that the sulfinylquinone **318a** pathway and Corey's method (quinone **369a**) might be used as potential routes, even though it appeared that only the most simple oxygenated diene **373a** was a suitable diene precursor for those two quinonoid systems. Nevertheless, optimisation of the Diels-Alder reaction of those two quinonoid systems with diene **373a** should give promising pathways.

On the other hand, the Evans's catalytic system did not work and it appeared the presence of substituent next to the ester, such as the methyl group in quinone **371a**, thwarted the reaction. The conformational issue observed with **371a** may be solved with the use of the new phthalide quinone **534**, whose synthesis, actually in progress, already gave promising results.

7.2 Outlook

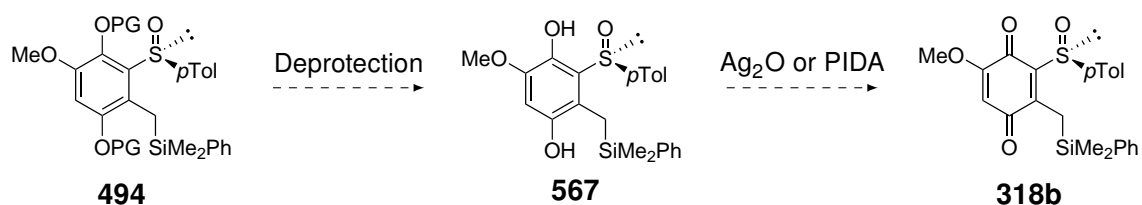
As said earlier, many interesting results have been obtained during this thesis. But a lot of work still needs to be done. Therefore, we will present in this section some ways of improvement for synthetic pathways already carried out or that have failed. We will also propose new ideas to give new perspectives to this project.

7.2.1 Synthesis of the silylated quinones

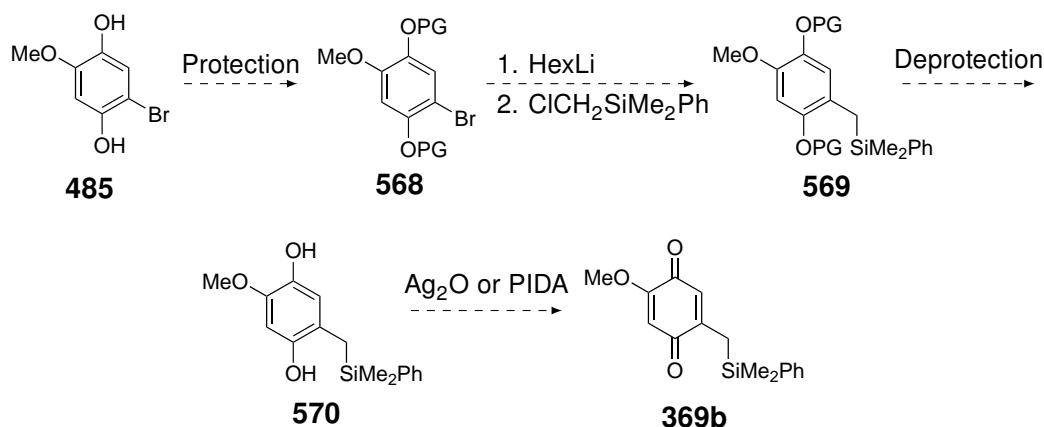
One of the parts of this project that needs attention is the synthesis of quinones with a dimethylphenylsilyl group, that was planned for the synthesis of momilactone B (**2**). Even though we were able to obtain silylated versions of the quinone precursor **494**, we did not succeed in oxidising the latter.

Published work suggested this oxidation would only work on the free hydroquinone **567**.^{18,19} Therefore, we planned a new synthetic route in which the protecting groups will be removed before the oxidation step (Scheme 7.8). Then, transformation of hydroquinone **567** into sulfinylquinone **318b** will be done with Ag₂O or PIDA, as proposed in the works cited above.

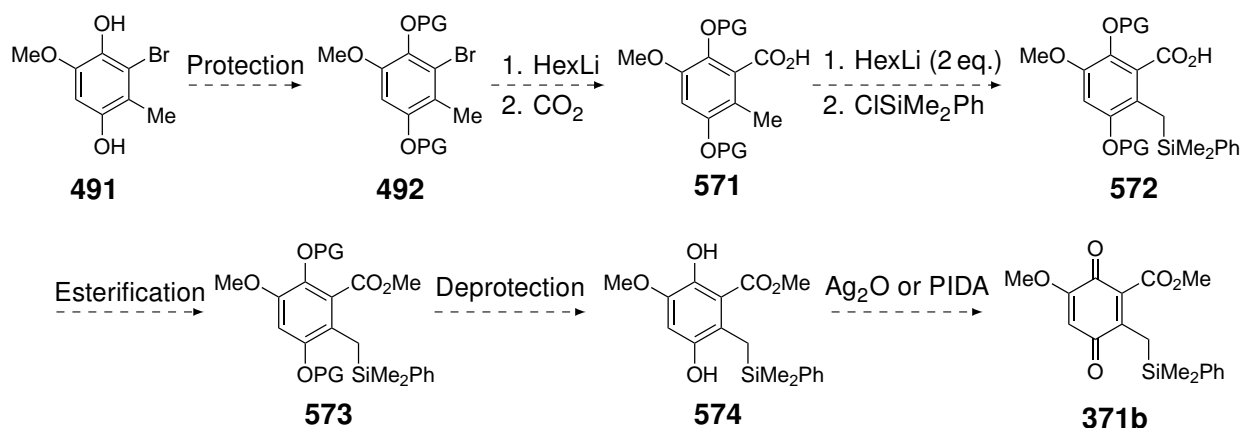
Consequently, the investigation of the protecting groups will be done in order to determine which ones can be inserted on the hydroquinone core and whose removal is compatible with the silyl group.

Scheme 7.8: New proposed pathway for the synthesis of silylated sulfinylquinone **318b**.

Similarly, the same investigation will be done with quinones **369b** and **371b**. For the former, the synthetic pathway will start with the protection of **485** (Scheme 7.9). Then, a bromine-lithium exchange, followed by the addition of (chloromethyl)dimethylphenylsilane will lead to the insertion of the silylated benzylic substituent. Intermediate **569** will later undergo deprotection and oxidation to give the silylated quinone **369b**.

Scheme 7.9: Proposed pathway for the synthesis of silylated quinone **369b**.

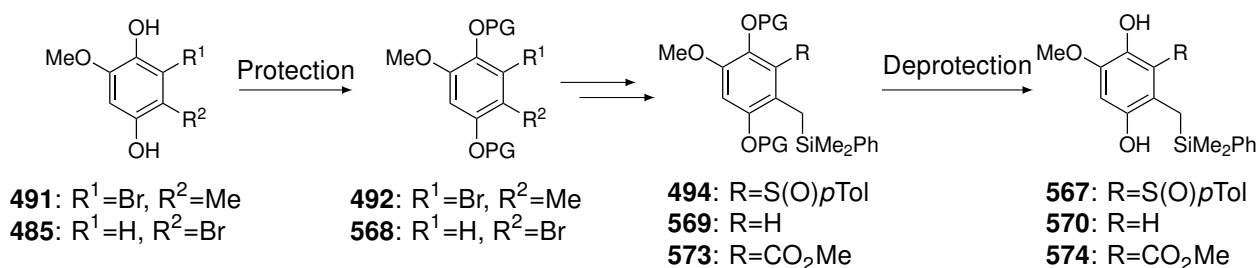
In the case of quinone **371b**, the synthesis will start with the protection of hydroquinone **491**. We will then insert a carboxylic acid by bromine-lithium exchange, followed by the addition of carbon dioxide. A lateral lithiation of benzoic acid **571** will allow the silylation of the benzylic position. The carboxylic acid will then be converted into a methyl ester and the hydroquinone core will be deprotected. The hydroquinone **574** will finally be oxidised into quinone **371b**.

Scheme 7.10: Proposed pathway for the synthesis of silylated quinone **371b**.

However, the synthesis of quinone **371b** might become irrelevant as, on one hand, the presence of a bulky substituent next to the ester group seemed to impair the course of the Evans catalysis and, on the other hand, we designed the new phthalide quinone **534** that could lead to both momilactones A (**1**) and B (**2**). Nevertheless, the synthesis of **371b** will remain interesting as very few examples of quinones bearing a methylsilyl group are reported. We could develop new methods for the synthesis of such compounds and establish the scope of substituents compatible with those methods.

By looking up in the literature, we found some reports on the deprotection of phenols on aromatic compounds bearing a methylsilyl substituent (Table 7.1). They reported the use of MOM^{19,20} and EOM²¹ that were deprotected in acidic media or the use of benzyl groups that were deprotected with thioanisole in TFA.^{22,23}

Table 7.1: Methods of formation and cleavage of potential protecting groups to be tested in the planned sequences for the synthesis of quinone **318b** (Scheme 7.8), **369b** (Scheme 7.9) and **371b** (Scheme 7.10).



PG	Formation	Cleavage
MOM	MOMCl, DIPEA, THF, 0 °C to rt	AcCl, MeOH, rt ¹⁹ TsOH (10 mol %), MeOH, 50 °C ²⁰
EOM	EOMCl, NaOH, BnEt ₃ NCl, THF, 0 °C to rt	PPTS, <i>i</i> PrOH, 70 °C ²¹
Bn	BnCl, K ₂ CO ₃ , DMF, 120 °C	PhSMe, TFA, 55 °C ^{22,23}

7.2.2 Computational study of the sulfinylquinones

A tremendous amount of work was already done on the theoretical study of the preferential conformation of the sulfinylquinones. But, it mainly concerned the effect of the substituents on the quinone core. The effect of the polarity of the solvent was also investigated, albeit implicit solvation was used. It will therefore be interesting to push the study further by performing the same study with an explicit solvation. This study should provide a better understanding of the solvent-sulfinylquinone interactions and how they impact the preferred conformation of the sulfinyl group.

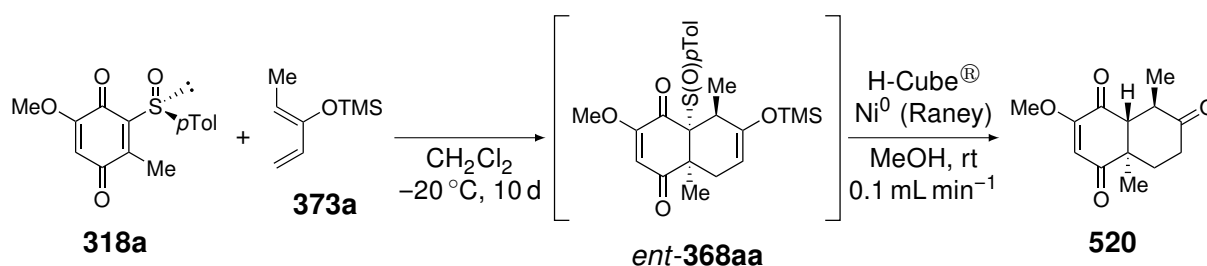
In addition to the theoretical study on the conformation of the sulfinylquinones, it will be of great interest to perform computational studies of the reaction pathways of the Diels-Alder reactions between sulfinylquinone and different dienes. The transition state energies of the reaction of a diene on both the *s*-cis and *s*-trans conformers of the sulfinylquinones will allow us to confirm or infirm the hypothesis that the *s*-cis conformation must be more reactive than the *s*-trans one. Those studies will also give some insights to explain why in some cases an inversion of facial diastereoselectivity is observed with cyclic dienes but not with acyclic ones.

7.2.3 Diels-Alder reactions for the synthesis of momilactones

Some progress on the asymmetric cycloadditions as key step for the total synthesis of momilactones has already been achieved. Nevertheless, all of them still need to be improved.

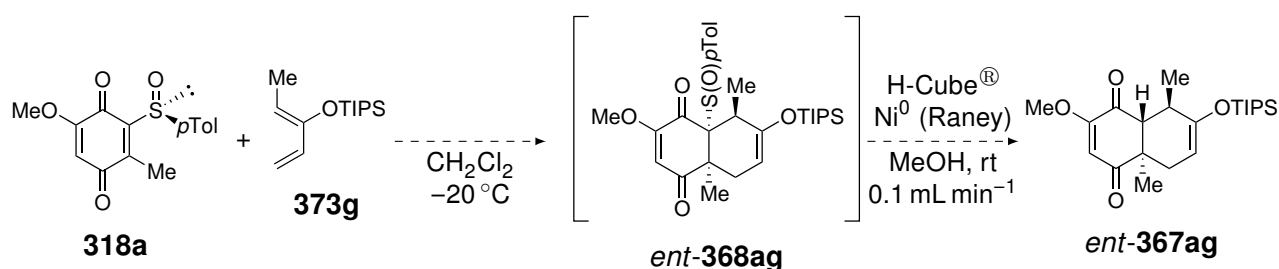
Sulfinylquinone pathway

In the case of sulfinylquinone **318a**, the most promising results were obtained with the oxygenated diene **373a**. As described, the use of H-Cube[®] system to reduce the carbon-sulfur bond, directly on the crude mixture of the cycloadduct *ent*-**368aa**, gave product **520**. Nevertheless, this method did not give satisfying enough results and we will take some interests in improving this method.



Scheme 7.11: Diels-Alder reaction of sulfinylquinone **318a** and diene **373a** and reduction of the adduct *ent*-**368aa** with the H-Cube[®] system.¹³

However, the use of this method with diene **373a**, that bears a trimethylsilyl enol ether, directly led to the desilylation of the cycloadduct. This might complicate the selective reduction of the carbonyl groups as a third one is present on the structure. In order to maintain the silyl enol ether after the Raney nickel reduction, we should test the same procedure with a more robust silyl group, such as a TIPS (diene **373g**).



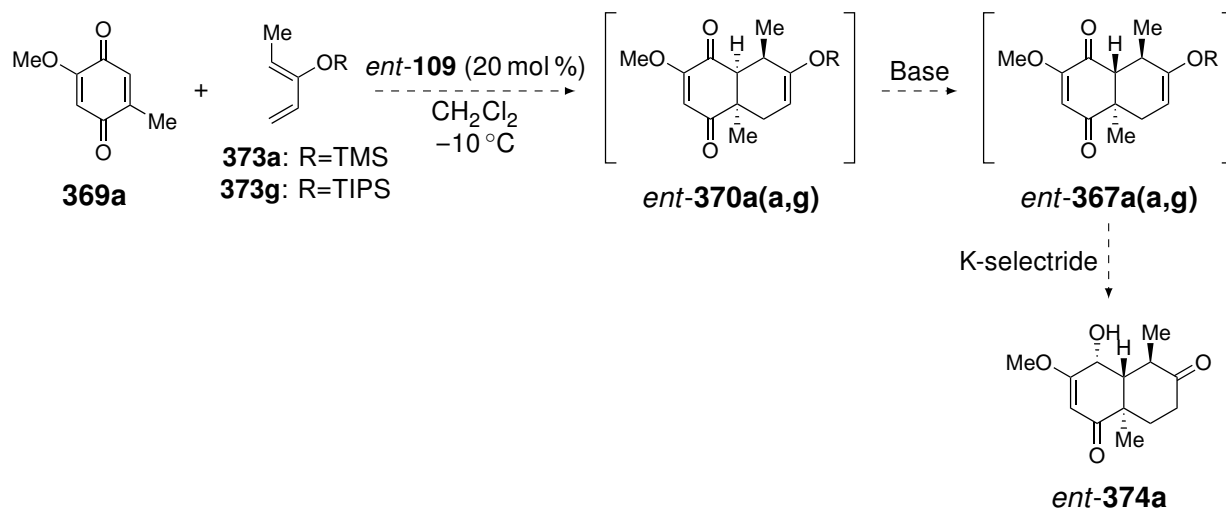
Scheme 7.12: Proposed Diels-Alder reaction of sulfinylquinone **318a** and diene **373g** and reduction of the adduct *ent*-**368ag** with the H-Cube[®] system.

Once triketone **520** or intermediate *ent*-**367ag** is obtained in good yields, the selective reduction of the different carbonyl groups will be studied. As soon as we find the best reagents to carry out the selective reductions, the rest of the synthesis will be continued as described in Chapter 3, including the development of the insertion of the oxidised carbon atom necessary for the lactone ring (Scheme 3.5).

Corey's asymmetric catalysis pathway

Similarly to the sulfinylquinone pathway, the best result we obtained for Corey's asymmetric catalysis was with diene **373a** (Scheme 7.5). But given the instability of the obtained product, we will test

that reaction again but without purifying the cycloadduct *ent*-**370aa**. Instead, the latter will be directly engaged in the epimerisation reaction and the reduction of the carbonyl group with K-selectride, that will likely lead to the cleavage of the silyl enol ether to give compound *ent*-**374a**. The latter will probably be more stable than the two previous intermediates and its analysis (determining the relative and absolute configurations, as well as the enantiomeric excess) will be more easily carried out.



Scheme 7.13: Corey's asymmetric catalysis for the Diels-Alder reactions of sulfanylquinone **369a** with dienes **373a** and **373g** and the next steps to intermediate *ent*-**374a**.

Another solution that we will try is the use of diene **373g** that possesses a TIPS instead of a TMS. Indeed, Corey's group reported the use of a diene bearing such a silyloxy group and the latter did not seem to suffer degradation.^{14,15} In doing so, we will maybe be able to determine the efficiency of Corey's catalysis on cycloadduct *ent*-**370ag** directly.

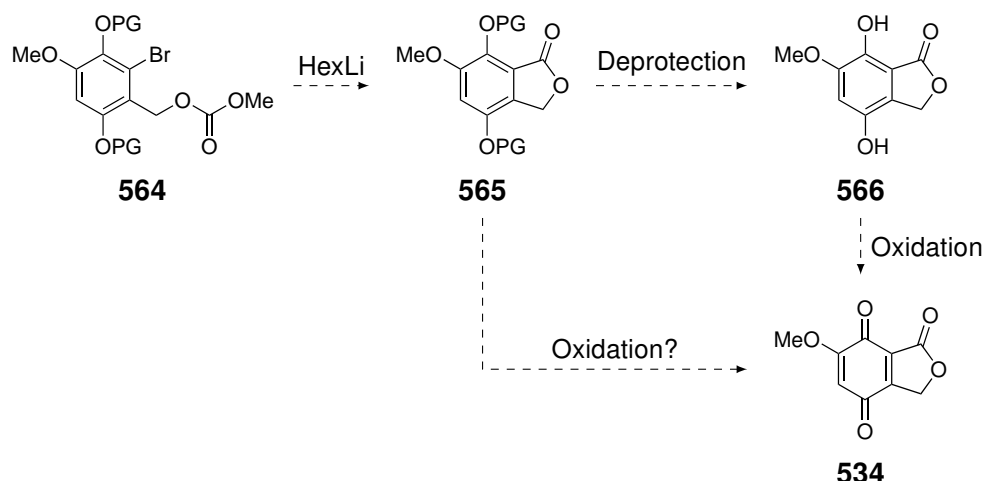
As soon as we optimise the use of Corey's catalysis for the total synthesis of momilactones, the next steps of the sequence planned in Chapter 3 will be followed (Scheme 3.5).

Evans asymmetric catalysis pathway

For this catalytic system, we already ruled out quinone **371a** as a suitable substrate and designed the phthalide quinone **534** as a surrogate. We will finish the synthesis of **534**, first with EOM as protecting groups (Scheme 7.14). We will determine if the oxidation can directly be done on the protected phthalide or if an early deprotection will be needed. In the event the EOM group is not the most appropriate, we will continue the investigation of other protecting groups.

We will then continue with the study of the Diels-Alder reactions of this quinone **534**. First, we will engage the latter in non-catalysed cycloadditions with model dienes and the chosen oxygenated dienes. We will then evaluate the same cycloadditions with achiral Lewis acids, as well as the use of HFIP as solvent. Finally, the Evans asymmetric catalysis will be used and the reactivity, along with the enantioselectivity, of quinone **534** will be assessed.

When we find the appropriate diene and conditions to apply that strategy in the synthesis of momilactones, the sequence proposed in Scheme 6.17 (Chapter 6) will be investigated.

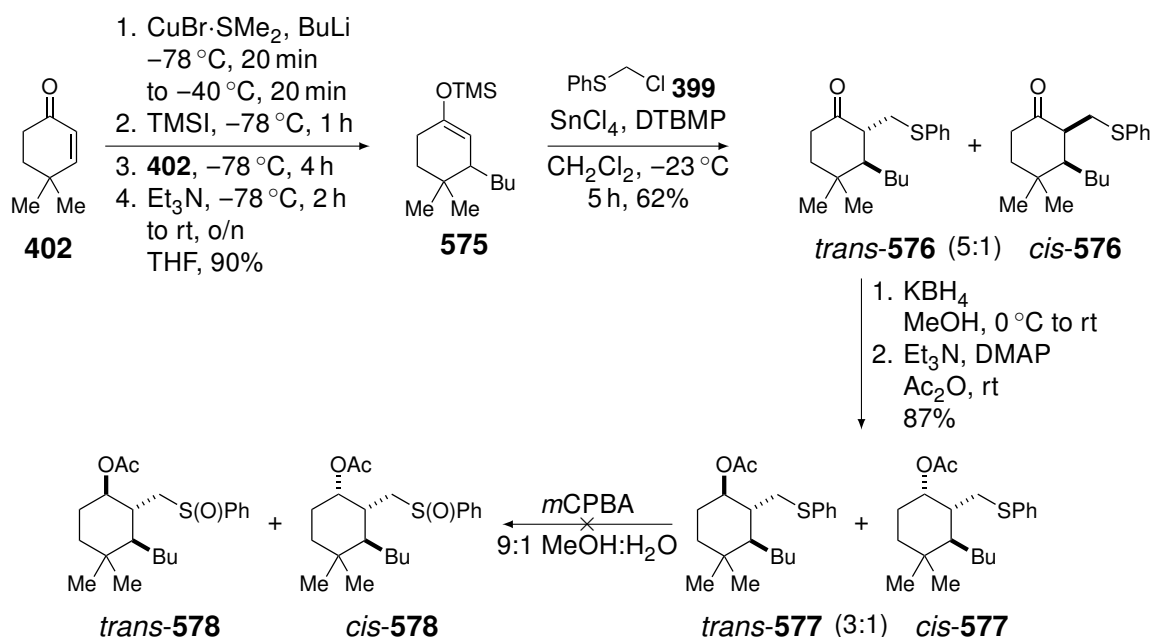


Scheme 7.14: Final steps for the synthesis of the phthalide quinone **534** from the protected phthalide **565**.

Once we find the best combination of the diene and the quinonoid system for the asymmetric Diels-Alder reaction as key step for the synthesis of momilactones, the investigation of the pathway to reach the common intermediate **377a** (Chapter 3, Schemes 3.5 to 3.10) will be pursued.

7.2.4 Model study for the formation of the third cycle of momilactones

The model study for the formation of the third ring of the momilactones was not achieved in this thesis (Chapter 3, Scheme 3.15). Nevertheless, some work was already done in a master thesis in 2014.²⁴ In that work, the student studied the conjugate addition of a butyl chain, as a model substituent for the allyl silyl chain. He started from 4,4-dimethylcyclohex-2-one as model substrate (**402**), to mimic the cyclohexenone part of intermediate **364** (Scheme 3.12), on which he performed the addition of the butyl copper, followed by the trapping of the intermediate enolate by trimethylsilyl iodide.²⁵

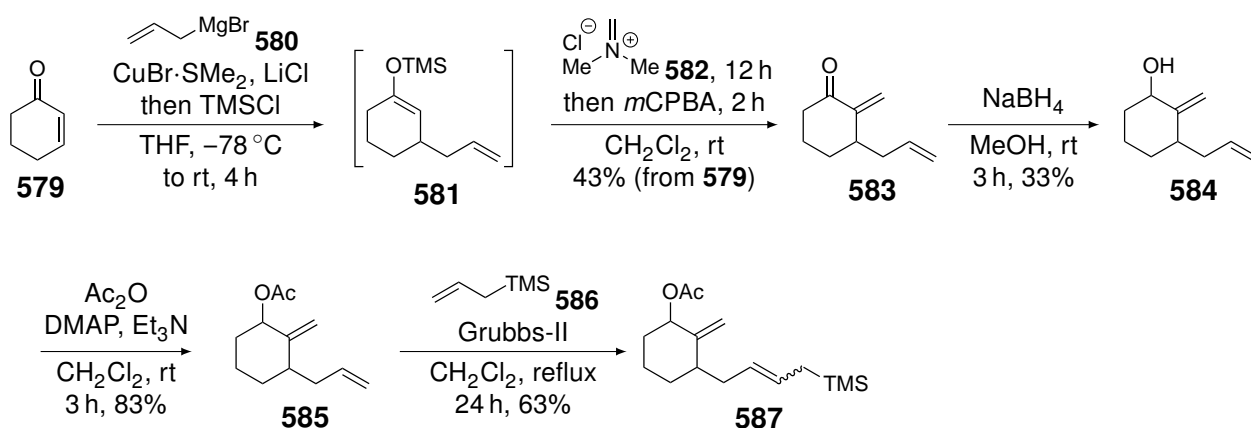


Scheme 7.15: Model study on cyclohexenone **402**, that mimics the cyclohexenone part of precursor **364** (Scheme 3.12), for the 1,4-conjugate addition of an alkyl chain and the formation of the exocyclic double bond.²⁴

Then, he alkylated enolate **575** with sulfide **399**^{26–28} to give cyclohexanone **576** in a 5:1 ratio of the *trans* and *cis* isomers with a 62% yield. On *trans*-**576**, a reduction with KBH_4 , followed by the acetylation of the resulting alcohol gave intermediate **577** in a 3:1 ratio of the 1,2-*trans*-**577** and 1,2-*cis*-**577** with a 87% yield. Finally, oxidation of the sulfide into the corresponding sulfoxide **578**, on the mixture of isomers of **577**, was attempted with *m*CPBA.^{28,29} Unfortunately, the oxidation did not stop to the sulfoxide but went on to the sulfone. The pyrolysis process, that would have led to the formation of the exocyclic double bond, could therefore not take place.

A few years later, a post-doctoral researcher at the École européenne de chimie, polymères et matériaux (ECPM, University of Strasbourg, France) worked on the same model study.³⁰ For the attempts on the Tsuji-Trost type reaction, he prepared three substrates.

He synthesised the first substrate **587** from the simpler cyclohexenone **579** on which the 1,4-conjugate addition of an allyl cuprate, prepared from allylmagnesium bromide (**580**), was performed, followed by the trapping of the enolate with TMSCl (Scheme 7.16).³¹ The intermediate enolate **581** underwent a nucleophilic addition on Eschenmoser's salt **582** and a subsequent oxidation with *m*CPBA led to the formation of the desired exocyclic double bond.^{32,33}



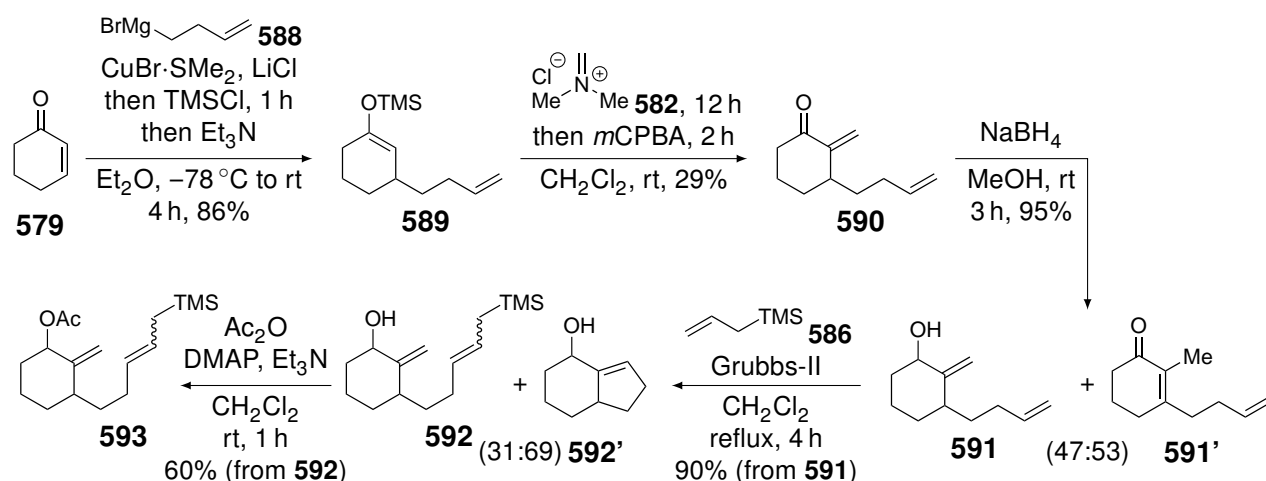
Scheme 7.16: Preparation of precursor **587** for the test of the Tsuji-Trost type annelation.³⁰

Enone **583** was then reduced into the allylic alcohol **584** with NaBH_4 . The alcohol was then acetylated and the cross-metathesis of intermediate **585** and allyl silane **586** led to substrate **587**.³⁴

With this substrate **587**, the carbocyclisation in the conditions of a Tsuji-Trost type reaction will lead to the formation of a five membered ring.

He then prepared substrate **593** following the same synthetic route. In this case, butenylmagnesium bromide **588**, generated *in situ*, was converted into the corresponding cuprate for its 1,4-conjugate addition on **579** (Scheme 7.17). As an additional carbon atom is present in the alkyl chain, the carbocyclisation will lead to the six membered ring.

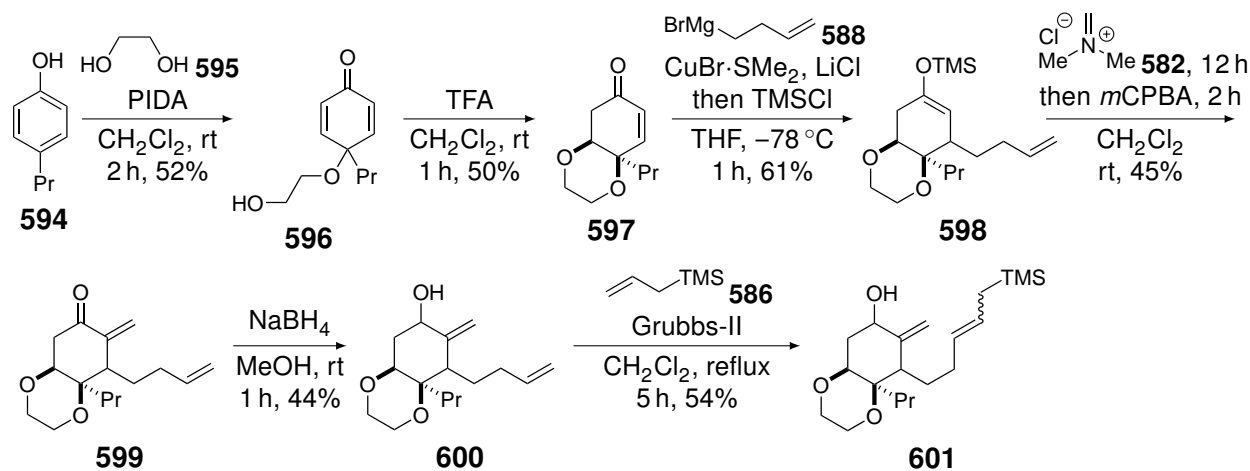
The rest of the synthesis was similar to the one presented in Scheme 7.16. However, he encountered some drawbacks during the reduction of enone **590** and obtained a 47:53 mixture of the allylic alcohol **591** and the isomerisation product **591'**. The cross-metathesis of **591** and allyl silane **586** also led to the RCM, giving **592'** in majority. Nevertheless, he could isolate the desired intermediate **592** that was engaged in an acetylation of the alcohol to reach substrate **593**.



Scheme 7.17: Preparation of precursor **593** for the test of the Tsuji-Trost type annelation.³⁰

Finally, the more complex substrate **601** was prepared from 4-propylphenol (**594**) that first underwent an oxidative dearomatisation with PIDA and ethylene glycol (**595**) (Scheme 7.18).³⁵ The cyclisation of the remaining alcohol on the quinonoid core led to intermediate **597**.³⁶

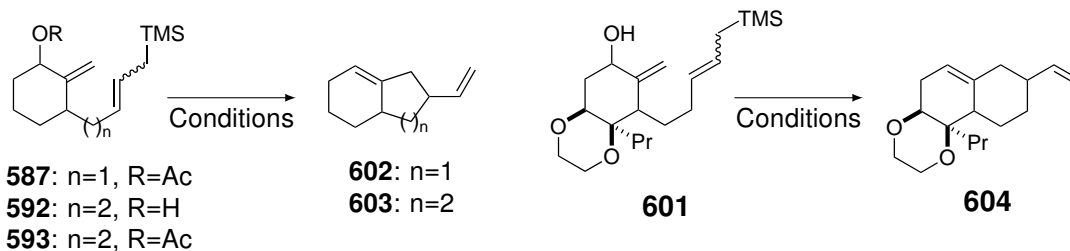
This cyclohexenone **597** was then submitted to the same synthetic pathway presented in Scheme 7.17 but, in this case, no undesired products were obtained in the reduction and the cross-coupling metathesis steps.



Scheme 7.18: Preparation of precursor **601** for the test of the Tsuji-Trost type annelation.³⁰

He then conducted the study on the intramolecular annelation with the different synthesised substrates **587**, **592**, **593** and **601** (Table 7.2). In the case of **587**, that would lead to the five membered ring **602**, he could not make any conditions work, whether with Lewis acids (entries 1 and 2),³⁷ a Brønsted acid (Tf_2NH , entry 3) or Bäckvall's conditions (entry 4).³⁸

He then moved on to the allylic alcohol **592**. The use of a palladium catalyst did not make the cyclisation work (entries 5 and 6). He decided to employ the catalytic system reported by Carreira for the carbocyclisation of allylic alcohols.³⁹ No reaction occurred in those conditions (entry 7) but when he replaced zinc triflate by scandium triflate (entry 8), the cyclisation product **603** was observed by NMR and gas chromatography. The use of $\text{BF}_3 \cdot \text{OEt}_2$ (entry 10) also seemed to lead to the same product but it was confirmed by GC only.

Table 7.2: Screening of conditions for the Tsuji-Trost type reaction with substrates **587**, **592**, **593** and **601**.³⁰

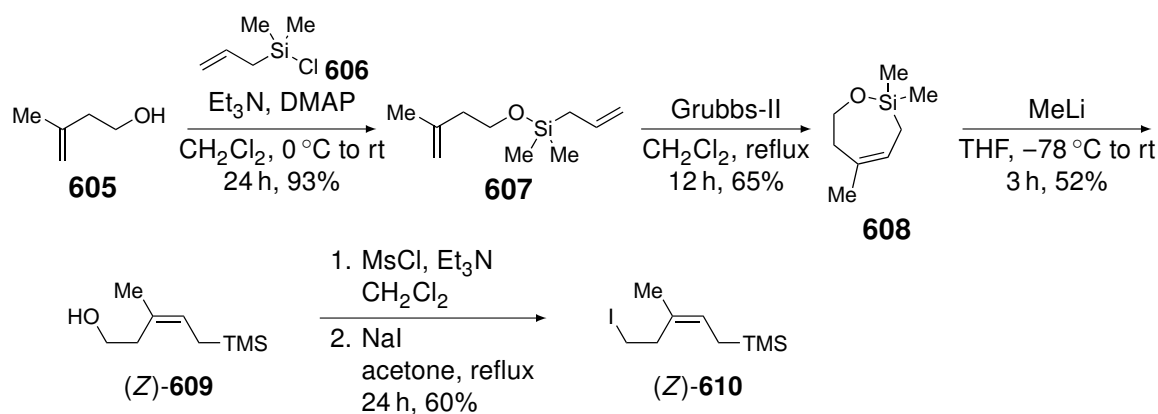
Entry	Substrate	Reagents	Solvent	Temp. (°C)	Time (h)	Result
1	587	BF ₃ ·OEt ₂ ³⁷	CH ₂ Cl ₂	rt	1	n.r.
2	587	SnCl ₄ ³⁷	CH ₂ Cl ₂	rt	1	n.r.
3	587	Tf ₂ NH	CH ₂ Cl ₂	rt	1	n.r.
4	587	PdCl ₂ (MeCN) ₂ , BQ, K ₂ CO ₃ ³⁸	acetone	rt	24	n.r.
5	592	Pd(OAc) ₂ , CsF	MeCN	rt	12	n.r.
6	592	Pd(OAc) ₂ , TBAF	THF	rt	12	n.r.
7	592	(Ir(cod)Cl) ₂ , Ligand, Zn(OTf) ₂ ³⁹	DCE	rt to reflux	36	n.r.
8	592	(Ir(cod)Cl) ₂ , Ligand, Sc(OTf) ₃	DCE	rt to reflux	36	Confirmed by NMR, GC
9	592	TBAF	THF	rt	12	Mixture
10	592	BF ₃ ·OEt ₂ ³⁷	CH ₂ Cl ₂	rt	1	Confirmed by GC only
11	593	Pd(PPh ₃) ₄ , TBAF	THF	60	24	Mixture of cyclised and desilylated products
12	593	Pd(PPh ₃) ₄ , DBU	PhMe	80	24	n.r.
13	593	Pd(PPh ₃) ₄ , DPEPhos, then TBAF	PhMe	rt	24/24	desilylation
14	601	(Ir(cod)Cl) ₂ , Ligand, Sc(OTf) ₃	DCE	reflux	3	Proto-desilylation

n.r. = no reaction

When he tried the same transformation with the acetylated **593**, the use of a palladium catalyst led to a mixture of cyclised and desilylated product (entry 11), no reaction at all (entry 12) or desilylation only (entry 13).

A last test was carried out on substrate **601** using the modified Carreira's conditions (entry 14). Contrariwise to **592**, no annelation reaction was observed and only the protodesilylation of **601** was obtained.

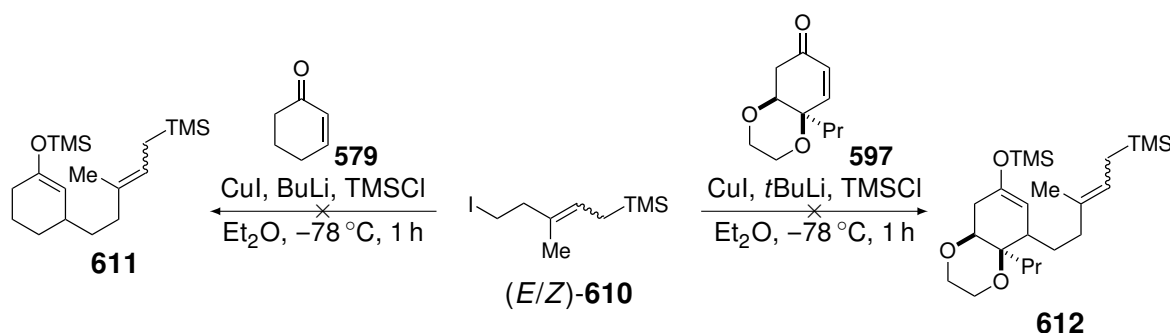
Besides the investigation of the preparation of the substrates bearing an exocyclic double bond and an allyl silane chain, that work also reported the stereoselective synthesis of *Z*-**610** (Scheme 7.19). That synthesis, whose first steps were already described,³⁴ started from isoprenol (**605**) that underwent a silylation reaction, followed by a RCM. Oxasilepine **608** was then opened by the nu-



Scheme 7.19: Stereoselective preparation of the iodide precursor (*Z*)-**610** that will be used to insert the allyl silyl chain planned in the total synthesis of momilactones.³⁰

cleophilic attack of methyllithium. The comparison of experimental data with the reported values confirmed the *Z* configuration of alcohol **609**. Finally, the alcohol was converted into the desired iodide (*Z*)-**610**.

The last part of that project focused on the 1,4-conjugate addition of the cuprate derivative of the allyl silane chain **610** on cyclohexenone substrates (Scheme 7.20). For those tests, a *E/Z* mixture of **610** (prepared *via* another pathway) was used and transformed into the corresponding cuprate *in situ*. Unfortunately, such an addition on cyclohexenones **579** and **597** did not give rise to any reactions.



Scheme 7.20: Attempts towards the 1,4-conjugate addition of the organolithium reagent derived from (*E/Z*)-**610** on hexenones **579** and **597**.³⁰

As a perspective for the model study of the carbocyclisation of the third cycle of momilactones, the conditions of the conjugate addition of the allyl silane chain on the cyclohexenone and the Tsuji-Trost type reaction must be optimised in order to propose a suitable method for the total synthesis of momilactones.

Moreover, it was proposed to prepare various *O*- and *C*-substituted cyclohexenone derivatives in the aim to determine the scope of the carbocyclisation. Indeed, this transformation could be used in many other total syntheses and not only momilactones.

7.2.5 Total synthesis of momilactones

Once we find the best conditions and partners for the asymmetric Diels-Alder reaction, in the course of the total synthesis of momilactones, investigation on the next steps will be undertaken as described in Chapter 3 (Schemes 3.5 to 3.10), until the common intermediate **364** is reached.

Similarly, when the optimisation of the carbocyclisation method is complete, the last steps of the total synthesis (Scheme 3.12) will be carried out with the method developed on the cyclohexenone substrates.

An additional perspective to the total synthesis of momilactones A (**1**) and B (**2**) will be the preparation of analogues of those two natural substances by en route insertions of other functional groups. The synthesis of such analogues will allow, on one hand, SAR studies in order to evaluate the mode of action of those metabolites and, on the other hand, the development of potential new drugs with a better activity than that the natural momilactones.

The journey is not over yet...

In the course of this thesis, we have explored several domains of the organic chemistry. The initial path that was planned was indeed strewn with pitfalls and many detours have been taken. But those detours were worth the effort as they forced us to be imaginative in order to overcome the problems encountered. We have therefore developed new synthetic pathways and methods, some by serendipity, and obtained many new compounds of interest, from simple to complex or even exotic.

Nevertheless, this project is far from over. Although we succeeded in synthesising compounds of interest and answered questions we were asking ourselves, we also have discovered new challenges and opened doors to new projects, whether they were related to momilactones or not. A lot of work has been done in this thesis and we have learned a great deal from the successes and the setbacks, but the road is not at an end and we have prepared the path for the next generation to work on this most challenging project.

References

- [1] Ackland, D. J.; Pinhey, J. T. The Chemistry of Aryl-lead(IV) Tricarboxylates. Reaction with Vinylogous β -Keto Esters. *J. Chem. Soc., Perkin Trans. 1* **1987**, 2689–2694.
- [2] Gebauer, J.; Blechert, S. Synthesis of γ,δ -Unsaturated- β -keto Lactones via Sequential Cross Metathesis-Lactonization: A Facile Entry to Macrolide Antibiotic (–)-A26771B. *J. Org. Chem.* **2006**, *71*, 2021–2025.
- [3] Rabe, P.; Klapschinski, T. A.; Brock, N. L.; Citron, C. A.; D'Alvise, P.; Gram, L.; Dickschat, J. S. Synthesis and bioactivity of analogues of the marine antibiotic tropodithietic acid. *Beilstein J. Org. Chem.* **2014**, *10*, 1796–1801.
- [4] Effenberger, F.; Ziegler, T.; Schönwälder, K.-H. Enoether, XVI. Synthese von 4-Hydroxy-2H-pyran-2-onen. *Chem. Ber.* **1985**, *118*, 741–752.
- [5] Effenberger, F.; Ziegler, T. Diels-Alder-Reaktionen mit 2H-Pyran-2-onen: Reaktivität und Selektivität. *Chem. Ber.* **1987**, *120*, 1339–1346.
- [6] Deneffe, B. Étude de la réactivité du 4-hydroxy-5-thiométhylènebuténolide dans des réactions de couplages organométalliques. M.Sc. thesis, Université de Namur, Belgium, 2021.
- [7] Lanfranchi, D. A.; Hanquet, G. Asymmetric Diels-Alder Reactions of a New Enantiomerically Pure Sulfinylquinone: A Straightforward Access to Functionalized Wieland-Miescher Ketone Analogues with (*R*) Absolute Configuration. *J. Org. Chem.* **2006**, *71*, 4854–4861.
- [8] Lanfranchi, D. A. Vers la synthèse totale de la salvinorine A et d'analogues structuraux. Ph.D. thesis, Université Louis Pasteur, Strasbourg, France, 2006.
- [9] Carreño, M. C.; García Ruano, J. L.; Urbano, A. Synthesis of Optically Active *p*-Tolylsulfinylquinones. *Synthesis* **1992**, 651–653.
- [10] Carreño, M. C.; García Ruano, J. L.; Toledo, M. A.; Urbano, A. Synthesis and Diels-Alder reactions of (*S*)-3-Chloro and (*S*)-3-Ethyl-2-*p*-tolylsulfinyl-1,4-benzoquinones. *Tetrahedron Lett.* **1994**, *35*, 9759–9762.
- [11] Carreño, M. C.; García Ruano, J. L.; Urbano, A. Asymmetric Diels-Alder Reactions of (*S*)-2-(*p*-Tolylsulfinyl)-1,4-naphthoquinones. *J. Org. Chem.* **1992**, *57*, 6870–6876.
- [12] Mambourg, K. Étude de la réaction de Diels-Alder utilisant une sulfinylquinone chirale comme diénophile et développement d'un modèle expliquant la stéréosélectivité. M.Sc. thesis, Université de Namur, Belgium, 2018.
- [13] Colas, L. Contribution à la synthèse totale de la momilactone A. Master internship at the Laboratoire de Chimie Organique de Synthèse, Faculté Universitaire Notre-Dame de la Paix, Namur, Belgium, 2010.
- [14] Ryu, D. H.; Corey, E. J. Triflimide Activation of a Chiral Oxazaborolidine Leads to a More General Catalytic System for Enantioselective Diels-Alder Addition. *J. Am. Chem. Soc.* **2003**, *125*, 6388–6390.
- [15] Ryu, D. H.; Zhou, G.; Corey, E. J. Enantioselective and Structure-Selective Diels-Alder Reactions of Unsymmetrical Quinones Catalyzed by a Chiral Oxazaborolidine Cation. Predictive Selection Rules. *J. Am. Chem. Soc.* **2004**, *126*, 4800–4802.
- [16] Evans, D. A.; Wu, J. Enantioselective Rare-Earth Catalyzed Quinone Diels-Alder Reactions. *J. Am. Chem. Soc.* **2003**, *125*, 10162–10163.
- [17] Traina, A. Catalytic asymmetric Diels-Alder reaction of a phthalide quinone. M.Sc. thesis, Université de Namur, Belgium, 2021–2022.
- [18] Taing, M.; Moore, H. W. *o*-Quinone Methides from 4-Alkenylcyclobutenones: Synthesis and Chemistry. *J. Org. Chem.* **1996**, *61*, 329–340.
- [19] Feldman, K. S.; Selfridge, B. R. Exploration of Braverman reaction chemistry. Synthesis of tricyclic dihydrothiophene dioxide derivatives from bispropargyl sulfones. *Heterocycles* **2010**, *81*, 117–143.
- [20] Uyanik, M.; Mutsuga, T.; Ishihara, K. 4,5-Dimethyl-2-Iodoxybenzenesulfonic Acid Catalyzed Site-Selective Oxidation of 2-Substituted Phenols to 1,2-Quinols. *Angew. Chem. Int. Ed.* **2017**, *56*, 3956–3960.
- [21] Yang, H.; Liu, Z.; Zhang, W. Multidentate Triphenolsilane-Based Alkyne Metathesis Catalysts. *Adv. Synth. Catal.* **2013**, *355*, 885–890.
- [22] Curran, D. P.; Du, W. Palladium-Promoted Cascade Reactions of Isonitriles and 6-Iodo-*N*-propargylpyridones: Synthesis of Mappicines, Camptothecins, and Homocamptothecins. *Org. Lett.* **2002**, *4*, 3215–3218.
- [23] Curran, D. P.; Du, W. Synthesis of polycyclic quinolines. WO 03/099825 A1. Dec. 4, 2003.
- [24] Pirenne, V. Vers la synthèse totale de la momilactone A. M.Sc. thesis, Université de Namur, Belgium, 2014.
- [25] Bergdhal, M.; Eriksson, M.; Nilsson, M.; Olsson, T. Iodotrimethylsilane-Promoted Additions of Monoorganocopper Compounds to α/β -Unsaturated Ketones, Esters, and Lactones. *J. Org. Chem.* **1993**, *58*, 7238–7244.
- [26] Paterson, I.; Fleming, I. Regiospecific α -methylenation and α -methylation of ketones: titanium tetrachloride promoted phenylthiomethylation of silyl enol ethers. *Tetrahedron Lett.* **1979**, 995–998.
- [27] Paterson, I.; Fleming, I. α -Alkylation and α -alkylidenation of carbonyl compounds: Lewis acid-promoted phenylthioalkylation of *O*-silylated enolates. *Tetrahedron Lett.* **1979**, 2179–2182.

- [28] Paterson, I. α -Alkylation and α -alkylidenation of carbonyl compounds by *O*-silylated enolate phenylthioalkylation. *Tetrahedron* **1988**, *44*, 4207–4219.
- [29] Ekhatov, I. V.; Silverton, J. V.; Robinson, C. H. An Unusual Stereochemical Outcome of a Peroxyacid Epoxydation Reaction: Stereospecific Synthesis of (4'*R*)-Spiro[oxirane-2,4'-5' α -cholestan-3' β -ol]. *J. Org. Chem.* **1988**, 2180–2183.
- [30] Nomula, R., Dr. Total Synthesis of Momilactones A and B. Scientific report, ECPM, Université de Strasbourg, France, 2019.
- [31] Waske, P. A.; Mattay, J. Synthesis of cyclopropyl silyl ethers and their facile ring opening by photoinduced electron transfer as key step in radical/radical cationic cascade reactions. *Tetrahedron* **2005**, *61*, 10321–10330.
- [32] Dauben, W. G.; Chollet, A. Acid catalyzed Cope rearrangement of 2-actl-1,5-dienes. *Tetrahedron Lett.* **1981**, *22*, 1583–1586.
- [33] Danishefsky, S. J.; Kahn, M.; Silvestri, M. An anomalous Mannich reaction of a trimethylsilyl enol ether. *Tetrahedron Lett.* **1982**, *23*, 1419–1422.
- [34] Tredwell, M.; Luft, J. A. R.; Schuler, M.; Tenza, K.; Houk, K. N.; Gouverneur, V. Fluorine-Directed Diastereoselective Iodocyclizations. *Angew. Chem. Int. Ed.* **2008**, *47*, 357–360.
- [35] Wu, W.; Li, X.; Huang, H.; Yuan, X.; Lu, J.; Zhu, K.; Ye, J. Asymmetric Intramolecular Oxa-Michael Reactions of Cyclohexadienones Catalyzed by a Primary Amine Salt. *Angew. Chem. Int. Ed.* **2013**, *52*, 1743–1747.
- [36] Giroux, M.-A.; Guérard, K. C.; Beaulieu, M.-A.; Sabot, C.; Canesi, S. Alternative Coupling Reaction with Unactivated Furan Derivatives. *Eur. J. Org. Chem.* **2009**, 3871–3874.
- [37] Rodgen, S. A.; Schaus, S. E. Efficient Construction of the Clerodane Decalin Core by an Asymmetric Morita–Baylis–Hillman Reaction/Lewis Acid Promoted Annulation Strategy. *Angew. Chem. Int. Ed.* **2006**, *45*, 4929–4932.
- [38] Castaño, A. M.; Persson, B. A.; Bäckvall, J.-E. Allylsilanes as Carbon Nucleophiles in the Palladium-Catalyzed 1,4-Oxidation of Conjugated Dienes. *Chem. Eur. J.* **1997**, *3*, 482–490.
- [39] Jeker, O. F.; Kravina, A. G.; Carreira, E. M. Total Synthesis of (+)-Asperolide C by Iridium-Catalyzed Enantioselective Polyene Cyclization. *Angew. Chem. Int. Ed.* **2013**, *52*, 12166–12169.

Part III

Experimental section

Chapter 8

Experimental

8 Experimental

8.1 General methods

8.1.1 Reagents, solvents and handling of the reactions

Reagents

Reagents were purchased as reagent grade from Merck (previously Sigma-Aldrich),¹ fluorochem,² TCI,³ Carbosynth,⁴ Fisher Scientific,⁵ or J&K Scientific⁶ and were used without further purification, unless indicated in the list below.

- 1,4-Benzoquinone: benzoquinone was recrystallised from boiling 95% ethanol and was stored away from light.⁷
- Cyclopentadiene: dicyclopentadiene was cracked ($\pm 150\text{ }^{\circ}\text{C}$) and cyclopentadiene was distilled ($\pm 45\text{ }^{\circ}\text{C}$ at atmospheric pressure) before use.⁷
- Diisopropylamine: DIPA was distilled from NaOH ($84\text{ }^{\circ}\text{C}$ at atmospheric pressure) and was stored in the fridge under argon atmosphere.⁷
- Sodium *para*-toluenesulfinate: sodium *para*-toluenesulfinate was dried in a Dean-Stark apparatus by azeotropic distillation with toluene for two days.⁸ The salt was filtered off, rinse with pentane and vacuum dried.
- Trimethylsilyl chloride: TMSCl was distilled from CaH_2 under argon atmosphere before use ($57\text{ }^{\circ}\text{C}$ at atmospheric pressure).⁷

Organolithium reagents were titrated using the Suffert's method with *N*-pivaloyl-*o*-benzylaniline as titrating agent.⁹

Solvents

Solvents were purchased from Fisher Scientific.⁵ Technical grade solvents (treatments and chromatography) were distilled and stored in dedicated 5 L glass bottles.

Toluene, diethyl ether, THF and dichloromethane were purified and dried using a MBraun SPS Compact solvent purification system when they were used for water sensitive reactions.

Absolute ethanol, methanol, isopropanol, acetone, acetonitrile, chloroform, hexane and acetic acid were purchased at reagent or analytical grade and used without further purification.

Deionised water was used as solvent and for the aqueous work-ups.

Deuterated solvents were purchased from Eurisotop.¹⁰

General procedures

All water sensitive reactions were carried out under dry argon atmosphere in heatgun-dried glassware. The introduction of the reagents in the liquid state (physical state of the reagent at room

temperature or in solution) was done with a syringe through a rubber stopper. The addition of solid reagents (if their introduction cannot be done before setting the inert atmosphere) was done by opening of the stopper with a light flux of argon gas. All reactions were magnetically stirred and monitored by thin layer chromatography (TLC) or NMR.

Cooled reactions were carried out using the following techniques:

- 0 °C: ice and water bath;
- -10 °C: ice mixed with sodium chloride and diluted with water until -10 °C was reached (or freezer set to -10 °C for long reaction times);
- -20 °C: ice mixed with sodium chloride (or in a freezer set to -20 °C for long reaction times);
- -78 °C: dry ice and acetone bath.

Microdistillation were performed using a Büchi GKR-50 bulb-to-bulb glass oven . Distillation under reduced pressure were performed by connecting the distillation set up to a vacuum pump PC 3001 VARIO pro (vacuubrand) with pressure control.

8.1.2 Chromatography

Thin layer chromatography

Thin layer chromatography (TLC) was performed on alumina sheets coated with silica gel 60 F₂₅₄ from Merck. The eluant for the TLC is indicated between parentheses and mixtures of solvents are given in volume/volume ratio.

After elution, the TLC plate was analysed under UV light at 254 nm, then by chemical stain followed by heating. The solutions for the chemical stain technique are:

- *p*-anisaldehyde: 3.7 mL of *para*-anisaldehyde, 1.1 mL of acetic acid and 3.7 mL of H₂SO₄ in 100 mL of absolute ethanol;
- KMnO₄: 3 g of KMnO₄, 20 g of K₂CO₄ and 5 mL of an 5% aqueous solution of NaOH in 300 mL of water.

The retention factor (R_f) of each spot was determined by dividing the distance the product traveled by the distance the solvent front traveled using the initial spotting site as reference.

Column chromatography

Flash (column) chromatography was performed under pressure of compressed air and on silica gel from 60 Merck (230-400 mesh, 0.040-0.063 mm).

Demetallated silica gel was prepared according to a reported procedure: silica gel was treated with a 10% aqueous hydrochloric bath and by stirring the mixture every half an hour for a day. The silica gel was then decanted, the supernatant was evacuated, and the remaining solution was diluted with water. The last step was repeated until the pH of the supernatant was neutral.¹¹

In the case of acid sensitive compounds, the purification by flash chromatography was carried out on silica gel treated with 1% volume of Et₃N during the preparation of the gel and conditioning of the column.¹²

8.1.3 Characterisation

NMR spectroscopy

NMR spectra (^1H and ^{13}C) were recorded on a Jeol JNM 400 MHz or 500 MHz (^1H NMR at 400 MHz or 500 MHz and ^{13}C NMR at 100 MHz or 126 MHz). The samples were prepared in standard quartz tubes (5 mm) in deuterated solvents and in room temperature. Chemical shifts were reported in ppm and calibrated on the chemical shift of the solvent residual peak reported in the table below.¹³

Solvent	δ (ppm) of solvent residual peak	
	^1H NMR	^{13}C NMR
CDCl_3	7.26	77.16
acetone- d_6	2.05	29.84 and 206.26
C_6D_6	7.16	128.06
DMSO- d_6	2.50	39.52
CD_3OD	3.31	49.00

Data for ^1H NMR were reported as (multiplicity, total number of protons, coupling constant(s) in Hz, assignment of the signals) with the following code for the multiplicity: s = singlet, d = doublet, t = triplet, q = quartet, m = multiplet and br = broad. All the ^{13}C NMR spectra were decoupled from the protons.

The assignment of the chemical shifts to the corresponding carbon and hydrogen atoms were done by DEPT analysis, ^1H - ^1H correlations (COSY, n.O.e and NEOSY) and ^1H - ^{13}C correlations (HMQC and HMBC).

Infrared spectroscopy

Infrared (IR) spectra were recorded on a "Spectrum Two" (Perkin Elmer) Fourier transform infrared spectrometer (FT-IR) using the Attenuated Total Reflection (ATR) technique. Wavenumbers ($\bar{\nu}$) were given in cm^{-1} .

Melting point

Melting points of solid compounds were measured with a Büchi Melting Point B-545 apparatus with a gradient of temperature of $10\text{ }^\circ\text{C min}^{-1}$. Samples were introduced inside the device *via* Rotilab[®] open capillary tubes (1.35 mm \times 80 mm). The indicated range of temperatures corresponds to the start of the melting and to the full melting of the compound.

Optical rotation

The specific optical rotations were measured using an MCP200 Polarimeter (Anton Paar) operating the sodium D line with a 1.0 dm long cell. The solutions were prepared using analytical grade solvents. The specific optical rotations of solutions were calculated according the Biot law : $[\alpha]_D^T = 100 \frac{\alpha}{c \cdot l}$

α : measured value by the polarimeter ($^\circ$)

T: temperature of the cell ($20\text{ }^\circ\text{C}$)

c: concentration of the solution (g/100 mL)

l: the length of the cell (1.0 dm);

and are reported as $[\alpha]_D^T$ (concentration, solvent).

High resolution mass spectrometry

HRMS were performed on a Bruker MaXis Impact mass spectrometer Q-TOF by the MaSUN platform of University of Namur. The analytes were dissolved in a suitable solvent at the concentration of 1 mg mL^{-1} and diluted 500 times in a mixture of MeCN/H₂O (50/50). The diluted solutions (200 μL) were delivered to the ESI source by a Harvard syringe pump at flow rate of $180 \mu\text{L min}^{-1}$. ESI conditions were as follows: capillary voltage was set at 4.5 kV; dry nitrogen was used as nebulizing gas at 0.4 bar and as drying gas at 180 °C. ESI-MS were recorded at 1 Hz in the range of 50-3000 m/z. Calibration was performed with ESI-TOF tuning mix from Agilent. Data were processed using Bruker DataAnalysis 4.1 software. The masses found for $[\text{M}+\text{H}]^+$, $[\text{M}+\text{Na}]^+$ or $[\text{M}+\text{K}]^+$ were compared to the calculated values.

X-ray diffraction

Single-crystal X-ray diffraction data were collected using the Oxford Diffraction Gemini R Ultra diffractometer Cu K_{α} , multilayer mirror, Ruby CCD area detector at 295(2) K. Data collection, unit cells determination and data reduction were carried out using CrysAlis PRO software package.¹⁴ Using Olex2¹⁵ and shelXle,¹⁶ the structure was solved with the SHELXT 2015¹⁷ structure solution program by Intrinsic Phasing methods and refined by full-matrix least squares on $|F|^2$ using SHELXL-2018/3.¹⁸ Non-hydrogen atoms were refined anisotropically. Hydrogen atoms, not involved in hydrogen bonding, were placed on calculated positions in riding mode with temperature factors fixed at 1.2 times U_{eq} of the parent carbon atoms (1.5 times for methyl groups). The parameters of the crystals are presented as:

- a, b, c: unit cell lengths (Å)
- α , β , γ : unit cell angles (°)
- V: unit cell volume (Å³)
- Z: number of molecules in the unit cell
- R: Resolution factor (%)
- Flack: Flack parameter

The color codes used to represent the atoms are:

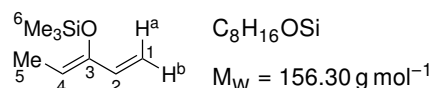
- H: white
- C: grey
- O: red
- S: yellow
- Cl: green
- Br: brown

Determination of the enantiomeric excess

Enantioselectivity was determined by HPLC analysis on an Agilent technologies 1200 Series device with a Daicel Chiralcel[®] OJ column (0.46 cm \times 25 cm). The samples were prepared in isopropanol at a concentration of 1 mg mL^{-1} . The elution was performed with 50% isopropanol in hexane at 0.2 mL min^{-1} and the compounds were detected at 254 nm.

8.2 Synthesis of the dienes

8.2.1 (Z)-Trimethyl(penta-1,3-dien-yloxy)silane (373a)



The title compound was synthesised according to Ackland and Pinhey.¹⁹

In a 50 mL two-neck flask under argon atmosphere and equipped with a condenser, a solution of ethyl vinyl ketone (**407**) (1.4 mL, 14.1 mmol, 1.0 eq.), TMSCl (4.3 mL, 33.9 mmol, 2.4 eq.) and Et₃N (4.7 mL, 33.7 mmol, 2.4 eq.) in 10 mL of DMF was heated up to 80 °C overnight. The mixture was then allowed to cool down to room temperature and the precipitate formed was filtered off. The filtrate was diluted with 20 mL of pentane and washed with a saturated solution of NaHCO₃. The aqueous phase was extracted with pentane. The organic phases were gathered and quickly washed with a 10% solution of HCl, then with saturated solutions of NaHCO₃ and NaCl. The organic phase was dried over Na₂SO₄ and the solvent evaporated. The crude was purified by distillation using a bulb-to-bulb glass oven (50 °C, 30 mbar) to give 1.366 g of the desired Z diene.

Aspect: colourless oil

Yield: 62%

¹H NMR (500 MHz, CDCl₃): δ (ppm) **6.17** (dd, 1H, *J* = 17.1; 10.6 Hz, C²H), **5.24** (d, 1H, *J* = 17.1 Hz, C¹H^a), **4.94** (d, 1H, *J* = 10.6 Hz, C¹H^b), **4.88** (q, 1H, *J* = 7.0 Hz, C⁴H), **1.65** (d, 3H, *J* = 7.0 Hz, C⁵H₃), **0.22** (s, 9H, 3 × C⁶H₃)

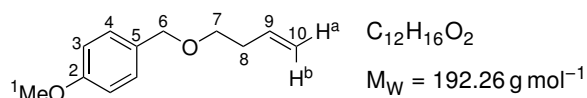
¹³C NMR (126 MHz, CDCl₃): δ (ppm) **149.84** (C³), **135.62** (C²H), **111.53** (C¹H₂), **110.44** (C⁴H), **11.76** (C⁵H₃), **0.77** (3 × C⁶H₃)

IR: $\bar{\nu}$ (cm⁻¹) 1651, 1606, 1251, 1203, 1084, 1051, 1016, 982, 898, 835, 798, 753

The experimental data were in agreement with those of the literature.¹⁹

8.2.2 (Z)-1-Methoxy-4-(((3-methoxypenta-2,4-dien-1-yl)oxy)methyl)benzene (373b)

1-((But-3-en-1-yloxy)methyl)-4-methoxybenzene (409)



The title compound was synthesised according to the procedure of Schrof and Altmann²⁰

in a 250 mL two-neck flask under argon atmosphere, NaH (60%) (4.995 g, 124.9 mmol, 5.4 eq.) was suspended in 100 mL anhydrous DMF and it was cooled down to 0 °C. A solution of but-3-en-1-ol (**408**) (2.0 mL, 23.2 mmol, 1.0 eq.) and PMBCl (5.6 mL, 41.1 mmol, 1.8 eq.) in 20 mL of anhydrous THF was added dropwise to the NaH suspension. The solution was allowed to warm up to room temperature and stirred for 20 h. The solution was then cooled down to 0 °C and quenched with a saturated solution of NH₄Cl. The phases were separated and the aqueous phase was extracted with diethyl ether. The organic phases were gathered and washed with brine, dried over MgSO₄ and the solvents were evaporated. The crude mixture was purified by flash chromatography (cHex/AcOEt: 98/2) to yield 4.442 g of the desired compound.

Aspect: colourless oil

Yield: quantitative

TLC: $R_f \approx 0.65$ (cHex/AcOEt: 8/2), visualised by UV and *p*-anisaldehyde

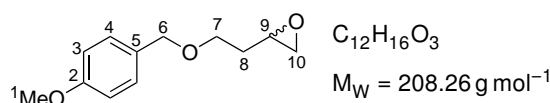
$^1\text{H NMR}$ (500 MHz, CDCl_3): δ (ppm) **7.27** (d, 2H, $J = 8.6$ Hz, C^4H), **6.88** (d, 2H, $J = 8.6$ Hz, C^3H), **5.83** (ddt, 1H, $J = 17.1; 10.3; 6.8$ Hz, C^9H), **5.10** (ddt, 1H, $J = 17.1, 1.5, 1.5$ Hz, C^{10}H^a), **5.04** (m, 1H, C^{10}H^b), **4.45** (s, 2H, C^6H_2), **3.81** (s, 3H, C^1H_3), **3.50** (t, 2H, $J = 6.8$ Hz, C^7H_2), **2.37** (tddd, 2H, $J = 6.8, 6.8, 1.5, 1.5$ Hz, C^8H_2)

$^{13}\text{C NMR}$ (126 MHz, CDCl_3): δ (ppm) **159.26** (C_q^2), **135.46** (C^9H), **130.66** (C_q^5), **129.42** ($2 \times \text{C}^4\text{H}$), **116.46** (C^{10}H_2), **113.88** ($2 \times \text{C}^3\text{H}$), **72.69** (C^6H_2), **69.42** (C^7H_2), **55.41** (C^1H_3), **34.38** (C^8H_2)

IR: $\bar{\nu}$ (cm^{-1}) 1612, 1512, 1245, 1092, 1034, 819

The experimental data were in agreement with those reported in the literature.²⁰

2-(2-((4-Methoxybenzyl)oxy)ethyl)oxirane (410)



The title compound as synthesised according to Gupta and Kumar.²¹

To a solution of alkene **409** (2.007 g, 10.4 mmol, 1.0 eq.) in 20 mL of dichloromethane cooled down to 0°C was added *m*CPBA (70%) (3.110 g, 12.6 mmol, 1.2 eq.). The solution was allowed to warm up to room temperature and stirred for 24 h. The solution was filtered off to remove the precipitate and the cake was washed with dichloromethane. The organic phase was washed with saturated solutions of $\text{Na}_2\text{S}_2\text{O}_3$, NaHCO_3 and brine. It was then dried over Na_2SO_4 and the solvent was evaporated. The crude oil was purified by flash chromatography (cHex/AcOEt: 95/5) to yield 1.662 g of the desired epoxide.

Aspect: colourless oil

Yield: 76%

TLC: $R_f \approx 0.33$ (cHex/AcOEt: 8/2), visualised by UV and *p*-anisaldehyde

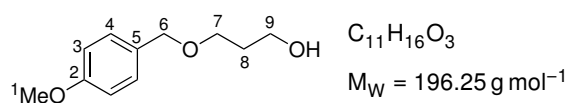
$^1\text{H NMR}$ (500 MHz, CDCl_3): δ (ppm) **7.27** (d, 2H, $J = 8.6$ Hz, $2 \times \text{C}^4\text{H}$), **6.88** (d, 2H, $J = 8.6$ Hz, $2 \times \text{C}^3\text{H}$), **4.46** (s, 2H, C^6H_2), **3.81** (s, 3H, C^1H_3), **3.62-3.64** (m, 2H, C^7H_2), **3.10-3.01** (m, 1H, C^9H), **2.78** (dd, 1H, $J = 5.0, 4.1$ Hz, $\frac{1}{2} \times \text{C}^{10}\text{H}_2$), **2.52** (dd, 1H, $J = 5.0, 2.7$ Hz, $\frac{1}{2} \times \text{C}^{10}\text{H}_2$), **1.93-1.71** (m, 2H, C^8H_2)

$^{13}\text{C NMR}$ (126 MHz, CDCl_3): δ (ppm) **159.31** (C_q^2), **130.46** (C_q^5), **129.42** ($2 \times \text{C}^4\text{H}$), **113.92** ($22 \times \text{C}^3\text{H}$), **72.91** (C^6H_2), **66.86** (C^7H_2), **55.42** (C^1H_3), **50.26** (C^9H), **47.28** (C^{10}H_2), **33.09** (C^8H_2)

IR: $\bar{\nu}$ (cm^{-1}) 1512, 1244, 1087, 1032, 819

The experimental data were in agreement with those reported in the literature.²¹

3-((4-Methoxybenzyl)oxy)propan-1-ol (412)



The title compound was synthesised according to a modified procedure of Mohapatra *et al.*²²

A solution of 1,3-propanediol (**411**) (10.843 g, 142.5 mmol, 5.1 eq.), PMBOH (3.898 g, 28.2 mmol, 1.0 eq.) and Amberlyst-A15 (1.010 g) in 75 mL of dichloromethane was refluxed overnight. The mix-

ture was filtered and the solid washed with dichloromethane. The organic phase was washed with water and brine, then dried over Na_2SO_4 . The solvent was evaporated and the crude was purified by flash chromatography (cHex/AcOEt: 8/2 to 6/4) to yield 4.418 g of desired compound.

Aspect: colourless oil

Yield: 80%

TLC: $R_f \approx 0.12$ (cHex/AcOEt: 7/3), visualised by UV and *p*-anisaldehyde

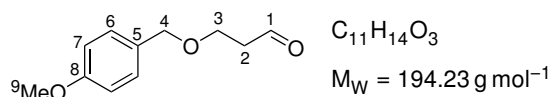
$^1\text{H NMR}$ (500 MHz, CDCl_3): δ (ppm) **7.25** (d, 2H, $J = 8.8$ Hz, $2 \times \text{C}^4\text{H}$), **6.88** (d, 2H, $J = 8.8$ Hz, $2 \times \text{C}^3\text{H}$), **4.45** (s, 2H, C^6H_2), **3.80** (s, 3H, C^1H_3), **3.78** (t, 2H, $J = 5.9$ Hz, C^9H_2), **3.64** (t, 2H, $J = 5.9$ Hz, C^7H_2), **1.85** (tt, 2H, $J = 5.9$; 5.9 Hz, C^8H_2)

$^{13}\text{C NMR}$ (126 MHz, CDCl_3): δ (ppm) **159.36** (C_q^2), **130.23** (C_q^5), **129.45** ($2 \times \text{C}^4\text{H}$), **113.96** ($2 \times \text{C}^3\text{H}$), **73.08** (C^6H_2), **69.38** (C^7H_2), **62.25** (C^9H_2), **55.41** (C^1H_3), **32.13** (C^8H_2)

IR: $\bar{\nu}$ (cm^{-1}) 3700-3200, 1612, 1512, 1244, 1083, 1032

The experimental data were in agreement with those reported in the literature.²²

3-((4-Methoxybenzyl)oxy)propanal (**413**)



The title compound was synthesised according to a modified procedure of Hayashi *et al.*²³

Under argon atmosphere, at 0°C , alcohol **412** (1.499 g, 7.38 mmol, 1.0 eq.) was dissolved in 5 mL of anhydrous dichloromethane. To that solution was added Et_3N (5.4 mL, 38.7 mmol, 5.3 eq.), DMSO (3.8 mL, 53.5 mmol, 7.3 eq.) and sulfur trioxide pyridine complex (3.525 g, 22.2 mmol, 3.0 eq.). The mixture was stirred 15 min at 0°C . It was then quenched with a saturated solution of NaHCO_3 . The phases were separated and the aqueous phase was extracted with AcOEt. The organic phases were gathered and washed with brine, dried over Na_2SO_4 and the solvent was evaporated. The crude product was purified by flash chromatography (cHex/AcOEt: 9/1 to 8/2) to yield 1.016 g of the desired aldehyde.

Aspect: colourless oil

Yield: 71%

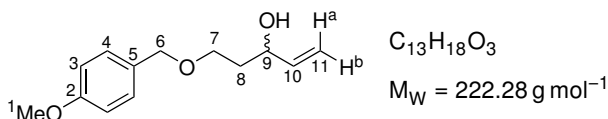
TLC: $R_f \approx 0.34$ (cHex/AcOEt: 7/3), visualised by UV and *p*-anisaldehyde

$^1\text{H NMR}$ (500 MHz, CDCl_3): δ (ppm) **9.79** (t, 1H, $J = 1.8$ Hz, C^1H), **7.25** (d, 2H, $J = 8.6$ Hz, $2 \times \text{C}^6\text{H}$), **6.88** (d, 2H, $J = 8.6$ Hz, $2 \times \text{C}^7\text{H}$), **4.46** (s, 2H, C^4H_2), **3.78** (s, 3H, C^9H_3), **3.81** (t, 2H, $J = 6.1$ Hz, C^3H_2), **2.68** (td, 2H, $J = 6.1$; 1.8 Hz, C^2H_2)

$^{13}\text{C NMR}$ (126 MHz, CDCl_3): δ (ppm) **201.42** (C^1H), **159.43** (C_q^8), **130.04** (C_q^5), **129.51** ($2 \times \text{C}^6\text{H}$), **113.97** ($2 \times \text{C}^7\text{H}$), **73.06** (C^4H_2), **63.64** (C^3H_2), **55.42** (C^9H_3), **44.02** (C^2H_2)

IR: $\bar{\nu}$ (cm^{-1}) 1722, 1612, 1512, 1244, 1173, 1088, 1031

The experimental data were in agreement with those reported in the literature.²³

5-((4-Methoxybenzyl)oxy)pent-1-en-3-ol (414)

Method A: the title compound was synthesised from epoxide according to a modified procedure of Seemand *et al.*²⁴

Under argon atmosphere, trimethylsulfonium iodide (3.919 g, 19.2 mmol, 3.9 eq.) was suspended into 60 mL of anhydrous THF and the resulting suspension was cooled down to $-20\text{ }^{\circ}\text{C}$. A 2.6 M solution of hexyllithium in hexanes (5.5 mL, 14.3 mmol, 2.9 eq.) was added dropwise over the sulfonium solution and the solution was stirred one hour at $-20\text{ }^{\circ}\text{C}$. A solution of the epoxide **410** (1.015 g, 4.87 mmol, 1.0 eq.) in 20 mL of anhydrous THF was added dropwise and the final mixture was stirred one hour at $-20\text{ }^{\circ}\text{C}$. The solution was then allowed to warm up to $0\text{ }^{\circ}\text{C}$ and quenched with a saturated solution of NH_4Cl . The phases were separated and the aqueous phase was extracted with diethyl ether. The organic phases were gathered and dried over Na_2SO_4 and the solvents were evaporated. The crude oil was purified by filtration over silica gel (cHex/AcOEt: 7/3) to yield 1.082 g of the desired allylic alcohol.

Aspect: colourless oil

Yield: quantitative

Method B: the title compound was synthesised from aldehyde according to a procedure of Matsubara and Jamison.²⁵

Under argon atmosphere, aldehyde **413** (837 mg, 4.31 mmol, 1.0 eq.) was dissolved in 10 mL of anhydrous THF and cooled down to $0\text{ }^{\circ}\text{C}$. A 1.0 M solution of vinyl Grignard in THF (5.2 mL, 5.2 mmol, 1.2 eq.) was added dropwise. The solution was allowed to warm up to room temperature and was stirred overnight. The mixture was quenched with a saturated solution of NH_4Cl and the phases were separated. The aqueous phase was extracted with diethyl ether. The organic phases were gathered, washed with brine, dried over Na_2SO_4 and the solvents were evaporated. The crude oil was filtered over silica gel (cHex/AcOEt: 7/3) to give 948 mg of desired allylic alcohol.

Aspect: colourless oil

Yield: quantitative

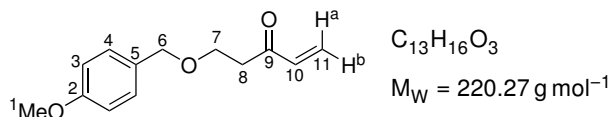
TLC: $R_f \approx 0.33$ (cHex/AcOEt: 7/3), visualised by UV and *p*-anisaldehyde

¹H NMR (500 MHz, CDCl_3): δ (ppm) **7.25** (d, 2H, $J = 8.7\text{ Hz}$, $2 \times \text{C}^4\text{H}$), **6.88** (d, 2H, $J = 8.7\text{ Hz}$, $2 \times \text{C}^3\text{H}$), **5.87** (ddd, 1H, $J = 17.2$; 10.5; 5.5 Hz, C^{10}H), **5.27** (ddd, 1H, $J = 17.2$, 1.6, 1.6 Hz, C^{11}H^a), **5.10** (ddd, 1H, $J = 10.5$, 1.6, 1.6 Hz, C^{11}H^b), **4.45** (s, 2H, C^6H_2), **4.37-4.29** (m, 1H, C^9H), **3.81** (s, 3H, C^1H_3), **3.65** (dddd, ABXY, 2H, $J_{AB} = 9.4\text{ Hz}$, $J_{AX} = 6.5\text{ Hz}$, $J_{AY} = 4.6\text{ Hz}$, $J_{BX} = 7.4\text{ Hz}$, $J_{BY} = 4.5\text{ Hz}$, $\Delta\nu_{AB} = 35.3\text{ Hz}$, C^7H_2), **3.03** (s (br), 1H, OH), **1.91-1.74** (m, ABXY, 2H, C^8H_2)

¹³C NMR (126 MHz, CDCl_3): δ (ppm) **159.40** (C_q^2), **140.63** (C^{10}H), **130.10** (C_q^5), **129.51** ($2 \times \text{C}^4\text{H}$), **114.50** (C^{11}H_2), **113.96** ($2 \times \text{C}^3\text{H}$), **73.11** (C^6H_2), **72.19** (C^9H), **68.26** (C^7H_2), **55.42** (C^1H_3), **36.35** (C^8H_2)

IR: $\bar{\nu}$ (cm^{-1}) 3600-3200, 1612, 1512, 1245, 1173, 1086, 1032

The experimental data are in agreement with those reported in the literature.²⁴

5-((4-Methoxybenzyl)oxy)pent-1-en-3-one (415)

Under argon atmosphere, allylic alcohol **414** (777 mg, 3.49 mmol, 1.0 eq.) was dissolved into 5 mL of anhydrous dichloromethane and the solution was cooled down to 0 °C. To that mixture was added Et₃N (2.5 mL, 17.9 mmol, 5.1 eq.), DMSO (1.8 mL, 25.3 mmol, 7.3 eq.) and sulfur trioxide pyridine complex (1.667 g, 10.5 mmol, 3.0 eq.) and the reaction mixture was stirred one hour at 0 °C. The reaction was then quenched with a saturated solution of NaHCO₃. The phases were separated and the aqueous phase was extracted with diethyl ether. The organic phases were gathered and washed with brine, dried over Na₂SO₄ and the solvents were evaporated. The crude was purified by filtration over silica gel (cHex/AcOEt: 7/3) to yield 669 mg of the desired enone.

Aspect: colourless oil

Yield: 87%

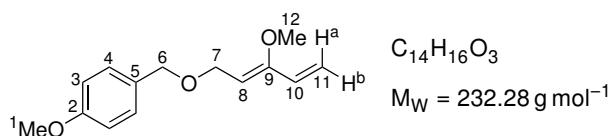
TLC: R_f ≈ 0.46 (cHex/AcOEt: 7/3), visualised by UV and *p*-anisaldehyde

¹H NMR (500 MHz, CDCl₃): δ (ppm) **7.25** (d, 2H, *J* = 8.6 Hz, 2 × C⁴H), **6.87** (d, 2H, *J* = 8.6 Hz, 2 × C³H), **6.37** (dd, 1H, *J* = 17.5; 10.6 Hz, C¹⁰H), **6.23** (d, 1H, *J* = 17.5 Hz, C¹¹H^a), **5.86** (d, 1H, *J* = 10.6 Hz, C¹¹H^b), **4.45** (s, 2H, C⁶H₂), **3.80** (s, 3H, C¹H₃), **3.77** (t, 2H, *J* = 6.5 Hz, C⁷H₂), **2.89** (t, 2H, *J* = 6.5 Hz, C⁸H₂)

¹³C NMR (126 MHz, CDCl₃): δ (ppm) **199.08** (C⁹), **159.33** (C²), **136.85** (C¹⁰H), **130.31** (C⁵), **129.49** (2 × C⁴H), **128.83** (C¹¹H₂), **113.90** (2 × C³H), **73.06** (C⁶H₂), **65.08** (C⁷H₂), **55.40** (C¹H₃), **39.77** (C⁸H₂)

IR: ν̄ (cm⁻¹) 1680, 1612, 1512, 1244, 1095, 1032, 945, 814

The experimental data were in agreement with those reported in the literature.²⁶

(Z)-1-Methoxy-4-(((3-methoxypenta-2,4-dien-1-yl)oxy)methyl)benzene (373b)

The synthesis of the title compound was inspired from the procedure of Xie and Saunders.²⁷

In a dried 100 mL two-neck flask, a 1 M solution of LiHMDS in THF/toluene (10.0 mL, 10.0 mmol, 3.0 eq.) and HMPA (5.3 mL, 30.5 mmol, 9.0 eq.) was dissolved in 30 mL of anhydrous THF and the resulting solution was cooled down to -78 °C. Enone **415** (745 mg, 3.38 mmol, 1.0 eq.) was dissolved in 3 mL of anhydrous THF and added dropwise into the base solution. After ten minutes at -78 °C, Me₃OBF₄ (2.578 g, 17.4 mmol, 5.2 eq.) was added portionwise. After three hours at that temperature, the mixture was quenched with a saturated aqueous solution of NaHCO₃. The phases were separated and the aqueous phase was extracted with diethyl ether. The organic phases were gathered and washed with water and brine, successively. The organic phase was then dried over Na₂SO₄ and the solvents were evaporated. The crude mixture was rapidly purified by flash chromatography on demetallated and neutralised silica gel (cHex/AcOEt: 9/1) to yield 545 mg of the desired *Z* diene.

Aspect: light yellow oil

Yield: 69%

TLC: $R_f \approx 0.61$ (cHex/AcOEt: 8/2), visualised by UV and KMnO_4

$^1\text{H NMR}$ (500 MHz, C_6D_6): δ (ppm) **7.25** (d, 2H, $J = 8.8$ Hz, $2 \times \text{C}^4\text{H}$), **6.80** (d, 2H, $J = 8.8$ Hz, $2 \times \text{C}^3\text{H}$), **5.96** (dd, 1H, $J = 17.2$; 10.8 Hz, C^{10}H), **5.47** (dd, 1H, $J = 17.2$, 1.6 Hz, C^{11}H^a), **5.20** (t, 1H, $J = 6.8$ Hz, C^8H), **4.96** (dd, 1H, $J = 10.8$, 1.6 Hz, C^{11}H^b), **4.37** (s, 2H, C^6H_2), **4.19** (d, 2H, $J = 6.8$ Hz, C^7H_2), **3.34** (s, 3H, C^{12}H_3), **3.30** (s, 3H, C^1H_3)

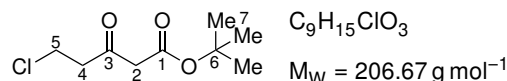
$^{13}\text{C NMR}$ (126 MHz, C_6D_6): δ (ppm) **159.69** (C_q^2), **156.88** (C_q^9), **132.83** (C^{10}H), **131.27** (C_q^5), **129.51** ($2 \times \text{C}^5\text{H}$), **115.47** (C^8H), **114.78** (C^{11}H_2), **114.04** ($2 \times \text{C}^3\text{H}$), **72.06** (C^6H_2), **64.37** (C^7H_2), **59.70** (C^{12}H_3), **54.76** (C^1H_3)

IR: $\bar{\nu}$ (cm^{-1}) 1611, 1512, 1245, 1173, 1087, 1056, 1033, 988, 916, 818

HRMS (ESI+): for $[\text{M}+\text{H}]^+$ calc.: 235.1334, found: 235.1329

8.2.3 6-Ethenyl-2,2-dimethyl-2,4-dihydro-1,3-dioxin-4-one (373c)

tert-Butyl 5-chloro-3-oxopentanoate (418)



This β -ketoester was synthesised according to a modified procedure of Ohta *et al.*²⁸

In a dry 100 mL two-neck flask under argon atmosphere, DIPA (2.8 mL, 20.0 mmol, 1.9 eq.) was dissolved in 40 mL of anhydrous THF and cooled down to -78°C . A solution of 2.5 M hexyllithium in hexane (8.0 mL, 20.0 mmol, 1.9 eq.) was added dropwise and the mixture was stirred at -78°C . After ten minutes, *tert*-butyl acetate (3.0 mL, 22.3 mmol, 2.1 eq.) was added dropwise at -78°C and the solution was stirred for 1h30. In a dry 250 mL two-neck flask under argon atmosphere, the ethyl 3-chloropropanoate (**417**) (1.4 mL, 10.3 mmol, 1.0 eq.) was dissolved in 25 mL of anhydrous THF and cooled down to -78°C . The enolate solution was added dropwise to the chloropropanoate solution and the final mixture was at -78°C . After thirty minutes, 5 mL of acetic acid was added dropwise. The mixture was allowed to warm up to room temperature and diluted with 150 mL of diethyl ether, followed by the addition of 50 mL of water. The phases were separated and the organic phase was washed with saturated solutions of NaHCO_3 and NaCl , successively. It was then dried over Na_2SO_4 and the solvents were evaporated to give 2.121 g of title compound **418** which is pure enough to be used in the next reaction without any further purification.

Aspect: Light yellow liquid

Yield: quantitative

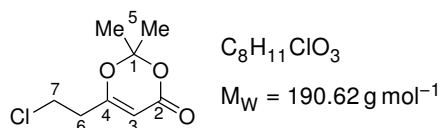
TLC: $R_f \approx 0.31$ (cHex/AcOEt: 9/1), visualised by *p*-anisaldehyde

$^1\text{H NMR}$ (500 MHz, CDCl_3): δ (ppm) **3.75** (t, 2H, $J = 6.6$ Hz, C^5H_2), **3.39** (s, 2H, C^2H_2), **3.03** (t, 2H, $J = 6.6$ Hz, C^4H_2), **1.47** (s, 9H, $3 \times \text{C}^7\text{H}_3$)

$^{13}\text{C NMR}$ (126 MHz, CDCl_3): δ (ppm) **200.08** (C_q^3), **166.02** (C_q^1), **82.50** (C_q^6), **50.92** (C^2H_2), **45.42** (C^2H_4), **37.87** (C^2H_5), **28.05** ($3 \times \text{C}^7\text{H}_3$)

IR: $\bar{\nu}$ (cm^{-1}) 1714, 1368, 1147

The experimental data were in agreement with those reported in the literature.²⁹

6-(2-Chloroethyl)-2,2-dimethyl-2,4-dihydro-1,3-dioxin-4-one (419)

This compound was synthesised according to the procedure of Gebauer and Blechert.³⁰

In a 50 mL two-neck flask under argon atmosphere, pentanoate **418** (1.009 g, 4.88 mmol, 1.0 eq.) was dissolved in 10 mL of acetone. The solution was cooled down to 0 °C and acetic anhydride (1.4 mL, 14.8 mmol, 3.0 eq.) and 0.27 mL of sulphuric acid (98%) was added dropwise. The reaction was allowed to warm up to room temperature and stirred overnight. It was then diluted with 50 mL of water and the aqueous phase was extracted with dichloromethane. The organic phase was then dried over $MgSO_4$ and the solvents were evaporated. The crude mixture was purified by flash chromatography on silica gel (cHex/AcOEt: 9/1) to give 705 mg of dioxinone **419**.

Aspect: yellowish oil

Yield: 76%

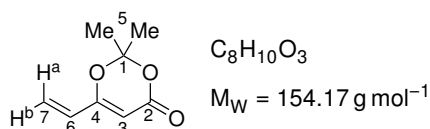
TLC: $R_f \approx 0.18$ (cHex/AcOEt: 9/1), visualised by UV and *p*-anisaldehyde

1H NMR (500 MHz, $CDCl_3$): δ (ppm) **5.36** (s, 1H, C^3H), **3.69** (t, 2H, $J = 6.3$ Hz, C^7H_2), **2.70** (t, 2H, $J = 6.3$ Hz, C^6H_2), **1.70** (s, 6H, $2 \times C^5H_3$)

^{13}C NMR (126 MHz, $CDCl_3$): δ (ppm) **167.18** (C_q^4), **160.89** (C_q^2), **107.09** (C_q^1), **95.85** (C^3H), **39.53** (C^7H_2), **36.64** (C^6H_2), **25.17** (C^5H_3)

IR: $\bar{\nu}$ (cm^{-1}) 1723, 1637, 1390, 1374, 1271, 1251, 1200, 1176, 1014

The experimental data were in agreement with those reported in the literature.³⁰

6-Ethenyl-2,2-dimethyl-2,4-dihydro-1,3-dioxin-4-one (373c)

This compound was synthesised according to the procedure of Gebauer and Blechert.³⁰

In a 25 mL round-bottom flask, dioxinone **419** (553 mg, 2.90 mmol, 1.0 eq.) was dissolved in 10 mL of dichloromethane and Et_3N (0.80 mL, 5.76 mmol, 2.0 eq.) was added dropwise. After three hours at room temperature, the mixture was diluted with 70 mL of dichloromethane and washed with HCl (5%). The organic phase was then dried over Na_2SO_4 and the solvent was evaporated. The crude mixture was purified by flash chromatography on silica gel (cHex/AcOEt: 9/1) to yield 445 mg of diene **373c**.

Aspect: yellowish oil

Yield: quantitative

TLC: $R_f \approx 0.34$ (cHex/AcOEt: 8/2), visualised by UV and *p*-anisaldehyde

1H NMR (500 MHz, $CDCl_3$): δ (ppm) **6.21** (dd, 1H, $J = 17.2$; 10.8 Hz, C^6H), **6.01** (d, 1H, $J = 17.2$ Hz, C^7H^a), **5.60** (d, 1H, $J = 10.8$ Hz, C^7H^b), **5.35** (s, 1H, C^3H), **1.72** (s, 6H, $2 \times C^5H_3$)

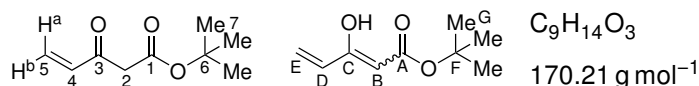
^{13}C NMR (126 MHz, $CDCl_3$): δ (ppm) **162.92** (C_q^2), **161.87** (C_q^4), **129.45** (C^6H), **124.00** (C^7H_2), **106.70** (C_q^1), **95.37** (C^3H), **25.13** ($2 \times C^5H_3$)

IR: $\bar{\nu}$ (cm⁻¹) 1725, 1645, 1581, 1390, 1375, 1272, 1251, 1202, 1172

The experimental data were in agreement with those reported in the literature.³⁰

8.2.4 *tert*-Butyl 3-((trimethylsilyl)oxy)penta-2,4-dienoate (373d)

tert-Butyl 3-oxopent-4-enoate (421)



This β -ketoester was synthesised according to a modified procedure of Ohta *et al.*²⁸

The exact same procedure as for the synthesis of 5-chloro-3-oxopentanoate **418** with the same quantity of 3-chloropropanoate **417** (1.4 mL, 10.3 mmol, 1.0 eq.). However, after the work up, the diethyl ether was not evaporated and Et₃N (7.0 mL, 50.4 mmol, 4.9 eq.) was added to the crude solution of 5-chloro-3-oxopentanoate **418**. The final mixture was stirred overnight at room temperature. The organic phase was then washed with HCl (5%) and brine. The phases were separated and the organic phase dried over Na₂SO₄ and the solvent was evaporated. The crude mixture was purified by distillation using a bulb-to-bulb glass oven (100 °C, 3 mbar) to give 1.597 g of pure **421**.

Aspect: colourless oil

Yield: 91%

TLC: R_f \approx 0.72 (cHex/AcOEt: 8/2), visualised by UV and *p*-anisaldehyde

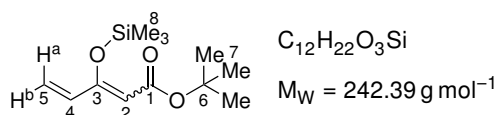
¹H NMR (500 MHz, CDCl₃): δ (ppm) **11.93** (s, 0.4H, OH (enol)), **6.41** (dd, 0.6H, $J = 17.7; 10.6$ Hz, C⁴H), **6.26** (d, 0.6H, $J = 17.7$ Hz, C⁵H^A), **6.09-6.04** (m, 0.8H, C^DH+ $\frac{1}{2} \times$ C^EH₂), **5.94** (d, 0.6H, $J = C^5H^B$), **5.50** (dd, 0.4H, $J = 7.0; 5.1$ Hz, $\frac{1}{2} \times$ C^EH₂), **4.99** (s, 0.4H, C^BH), **3.53** (s, 1.2H, C²H₃), **1.49** (s, 3.6H, 3 \times C^GH₃), **1.46** (s, 5.4H, 3 \times C⁷H₃)

¹³C NMR (126 MHz, CDCl₃): δ (ppm) **193.29** (C_q³), **172.75** (C_q^A), **168.26** (C_q^C), **166.54** (C_q¹), **136.04** (C⁴H), **131.58** (C^DH), **130.01** (C⁵H₂), **122.10** (C^EH₂), **93.61** (C^BH), **82.20** (C_q⁶), **81.29** (C_q^F), **48.03** (C²H₂), **28.43** (3 \times C^GH₃), **28.07** (3 \times C⁷H₃)

IR: $\bar{\nu}$ (cm⁻¹) 3600-3200, 2965, 1713, 1651, 1588, 1457, 1415, 1395, 1369, 1321, 1256, 1144, 1085, 1014, 800

The experimental data were in agreement with those reported in the literature.³¹

tert-Butyl 3-((trimethylsilyl)oxy)penta-2,4-dienoate (373d)



The title compound was prepared according to Dickschat *et al.*³¹

In a dry 50 mL two-neck flask under argon atmosphere, β -ketoester **421** (410 mg, 2.41 mmol, 1.0 eq.) was dissolved in 10 mL of anhydrous toluene. Et₃N (0.50 mL, 3.59 mmol, 1.5 eq.) and TMSCl (0.46 mL, 3.62 mmol, 1.5 eq.) were added to the solution that was stirred 24 h at room temperature. The reaction mixture was quenched with water, the phases were separated and the aqueous phase was extracted with ethyl acetate. The organic phases were gathered, dried over Na₂SO₄ and the solvent were evaporated to give 520 mg of **373d** in a mixture of *E* and *Z* isomers (2:1, not assigned).

Aspect: colourless oil

Yield: 89%

TLC: $R_f \approx 0.68$ (cHex/AcOEt: 95/5), visualised by UV and *p*-anisaldehyde

$^1\text{H NMR}$ (500 MHz, CDCl_3): δ (ppm) **7.58** (dd, 0.66H, $J = 17.2$; 10.6 Hz, C^4H (major isomer)), **6.15** (dd, 0.33H, $J = 17.2$; 10.5 Hz, C^4H (minor isomer)), **5.81** (ddd, 0.66H, $J = 17.2$; 2.2; 0.6 Hz, C^5H^a (major isomer)), **5.74** (ddd, 0.33H, $J = 17.2$; 1.3; 0.5 Hz, C^5H^a (minor isomer)), **5.42** (ddd, 0.66H, $J = 10.6$; 2.2; 1.5 Hz, C^5H^b (major isomer)), **5.32** (ddd, 0.33H, $J = 10.5$; 1.3; 0.5 Hz, C^5H^b (minor isomer)), **5.18** (s, 0.33H, C^2H (minor isomer)), **4.96** (d, 0.66H, $J = 1.5$ Hz, C^2H (major isomer)), **1.49** (s, 6H, $3 \times \text{C}^7\text{H}_3$ (major isomer)), **1.46** (s, 3H, $3 \times \text{C}^7\text{H}_3$ (minor isomer)), **0.27** (s, 6H, $3 \times \text{C}^8\text{H}_3$ (major isomer)), **1.46** (s, 3H, $3 \times \text{C}^8\text{H}_3$ (minor isomer))

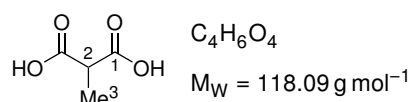
$^{13}\text{C NMR}$ (126 MHz, CDCl_3): δ (ppm) **166.48** (C_q^1 (major isomer)), **165.02** (C_q^1 (minor isomer)), **162.12** (C_q^3 (major isomer)), **160.04** (C_q^3 (minor isomer)), **135.87** (C^4H (minor isomer)), **130.73** (C^4H (major isomer)), **121.01** (C^5H_2 (major isomer)), **120.18** (C^5H_2 (minor isomer)), **104.94** (C^2H (minor isomer)), **103.21** (C^2H (major isomer)), **79.65** (C_q^6 (major isomer)), **79.16** (C_q^6 (minor isomer)), **28.32** ($3 \times \text{C}^7\text{H}_3$ (major isomer)), **28.19** ($3 \times \text{C}^7\text{H}_3$ (minor isomer)), **0.64** ($3 \times \text{C}^8\text{H}_3$ (minor isomer)), **0.09** ($3 \times \text{C}^8\text{H}_3$ (major isomer))

IR: $\bar{\nu}$ (cm^{-1}) 2979, 2934, 1734, 1703, 1655, 1635, 1586, 1574, 1456, 1415, 1368, 1301, 1249, 1129, 1064, 1042, 997, 984, 940, 884, 813

The experimental data were in agreement with those reported in the literature.³¹

8.2.5 4-methoxy-3-methyl- α -pyrone (373e)

2-Methylmalonic acid (426)



This compound was synthesised according to the protocol of Ng *et al.*³²

In a 500 mL flask equipped with a condenser, a solution of KOH (10.003 g, 152 mmol, 2.6 eq.) dissolved in 150 mL of absolute ethanol were added over a solution of diethyl 2-methylmalonate (10 mL, 58.13 mmol, 1.0 eq.) dissolved in 50 mL of absolute ethanol. The resulting mixture was refluxed for two hours. The solution was allowed to cool down to room temperature and was stirred overnight. The salts were filtered and dissolved in 150 mL of water. This solution was cooled down to 0 °C and a solution of HCl (37%) was added dropwise until a pH value below 2 was reached. The aqueous phase was extracted with ethyl acetate. Then the organic phase was dried over MgSO_4 , filtered off and the solvent was evaporated to give 6.583 g of a white solid.

Aspect: white solid

Yield: 96%

TLC: $R_f \approx 0$ (AcOEt), visualised by UV and KMnO_4

m_p : 128-130 °C

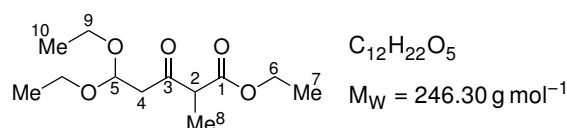
$^1\text{H NMR}$ (400 MHz, $\text{DMSO}-d_6$): δ (ppm) **3.27** (q, 1H, $J = 7.1$ Hz, C^2H), **1.17** (d, 3H, $J = 7.1$ Hz, C^3H_3)

$^{13}\text{C NMR}$ (400 MHz, $\text{DMSO}-d_6$): δ (ppm) **172.11** ($2 \times \text{C}_q^1$), **46.13** (C^2H), **14.07** (C^3H_3)

IR: $\bar{\nu}$ (cm⁻¹) 3200-2500, 1688, 1411, 1289, 1245, 896

The experimental data were in agreement with those reported in the literature.³²

Ethyl 5,5-diethoxy-2-methyl-3-oxopentanoate (423)



This compound was synthesised according to the combined protocols of Körner *et al.*³³ and Minich *et al.*³⁴

In a 250 mL two-neck flask under argon atmosphere, diacid **426** (5.125 g, 43.39 mmol, 1.0 eq.) was suspended in 50 mL of anhydrous dichloromethane and cooled down to 0 °C. DMF (0.5 mL, 6.46 mmol, 0.15 eq.) and (COCl)₂ (11.5 mL, 136 mmol, 3.1 eq.) was added dropwise (the solution directly started to bubble). The solution was allowed to warm up to room temperature and was stirred overnight. The solvents were then evaporated and the golden oil was dissolved in 25 mL of anhydrous THF. Ethyl vinyl ether (21 mL, 220 mmol, 5.1 eq.) was dissolved in 15 mL of anhydrous THF and cooled down to 0 °C and the malonyl chloride solution was added dropwise. The mixture was stirred one hour at 0 °C and absolute ethanol (20.5 mL, 352 mmol, 8.1 eq.) was added dropwise. After 15 minutes at 0 °C, Et₃N (12.5 mL, 89.2 mmol, 2.1 eq.), dissolved in 15 mL of anhydrous THF, was added dropwise and the solution was allowed to warm up to room temperature. The ammonium salts were filtered, and the solvents were evaporated to obtain a golden oil which was purified by flash chromatography on demetallated and neutralised silica gel (cHex/AcOEt: 100/0 → 99/1 → 98/2) to give 5.492 g of **423**.

Aspect: golden oil

Yield: 51%

TLC: $R_f \approx 0.63$ (cHex/AcOEt: 7/3), visualised by UV and *p*-anisaldehyde

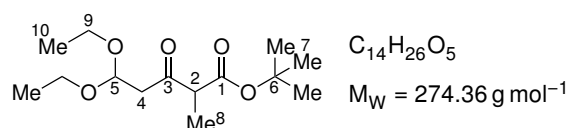
¹H NMR (400 MHz, CDCl₃): δ (ppm) **4.89** (dd, 1H, ABX, $J_{AX} = 5.7 \text{ Hz}$, $J_{BX} = 5.5 \text{ Hz}$, C⁵H), **4.17** (q, 2H, $J = 7.1 \text{ Hz}$, C⁶H₂), **3.73-3.47** (m, 5H, 2 × C⁹H₂ + C²H), **2.87** (2 × dd, ABX, $J_{AX} = 5.7 \text{ Hz}$, $J_{BX} = 5.5 \text{ Hz}$, $J_{AB} = 15.0 \text{ Hz}$, $\Delta\nu_{AB} = 20 \text{ Hz}$, C⁴H₂), **1.31** (d, 3H, $J = 7.1 \text{ Hz}$, C⁸H₃), **1.29-1.14** (m, 9H, C⁷H₃ + 2 × C¹⁰H₃)

¹³C NMR (100 MHz, CDCl₃): δ (ppm) **202.28** (C_q³), **170.03** (C_q¹), **99.82** (C⁵H), **62.50** (C⁹H₂), **62.11** (C⁹H₂), **61.06** (C⁶H₂), **53.38** (C²H), **46.19** (C⁴H₂), **15.03** (2 × C¹⁰H₃), **13.87** (C⁷H₃), **12.09** (C⁸H₃)

IR: $\bar{\nu}$ (cm⁻¹) 2979, 1743, 1716, 1244, 1195, 1123, 1057

The experimental data were in agreement with those reported in the literature.³⁵

tert-Butyl 5,5-diethoxy-2-methyl-3-oxopentanoate (461)



In a dry 500 mL two-neck flask, DIPA (4.4 mL, 31.4 mmol, 1.5 eq.) was dissolved in 160 mL of anhydrous THF and cooled down to -78 °C. A 2.5 M solution of *n*-hexyllithium in hexane (12.5 mL,

31.3 mmol, 1.5 eq.) was added dropwise and the solution was stirred for ten minutes at $-78\text{ }^{\circ}\text{C}$. Then, *tert*-butylpropionate (**440**) (4.6 mL, 30.6 mmol, 1.5 eq.) was added dropwise and the mixture was stirred for half an hour. Ethyl 3,3-diethoxypropanoate (**460**) (4.0 mL, 20.6 mmol, 1.0 eq.) was added dropwise to the solution at $-78\text{ }^{\circ}\text{C}$. The resulting mixture was warmed up over two hours to room temperature and stirred overnight. The yellow solution was cooled down to $0\text{ }^{\circ}\text{C}$ and quenched with water. The phases were separated and the aqueous phase was extracted with diethyl ether. The organic phases were gathered, washed with a saturated solution of NH_4Cl and dried over MgSO_4 . The solvents were evaporated and the crude golden oil was purified by flash chromatography on demetallated and neutralised silica gel (cHex/AcOEt: 100/0 \rightarrow 98/2 \rightarrow 95/5) to give 3.949 g of pentanoate **461**. The crude oil can also be used directly in the next step without purification.

Aspect: colourless liquid

Yield: 70%

TLC: $R_f \approx 61$ (cHex/AcOEt: 8/2), visualised by UV and KMnO_4

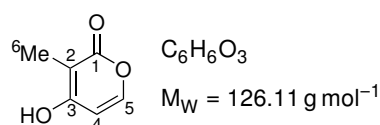
^1H NMR (500 MHz, CDCl_3): δ (ppm) **4.91** (dd, 1H, ABX, $J_{\text{AX}} = 6.3\text{ Hz}$, $J_{\text{BX}} = 5.7\text{ Hz}$, C^5H), **3.72-6.61** (m, 2H, C^9H_2), **3.58-3.45** (m, 3H, $\text{C}^9\text{H}_2 + \text{C}^2\text{H}$), **2.86** (ddd, 2H, ABX, $J_{\text{AB}} = 15.5\text{ Hz}$, $J_{\text{AX}} = 6.3\text{ Hz}$, $J_{\text{BX}} = 5.7\text{ Hz}$, $\Delta\nu_{\text{AB}} = 23.2\text{ Hz}$, C^4H_2), **1.45** (s, 9H, $3 \times \text{C}^7\text{H}_3$), **1.27** (d, 3H, $J = 7.45\text{ Hz}$, C^8H_3), **1.24-1.12** (m, 6H, $2 \times \text{C}^{10}\text{H}_3$)

^{13}C NMR (126 MHz, CDCl_3): δ (ppm) **203.45** (C_q^3), **169.60** (C_q^1), **100.16** (C^5H), **81.98** (C_q^6), **62.99** (C^9H_2), **62.53** (C^9H_2), **54.73** (C^2H), **46.53** (C^4H_2), **28.04** ($3 \times \text{C}^7\text{H}_3$), **15.41** (C^{10}H_3), **15.38** (C^{10}H_3), **12.41** (C^8H_3)

IR: $\bar{\nu}$ (cm^{-1}) 1715, 1251, 1215, 1058, 1006

HRMS (ESI+): for $[\text{M}+\text{H}]^+$ calc.: 275.1858, found: 275.1853

4-Hydroxy-3-methyl-2H-pyran-2-one (**424**)



From pentanoate **423** (according to Effenberger *et al.*³⁵). In a 50 mL two-neck flask under argon atmosphere, pentanoate **423** (1.000 g, 4.06 mmol, 1.0 eq.) was dissolved in 10 mL of absolute ethanol. A 2 M solution of KOH in absolute ethanol (5 mL, 10.0 mmol, 2.5 eq.) was added and the mixture was stirred at room temperature overnight. The ethanol was evaporated and the residue replaced under argon atmosphere and was cooled down to $0\text{ }^{\circ}\text{C}$. Carefully, 10 mL of fuming sulfuric acid (20% in SO_3). The mixture was heated up to $100\text{ }^{\circ}\text{C}$ and was stirred for one hour. The hot mixture was directly poured on 100 mL of water. The aqueous phase was extracted with ethyl acetate. The organic phase was washed with brine, dried over MgSO_4 , filtered off and the solvent was evaporated to give a black sticky solid. The crude was purified by flash chromatography on silica gel (cHex/AcOEt: 10/0 \rightarrow 8/2 \rightarrow 6/4 \rightarrow 5/5 \rightarrow 4/6 \rightarrow 2/8) to give 0.174 g of hydroxypyron **424**. Crystals of this compound were obtained from recrystallisation from boiling AcOEt.

Aspect: brown solid

Yield: 34%

From pentanoate 461. In a 50 mL flask, pentanoate **461** (1.359 g, 4.95 mmol) was dissolved at 0 °C with 15 mL of concentrated H₂SO₄ (98%). The reaction was allowed to warm up to room temperature and was stirred two hours. The mixture was then poured into 150 mL of water. The aqueous phase was extracted with AcOEt. The organic phase was washed with brine, dried over Na₂SO₄ and the solvent was evaporated. The resulting brown slushy solid was triturated with dichloromethane and the precipitate was filtered, thoroughly washed with dichloromethane and dried under vacuum to give 317 mg of hydroxypyronone **424**.

Aspect: white solid

Yield: 51% (39% over two steps if pentanoate **461** is not isolated)

TLC: R_f ≈ 0.47 (AcOEt), visualised by UV and KMnO₄

m_p: 218-220 °C (decomposition)

¹H NMR (500 MHz, acetone-*d*₆): δ (ppm) **7.47** (d, 1H, *J* = 5.7 Hz, C⁵H), **6.22** (d, 1H, *J* = 5.7 Hz, C⁴H), **1.86** (s, 3H, C⁶H₃)

¹³C NMR (500 MHz, acetone-*d*₆): δ (ppm) **165.50** (C_q¹), **164.03** (C_q³), **150.58** (C⁵H), **103.63** (C⁴H), **101.76** (C_q²), **8.79** (C⁶H₃)

IR: ν̄ (cm⁻¹) 3300-2800, 1663, 1618, 1340, 1291, 1218, 1149

The experimental data were in agreement with those reported in the literature.³⁵

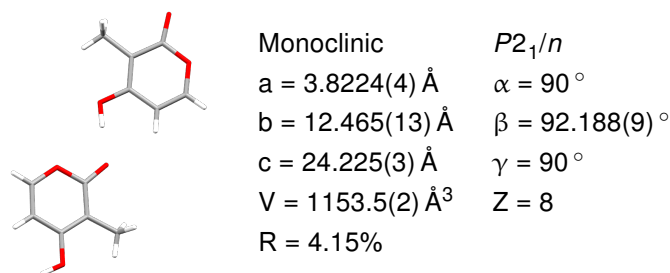
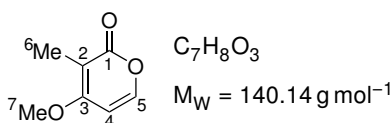


Figure 8.1: X-ray structure of **424** and parameters of the crystal. Recrystallisation from boiling ethyl acetate.

4-Methoxy-3-methyl-2*H*-pyran-2-one (**373e**)



This compound was synthesised according to Effenberger *et al.*³⁶

In a 250 mL two-neck flask under argon atmosphere and equipped with a condenser, hydroxypyronone **424** (1.953 g, 15.5 mmol, 1.0 eq.) was dissolved in 65 mL of acetone. Anhydrous potassium carbonate (5.369 g, 38.8 mmol, 2.5 eq.) and dimethyl sulfate (1.5 mL, 15.9 mmol, 1.0 eq.) were added to the solution and the mixture was heated up to 50 °C. After 30 min, a TLC analysis indicated the complete conversion of the starting material. The mixture was allowed to cooled down to room temperature and the solid was filtered off and washed with acetone. The solvents were evaporated and the crude was purified by flash chromatography on demetallated silica gel (cHex/AcOEt: 5/5) to give 1.666 g of methoxypyronone **373e**.

Aspect: pale yellow solid

Yield: 77%

TLC: $R_f \approx 0.38$ (cHex/AcOEt: 3/7), visualised by UV and KMnO_4

m_p : 86-88 °C

$^1\text{H NMR}$ (500 MHz, CDCl_3): δ (ppm) **7.42** (d, 1H, $J = 6.0$ Hz, C^5H), **6.25** (d, 1H, $J = 6.0$ Hz, C^4H), **3.89** (s, 3H, C^7H_3), **1.93** (s, 3H, C^6H_3)

$^{13}\text{C NMR}$ (126 MHz, CDCl_3): δ (ppm) **165.34** (C_q^1), **164.79** (C_q^3), **145.00** (C^5H), **104.67** (C_q^2), **97.92** (C^4H), **56.50** (C^7H_3), **8.76** (C^6H_3)

IR: $\bar{\nu}$ (cm^{-1}) 1678, 1629, 1323, 1295, 1168, 1004

The experimental data were in agreement with those reported in the literature.³⁶

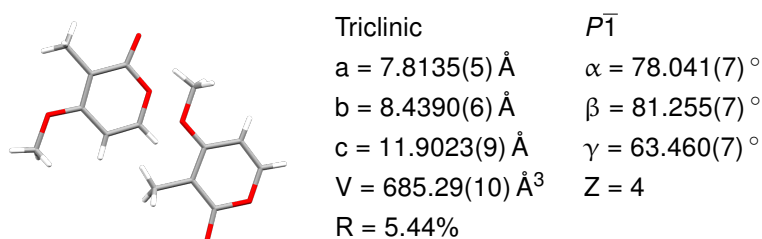
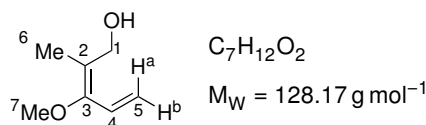


Figure 8.2: X-ray structure of **373e** and parameters of the crystal. Recrystallisation from boiling hexane.

8.2.6 (*E*)-3-Methoxy-2-methylpenta-2,4-dien-1-ol (**373f**)



In a dry 50 mL two-neck flask, pyrone **373e** (514 mg, 3.67 mmol, 1.0 eq.) was dissolved in 10 mL of anhydrous THF and the solution was cooled down to 0 °C. A 2.0 M solution of LiAlH_4 in THF (2.4 mL, 4.80 mmol, 1.3 eq.) was added dropwise to the solution. After 30 min at 0 °C, the solution was diluted with 10 mL of diethyl ether and the reaction was quenched with iced water. The phases were separated and the aqueous phase was extracted with diethyl ether. The organic phases were gathered, washed with brine, dried over Na_2SO_4 and the solvents were evaporated to give 402 mg of the title compound that was pure enough to be engaged in other reactions.

Aspect: colourless oil

Yield: 86%

TLC: $R_f \approx 0.52$ (cHex/AcOEt: 5/5), visualised by UV and KMnO_4

$^1\text{H NMR}$ (500 MHz, C_6D_6): δ (ppm) **6.38** (dd, 1H, $J = 17.0$; 10.8 Hz, C^4H), **5.49** (d, 1H, $J = 17.0$ Hz, C^5H^a), **5.02** (d, 1H, $J = 10.8$ Hz, C^5H^b), **3.94** (s, 2H, C^1H_2), **3.32** (s, 3H, C^7H_3), **1.83** (s, 3H, C^6H_3)

$^{13}\text{C NMR}$ (126 MHz, C_6D_6): δ (ppm) **151.75** (C_q^3), **127.83** (C^4H), **124.74** (C_q^2), **114.40** (C^5H_2), **62.09** (C^1H_2), **58.43** (C^7H_3), **14.07** (C^6H_3)

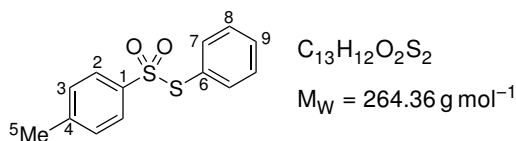
IR: $\bar{\nu}$ (cm^{-1}) 3200-2800, 1608, 1515, 1237, 1176, 1063, 975

HRMS (ESI+): for $[\text{M}+\text{H}]^+$ calc.: 129.0916, found: 129.0918

8.3 Synthesis of the 5-thiomethylenefuran-2-ones

8.3.1 Phenylthiomethylenefuranone 455a

S-Phenyl 4-methylbenzenethiosulfonate (452a)



The compound was prepared according to the procedure reported by Fujiki *et al.*³⁷

In a 500 mL two-neck flask under argon atmosphere, diphenyl disulfide (5.085 g, 23.3 mmol, 1.0 eq.) was dissolved in 120 mL of CH_2Cl_2 . Sodium *para*-toluenesulfinate (16.367 g, 91.9 mmol, 3.9 eq.) and iodine (23.468 g, 92.5 mmol, 4.0 eq.) were added to the solution. The mixture darkened and was stirred overnight. The solution was diluted with 50 mL of dichloromethane and a saturated solution of $Na_2S_2O_3$ was added until discolouration of the mixture. The phases were separated and the aqueous phase was extracted with dichloromethane. The organic phases were gathered, washed with brine, dried over $MgSO_4$, filtered off and the solvents were evaporated. The crude was recrystallised in boiling methanol to obtain 9.735 g of slightly yellow needles.

Aspect: yellowish needles

Yield: 79%

TLC: $R_f \approx 0.51$ (cHex/AcOEt: 8/2), visualised by UV and $KMnO_4$

m_p : 78–80 °C

1H NMR (500 MHz, $CDCl_3$): δ (ppm) **7.50–7.45** (m, 1H, C^9H), **7.44** (d, 2H, $J = 8.1$ Hz, $2 \times C^2H$), **7.40–7.29** (m, 4H, $2 \times C^7H + 2 \times C^8H$), **7.20** (d, 2H, $J = 8.1$ Hz, $2 \times C^3H$), **2.41** (s, 3H, C^5H_3)

^{13}C NMR (126 MHz, $CDCl_3$): δ (ppm) **144.85** (C^4_q), **140.41** (C^1_q), **136.72** ($2 \times C^8H$), **131.45** (C^9H), **129.53** ($2 \times C^3H$ or $2 \times C^7H$), **129.51** ($2 \times C^3H$ or $2 \times C^7H$), **128.15** (C^6_q), **127.72** ($2 \times C^2H$), **21.80** (C^5H_3)

IR: $\bar{\nu}$ (cm^{-1}) 1326, 1137, 815, 750, 701

The experimental data were in agreement with those reported in the literature.³⁷

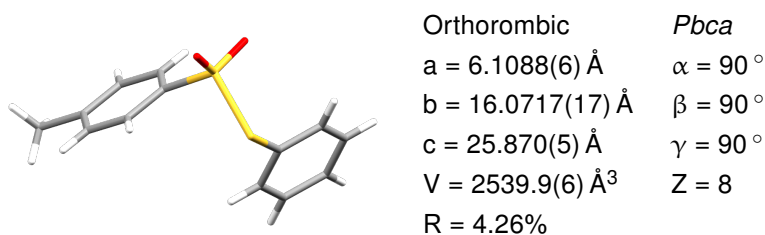
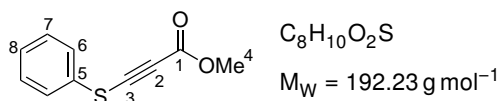


Figure 8.3: X-ray structure of **452a** and parameters of the crystal. Recrystallisation from boiling methanol.

Methyl 3-(phenylthio)propiolate (453a)

This compound was synthesised according to Minakata *et al.*³⁸

In a dry 100 mL two-neck flask under argon atmosphere, a solution of DIPA (3.2 mL, 22.8 mmol, 2.0 eq.) in 15 mL of anhydrous THF was cooled down to -78°C . A solution of 2.5 M hexyllithium in hexanes (4.5 mL, 11.3 mmol, 1.0 eq.) was added dropwise and the solution was stirred for ten minutes at -78°C . Methyl propiolate (**441**) (1.0 mL, 11.2 mmol, 1.0 eq.) was added dropwise. The mixture yellowed and was stirred for thirty minutes at -78°C . A solution of thiosulfonate **452a** (3.002 g, 11.4 mmol, 1.0 eq.) in 20 mL of anhydrous THF was added dropwise and the mixture was stirred for thirty minutes at -78°C , then allowed to warm up to room temperature and stirred for another thirty minutes. The reaction was quenched with a saturated solution of NH_4Cl . The phases were separated and the aqueous phase was extracted with dichloromethane. The organic phases were gathered, dried over MgSO_4 , filtered off and the solvents were evaporated. The crude oil was purified by flash chromatography on silica gel (cHex/TBME : 99/1) to give 1.611 g of propiolate **453a**.

Aspect: orangish liquid

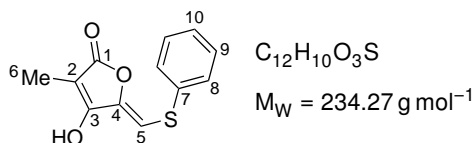
Yield: 75%

TLC: $R_f \approx 0.73$ (cHex/AcOEt: 7/3), visualised by UV and *p*-anisaldehyde

$^1\text{H NMR}$ (500 MHz, CDCl_3): δ (ppm) **7.50-7.44** (m, 2H, $2 \times C^6\text{H}$), **7.437.35** (m, 2H, $2 \times C^7\text{H}$), **7.35-7.27** (m, 1H, $C^8\text{H}$), **3.81** (s, 3H, $C^4\text{H}_3$)

$^{13}\text{C NMR}$ (126 MHz, CDCl_3): δ (ppm) **153.44** (C^1_q), **129.84** ($2 \times C^7\text{H}$), **129.49** (C^5_q), **128.08** ($C^8\text{H}$), **127.58** ($2 \times C^6\text{H}$), **91.47** (C^2_q or C^3_q), **80.55** (C^2_q or C^3_q), **52.81** ($C^4\text{H}_3$)

IR: $\bar{\nu}$ (cm^{-1}) 2159, 1703, 1233, 1022, 736, 685, 567

(Z)-4-Hydroxy-3-methyl-5-((methylthio)methylene)furan-2(5H)-one (455a)

In a dry 500 mL two-neck flask under argon atmosphere, a solution of DIPA (3.4 mL, 24.3 mmol, 1.5 eq.) in 150 mL of anhydrous THF was cooled down to -78°C . A 2.5 M solution of hexyllithium in hexanes (6.5 mL, 16.3 mmol, 1.0 eq.) was added dropwise and the solution was stirred ten minutes at -78°C . To the mixture, *tert*-butyl propionate (**440**) (2.4 mL, 16.0 mmol, 1.0 eq.) was added dropwise and the solution was stirred thirty minutes at -78°C . A solution of propiolate **453a** (3.088 g, 16.1 mmol, 1.0 eq.) in 25 mL of anhydrous THF was added dropwise on the enolate solution. The mixture was stirred one hour at -78°C . It was then allowed to warm up at room temperature and quenched with a saturated solution of NH_4Cl . The phases were separated and the aqueous phase was extracted with diethyl ether. The organic phases were gathered, dried over MgSO_4 , filtered off and the solvents were evaporated. The crude oil was dried under vacuum and dissolved in 50 mL

of dichloromethane. Carefully, TFA (0.50 mL, 9.02 mmol, 0.56 eq.) was added dropwise and a yellow precipitate appeared. The solution was stirred overnight at room temperature. The solid was filtered, washed with dichloromethane and pentane, and dried under vacuum to give 1.640 g of butenolide **455a**.

Aspect: white powder

Yield: 44%

TLC: $R_f \approx 0.47$ (cHex/AcOEt/AcOH : 7/3/0.5), visualised by UV and KMnO_4

m_p: 220-222 °C

¹H NMR (500 MHz, acetone-*d*₆): δ (ppm) **7.57-7.50** (m, 2H, 2 × C⁸H), **7.49-7.40** (m, 2H, 2 × C⁹H), **7.40-7.32** (m, 1H, C¹⁰H), **6.43** (s, 1H, C⁵H), **1.78** (s, 3H, C⁶H₃)

¹³C NMR (500 MHz, acetone-*d*₆): δ (ppm) **169.58** (C_q¹), **161.36** (C_q³), **142.93** (C_q⁴), **134.84** (C_q⁷), **130.48** (2 × C⁸H or 2 × C⁹H), **128.52** (C¹⁰H), **104.32** (C⁵H), **94.42** (C_q²), **6.52** (C⁶H₃)

IR: $\bar{\nu}$ (cm⁻¹) 330-2900, 1722, 1603, 1276, 1204, 832, 745, 687

HRMS (ESI+): for [M+H]⁺ calc.: 235.0429, found: 235.0423

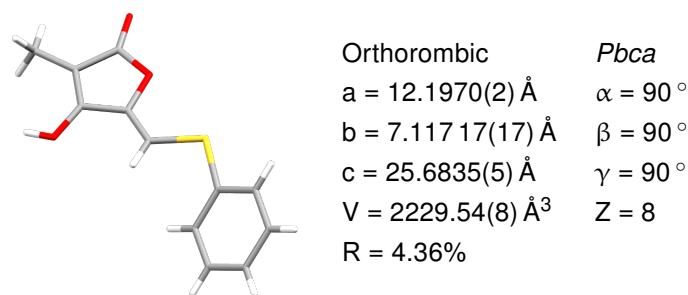
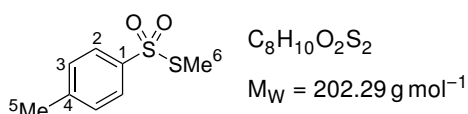


Figure 8.4: X-ray structure of **455a** and parameters of the crystal. Recrystallisation from boiling ethyl acetate.

8.3.2 Methylthiomethylenefuranone **455b**

S-Methyl 4-methylbenzenesulfonothioate (**452b**)



This compound was prepared following a procedure described by Fujiki *et al.*³⁷

In a 250 mL two-neck flask under argon atmosphere, sodium *para*-toluenesulfinate (8.445 g, 47.4 mmol, 3.0 eq.) was suspended in 75 mL of dichloromethane. Over the suspension, dimethyl disulfide (1.4 mL, 15.8 mmol, 1.0 eq.) was added, followed by the slow addition of iodine (10.101 g, 39.8 mmol, 2.5 eq.). The solution darkened and was stirred overnight at room temperature. The solution was then diluted with 50 mL of dichloromethane and a saturated solution of $\text{Na}_2\text{S}_2\text{O}_3$ was added until discolouration of the mixture. The phases were separated and the aqueous phase was extracted with dichloromethane. The organic phases were gathered and washed with brine, dried over MgSO_4 and the solvent were evaporated. The solid crude were recrystallised in boiling methanol to afford 5.724 g of thiosulfonate **452b**.

Aspect: white needles

Yield: 90%

TLC: $R_f \approx 0.45$ (cHex/AcOEt: 9/1), visualised by UV and KMnO_4

m_p : 51–53 °C

$^1\text{H NMR}$ (500 MHz, CDCl_3): δ (ppm) **7.81** (d, 2H, $J = 8.2$ Hz, $2 \times \text{C}^2\text{H}$), **7.35** (d, 2H, $J = 8.2$ Hz, $2 \times \text{C}^3\text{H}$), **2.50** (s, 3H, C^6H_3), **2.46** (s, 3H, C^5H_3)

$^{13}\text{C NMR}$ (126 MHz, CDCl_3): δ (ppm) **144.95** (C_q^4), **141.15** (C_q^1), **129.98** ($2 \times \text{C}^3\text{H}$), **127.34** ($2 \times \text{C}^2\text{H}$), **21.78** (C^6H_3), **18.13** (C^5H_3)

IR: $\bar{\nu}$ (cm^{-1}) 1425, 1326, 1291, 1138, 809

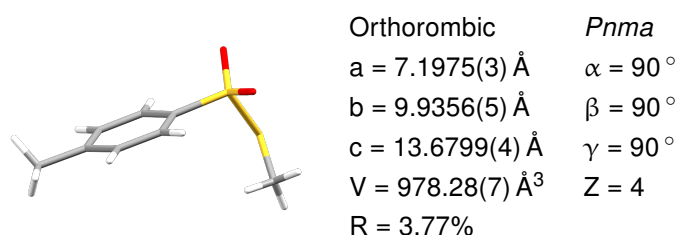
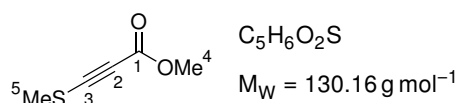


Figure 8.5: X-ray structure of **452b** and parameters of the crystal. Recrystallisation from boiling methanol.

Methyl 3-(methylthio)propiolate (**453b**)



This compound was synthesised according to Minakata *et al.*³⁸

In a dry 250 mL two-neck flask under argon atmosphere, a solution of DIPA (9.5 mL, 67.8 mmol, 2.0 eq.) in 45 mL of anhydrous THF was cooled down to -78°C . A solution of hexyllithium 2.5 M in hexanes (13.5 mL, 33.8 mmol, 1.0 eq.) was added dropwise and the solution was stirred ten minutes at -78°C . Methyl propiolate (**441**) (3.0 mL, 33.7 mmol, 1.0 eq.) was added dropwise and the mixture was stirred thirty minutes at -78°C . A solution of thiosulfonate **452b** (6.897 g, 34.1 mmol, 1.0 eq.) dissolved in 60 mL of anhydrous THF was added dropwise. The resulting mixture was stirred thirty minutes at -78°C , then allowed to warm up to room temperature and stirred for another thirty minutes. The reaction was quenched with a saturated solution of NH_4Cl and the phases were separated. The aqueous phase was extracted with dichloromethane. The organic phase was dried over MgSO_4 , filtered off and the solvents were evaporated. The crude oil was purified by flash chromatography on silica gel (cHex/AcOEt: 100/0 \rightarrow 99/1 \rightarrow 98/2) to give 3.253 g of propiolate **453b**.

Aspect: colourless liquid

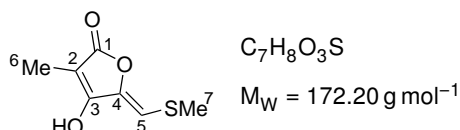
Yield: 74%

TLC: $R_f \approx 0.54$ (cHex/AcOEt: 8/2), visualised by UV and *p*-anisaldehyde

$^1\text{H NMR}$ (500 MHz, CDCl_3): δ (ppm) **3.77** (s, 3H, C^4H_3), **2.49** (s, 3H, C^5H_3)

$^{13}\text{C NMR}$ (126 MHz, CDCl_3): δ (ppm) **153.51** (C_q^1), **86.41** (C_q^2), **85.83** (C_q^3), **52.63** (C^4H_3), **18.74** (C^5H_3)

IR: $\bar{\nu}$ (cm^{-1}) 2154, 1699, 1433, 1231, 740

(Z)-5-((Methylthio)methylene)-4-hydroxy-3-methylfuran-2(5H)-one (455b)

In a dry 500 mL two-neck flask under argon atmosphere, DIPA (4.8 mL, 34.3 mmol, 1.5 eq.) was dissolved in 150 mL of anhydrous THF and cooled down to -78°C . A solution of hexyllithium 2.5 M in hexane (9.4 mL, 23.5 mmol, 1.0 eq.) was added dropwise and the solution was stirred for ten minutes at -78°C . Then, *tert*-butyl propionate (**440**) (3.5 mL, 23.6 mmol, 1.0 eq.) was added dropwise and the resulting mixture was stirred for thirty minutes at -78°C . A solution of propiolate **453b** (3.007 g, 23.1 mmol, 1.0 eq.) dissolved in 40 mL of anhydrous THF was added dropwise. The solution turned yellow and was stirred thirty minutes at -78°C . The reaction mixture was allowed to warm up to room temperature and was quenched with a saturated solution of NH_4Cl . The phases were separated and the aqueous phase was extracted with dichloromethane. The organic phases were gathered, dried over MgSO_4 , filtered off and the solvents were evaporated. The crude oil was dried under vacuum, then dissolved in 50 mL of dichloromethane. TFA (0.65 mL, 11.7 mmol, 0.51 eq.) was added dropwise at room temperature and a precipitate appeared. The mixture was stirred overnight. The solid formed was filtered, washed with dichloromethane and pentane to give 1.331 g of **455b**.

Aspect: white powder

Yield: 33%

TLC: $R_f \approx 0.28$ (cHex/AcOEt/AcOH: 7/3/0.5), visualised by UV and KMnO_4

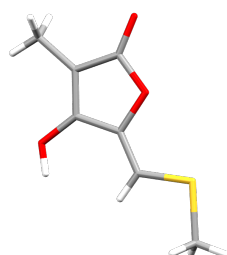
m_p: 196-199 $^{\circ}\text{C}$

¹H NMR (500 MHz, acetone-*d*₆): δ (ppm) **6.20** (s, 1H, C⁵H), **2.46** (s, 3H, C⁷H₃), **1.73** (s, 3H, C⁶H₃)

¹³C NMR (500 MHz, acetone-*d*₆): δ (ppm) **172.73** (C_q¹), **163.07** (C_q³), **141.81** (C_q⁴), **110.43** (C⁵H), **97.62** (C_q²), **17.22** (C⁷H₃), **6.11** (C⁶H₃)

IR: $\bar{\nu}$ (cm⁻¹) 3400-3100, 3051, 1717, 1644, 1623, 1421, 1371, 1292, 1141, 1067, 824

HRMS (ESI+): for $[\text{M}+\text{H}]^+$ calc.: 173.0272, found: 173.0267

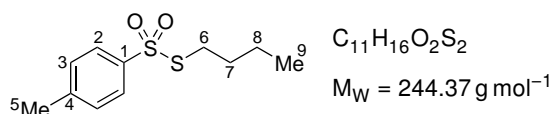


Monoclinic $P2_1/m$
 $a = 6.7967(4) \text{ \AA}$ $\alpha = 90^{\circ}$
 $b = 6.2975(5) \text{ \AA}$ $\beta = 91.117(6)^{\circ}$
 $c = 9.0648(5) \text{ \AA}$ $\gamma = 90^{\circ}$
 $V = 387.92(4) \text{ \AA}^3$ $Z = 2$
 $R = 4.24\%$

Figure 8.6: X-ray structure of **455b** and parameters of the crystal. Recrystallisation from boiling ethyl acetate.

8.3.3 Butylthiomethylenefuranone 455c

S-Butyl 4-methylbenzenesulfonothioate (452c)



The compound was prepared according to the procedure reported by Fujiki *et al.*³⁷

In a 250 mL two-neck flask under argon atmosphere, butyl disulfide (3.0 mL, 15.8 mmol, 1.0 eq.) was dissolved in 100 mL of dichloromethane and sodium *p*-toluene sulfinate (8.390 g, 47.1 mmol, 3.0 eq.) was added (as suspension) to the solution. Iodine (10.059 g, 39.6 mmol, 2.5 eq.) was then added and the dark resulting mixture was stirred overnight at room temperature. A saturated solution of Na₂S₂O₃ was added until the decolouration of the solution and the phases were separated. The aqueous phase was extracted with dichloromethane and the gathered organic phases were washed with brine. The organic phase was then dried over MgSO₄ and the solvent evaporated to give a golden oil. The crude was filtered through a short pad of silica using dichloromethane as eluant and the solvent was evaporated to give 7.653 g of thiosulfonate **452c**.

Aspect: golden oil

Yield: quantitative

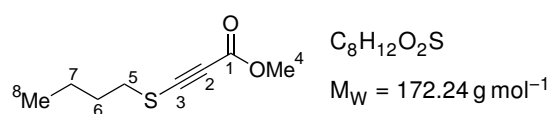
TLC: R_f ≈ 0.59 (cHex/AcOEt: 8/2), visualised by UV and KMnO₄

¹H NMR (500 MHz, CDCl₃): δ (ppm) **7.80** (d, 2H, *J* = 8.2 Hz, 2 × C²H), **7.34** (d, 2H, *J* = 8.2 Hz, 2 × C³H), **2.97** (t, 2H, *J* = 7.5 Hz, C⁶H₂), **2.44** (s, 3H, C⁵H₃), **1.57** (tt, 2H, *J* = 7.5; 7.5 Hz, C⁷H₂), **1.32** (qt, 2H, *J* = 7.5; 7.5 Hz, C⁸H₂), **0.84** (t, 3H, *J* = 7.5 Hz, C⁹H₃)

¹³C NMR (126 MHz, CDCl₃): δ (ppm) **144.77** (C_q⁴), **142.11** (C_q¹), **129.91** (2 × C³H), **127.11** (2 × C²H), **35.79** (C⁶H₂), **30.66** (C⁷H₂), **21.80** (C⁸H₂), **21.76** (C⁵H₃), **13.50** (C⁹H₃)

IR: ν̄ (cm⁻¹) 1594, 1323, 1138, 812

Methyl 3-(butylthio)propionate (453c)



This compound was synthesised according to Minakata *et al.*³⁸

In a dry 100 mL two-neck flask under argon atmosphere, DIPA (1.6 mL, 11.4 mmol, 1.0 eq.) was dissolved in 15 mL of anhydrous THF and cooled down to -78 °C. A 2.5 M solution of hexyllithium in hexane (4.5 mL, 11.25 mmol, 1.0 eq.) was added dropwise and the solution was stirred ten minutes at -78 °C. Methyl propionate (**441**) (1.0 mL, 11.24 mmol, 1.0 eq.) was added dropwise and the mixture was stirred half an hour at -78 °C. A solution of thiosulfonate **452c** (2.768 g, 11.3 mmol, 1.0 eq.) dissolved in 20 mL of anhydrous THF was added dropwise to the solution which was stirred for thirty minutes at -78 °C, then warmed up to room temperature and stirred for an extra thirty minutes. The mixture was quenched with a saturated solution of NH₄Cl and the phases were separated. The aqueous phase was extracted with diethyl ether and the gathered organic phases were dried over MgSO₄, then the solvent was evaporated. The crude oil was purified by flash chromatography on silica gel (cHex/AcOEt: 99/1) to give 1.4142 g of propionate **453c**.

Aspect: golden oil

Yield: 73%

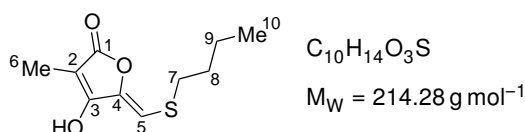
TLC: $R_f \approx 0.70$ (cHex/AcOEt: 8/2), visualised by UV and KMnO_4

$^1\text{H NMR}$ (500 MHz, CDCl_3): δ (ppm) **3.76** (s, 3H, C^4H_3), **2.82** (t, 2H, $J = 7.5$ Hz, C^5H_2), **1.74** (tt, 2H, $J = 7.5$; 7.5 Hz, C^6H_2), **1.44** (qt, 2H, $J = 7.5$; 7.5 Hz, C^7H_2), **0.94** (t, 3H, $J = 7.5$ Hz, C^8H_3)

$^{13}\text{C NMR}$ (126 MHz, CDCl_3): δ (ppm) **153.57** (C_q^1), **87.36** (C_q^2), **84.98** (C_q^3), **56.60** (C^4H_3), **35.39** (C^5H_2), **31.39** (C^6H_2), **21.40** (C^7H_2), **13.60** (C^8H_3)

IR: $\bar{\nu}$ (cm^{-1}) 2155, 1702, 1433, 1235

(Z)-5-((Butylthio)methylene)-4-hydroxy-3-methylfuran-2(5H)-one (455c)



In a dry 100 mL two-neck flask under argon atmosphere, DIPA (0.75 mL, 5.35 mmol, 1.3 eq.) was dissolved in 35 mL of anhydrous THF and cooled down to -78°C . A 2.5 M solution of hexyllithium (2.0 mL, 5.0 mmol, 1.2 eq.) in hexane was added dropwise and the mixture was stirred ten minutes at -78°C . Then, *tert*-butyl propionate (**440**) (0.65 mL, 4.32 mmol, 1.1 eq.) was added dropwise and the solution was stirred thirty minutes at -78°C . A solution of propiolate **453c** (700 mg, 4.06 mmol, 1.0 eq.) in 15 mL of anhydrous THF was added dropwise and the solution was stirred half an hour at -78°C . The solution was then warmed up to room temperature and quenched with a saturated solution of NH_4Cl . The phases were separated and the aqueous phase was extracted with diethyl ether. The organic phases were gathered, dried over MgSO_4 and the solvents were evaporated. The crude oil was transferred in a 50 mL flask and dissolved in 10 mL of dichloromethane. TFA (0.50 mL, 9.02 mmol, 2.0 eq.) was added dropwise and the solution was stirred overnight at room temperature. Addition of pentane allowed a precipitate to form. The solid was filtered off, washed with pentane, and vacuum dried to give 317 mg of butenolide **455c**.

Aspect: white powder

Yield: 36%

TLC: $R_f \approx 0.42$ (cHex/AcOEt/AcOH: 5/5/0.5), visualised by UV and KMnO_4

m_p : 117-119 $^\circ\text{C}$

$^1\text{H NMR}$ (500 MHz, acetone- d_6): δ (ppm) **10.26** (s, broad, 1H, OH), **6.24** (s, 1H, C^5H), **2.91** (t, 2H, $J = 7.4$ Hz, C^7H_2), **1.73** (s, 3H, C^6H_3), **1.67** (m, 2H, C^8H_2), **1.45** (m, 2H, C^9H_2), **0.92** (t, 3H, $J = 7.4$ Hz, C^{10}H_3)

$^{13}\text{C NMR}$ (500 MHz, acetone- d_6): δ (ppm) **169.93** (C_q^1), **161.23** (C_q^3), **141.52** (C_q^4), **107.29** (C^5H), **98.12** (C_q^2), **34.16** (C^7H_2), **33.30** (C^8H_2), **22.13** (C^9H_2), **13.83** (C^{10}H_3), **6.41** (C^6H_3)

IR: $\bar{\nu}$ (cm^{-1}) 3300-3100, 1707, 1642, 1622, 1421, 1296, 1147, 1066

HRMS (ESI+): for $[\text{M}+\text{H}]^+$ calc.: 215.0736, found: 215.0740

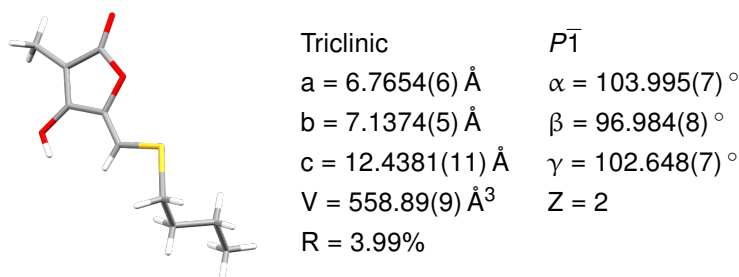
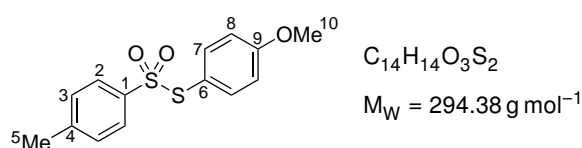


Figure 8.7: X-ray structure of **455c** and parameters of the crystal. Crystallisation by slow evaporation from dichloromethane.

8.3.4 (4-Methoxyphenyl)thiomethylenefuranone **455d**

S-(4-Methoxyphenyl) 4-methylbenzenesulfonothioate (**452d**)



The compound was prepared according to the procedure reported by Fujiki *et al.*³⁷

In a 250 mL two-neck flash under argon atmosphere, 4-methoxythiophenol (2.0 mL, 16.3 mmol, 1.0 eq.) was dissolved in 100 mL of dichloromethane. Then, Et_3N (2.4 mL, 17.3 mmol, 1.1 eq.), sodium *p*-toluenesulfinate (8.714 g, 48.9 mmol, 3.0 eq.) and iodine (12.391 g, 48.8 mmol, 3.0 eq.) were added, respectively. The solution turned dark and was stirred overnight at room temperature. It was then quenched with a saturated solution of $Na_2S_2O_3$ (until decolouration) and the phases were separated and the aqueous phase was extracted with dichloromethane. The organic phases were gathered and dried over $MgSO_4$ to give a yellowish oil. This oil was dissolved in 30 mL of methanol and let in the fridge overnight to crystallise. The crystals were filtered off and washed with cold methanol to give 3.184 g of thiosulfonate **452d**.

Aspect: white crystals

Yield: 67%

TLC: $R_f \approx 0.33$ (cHex/AcOEt: 8/2), visualised by UV and $KMnO_4$

m_p : 45-47 °C

1H NMR (500 MHz, $CDCl_3$): δ (ppm) **7.43** (d, 2H, $J = 8.1$ Hz, $2 \times C^2H$), **7.25** (d, 2H, $J = 8.4$ Hz, $2 \times C^7H$), **7.20** (d, 2H, $J = 8.1$ Hz, $2 \times C^3H$), **6.83** (d, 2H, $J = 8.4$ Hz, $2 \times C^8H$), **3.81** (s, 3H, $C^{10}H_3$), **2.41** (s, 3H, C^5H_3)

^{13}C NMR (126 MHz, $CDCl_3$): δ (ppm) **162.33** (C^9_q), **144.70** (C^4_q), **140.34** (C^1_q), **138.42** ($2 \times C^7H$), **129.49** ($2 \times C^3H$), **127.69** ($2 \times C^2H$), **118.76** (C^6_q), **115.03** ($2 \times C^8H$), **55.58** ($C^{10}H_3$), **21.78** (C^5H_3)

IR: $\bar{\nu}$ (cm^{-1}) 1586, 1569, 1489, 1330, 1249, 1134, 835, 812

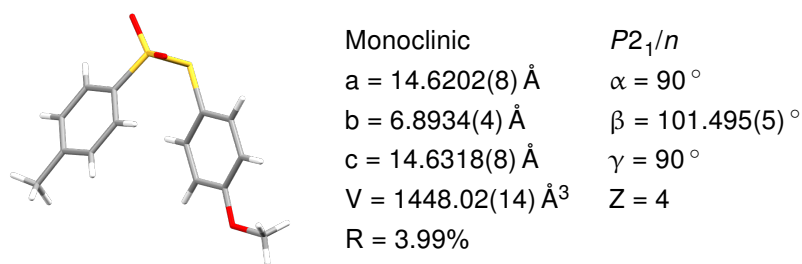
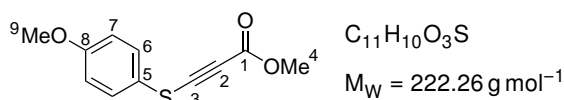


Figure 8.8: X-ray structure of **452d** and parameters of the crystal. Crystallisation in cold methanol.

Methyl 3-((4-methoxyphenyl)thio)propiolate (**453d**)



This compound was synthesised according to Minakata *et al.*³⁸

In a 100 mL two-neck flask under argon atmosphere, DIPA (1.8 mL, 12.8 mmol, 1.1 eq.) was dissolved in 15 mL of anhydrous THF and cooled down to -78°C . A 2.5 M solution of hexyllithium in hexane (4.5 mL, 11.3 mmol, 1.0 eq.) was added dropwise and the resulting mixture was stirred ten minutes at -78°C . Methyl propiolate (**441**) (1.0 mL, 11.24 mmol, 1.0 eq.) was then added dropwise and the mixture was stirred half an hour at -78°C . A solution of thiosulfonate **452d** (3.329 g, 11.3 mmol, 1.0 eq.) in 20 mL of anhydrous THF was added dropwise at -78°C and the solution was stirred half an hour at that temperature and then warmed up to room temperature and stirred for an extra thirty minutes. The mixture was quenched with a saturated solution of NH_4Cl , the phases were separated and the aqueous phase was extracted with diethyl ether. The organic phases were gathered, dried over MgSO_4 and the solvent evaporated. The crude dark oil was purified by flash chromatography on silica gel (cHex/AcOEt: 100/0 \rightarrow 99/1 \rightarrow 98/2) to give 915 mg of propiolate **453d**.

Aspect: dark red oil

Yield: 37%

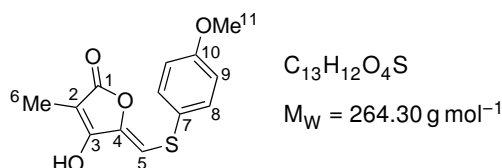
TLC: $R_f \approx 0.43$ (cHex/AcOEt: 8/2), visualised by UV and KMnO_4

$^1\text{H NMR}$ (500 MHz, CDCl_3): δ (ppm) **7.41** (d, 2H, $J = 8.9 \text{ Hz}$, $2 \times C^6\text{H}$), **6.92** (d, 2H, $J = 8.9 \text{ Hz}$, $2 \times C^7\text{H}$), **3.81** (s, 3H, $C^9\text{H}_3$), **3.78** (s, 3H, $C^4\text{H}_3$)

$^{13}\text{C NMR}$ (126 MHz, CDCl_3): δ (ppm) **160.16** (C^8_{q}), **153.52** (C^1_{q}), **130.67** ($2 \times C^6\text{H}$), **119.33** (C^5_{q}), **115.54** ($2 \times C^7\text{H}$), **89.74** (C^2_{q} or C^3_{q}), **82.40** (C^2_{q} or C^3_{q}), **55.60** ($C^9\text{H}_3$), **52.73** ($C^4\text{H}_3$)

IR: $\bar{\nu}$ (cm^{-1}) 2157, 1702, 1591, 1493, 1234, 1173, 1024, 822

(*Z*)-4-Hydroxy-5-(((4-methoxyphenyl)thio)methylene)-3-methylfuran-2(5*H*)-one (**455d**)



In a 100 mL two-neck flask under argon atmosphere, DIPA (0.40 mL, 2.85 mmol, 1.2 eq.) was dissolved in 20 mL of anhydrous THF and cooled down to -78°C . A 2.5 M solution of hexyllithium

in hexane (1.1 mL, 2.75 mmol, 1.2 eq.) was added dropwise and the resulting mixture was stirred for ten minutes at $-78\text{ }^{\circ}\text{C}$. Then, *tert*-butyl propionate (**440**) (0.40 mL, 2.66 mmol, 1.2 eq.) was added dropwise and the mixture was stirred half an hour. A solution of propionate **453d** (510 mg, 2.29 mmol, 1.0 eq.) dissolved in 10 mL of anhydrous THF was added to the solution at $-78\text{ }^{\circ}\text{C}$ and stirred one hour. The mixture was warmed up to room temperature and quenched with a saturated solution of NH_4Cl . The phases were separated and the aqueous phase extracted with diethyl ether. The organic phases were gathered, dried over MgSO_4 and the solvent evaporated. The orange oil was transferred to a 50 mL flask and dissolved in 10 mL of dichloromethane. TFA (0.20 mL, 3.61 mmol, 1.6 eq.) was added dropwise and a yellow solid precipitated. The precipitate was filtered, washed with dichloromethane and pentane, and vacuum dried. It was recrystallised from boiling AcOEt to give 229 mg of **455d** as yellow needles.

Aspect: yellow needles

Yield: 38%

TLC: $R_f \approx 0.48$ (cHex/AcOEt/AcOH: 5/5/0.5), visualised by UV and KMnO_4

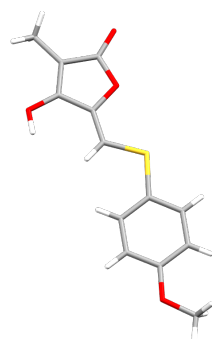
m_p : 178-181 $^{\circ}\text{C}$

$^1\text{H NMR}$ (500 MHz, CDCl_3): δ (ppm) **10.35** (s, 1H, OH), **7.47** (d, 2H, $J = 8.8\text{ Hz}$, $2 \times \text{C}^8\text{H}$), **7.00** (d, 2H, $J = 8.8\text{ Hz}$, $2 \times \text{C}^9\text{H}$), **6.28** (s, 1H, C^5H), **3.82** (s, 3H, C^{11}H_3), **1.76** (s, 3H, C^6H_3)

$^{13}\text{C NMR}$ (126 MHz, CDCl_3): δ (ppm) **169.67** (C_q^1), **161.41** (C_q^3), **160.95** (C_q^{10}), **141.55** (C_q^4), **133.52** ($2 \times \text{C}^8\text{H}$), **124.81** (C_q^7), **115.99** ($2 \times \text{C}^9\text{H}$), **107.04** (C^5H), **99.07** (C_q^2), **55.77** (C^{11}H_3), **6.48** (C^6H_3)

IR: $\bar{\nu}$ (cm^{-1}) 3100-2700, 1706, 1642, 1612, 1498, 1243, 1062, 814

HRMS (ESI+): for $[\text{M}+\text{H}]^+$ calc.: 265.0529, found: 265.0517

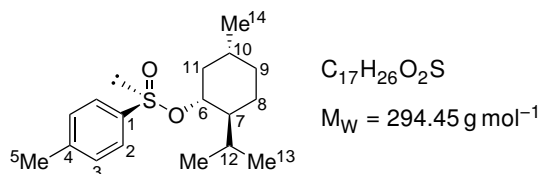


Monoclinic	$P2_1/n$
$a = 7.5237(3)\text{ \AA}$	$\alpha = 90^\circ$
$b = 14.2157(6)\text{ \AA}$	$\beta = 97.566(4)^\circ$
$c = 11.6448(4)\text{ \AA}$	$\gamma = 90^\circ$
$V = 1234.63(9)\text{ \AA}^3$	$Z = 4$
$R = 4.42\%$	

Figure 8.9: X-ray structure of **455d** and parameters of the crystal. Recrystallisation from boiling ethyl acetate.

8.4 Synthesis of the sulfinylquinones

8.4.1 (*l*)-Menthyl (–)-(SS)-*para*-toluenesulfinate ((SS)-292)



This compound was prepared following the procedure reported by Solladié *et al.*³⁹

In a 1 L three-neck flask under argon atmosphere, SOCl₂ (62 mL, 850 mmol, 3.0 eq.) were dissolved in 175 mL of anhydrous toluene. Sodium *p*-toluenesulfinate (**451**) (50.232 g, 282 mmol, 1.0 eq.) was added portionwise to the solution, which turned yellow and warmed up a bit. After two hours of agitation at room temperature, the solvents were evaporated under reduced pressure (to one third). The resulting residue was dissolved with 100 mL of anhydrous diethyl ether (the precipitation of NaCl was observed) and cooled down to 0 °C.

A solution of *l*-menthol (**472**) (48.536 g, 311 mmol, 1.1 eq.), dissolved in 50 mL of pyridine, was added over thirty minutes to the chloride solution. When the addition was finished, the mixture was stirred for two hours at room temperature.

The reaction mixture was carefully quenched at 0 °C with 100 mL of water. The phases were separated and the aqueous phase was extracted with diethyl ether. The organic phase was washed a solution of HCl (10%) and brine. It was then dried over MgSO₄, filtered off and the solvents were evaporated. The resulting golden oil was diluted with 40 mL of diethyl ether and was allowed to crystallise overnight. The white crystals were filtered and the solvents of the filtrate were evaporated. The residue was diluted with 75 mL of acetone, treated with 1 mL of 1 mL of HCl (37%) and left in the fridge to crystallise overnight. The process was repeated until wearing out of the mother liquors.

Aspect: white crystals

Yield: 79%

TLC: R_f ≈ 0.72 (cHex/AcOEt: 8/2), visualised by UV and *p*-anisaldehyde

m_p: 100-102 °C

[α]_D²⁰: –201.1 ° (c = 2.0; acetone)

¹H NMR (400 MHz, CDCl₃): δ (ppm) **7.60** (d, 2H, *J* = 8.3 Hz, × 2 C²H), **7.32** (d, 2H, *J* = 8.3 Hz, 2 × C³H), **4.12** (td, 1H, *J* = 10.8; 4.5 Hz, C⁶H), **2.41** (s, 3H, C⁵H₃), **2.31-2.24** (m, 1H, 1/2 × C¹¹H₂), **2.18-2.07** (m, 1H, C¹²H), **1.72-1.64** (m, 2H, 1/2 × C⁸H₂ + 1/2 × C⁹H₂), **1.55-1.41** (m, 1H, C¹⁰H), **1.40-1.30** (m, 1H, C⁷H), **1.22** (dd, 1H, *J* = 23.3; 12.0 Hz, 1/2 × C¹¹H₂), **1.09-0.97** (m, 1H, 1/2 × C⁸H₂), **0.96** (d, 3H, *J* = 6.5 Hz, C¹⁴H₃), **0.93-0.80** (m, 1H, 1/2 × C⁹H₂), **0.86** (d, 3H, *J* = 7.0 Hz, C¹³H₃), **0.71** (d, 3H, *J* = 7.0 Hz, C¹³H₃)

¹³C NMR (100 MHz, CDCl₃): δ (ppm) **143.07** (C_q¹), **142.27** (C_q⁴), **129.52** (2 × C³H), **124.90** (2 × C²H), **79.93** (C⁶H), **47.76** (C⁷H), **42.88** (C¹¹H₂), **33.93** (C⁹H₂), **31.63** (C¹⁰H), **25.11** (C¹²H), **23.05** (C⁸H₂), **22.02** (C¹⁴H₃), **21.41** (C⁵H₃), **20.81** (C¹³H₃), **15.40** (C¹³H₃)

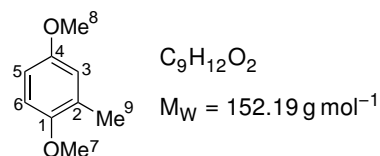
IR: ν̄ (cm⁻¹) 2948-2846, 1456, 1388, 1370, 1341, 1180, 1129, 1106, 1080, 1040, 1006, 951, 916, 881, 821, 778, 755

The experimental data were in agreement with those reported in the literature.³⁹

8.4.2 Sulfinylquinone 318a/SQ1

This sulfinylquinone was prepared following the synthetic sequence reported by Hanquet *et al.*^{8,40}

1,4-Dimethoxy-2-methylbenzene (474)



Into 500 mL two-neck flask under argon, methylhydroquinone (**473**) (9.995 g, 80.5 mmol, 1.0 eq.) was suspended into 200 mL of dichloromethane. An aqueous solution of NaOH (9.661 g, 255.3 mmol, 3.0 eq.) in 60 mL of water, was then added. After ten minutes, tetradecylammonium bromide (0.941 g, 1.439 mmol, 0.02 eq.) was added at once and Me_2SO_4 (31 mL, 327.6 mmol, 4.1 eq.) was added dropwise. After 45 minutes, NaOH (6.440 g, 161.0 mmol, 2.0 eq.) was added and the solution was vigorously stirred overnight. The next day, the phases were separated and the aqueous phase was extracted with dichloromethane. The organic phases were gathered and dried over MgSO_4 . The solution was filtered and the solvents were evaporated to give a colourless liquid. The filtration of this liquid through silica, using dichloromethane as eluent, gave 12.083 g of dimethoxytoluene **474**.

Aspect: colourless liquid

Yield: 98%

TLC: $R_f \approx 0.68$ (cHex/AcOEt: 8/2), visualised by UV and *p*-anisaldehyde

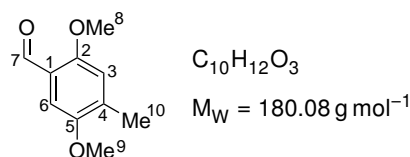
¹H NMR (400 MHz, CDCl_3): δ (ppm) **6.75** (d, 1H, $J = 8.7$ Hz, C^6H), **6.74** (d, 1H, $J = 3.1$ Hz, C^3H), **6.68** (dd, 1H, $J = 8.7$; 3.1 Hz, C^5H), **3.79** (s, 3H, C^7H_3), **3.76** (s, 3H, C^8H_3), **2.21** (s, 3H, C^9H_3)

¹³C NMR (100 MHz, CDCl_3): δ (ppm) **153.36** (C_q^4), **152.01** (C_q^1), **127.67** (C_q^2), **117.01** (C^3H), **110.71** (C^5H), **110.60** (C^6H), **55.62** (C^7H_3), **55.39** (C^8H_3), **16.32** (C^9H_3)

IR: $\bar{\nu}$ (cm^{-1}) 1498, 1464, 1442, 1280, 1218, 1179, 1156, 1129, 1047, 1030, 795, 710, 699

The experimental data were in agreement with those reported in the literature.^{8,40}

2,5-Dimethoxy-4-methylbenzaldehyde (475)



In a 250 mL two-neck flask under argon atmosphere and equipped with a condenser, POCl_3 (11.5 mL, 123.4 mmol, 1.7 eq.) was added dropwise on *N*-methylformanilide (15 mL, 121.5 mmol, 1.6 eq.). After ten minutes, dimethoxytoluene **474** (11.375 g, 74.7 mmol, 1.0 eq.) was added dropwise over the yellow mixture and the solution was heated up at 60 °C for 30 min. The mixture turned black and solidified. The solid was then broken into pieces and poured into 200 mL of iced water. The mixture was allowed to hydrolyse overnight. The next day, the solution was filtered and the solid rinsed with water. It was then dissolved in dichloromethane and the organic phase was dried over MgSO_4 and filtered. The solvents were evaporated to give a yellowish solid. This solid was purified by filtration over silica, using dichloromethane as eluent, to give 12.297 g of benzaldehyde **475**.

Aspect: Yellow solid

Yield: 92%

TLC: $R_f \approx 0.47$ (cHex/AcOEt: 8/2), visualised by UV and *p*-anisaldehyde

m_p : 77-78 °C

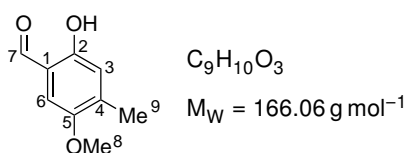
$^1\text{H NMR}$ (400 MHz, CDCl_3): δ (ppm) **10.39** (s, 1H, C^7H), **7.25** (s, 1H, C^6H), **6.81** (s, 1H, C^3H), **3.88** (s, 3H, C^8H_3), **3.83** (s, 3H, C^9H_3), **2.28** (s, 3H, C^{10}H_3)

$^{13}\text{C NMR}$ (100 MHz, CDCl_3): δ (ppm) **189.37** (C^7), **156.69** (C_q^2), **152.04** (C_q^5), **136.67** (C_q^4), **122.88** (C_q^1), **114.76** (C^3H), **107.68** (C^6H), **56.21** (C^8H_3), **55.82** (C^9H_3), **17.39** (C^{10}H_3)

IR: $\bar{\nu}$ (cm^{-1}) 1658, 1610, 1498, 1468, 1403, 1372, 1268, 1252, 1211, 1169, 1121, 1041

The experimental data were in agreement with those reported in the literature.^{8,40}

2-Hydroxy-5-methoxy-4-methylbenzaldehyde (476)



In a 500 mL two-neck flask under argon, equipped with a condenser and a dropping funnel, anhydrous AlCl_3 (9.830 g, 66.8 mmol, 1.0 eq.) was dissolved in 100 mL of MeCN. A solution of benzaldehyde **475** (12.052 g, 66.9 mmol, 1.0 eq.) into 100 mL of MeCN was added dropwise through the dropping funnel. The solution was heated up to 45 °C and anhydrous NaI (15.294 g, 102.0 mmol, 1.5 eq.) was added. The mixture was refluxed for two hours. The solution was cooled down to room temperature and the yellow solid formed during the reaction was filtered. The filtrate was evaporated to give a curry yellow solid. Both solids from the cake and the filtrate were dissolved in 200 mL of ethyl acetate and treated with 200 mL of a saturated solution of sodium potassium tartrate. The solution was vigorously stirred for two hours. The phases were separated and the aqueous phase was extracted with ethyl acetate. Organic phases were gathered and washed with a saturated solution of $\text{Na}_2\text{S}_2\text{O}_3$ (the organic phase cleared), then with brine, and were dried over MgSO_4 . The filtration and evaporation of the solution gave 11.069 g of yellow needles that can be used in the next reaction without any further purification. The analytic sample can be obtained by filtration over silica (using dichloromethane as eluent) or by recrystallisation in petroleum ether.

Aspect: yellow needles

Yield: 99%

TLC: $R_f \approx 0.45$ (cHex/AcOEt: 8/2), visualised by UV and *p*-anisaldehyde

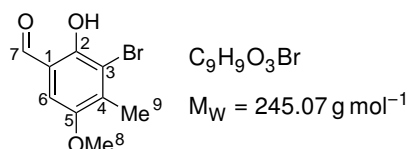
m_p : 103-105 °C

$^1\text{H NMR}$ (400 MHz, CDCl_3): δ (ppm) **10.78** (s, 1H, OH (phenol)), **9.81** (s, 1H, C^7H), **6.86** (s, 1H, C^6H), **6.80** (s, 1H, C^3H), **3.84** (s, 3H, C^8H_3), **2.26** (s, 3H, C^9H_3)

$^{13}\text{C NMR}$ (100 MHz, CDCl_3): δ (ppm) **195.52** (C^7), **156.32** (C_q^2), **151.40** (C_q^5), **139.14** (C_q^4), **119.67** (C^3H), **118.19** (C_q^1), **111.83** (C^6H), **55.87** (C^8H_3), **17.23** (C^9H_3)

IR: $\bar{\nu}$ (cm^{-1}) 1651, 1621, 1499, 1486, 1471, 1320, 1247, 1210, 1193, 1172, 1122, 1016, 789, 706

The experimental data were in agreement with those reported in the literature.^{8,40}

3-Bromo-2-hydroxy-5-methoxy-4-methylbenzaldehyde (477)

In a 500 mL two-neck flask under argon, equipped with a dropping funnel, benzaldehyde **476** (10.375 g, 62.5 mmol, 1.0 eq.) and anhydrous sodium acetate (7.908 g, 96.4 mmol, 1.5 eq.) were dissolved in 200 mL of glacial acetic acid. After a complete dissolution, a solution of Br_2 (3.25 mL, 63.3 mmol 1.0 eq.), in 15 mL of glacial acetic acid was added dropwise through the dropping funnel. After one hour, a precipitate appeared. After three hours, the mixture was filtered and the filtrate was evaporated to give a yellowish solid. Both solids from the cake and the filtrate were dissolved in dichloromethane and the organic phase was washed with saturated solutions of $Na_2S_2O_3$, $NaHCO_3$, and $NaCl$, successively. The organic phase was dried over $MgSO_4$, filtered, and the solvents were evaporated to give a yellow solid. The recrystallisation in boiling methanol gave 14.786 g of yellow crystals.

Aspect: Yellow crystals

Yield: 97%

TLC: $R_f \approx 0.58$ (cHex/AcOEt: 7/3), visualised by UV and *p*-anisaldehyde

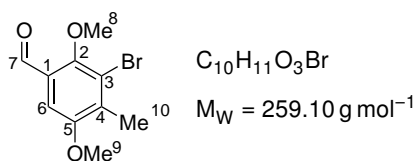
m_p : 106-107 °C

1H NMR (400 MHz, $CDCl_3$): δ (ppm) **11.43** (s, 1H, OH (phenol)), **9.80** (s, 1H, C^7H_3), **6.92** (s, 1H, C^6H), **3.86** (s, 3H, C^8H_3), **2.42** (s, 3H, C^9H_3)

^{13}C NMR (100 MHz, $CDCl_3$): δ (ppm) **195.21** (C^7), **153.16** (C^2_q), **151.43** (C^5_q), **138.66** (C^4_q), **117.89** (C^1_q), **115.01** (C^3_q), **111.36** (C^6H), **56.36** (C^8H_3), **17.12** (C^9H_3)

IR: $\bar{\nu}$ (cm^{-1}) 1647, 1616, 1459, 1359, 1323, 1210, 1196, 1122, 1033, 881, 843, 760, 650

The experimental data were in agreement with those reported in the literature.^{8,40}

3-Bromo-2,5-dimethoxy-4-methylbenzaldehyde (478)

In a 500 mL two-neck flask under argon atmosphere, bromophenol **477** (11.778 g, 48.1 mmol, 1.0 eq.) was dissolved in 100 mL of dichloromethane. An solution of $NaOH$ (2.885 g, 72.1 mmol, 1.5 eq.), in 50 mL of water, was added dropwise to the yellow solution. After ten minutes of agitation, tetradecylammonium bromide (1.507 g, 2.29 mmol, 0.05 eq.) was added at once and Me_2SO_4 (10.0 mL, 105.7 mmol, 2.2 eq.) was added dropwise. The mixture was vigorously stirred. After one hour, $NaOH$ (2.952 g, 73.8 mmol, 1.5 eq.) was added and the mixture was allowed to stir overnight. The next day, phases were separated and the aqueous phase was extracted with dichloromethane. The organic phases were gathered, washed with brine, and dried over $MgSO_4$. After evaporation of the solvent, a white solid was obtained. The crude was purified by filtration over silica gel using dichloromethane as eluent. After evaporation, 11.936 g of pure benzaldehyde **478** was obtained.

Aspect: White solid

Yield: 96%

TLC: $R_f \approx 0.59$ (cHex/AcOEt: 7/3), visualised by UV and *p*-anisaldehyde

m_p : 93–94 °C

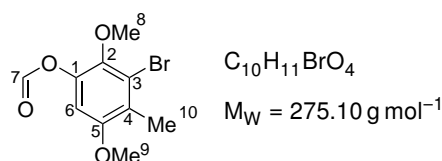
$^1\text{H NMR}$ (400 MHz, CDCl_3): δ (ppm) **10.31** (s, 1H, C^7H), **7.22** (s, 1H, C^6H), **3.93** (s, 3H, C^8H_3), **3.86** (s, 3H, C^9H_3), **2.39** (s, 3H, C^{10}H_3)

$^{13}\text{C NMR}$ (100 MHz, CDCl_3): δ (ppm) **189.29** (C^7H), **154.95** (C_q^2 ou C_q^5), **154.93** (C_q^2 ou C_q^5), **136.81** (C_q^4), **127.83** (C_q^1), **121.95** (C_q^3), **106.39** (C^6H), **64.05** (C^8H_3), **56.24** (C^9H_3), **17.08** (C^{10}H_3)

IR: $\bar{\nu}$ (cm^{-1}) 1688, 1596, 1466, 1388, 1368, 1216, 1195, 1109, 1037, 873, 697

The experimental data were in agreement with those reported in the literature.^{8,40}

3-Bromo-2,5-dimethoxy-4-methylphenyl formate



In a 500 mL two-neck flask under argon, *m*CPBA (70%) (13.656 g, 79.1 mmol, 1.7 eq.) was dissolved in 30 mL of dichloromethane. When *m*CPBA was completely dissolved, benzaldehyde **478** (11.864 g, 45.8 mmol, 1.0 eq.), dissolved in 150 mL of dichloromethane, was added dropwise to the solution. The mixture was stirred for 24 hours. The *meta*-chlorobenzoic acid precipitate formed during the reaction was filtered and washed with CH_2Cl_2 . The organic phase was washed with saturated solutions of $\text{Na}_2\text{S}_2\text{O}_3$, NaHCO_3 and NaCl , successively. The organic phase was dried over MgSO_4 and the solvent were evaporated to obtain 12.480 g of an orangish solid which was directly used in the next reaction without any further purification.

Aspect: Orangish solid

Yield: quantitative

TLC: $R_f \approx 0.57$ (cHex/AcOEt: 7/3), visualised by UV and *p*-anisaldehyde

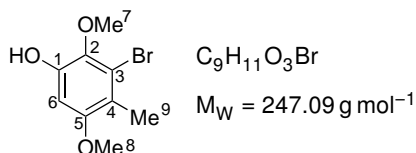
m_p : 82–84 °C

$^1\text{H NMR}$ (400 MHz, CDCl_3): δ (ppm) **8.28** (s, 1H, C^7H), **6.61** (s, 1H, C^6H), **3.79** (s, 3H, C^9H_3), **3.76** (s, 3H, C^8H_3), **2.31** (s, 3H, C^{10}H_3)

$^{13}\text{C NMR}$ (100 MHz, CDCl_3): δ (ppm) **159.31** (C^7H), **154.40** (C_q^5), **142.57** (C_q^2), **141.38** (C_q^1), **126.61** (C_q^4), **121.80** (C_q^3), **104.31** (C^6H), **61.18** (C^8H_3), **56.25** (C^9H_3), **16.02** (C^{10}H_3)

IR: $\bar{\nu}$ (cm^{-1}) 1765, 1469, 1443, 1394, 1375, 1331, 1216, 1132, 1119, 1083, 1039, 975, 885, 849, 742

The experimental data were in agreement with those reported in the literature.^{8,40}

3-Bromo-2,5-dimethoxy-4-methylphenol (479)

In a 250 mL flask equipped with a reirigerant, the previously synthesised 3-Bromo-2,5-dimethoxy-4-methylphenyl formate (9.327 g, 33.9 mmol, 1.0 eq.) was dissolved in 75 mL of refluxing methanol. An aqueous solution of NaOH (1.424 g, 35.6 mmol, 1.0 eq., dissolved in 15 mL of water, was added and the mixture directly darkened. After five minutes, the reaction mixture was cooled down to room temperature, the methanol was evaporated and the resulting black oil was dissolved in 100 mL of water. The solution was cooled down to 0 °C and HCl (37%) was added dropwise until the solution reached a pH value below 2. The light brown precipitate formed during acidification was filtered off and washed with cold water. The mother liquors were extracted with dichloromethane and the organic phase was evaporated to give a yellowish solid. Both solid were gathered and dissolved in dichloromethane and the organic phase was washed with brine and dried over $MgSO_4$. The evaporation of the solvent gave a yellow solid which was purified by recrystallisation from a hot 50/50 mixture of pentane and cyclohexane. After filtration, 7.306 g of yellow needles were obtained.

Aspect: Yellow needles

Yield: 93%

TLC: $R_f \approx 0.35$ (cHex/AcOEt: 8/2), visualised by UV and *p*-anisaldehyde

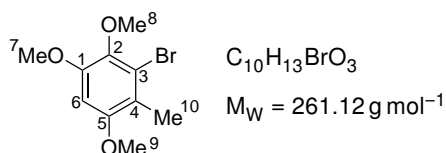
m_p : 91-92 °C

1H NMR (400 MHz, $CDCl_3$): δ (ppm) **6.50** (s, 1H, C^6H), **5.59** (s, 1H, OH (phenol)), **3.83** (s, 3H, C^2H_3), **3.77** (s, 3H, C^5H_3), **2.23** (s, 3H, C^9H_3)

^{13}C NMR (100 MHz, $CDCl_3$): δ (ppm) **154.98** (C^5_q), **147.60** (C^1_q), **137.97** (C^2_q), **119.60** (C^3_q), **119.01** (C^4_q), **98.27** (C^6H), **61.26** (C^7H_3), **56.14** (C^8H_3), **15.30** (C^9H_3)

IR: $\bar{\nu}$ (cm^{-1}) 3500-3200, 1606, 1582, 1483, 1446, 1409, 1378, 1314, 1202, 1167, 1123, 1035, 971, 863, 836, 812, 740, 696

The experimental data were in agreement with those reported in the literature.^{8,40}

3-Bromo-1,2,5-trimethoxy-4-methylbenzene (480)

In a 250 mL two-neck flask under argon atmosphere, phenol **479** (7.279 g, 29.5 mmol, 1.0 eq.) was dissolved in 100 mL of dichloromethane. An aqueous solution of NaOH (3.712 g, 92.8 mmol, 3.1 eq.), in 40 mL of water, was added dropwise. After ten minutes, tetradecylammonium bromide (1.090 g, 1.41 mmol, 0.05 eq.) was added at once and Me_2SO_4 (6.0 mmol, 63.4 mmol, 2.2 eq.) was added dropwise. After 30 minutes, NaOH (2.388 g, 59.7 mmol, 2.0 eq.) and the mixture was vigorously stirred overnight. The next day, the phases were separated and the aqueous phase was extracted with dichloromethane. The organic phases were gathered, washed with brine and dried over $MgSO_4$.

Evaporation of the solvent gave a white solid purified by filtration over silica using dichloromethane as eluent. After evaporation of the solvent, 7.259 g of trimethoxytoluene **480** was obtained.

Aspect: White solid

Yield: 95%

TLC: $R_f \approx 0.45$ (cHex/AcOEt: 8/2), visualised by UV and *p*-anisaldehyde

m_p: 58–60 °C

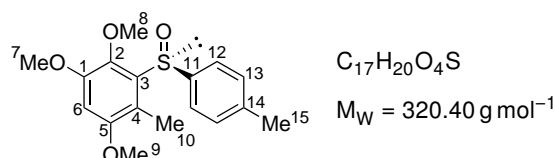
¹H NMR (400 MHz, CDCl₃): δ (ppm) **6.47** (s, 1H, C⁶H), **3.87** (s, 3H, C⁷H₃), **3.81** (s, 3H, C⁹H₃), **3.79** (s, 3H, C⁸H₃), **2.25** (s, 3H, C¹⁰H₃)

¹³C NMR (100 MHz, CDCl₃): δ (ppm) **154.29** (C⁵_q), **151.46** (C¹_q), **140.55** (C²_q), **121.72** (C³_q), **119.42** (C⁴_q), **96.86** (C⁶H), **60.70** (C⁸H₃), **56.56** (C⁷H₃), **56.41** (C⁹H₃), **15.45** (C¹⁰H₃)

IR: $\bar{\nu}$ (cm⁻¹) 1593, 1569, 1495, 1484, 1468, 1453, 1436, 1387, 1324, 1294, 1259, 1214, 1199, 1183, 1151, 1125, 1029, 1000, 971, 857, 819, 806, 740, 687

The experimental data were in agreement with those reported in the literature.^{8,40}

(–)-(S)-1,2,5-Trimethoxy-4-methyl-3-(*p*-tolylsulfinyl)benzene (**481**)



In a dry 100 mL two-neck flask under argon atmosphere equipped with a condenser, magnesium (819 mg, 33.6 mmol, 1.2 eq.) was suspended in 20 mL of dry THF. To that solution, bromide **481** (7.205 g, 27.6 mmol, 1.0 eq.), dissolved in 15 mL of dry THF, was added dropwise to the magnesium suspension. An iodine crystal was added to activate the magnesium. Once the organomagnesium was activated, the mixture was stirred for three to four hours.

The solution, containing the Grignard's reagent, was cooled down to 0 °C and cannulated over a solution of 8.142 g of (–)-(SS)-menthyl sulfinate (SS)-**292** (27.65 mmol, 1.0 eq.) (dissolved in 50 mL of dry THF under argon atmosphere and cooled down to 0 °C). The reaction was stirred overnight.

The next day, the reaction was slowly hydrolysed at 0 °C with 50 mL of a saturated solution of NH₄Cl. The phases were separated and the aqueous phase was extracted with diethyl ether. Organic phases were gathered, washed with brine and dried over MgSO₄. After evaporation of the solvent, a waxy solid was obtained. Trituration of this solid with diethyl ether gave 4.458 g of a light brown powder after filtration.

Aspect: light brown powder

Yield: 51%

TLC: $R_f \approx 0.22$ (cHex/AcOEt: 7/3), visualised by UV and *p*-anisaldehyde

m_p: 125–127 °C

[α]_D²⁰: –155.9° (c = 1.35; acetone)

¹H NMR (400 MHz, CDCl₃): δ (ppm) **7.47** (d, 2H, *J* = 7.3 Hz, 2 × C¹²H), **7.22** (d, 2H, *J* = 7.3 Hz, 2 × C¹³H), **6.58** (s, 1H, C⁶H), **3.87** (s, 3H, C⁷H₃), **3.82** (s, 3H, C⁸H₃), **3.78** (s, 3H, C⁹H₃), **2.35** (s, 3H, C¹⁵H₃), **2.26** (s, 3H, C¹⁰H₃)

¹³C NMR (100 MHz, CDCl₃): δ (ppm) **154.73** (C⁵_q), **151.13** (C¹_q), **141.84** (C²_q), **141.60** (C¹¹), **139.93** (C¹⁴), **137.49** (C³_q), **129.59** (2 × C¹³H), **124.42** (2 × C¹²H), **119.96** (C⁴_q), **100.65** (C⁶H), **61.82** (C⁸H₃)

56.47 (C^9H_3), **56.35** (C^7H_3), **21.41** ($C^{15}H_3$), **10.02** ($C^{10}H_3$)

IR: $\bar{\nu}$ (cm^{-1}) 1593, 1479, 1313, 1216, 1198, 1180, 1124, 1081, 1038, 973, 859, 818, 621

The experimental data were in agreement with those reported in the literature.^{8,40}

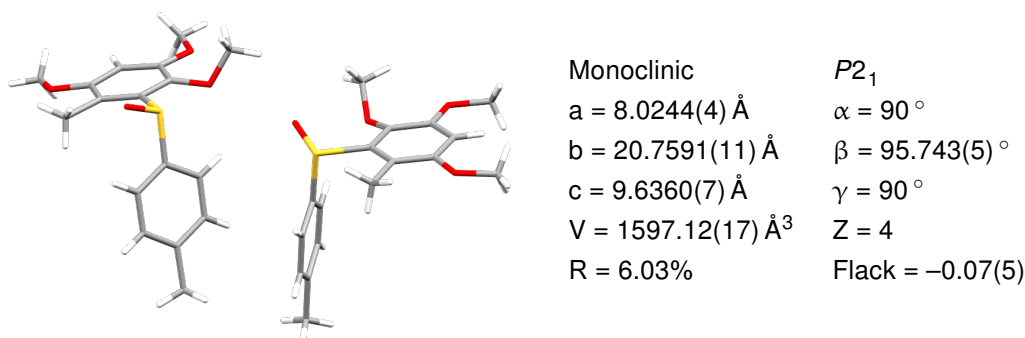
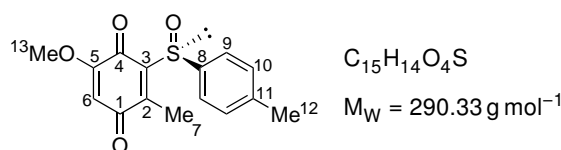


Figure 8.10: X-ray structure of **481** and parameters of the crystal. Crystallisation by slow evaporation from dichloromethane.

(+)-(S)-5-Methoxy-2-methyl-3-(*p*-tolylsulfinyl)cyclohexa-2,5-diene-1,4-dione (318a/SQ1)



In a 500 mL flask, sulfoxide **481** (4.344 g, 13.6 mmol, 1.0 eq.) was dissolved in 150 mL of acetonitrile. A aqueous solution of CAN (18.703 g, 34.1 mmol, 2.5 eq.) in 150 mL of water was quickly added to the first mixture. The solution turned bright red. After 40 minutes, the solvents were evaporated and the aqueous phase was extracted with dichloromethane. Organic phases were gathered, washed with brine and dried over $MgSO_4$. The evaporation of the solvents gave a red solid which was purified by recrystallisation from boiling methanol. The crystals were filtered to obtain 3.738 g of red needles.

Aspect: Red needles

Yield: 95%

TLC: $R_f \approx 0.43$ (cHex/AcOEt: 5/5), visualised by UV and *p*-anisaldehyde

m_p : 130-132 °C

$[\alpha]_D^{20}$: +469.4 ° ($c = 0.98$; CH_2Cl_2)

1H NMR (500 MHz, $CDCl_3$): δ (ppm) **7.64** (d, 2H, $J = 8.1$ Hz, $2 \times C^9H$), **7.29** (d, 2H, $J = 8.1$ Hz, $2 \times C^{10}H$), **5.96** (s, 1H, C^6H), **3.79** (s, 3H, $C^{13}H_3$), **2.50** (s, 3H, C^7H_3), **2.39** (s, 3H, $C^{12}H_3$)

^{13}C NMR (126 MHz, $CDCl_3$): δ (ppm) **185.37** (C_q^1), **179.30** (C_q^4), **157.96** (C_q^5), **148.23** (C_q^2), **144.67** (C_q^3), **141.89** (C_q^{11}), **139.48** (C_q^8), **130.24** ($2 \times C^{10}H$), **125.02** ($2 \times C^9H$), **108.06** (C^6H), **56.68** ($C^{13}H_3$), **21.54** ($C^{12}H_3$), **9.55** (C^7H_3)

IR: $\bar{\nu}$ (cm^{-1}) 1665, 1629, 1593, 1354, 1305, 1200, 1184, 1081, 1046, 1013, 993, 861, 814, 796, 765, 704

The experimental data were in agreement with those reported in the literature.^{8,40}

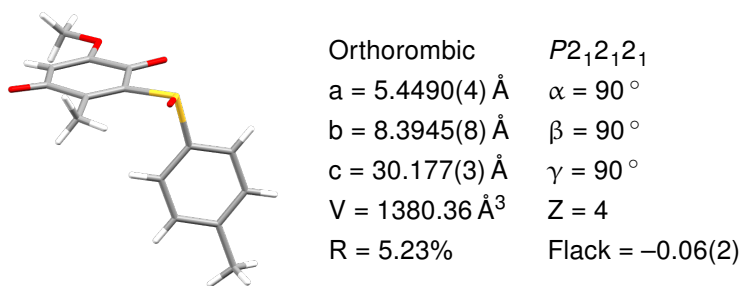
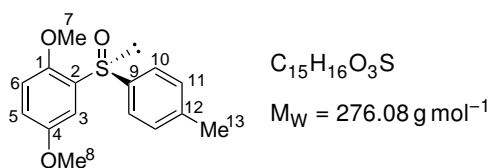


Figure 8.11: X-ray structure of **318a** and parameters of the crystal. Recrystallisation from boiling methanol.

8.4.3 Sulfinylquinone 297/SQ2

(-)-(S)-1,4-Dimethoxy-2-(*p*-tolylsulfinyl)benzene (**295**)



The protocol of Carreño *et al.* has been used with slight modifications.⁴¹

In a 250 mL two-neck flask under argon atmosphere, dimethoxybenzene **298** (2.059 g, 15.0 mmol, 1.0 eq.) was dissolved in 60 mL of anhydrous THF. The solution was cooled down to 0 °C and a 2.5 M hexyllithium solution in hexane (6.0 mL, 15.0 mmol, 1.0 eq.) was added dropwise. The solution was stirred for one hour at 0 °C, then cooled down to -78 °C and quickly cannulated over a solution of (-)-(SS)-menthyl sulfinatate (SS)-**292** (4.483 g, 15.0 mmol, 1.0 eq.) in 40 mL of anhydrous THF (also cooled down to -78 °C). The mixture was stirred for two hours at -78 °C. The solution was allowed to warm up to room temperature and quenched with 100 mL of water. The phases were separated and the aqueous phase was extracted with dichloromethane. The organic phase was dried over MgSO_4 , filtered off and evaporated. The crude was purified by flash chromatography on silica gel (cyclohexane/AcOEt: 9/1 \rightarrow 8/2 \rightarrow 7/3) to give 3.188 g of sulfoxide **295**.

Aspect: white solid

Yield: 77%

TLC: $R_f \approx 0.54$ (cHex/AcOEt: 5/5), visualised by UV and *p*-anisaldehyde

m_p : 75-77 °C

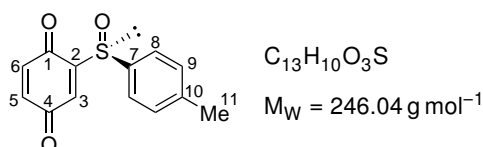
$[\alpha]_D^{20}$: -20.6 ° (c = 1.06; CHCl_3)

$^1\text{H NMR}$ (400 MHz, CDCl_3): δ (ppm) **7.58** (d, 2H, $J = 8.1$ Hz, $2 \times \text{C}^{10}\text{H}$), **7.48** (d, 1H, $J = 3.1$ Hz, C^3H), **7.21** (d, 2H, $J = 8.1$ Hz, $2 \times \text{C}^{11}\text{H}$), **6.90** (dd, 1H, $J = 8.9$; 3.1 Hz, C^5H), **6.77** (d, 1H, $J = 8.9$ Hz, C^6H), **3.82** (s, 3H, C^8H_3), **3.72** (s, 3H, C^7H_3), **2.34** (s, 3H, C^{13}H_3)

$^{13}\text{C NMR}$ (100 MHz, CDCl_3): δ (ppm) **154.73** (C_q^4), **149.67** (C_q^1), **142.38** (C_q^9), **141.47** (C_q^{12}), **134.11** (C_q^2), **129.77** ($2 \times \text{C}^{11}\text{H}$), **125.49** ($2 \times \text{C}^{10}\text{H}$), **118.13** (C^5H), **112.71** (C^6H), **108.68** (C^3H), **56.33** (C^7H_3), **56.13** (C^8H_3), **21.53** (C^{13}H_3)

IR: $\bar{\nu}$ (cm^{-1}) 1487, 1460, 1438, 1268, 1042, 1029, 806, 685

The experimental data were in agreement with those reported in the literature.⁴¹

(+)-(S)-2-(*p*-Tolylsulfinyl)cyclohexa-2,5-diene-1,4-dione (297/SQ2)

This molecule was synthesised according to Carreño *et al.* protocol.⁴¹

In a 500 mL flask, sulfoxide **295** (2.520 g, 9.12 mmol, 1.0 eq.) was dissolved in 100 mL of acetonitrile. A solution of CAN (12.627 g, 23.0 mmol, 2.5 eq.) in 100 mL of water was added at once over the sulfoxide solution and stirred for one hour at room temperature. Acetonitrile was then evaporated and the aqueous residue was extracted with dichloromethane. The organic phase was dried over MgSO₄, filtered off and evaporated to yield 2.183 g of the desired sulfinylquinone. Recrystallisation from hot diethyl ether gave blood red needles.

Aspect: red needles

Yield: 97% (before recrystallisation)

TLC: R_f ≈ 0.63 ((), visualised by cHex/AcOEt: 5/5), revealed by UV and *p*-anisaldehyde

m_p: 124-126 °C

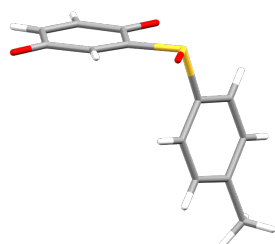
[α]_D²⁰: +1011 ° (c = 1.00; CHCl₃)

¹H NMR (400 MHz, CDCl₃): δ (ppm) **7.66** (d, 2H, *J* = 8.1 Hz, 2 × C⁸H), **7.43** (d, 1H, *J* = 2.5 Hz, C³H), **7.29** (d, 2H, *J* = 8.1 Hz, 2 × C⁹H), **6.79** (dd, 1H, *J* = 10.1; 2.5 Hz, C⁵H), **6.71** (d, 1H, *J* = 10.1 Hz, C⁶H), **2.39** (s, 3H, C¹¹H₃)

¹³C NMR (100 MHz, CDCl₃): δ (ppm) **185.23** (C_q⁴), **183.71** (C_q¹), **155.46** (C_q²), **143.09** (C_q¹⁰), **138.31** (C_q⁷), **137.53** (C⁵H), **136.58** (C⁶H), **131.69** (C³H), **130.39** (2 × C⁹H), **125.94** (2 × C⁸H), **21.62** (C¹¹H₃)

IR: $\bar{\nu}$ (cm⁻¹) 1657, 1591, 1057, 806

The experimental data were in agreement with those reported in the literature.⁴¹

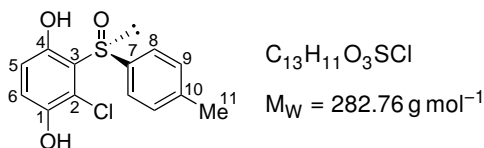


Orthorhombic	<i>P</i> 2 ₁ 2 ₁ 2 ₁
a = 6.6870(1) Å	α = 90 °
b = 13.2586(2) Å	β = 90 °
c = 13.4136(2) Å	γ = 90 °
V = 1189.25(3) Å ³	Z = 4
R = 2.73%	Flack = -0.012(16)

Figure 8.12: X-ray structure of **297** and paramaters of the crystal. Recrystallisation from boiling diethyl ether.

8.4.4 Sulfinylquinone 307a/SQ4

(-)-(S)-2-Chloro-3-(*p*-tolylsulfinyl)benzene-1,4-diol (**482**)



The title compound was cited by Carreño *et al.* although no experimental procedure was given.⁴²

In a 250 mL two-neck flask under argon atmosphere, sulfinylquinone **297** (1.996 g, 8.10 mmol, 1.0 eq.) was dissolved in 150 mL of anhydrous dichloromethane and cooled down to 0 °C and TiCl₄ (2.5 mL, 22.8 mmol, 2.8 eq.) was added dropwise. The dark red solution was allowed to warm up to room temperature and was stirred overnight. Hydrolysis was performed by addition of 100 mL of a saturated solution of sodium potassium tartrate and a vigorous stirring for five hours. The phases were separated and the aqueous phase was extracted with dichloromethane. Organic phases were gathered and washed with a saturated solution of Na₂S₂O₃ and brine, successively. The organic phase was then dried over MgSO₄, filtered off and evaporated. The crude was purified by flash chromatography on demetallated silica gel (cyclohexane/AcOEt: 9/1 → 8/2) to give 1.001 g of a pale yellow solid.

Aspect: pale yellow solid

Yield: 44%

TLC: R_f ≈ 0.60 (cHex/AcOEt: 5/5), visualised by UV and *p*-anisaldehyde

m_p: 173-176 °C

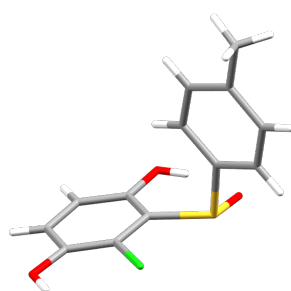
[α]_D²⁰: -95° (c = 1.0; acetone)

¹H NMR (500 MHz, CDCl₃): δ (ppm) **10.85** (s, broad, 1H, OH), **7.73** (d, 2H, *J* = 8.2 Hz, 2 × C⁸H), **7.31** (d, 2H, *J* = 8.2 Hz, 2 × C⁹H), **7.00** (d, 1H, *J* = 9.0 Hz, C⁵H or C⁶H), **6.77** (d, 1H, *J* = 9.0 Hz, C⁵H or C⁶H), **5.44** (s, br, 1H, OH), **2.40** (s, 3H, C¹¹H₃)

¹³C NMR (126 MHz, CDCl₃): δ (ppm) **154.58** (C_q¹ or C_q⁴), **144.98** (C_q¹ or C_q⁴), **143.35** (C_q¹⁰), **139.52** (C_q⁷), **130.54** (2 × C⁹H), **126.22** (2 × C⁸H), **120.61** (C⁵H or C⁶H), **120.37** (C_q² or C_{3q}), **119.63** (C⁵H or C⁶H), **115.87** (C_q² or C_{3q}), **21.67** (C¹¹H₃)

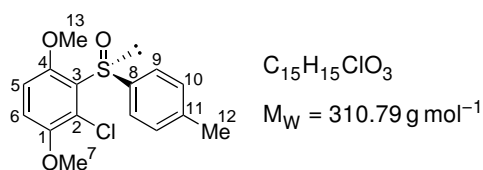
IR: ν̄ (cm⁻¹) 3400-2800, 1286, 1207, 966, 805

The experimental data were in agreement with those reported in the literature.⁴²



Orthorhombic	<i>P</i> 2 ₁ 2 ₁ 2 ₁
a = 7.5344(5) Å	α = 90°
b = 7.6908(8) Å	β = 90°
c = 21.7319(12) Å	γ = 90°
V = 1259.26(17) Å ³	Z = 4
R = 4.75%	Flack = 0.01(3)

Figure 8.13: X-ray structure of **482** and parameters of the crystal. Crystallisation by slow evaporation from dichloromethane.

(-)-(S)-2-Chloro-1,4-dimethoxy-3-(*p*-tolylsulfinyl)benzene (499)

In a 50 mL two-neck flask under argon atmosphere and equipped with a condenser, hydroquinone **482** (207 mg, 0.732 mmol, 1.0 eq.) was dissolved in 10 mL of acetone. Potassium carbonate (505 mg, 3.66 mmol, 5.0 eq.) and dimethyl sulfate (0.15 mL, 1.58 mmol, 2.2 eq.) were added to the solution and the mixture was heated up at 55 °C for two hours. The reaction mixture was cooled down to room temperature and filtered to remove the potassium salts. The solid was thoroughly washed with acetone and the solvent was evaporated. The crude was then dissolved in 10 mL of dichloromethane and 10 mL of water was added. Sodium hydroxide (63 mg, 1.58 mmol, 2.2 eq.) was added and the final mixture was vigorously stirred for thirty minutes. The phases were separated and the aqueous phase was extracted with dichloromethane. The organic phases were gathered, dried over $MgSO_4$ and filtered. The crude was purified by filtration on silica gel, using ethyl acetate as eluent. Evaporation of the solvents gave 174 mg of dimethoxybenzene **499**.

Aspect: white crystals

Yield: 77%

TLC: $R_f \approx 0.17$ (cHex/AcOEt: 5/5), visualised by UV and *p*-anisaldehyde

m_p : 171-174 °C

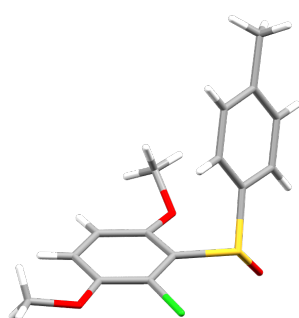
$[\alpha]_D^{20}$: -133° ($c = 1.0$; $CHCl_3$)

1H NMR (500 MHz, $CDCl_3$): δ (ppm) **7.54** (d, 2H, $J = 8.6$ Hz, $2 \times C^9H$), **7.23** (d, 2H, $J = 8.6$ Hz, $2 \times C^{10}H$), **6.98** (d, 1H, $J = 8.6$ Hz, C^5H or C^6H), **6.78** (d, 1H, $J = 8.6$ Hz, C^5H or C^6H), **3.85** (s, 3H, C^7H_3 or $C^{13}H_3$), **3.67** (s, 3H, C^7H_3 or $C^{13}H_3$), **2.37** (s, 3H, $C^{12}H_3$)

^{13}C NMR (126 MHz, $CDCl_3$): δ (ppm) **153.72** (C_q^1 or C_q^4), **149.85** (C_q^1 or C_q^4), **140.59** (C_q^8), **140.26** (C_q^{11}), **132.29** (C_q^2 or C_q^3), **129.34** ($2 \times C^{10}H$), **124.57** (C_q^2 or C_q^3), **124.44** ($2 \times C^9H$), **116.02** (C^5H or C^6H), **111.88** (C^5H or C^6H), **57.15** (C^7H_3 or $C^{13}H_3$), **56.84** (C^7H_3 or $C^{13}H_3$), **21.50** ($C^{12}H_3$)

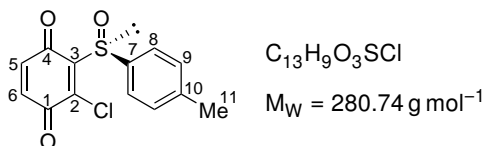
IR: $\bar{\nu}$ (cm^{-1}) 1563, 1462, 1429, 1269, 1049, 1031, 1014, 819

HRMS (ESI+): for $[M+H]^+$ calc.: 311.0503, found: 311.0499



Orthorhombic	$P2_12_12_1$
$a = 7.3892(2) \text{ \AA}$	$\alpha = 90^\circ$
$b = 8.1936(3) \text{ \AA}$	$\beta = 90^\circ$
$c = 24.3849(8) \text{ \AA}$	$\gamma = 90^\circ$
$V = 1476.35(9) \text{ \AA}^3$	$Z = 4$
$R = 3.91\%$	Flack = $-0.02(3)$

Figure 8.14: X-ray structure of **499** and parameters of the crystal. Recrystallisation from boiling isopropanol.

(+)-(S)-2-Chloro-3-(*p*-tolylsulfinyl)cyclohexa-2,5-diene-1,4-dione (307a/SQ4)

This compound was cited by Carreño *et al.* although no experimental procedure was given.⁴² Therefore, the general procedure for the oxidation of hydroquinone was used.

In a 100 mL flask, sulfinylhydroquinone **482** (602 mg, 2.13 mmol, 1.0 eq.) was dissolved in 40 mL of acetonitrile. A solution of CAN (2.942 g, 5.37 mmol, 2.5 eq.) in 40 mL of water was added at once over the sulfoxide solution. After one hour, the acetonitrile was evaporated and the aqueous residue was extracted with dichloromethane. The organic phase was dried over MgSO₄, filtered off and evaporated to give 578 mg of sulfinylquinone **307a**.

Aspect: red needles

Yield: 97%

TLC: R_f ≈ 0.41 (cHex/AcOEt: 5/5), visualised by UV and *p*-anisaldehyde

m_p: 138-140 °C

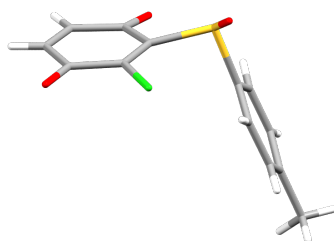
[α]_D²⁰: +638 ° (c = 1.0; CHCl₃)

¹H NMR (500 MHz, CDCl₃): δ (ppm) **7.72** (d, 2H, *J* = 8.2 Hz, 2 × C⁸H), **7.33** (d, 2H, *J* = 8.2 Hz, 2 × C⁹H), **6.91** (d, 1H, *J* = 10.1 Hz, C⁵H or C⁶H), **6.78** (d, 1H, *J* = 10.1 Hz, C⁵H or C⁶H), **2.40** (s, 3H, C¹¹H₃)

¹³C NMR (126 MHz, CDCl₃): δ (ppm) **181.27** (C_q¹ or C_q⁴), **177.91** (C_q¹ or C_q⁴), **146.28** (C_q² or C_q³), **143.71** (C_q² or C_q³), **142.61** (C_q¹⁰), **138.03** (C_q⁷), **130.34** (2 × C⁹H), **125.17** (2 × C⁸H), **21.63** (C¹¹H₃)

IR: ν̄ (cm⁻¹) 1676, 1652, 1063, 836

The experimental data were in agreement with those reported in the literature.⁴²

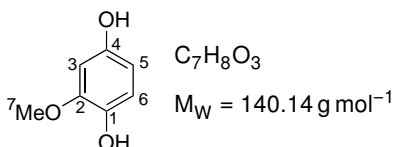


Orthorhombic	<i>P</i> 2 ₁ 2 ₁ 2 ₁
<i>a</i> = 10.1899(5) Å	α = 90 °
<i>b</i> = 10.1885(4) Å	β = 90 °
<i>c</i> = 11.8334(5) Å	γ = 90 °
<i>V</i> = 1228.54(9) Å ³	<i>Z</i> = 4
<i>R</i> = 2.88%	Flack = 0.01(4)

Figure 8.15: X-ray structure of **307a** and parameters of the crystal. Recrystallisation from a boiling mixture of pentane and toluene.

8.4.5 Sulfinylquinone 488/SQ3

2-Methoxybenzene-1,4-diol (484)



Compound **484** was obtained using a modified version of the protocol of Ferreira *et al.*⁴³

In a 100 mL two-neck flask, a solution of NaOH (1.574 g, 39.4 mmol, 1.2 eq.) in 40 mL of water was used to dissolve vanillin (**483**) (5.163 g, 33.9 mmol, 1.0 eq.). Through a dropping funnel, an aqueous solution of H₂O₂ (37%), (3.3 mL, 40.6 mmol, 1.2 eq.) diluted with 20 mL of water was added dropwise to the phenolate solution. The mixture directly turned dark and was stirred overnight at room temperature. The solution was acidified with 20 mL of HCl (10%) and extracted with ethyl acetate. The organic phase was washed with a saturated solution of Na₂S₂O₃, dried over MgSO₄, filtered off and evaporated to provide a dark oil which was purified by flash chromatography on silica gel (cHex/AcOEt: 8/2) to give 3.633 g of **484** as a white solid.

Aspect: greyish powder

Yield: 76%

TLC: $R_f \approx 0.43$ (cHex/AcOEt: 5/5), visualised by UV and KMnO₄

m_p: 85-86 °C

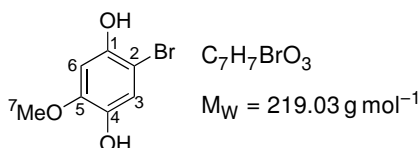
¹H NMR (400 MHz, CD₃OD): δ (ppm) **6.61** (d, 1H, $J = 8.5$ Hz, C⁶H), **6.42** (d, 1H, $J = 2.7$ Hz, C³H), **6.22** (dd, 1H, $J = 8.5; 2.7$ Hz, C⁵H), **3.80** (s, 3H, C⁷H₃)

¹³C NMR (400 MHz, CD₃OD): δ (ppm) **151.74** (C_q⁴), **149.46** (C_q²), **140.28** (C_q¹), **116.36** (C⁶H), **107.43** (C⁵H), **101.22** (C³H), **56.16** (C⁷H₃)

IR: $\bar{\nu}$ (cm⁻¹) 3500-3000, 1509, 1451, 1371, 1289, 1241, 1217, 1191, 1158, 1110, 1032, 945, 832, 795

The experimental data were in agreement with those reported in the literature.⁴³

2-Bromo-5-methoxybenzene-1,4-diol (485)



This compound was synthesised according to Keana *et al.*⁴⁴

In a 500 mL two-neck flask, equipped with a dropping funnel, under argon atmosphere, 3.506 g of hydroquinone **484** (3.506 g, 25.0 mmol, 1.0 eq.) was dissolved in 150 mL of glacial acetic acid. The solution was cooled down using an iced-water bath. Bromine (1.3 mL, 25.3 mmol, 1.0 eq.), dissolved in 30 mL of glacial acetic acid, was added dropwise through the dropping funnel. The mixture was stirred for four hours. Then, the solvent was evaporated under reduced pressure and the residue was dissolved in ethyl acetate. The organic phase was washed with saturated solutions of Na₂S₂O₃,

NaHCO₃ and brine, successively, then dried over MgSO₄, filtered off and evaporated. The crude was purified by recrystallisation in hot toluene (80 °C) to give 4.582 g of **485**.

Aspect: white crystals

Yield: 83%

TLC: R_f ≈ 0.46 (cHex/AcOEt: 5/5), visualised by UV and *p*-anisaldehyde

m_p: 120-122 °C

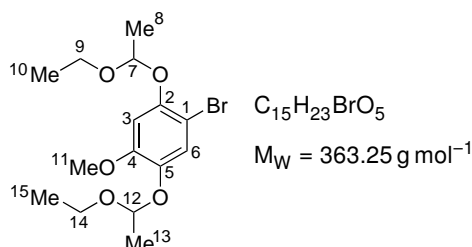
¹H NMR (400 MHz, CD₃OD): δ (ppm) **6.86** (s, 1H, C³H), **6.53** (s, 1H, C⁶H), **3.79** (s, 3H, C⁷H₃)

¹³C NMR (100 MHz, CD₃OD): δ (ppm) **149.17** (C_q⁵), **148.19** (C_q¹), **141.27** (C_q⁴), **119.57** (C³H), **102.03** (C⁶H), **100.05** (C_q²), **56.40** (C⁷H₃)

IR: ν̄ (cm⁻¹) 3500-3000, 1512, 1443, 1274, 1197, 1165, 974, 820

The experimental data were in agreement with those reported in the literature.⁴⁴

1-Bromo-2,5-bis(1-ethoxyethoxy)-4-methoxybenzene (**486a**)



In a 100 mL two-neck flask under argon atmosphere, hydroquinone **485** (1.415 g, 6.46 mmol, 1.0 eq.) were suspended into 25 mL of anhydrous dichloromethane. To that suspension, ethyl vinyl ether (3.4 mL, 35.6 mmol, 5.5 eq.) was added dropwise. After five minutes, PPTS (42 mg, 0.167 mmol, 0.025 eq.) was added. The solid was dissolved after a few minutes. The reaction was stirred overnight at room temperature and a saturated solution of NaHCO₃ was added to quench the reaction. The phases were separated and the aqueous phase was extracted with diethyl ether. The organic phases were gathered and dried over MgSO₄, then filtered off and the solvents were evaporated. The crude was purified by filtration over a silica gel pad, using a cHex/Et₂O mixture in 4/1 ratio as eluent. The solvents were evaporated to give 2.344 g of **486a** as a yellow oil.

Aspect: golden oil

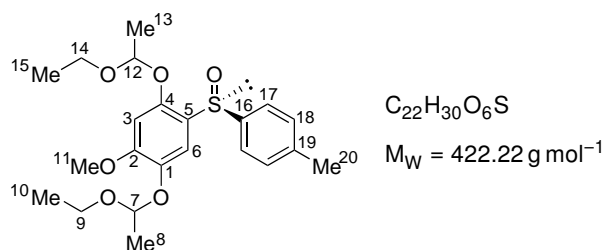
Yield: quantitative

TLC: R_f ≈ 0.53 (cHex/AcOEt: 7/3), visualised by UV and *p*-anisaldehyde

¹H NMR (400 MHz, CDCl₃): δ (ppm) **7.22(3)** (s, 0.5H, C⁶H), **7.22(0)** (s, 0.5H, C⁶H), **6.78** (s, 1H, C³H), **5.34-5.27** (m, 1H, C⁷H or C¹²H), **5.27-5.20** (m, 1H, C⁷H or C¹²H), **3.89-3.76** (m, 2H, C⁹H₂ or C¹⁴H₂), **3.80** (s, 3H, C¹¹H₃), **3.65-3.53** (m, 2H, C⁹H₂ or C¹⁴H₂), **1.51-1.48** (m, 3H, C⁸H or C¹³H), **1.47-1.44** (m, 3H, C⁸H or C¹³H), **1.24-1.18** (m, 6H, C¹⁰H₃ + C¹⁵H₃)

¹³C NMR (100 MHz, CDCl₃): δ (ppm) **151.03** (C_q⁴), **149.01 + 148.98** (C_q² or C_q⁵), **141.48 + 141.46** (C_q² or C_q⁵), **124.03** (C⁶H), **105.11 + 105.10** (C³H), **104.22** (C_q¹), **101.90 + 101.86** (C⁷H or C¹²H), **101.74 + 101.70** (C⁷H or C¹²H), **62.35 + 62.31** (C⁹H₂ or C¹⁴H₂), **61.80 + 61.77** (C⁹H₂ or C¹⁴H₂), **56.14** (C¹¹H₃), **20.33 + 20.30** (C⁸H₃ or C¹³H₃), **20.25 + 20.23** (C⁸H₃ or C¹³H₃), **15.36** (C¹⁰H₃ or C¹⁵H₃), **15.25** (C¹⁰H₃ or C¹⁵H₃)

IR: ν̄ (cm⁻¹) 1198-1040, 988-891, 820

1,4-Bis(1-ethoxyethoxy)-2-methoxy-5-((S)-*p*-tolylsulfinyl)benzene (487a)

In a 100 mL two-neck flask under argon atmosphere, a 2.5 M hexyllithium solution in hexane (1.60 mL, 4.00 mmol, 1.0 eq.) were dissolved in 15 mL of anhydrous THF and cooled down to -78°C . A solution of bromide **486a** (1.423 g, 3.919 mmol, 1.0 eq.), dissolved in 25 mL of anhydrous THF, was added dropwise to the lithium solution. The golden mixture was stirred for one hour at -78°C . After 15 minutes, the solution turned light green. In a 250 mL two-neck flask under argon atmosphere, 1.399 g of (–)-menthyl sulfinate (SS)-**292** (1.399 g, 4.76 mmol, 1.2 eq.) was dissolved in 45 mL of anhydrous THF and cooled down to -78°C . The lithium solution was quickly cannulated over the sulfinate solution and the final mixture was stirred for two hours at -78°C . The solution was allowed to warm up to room temperature and was quenched with water. The phases were separated and the aqueous phase was extracted with diethyl ether. The organic phase was dried over MgSO_4 , filtered off and evaporated. The crude was purified by flash chromatography on silica gel (cHex/AcOEt: 9/1 \rightarrow 8/2) to give 916 mg of **487a** as a orange oil.

Aspect: golden oil

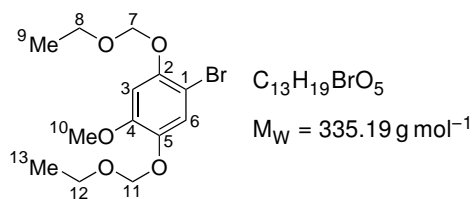
Yield: 55%

TLC: $R_f \approx 0.50$ (cHex/AcOEt: 4/6), visualised by UV and *p*-anisaldehyde

¹H NMR (400 MHz, CDCl_3): δ (ppm) **7.62-7.51** (m, 2H, $2 \times \text{C}^{17}\text{H}$), **7.32-7.26** (m, 2H, C^{18}H), **6.93 + 6.89 + 6.70** ($3 \times \text{s}$, 1H, C^6H), **6.42 + 6.41 + 6.40** ($3 \times \text{s}$, 1H, C^3H), **5.37-5.27** (m, 1H, C^7H or C^{12}H), **5.24-5.14** (m, 1H, C^7H or C^{12}H), **3.91-3.72** (m, 5H, $\text{C}^{11}\text{H}_3 + \text{C}^9\text{H}_2$ or C^{14}H_2), **3.67-3.45** (m, 2H, C^9H_2 or C^{14}H_2), **2.37** (s, 3H, C^{20}H_3), **1.45-1.09** (m, 12H, $\text{C}^8\text{H}_3 + \text{C}^{10}\text{H}_3 + \text{C}^{13}\text{H}_3 + \text{C}^{15}\text{H}_3$)

¹³C NMR (100 MHz, CDCl_3): δ (ppm) **153.96 + 153.86 + 153.84** (C_q^2), **148.95 + 148.86 + 148.80 + 148.68** (C_q^{Ar}), **142.82 + 148.81 + 148.78 + 148.76** (C_q^{Ar}), **141.33 + 141.30 + 141.27 + 141.24** (C_q^{Ar}), **141.11 + 141.09** (C_q^{Ar}), **129.58** ($2 \times \text{C}^{\text{pTolH}}$), **125.65+126.61** (C^6H), **125.21** ($2 \times \text{C}^{\text{pTolH}}$), **115.45 + 115.32 + 115.09 + 114.6** (C_q^{Ar}), **101.99 + 101.97** (C^3H), **101.67 + 101.60 + 101.57 + 101.54** (C^7H or C^{12}H), **100.35 + 100.26 + 100.17 + 100.16** (C^7H or C^{12}H), **62.62 + 62.58 + 62.26 + 62.20** (C^9H_2 or C^{14}H_2), **61.15 + 61.12 + 60.31 + 60.24** (C^9H_2 or C^{14}H_2), **56.11 + 56.10 + 56.08** (C^{11}H_3), **21.37** (C^{20}H_3), **20.53 + 20.37 + 20.34** (C^8H_3 or C^{13}H_3), **19.82 + 19.80 + 19.55 + 19.50** (C^8H_3 or C^{13}H_3), **15.23 + 15.18 + 15.14** ($\text{C}^{10}\text{H}_3 + \text{C}^{15}\text{H}_3$)

IR: $\bar{\nu}$ (cm^{-1}) 2996-2879, 1197-1081, 1046, 994-906

1-Bromo-2,5-bis(ethoxymethoxy)-4-methoxybenzene (486b)

In a 100 mL two-neck flask under argon atmosphere, a solution of hydroquinone **485** (2.501 g, 11.4 mmol, 1.0 eq.) and BnEt_3NCl (267 mg, 1.17 mmol, 0.10 eq.), dissolved in 25 mL of anhydrous THF, was cooled down to 0 °C. Solid sodium hydroxide (2.761 g, 69.0 mmol, 6.0 eq.) was added to the solution, followed by ethoxymethyl chloride (4.2 mL, 45.3 mmol, 4.0 eq.). The resulting mixture was stirred one hour at 0 °C, then one hour at room temperature. The reaction mixture was then poured into 25 mL of water and the biphasic mixture was stirred for ten minutes. The phases were separated and the organic layer was washed with brine, dried over MgSO_4 and evaporated. The crude oil was filtered over silica gel (eluent: *c*Hex/*Ac*OEt: 9/1) to yield 2.8055 g of the desired compound.

Aspect: Yellowish oil

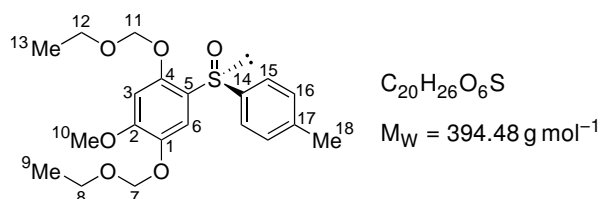
Yield: 73%

TLC: $R_f \approx 0.57$ (*c*Hex/*Ac*OEt: 7/3), visualised by UV and *p*-anisaldehyde

$^1\text{H NMR}$ (500 MHz, CDCl_3): δ (ppm) **7.32** (s, 1H, C^6H), **6.82** (s, 1H, C^3H), **5.22** (s, 2H, C^7H_2), **5.18** (s, 2H, C^{11}H_2), **3.84** (s, 3H, C^{10}H_3), **3.80** (q, 2H, $J = 7.1 \text{ Hz}$, C^8H_2 or C^{12}H_2), **3.80** (q, 2H, $J = 7.1 \text{ Hz}$, C^{11}H_2 or C^8H_2), **1.24** (t, 3H, $J = 7.1 \text{ Hz}$, C^9H_3 or C^{13}H_3), **1.23** (t, 3H, $J = 7.1 \text{ Hz}$, C^{13}H_3 or C^9H_3)

$^{13}\text{C NMR}$ (126 MHz, CDCl_3): δ (ppm) **150.08** (C_q^4), **149.57** (C_q^2), **142.26** (C_q^5), **121.41** (C^6H), **102.72** (C_q^1), **102.60** (C^3H), **95.00** (C^7H_2 or C^{11}H_2), **94.92** (C^{11}H_2 or C^7H_2), **64.68** (C^8H_2 or C^{12}H_2), **64.68** (C^{12}H_2 or C^8H_2), **56.27** (C^{10}H_3), **15.22** (C^9H_3 or C^{13}H_3), **15.18** (C^{13}H_3 or C^9H_3)

IR: $\bar{\nu}$ (cm^{-1}) 1502, 1263, 1196, 1156, 1100, 1083, 974

(-)-(S)-1,4-Bis(ethoxymethoxy)-2-methoxy-5-(*p*-tolylsulfinyl)benzene (487b)

In a dry 250 mL two-neck flask under argon atmosphere, bromide **486b** (2.061 g, 6.15 mmol, 1.0 eq.) was dissolved in 60 mL of anhydrous THF and cooled down to -78 °C. A 2.3 M solution of hexyllithium in hexane (2.7 mL, 6.21 mmol, 1.0 eq.) was added dropwise and the solution was stirred thirty minutes at -78 °C. The solution was then cannulated over a solution of sulfinate (SS)-**292** (1.878 g, 6.38 mmol, 1.0 eq.) dissolved in 60 mL of anhydrous THF and cooled down to -78 °C. The resulting mixture was stirred one hour at -78 °C and one hour at room temperature. It was then quenched with a saturated solution of NH_4Cl and the phases were separated. The aqueous layer was extracted with diethyl ether and the gathered organic layers were washed with brine, dried over

MgSO₄, and evaporated. The crude oil was purified by flash chromatography over silica gel (eluent: cHex/AcOEt: 8/2 → 6/4) to yield 1.674 g of desired sulfoxide.

Aspect: yellowish oil

Yield: 69%

TLC: R_f ≈ 0.11 (cHex/AcOEt: 7/3), visualised by UV and *p*-anisaldehyde

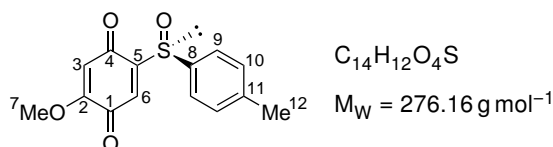
[α]_D²⁰: -75.2° (c = 1.0; CHCl₃)

¹H NMR (500 MHz, CDCl₃): δ (ppm) **7.57** (s, 1H, C⁶H), **7.55** (d, 2H, *J* = 8.1 Hz, C¹⁵H₂), **7.21** (d, 2H, *J* = 8.1 Hz, C¹⁶H₂), **6.73** (s, 1H, C³H), **5.21** (dd, *AB*, 2H, *J*_{AB} = 6.6 Hz, Δ*ν*_{AB} = 10.7 Hz, C⁷H₂), **5.14** (dd, *A'B'*, 2H, *J*_{A'B'} = 7.1 Hz, Δ*ν*_{A'B'} = 19.2 Hz, C¹¹H₂), **3.84** (s, 3H, C¹⁰H₃), **3.75** (q, 2H, *J* = 7.1 Hz, C⁸H₂), **3.58** (ddq, *CDX*, 2H, *J*_{CD} = 9.6 Hz, *J*_{CX} = *J*_{DX} = 7.1 Hz, Δ*ν*_{CD} = 45.2 Hz, C¹²H₂), **2.34** (s, 3H, C¹⁸H₃), **1.19** (t, 3H, *J* = 7.1 Hz, C⁹H₃), **1.15** (t, *CDX*, 3H, *J*_{CX} = *J*_{DX} = 7.1 Hz, C¹³H₂)

¹³C NMR (126 MHz, CDCl₃): δ (ppm) **153.43** (C_q²), **149.68** (C_q⁴), **142.09** (C_q¹ + C_q¹⁴), **141.24** (C_q¹⁷), **129.74** (2 × C¹⁶H), **125.34** (C_q⁵ + 2 × C¹⁵H), **113.73** (C⁶H), **100.24** (C³H), **94.97** (C⁷H₂), **93.95** (C¹¹H₂), **64.65** (C⁸H₂ or C¹²H₂), **64.65** (C¹²H₂ or C⁸H₂), **56.31** (C¹⁰H₃), **21.50** (C¹⁸H₃), **15.16** (C⁹H₃ or C¹³H₃), **15.13** (C¹³H₃ or C⁹H₃)

IR: $\bar{\nu}$ (cm⁻¹) 1493, 1272, 1195, 1148, 1106, 1081, 1049

(+)-(S)-2-Methoxy-5-(*p*-tolylsulfinyl)cyclohexa-2,5-diene-1,4-dione (488/SQ3)



From sulfoxide 487a. In a 50 mL flask, sulfoxide **487a** (604 mg, 1.43 mmol, 1.0 eq.) was dissolved in 15 mL of acetonitrile. A solution of CAN (2.178 g, 3.97 mmol, 2.8 eq.) dissolved in 10 mL of water was quickly poured on the sulfoxide solution. After 20 minutes, a TLC analysis indicated the complete conversion of the starting material. The acetonitrile was evaporated and the aqueous residue was extracted with dichloromethane. The organic phase was dried over MgSO₄, filtered off and evaporated to give 375 mg of a light orange solid which was recrystallised from hot ethanol.

Aspect: orange needles

Yield: 95%

From sulfoxide 487b. In a 250 mL round bottom flask, sulfoxide **487b** (1.500 g, 3.80 mmol, 1.0 eq.) was dissolved in 50 mL of acetonitrile. A solution of CAN (5.267 g, 9.61 mmol, 2.5 eq.) in 25 mL of water was added on the sulfoxide solution and the final mixture was stirred for thirty minutes. Acetonitrile was evaporated and the aqueous phase was extracted with dichloromethane. The organic phase was dried over Na₂SO₄ and the solvent was evaporated. The orange solid was recrystallised from boiling ethanol to give 936 mg of orange needles of sulfinylquinones **488**.

Aspect: orange needles

Yield: 89%

TLC: R_f ≈ 0.20 (cHex/TBME: 5/5), visualised by UV and *p*-anisaldehyde

m_p: 121-123 °C

[α]_D²⁰: +428.8° (c = 1.0; CHCl₃)

$^1\text{H NMR}$ (500 MHz, CDCl_3): δ (ppm) **7.65** (d, 2H, $J = 8.2$ Hz, $2 \times \text{C}^9\text{H}$), **7.34** (s, 1H, C^6H), **7.29** (d, 2H, $J = 8.2$ Hz, $2 \times \text{C}^{10}\text{H}$), **5.85** (s, 1H, C^3H), **3.81** (s, 3H, C^7H_3), **2.38** (s, 3H, C^{12}H_3)

$^{13}\text{C NMR}$ (126 MHz, CDCl_3): δ (ppm) **183.65** (C_q^1), **179.70** (C_q^4), **159.73** (C_q^2), **156.54** (C_q^5), **149.94** (C_q^{11}), **138.54** (C_q^8), **130.35** ($2 \times \text{C}^{10}\text{H}$), **129.73** (C^6H), **125.98** ($2 \times \text{C}^9\text{H}$), **107.64** (C^3H), **56.87** (C^7H_3), **21.60** (C^{12}H_3)

IR: $\bar{\nu}$ (cm^{-1}) 1676, 1634, 1634, 1079, 1055

HRMS (ESI+): for $[\text{M}+\text{H}]^+$ calc.: 277.0535, found: 277.0529

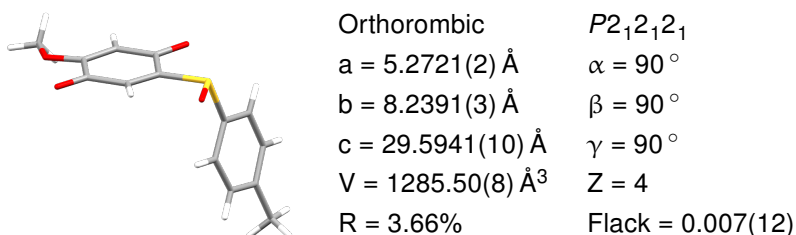
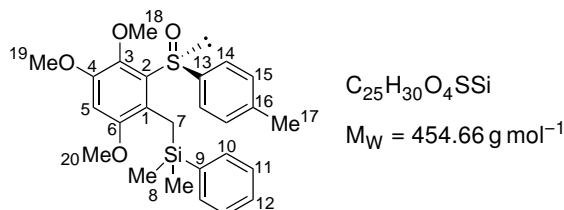


Figure 8.16: X-ray structure of **488** and parameters of the crystals. Recrystallisation from boiling ethanol.

8.4.6 Silylated sulfinylquinone **318b**

(-)-(S)-Dimethyl(phenyl)(3,4,6-trimethoxy-2-(*p*-tolylsulfinyl)benzyl)silane (**489**)



This compound was prepared following the procedure reported by García Ruano *et al.*^{45,46}

In a dry 150 mL three-neck flask under argon atmosphere, DIPA (1.2 mL, 8.56 mmol, 1.8 eq.) was dissolved in 30 mL of anhydrous THF. The solution was cooled down to 0°C and a 2.5 M solution of hexyllithium in hexanes (2.3 mL, 5.75 mmol, 1.2 eq.) was added dropwise. The mixture was stirred ten minutes at 0°C and then cooled down to -78°C . The sulfoxide **481** (1.501 g, 4.69 mmol, 1.0 eq.) was dissolved in 30 mL of anhydrous THF and added dropwise to the LDA solution which turned dark. After stirring one hour at -78°C , chlorodimethylphenylsilane (2.4 mL, 14.3 mmol, 3.1 eq.) was added dropwise at -78°C and the solution immediately lightened. After five minutes at -78°C , the solution was warmed up to room temperature and quenched with a saturated solution of NH_4Cl . The phases were separated and the aqueous phase was extracted with diethyl ether. Organic phases were gathered, dried over MgSO_4 and the solvents were evaporated. The crude oil was purified by flash chromatography on neutralised silica gel (cHex/AcOEt: 100/0 \rightarrow 95/5 \rightarrow 90/10) to obtain 1.469 g of silane **489**.

Aspect: golden oil

Yield: 69%

TLC: $R_f \approx 0.39$ (cHex/AcOEt: 7/3), visualised by UV and *para*-anisaldehyde

$[\alpha]_D^{20}$: -54.4° ($c = 1.0$; CHCl_3)

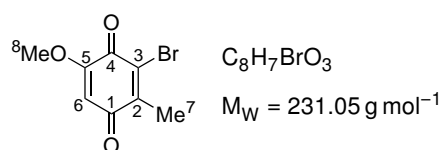
¹H NMR (500 MHz, CDCl₃): δ (ppm) **7.52-7.47** (m, 2H, 2 × C¹⁰H), **7.39** (d, 2H, *J* = 8.3 Hz, 2 × C¹⁴H), **7.35-7.25** (m, 3H, 2 × C¹¹H + C¹²H), **7.16** (d, 2H, *J* = 8.3 Hz, 2 × C¹⁵H), **6.47** (s, 1H, C⁵H), **3.82** (s, 3H, C¹⁹H₃), **3.68** (s, 3H, C¹⁸H₃), **3.56** (s, 3H, C²⁰H₃), **2.66** (2H, AB, *J*_{AB} = 13.4 Hz, Δ*ν*_{AB} = 55.4 Hz, C⁷H₂) **2.33** (s, 3H, C¹⁷H₃), **0.24** (s, 3H, C⁸H₃), **0.22** (s, 3H, C⁸H₃)

¹³C NMR (126 MHz, CDCl₃): δ (ppm) **153.04** (C_q⁶), **150.11** (C_q⁴), **142.05** (C_q¹³), **141.89** (C_q³), **140.05** (C_q⁹), **139.64** (C_q¹⁶), **136.22** (C_q²), **133.74** (2 × C¹⁰H), **129.48** (2 × C¹⁵H), **128.70** (C¹²H), **127.55** (2 × C¹¹H), **124.38** (2 × C¹⁴H), **123.24** (C_q¹), **99.99** (C⁵H), **61.62** (C¹⁸H₃), **56.47** (C¹⁹H₃), **55.20** (C²⁰H₃), **21.41** (C¹⁷H₃), **15.03** (C⁷H₂), **-2.06** (C⁸H₃), **-2.20** (C⁸H₃)

IR: $\bar{\nu}$ (cm⁻¹) 1591, 1477, 1462, 1428, 1317, 1225, 1198, 1033, 870, 808, 729, 699

HRMS (ESI+): for [M+H]⁺ calc.: 455.1712, found: 455.1708

3-Bromo-5-methoxy-2-methylcyclohexa-2,5-diene-1,4-dione (490/Q6)



In a 1 L flask, compound **480** (5.002 g, 19.2 mmol, 1.0 eq.) was dissolved in 250 mL of acetonitrile. A solution of CAN (26.306 g, 48.0 mmol, 2.5 eq.) in 250 mL of water was poured at once over the aromatic solution. After stirring thirty minutes at room temperature, the acetonitrile was evaporated and the aqueous residue was extracted with dichloromethane. The organic phase was dried over MgSO₄ and the solvents were evaporated. The crude was purified by recrystallisation from boiling absolute ethanol to obtain 4.055 g of yellow needles.

Aspect: yellow needles

Yield: 92%

TLC: R_f ≈ 0.54 (cHex/AcOEt: 5/5), visualised by UV and *para*-anisaldehyde

m_p: 101-104 °C

¹H NMR (500 MHz, CDCl₃): δ (ppm) **5.96** (s, 1H, C⁶H), **3.84** (s, 3H, C⁸H₃), **2.23** (s, 3H, C⁷H₃)

¹³C NMR (126 MHz, CDCl₃): δ (ppm) **184.11** (C_q¹), **174.74** (C_q⁴), **158.42** (C_q⁵), **146.78** (C_q²), **133.13** (C_q³), **107.39** (C⁶H), **56.82** (C⁸H₃), **17.23** (C⁷H₃)

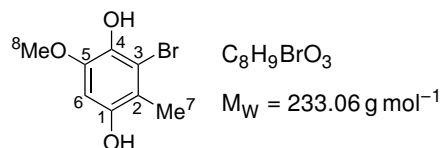
IR: $\bar{\nu}$ (cm⁻¹) 1683, 1634, 1244, 981, 848

HRMS (ESI+): for [M+H]⁺ calc.: 230.9657, found: 230.9651



Monoclinic	<i>P</i> 2 ₁ / <i>n</i>
<i>a</i> = 4.0250(4) Å	α = 90 °
<i>b</i> = 7.0107(6) Å	β = 91.100(9) °
<i>c</i> = 30.152(3) Å	γ = 90 °
<i>V</i> = 850.69(14) Å ³	<i>Z</i> = 4
<i>R</i> = 3.84%	

Figure 8.17: X-ray structure of **490** and parameters of the crystal. Recrystallisation from boiling ethanol.

3-Bromo-5-methoxy-2-methylbenzene-1,4-diol (491)

In a 250 mL two-neck flask under argon atmosphere, quinone **490** (3.942 g, 17.1 mmol, 1.0 eq.) was suspended in 100 mL of absolute ethanol. The solution was cooled down to 0 °C and NaBH_4 (2.286 g, 60.4 mmol, 3.5 eq.) was added portionwise. The mixture darkened, then lightened after a few minutes into a light orange solution. After half an hour, 40 mL of a HCl solution (10%) were added at 0 °C and the mixture turned colourless. The phases were separated and the aqueous phase was extracted with diethyl ether and dichloromethane. The organic phases were gathered and dried over MgSO_4 , filtered off and the solvents were evaporated to give 3.743 g of hydroquinone **491**.

Aspect: white powder

Yield: 94%

TLC: $R_f \approx 0.43$ (cHex/AcOEt: 5/5), visualised by UV and *p*-anisaldehyde

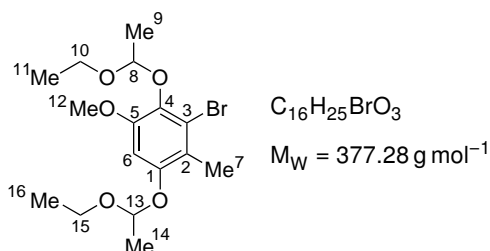
m_p : 168-170 °C

$^1\text{H NMR}$ (500 MHz, acetone- d_6): δ (ppm) **7.94** (s, 1H, OH), **7.44** (s, 1H, OH), **6.56** (s, 1H, $C^6\text{H}$), **3.77** (s, 3H, $C^8\text{H}_3$), **2.21** (s, 3H, $C^7\text{H}_3$)

$^{13}\text{C NMR}$ (500 MHz, acetone- d_6): δ (ppm) **148.37** (C^1_q), **145.56** (C^5_q), **136.77** (C^4_q), **116.73** (C^2_q), **112.92** (C^3_q), **99.90** ($C^6\text{H}$), **56.65** ($C^8\text{H}_3$), **15.58** ($C^7\text{H}_3$)

IR: $\bar{\nu}$ (cm^{-1}) 3500-3100, 1617, 1502, 1243, 1198, 1178, 1012, 829

HRMS (ESI+): for $[\text{M}+\text{H}]^+$ calc.: 232.9813, found: 232.9808

3-Bromo-1,4-bis(1-ethoxyethoxy)-5-methoxy-2-methylbenzene (492a)

In a 150 mL two-neck flask under argon atmosphere, hydroquinone **491** (1.349 g, 5.79 mmol, 1.0 eq.) was suspended in 40 mL of dichloromethane. Ethyl vinyl ether (**185**) (3.0 mL, 31.4 mmol, 5.4 eq.) was added dropwise, followed by the addition of PPTS (38 mg, 0.150 mmol, 0.025 eq.) and the reaction was stirred overnight. The reaction was then quenched with a saturated solution of NaHCO_3 and the phases were separated. The aqueous phase was extracted with dichloromethane. The organic phases were gathered, dried over MgSO_4 and the solvents were evaporated. The crude was purified by filtration over silica gel (cHex/ Et_2O : 8/2) and the solvent was evaporated to give 2.183 g of **492a**.

Aspect: golden oil

Yield: quantitative

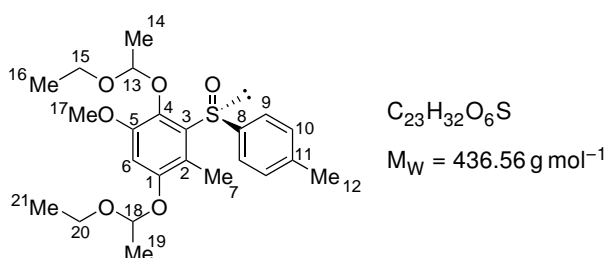
TLC: $R_f \approx 0.66$ (cHex/AcOEt: 8/2), visualised by UV and *p*-anisaldehyde

^1H NMR (500 MHz, CDCl_3): δ (ppm) **6.70** (s, 1H, C^6H), **5.36** (q, 1H, $J = 5.3$ Hz, C^8H), **5.27** (q, 1H, $J = 5.3$ Hz, C^{13}H), **3.80** (s, 3H, C^{12}H_3), **3.77-3.63** (m, 4H, C^{10}H_2 or C^{15}H_2), **2.27** (s, 3H, C^7H_3), **1.51-1.43** (m, 6H, C^9H_3 or C^{14}H_3), **1.24-1.14** (m, 6H, C^{11}H_3 or C^{16}H_3)

^{13}C NMR (126 MHz, CDCl_3): δ (ppm) **151.15** (C_q^1 or C_q^5), **151.10** (C_q^1 or C_q^5), **138.82+138.77** (C_q^4), **121.87+121.83** (C_q^2), **103.36+103.33** (C^8H), **102.34+102.32** (C^6H), **101.65** (C_q^3), **101.00+100.99** (C^{13}H), **63.58+63.55** (C^{10}H_2), **61.44+61.43** (C^{15}H_2), **56.25** (C^{12}H_3), **21.09+21.08** (C^9H_3 or C^{14}H_3), **20.41** (C^9H_3 or C^{14}H_3), **16.21** (C^7H_3), **15.42** (C^{11}H_3 or C^{16}H_3), **15.41** (C^{11}H_3 or C^{16}H_3)

IR: $\bar{\nu}$ (cm^{-1}) 2975, 2934, 1595, 1481, 1444, 1379, 1338, 1211, 1179, 1136, 1102, 1074, 1042, 1008, 941, 867

1,4-Bis(1-ethoxyethoxy)-5-methoxy-2-methyl-3-((*S*)-*p*-tolylsulfinyl)benzene (493a)



In a dry 150 mL two-neck flask under argon atmosphere, a solution of bromide **492a** (2.037 g, 5.40 mmol, 1.0 eq.) in 75 mL of anhydrous THF was cooled down to -78°C . A 2.4 M solution of hexyl-lithium in hexanes (2.3 mL, 5.52 mmol, 1.0 eq.) was added dropwise and the mixture was stirred at -78°C for thirty minutes. In a dry 250 mL two-neck flask under argon atmosphere, sulfinate (SS)-**292** (1.603 g, 5.44 mmol, 1.0 eq.) in 80 mL of THF was cooled down to -78°C . The aryllithium solution was rapidly cannulated over the sulfinate solution and the final reaction mixture was stirred for two hours at -78°C . The reaction was warmed up to room temperature and quenched with a saturated solution of NH_4Cl . The phases were separated and the aqueous phase was extracted with dichloromethane. The organic phases were gathered, dried over MgSO_4 and the solvents were evaporated. The crude oil was purified by flash chromatography on demetallated silica gel (cHex/AcOEt: 9/1 \rightarrow 8/2) to give 1.126 g of sulfoxide **493a**.

Aspect: golden oil

Yield: 48%

TLC: $R_f \approx 0.59$ (cHex/AcOEt: 5/5), visualised by UV and *p*-anisaldehyde

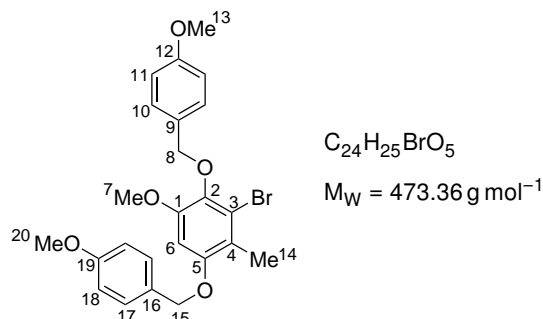
^1H NMR (400 MHz, CDCl_3): δ (ppm) **7.58-7.49** (m, 2H, $2 \times \text{C}^9\text{H}$), **7.30-7.24** (m, 2H, C^{10}H), **6.44 + 6.42 + 6.41** ($3 \times$ s, 1H, C^6H), **5.42-5.30** (m, 1H, C^{13}H or C^{18}H), **5.21-5.11** (m, 1H, C^{13}H or C^{18}H), **3.95-3.71** (m, 5H, $\text{C}^{17}\text{H}_2 + \text{C}^{15}\text{H}_3$ or C^{20}H_2), **3.64-3.39** (m, 2H, C^{15}H_2 or C^{20}H_2), **2.29** (s, 3H, C^{12}H_3), **2.21** (s, 3H, C^7H_3), **1.36-1.10** (m, 12H, $\text{C}^{14}\text{H}_3 + \text{C}^{16}\text{H}_3 + \text{C}^{19}\text{H}_3 + \text{C}^{21}\text{H}_3$)

^{13}C NMR (100 MHz, CDCl_3): δ (ppm) **152.96 + 152.89 + 152.81** (C_q^5), **149.23 + 149.05 + 148.96 + 148.91** (C_q^{Ar}), **142.84 + 148.80 + 148.76 + 148.73** (C_q^{Ar}), **141.15 + 141.06 + 140.99 + 140.92** (C_q^{Ar}), **140.52 + 140.48** (C_q^{Ar}), **129.65** ($2 \times \text{C}^{\text{OTolH}}$), **124.99** ($2 \times \text{C}^{\text{OTolH}}$), **116.12 + 116.02 + 115.97 + 115.93** (C_q^{Ar}), **101.89 + 101.86** (C^6H), **101.67 + 101.60 + 101.57 + 101.54** (C^{13}H or C^{18}H), **100.35 + 100.26 + 100.17 + 100.16** (C^{13}H or C^{18}H), **62.58 + 62.54 + 62.21 + 62.16** (C^{15}H_2 or C^{20}H_2), **61.20 + 61.16 + 60.36 + 60.30** (C^{15}H_2 or C^{20}H_2), **56.15 + 56.12 + 56.09** (C^{17}H_3), **21.42** (C^{12}H_3), **20.46 + 20.36 +**

20.32 ($C^{14}H_3$ or $C^{19}H_3$), **19.79 + 19.76 + 19.49 + 19.46** ($C^{14}H_3$ or $C^{19}H_3$), **15.21 + 15.16 + 15.11** ($C^{16}H_3 + C^{21}H_3$) **10.12 + 10.02 + 9.99** (C^7H_3)

IR: $\bar{\nu}$ (cm^{-1}) 2987-2880, 1201-1065, 1039, 989-903

3-Bromo-1-methoxy-2,5-bis[(4-methoxyphenyl)methoxy]-4-methylbenzene (**492b**)



In a 100 mL two-neck flask under argon atmosphere and equipped with a condenser, hydroquinone **491** (2.972 g, 12.8 mmol, 1.0 eq.) was dissolved in 30 mL of DMF. After the addition of K_2CO_3 (8.816 g, 63.8 mmol, 5.0 eq.) and PMBCl (7.0 mL, 51.6 mmol, 4.0 eq.), the mixture was heat up at $120^\circ C$ for two hours. The solution was cooled down to room temperature and poured into 270 mL of water. The precipitate formed was filtered and rinsed with water. The latter was recrystallised from boiling hexane to give 5.185 g of **492b** as white needles.

Aspect: white needles

Yield: 86%

TLC: $R_f \approx 0.63$ (cHex/AcOEt: 7/3), visualised by UV and *p*-anisaldehyde

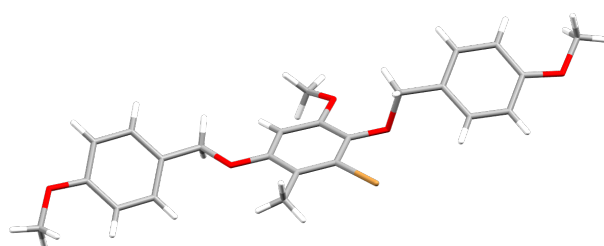
m_p : 113-115 $^\circ C$

1H NMR (500 MHz, $CDCl_3$): δ (ppm) **7.49** (d, 2H, $J = 8.6 \text{ Hz}$, $2 \times C^{10}H$), **7.36** (d, 2H, $J = 8.6 \text{ Hz}$, $2 \times C^{17}H$), **6.93** (d, 2H, $J = 8.6 \text{ Hz}$, $2 \times C^{11}H$ or $2 \times C^{18}H$), **6.91** (d, 2H, $J = 8.6 \text{ Hz}$, $2 \times C^{11}H$ or $2 \times C^{18}H$), **6.54** (s, 1H, C^6H), **4.98** (s, 2H, $C^{15}H_2$), **4.98** (s, 2H, C^8H_2), **3.83** (s, 6H, $2 \times OCH_3$), **3.82** (s, 3H, OCH_3), **2.30** (s, 3H, $C^{14}H_3$)

^{13}C NMR (126 MHz, $CDCl_3$): δ (ppm) **159.62** (C_q^{12} or C_q^{19}), **159.60** (C_q^{12} or C_q^{19}), **153.45** (C_q^5), **151.64** (C_q^1), **139.83** (C_q^2), **130.33** ($2 \times C^{10}H$), **129.83** (C_q^9 or C_q^{16}), **129.18** ($2 \times C^{17}H$), **129.13** (C_q^9 or C_q^{16}), **114.13** ($2 \times C^{18}H$), **113.81** ($2 \times C^{11}H$), **74.61** (C^8H_2), **71.35** ($C^{15}H_2$), **56.65** (OCH_3), **55.43** ($2 \times OCH_3$), **15.82** ($C^{14}H_3$)

IR: $\bar{\nu}$ (cm^{-1}) 1612, 1595, 1514, 1491, 1459, 1255, 1222, 1206, 1028, 817

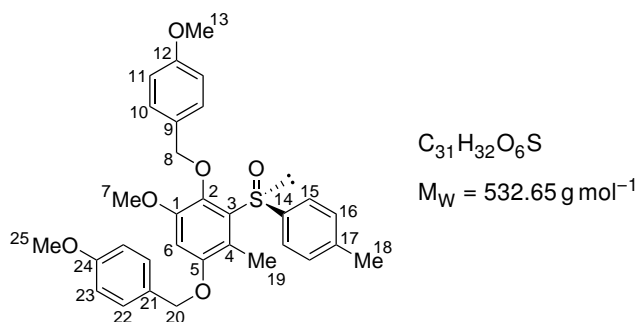
HRMS (ESI+): for $[M+H]^+$ calc.: 473.0964, found: 473.0958



Triclinic	$P\bar{1}$
$a = 7.41186(13) \text{ \AA}$	$\alpha = 109.0828(13)^\circ$
$b = 16.5746(2) \text{ \AA}$	$\beta = 93.9318(13)^\circ$
$c = 18.3483(3) \text{ \AA}$	$\gamma = 91.2656(13)^\circ$
$V = 2122.93(6) \text{ \AA}^3$	$Z = 4$
$R = 2.47\%$	

Figure 8.18: X-ray structure of **492b** and parameters of the crystal. Recrystallisation from boiling hexane.

(-)-1-Methoxy-2,5-bis[(4-methoxyphenyl)methoxy]-4-methyl-3-((S)-*p*-tolylsulfinyl)benzene (493b)



In a 100 mL two-neck flask under argon atmosphere, bromide **492b** (2.013 g, 4.26 mmol, 1.0 eq.) was dissolved in 40 mL of anhydrous THF and the solution was cooled down to -78°C . A solution of butyllithium 2.42 M in hexane (2.0 mL, 4.84 mmol, 1.1 eq.) was added dropwise and the mixture was stirred for thirty minutes at -78°C . In a 250 mL two-neck flask under argon atmosphere, sulfinic acid (S)-**292** (1.255 g, 4.26 mmol, 1.0 eq.) was dissolved in 40 mL of anhydrous THF and cooled down to -78°C . The lithium solution was quickly cannulated over the sulfinic acid solution and the final mixture was stirred for two hours at -78°C . The reaction was then warmed up to room temperature and quenched with a saturated solution of NH_4Cl . The phases were separated and the aqueous phase was extracted with dichloromethane. The organic phases were gathered, dried over MgSO_4 , filtered off and the solvents were evaporated. The crude oil was purified by flash chromatography on demetallated silica gel (cHex/AcOEt: 9/1 \rightarrow 8/2) to give 1.607 g of sulfoxide **493b**.

Aspect: white solid

Yield: 71%

TLC: $R_f \approx 0.37$ (cHex/AcOEt: 7/3), visualised by UV and *p*-anisaldehyde

m_p: 104-106 $^{\circ}\text{C}$

$[\alpha]_{\text{D}}^{20}$: -85.0° ($c = 1.0$; CHCl_3)

$^1\text{H NMR}$ (500 MHz, CDCl_3): δ (ppm) **7.45** (d, 2H, $J = 8.6$ Hz, $2 \times \text{C}^{10}\text{H}$), **7.43** (d, 2H, $J = 8.3$ Hz, $2 \times \text{C}^{15}\text{H}$), **7.30** (d, 2H, $J = 8.6$ Hz, $2 \times \text{C}^{22}\text{H}$), **7.17** (d, 2H, $J = 8.3$ Hz, $2 \times \text{C}^{16}\text{H}$), **6.90** (d, 2H, $J = 8.6$ Hz, C^{11}H), **6.89** (d, 2H, $J = 8.6$ Hz, C^{23}H), **6.65** (s, 1H, C^6H), **5.04** (dd, 2H, AB, $J_{\text{AB}} = 10.0$ Hz, $\Delta\nu_{\text{AB}} = 61.8$ Hz, C^8H_2), **4.94** (dd, 2H, AB, $J_{\text{AB}} = 11.4$ Hz, $\Delta\nu_{\text{AB}} = 13.8$ Hz, C^{20}H_2), **3.85** (s, 3H, C^7H_3), **3.81(2)** (s, 3H, C^{13}H_3 or C^{25}H_3), **3.80(6)** (s, 3H, C^{13}H_3 or C^{25}H_3), **2.33** (s, 3H, C^{18}H_3), **2.26** (s, 3H, C^{19}H_3)

$^{13}\text{C NMR}$ (126 MHz, CDCl_3): δ (ppm) **159.71** (C_q^{12}), **159.59** (C_q^{24}), **154.16** (C_q^5), **151.05** (C_q^1), **141.53** (C_q^{14}), **140.83** (C_q^2), **139.86** (C_q^{17}), **137.68** (C_q^3), **130.50** ($2 \times \text{C}^{10}\text{H}$), **129.54** ($2 \times \text{C}^{16}\text{H}$), **129.41** (C_q^{21}), **129.12** ($2 \times \text{C}^{22}\text{H}$), **128.91** (C_q^9), **124.56** ($2 \times \text{C}^{15}\text{H}$), **120.65** (C_q^4), **114.10** ($2 \times \text{C}^{11}\text{H}$ or $2 \times \text{C}^{23}\text{H}$), **113.88** ($2 \times \text{C}^{11}\text{H}$ or $2 \times \text{C}^{23}\text{H}$), **102.45** (C^6H), **75.90** (C^8H_2), **71.39** (C^{20}H_2), **56.27** (C^7H_3), **55.42** (C^{13}H_3 or C^{25}H_3), **55.40** (C^{13}H_3 or C^{25}H_3), **21.37** (C^{18}H_3), **9.90** (C^{19}H_3)

IR: $\bar{\nu}$ (cm^{-1}) 3000-2800, 1612, 1587, 1513, 1464, 1442, 1303, 1246, 1211, 1172, 1124, 1081, 1027, 808

HRMS (ESI+): for $[\text{M}+\text{H}]^+$ calc.: 533.1998, found: 533.1992

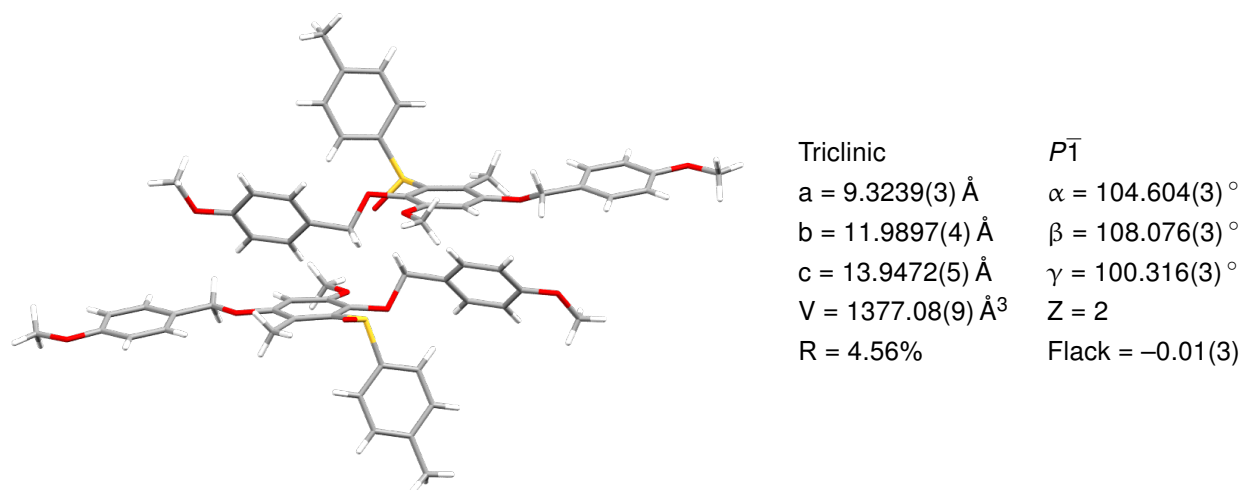
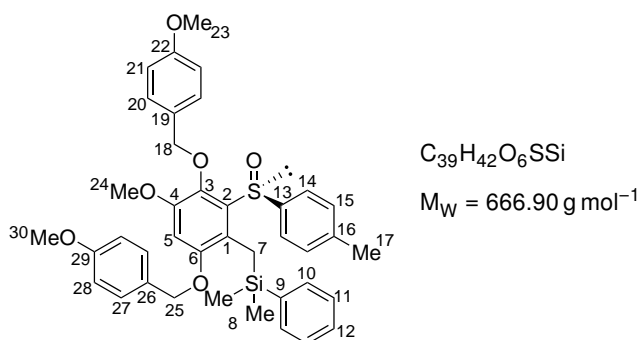


Figure 8.19: X-ray structure of **493b** and parameters of the crystal. Crystallisation by slow evaporation from dichloromethane.

(S)-(4-Methoxy-3,6-bis((4-methoxybenzyl)oxy)-2-(*p*-tolylsulfinyl)benzyl)dimethyl(phenyl)silane (494b)



This compound was prepared following the procedure reported by García Ruano *et al.*^{45,46}

In a 25 mL two-neck flask under argon atmosphere, A solution of DIPA (0.10 mL, 0.714 mmol, 1.85 eq.) in 5 mL of anhydrous THF was cooled down to -78°C . A 2.5 M solution of hexyllithium in hexanes (0.20 mL, 0.500 mmol, 1.3 eq.) was added dropwise. After ten minutes, a solution of sulfoxide **493b** (205 mg, 0.386 mmol, 1.0 eq.) in 5 mL of anhydrous THF was added dropwise the solution of LDA. After 45 min at -78°C , ClSiMe_2Ph (0.20 mL, 1.19 mmol, 3.1 eq.) was added dropwise and the final mixture was stirred for five minutes at -79°C . The reaction was allowed to warm up to room temperature and was quenched with a saturated solution of NH_4Cl . The phases were separated and the aqueous phase was extracted with dichloromethane. The organic phases were gathered, dried over MgSO_4 and the solvents were evaporated. the crude was purified by flash chromatography on demetallated silica gel (cHex/AcOEt: 9/1) to give 176 mg of **494b**.

Aspect: viscous yellow oil

Yield: 68%

TLC: $R_f \approx 0.54$ (cHex/AcOEt: 7/3), visualised by UV and *p*-anisaldehyde

$[\alpha]_D^{20}$: -29.7° ($c = 0.5$; CHCl_3)

$^1\text{H NMR}$ (400 MHz, CDCl_3): δ (ppm) **7.44-7.34** (m, 5H, $5 \times \text{C}^{\text{Ar}}\text{H}$), **7.30-7.18** (m, 4H, $\text{C}^{\text{Ar}}\text{H}$), **7.08** (d, 2H, $J = 8.0 \text{ Hz}$, $2 \times \text{C}^{15}\text{H}$), **6.87** (d, 4H, $J = 8.4 \text{ Hz}$, $2 \times \text{C}^{21}\text{H} + 2 \times \text{C}^{28}\text{H}$), **6.57** (s, 1H, C^5H),

4.96 (dd, 2H, AB, $J_{AB} = 9.8$ Hz, $\Delta\nu_{AB} = 93.7$ Hz, $C^{18}H_2$), **4.78** (dd, 2H, AB, $J_{AB} = 11.5$ Hz, $\Delta\nu_{AB} = 6.61$ Hz, $C^{25}H_2$), **3.83** (s, 3H, $C^{23}H_3$ or $C^{24}H_3$ or $C^{30}H_3$), **3.81** (s, 3H, $C^{23}H_3$ or $C^{24}H_3$ or $C^{30}H_3$), **3.79** (s, 3H, $C^{23}H_3$ or $C^{24}H_3$ or $C^{30}H_3$), **2.67** (dd, 2H, AB, $J_{AB} = 13.3$ Hz, $\Delta\nu_{AB} = 72.8$ Hz, C^7H_2), **2.29** (s, 3H, $C^{17}H_3$), **0.19** (s, 3H, C^8H_3), **0.16** (s, 3H, C^8H_3)

^{13}C NMR (100 MHz, $CDCl_3$): δ (ppm) **159.61** (C_q^{22}), **159.55** (C_q^{29}), **152.47** (C_q^6), **150.03** (C_q^4), **141.98** (C_q^{13}), **140.88** (C_q^3), **140.08** (C_q^9), **139.57** (C_q^{16}), **136.41** (C_q^2), **131.52** ($2 \times C^{10}H$), **129.90** ($2 \times C^{20}H$), **129.43** ($2 \times C^{15}H$), **129.21** (C_q^{26}), **129.05** ($C^{12}H$), **128.96** (C_q^{19}), **129.92** ($2 \times C^{27}H$), **128.23** ($2 \times C^{11}H$), **124.52** ($2 \times C^{14}H$), **123.93** (C_q^1), **114.30** ($2 \times C^{21}H$ or $2 \times C^{28}H$), **114.19** ($2 \times C^{21}H$ or $2 \times C^{28}H$), **101.79** (C^5H), **75.70** ($C^{18}H_2$), **70.12** ($C^{25}H_2$), **56.39** ($C^{24}H_3$), **55.61** ($C^{23}H_3$ or $C^{30}H_3$), **55.58** ($C^{23}H_3$ or $C^{30}H_3$), **21.37** ($C^{17}H_3$), **14.91** (C^7H_3), **-2.08** (C^8H_3), **-2.16** (C^8H_3)

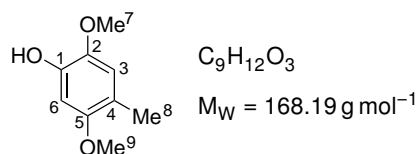
IR: $\bar{\nu}$ (cm^{-1}) 3000-2800, 1615, 1592, 1508, 1463, 1439, 1299, 1248, 1211, 1163, 1092, 1015, 875, 806, 732, 701

HRMS (ESI+): for $[M+H]^+$ calc.: 667.2550, found: 667.2546

8.5 Synthesis of the quinones

8.5.1 Quinone 369a/Q3

2,5-Dimethoxy-4-methylphenol (495)



This compound was prepared following a procedure reported by Shishido *et al.*⁴⁷

In a 100 mL round bottom flask, a solution of aldehyde **475** (5.030 g, 27.9 mmol, 1.0 eq.) and NaHCO₃ (6.342 g, 75.5 mmol, 2.7 eq.) was cooled down to -10 °C. Solid *m*CPBA (70%) (8.334 g, 33.8 mmol, 1.2 eq.) was added and the reaction mixture was stirred one hour. The solution was treated with water, the phases were separated the aqueous phase was extracted with dichloromethane. The organic phase was then washed with a saturated solution of NaHCO₃ and brine. The latter was then dried over Na₂SO₄ and the solvent was evaporated. The resulting orange oil was then dissolved in 100 mL of methanol and a solution of KOH (1.958 g, 34.9 mmol, 1.2 eq.) in 20 mL in methanol was added. After thirty minutes, the solvent was evaporated and the resulting solid was dissolved in 100 mL of water. Acidification of the solution with HCl (37%) was done until a pH below 2 was reached. The precipitate formed was filtered and rinsed with water. The solid was then dissolved in ethyl acetate, the organic phase was dried over Na₂SO₄ and the solvent was evaporated to give 3.765 g of **495**

Aspect: white solid

Yield: 80%

TLC: R_f ≈ 0.45 (cHe/AcOEt: 8/2), visualised by UV and *p*-anisaldehyde

m_p: 78-79 °C

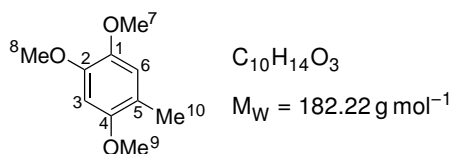
¹H NMR (500 MHz, CDCl₃): δ (ppm) **6.68** (s, 1H, C⁶H), **6.53** (s, 1H, C³H), **5.52** (s, 1H, OH), **3.83** (s, 3H, C⁷H₃), **3.76** (s, 3H, C⁹H₃), **2.15** (s, 3H, C⁸H₃)

¹³C NMR (126 MHz, CDCl₃): δ (ppm) **152.21** (C⁵_q), **144.16** (C¹_q), **139.98** (C²_q), **117.17** (C⁴_q), **114.14** (C³H), **99.23** (C⁶H), **56.89** (C⁷H₃), **56.09** (C⁹H₃), **15.78** (C⁸H₃)

IR: ν̄ (cm⁻¹) 3600-3100, 2959, 2936, 2838, 1601, 1519, 1414, 1311, 1225, 1195, 1168, 1119, 1039, 1003, 838

The experimental data were in agreement with those reported in the literature.⁴⁷

1,2,4-Trimethoxy-5-methylbenzene (496)



In a 250 mL two-neck flask under argon atmosphere, phenol **495** (3.496 g, 20.8 mmol, 1.0 eq.) was dissolved in 50 mL of dichloromethane. A solution of NaOH (1.248 g, 31.2 mmol, 1.5 eq.) in water was added. After ten minutes, Bu₄NBr (344 mg, 1.07 mmol, 0.05 eq.) was added, followed

by the dropwise addition of Me_2SO_4 (4.0 mL, 42.3 mmol, 2.0 eq.). After two hours, NaOH (1.682 g, 42.1 mmol, 2.0 eq.) was added and the solution was vigorously stirred overnight. The phases were then separated and the aqueous phase was extracted with dichloromethane. The organic phases were gathered, washed with brine and dried over MgSO_4 . The solvent was evaporated and the crude product was purified by filtration over silica gel, using dichloromethane as eluent, to give 3.635 g of trimethoxytoluene **496**.

Aspect: white solid

Yield: 96%

TLC: $R_f \approx 0.50$ (cHex/AcOEt: 8/2), visualised by UV and *p*-anisaldehyde

m_p : 53-56 °C

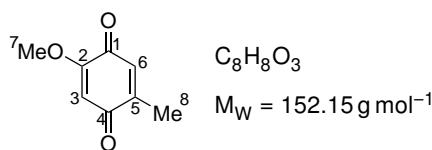
$^1\text{H NMR}$ (500 MHz, CDCl_3): δ (ppm) **6.70** (s, 1H, C^6H), **6.51** (s, 1H, C^3H), **3.87** (s, 3H, C^7H_3), **3.83** (s, 3H, C^8H_3), **3.80** (s, 3H, C^9H_3), **2.17** (s, 3H, C^{10}H_3)

$^{13}\text{C NMR}$ (126 MHz, CDCl_3): δ (ppm) **151.73** (C_q^4), **147.53** (C_q^1), **142.82** (C_q^2), **118.02** (C_q^5), **114.97** (C^6H), **97.93** (C^3H), **56.70** (C^7H_3 or C^8H_3 or C^9H_3), **56.49** (C^7H_3 or C^8H_3 or C^9H_3), **56.41** (C^7H_3 or C^8H_3 or C^9H_3), **15.66** (C^{10}H_3)

IR: $\bar{\nu}$ (cm^{-1}) 2957, 2834, 1515, 1454, 1220, 1199, 1043, 1030, 853, 818

The experimental data were in agreement with those reported in the literature.⁴⁸

2-Methoxy-5-methylcyclohexa-2,5-diene-1,4-dione (**369a/Q3**)



In a 500 mL round bottom flask, a solution of CAN (23.324 g, 42.5 mmol, 2.5 eq.) in 180 mL of water was poured on a solution of **496** (3.080 g, 19.9 mmol, 1.0 eq.) in 180 mL of MeCN. After 10 min, MeCN was evaporated and the aqueous phase was extracted with dichloromethane. The organic phase was dried over MgSO_4 and the solvent was evaporated to give 2.367 g of quinone **369a**.

Aspect: yellow powder

Yield: 92%

TLC: $R_f \approx 0.18$ (cHex/AcOEt: 8/2), visualised by UV and *p*-anisaldehyde

m_p : 170-172 °C

$^1\text{H NMR}$ (500 MHz, CDCl_3): δ (ppm) **6.54** (q, 1H, $J = 1.6 \text{ Hz}$, C^6H), **5.91** (s, 1H, C^3H), **3.80** (s, 3H, C^7H_3), **2.05** (d, 1H, $J = 1.6 \text{ Hz}$, C^8H)

$^{13}\text{C NMR}$ (126 MHz, CDCl_3): δ (ppm) **187.79** (C_q^4), **182.26** (C_q^1), **158.81** (C_q^5), **146.99** (C_q^5), **131.37** (C^6H), **107.68** (C^3H), **56.35** (C^7H_3), **15.91** (C^8H_3)

IR: $\bar{\nu}$ (cm^{-1}) 1670, 1648, 1598, 1466, 1365, 1235, 1205, 975, 910, 859

The experimental data were in agreement with those reported in the literature.⁴⁸

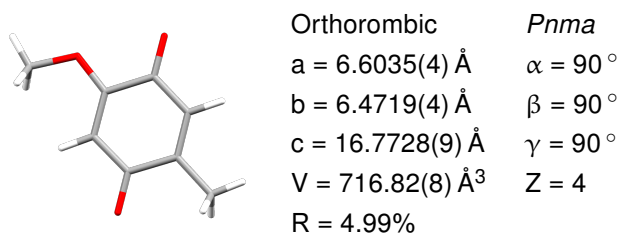
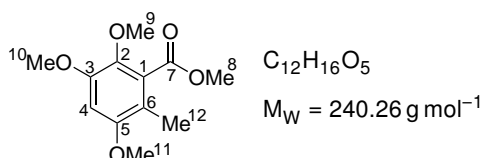


Figure 8.20: X-ray structure of **369a** and parameters of the crystal. Recrystallisation from boiling ethanol.

8.5.2 Quinone 371a/Q8

Methyl 2,3,5-trimethoxy-6-methylbenzoate (497)



In a dry 250 mL two-neck flask under argon atmosphere, a solution of bromide **480** (3.06 g, 11.7 mmol, 1.0 eq.) in 100 mL of anhydrous THF was cooled down to -78°C . A 2.3 M solution of hexyllithium in hexanes (6.5 mL, 15.0 mmol, 1.3 eq.) was added dropwise to the bromide solution. After ten minutes, methyl chloroformate (1.2 mL, 15.5 mmol, 1.3 eq.) was added dropwise and the reaction mixture was allowed to warm up to room temperature. After one hour, the mixture was cooled down to 0°C , quenched with water and diluted with diethyl ether. The phases were separated, the organic phase was dried over Na_2SO_4 and the solvents were evaporated. The crude mixture was purified by flash chromatography on silica gel (cHex/AcOEt: 95/5) to give 2.330 g of **497**.

Aspect: white powder

Yield: 83%

TLC: $R_f \approx 0.36$ (cHex/AcOEt: 8/2), visualised by UV and *p*-anisaldehyde

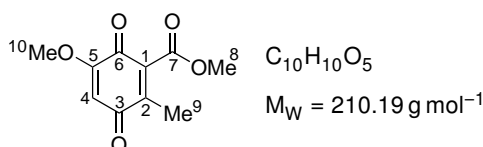
m_p : $51\text{--}53^\circ\text{C}$

$^1\text{H NMR}$ (500 MHz, CDCl_3): δ (ppm) **6.52** (s, 3H, C^4H_3), **3.92** (s, 3H, C^8H_3), **3.87** (s, 3H, C^{10}H_3), **3.81** (s, 3H, C^{11}H_3), **3.80** (s, 3H, C^9H_3), **2.06** (s, 3H, C^{12}H_3)

$^{13}\text{C NMR}$ (126 MHz, CDCl_3): δ (ppm) **168.46** (C_q^7), **154.20** (C_q^5), **151.00** (C_q^3), **139.39** (C_q^2), **130.39** (C_q^1), **115.71** (C_q^6), **98.92** (C^4H), **61.84** (C^9H_3), **56.53** (C^{10}H_3), **56.36** (C^{11}H_3), **52.39** (C^8H_3)

IR: $\bar{\nu}$ (cm^{-1}) 2948, 1728, 1438, 1334, 1267, 1195, 1063, 967

Methyl 5-methoxy-2-methyl-3,6-dioxocyclohexa-1,4-diene-1-carboxylate (371a/Q8)



A solution of CAN (12.91 g, 23.5 mmol, 2.5 eq.) in 100 mL of water was added to a solution of benzoate **497** (2.24 g, 9.33 mmol, 1.0 eq.) in 100 mL of acetonitrile. After fifteen minute at room

temperature, acetonitrile was evaporated and the aqueous phase was extracted with dichloromethane. The organic phase was then dried over Na_2SO_4 and the solvents were evaporated. The crude mixture was dissolved in a minimum of dichloromethane and the product was precipitated by the addition of pentane. The yellow precipitate was filtered, washed with pentane and dried under vacuum to yield 1.62 g of quinone **371a**.

Aspect: bright yellow powder

Yield: 83%

TLC: $R_f \approx 0.38$ (cHex/AcOEt: 7/3), visualised by UV and *p*-anisaldehyde

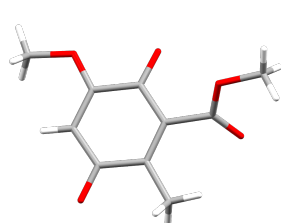
m_p : 98–100 °C

$^1\text{H NMR}$ (500 MHz, CDCl_3): δ (ppm) **5.98** (s, 1H, C^4H), **3.92** (s, 3H, C^8H_3), **3.83** (s, 3H, C^{10}H_3), **2.06** (s, 3H, C^9H_3)

$^{13}\text{C NMR}$ (126 MHz, CDCl_3): δ (ppm) **186.42** (C_q^3), **178.65** (C_q^6), **164.48** (C_q^7), **158.14** (C_q^5), **143.44** (C_q^2), **135.81** (C_q^1), **107.71** (C^4H), **56.58** (C^{10}H_3), **53.00** (C^8H_3), **13.59** (C^9H_3)

IR: $\bar{\nu}$ (cm^{-1}) 1716, 1683, 1648, 1607, 1436, 1369, 1292, 1249, 1222, 1059, 1009, 865

HRMS (ESI+): for $[\text{M}+\text{Na}]^+$ calc.: 233.0420, found: 233.0412

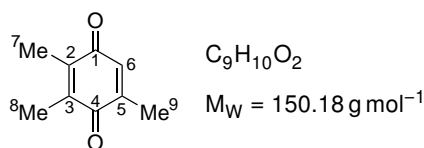


Monoclinic	$P2_1/n$
$a = 3.9749(3) \text{ \AA}$	$\alpha = 90^\circ$
$b = 14.4461(8) \text{ \AA}$	$\beta = 91.309(5)^\circ$
$c = 17.1695(8) \text{ \AA}$	$\gamma = 90^\circ$
$V = 982.64(10) \text{ \AA}^3$	$Z = 4$
$R = 5.86\%$	

Figure 8.21: X-ray structure of **371a** and parameters of the crystal. Crystallisation by slow evaporation from dichloromethane.

8.5.3 Quinone Q2

2,3,5-Trimethylcyclohex-2,5-diene-1,4-dione (Q2)



Into a 1 L round-bottomed flask, 2,3,5-trimethylhydroquinone (3.074 g, 20.2 mL, 1.0 eq.), was dissolved in 300 mL of acetonitrile. A solution of CAN (27.898 g, 50.9 mmol, 2.5 eq.) dissolved in 150 mL of water was quickly added. The solution directly turned yellow. After ten minutes, the acetonitrile was evaporated and the aqueous residue was extracted with dichloromethane. The organic phase was washed with water and brine. It was then dried over MgSO_4 and the solvents were evaporated to give 2.001 g of a yellow solid.

Aspect: yellow powder

Yield: 66%

TLC: $R_f \approx 0.64$ (cHex/AcOEt: 6/4), visualised by UV and *p*-anisaldehyde

m_p : 34–36 °C

$^1\text{H NMR}$ (500 MHz, CDCl_3): δ (ppm) **6.54** (q, 1H, $J = 1.6 \text{ Hz}$, C^6H), **2.02** (d, 3H, $J = 1.6 \text{ Hz}$, C^9H_3),

2.01 (dd, 3H, $J = 2.3; 1.2$ Hz, C^8H_3), **1.99** (dd, 3H, $J = 2.3; 1.2$ Hz, C^7H_3)

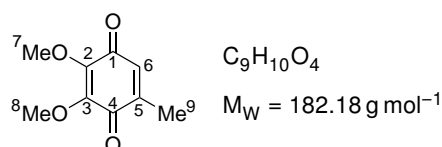
^{13}C NMR (126 MHz, $CDCl_3$): δ (ppm) **188.01** (C_q^4), **187.63** (C_q^1), **145.45** (C_q^5), **141.02** (C_q^2), **140.85** (C_q^3), **133.19** (C^6H), **16.00** (C^9H_3), **12.47** (C^8H_3), **12.17** (C^7H_3)

IR: $\bar{\nu}$ (cm^{-1}) 1643, 1615, 1371, 1316, 1261, 1191, 903, 889, 675

The experimental data were in agreement with those reported in the literature.⁴⁹

8.5.4 Quinone Q4

2,3-Dimethoxy-5-methyl-cyclohexa-2,5-diene-1,4-dione (Q4)



Into a 250 mL round-bottomed flask, 1,2,3,4-tetramethoxy-5-methylbenzene (1.013 g, 4.77 mmol, 1.0 eq.) was dissolved in 75 mL of acetonitrile. A solution of CAN (6.631 g, 12.1 mmol, 2.5 eq.) in 75 mL of water was quickly added. After twenty minutes, the acetonitrile was evaporated and the aqueous residue was extracted with dichloromethane. The organic phase was washed with water and brine. It was then dried over $MgSO_4$ and the solvents were evaporated to give 815 mg of desired benzoquinone.

Aspect: dark red solid

Yield: 94%

TLC: $R_f \approx 0.56$ (cHex/AcOEt: 7/3), visualised by UV and *p*-anisaldehyde

m_p : 58-60 °C

1H NMR (500 MHz, $CDCl_3$): δ (ppm) **6.43** (q, 1H, $J = 1.6$ Hz, C^6H), **4.02** (s, 3H, C^7H_3 or C^8H_3), **3.99** (s, 3H, C^8H_3 or C^7H_3), **2.03** (d, 3H, $J = 1.6$ Hz, C^9H_3)

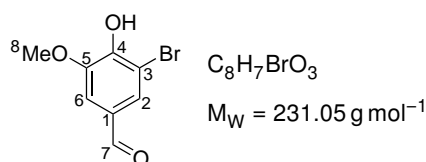
^{13}C NMR (126 MHz, $CDCl_3$): δ (ppm) **184.56** (C_q^1 or C_q^4), **184.34** (C_q^4 or C_q^1), **145.16** (C_q^2 or C_q^3), **144.98** (C_q^3 or C_q^2), **144.19** (C_q^5), **131.43** (C^6H), **61.40** (C^7H_3 or C^8H_3), **61.33** (C^8H_3 or C^7H_3), **15.62** (C^9H_3)

IR: $\bar{\nu}$ (cm^{-1}) 1669, 1653, 1640, 1600, 1458, 1430, 1318, 1277, 1215, 1199, 1125, 1089, 991, 943, 898, 884, 721, 675, 461

The experimental data were in agreement with those reported in the literature.⁵⁰

8.5.5 Quinone Q5

3-Bromo-4-hydroxy-5-methoxybenzaldehyde (550)



Into a three-neck 1 L flask under argon atmosphere, equipped with a dropping funnel, vanillin (**483**) (10.328 g, 67.88 mmol, 1.0 eq.) and sodium acetate (8.362 g, 101.9 mmol, 1.5 eq.) were dissolved in 250 mL of glacial acetic acid. Through the dropping funnel, a solution of Br_2 (3.5 mL, 68.13 mmol, 1.0 eq.) in 25 mL of glacial acetic acid were added dropwise. After three hours, the solid formed during the reaction was filtered and the filtrate were evaporated to give a brownish solid. Both solid

were dissolved in dichloromethane and the organic phase was washed with saturated solutions of $\text{Na}_2\text{S}_2\text{O}_3$, NaHCO_3 and NaCl , successively. The organic phase was dried over MgSO_4 and the solvent was evaporated to give 12.982 g of a yellowish solid. The analytical sample could be obtained by recrystallisation from boiling methanol.

Aspect: Yellowish crystals

Yield: 83%

TLC: $R_f \approx 0.61$ (cHex/TBME : 4/6), visualised by UV and *p*-anisaldehyde

m_p : 160-163 °C

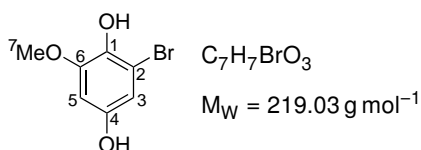
$^1\text{H NMR}$ (400 MHz, $\text{DMSO}-d_6$): δ (ppm) **9.77** (s, 1H, C^7H), **7.72** (d, 1H, $J = 1.8$ Hz, C^2H), **7.41** (d, 1H, $J = 1.8$ Hz, C^6H), **3.91** (s, 3H, C^8H_3)

$^{13}\text{C NMR}$ (400 MHz, $\text{DMSO}-d_6$): δ (ppm) **190.48** (C^7H), **149.83** (C^4_q), **148.67** (C^5_q), **128.94** (C^3_q), **128.80** (C^2H), **109.55** (C^6H), **109.24** (C^1_q), **56.37** (C^8H_3)

IR: $\bar{\nu}$ (cm^{-1}) 3500-3000, 1673, 1423, 1289, 1045, 854

The experimental data were in agreement with those reported in the literature.⁵¹

2-Bromo-6-methoxybenzene-1,4-diol (551)



This compound was prepared following a procedure reported by Cross and Zammit.⁵²

Into a 250 mL two-neck flask equipped with a dropping funnel, benzaldehyde **550** (6.340 g of phenol, 24.28 mmol, 1.0 eq.) was dissolved in of a 1 M aqueous solution of NaOH (25 mL, 25.00 mmol, 1.0 eq.). Through the dropping funnel, a 5% aqueous solution of H_2O_2 (20 mL, 30.00 mmol, 1.2 eq.) was added dropwise. The solution darkened and heated up and a pink solid precipitated. The mixture was stirred overnight. The next day, the solid was filtered and washed with water. After deep drying under vacuum, 5.021 g of a light gray solid were obtained.

Aspect: light grey powder

Yield: 95%

TLC: $R_f \approx 0.45$ (cHex/AcOEt: 4/6), visualised by UV and *p*-anisaldehyde

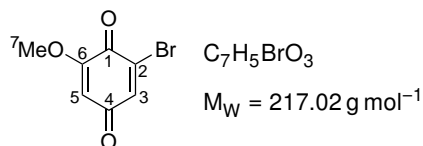
m_p : 138-141 °C

$^1\text{H NMR}$ (400 MHz, CD_3OD): δ (ppm) **6.49** (d, 1H, $J = 2.7$ Hz, C^3H), **6.40** (d, 1H, $J = 2.7$ Hz, C^5H), **3.81** (s, 3H, C^7H_3)

$^{13}\text{C NMR}$ (400 MHz, CD_3OD): δ (ppm) **151.90** (C^4_q), **150.23** (C^6_q), **138.21** (C^1_q), **111.12** (C^3H), **110.07** (C^2_q), **100.46** (C^5H), **56.52** (C^7H_3)

IR: $\bar{\nu}$ (cm^{-1}) 3400-3000, 1470, 1430, 1214, 1190, 1134, 1036, 842

The experimental data were in agreement with those reported in the literature.⁵³

2-Bromo-6-methoxycyclohexa-2,5-diene-1,4-dione (Q5)

Into a 500 mL round-bottom flask, hydroquinone **551** (2.013 g, 9.19 mmol, 1.0 eq.) was dissolved in 150 mL of acetonitrile. A solution of CAN (12.700 g, 23.2 mmol, 2.5 eq.) in 150 mL of water was quickly added and the orange mixture was stirred one hour at room temperature. The acetonitrile was then evaporated under reduced pressure and the aqueous phase was extracted with dichloromethane. The organic phase was dried over $MgSO_4$ and the solvents were evaporated. The crude was recrystallised in boiling ethanol to yield 1.640 g of quinone.

Aspect: orange needles

Yield: 72%

TLC: $R_f \approx 0.37$ (cHex/AcOEt: 6/4), visualised by UV and *p*-anisaldehyde

m_p : 167-169 °C

1H NMR (500 MHz, $CDCl_3$): δ (ppm) **7.20** (d, 1H, $J = 2.3$ Hz, C^3H), **5.96** (d, 1H, $J = 2.3$ Hz, C^5H), **3.85** (s, 3H, C^7H_3)

^{13}C NMR (126 MHz, $CDCl_3$): δ (ppm) **184.76** (C^1_q), **174.67** (C^4_q), **158.38** (C^6_q), **138.61** (C^3H), **134.39** (C^2_q), **107.76** (C^5H), **56.95** (C^7H_3)

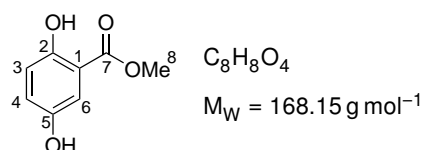
IR: $\bar{\nu}$ (cm^{-1}) 1686, 1620, 1571, 1309, 1228, 1131, 991, 903, 788

The experimental data were in agreement with literature.⁵³



Monoclinic $P2_1/c$
 $a = 3.84287(14) \text{ \AA}$ $\alpha = 90^\circ$
 $b = 19.5438(7) \text{ \AA}$ $\beta = 99.648(3)^\circ$
 $c = 9.7482(3) \text{ \AA}$ $\gamma = 90^\circ$
 $V = 721.78(4) \text{ \AA}^3$ $Z = 4$
 $R = 3.68\%$

Figure 8.22: X-ray structure of **Q5** and parameters of the crystal. Recrystallisation from boiling ethanol.

8.5.6 Quinone Q7**Methyl 2,5-dihydroxybenzoate**

Into a 250 mL round-bottomed flask, 2,5-dihydroxybenzoic acid (10.039 g, 65.1 mmol, 1.0 eq.) was dissolved in 70 mL of methanol. Afterwards, 5 mL of sulfuric acid was added and the final mixture was refluxed overnight. The methanol was evaporated and the residue was dissolved in dichloromethane.

The organic phase was washed with water and a saturated solution of NaHCO_3 and then, dried over Na_2SO_4 . The solvents were evaporated to give 9.704 g of the desired methyl ester.

Aspect: white solid

Yield: 89%

TLC: $R_f \approx 0.60$ (PhMe/AcOEt: 7/3), visualised by UV and KMnO_4

m_p : 89-92 °C

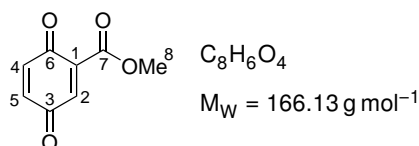
$^1\text{H NMR}$ (500 MHz, CDCl_3): δ (ppm) **7.24** (d, 1H, $J = 3.3$ Hz, C^6H), **6.99** (dd, 1H, $J = 9.0$; 3.3 Hz, C^4H), **6.84** (d, 1H, $J = 9.0$ Hz, C^3H), **3.89** (s, 3H, C^8H_3)

$^{13}\text{C NMR}$ (126 MHz, CDCl_3): δ (ppm) **170.37** (C_q^7), **155.34** (C_q^2 or C_q^5), **148.29** (C_q^5 or C_q^2), **124.26** (C^4H), **118.41** (C^3H), **114.85** (C^6H), **112.24** (C_q^1), **52.47** (C^8H_3)

IR: $\bar{\nu}$ (cm^{-1}) 3500-3100, 1683, 1616, 1505, 1437, 1337, 1213, 1187, 1077, 872, 781, 681

The experimental data were in agreement with those reported in the literature.⁵⁴

Methyl 3,6-dioxocyclohexa-1,4-diene-1-carboxylate (Q7)



Into a 100 mL round-bottomed under argon atmosphere, methyl 2,5-dihydroxybenzoate (2.001 g, 11.9 mmol, 1.0 eq.) was dissolved in 20 mL of diethyl ether, followed by the addition of MgSO_4 (4.101 g, 34.1 mmol, 2.9 eq.) and Ag_2O (4.061 g, 17.5 mmol, 1.5 eq.). After four hours, the solution was filtered over Celite[®] and the solvent was evaporated to give 1.875 g of desired benzoquinone.

Aspect: orange solid

Yield: 95%

TLC: $R_f \approx 0.65$ (PhMe/AcOEt: 7/3), visualised by UV and KMnO_4

m_p : 51-52 °C

$^1\text{H NMR}$ (500 MHz, CDCl_3): δ (ppm) **7.11** (dd, 1H, $J = 2.0$; 0.5 Hz, C^4H), **6.83** (d, 1H, $J = 2.0$ Hz, C^5H), **6.82** (d, 1H, $J = 0.5$ Hz, C^2H), **3.91** (s, 3H, C^8H_3)

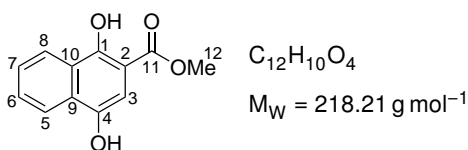
$^{13}\text{C NMR}$ (126 MHz, CDCl_3): δ (ppm) **186.95** (C_q^3), **183.11** (C_q^6), **163.27** (C_q^7), **137.14** (C_q^1), **137.07** (C^2H), **136.70** (C^4H), **136.28** (C^5H), **53.28** (C^8H_3)

IR: $\bar{\nu}$ (cm^{-1}) 1737, 1710, 1662, 1601, 1438, 1338, 1243, 1225, 1205, 1043, 962, 841, 793, 779, 560

The experimental data were in agreement with those reported in the literature.⁵⁵

8.5.7 Naphthoquinone Q9

Methyl 1,4-dihydroxynaphthalene-2-carboxylate



Into a 250 mL two-neck flask under argon atmosphere, 1,4-dihydroxy-2-naphthoic acid (10.019 g, 49.1 mmol, 1.0 eq.) was dissolved in 70 mL of anhydrous DMF. Afterwards, NaHCO_3 (8.369 g, 99.6 mmol,

2.0 eq.) and iodomethane (3.1 mL, 49.8 mmol, 1.0 eq.) was added to the solution. After seven hours, the reaction mixture was poured into 350 mL of water. The precipitate was filtered off and thoroughly washed with water. It was dissolved in ethyl acetate and dried over Na_2SO_4 . The solvent was then evaporated to give 7.690 g of desired product.

Aspect: greenish powder

Yield: 72%

TLC: $R_f \approx 0.66$ (PhMe/AcOEt/AcOH: 8/2/0.5), visualised by UV and KMnO_4

m_p : 195-197 °C

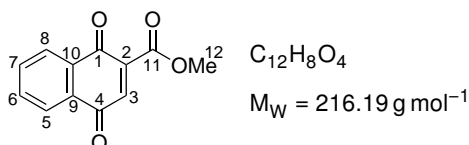
$^1\text{H NMR}$ (500 MHz, CDCl_3): δ (ppm) **11.33** (s, 1H, OH), **8.21** (d, 1H, $J = 8.3$ Hz, C^9H), **8.07** (d, 1H, $J = 8.3$ Hz, C^6H), **7.52-7.44** (m, 1H, C^7H), **7.44-7.36** (m, 1H, C^8H), **7.01** (s, 1H, C^3H), **3.83** (s, 3H, C^{12}H_3)

$^{13}\text{C NMR}$ (126 MHz, CDCl_3): δ (ppm) **171.16** (C_q^{11}), **154.16** (C_q^1), **144.86** (C_q^4), **129.52** (C_q^5), **128.30** (C^7H), **125.81** (C^8H), **125.22** (C_q^{10}), **123.42** (C^9H), **122.16** (C^6H), **104.53** (C_q^2), **104.28** (C^3H), **52.03** (C^{12}H_3)

IR: $\bar{\nu}$ (cm^{-1}) 3500-3200, 1648, 1634, 1599, 1438, 1354, 1292, 1255, 1216, 1148, 1073, 991, 845, 792, 762, 664, 644, 600

The experimental data were in agreement with those reported in the literature.⁵⁶

Methyl 1,4-dioxonaphthalene-2-carboxylate (Q9)



Into a 100 mL round-bottomed flask under argon atmosphere, methyl 1,4-dihydroxynaphthalene-2-carboxylate (2.671 g, 12.4 mmol, 1.0 eq.) was dissolved in 20 mL of diethyl ether, followed by the addition of MgSO_4 (4.214 g, 35.0 mmol, 2.9 eq.) and Ag_2O (8.630 g, 37.2 mmol, 3.0 eq.). The resulting mixture was stirred overnight. The solution was filtered over Celite[®] and the solvent was evaporated to give 1.843 g of desired naphthoquinone.

Aspect: orange solid

Yield: 70%

TLC: $R_f \approx 0.47$ (cHex/AcOEt: 7/3), visualised by UV and KMnO_4

m_p : 88-90 °C

$^1\text{H NMR}$ (500 MHz, CDCl_3): δ (ppm) **8.15-8.06** (m, 1H, C^9H), **8.09-8.04** (m, 1H, C^6H), **7.83-7.74** (m, 2H, $\text{C}^7\text{H} + \text{C}^8\text{H}$), **7.26** (s, 1H, C^3H), **3.94** (s, 3H, C^{12}H_3)

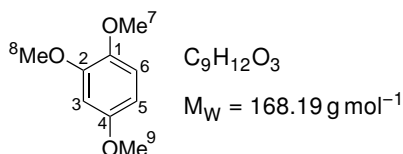
$^{13}\text{C NMR}$ (126 MHz, CDCl_3): δ (ppm) **184.68** (C_q^4), **181.24** (C_q^1), **163.91** (C_q^{11}), **139.54** (C_q^2), **138.45** (C^3H), **134.70** (C^8H), **134.38** (C^7H), **131.88** (C_q^{10}), **131.69** (C_q^5), **127.14** (C^9H), **126.42** (C^6H), **53.27** (C^{12}H_3)

IR: $\bar{\nu}$ (cm^{-1}) 1719, 1658, 1588, 1432, 1351, 1292, 1258, 1124, 963, 918, 784, 756, 711, 690

The experimental data were in agreement with those reported in the literature.⁵⁵

8.5.8 Phthalide quinone 534

1,2,4-Trimethoxybenzene (543)



In a 500 mL two-neck flask under argon atmosphere, hydroquinone **484** (3.620 g, 25.8 mmol, 1.0 eq.) was suspended in 100 mL of dichloromethane. A solution of NaOH (2.904 g, 72.3 mmol, 2.8 eq.) in 100 mL of water was added. After ten minutes, Bu₄NBr (416 mg, 1.29 mmol, 0.06 eq.) was added, followed by the dropwise addition of Me₂SO₄ (10 mL, 105.4 mmol, 4.0 eq.). After two hours, solid NaOH (3.004 g, 75.1 mmol, 2.9 eq.) was added to the reaction and the mixture was vigorously stirred overnight. The phases were separated and the aqueous phase was extracted with dichloromethane. The organic phase was washed with brine, dried over MgSO₄ and the solvent was evaporated. The crude oil was purified by filtration over silica gel using dichloromethane as eluent and the solvent was evaporated to yield 3.646 g of trimethoxybenzene **543**.

Aspect: yellow oil

Yield: 84%

TLC: $R_f \approx 0.48$ (cHex/AcOEt: 5/5), visualised by UV and *p*-anisaldehyde

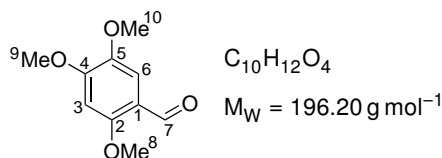
¹H NMR (500 MHz, CDCl₃): δ (ppm) **6.78** (d, 1H, $J = 8.7$ Hz, C⁶H), **6.51** (d, 1H, $J = 2.8$ Hz, C³H), **6.39** (dd, 1H, $J = 8.7; 2.8$ Hz, C⁵H), **3.85** (s, 3H, C⁸H₃), **3.83** (s, 3H, C⁷H₃ or C⁹H₃), **3.77** (s, 3H, C⁷H₃ or C⁹H₃)

¹³C NMR (126 MHz, CDCl₃): δ (ppm) **154.30** (C_q¹ or C_q⁴), **149.91** (C_q²), **143.51** (C_q¹ or C_q⁴), **111.77** (C⁶H), **102.83** (C⁵H), **100.38** (C³H), **56.51** (C⁷H₃ or C⁸H₃ or C⁹H₃), **55.90** (C⁷H₃ or C⁸H₃ or C⁹H₃), **55.75** (C⁷H₃ or C⁸H₃ or C⁹H₃)

IR: $\bar{\nu}$ (cm⁻¹) 2938, 2833, 1596, 1508, 1455, 1437, 1281, 1261, 1226, 1205, 1181, 1155, 1137, 1122, 1047, 1024, 921, 830

The experimental data were in agreement with those reported in the literature.⁵⁷

2,4,5-Trimethoxybenzaldehyde (544)



In a 100 mL two-neck flask under argon atmosphere and equipped with a condenser, POCl₃ (3.4 mL, 36.5 mmol, 1.8 eq.) was added dropwise on *N*-methylformanilide (4.2 mL, 34.0 mmol, 1.7 eq.). After fifteen minutes, trimethoxybenzene **543** (3.413 g, 20.3 mmol, 1.0 eq.) was added dropwise to the yellow oil and the final mixture is heated up to 60 °C. The solution slowly darkened and solidified. After 35 min, the solution was cooled down to room temperature and 20 mL of iced water were added. The mixture was stirred at room temperature overnight. The yellow precipitate was then filtered and rinsed with water. The solide was dissolved in dichloromethane and the aqueous phase was extracted with dichloromethane. The organic phases were gathered, dried over MgSO₄ and the solvent was

evaporated. The crude product was purified by filtration over silica gel using ethyl acetate as eluent. The solvent was evaporated to give 3.178 g of benzaldehyde **544**

Aspect: white solid

Yield: 80%

TLC: $R_f \approx 0.57$ (cHex/AcOEt: 8/2), visualised by UV and *p*-anisaldehyde

m_p: 113-115 °C

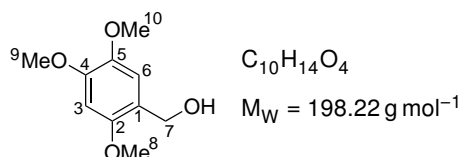
¹H NMR (126 MHz, CDCl₃): δ (ppm) **10.31** (s, 1H, C⁷H), **7.33** (s, 1H, C⁶H), **6.49** (s, 1H, C³H), **3.98** (C⁸H₃, C⁹H₃, C¹⁰H₃), **3.93** (C⁸H₃, C⁹H₃, C¹⁰H₃), **3.88** (C⁸H₃, C⁹H₃, C¹⁰H₃)

¹³C NMR (126 MHz, CDCl₃): δ (ppm) **188.2** (C⁷H), **158.77** (C_q² or C_q⁴ or C_q⁵), **155.90** (C_q² or C_q⁴ or C_q⁵), **143.68** (C_q² or C_q⁴ or C_q⁵), **117.45** (C_q¹), **109.08** (C⁶H), **96.01** (C³H), **56.43** (C⁸H₃ or C⁹H₃ or C¹⁰H₃), **56.36** (C⁸H₃ or C⁹H₃ or C¹⁰H₃), **56.34** (C⁸H₃ or C⁹H₃ or C¹⁰H₃)

IR: $\bar{\nu}$ (cm⁻¹) 2931, 2864, 2833, 1657, 1607, 1516, 1478, 1357, 1290, 1263, 1213, 1187, 1126, 1041, 1024, 995, 863, 823

The experimental data were in agreement with those reported in the literature.⁵⁸

(2,4,5-Trimethoxyphenyl)methanol (**545**)



In a 250 mL two-neck flask under argon atmosphere, benzaldehyde **544** (3.178 g, 16.2 mmol, 1.0 eq.) was suspended in 100 mL of methanol. Then, NaBH₄ (672 mg, 17.8 mmol, 1.1 eq.) was added by portions at 0 °C and the mixture was allowed to warm up to room temperature. After 35 min, the reaction mixture was cooled down to 0 °C and 20 mL of water were added. Methanol was evaporated and the aqueous phase was extracted with diethyl ether. The organic phase was then washed with brine, dried over MgSO₄ and the solvent was evaporated to give 2.819 g of benzyl alcohol **545**.

Aspect: white solid

Yield: 88%

TLC: $R_f \approx 0.20$ (cHex/AcOEt: 5/5), visualised by UV and *p*-anisaldehyde

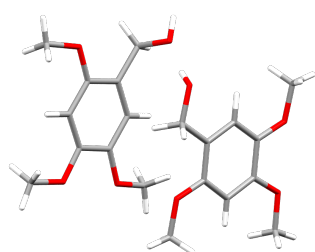
m_p: 68-70 °C

¹H NMR (500 MHz, CDCl₃): δ (ppm) **6.85** (s, 1H, C⁶H), **6.52** (s, 1H, C³H), **4.61** (d, 2H, $J = 4.0$ Hz, C⁷H₂), **3.88** (s, 3H, C⁸H₃), **3.83** (s, 3H, C⁹H₃ or C¹⁰H₃), **3.83** (s, 3H, C⁹H₃ or C¹⁰H₃), **2.26** (s (br), 1H, OH)

¹³C NMR (126 MHz, CDCl₃): δ (ppm) **152.28** (C_q⁴ or C_q⁵), **149.75** (C_q²), **143.39** (C_q⁴ or C_q⁵), **121.12** (C_q¹), **113.74** (C⁶H), **97.82** (C³H), **62.13** (C⁷H₂), **57.19** (C⁸H₃ or C⁹H₃ or C¹⁰H₃), **56.85** (C⁸H₃ or C⁹H₃ or C¹⁰H₃), **56.74** (C⁸H₃ or C⁹H₃ or C¹⁰H₃)

IR: $\bar{\nu}$ (cm⁻¹) 3486, 3367, 2937, 2835, 1509, 1439, 1122, 1030, 1001, 847, 810

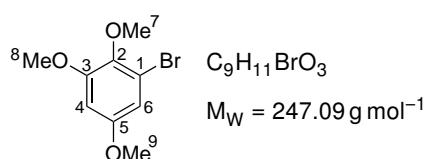
The experimental data were in agreement with those reported in the literature.⁵⁹



Monoclinic $P2_1/c$
 $a = 7.6272(3) \text{ \AA}$ $\alpha = 90^\circ$
 $b = 8.4191(4) \text{ \AA}$ $\beta = 95.452(4)^\circ$
 $c = 31.0409(14) \text{ \AA}$ $\gamma = 90^\circ$
 $V = 1984.24(15) \text{ \AA}^3$ $Z = 8$
 $R = 4.35\%$

Figure 8.23: X-ray structure of **545** and parameters of the crystal. Recrystallised from a boiling mixture of hexane and ethyl acetate.

1-Bromo-2,3,5-trimethoxybenzene (**552**)



In a 250 mL two-neck flask under argon atmosphere, hydroquinone **551** (2.023 g, 9.24 mmol, 1.0 eq.) was dissolved in 50 mL of dichloromethane. A solution of NaOH (1.068 g, 26.7 mmol, 2.9 eq.) in 50 mL of water was added. After ten minutes, Bu_4NBr (149 mg, 0.462 mmol, 0.05 eq.) was added to the biphasic mixture, followed by the dropwise addition of Me_2SO_4 (3.5 mL, 36.9 mmol, 4.0 eq.). After one hour, solid NaOH (1.100 g, 27.5 mmol, 3.0 eq.) was added to the reaction and the final mixture was vigorously stirred overnight. The phases were then separated and the organic phase was washed with brine, dried over $MgSO_4$ and the solvent was evaporated. The crude product was purified by filtration over silica gel using dichloromethane as eluent to yield 2.002 g of **552**.

Aspect: orange oil

Yield: 88%

TLC: $R_f \approx 0.59$ (cHex/AcOEt: 7/3), visualised by UV and $KMnO_4$

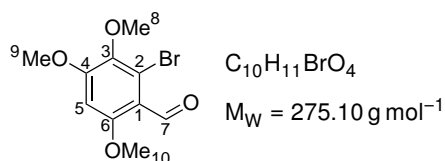
1H NMR (500 MHz, $CDCl_3$): δ (ppm) **6.63** (d, 1H, $J = 2.8 \text{ Hz}$, C^6H), **6.44** (d, 1H, $J = 2.8 \text{ Hz}$, C^4H), **3.83** (s, 3H, C^7H_3 or C^8H_3 or C^9H_3), **3.79** (s, 3H, C^7H_3 or C^8H_3 or C^9H_3), **3.76** (s, 3H, C^7H_3 or C^8H_3 or C^9H_3)

^{13}C NMR (126 MHz, $CDCl_3$): δ (ppm) **156.55** (C_q^2 or C_q^3 or C_q^5), **154.22** (C_q^2 or C_q^3 or C_q^5), **140.87** (C_q^2 or C_q^3 or C_q^5), **117.62** (C_q^1), **107.91** (C^6H), **100.08** (C^4H), **60.85** (C^7H_3 or C^8H_3 or C^9H_3), **56.13** (C^7H_3 or C^8H_3 or C^9H_3), **55.88** (C^7H_3 or C^8H_3 or C^9H_3)

IR: $\bar{\nu}$ (cm^{-1}) 2938, 2834, 1598, 1570, 1489, 1454, 1426, 1231, 1212, 1447, 1034, 999, 821

The experimental data were in agreement with those reported in the literature.⁶⁰

2-Bromo-3,4,6-trimethoxybenzaldehyde (**553**)



In a 100 mL two-neck flash under argon atmosphere and equipped with a condenser, $POCl_3$ (0.64 mL, 6.93 mmol, 1.7 eq.) was added dropwise on *N*-methylformanilide (0.80 mL, 6.52 mmol, 1.6 eq.).

After ten minutes, bromotrimethoxybenzene **552** (1.101 g, 4.08 mmol, 1.0 eq.) was added dropwise on the yellow oil and the reaction was heated up to 60 °C. The mixture darkened and solidified. After 1.75 h, the reaction was cooled down to room temperature and 60 mL of iced water was added. The solution was stirred overnight and the solid that precipitated was filtered and rinsed with water. The solid was dissolved in dichloromethane and the aqueous phase was extracted with dichloromethane. The organic phases were gathered, dried over MgSO_4 and the solvent was evaporated. The crude product was purified by filtration over silica gel using ethyl acetate as eluent and the solvent was evaporated to give 1.003 g benzaldehyde **553**.

Aspect: light brown solid

Yield: 89%

TLC: $R_f \approx 0.74$ (cHex/AcOEt: 6/4), visualised by UV and KMnO_4

m_p : 120-122 °C

$^1\text{H NMR}$ (500 MHz, CDCl_3): δ (ppm) **10.31** (s, 1H, C^7H), **6.47** (s, 1H, C^5H), **3.96** (s, 3H, C^8H_3 or C^9H_3 or C^{10}H_3), **3.91** (s, 3H, C^8H_3 or C^9H_3 or C^{10}H_3), **3.79** (s, 3H, C^8H_3 or C^9H_3 or C^{10}H_3)

$^{13}\text{C NMR}$ (126 MHz, CDCl_3): δ (ppm) **189.56** (C^7), **160.07** (C_q^6), **158.34** (C_q^4), **140.92** (C_q^3), **121.81** (C_q^2), **116.17** (C_q^1), **95.70** (C^5H), **60.77** (C^8H_3 or C^9H_3 or C^{10}H_3), **56.62** (C^8H_3 or C^9H_3 or C^{10}H_3), **56.33** (C^8H_3 or C^9H_3 or C^{10}H_3)

IR: $\bar{\nu}$ (cm^{-1}) 2925, 1673, 1590, 1439, 1398, 1323, 1277, 1231, 1213, 1125, 1025, 971, 821

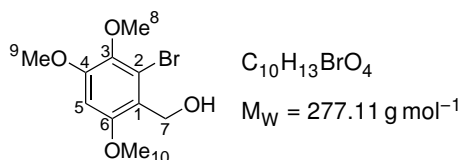
HRMS (ESI+): for $[\text{M}+\text{H}]^+$ calc.: 274.9913, found: 274.9924



Monoclinic	$P2_1/c$
$a = 4.0205(1) \text{ \AA}$	$\alpha = 90^\circ$
$b = 14.8887(3) \text{ \AA}$	$\beta = 93.408(2)^\circ$
$c = 18.0394(3) \text{ \AA}$	$\gamma = 90^\circ$
$V = 1077.93(4) \text{ \AA}^3$	$Z = 4$
$R = 1.9\%$	

Figure 8.24: X-ray structure of **553** and parameters of the crystal. Crystallisation by slow evaporation from dichloromethane.

(2-Bromo-3,4,6-trimethoxyphenyl)methanol (**554**)



In a 100 mL two-neck flask under argon atmosphere, benzaldehyde **553** (505 mg, 1.84 mmol, 1.0 eq.) was suspended in 50 mL of methanol. At 0 °C, NaBH_4 (147 mg, 3.89 mmol, 2.1 eq.) was added, the reaction was warmed up to room temperature and stirred overnight. The solvent was then evaporated and the solid was treated with 50 mL of water at 0 °C. The mixture was stirred ten minutes and dichloromethane was used to dissolve the solid. The phases were separated and the aqueous phase was extracted with dichloromethane. The organic phases were gathered, dried over MgSO_4 and the solvent was evaporated to give 490 mg of benzyl alcohol **554**.

Aspect: white solid

Yield: 96%

TLC: $R_f \approx 0.63$ (cHex/AcOEt: 2/8), visualised by UV and KMnO_4

m_p : 107-109 °C

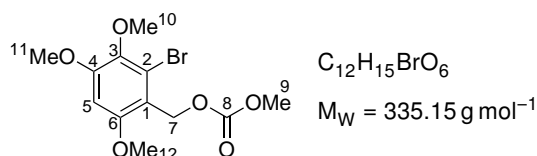
$^1\text{H NMR}$ (500 MHz, CDCl_3): δ (ppm) **6.49** (s, 1H, C^5H), **4.84** (d, 1H, $J = 5.8$ Hz, C^7H), **3.90** (s, 3H, C^8H_3 or C^9H_3 or C^{10}H_3), **3.87** (s, 3H, C^8H_3 or C^9H_3 or C^{10}H_3), **3.79** (s, 3H, C^8H_3 or C^9H_3 or C^{10}H_3)

$^{13}\text{C NMR}$ (126 MHz, CDCl_3): δ (ppm) **155.11** (C_q^6), **153.69** (C_q^3 or C_q^4), **140.53** (C_q^3 or C_q^4), **121.36** (C_q^1 or C_q^2), **121.09** (C_q^1 or C_q^2), **96.46** (C^5H), **60.80** (C^8H_3 or C^9H_3 or C^{10}H_3), **60.12** (C^7H_2), **56.42** (C^8H_3 or C^9H_3 or C^{10}H_3), **56.40** (C^8H_3 or C^9H_3 or C^{10}H_3)

IR: $\bar{\nu}$ (cm^{-1}) 3500-3300, 2924, 2851, 1591, 1564, 1434, 1396, 1322, 1201, 1029, 997, 965, 809

HRMS (ESI+): for $[\text{M}+\text{H}]^+$ calc.: 277.0070, found: 276.9901

2-Bromo-3,4,6-trimethoxybenzyl methyl carbonate (557)



In a 25 mL two-neck flask under argon atmosphere, benzyl alcohol **554** (223 mg, 0.805 mmol, 1.0 eq.) and pyridine (0.22 mL, 2.74 mmol, 3.4 eq.) were dissolved in 2 mL of dichloromethane. The solution was cooled down to 0 °C and methyl chloroformate (0.12 mL, 1.53 mmol, 1.9 eq.) was added dropwise. The reaction was warmed up to room temperature and a precipitate was formed. The solution was diluted with a minimum of dichloromethane to dissolve the solid and the organic phase was washed with HCl (1 M), a saturated solution of NaHCO_3 and brine, successively. The organic phase were then dried over MgSO_4 and the solvent was evaporated. The crude solid was purified by flash chromatography on silica gel (cHex/AcOEt: 8/2) to give 231 mg of carbonate **557**

Aspect: light brown solid

Yield: 86%

TLC: $R_f \approx 0.61$ (cHex/AcOEt: 5/5), visualised by UV and KMnO_4

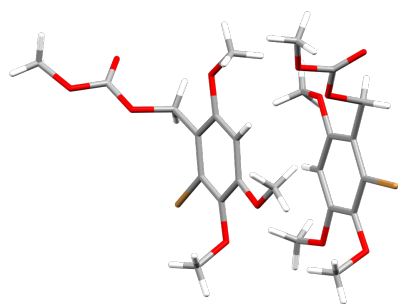
m_p : 77-79 °C

$^1\text{H NMR}$ (500 MHz, CDCl_3): δ (ppm) **6.47** (s, 1H, C^5H), **5.36** (s, 1H, C^7H), **3.90** (s, 3H, C^{10}H_3 or C^{11}H_3), **3.84** (s, 3H, C^{10}H_3 or C^{11}H_3), **3.80** (s, 3H, C^9H_3 or C^{12}H_3), **3.79** (s, 3H, C^{10}H_3 or C^{11}H_3)

$^{13}\text{C NMR}$ (126 MHz, CDCl_3): δ (ppm) **156.49** (C_q^4), **156.21** (C_q^3 or C_q^4), **155.16** (C_q^3 or C_q^4), **123.29** (C_q^8), **122.44** (C_q^2), **115.64** (C_q^1), **96.63** (C^5H), **64.86** (C^7H_2), **61.13** (C^9H_3 or C^{10}H_3 or C^{11}H_3 or C^{12}H_3), **56.91** (C^9H_3 or C^{10}H_3 or C^{11}H_3 or C^{12}H_3), **56.69** (C^9H_3 or C^{10}H_3 or C^{11}H_3 or C^{12}H_3), **55.26** (C^9H_3 or C^{10}H_3 or C^{11}H_3 or C^{12}H_3)

IR: $\bar{\nu}$ (cm^{-1}) 2952, 2923, 2853, 1742, 1598, 1438, 1253, 1226, 1134, 1035, 927, 817

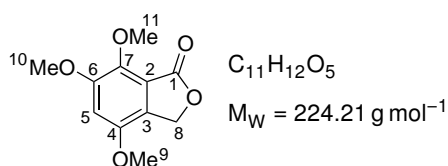
HRMS (ESI+): for $[\text{M}+\text{H}]^+$ calc.: 335.0130, found: 335.0080



Triclinic	$P\bar{1}$
$a = 7.3571(1) \text{ \AA}$	$\alpha = 100.495(2)^\circ$
$b = 12.6102(3) \text{ \AA}$	$\beta = 91.521(2)^\circ$
$c = 15.8618(3) \text{ \AA}$	$\gamma = 105.503(2)^\circ$
$V = 1389.90(5) \text{ \AA}^3$	$Z = 4$
$R = 2.2\%$	

Figure 8.25: X-ray structure of **557** and parameters of the crystal. Crystallisation by slow evaporation from dichloromethane.

4,6,7-Trimethoxyisobenzofuran-1(3H)-one (**546**)



Method A: from benzyl alcohol 545. In a dry 50 mL two-neck flask under argon atmosphere and equipped with a condenser, benzyl alcohol **545** (693 mg, 3.49 mmol, 1.0 eq.) was dissolved in 15 mL of anhydrous THF and the solution was cooled down to -78°C . A 2.4 M solution of hexyllithium in hexanes (3.2 mL, 7.68 mmol, 2.2 eq.) was added dropwise. After one hour, the reaction mixture is heated up to 70°C for 1.5 h. the solution is cooled down to 0°C and dry ice was added and the mixture was stirred 30 min. Then, 10 mL of HCl (10%) was added and the reaction mixture was warmed up to room temperature. The aqueous phase was extracted with dichloromethane. The organic phases were gathered and washed with water and brine. The solvent was then evaporated and the yellow oil was triturated with a minimum of dichloromethane. The precipitate formed was filtered and rinsed with dichloromethane. The filtrate was concentrated and the crude oil was purified by flash chromatography on silica gel to isolate 86 mg of **546** in the first fraction (cHex/AcOEt: 8/2).

Aspect: orange solid

Yield: 11%

Method B: from benzyl alcohol 557. In a dry 100 mL two-neck flask under argon atmosphere, benzyl alcohol **557** (106 mg, 0.317 mmol, 1.0 eq.) was dissolved in 20 mL of anhydrous THF and the solution was cooled down to -78°C . A 2.40 M solution of hexyllithium in hexanes (0.20 mL, 0.384 mmol, 1.2 eq.) was added dropwise. The mixture was allowed to warm up to room temperature and was stirred for three hours. The reaction was then quenched with a saturated solution of NH_4Cl and the final mixture was stirred thirty minutes. The organic solvent was evaporated and the aqueous phase was extracted with ethyl acetate. The organic phases were gathered, dried over MgSO_4 , and the solvent was evaporated to give 10 mg of phthalide **546**.

Aspect: white solid

Yield: 13%

TLC: $R_f \approx 0.19$ (cHex/AcOEt: 7/3), visualised by UV and *p*-anisaldehyde

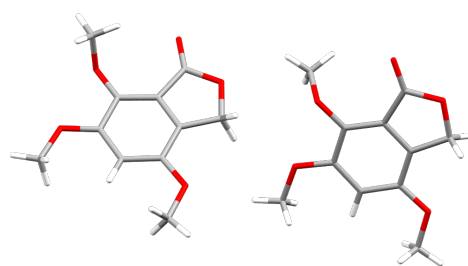
m_p : $153\text{--}156^\circ\text{C}$

¹H NMR (500 MHz, CDCl₃): δ (ppm) **6.74** (s, 1H, C⁵H), **5.14** (s, 2H, C⁸H₂), **3.98** (s, 3H, C¹⁰H₃), **3.93** (s, 3H, C⁹H₃ or C¹¹H₃), **3.88** (C⁹H₃ or C¹¹H₃)

¹³C NMR (126 MHz, CDCl₃): δ (ppm) **167.79** (C_q¹), **153.86** (C_q⁴ or C_q⁷), **149.61** (C_q⁴ or C_q⁷), **141.73** (C_q⁶), **126.68** (C_q³), **119.31** (C_q²), **103.26** (C⁵H), **67.19** (C⁸H₂), **62.54** (C¹⁰H₃), **57.44** (C⁹H₃ or C¹¹H₃), **56.05** (C⁹H₃ or C¹¹H₃)

IR: $\bar{\nu}$ (cm⁻¹) 2935, 2843, 1758, 1505, 1453, 1340, 104, 1203, 1123, 1039, 1004, 981, 888, 852

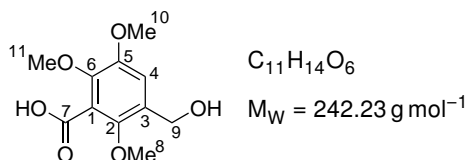
HRMS (ESI⁺): for [M+H]⁺ calc.: 225.0757, found: 225.0767



Monoclinic *P*2₁/*c*
 $a = 33.222(7) \text{ \AA}$ $\alpha = 90^\circ$
 $b = 3.97699(10) \text{ \AA}$ $\beta = 100.648(2)^\circ$
 $c = 16.0441(3) \text{ \AA}$ $\gamma = 90^\circ$
 $V = 2083.31(8) \text{ \AA}^3$ $Z = 8$
 $R = 2.6\%$

Figure 8.26: X-ray structure of **546** and parameters of the crystal. Crystallisation by slow evaporation from dichloromethane.

3-(Hydroxymethyl)-2,5,6-trimethoxybenzoic acid (**547**)



This compound was obtained following the same procedure as the method A for the synthesis of phthalide **546**. The solid obtained from the filtration and the one isolated in the second fraction of the chromatography (cHex/AcOEt/AcOH: 5/5/0.25) were gathered to give 244 mg of benzoic acid **547**.

Aspect: white solid

Yield: 29%

TLC: $R_f \approx 0.22$ (cHex/AcOEt/AcOH: 5/5/0.25), visualised by UV and *p*-anisaldehyde

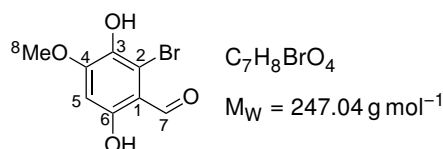
m_p : 115-116 °C

¹H NMR (500 MHz, acetone-*d*₆): δ (ppm) **7.20** (s, 1H, C⁴H), **4.63** (s, 2H, C⁹H₂), **3.86** (s, 1H, C¹⁰H₃ or C¹¹H₃), **3.81** (s, 1H, C¹⁰H₃ or C¹¹H₃), **3.76** (s, 3H, C⁸H₃)

¹³C NMR (126 MHz, acetone-*d*₆): δ (ppm) **167.09** (C_q⁷), **150.06** (C_q⁵ or C_q⁶), **148.05** (C_q²), **145.75** (C_q⁵ or C_q⁶), **132.09** (C_q³), **125.68** (C_q¹), **114.20** (C⁴H), **63.09** (C⁸H₂), **61.42** (C¹⁰H₃ or C¹¹H₃), **59.06** (C⁹H₃), **56.50** (C¹⁰H₃ or C¹¹H₃)

IR: $\bar{\nu}$ (cm⁻¹) 3500-3200, 1716, 1486, 1274, 1122, 1056, 1012, 968, 856

HRMS: pending

2-Bromo-3,6-dihydroxy-4-methoxybenzaldehyde (558)

In a 50 mL two-neck flask under argon atmosphere and equipped with a condenser, hydroquinone **551** (208 mg, 0.950 mmol, 1.0 eq.) and hexamine (128 mg, 0.917 mmol, 1.0 eq.) was dissolved in 5 mL of TFA and the solution was refluxed overnight. The mixture was cooled down to room temperature and the solvent was evaporated. The solid was treated with 100 mL of water at 60 °C for six hours. The solution was cooled down to room temperature and the aqueous phase was extracted with ethyl acetate. The organic phase was washed with brine, dried over $MgSO_4$ and the solvent was evaporated to yield 190 mg benzaldehyde **558**.

Aspect: brown solid

Yield: 81%

TLC: $R_f \approx 0.15$ (cHex/AcOEt: 5/5), visualised by UV and $KMnO_4$

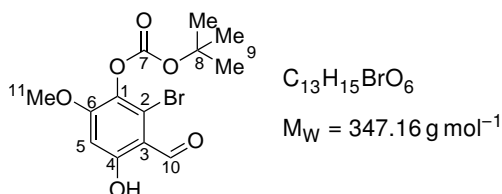
m_p : 199-201 °C

1H NMR (500 MHz, acetone- d_6): δ (ppm) **10.13** (s, 1H, C^7H), **6.56** (s, 1H, C^5H), **3.99** (s, 3H, C^8H_3)

^{13}C NMR (126 MHz, $CDCl_3$): δ (ppm) **196.75** (C_q^7), **161.06** (C_q^6), **156.8** (C_q^4), **138.88** (C_q^3), **111.70** (C_q^1 or C_q^3), **111.64** (C_q^1 or C_q^3), **99.71** (C^5H), **57.16** (C^8H_3)

IR: $\bar{\nu}$ (cm^{-1}) 3400-3000, 1628, 1488, 1432, 1251, 1206, 1158, 1018, 897

HRMS: pending

2-Bromo-3-formyl-4-hydroxy-6-methoxyphenyl *tert*-butyl carbonate (559)

In a 50 mL two-neck flask under argon atmosphere, hydroquinone **558** (128 mg, 0.517 mmol, 1.0 eq.) and Boc_2O (256 mg, 1.175 mg, 2.2 eq.) were placed in 5 mL of hexane. To that solution, DMAP (5 mg, 38.5 mmol, 0.07 eq.) and the reaction was stirred for one hour. The reaction mixture was partitioned between ethyl acetate, brine and HCl (1 M). The phases were separated and the organic phase was washed with a saturated solution of $NaHCO_3$. The latter was then dried over Na_2SO_4 and the solvents were evaporated. The crude product was purified by filtration over silica gel (cHex/AcOEt: 5/5) to give 154 mg of the mono-protected hydroquinone **559**.

Aspect: brown solid

Yield: 86%

TLC: $R_f \approx 0.82$ (cHex/AcOEt: 5/5), visualised by UV and $KMnO_4$

m_p : 99-103 °C

1H NMR (500 MHz, $CDCl_3$): δ (ppm) : **12.53** (s, 1H, OH), **6.46** (s, 1H, $C^{10}H$), **6.46** (s, 1H, C^5H), **3.91** (s, 3H, $C^{11}H_3$), **1.56** (s, 9H, $3 \times C^9H_3$)

^{13}C NMR (126 MHz, CDCl_3): δ (ppm) **195.86** (C^{10}H), **164.35** (C_q^4), **159.44** (C_q^6), **150.59** (C_q^7), **132.22** (C_q^1), **122.11** (C_q^2), **111.40** (C_q^3), **99.33** (C^5H), **84.61** (C_q^8), **56.80** (C^{11}H_3), **27.72** ($3 \times \text{C}^9\text{H}_3$)
IR: $\bar{\nu}$ (cm^{-1}) 2982, 2927, 1756, 1627, 1489, 1438, 1370, 1272, 1254, 1214, 1138, 803
HRMS (ESI+): for $[\text{M}+\text{H}]^+$ calc.: 347.0125, found: 347.0134

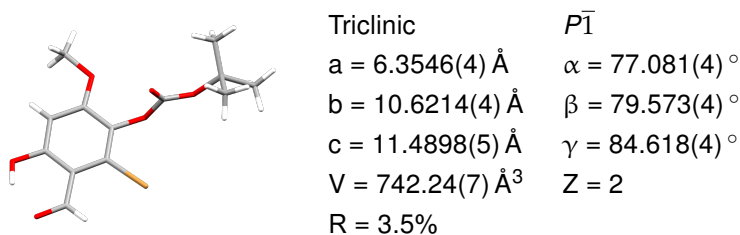
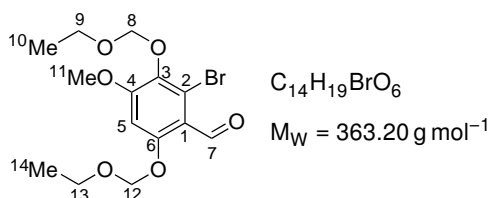


Figure 8.27: X-ray structure of **559** and parameters of the crystal. Crystallisation by slow evaporation from dichloromethane.

2-Bromo-3,6-bis(ethoxymethoxy)-4-methoxybenzaldehyde (**562**)



In a 50 mL two-neck flask under argon atmosphere, hydroquinone **558** (212 mg, 0.857 mmol, 1.0 eq.) was dissolved in 5 mL of acetone. To that solution, K_2CO_3 (476 millig, 3.442 mmol, 4.0 eq.) was added, followed by the dropwise addition of ethoxymethyl chloride (0.17 mL, 1.834 mmol, 2.1 eq.). The solution was refluxed overnight. The reaction was cooled down to room temperature and 1 mL of water was added and the mixture was stirred one hour. The formed precipitate was filtered and the filtrate was evaporated. The crude oil was purified by flash chromatography on silica gel (cHex/AcOEt: 8/2) to give 192 mg of the protected hydroquinone **562**.

Aspect: yellow oil

Yield: 62%

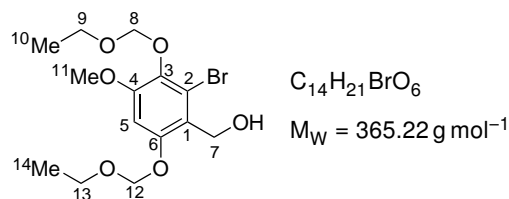
TLC: $R_f \approx 0.64$ (cHex/AcOEt: 6/4), visualised by UV and KMnO_4

^1H NMR (500 MHz, CDCl_3): δ (ppm) **10.31** (s, 1H, C^7H), **6.82** (s, 1H, C^5H), **5.29** (s, 2H, C^{12}H_2), **5.13** (s, 2H, C^8H_2), **3.94** (q, 2H, $J = 7.1 \text{ Hz}$, C^9H_2), **3.90** (s, 3H, C^{11}H_3), **3.76** (q, 2H, $J = 7.0 \text{ Hz}$, C^{13}H_2), **1.27-1.19** (m, 6H, $\text{C}^{10}\text{H}_3 + \text{C}^{14}\text{H}_3$)

^{13}C NMR (126 MHz, CDCl_3): δ (ppm) **189.45** (C^7H), **158.05** (C_q^4 or C_q^6), **157.95** (C_q^4 or C_q^6), **138.80** (C_q^3), **121.04** (C_q^2), **117.39** (C_q^1), **99.66** (C^5H), **97.23** (C^8H_2), **94.45** (C^2H_{12}), **66.08** (C^9H_2), **65.02** (C^{13}H_2), **56.31** (C^{11}H_3), **15.18** (C^{10}H_3 or C^{14}H_3), **15.14** (C^{10}H_3 or C^{14}H_3)

IR: $\bar{\nu}$ (cm^{-1}) 2976, 2930, 1688, 1587, 1480, 1445, 1383, 1316, 1265, 1195, 1108, 969, 942

HRMS: pending

(2-Bromo-3,6-bis(ethoxymethoxy)-4-methoxyphenyl)methanol (563)

In a 50 mL two-neck flask under argon atmosphere, benzaldehyde **562** (129 mg, 0.355 mmol, 1.0 eq.) was dissolved in 15 mL of methanol. The solution was cooled down and NaBH_4 (15 mg, 0.397 mmol, 1.1 eq.) was added. After 1.25 h, the solvent was evaporated and replaced by 15 mL of water. The aqueous phase was extracted with dichloromethane and the organic phase was then washed with water. The organic phase was dried over Na_2SO_4 and the solvent was evaporated. The crude oil was purified by filtration over silica gel, using dichloromethane as eluent, to give 68 mg of the benzyl alcohol **563**.

Aspect: yellow oil

Yield: 53%

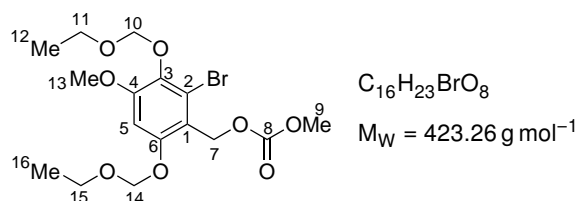
TLC: $R_f \approx 0.37$ (cHex/AcOEt: 6/4), visualised by UV and KMnO_4

$^1\text{H NMR}$ (500 MHz, CDCl_3): δ (ppm) **6.79** (s, 1H, C^5H), **5.24** (s, 2H, C^{12}H_2), **5.13** (s, 2H, C^8H_2), **4.83** (s, 2H, C^7H_2), **3.94** (q, 2H, $J = 7.1 \text{ Hz}$, C^9H_2), **3.84** (s, 3H, C^{11}H_3), **3.75** (q, 2H, $J = 7.1 \text{ Hz}$, C^{13}H_2), **1.25** (t, 3H, $J = 7.1 \text{ Hz}$, C^{10}H_3), **1.23** (t, 3H, $J = 7.1 \text{ Hz}$, C^{14}H_3)

$^{13}\text{C NMR}$ (500 MHz, CDCl_3): δ (ppm) **153.55** (C_q^4), **153.31** (C_q^6), **138.49** (C_q^3), **122.52** (C_q^1), **121.28** (C_q^2), **100.48** (C^5H), **97.24** (C^8H_2), **94.68** (C^{12}H_2), **65.96** (C^9H_2), **64.82** (C^{13}H_2), **60.11** (C^7H_2), **56.27** (C^{11}H_3), **15.21** ($\text{C}^{10}\text{H}_3 + \text{C}^{14}\text{H}_3$)

IR: $\bar{\nu}$ (cm^{-1}) 3600-3300, 2976, 2935, 2987, 1595, 1569, 1482, 1446, 1385, 1214, 1148, 1128, 1105, 1075, 988, 941, 844, 812, 733

HRMS: pending

2-Bromo-3,6-bis(ethoxymethoxy)-4-methoxybenzyl methyl carbonate (564)

In a 50 mL two-neck flask under argon atmosphere, benzyl alcohol **563** (503 mg, 1.815 mmol, 1.0 eq.) and pyridine (0.50 mL, 6.21 mmol, 3.4 eq.) were dissolved in 5 mL of dichloromethane. The solution was cooled down to 0°C and methyl chloroformate (0.27 mL, 3.49 mmol, 1.9 eq.) was added dropwise, the reaction was warmed up to room temperature and a precipitate was formed. The solution was diluted with a minimum of dichloromethane to dissolve the solid and the organic phase was washed with HCl (1 M), then a saturated solution of NaHCO_3 and brine. The organic phase was dried over MgSO_4 and the solvent was evaporated. The crude oil was purified by flash chromatography on silica gel (cHex/AcOEt: 8/2) to give 498 mg of carbonate **564**.

Aspect: yellow oil

Yield: 82%

TLC: $R_f \approx 0.65$ (cHex/AcOEt: 5/5), visualised by UV and KMnO_4

$^1\text{H NMR}$ (500 MHz, CDCl_3): δ (ppm) **6.80** (s, 1H, C^5H), **5.36** (s, 2H, C^7H_2), **5.22** (s, 2H, C^{14}H_2), **5.12** (s, 2H, C^{10}H_2), **3.94** (q, 2H, $J = 7.1$ Hz, C^{11}H_2), **3.84** (s, 3H, C^{13}H_3), **3.79** (s, 3H, C^9H_3), **3.73** (q, 2H, $J = 7.1$ Hz, C^{15}H_2), **1.26-1.23** (m, 6H, $\text{C}^{12}\text{H}_3 + \text{C}^{16}\text{H}_3$)

$^{13}\text{C NMR}$ (126 MHz, CDCl_3): δ (ppm) **155.84** (C_q^8), **154.62** (C_q^4 or C_q^6), **154.25** (C_q^4 or C_q^6), **138.34** (C_q^3), **122.65** (C_q^2), **116.26** (C_q^1), **99.61** (C^5H), **97.21** (C^{10}H_2), **94.18** (C^{14}H_2), **65.94** (C^{11}H_2), **64.65** (C^7H_2 or C^{15}H_2), **64.62** (C^7H_2 or C^{15}H_2), **56.21** (C^{13}H_3), **54.88** (C^9H_3), **15.22** (C^{12}H_3 or C^{16}H_3), **15.19** (C^{12}H_3 or C^{16}H_3)

IR: $\bar{\nu}$ (cm^{-1}) 2926, 1747, 1597, 1486, 1443, 1257, 1135, 1005, 938

HRMS: pending

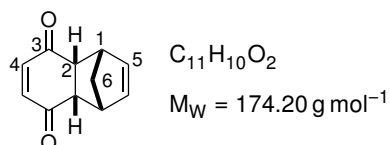
8.6 Diels-Alder reactions

General procedure

The quinone was dissolved in dichloromethane or HFIP (10 mL/mmol). The diene was then added (1 or 2 equivalents) at room temperature. The reaction was then monitored by TLC. Once the reaction reached completion or maximum conversion, the solvent was evaporated and the crude product purified if necessary (otherwise it was pure enough to be analysed without any further purification). Reaction times are reported in Tables 5.4, 5.5, 5.6 and 5.7 in Chapter 5.

8.6.1 Solvent study: expected cycloadducts and pyrolysed adducts

(1*R*,4*S*,4*aR*,8*aR*)-1,4,4*a*,8*a*-Tetrahydro-1,4-methanonaphthalene-5,8-dione (**Q1D1**)



Quinone **Q1** (CH₂Cl₂: 208 mg, 1.92 mmol, 1.0 eq.; HFIP: 51 mg, 0.476 mmol, 1.0 eq.) and diene **D1** (CH₂Cl₂: 0.33 mL, 3.92 mmol, 2.0 eq.; HFIP: 0.04 mL, 0.476 mmol, 1.0 eq.) were reacted following general procedure to give **Q1D1** (CH₂Cl₂: 326 mg; HFIP: 83 mg).

Aspect: greyish powder

Yield: CH₂Cl₂: 94%; HFIP: quantitative

TLC: R_f ≈ 0.26 (cHex/AcOEt: 8/2), visualised by UV and *p*-anisaldehyde

m_p: 66–69 °C

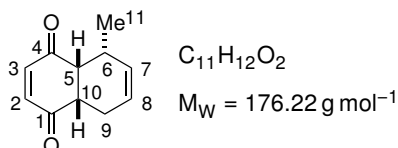
¹H NMR (500 MHz, CDCl₃): δ (ppm) **6.57** (s, 2H, 2 × C⁴H), **6.06** (dd, 2H, ABXYZ, J_{AX} = J_{AY} = 1.8 Hz, 2 × C⁵H), **3.54** (m, 2H, ABXYZ 2 × C¹H), **3.22** (dd, 2H, ABXYZ, J_{YZ} = 2.3 Hz, J_{BZ} = 1.5 Hz, 2 × C²H), **1.48** (2 × ddd, 2H, ABXYZ, J_{AX} = 1.8 Hz, J_{BZ} = 1.5 Hz, J_{AB} = 8.8 Hz, Δ_ν_{AB} = 55.7 Hz, C⁶H₂)

¹³C NMR (126 MHz, CDCl₃): δ (ppm) **199.62** (2 × C_q³), **142.20** (2 × C⁴H), **135.43** (2 × C⁵H), **48.91** (2 × C¹H), **48.85** (C⁶H₂), **48.47** (2 × C²H)

IR: ν̄ (cm⁻¹) 1748, 1720, 1667, 1301, 1279, 1055, 862, 734, 455

The experimental data were in agreement with those reported in the literature.⁶¹

(±)-*rel*-(4*aR*,5*R*,8*aS*)-5-Methyl-4*a*,5,8,8*a*-tetrahydronaphthalene-1,4-dione (**Q1D2**)



Quinone **Q1** (CH₂Cl₂: 217 mg, 2.01 mmol, 1.0 eq.; HFIP: 56 mg, 0.516 mmol, 1.0 eq.) and diene **D2** (CH₂Cl₂: 0.40 mL, 4.01 mmol, 2.0 eq.; HFIP: 0.10 mL, 1.00 mmol, 1.9 eq.) were reacted following the general procedure to give **Q1D2** (CH₂Cl₂: 324 mg; HFIP: 88 mg).

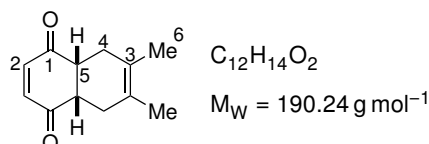
Aspect: greyish oil

Yield: CH₂Cl₂: 92%; HFIP: 97%

TLC: R_f ≈ 0.50 (cyclohex./AcOEt: 7/3), visualised by UV and *p*-anisaldehyde

^1H NMR (500 MHz, CDCl_3): δ (ppm) **6.75** (d, 1H, $J = 10.3$ Hz, C^2H), **6.69** (d, 1H, $J = 10.3$ Hz, C^3H), **5.70-5.65** (m, 1H, C^7H), **5.64-5.59** (m, 1H, C^8H), **3.34** (dd, 1H, $J = 6.0; 5.9$ Hz, C^5H), **3.24** (ddd, 1H, $J = 7.5; 5.9; 3.9$ Hz, C^{10}H), **2.57** (m, 1H, C^6H), **2.49** (m, 2H, C^9H_2), **0.94** (d, 3H, $J = 7.4$ Hz, C^{11}H_3)
 ^{13}C NMR (126 MHz, CDCl_3): δ (ppm) **201.31** (C_q^4), **199.71** (C_q^1), **141.21** (C^3H), **140.60** (C^2H), **130.99** (C^7H), **123.48** (C^8H), **50.52** (C^5H), **45.49** (C^{10}H), **31.86** (C^6H), **22.50** (C^9H_2), **18.69** (C^{11}H_3)
IR: $\bar{\nu}$ (cm^{-1}) 2961, 2924, 2868, 1669, 1487, 1460, 1264, 1180, 1094, 1040, 932, 867, 805, 737, 703
 The experimental data were in agreement with those reported in the literature.⁶²

(4a*R*,8a*S*)-6,7-Dimethyl-1,4,4a,5,8,8a-hexahydronaphthalene-1,4-dione (Q1D3)



Quinone **Q1** (CH_2Cl_2 : 206 mg, 1.90 mmol, 1.0 eq.; HFIP: 56 mg, 0.521 mmol, 1.0 eq.) and diene **D3** (CH_2Cl_2 : 0.43 mL, 3.80 mmol, 2.0 eq.; HFIP: 0.12 mL, 1.06 mmol, 2.0 eq.) were reacted following the general procedure to give **Q1D3** (CH_2Cl_2 : 288 mg; HFIP 95 mg).

Aspect: greyish powder

Yield: CH_2Cl_2 : 80%; HFIP: 95%

TLC: $R_f \approx 0.59$ (cHex/AcOEt: 7/3), visualised by UV and *p*-anisaldehyde

m_p : 120-123 °C

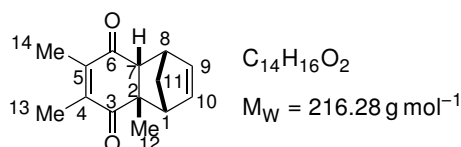
^1H NMR (500 MHz, CDCl_3): δ (ppm) **6.65** (s, 2H, $2 \times \text{C}^2\text{H}$), **3.24-3.12** (m, 2H, $2 \times \text{C}^5\text{H}$), **2.21** (m, 4H, *AB*, $J_{AB} = 17.4$ Hz, $\Delta\nu_{AB} = 158.7$ Hz, $2 \times \text{C}^4\text{H}_2$), **1.62** (s, 6H, $2 \times \text{C}^6\text{H}_3$)

^{13}C NMR (126 MHz, CDCl_3): δ (ppm) **200.42** ($2 \times \text{C}_q^1$), **139.45** ($2 \times \text{C}^2\text{H}$), **123.41** ($2 \times \text{C}_q^3$), **47.18** ($2 \times \text{C}^5\text{H}$), **30.55** ($2 \times \text{C}^4\text{H}_2$), **18.97** ($2 \times \text{C}^6\text{H}_3$)

IR: $\bar{\nu}$ (cm^{-1}) 2881, 1708, 1231, 1137

The experimental data were in agreement with those reported in the literature.⁶³

(±)-*rel*-(1*R*,4*S*,4a*R*,8a*S*)-4a,6,7-Trimethyl-1,4,4a,8a-tetrahydro-1,4-methanonaphthalene-5,8-dione (Q2D1)



Quinone **Q2** (CH_2Cl_2 : 118 mg, 0.783 mmol, 1.0 eq.; HFIP: 52 mg, 0.345 mmol, 1.0 eq.) and diene **D1** (CH_2Cl_2 : 0.13 mL, 1.55 mmol, 1.98 eq.; HFIP: 0.06 mL, 0.713 mmol, 2.1 eq.) were reacted following the general procedure. The crude product was purified by flash chromatography on silica gel (PhMe/AcOEt: 95/5) to give **Q2D1** (CH_2Cl_2 : 101 mg; HFIP: 75 mg).

Aspect: pale yellow oil

Yield: CH_2Cl_2 : 60%; HFIP: quantitative

TLC: $R_f \approx 0.73$ (PhMe/AcOEt: 8/2), visualised by UV and KMnO_4

^1H NMR (500 MHz, CDCl_3): δ (ppm) **6.06** (dd, 1H, $J = 5.6; 2.9$ Hz, C^{10}H), **5.92** (dd, 1H, $J = 5.6; 2.8$ Hz, C^9H), **3.43-3.36** (m, 1H, C^8H), **3.09-3.02** (m, 1H, C^1H), **2.81** (d, 7H, $J = 3.9$ Hz, C^7H_7), **1.91**

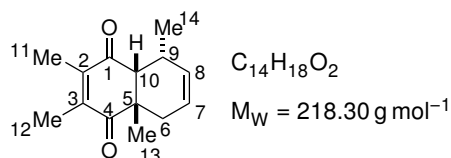
(s, 6H, $C^{13}H_3 + C^{14}H_3$), **1.57** (dddd, 2H, ABXY, $J_{AB} = 9.0$ Hz, $J_{AX} = J_{AY} = 1.7$ Hz, $J_{BX} = J_{BY} = 1.5$ Hz, $\Delta\nu_{AB} = 78.9$ Hz, $C^{11}H_2$), **1.43** (s, 3H, $C^{12}H_3$)

^{13}C NMR (126 MHz, $CDCl_3$): δ (ppm) **202.48** (C_q^3), **199.14** (C_q^6), **147.06** (C_q^4 or C_q^5), **146.82** (C_q^5 or C_q^4), **138.28** ($C^{10}H$), **134.82** (C^9H), **56.96** (C^7H_7), **53.68** (C^1H), **52.47** (C_q^2), **49.09** (C^8H), **46.40** ($C^{11}H_2$), **26.92** ($C^{12}H_3$), **13.50** ($C^{13}H_3$ or $C^{14}H_3$), **13.12** ($C^{14}H_3$ or $C^{13}H_3$)

IR: $\bar{\nu}$ (cm^{-1}) 2963, 1742, 1728, 1660, 1455, 1379

HRMS (ESI+): for $[M+H]^+$ calc.: 217.1229, found: 217.1223

(±)-rel-(4aR,8S,8aS)-2,3,4a,8-Tetramethyl-4a,5,8,8a-tetrahydronaphthalene-1,4-dione (Q2D2)



Quinone **Q2** (CH_2Cl_2 : 215 mg, 1.43 mmol, 1.0 eq.; HFIP: 86 mg, 0.569 mmol, 1.0 eq.) and diene **D2** (CH_2Cl_2 : 0.29 mL, 2.91 mmol, 2.0 eq.; HFIP: 0.11 mL, 1.10 mmol, 1.9 eq.) were reacted following the general procedure. The crude product was purified by flash chromatography on silica gel (cyclohex./ CH_2Cl_2 /acetone: 8/2/0.1) to give **Q2D2** (CH_2Cl_2 : 97 mg; HFIP: 124 mg).

Aspect: pale yellow oil

Yield: CH_2Cl_2 : 31%; HFIP: quantitative

TLC: $R_f \approx 0.70$ (CH_2Cl_2 /cyclohex./acetone: 6/4/0.2), visualised by UV and $KMnO_4$

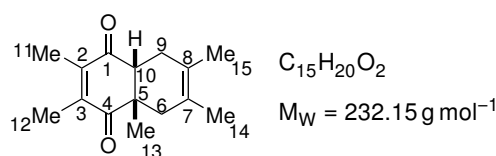
1H NMR (500 MHz, $CDCl_3$): δ (ppm) **5.67-5.59** (m, 1H, C^7H), **5.59-5.52** (m, 1H, C^8H), **2.93-2.82** (m, 2H, $\frac{1}{2} \times C^6H_2 + C^{10}H$), **2.15-2.02** (m, 2H, $\frac{1}{2} \times C^6H_2 + C^9H$), **2.00** (q, 3H, $J = 1.0$ Hz, $C^{11}H_3$), **1.98** (q, 3H, $J = 1.0$ Hz, $C^{12}H_3$), **1.40** (s, 3H, $C^{13}H_3$), **0.72** (d, 3H, $J = 7.3$ Hz, $C^{14}H_3$)

^{13}C NMR (126 MHz, $CDCl_3$): δ (ppm) **203.25** (C_q^4), **199.43** (C_q^1), **146.07** (C_q^2 or C_q^3), **144.75** (C_q^3 or C_q^2), **130.17** (C^8H), **122.79** (C^7H), **50.34** (C_q^5), **50.02** ($C^{10}H$), **39.56** (C^9H), **24.29** ($C^{13}H_3$), **20.93** (C^6H_2), **19.34** ($C^{14}H_3$), **13.36** ($C^{11}H_3$), **12.80** ($C^{12}H_3$)

IR: $\bar{\nu}$ (cm^{-1}) 2973, 2934, 1667, 1374, 1287, 1249, 1224, 1180, 1100, 1070, 708

HRMS (ESI+): for $[M+H]^+$ calc.: 219.1385, found: 219.1380

(±)-cis-2,3,4a,6,7-Pentamethyl-4a,5,8,8a-tetrahydronaphthalene-1,4-dione (Q2D3)



Quinone **Q2** (HFIP: 176 mg, 1.17 mmol, 1.0 eq.) and diene **D3** (HFIP: 0.26 mL, 2.30 mmol, 2.0 eq.) were reacted following the general procedure. The crude product was purified by flash chromatography on silica gel (cyclohex./AcOEt: 99/1) to give **Q2D3** (HFIP: 269 mg).

Aspect: pale yellow oil

Yield: quantitative

TLC: $R_f \approx 0.66$ (cyclohex./AcOEt: 8/2), visualised by UV and $KMnO_4$

1H NMR (500 MHz, $CDCl_3$): δ (ppm) **2.81** (t, 1H, $J = 5.9$ Hz, $C^{10}H$), **2.52-2.43** (m, 1H, $\frac{1}{2} \times C^9H_2$),

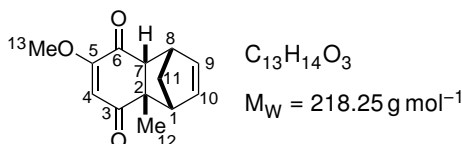
2.40 (d, 1H, $J = 17.2$ Hz, $\frac{1}{2} \times C^6H_2$), **2.11-2.03** (m, 1H, C^9H_2), **1.97** (s, 6H, $C^{11}H_3 + C^{12}H_3$), **1.66** (d, 1H, $J = 17.2$ Hz, $\frac{1}{2} \times C^6H_2$), **1.62** (s, 3H, $C^{15}H_3$), **1.57** (s, 3H, $C^{14}H_3$), **1.26** (s, 3H, $C^{13}H_3$)

^{13}C NMR (126 MHz, $CDCl_3$): δ (ppm) **202.70** (C_q^4), **200.20** (C_q^1), **143.37** (C^2H or C^3H), **142.56** (C_q^3 or C_q^2), **122.97** (C_q^7 or C_q^8), **122.87** (C_q^8 or C_q^7), **52.80** ($C^{10}H$), **48.16** (C^5), **39.18** (C^6H_2), **30.17** (C^9H_2), **23.39** ($C^{13}H_3$), **19.08** ($C^{14}H_3$), **18.72** ($C^{15}H_3$), **13.26** ($C^{11}H_3$ or $C^{12}H_3$), **13.02** ($C^{12}H_3$ or $C^{11}H_3$)

IR: $\bar{\nu}$ (cm^{-1}) 2918, 1673, 1373, 1288, 1234, 1074, 1026, 753

HRMS (ESI+): for $[M+H]^+$ calc.: 233.1542, found: 233.1536

(±)-rel-(1R,4S,4aR,8aS)-7-Methoxy-4a-methyl-1,4,4a,8a-tetrahydro-1,4-methanonaphthalene-5,8-dione (Q3D1)



Quinone **Q3** (CH_2Cl_2 : 137 mg, 0.900 mmol, 1.0 eq.; HFIP: 100 mg, 0.655 mmol, 1.0 eq.) and diene **D1** (CH_2Cl_2 : 0.15 mL, 1.78 mmol, 2.0 eq.) were reacted following the general procedure. The crude product was purified by flash chromatography on silica gel (cHex/AcOEt: 7/3) to give **Q3D1** (CH_2Cl_2 : 196 mg; HFIP: 133 mg).

Aspect: white powder

Yield: CH_2Cl_2 : quantitative; HFIP: 93%

TLC: $R_f \approx 0.24$ (cHex/AcOEt: 7/3), visualised by UV and *p*-anisaldehyde

m_p : 107-109 °C

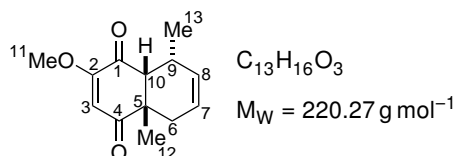
1H NMR (400 MHz, $CDCl_3$): δ (ppm) **6.16** (dd, 1H, $J = 5.7$; 2.9 Hz, $C^{10}H$), **5.98** (dd, 1H, $J = 5.7$; 2.8 Hz, C^9H), **5.85** (s, 1H, C^4H), **3.72** (s, 3H, $C^{13}H_3$), **3.45** (s (br), 1H, C^8H), **3.07** (s (br), 1H, C^1H), **2.88** (d, 1H, $J = 3.9$ Hz, C^7H), **1.60** (ddt, 2H, ABX, $J_{AB} = 9.2$ Hz, $J_{AX} = 1.4$ Hz, $J_{BX} = 1.7$ Hz, $\Delta\nu_{AB} = 56.8$ Hz, $C^{11}H_2$), **1.47** (s, 3H, $C^{12}H_3$)

^{13}C NMR (126 MHz, $CDCl_3$): δ (ppm) **202.46** (C_q^3), **194.56** (C_q^6), **162.60** (C_q^5), **138.70** ($C^{10}H$), **134.09** (C^9H), **114.13** (C^4H), **57.20** (C^7H), **56.46** ($C^{13}H_3$), **53.50** (C_q^2), **53.48** (C^1H), **49.65** (C^8H), **46.58** ($C^{11}H_2$), **26.68** ($C^{12}H_3$)

IR: $\bar{\nu}$ (cm^{-1}) 2954, 1756, 1735, 1679, 1647, 1606, 1452, 1370, 1330, 1237, 1175, 1126, 1091, 995

HRMS (ESI+): for $[M+H]^+$ calc.: 219.1016, found: 219.1008

(±)-rel-(4aR,8S,8aS)-2-Methoxy-4a,8-dimethyl-4a,5,8,8a-tetrahydronaphthalene-1,4-dione (Q3D2)



Quinone **Q3** (HFIP: 152 mg, 1.00 mmol, 1.0 eq.) and diene **D1** (CH_2Cl_2 : 0.20 mL, 2.00 mmol, 2.0 eq.) were reacted following the general procedure. The crude product was purified by flash chromatography on silica gel (cHex/AcOEt/acetone: 7/3/0.1) to give 177 mg of **Q3D1**.

Aspect: white powder

Yield: 81%

TLC: $R_f \approx 0.41$ (cHex/AcOEt/actone: 7/3/0.5), visualised by UV and *p*-anisaldehyde

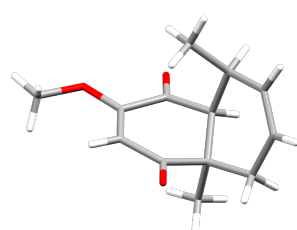
m_p : 52-54 °C

$^1\text{H NMR}$ (500 MHz, CDCl_3): δ (ppm) **5.82** (s, 1H, C^3H), **5.67-5.61** (m, 1H, C^8H), **5.61-5.55** (m, 1H, C^7H), **3.78** (s, 3H, C^{11}H_3), **3.01** (d, 1H, $J = 5.7$ Hz, C^{10}H), **2.68-2.56** (m, 2H, $\frac{1}{2} \times \text{C}^6\text{H}_2 + \text{C}^9\text{H}$), **1.86-1.75** (m, 1H, $\frac{1}{2} \times \text{C}^6\text{H}_2$), **1.33** (s, 3H, C^{12}H_3), **1.10** (d, 3H, $J = 7.4$ Hz, C^{13}H_3)

$^{13}\text{C NMR}$ (126 MHz, CDCl_3): δ (ppm) **201.74** (C_q^4), **195.88** (C_q^1), **162.26** (C_q^2), **130.43** (C^8H), **123.24** (C^7H), **109.30** (C^3H), **56.72** (C^{10}H), **56.50** (C^{11}H_3), **48.13** (C_q^5), **32.36** (C^6H_2), **30.74** (C^9H), **25.80** (C^{12}H_3), **18.35** (C^{13}H_3)

IR: $\bar{\nu}$ (cm^{-1}) 2967, 2935, 2875, 1700, 1661, 1602, 1459, 1343, 1213, 1173, 1145, 986, 874, 717

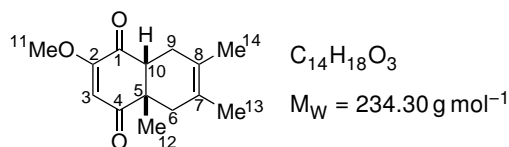
HRMS (ESI+): for $[\text{M}+\text{H}]^+$ calc.: 221.1172, found: 221.1171



Tetragonal $P4_12_12$
 $a = 7.694\ 62(15)$ Å $\alpha = 90^\circ$
 $b = 7.694\ 62(15)$ Å $\beta = 90^\circ$
 $c = 38.8358(10)$ Å $\gamma = 90^\circ$
 $V = 2299.36(11)$ Å³ $Z = 8$
 $R = 4.49\%$

Figure 8.28: X-ray structure of **Q3D2** and parameters of the crystal. Crystallisation by slow evaporation from dichloromethane.

(±)-*cis*-2-Methoxy-4a,6,7-trimethyl-4a,5,8,8a-tetrahydronaphthalene-1,4-dione (**Q3D3**)



Quinone **Q3** (HFIP: 153 mg, 1.01 mmol, 1.0 eq.) and diene **D1** (CH_2Cl_2 : 0.23 mL, 2.03 mmol, 2.0 eq.) were reacted following the general procedure. The crude product was purified by flash chromatography on silica gel (cHex/AcOEt/acetone: 7/3/0.1) to give 229 mg of **Q3D1**.

Aspect: white powder

Yield: 97%

TLC: $R_f \approx 0.41$ (cHex/AcOEt/actone: 7/3/0.5), visualised by UV and *p*-anisaldehyde

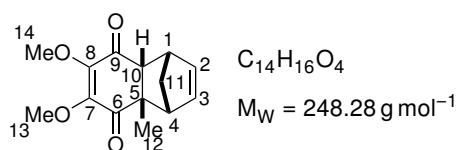
m_p : 60-62 °C

$^1\text{H NMR}$ (500 MHz, CDCl_3): δ (ppm) **5.81** (s, 1H, C^3H), **3.78** (s, 3H, C^{11}H_3), **2.86** (t, 1H, $J = 6.0$ Hz, C^{10}H), **2.60** (m, 1H; $\frac{1}{2} \times \text{C}^9\text{H}_2$), **2.44** (d, 1H, $J = 17.4$ Hz, $\frac{1}{2} \times \text{C}^6\text{H}_2$), **2.17-2.03** (m, 1H, $\frac{1}{2} \times \text{C}^9\text{H}_2$), **1.73** (d, 1H, $J = 17.4$ Hz, $\frac{1}{2} \times \text{C}^6\text{H}_2$), **1.63** (s, 3H, C^{14}H_3), **1.58** (s, 3H, C^{13}H_3), **1.28** (s, 3H, C^{12}H_3)

$^{13}\text{C NMR}$ (126 MHz, CDCl_3): δ (ppm) **202.46** (C_q^4), **195.25** (C_q^1), **160.85** (C_q^2), **123.13** (C_q^7), **122.54** (C_q^8), **109.24** (C^3H), **56.40** (C^{11}H_3), **52.69** (C^{10}H), **48.37** (C_q^5), **39.32** (C^6H_2), **29.79** (C^9H_2), **23.61** (C^{12}H_3), **19.09** (C^{13}H_3), **18.69** (C^{14}H_3)

IR: $\bar{\nu}$ (cm^{-1}) 2926, 2908, 2836, 1699, 1661, 1610, 1464, 1427, 1357, 1228, 1175, 1121, 1102, 1029, 851

HRMS (ESI+): for $[\text{M}+\text{H}]^+$ calc.: 235.1329, found: 235.1323

(±)-rel-(1*R*,4*S*,4*aR*,8*aS*)-6,7-Dimethoxy-4*a*-methyl-1,4,4*a*,8*a*-tetrahydro-1,4-methanonaphthalene-5,8-dione (Q4D1)

Quinone **Q4** (CH₂Cl₂: 43 mg, 0.236 mmol, 1.0 eq.; HFIP: 50 mg, 0.276 mmol, 1.0 eq.) and diene **D1** (CH₂Cl₂: 0.04 mL, 0.476 mmol, 2.0 eq.; HFIP: 0.05 mL, 0.595 mmol, 2.2 eq.) were reacted following the general procedure to give **Q4D1** (CH₂Cl₂: 58 mg; HFIP: 68 mg).

Aspect: viscous yellow oil

Yield: CH₂Cl₂: 98%; HFIP: quantitative

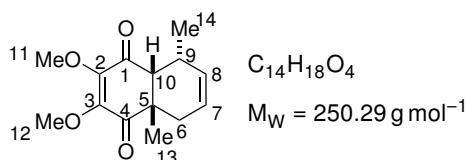
TLC: R_f ≈ 0.38 (cyclohex./AcOEt: 7/3), visualised by UV and KMnO₄

¹H NMR (500 MHz, CDCl₃): δ (ppm) **6.09** (dd, 1H, *J* = 5.6; 2.9 Hz, C³H), **5.95** (dd, 1H, *J* = 5.6; 2.8 Hz, C²H), **3.88** (s, 3H, C¹³H₃ or C¹⁴H₃), **3.87** (s, 3H, C¹⁴H₃ or C¹³H₃), **3.36** (s (br), 1H, C¹H), **3.02** (s (br), 4H, C¹H₄), **2.78** (d, 1H, *J* = 3.9 Hz, C¹⁰H), **1.55** (m, 2H, C¹¹H₂), **1.43** (s, 3H, C¹²H₃)

¹³C NMR (126 MHz, CDCl₃): δ (ppm) **198.49** (C_q⁶), **194.89** (C_q⁹), **150.60** (C_q⁷ or C_q⁸), **150.54** (C_q⁸ or C_q⁷), **138.15** (C³H), **134.52** (C²H), **60.66** (C¹³H₃ or C¹⁴H₃), **60.64** (C¹⁴H₃ or C¹³H₃), **57.05** (C¹⁰H), **53.41** (C⁴H), **52.56** (C_q⁵), **48.83** (C¹H), **46.34** (C¹¹H₂), **26.51** (C¹²H₃)

IR: ν̄ (cm⁻¹) 2949, 1661, 1594, 1450, 1332, 1287, 1254, 1206, 1128, 1110, 1078, 1029, 1006, 995, 974, 914, 709

The experimental data were in agreement with those reported in the literature.⁵⁰

(±)-rel-(4*aR*,8*S*,8*aS*)-2,3-Dimethoxy-4*a*,8-dimethyl-4*a*,5,8,8*a*-tetrahydronaphthalene-1,4-dione (Q4D2)

Quinone **Q4** (CH₂Cl₂: 150 mg, 0.821 mmol, 1.0 eq.; HFIP: 173 mg, 0.847 mmol, 1.0 eq.) and diene **D2** (CH₂Cl₂: 0.13 mL, 1.65 mmol, 2.0 eq.; HFIP: 0.15 mL, 1.90 mmol, 2.3 eq.) were reacted following the general procedure. The crude product was purified by flash chromatography on silica gel (cyclohex./CH₂Cl₂: 5/5) to give **Q4D2** (CH₂Cl₂: 47 mg; HFIP: 225 mg).

Aspect: yellow viscous oil.

Yield: CH₂Cl₂: 23%; HFIP: 95%

TLC: R_f ≈ 0.46 (cyclohex./CH₂Cl₂/acetone: 5/5/0.2), visualised by UV and KMnO₄

¹H NMR (500 MHz, CDCl₃): δ (ppm) **5.66-5.60** (m, 1H, C⁷H), **5.60-5.53** (m, 1H, C⁸H), **3.98** (s, 3H, C¹¹H₃ or C¹²H₃), **3.97** (s, 3H, C¹²H₃ or C¹¹H₃), **2.97-2.86** (m, 1H, 1/2 × C⁶H₂), **2.80** (dd, 1H, *J* = 7.3; 1.8 Hz, C¹⁰H), **2.21-2.12** (m, 1H, C⁹H), **2.10-2.02** (m, 1H, 1/2 × C⁶H₂), **1.41** (s, 3H, C¹³H₃), **0.85** (d, 3H, *J* = 7.3 Hz, C¹⁴H₃)

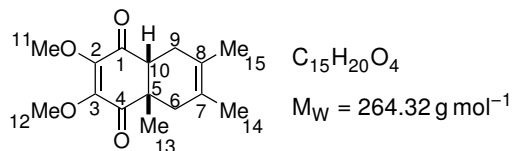
¹³C NMR (126 MHz, CDCl₃): δ (ppm) **199.53** (C_q⁴), **194.88** (C_q¹), **150.42** (C_q² or C_q³), **148.92** (C_q³ or C_q²), **130.09** (C⁸H), **122.48** (C⁷H), **60.87** (C¹¹H₃ or C¹²H₃), **60.51** (C¹²H₃ or C¹¹H₃), **49.54** (C¹⁰H),

39.55 (C_q^5), **39.55** (C^9H), **23.99** ($C^{13}H_3$), **20.48** (C^6H_2), **19.36** ($C^{14}H_3$)

IR: $\bar{\nu}$ (cm^{-1}) 2936, 1672, 1598, 1451, 1276, 1206, 1123, 1102, 1093, 1075, 1043, 1002, 716, 698

HRMS (ESI+): for $[M+H]^+$ calc.: 251.1283, found: 251.1278

(±)-cis-2,3-Dimethoxy-4a,6,7-trimethyl-4a,5,8,8a-tetrahydronaphthalene-1,4-dione (Q4D3)



Quinone **Q4** (HFIP: 245 mg, 1.35 mmol, 1.0 eq.) and diene **D3** (HFIP: 0.30 mL, 2.65 mmol, 2.0 eq.) were reacted following the general procedure. The crude product as purified by flash chromatography on silica gel (cyclohex./AcOEt: 9/1) to give **Q4D3** (HFIP: 246 mg).

Aspect: yellow oil

Yield: 70%

TLC: $R_f \approx 0.78$ (PhMe/AcOEt: 5/5), visualised by UV and $KMnO_4$

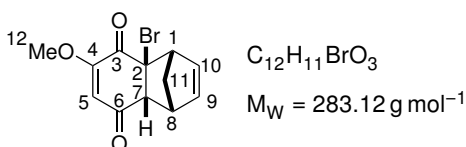
1H NMR (500 MHz, $CDCl_3$): δ (ppm) **3.96** (s, 3H, $C^{11}H_3$ or $C^{12}H_3$), **3.95** (s, 3H, $C^{12}H_3$ or $C^{11}H_3$), **2.76** (ddd, 1H, $J = 6.1; 5.2; 0.6$ Hz, $C^{10}H$), **2.56-2.47** (m, 1H, $\frac{1}{2} \times C^9H_2$), **2.43** (d, 1H, $J = 17.2$ Hz, $\frac{1}{2} \times C^6H_2$), **2.16-2.02** (m, 1H, $\frac{1}{2} \times C^9H_2$), **1.70** (d, 1H, $J = 17.2$ Hz, $\frac{1}{2} \times C^6H_2$), **1.63** (ddt, 3H, $J = 2.8; 2.0; 1.0$ Hz, $C^{15}H_{3H}$), **1.58** (ddt, 3H, $J = 2.8; 2.0; 1.0$ Hz, $C^{14}H_3$), **1.29** (s, 3H, $C^{13}H_3$)

^{13}C NMR (126 MHz, $CDCl_3$): δ (ppm) **198.77** (C_q^4), **195.94** (C_q^1), **147.70** (C_q^2 or C_q^3), **147.08** (C_q^3 or C_q^2), **122.84** (C_q^7 or C_q^8), **122.73** (C_q^8 or C_q^7), **60.72** ($C^{11}H_3$ or $C^{12}H_3$), **60.62** ($C^{12}H_3$ or $C^{11}H_3$), **51.80** ($C^{10}H$), **47.41** (C_q^5), **39.13** (C^6H_2), **29.89** (C^9H_2), **23.28** ($C^{13}H_3$), **19.06** ($C^{14}H_3$), **18.70** ($C^{15}H_3$)

IR: $\bar{\nu}$ (cm^{-1}) 2916, 1674, 1597, 1449, 1330, 1282, 1218, 1194, 1134, 1112, 1076, 1031, 995, 944

HRMS (ESI+): for $[M+H]^+$ calc.: 265.1440, found: 265.1434

(±)-rel-(1R,4S,4aS,8aR)-4a-Bromo-6-methoxy-1,4,4a,8a-tetrahydro-1,4-methanonaphthalene-5,8-dione (Q5D1)



Quinone **Q5** (CH_2Cl_2 : 200 mg, 0.923 mmol, 1.0 eq.; HFIP: 50 mg, 0.230 mmol, 1.0 eq.) and diene **D1** (CH_2Cl_2 : 0.16 mL, 1.90 mmol, 2.1 eq.; HFIP: 0.04 mL, 0.476 mmol, 2.1 eq.) were reacted following the general procedure to give **Q5D1** (CH_2Cl_2 : 261 mg; HFIP: 65 mg).

Aspect: white powder

Yield: CH_2Cl_2 : quantitative; HFIP: quantitative

TLC: $R_f \approx 0.45$ (PhMe/AcOEt: 8/2), visualised by UV and *p*-anisaldehyde

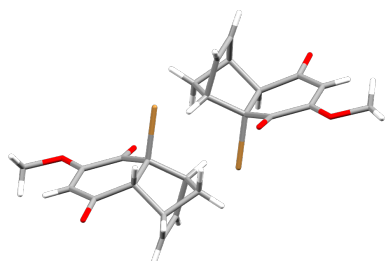
m_p : 103-105 °C

1H NMR (500 MHz, $CDCl_3$): δ (ppm) **6.18** (dd, 1H, $J = 5.6; 2.8$ Hz, C^9H), **6.06** (dd, 1H, $J = 5.6; 3.0$ Hz, $C^{10}H$), **5.97** (s, 1H, C^5H), **3.79** (s, 3H, $C^{12}H_3$), **3.75-3.70** (m, 1H, C^1H), **3.67** (d, 1H, $J = 3.9$ Hz, C^7H), **3.56-3.48** (m, 1H, C^8H), **2.06** (dddd, 2H, $ABXY$, $J_{AX} = 1.3$ Hz, $J_{AY} = 0.6$ Hz, $J_{BX} = J_{BY} = 1.8$ Hz, $J_{AB} = 9.4$ Hz, $\Delta\nu_{AB} = 136.6$ Hz, $C^{11}H_2$)

^{13}C NMR (126 MHz, CDCl_3): δ (ppm) **194.75** (C_q^6), **186.92** (C_q^3), **162.31** (C_q^4), **138.02** (C^9H), **135.39** (C^{10}H), **114.39** (C^5H), **62.44** (C^7H), **61.51** (C_q^2), **56.93** (C^{12}H_3), **54.79** (C^1H), **47.61** (C^8H), **47.27** (C^{11}H_2)

IR: $\bar{\nu}$ (cm^{-1}) 1703, 1648, 1600, 1356, 1328, 1257, 1230, 1195, 1166, 1100, 1082, 1017, 911, 883, 724, 676, 500

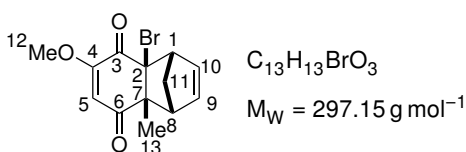
HRMS (ESI+): for $[\text{M}+\text{H}]^+$ calc.: 282.9964, found: 282.9954



Triclinic $P\bar{1}$
 $a = 7.5195(5) \text{ \AA}$ $\alpha = 104.395(5)^\circ$
 $b = 9.1616(5) \text{ \AA}$ $\beta = 97.604(5)^\circ$
 $c = 9.3920(6) \text{ \AA}$ $\gamma = 111.966(6)^\circ$
 $V = 562.63(7) \text{ \AA}^3$ $Z = 2$
 $R = 3.59\%$

Figure 8.29: X-ray structure of **Q5D1** and parameters of the crystal. Crystallisation by slow evaporation from dichloromethane.

(±)-rel-(1*R*,4*S*,4*aS*,8*aR*)-4*a*-Bromo-6-methoxy-8*a*-methyl-1,4,4*a*,8*a*-tetrahydro-1,4-methano-naphthalene-5,8-dione (Q6D1**)**



Quinone **Q6** (HFIP: 209 mg, 0.903 mmol, 1.0 eq.) and diene **D1** (HFIP: 0.15 mL, 1.78 mmol, 2.0 eq.) were reacted following the general procedure to give **Q6D1** (HFIP: 265 mg).

Aspect: greyish powder

Yield: quantitative

TLC: $R_f \approx 0.43$ (cyclohex./AcOEt: 7/3), visualised by UV and *p*-anisaldehyde

m_p : 93-96 °C

^1H NMR (500 MHz, CDCl_3): δ (ppm) **6.24** (dd, 1H, $J = 5.5$; 2.8 Hz, C^9H), **5.96** (dd, 1H, $J = 5.5$; 3.1 Hz, C^{10}H), **5.88** (s, 1H, C^5H), **3.79** (s, 3H, C^{12}H_3), **3.72** (3.66, 1H, C^1H), **3.14-3.08** (m, 1H, C^8H), **2.06** (dddd, 2H, ABXY, $J_{AX} = J_{AY} = 1.6$ Hz, $J_{BX} = 0.75$ Hz, $J_{BY} = 1.7$ Hz, $J_{AB} = 9.7$ Hz, $\Delta\nu_{AB} = 189.9$ Hz, C^{11}H_2), **1.69** (s, 3H, C^{13}H_3)

^{13}C NMR (126 MHz, CDCl_3): δ (ppm) **198.62** (C_q^6), **187.17** (C_q^3), **162.47** (C_q^4), **140.89** (C^9H_3), **134.63** (C^{10}H), **113.06** (C^5H), **71.17** (C_q^2), **59.25** (C_q^7), **56.86** (C^{12}H_3), **56.31** (C^1H), **52.84** (C^8H), **44.75** (C^{11}H_2), **30.83** (C^{13}H_3)

IR: $\bar{\nu}$ (cm^{-1}) 1698, 1660, 1603, 1358, 1244, 1180, 1162, 1085, 1007, 914, 835, 730, 719, 689, 665

HRMS (ESI+): for $[\text{M}+\text{H}]^+$ calc.: 299.0283, found: 299.0277

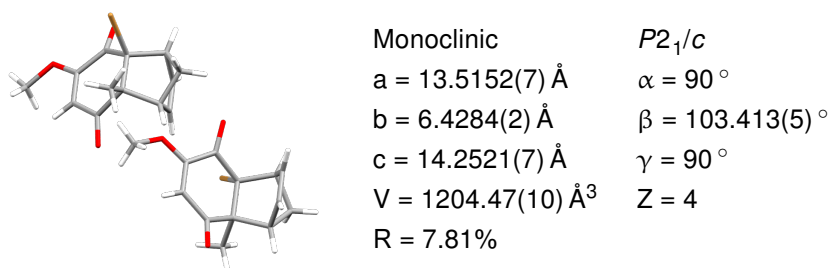
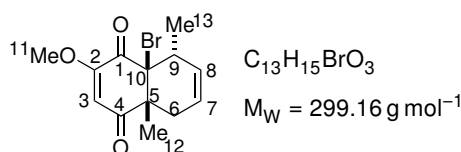


Figure 8.30: X-ray structure of **Q6D1** and crystal parameters. Crystallisation by slow evaporation from dichloromethane.

(±)-rel-(4a*R*,8*R*,8a*S*)-8a-Bromo-2-methoxy-4a,8-dimethyl-4a,5,8,8a-tetrahydronaphthalene-1,4-dione (Q6D2)



Quinone **Q6** (CH_2Cl_2 : 207 mg, 0.895 mmol, 1.0 eq.; HFIP: 208 mg, 0.902 mmol, 1.0 eq.) and diene **D2** (CH_2Cl_2 : 0.14 mL, 1.77 mmol, 2.0 eq.; HFIP: 0.14 mL, 1.77 mmol, 2.0 eq.) were reacted following the general procedure to give **Q6D2** (HFIP: 268 mg). The conversion being too low in dichloromethane (13%), we did not try to isolate the adduct.

Aspect: greyish oil

Yield: HFIP: quantitative

TLC: $R_f \approx 0.64$ (cyclohex./AcOEt: 7/3), visualised by UV and *p*-anisaldehyde

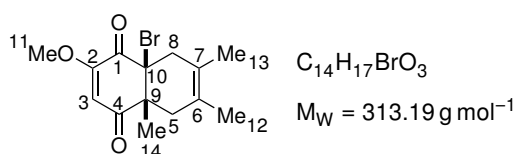
1H NMR (500 MHz, $CDCl_3$): δ (ppm) **5.64** (s, 1H, C^3H), **5.63-5.59** (m, 1H, C^8H), **5.58-5.51** (m, 1H, C^7H), **3.80** (s, 3H, $C^{11}H_3$), **2.99-2.88** (m, 1H, C^9H), **2.54-2.16** (m, 2H, C^6H_2), **1.56** (d, 3H, $J = 0.8$ Hz, $C^{12}H_3$), **1.53** (d, 3H, $J = 7.4$ Hz, $C^{13}H_3$)

^{13}C NMR (126 MHz, $CDCl_3$): δ (ppm) **198.34** (C^4_q), **186.49** (C^1_q), **159.87** (C^2_q), **130.15** (C^8H), **122.17** (C^7H), **105.96** (C^3H), **74.92** (C^{10}_q), **56.67** ($C^{11}H_3$), **55.05** (C^5_q), **38.68** (C^9H), **36.40** (C^6H_2), **17.31** ($C^{12}H_3$), **16.59** ($C^{13}H_3$)

IR: $\bar{\nu}$ (cm^{-1}) 2983, 2941, 2845, 1716, 1671, 1611, 1455, 1376, 1351, 1244, 1213, 1172, 1147, 1087, 1055, 1000, 965, 853, 735, 687, 673, 647

HRMS (ESI+): for $[M+H]^+$ calc.: 299.0283, found: 299.0277

(±)-cis-8a-Bromo-2-methoxy-4a,6,7-trimethyl-4a,5,8,8a-tetrahydronaphthalene-1,4-dione (Q6D3)



Quinone **Q6** (HFIP: 106 mg, 0.458 mmol, 1.0 eq.) and diene **D3** (HFIP: 0.10 mL, 0.884 mmol, 1.9 eq.) were reacted following the general procedure. The crude product was purified by flash chromatography (cyclohex./AcOEt: 9/1) to give **Q6D3** (HFIP: 52 mg).

Aspect: greyish oil

Yield: 36%

TLC: $R_f \approx 0.59$ (cyclohex./AcOEt: 7/3), visualised by UV and *p*-anisaldehyde

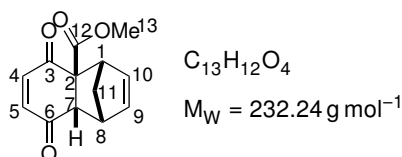
$^1\text{H NMR}$ (500 MHz, CDCl_3): δ (ppm) **5.71** (s, 1H, C^3H), **3.81** (s, 3H, C^{11}H_3), **3.18** (d, 1H, $J = 17.2$ Hz, $\frac{1}{2} \times \text{C}^9\text{H}_2$), **2.63** (d, 1H, $J = 17.2$ Hz, $\frac{1}{2} \times \text{C}^9\text{H}_2$), **2.46** (d, 1H, $J = 17.6$ Hz, $\frac{1}{2} \times \text{C}^6\text{H}_2$), **2.02** (d, 1H, $J = 17.6$ Hz, $\frac{1}{2} \times \text{C}^6\text{H}_2$), **1.67** (s, 3H, C^{14}H_3), **1.51** (s, 3H, C^{13}H_3), **1.49** (s, 3H, C^{12}H_3)

$^{13}\text{C NMR}$ (126 MHz, CDCl_3): δ (ppm) **198.85** (C_q^4), **185.75** (C_q^1), **159.26** (C_q^2), **124.31** (C_q^7 or C_q^8), **122.11** (C_q^8 or C_q^7), **107.26** (C^3H), **69.31** (C_q^{10}), **56.60** (C^{11}H_3), **53.21** (C_q^5), **42.26** (C^6H_2), **38.59** (C^9H_2), **18.50** (C^{13}H_3 or C^{14}H_3), **18.48** (C^{14}H_3 or C^{13}H_3), **18.02** (C^{12}H_3)

IR: $\bar{\nu}$ (cm^{-1}) 2911, 1717, 1662, 1612, 1450, 1367, 1349, 1263, 1221, 1156, 1112, 1099, 1074, 1023, 965, 867, 732

HRMS (ESI+): for $[\text{M}+\text{H}]^+$ calc.: 313.0439, found: 313.0435

Methyl (\pm)-*rel*-(1*R*,4*S*,4*aS*,8*aS*)-5,8-Dioxo-1,5,8,8*a*-tetrahydro-1,4-methanonaphthalene-4*a*(4*H*)-carboxylate (Q7D1)



Quinone **Q7** (CH_2Cl_2 : 230 mg, 1.38 mmol, 1.0 eq.; HFIP: 55 mg, 0.333 mmol, 1.0 eq.) and diene **D1** (CH_2Cl_2 : 0.23 mL, 2.74 mmol, 2.0 eq.; HFIP: 0.06 mL, 0.712 mmol, 2.1 eq.) were reacted following the general procedure. The crude product was purified by flash chromatography on silica gel (cyclohex./AcOEt: 9/1) to give **Q7D1** (CH_2Cl_2 : 281 mg; HFIP: 71 mg)

Aspect: yellow oil

Yield: CH_2Cl_2 : 88%; HFIP: 92%

TLC: $R_f \approx 0.47$ (cyclohex./AcOEt: 7/3), visualised by UV and *p*-anisaldehyde

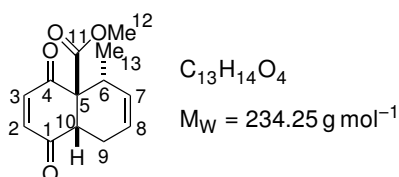
$^1\text{H NMR}$ (500 MHz, CDCl_3): δ (ppm) **6.61** (dd, $A'B'$, 2H, $J_{A'B'} = 10.4$ Hz, $\Delta\nu_{A'B'} = 4.6$ Hz, $\text{C}^4\text{H} + \text{C}^5\text{H}$), **6.12** (dd, 1H, $J = 5.6$; 2.8 Hz, C^9H), **6.09** (dd, 1H, $J = 5.6$; 2.9 Hz, C^{10}H), **3.82-3.76** (m, 1H, C^1H), **3.73** (s, 3H, C^{13}H_3), **3.52-3.44** (m, 1H, C^8H), **3.38** (d, 1H, $J = 4.0$ Hz, C^7H), **1.65** (dddd, $ABXY$, 2H, $J_{AB} = 9.3$ Hz, $J_{AX} = J_{AY} = 1.4$ Hz, $J_{BX} = J_{BY} = 1.7$ Hz, $\Delta\nu_{AB} = 21.9$ Hz)

$^{13}\text{C NMR}$ (126 MHz, CDCl_3): δ (ppm) **197.58** (C_q^3 or C_q^6), **194.98** (C_q^6 or C_q^3), **171.16** (C_q^{12}), **141.45** (C^4H or C^5H), **141.42** (C^5H or C^4H), **137.20** (C^9H), **136.45** (C^{10}H), **54.26** (C_q^7), **53.37** (C^{13}H_3), **52.07** (C^1H), **48.33** (C^8H), **48.10** (C^{11}H_2)

IR: $\bar{\nu}$ (cm^{-1}) 2955, 1732, 1673, 1435, 1316, 1286, 1250, 1228, 1153, 1113, 1070, 1040, 1012, 996

The experimental data were in agreement with those reported in the literature.⁶⁴

Methyl (\pm)-*rel*-(4*aR*,5*S*,8*aR*)-5-Methyl-1,4-dioxo-1,5,8,8*a*-tetrahydronaphthalene-4*a*(4*H*)-carboxylate (Q7D2)



Quinone **Q7** (CH_2Cl_2 : 213 mg, 1.29 mmol, 1.0 eq.; HFIP: 67 mg, 0.403 mmol, 1.0 eq.) and diene **D2** (CH_2Cl_2 : 0.26 mL, 2.61 mmol, 2.0 eq.; HFIP: 0.08 mL, 0.802 mmol, 2.0 eq.) were reacted following the general procedure to give **Q7D2** (CH_2Cl_2 : 300 mg; HFIP: 94 mg).

Aspect: pale yellow oil

Yield: CH_2Cl_2 : quantitative; HFIP: quantitative

TLC: $R_f \approx 0.46$ (cyclohex./AcOEt: 7/3), visualised by UV and $KMnO_4$

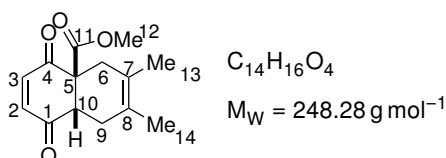
1H NMR (500 MHz, $CDCl_3$): δ (ppm) **6.74** (dd, 2H, AB, $J_{AB} = 10.3$ Hz, $\Delta\nu_{AB} = 16.6$ Hz, $C^2H + C^3H$), **5.67-5.62** (m, 1H, C^7H), **5.61-5.56** (m, 8H, C^1H_8), **3.78** (s, 3H, $C^{12}H_3$), **3.78** (dd, 1H, $J = 7.4$; 4.2 Hz, $C^{10}H$), **3.07-2.94** (m, 1H, C^6H), **2.66** (dt, 1H, $J = 18.7$, 4.2, 1.9 Hz, $\frac{1}{2} \times C^9H_2$), **2.09** (ddq, 1H, $J = 18.7$, 7.4, 2.6 Hz, $\frac{1}{2} \times C^9H_2$), **0.99** (d, 3H, $J = 7.5$ Hz, $C^{13}H_3$)

^{13}C NMR (126 MHz, $CDCl_3$): δ (ppm) **197.74** (C_q^1), **196.65** (C_q^4), **170.75** (C_q^{11}), **140.29** (C^2H or C^3H), **140.17** (C^3H or C^2H), **130.55** (C^7H), **122.65** (C^8H), **63.13** (C_q^5), **53.36** ($C^{12}H_3$), **48.20** ($C^{10}H$), **34.65** (C^6H), **22.16** (C^9H_2), **18.42** ($C^{13}H_3$)

IR: $\bar{\nu}$ (cm^{-1}) 2957, 1745, 1727, 1697, 1678, 1434, 1253, 1225, 1109, 1080, 1028, 806, 737, 709

The experimental data were in agreement with those reported in the literature.⁶⁵

Methyl (\pm)-*cis*-6,7-Dimethyl-1,4-dioxo-1,5,8,8*a*-tetrahydronaphthalene-4*a*(4*H*)-carboxylate (Q7D3)



Quinone **Q7** (CH_2Cl_2 : 216 mg, 1.30 mmol, 1.0 eq.; HFIP: 52 mg, 0.312 mmol, 1.0 eq.) and diene **D3** (CH_2Cl_2 : 0.30 mL, 2.65 mmol, 2.0 eq.; HFIP: 0.07 mL, 0.619 mmol, 2.0 eq.) were reacted following the general procedure to give **Q7D3** (CH_2Cl_2 : 321 mg; HFIP: 76 mg).

Aspect: grey powder

Yield: CH_2Cl_2 : quantitative; HFIP: 98%

TLC: $R_f \approx 0.46$ (cHex/AcOEt: 7/3), visualised by UV and *p*-anisaldehyde

m_p : 104-107 °C

1H NMR (500 MHz, $CDCl_3$): δ (ppm) **6.66** (dd, AB, 2H, $J_{AB} = 10.5$ Hz, $\Delta\nu_{AB} = 4.8$ Hz, $C^2H + C^3H$), **3.74** (s, 3H, $C^{12}H_3$), **3.54** (dd, 1H, $J = 7.2$; 6.5 Hz, $C^{10}H$), **2.62-2.54** (m, 1H, $\frac{1}{2} \times C^6H_2$), **2.38-2.30** (m, 2H, $\frac{1}{2} \times C^6H_2 + \frac{1}{2} \times C^9H_2$), **2.16-2.01** (m, 1H, $\frac{1}{2} \times C^9H_2$), **1.67-1.61** (m, 3H, $C^{13}H_3$), **1.61** (1.55, 3H, $C^{14}H_3$)

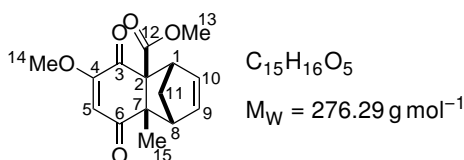
^{13}C NMR (126 MHz, $CDCl_3$): δ (ppm) **198.15** (C_q^1), **195.17** (C_q^4), **170.65** (C_q^{11}), **139.63** (C^2H or C^3H), **138.07** (C^3H or C^2H), **123.08** (C_q^8), **122.78** (C_q^7), **60.84** (C_q^5), **53.32** ($C^{12}H_3$), **49.04** ($C^{10}H$), **33.96**

(C^6H_2), **30.21** (C^9H_2), **18.83** ($C^{13}H_3$ or $C^{14}H_3$), **18.77** ($C^{14}H_3$ or $C^{13}H_3$)

IR: $\bar{\nu}$ (cm^{-1}) 2899, 1743, 1677, 1439, 1291, 1262, 1248, 1229, 1211, 1195, 1095, 1070, 1049, 854

The experimental data were in agreement with those reported in the literature.⁶⁶

Methyl (\pm)-*rel*-(1*R*,4*S*,4*aS*,8*aS*)-6-methoxy-8*a*-methyl-5,8-dioxo-1,5,8,8*a*-tetrahydro-1,4-methanonaphthalene-4*a*(4*H*)-carboxylate (Q8D1)



Quinone **Q8** (CH_2Cl_2 : 130 mg, 0.619 mmol, 1.0 eq.; HFIP: 118 mg, 0.561 mmol, 1.0 eq.) and diene **D1** (CH_2Cl_2 : 0.10 mL, 1.19 mmol, 1.9 eq.; HFIP: 0.10 mL, 1.19 mmol, 2.1 eq.) were reacted following the general procedure. After evaporation of the solvent, the crude mixture was triturated with diethyl ether, filtered and dried under vacuum to give **Q8D1** (CH_2Cl_2 : 142 mg; HFIP: 125 mg).

Aspect: white powder

Yield: CH_2Cl_2 : 85%; HFIP: 82%

TLC: $R_f \approx 0.55$ (cHex/AcOEt: 7/3), visualised by UV and $KMnO_4$

m_p : 164-166 °C

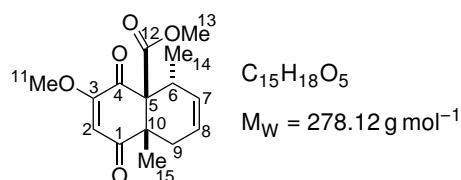
1H NMR (500 MHz, $CDCl_3$): δ (ppm) **6.18** (dd, 1H, $J = 5.7; 3.0$ Hz, C^9H or $C^{10}H$), **6.02** (dd, 1H, $J = 5.7; 2.9$ Hz, C^9H or $C^{10}H$), **5.88** (s, 1H, C^5H), **3.77** (s, 3H, $C^{14}H_3$), **3.70** (s, 3H, $C^{13}H_3$), **3.65-3.62** (m, 1H, C^1H), **3.04** (m, 1H, C^8H), **2.10** (dt, 1H, $J = 9.7; 1.4$ Hz, $\frac{1}{2} \times C^{11}H_2$), **1.60** (dt, 1H, $J = 9.7; 1.7$ Hz, $\frac{1}{2} \times C^{11}H_2$), **1.40** (s, 3H, $C^{15}H_3$)

^{13}C NMR (126 MHz, $CDCl_3$): δ (ppm) **200.20** (C_q^6), **191.73** (C_q^3), **171.31** (C_q^{12}), **162.42** (C_q^4), **140.02** (C^9H or $C^{10}H$), **136.05** (C^9H or $C^{10}H$), **113.10** (C^5H), **66.95** (C_q^2), **57.48** (C_q^7), **56.62** ($C^{14}H_3$), **54.06** (C^8H), **52.77** ($C^{13}H_3$), **52.61** (C^1H), **45.79** ($C^{11}H_2$), **23.64** ($C^{15}H_3$)

IR: $\bar{\nu}$ (cm^{-1}) 2958, 1736, 1694, 1649, 1607, 1435, 1363, 1225, 1169, 1030

HRMS (ESI⁺): for $[M+Na]^+$ calc.: 299.0890, found: 299.0878

Methyl (\pm)-*rel*-(4*aR*,5*S*,8*aR*)-3-methoxy-5,8*a*-dimethyl-1,4-dioxo-1,5,8,8*a*-tetrahydronaphthalene-4*a*(4*H*)-carboxylate (Q8D2)



Quinone **Q8** (HFIP: 127 mg, 0.605 mmol, 1.0 eq.) and diene **D2** (HFIP: 0.12 mL, 1.20 mmol, 1.9 eq.) were reacted following the general procedure. After evaporation of the solvent, the crude mixture was triturated with diethyl ether, filtered and dried under vacuum to give **Q8D2** (HFIP: 132 mg).

Aspect: White powder

Yield: 79%

TLC: $R_f \approx 0.47$ (cHex/ CH_2Cl_2 /acetone: 5/5/0.5), visualised by UV and $KMnO_4$

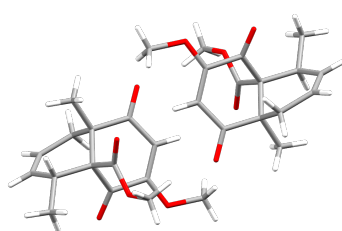
m_p : 133-134 °C

¹H NMR (500 MHz, CDCl₃): δ (ppm) **5.68** (s, 1H, C²H), **5.66** (ddt, 1H, *J* = 10.2; 2.5; 1.8 Hz, C⁷H), **5.52** (ddt, 1H, *J* = 10.2; 5.1; 2.6 Hz, C⁸H), **3.79** (s, 3H, C¹¹H₃), **3.69** (s, 3H, C¹³H₃), **2.86-2.76** (m, 1H, C⁶H), **2.35-2.24** (m, 1H, 1/2 × C⁹H₂), **2.00-1.88** (m, 1H, 1/2 × C⁹H₂), **1.52** (s, 3H, C¹⁵H₃), **1.33** (d, 3H, *J* = 7.5 Hz, C¹⁴H₃)

¹³C NMR (126 MHz, CDCl₃): δ (ppm) **199.95** (C_q¹), **189.79** (C_q⁴), **170.88** (C_q¹²), **162.98** (C_q³), **130.52** (C⁷H), **121.63** (C⁸H), **106.65** (C²H), **65.19** (C_q⁵), **56.75** (C¹¹H₃), **52.73** (C¹³H₃), **52.61** (C_q¹⁰), **37.41** (C⁹H₂), **33.43** (C⁶H), **17.01** (C¹⁵H₃), **16.05** (C¹⁴H₃)

IR: $\bar{\nu}$ (cm⁻¹) 2953, 1720, 1667, 1601, 1438, 1348, 1213, 1042, 859

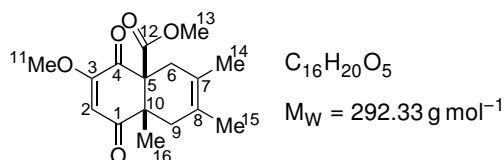
HRMS (ESI+): for [M+Na]⁺ calc.: 301.1046, found: 301.1037



Monoclinic *P*2₁/*c*
a = 10.6822(6) Å *α* = 90°
b = 11.3107(4) Å *β* = 114.202(6)°
c = 12.8714(6) Å *γ* = 90°
V = 1418.48(13) Å³ *Z* = 4
R = 4.66%

Figure 8.31: X-ray structure of **Q8D2** and parameters of the crystal. Crystallisation by slow evaporation from dichloromethane.

Methyl (±)-*cis*-3-methoxy-6,7,8a-trimethyl-1,4-dioxo-1,5,8,8a-tetrahydronaphthalene-4a(4*H*)-carboxylate (**Q8D3**)



Quinone **Q8** (HFIP: 139 mg, 0.663 mmol, 1.0 eq.) and diene **D3** (HFIP: 0.15 mL, 1.33 mmol, 2.0 eq.) were reacted following the general procedure. After evaporation of the solvent, the crude mixture was triturated with diethyl ether, filtered and dried under vacuum to give **Q8D3** (HFIP: 159 mg).

Aspect: white powder

Yield: 82%

TLC: *R_f* ≈ 0.47 (cHex/CH₂Cl₂/acetone: 5/5/0.5), visualised by UV and KMnO₄

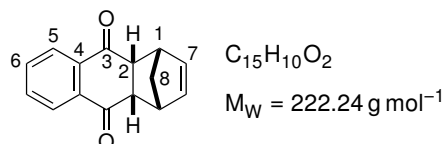
***m_p*:** 112-114 °C

¹H NMR (500 MHz, CDCl₃): δ (ppm) **5.91** (s, 1H, C²H), **3.75** (s, 3H, C¹¹H₃), **3.66** (s, 3H, C¹³H₃), **3.07** (d, 1H, *J* = 17.8 Hz, 1/2 × C⁶H₂), **2.41-2.20** (m, 2H, 1/2 × C⁶H₂ + 1/2 × C⁹H₂), **3.07** (d, 1H, *J* = 17.7 Hz, 1/2 × C⁹H₂), **1.79** (s, 3H, C¹⁴H₃), **1.52** (s, 3H, C¹⁵H₃), **1.29** (s, 3H, C¹⁶H₃)

¹³C NMR (126 MHz, CDCl₃): δ (ppm) **200.59** (C_q¹), **188.99** (C_q⁴), **169.52** (C_q¹²), **158.97** (C_q³), **122.76** (C_q⁷ or C_q⁸), **110.55** (C¹H₂), **65.34** (C_q⁵), **56.41** (C¹¹H₃), **53.34** (C¹³H₃), **50.57** (C_q¹⁰), **42.74** (C⁹H₂), **31.66** (C⁶H₂), **18.75** (C¹⁴H₃ or C¹⁵H₃), **18.72** (C¹⁴H₃ or C¹⁵H₃), **17.62** (C¹⁶H₃)

IR: $\bar{\nu}$ (cm⁻¹) 2893, 1733, 1705, 1668, 1603, 1433, 1348, 1231, 1193, 1075, 884

HRMS (ESI+): for [M+Na]⁺ calc.: 315.1203, found: 315.1200

(1R,4S,4aR,9aS)-1,4,4a,9a-Tetrahydro-1,4-methanoanthracene-9,10-dione (Q9D1)

Quinone **Q9** (CH_2Cl_2 : 195 mg, 1.23 mmol, 1.0 eq.; HFIP: 51 mg, 0.323 mmol, 1.0 eq.) and diene **D1** (CH_2Cl_2 : 0.21 mL, 2.50 mmol, 2.0 eq.; HFIP: 0.06 mL, 0.714 mmol, 2.2 eq.) were reacted following the general procedure to give **Q9D1** (CH_2Cl_2 : 257 mg; HFIP: 72 mg).

Aspect: brown powder

Yield: CH_2Cl_2 : 93%; HFIP: quantitative

TLC: $R_f \approx 0.33$ (cHex/AcOEt: 8/2), visualised by UV and *p*-anisaldehyde

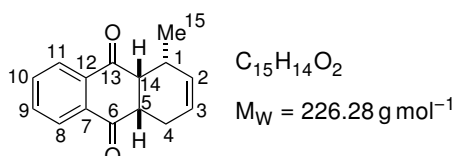
m_p : 108-110 °C

1H NMR (500 MHz, $CDCl_3$): δ (ppm) **8.02** (dd, 2H, $J = 5.9 \text{ Hz}$; 3.3 Hz, $2 \times C^5H$ or $2 \times C^6H$), **7.69** (dd, 2H, $J = 5.9 \text{ Hz}$; 3.3 Hz, $2 \times C^6H$ or $2 \times C^5H$), **5.98** (dd, 2H, ABXYZ, $J_{AX} = J_{XY} = 1.8 \text{ Hz}$, $2 \times C^7H$), **3.66** (m, 2H, ABXYZ, $2 \times C^1H$), **3.45** (dd, 2H, ABXYZ, $J_{YZ} = 2.5 \text{ Hz}$, $J_{BY} = 1.4 \text{ Hz}$, $2 \times C^2H$), **1.55** (dddd, 2H, ABXYZ, $J_{AX} = 1.8 \text{ Hz}$, $J_{BZ} = 1.4 \text{ Hz}$, $J_{AB} = 8.6 \text{ Hz}$, $\Delta\nu_{AB} = 17.2 \text{ Hz}$, C^8H_2)

^{13}C NMR (126 MHz, $CDCl_3$): δ (ppm) **197.97** ($2 \times C_q^3$), **135.93** ($2 \times C_q^4$), **135.86** ($2 \times C_7H$), **134.24** ($2 \times C^6H$ or $2 \times C^5H$), **126.98** ($2 \times C^5H$ or $2 \times C^6H$), **49.66** ($2 \times C^1H$), **49.63** ($2 \times C^2H$), **49.35** (C^8H_2)

IR: $\bar{\nu}$ (cm^{-1}) 1672, 1586, 1298, 1269, 751, 702, 657, 548

The experimental data were in agreement with those reported in the literature.⁶⁷

(±)-rel-(1R,4aS,9aR)-1-Methyl-1,4,4a,9a-tetrahydroanthracene-9,10-dione (Q9D2)

Quinone **Q9** (CH_2Cl_2 : 208 mg, 1.32 mmol, 1.0 eq.; HFIP: 66 mg, 0.419 mmol, 1.0 eq.) and diene **D2** (CH_2Cl_2 : 0.26 mL, 2.61 mmol, 2.0 eq.; HFIP: 0.08 mL, 0.802 mmol, 1.9 eq.) were reacted following the general procedure to give **Q9D2** (CH_2Cl_2 : 300 mg; HFIP: 96 mg).

Aspect: greyish oil

Yield: CH_2Cl_2 : quantitative; HFIP: quantitative

TLC: $R_f \approx 0.81$ (cyclohex./AcOEt: 7/3), visualised by UV and *p*-anisaldehyde

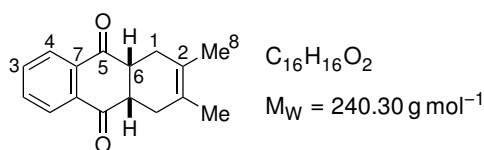
1H NMR (500 MHz, $CDCl_3$): δ (ppm) **8.09-8.00** (m, 2H, $C^8H + C^{11}H$ or $C^9H + C^{10}H$), **7.77-7.71** (m, 2H, $C^9H + C^{10}H$ or $C^8H + C^{11}H$), **5.76-5.65** (m, 2H, $C^2H + C^3H$), **3.51** (dd, 1H, $J = 5.9$; 5.8 Hz, $C^{14}H$), **3.43-3.38** (m, 1H, C^5H), **2.85-2.75** (m, 1H, $\frac{1}{2} \times C^4H_2$), **2.73-2.55** (m, 1H, C^1H), **2.26-2.18** (m, 1H, $\frac{1}{2} \times C^4H_2$), **0.84** (d, 3H, $J = 7.4 \text{ Hz}$, $C^{15}H_3$)

^{13}C NMR (126 MHz, $CDCl_3$): δ (ppm) **199.14** (C_q^{13}), **198.35** (C_q^6), **135.90** (C_q^7 or C_q^{12}), **135.43** (C_q^{12} or C_q^7), **134.33** (C^8H or C^9H or $C^{10}H$ or $C^{11}H$), **134.24** (C^8H or C^9H or $C^{10}H$ or $C^{11}H$), **131.29** (C^2H), **126.76** (C^8H or C^9H or $C^{10}H$ or $C^{11}H$), **126.63** (C^8H or C^9H or $C^{10}H$ or $C^{11}H$), **123.65** (C^3H), **50.90** ($C^{14}H$), **46.03** (C^5H), **23.09** (C^4H_2), **18.49** ($C^{15}H_3$)

IR: $\bar{\nu}$ (cm⁻¹) 2964, 2929, 2875, 1688, 1659, 1619, 1591, 1326, 1247, 1215, 1180, 1101, 913, 710

The experimental data were in agreement with those reported in the literature.⁶⁸

(4a*R*,9a*S*)-2,3-Dimethyl-1,4,4a,9a-tetrahydroanthracene-9,10-dione (Q9D3)



Quinone **Q9** (CH₂Cl₂: 196 mg, 1.24 mmol, 1.0 eq.; HFIP: 56 mg, 0.354 mmol, 1.0 eq.) and diene **D3** (CH₂Cl₂: 0.28 mL, 2.47 mmol, 2.0 eq.; HFIP: 0.08 mL, 0.707 mmol, 2.0 eq.) were reacted following the general procedure. The crude was purified by flash chromatography on silica gel (cyclohex./AcOEt: 9/1) to give **Q9D3** (CH₂Cl₂: 176 mg; HFIP: 81 mg).

Aspect: brown powder

Yield: CH₂Cl₂: 59%; HFIP: 95%

TLC: R_f ≈ 0.70 (cHex/AcOEt: 7/3), visualised by UV and *p*-anisaldehyde

m_p: 146-149 °C

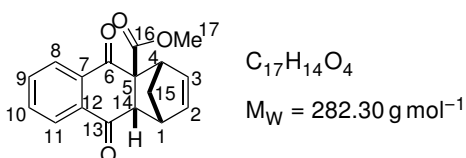
¹H NMR (500 MHz, CDCl₃): δ (ppm) **8.04** (dd, 2H, *J* = 5.8 Hz; 3.3 Hz, 2 × C³H or 2 × C⁴H), **7.73** (dd, 2H, *J* = 5.8 Hz; 3.3 Hz, 2 × C⁴H or 2 × C³H), **3.40-3.29** (m, 2H, 2 × C⁶H), **2.28** (m, 4H, AB, *J*_{AB} = 15.5 Hz, Δ*v*_{AB} = 153.9 Hz, 2 × C¹H₂), **1.64** (s, 6H, 2 × C⁸H₃)

¹³C NMR (126 MHz, CDCl₃): δ (ppm) **198.55** (2 × C⁵_q), **134.37** (2 × C³H or 2 × C⁴H), **134.22** (2 × C⁷_q), **126.97** (2 × C⁴H or 2 × C³H), **123.60** (2 × C²_q), **47.48** (2 × C⁶H), **30.79** (2 × C¹H₂), **19.04** (2 × C⁸H₃)

IR: $\bar{\nu}$ (cm⁻¹) 2889, 1685, 1593, 1285, 1252, 777, 744, 719, 555

The experimental data were in agreement with those reported in the literature.⁶³

Methyl (±)-*rel*-(1*R*,4*S*,4a*S*,9a*S*)-9,10-dioxo-1,9,9a,10-tetrahydro-1,4-methanonaphthalene-4a(4*H*)-carboxylate (Q10D1)



Quinone **Q10** (CH₂Cl₂: 205 mg, 0.949 mmol, 1.0 eq.; HFIP: 51 mg, 0.237 mmol, 1.0 eq.) and diene **D1** (CH₂Cl₂: 0.16 mL, 1.90 mmol, 2.0 eq.; HFIP: 0.04 mL, 0.476 mmol, 2.0 eq.) were reacted following the general procedure. The crude product was purified by flash chromatography on silica gel (cyclohex./AcOEt: 8/2) to give **Q10D1** (CH₂Cl₂: 256 mg; HFIP: 65 mg).

Aspect: pale yellow viscous oil

Yield: CH₂Cl₂: 95%; HFIP: 97%

TLC: R_f ≈ 0.55 (cyclohex./AcOEt: 7/3), visualised by UV and KMnO₄

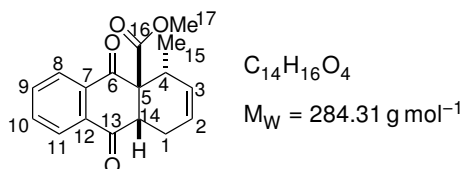
¹H NMR (500 MHz, CDCl₃): δ (ppm) **8.09-8.00** (m, 2H, C⁸H + C¹¹H), **7.75-7.69** (m, 2H, C⁹H + C¹⁰H), **6.03** (2H, ddd, ABXY, *J*_{AX} = 2.9 Hz, *J*_{BY} = 2.6 Hz, *J*_{AB} = 5.6 Hz, Δ*v*_{AB} = 13.1 Hz, C²H + C³H), **3.95-3.88** (m, 1H, C¹H), **3.70** (s, 3H, C¹⁷H₃), **3.63-3.49** (m, 2H, C⁴H + C¹⁴H), **1.68** (dddd, 2H, A'B'X'Y', *J*_{A'X'} = *J*_{A'Y'} = *J*_{B'X'} = *J*_{B'Y'} = 1.5 Hz, *J*_{A'B'} = 9.2 Hz, Δ*v*_{A'B'} = 53.5 Hz, C¹⁵H₂)

^{13}C NMR (126 MHz, CDCl_3): δ (ppm) **195.92** (C_q^6 or C_q^{13}), **193.68** (C_q^{13} or C_q^6), **171.78** (C_q^{16}), **137.39** (C^2H or C^3H), **136.61** (C^3H or C^2H), **135.27** (C_q^7 or C_q^{12}), **134.99** (C_q^{12} or C_q^7), **134.60** (C^9H or C^{10}H), **134.48** (C^{10}H or C^9H), **127.49** (C^8H or C^{11}H), **127.16** (C^{11}H or C^8H), **64.37** (C_q^5), **55.29** (C^{14}H), **52.80** ($\text{C}^1\text{H} + \text{C}^{17}\text{H}_3$), **49.05** (C^4H), **48.63** (C^{15}H_2)

IR: $\bar{\nu}$ (cm^{-1}) 2959, 2930, 1737, 1671, 1588, 1267, 1219, 1155, 1049, 808, 775

HRMS (ESI+): for $[\text{M}+\text{H}]^+$ calc.: 283.0965, found: 283.0961

Methyl (\pm)-*rel*-(4*R*,4*aS*,9*aS*)-4-methyl-9,10-dioxo-1,9,9*a*,10-tetrahydroanthracene-4*a*(4*H*)-carboxylate (Q10D2**)**



Quinone **Q10** (CH_2Cl_2 : 205 mg, 0.948 mmol, 1.0 eq.; HFIP: 62 mg, 0.286 mmol, 1.0 eq.) and diene **D2** (CH_2Cl_2 : 0.15 mL, 1.90 mmol, 2.0 eq.; HFIP: 0.06 mL, 0.602 mmol, 2.1 eq.) were reacted following the general procedure to give **Q10D2** (CH_2Cl_2 : 266 mg; HFIP: 80 mg).

Aspect: grey powder

Yield: CH_2Cl_2 : quantitative; HFIP: quantitative

TLC: $R_f \approx 0.71$ (cyclohex./AcOEt: 7/3), visualised by UV and KMnO_4

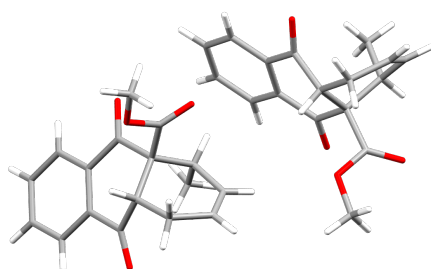
m_p : 98–101 °C

^1H NMR (500 MHz, CDCl_3): δ (ppm) **8.10–8.01** (m, 2H, $\text{C}^8\text{H} + \text{C}^{11}\text{H}$), **7.79–7.71** (m, 2H, $\text{C}^9\text{H} + \text{C}^{10}\text{H}$), **5.73–5.68** (m, 1H, C^3H), **5.68–5.60** (m, 1H, C^2H), **3.89** (dd, 1H, $J = 6.8; 4.6$ Hz, C^{14}H), **3.74** (s, 3H, C^{17}H_3), **3.16–3.04** (m, 1H, C^4H), **2.80–2.70** (m, 1H, $\frac{1}{2} \times \text{C}^1\text{H}_2$), **2.20–2.12** (m, 1H, $\frac{1}{2} \times \text{C}^1\text{H}_2$), **0.89** (d, 3H, $J = 7.5$ Hz, C^{15}H_3)

^{13}C NMR (126 MHz, CDCl_3): δ (ppm) **196.34** (C_q^{13}), **194.95** (C_q^6), **171.11** (C_q^{16}), **135.01** (C_q^7 or C_q^{12}), **134.77** (C_q^{12} or C_q^7), **134.67** (C^9H or C^{10}), **134.54** (C^{10}H or C^9), **130.85** (C^3H), **127.22** (C^8H or C^{11}), **126.64** (C^{11}H or C^8), **122.80** (C^2H), **63.23** (C_q^5), **53.24** (C^{17}H_3), **48.59** (C^{14}H), **34.83** (C^4H), **22.64** (C^1H_2), **18.04** (C^{15}H_2)

IR: $\bar{\nu}$ (cm^{-1}) 2982, 2887, 1742, 1705, 1681, 1591, 1438, 1275, 1252, 1229, 1199, 1133, 1073, 1020, 942, 786

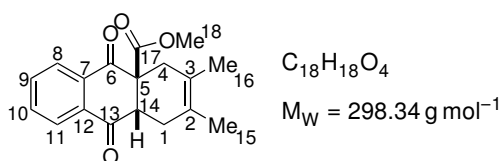
The experimental data were in agreement with those reported in the literature.⁶⁵



Monoclinic	$P2_1/c$
$a = 7.5455(3) \text{ \AA}$	$\alpha = 90^\circ$
$b = 14.8987(5) \text{ \AA}$	$\beta = 90.430(3)^\circ$
$c = 12.7722(4) \text{ \AA}$	$\gamma = 90^\circ$
$V = 1435.79(8) \text{ \AA}^3$	$Z = 4$
$R = 4.13\%$	

Figure 8.32: X-ray structure of **Q10D2** and parameters of the crystal. Crystallisation by slow evaporation from dichloromethane.

Methyl (\pm)-*cis*-2,3-dimethyl-9,10-dioxo-1,9,9a,10-tetrahydroanthracene-4a-(4*H*)-carboxylate (Q10D3)



Quinone **Q10** (CH₂Cl₂: 217 mg, 1.00 mmol, 1.0 eq.; HFIP: 63 mg, 0.291 mmol, 1.0 eq.) and diene **D3** (CH₂Cl₂: 0.23 mL, 2.03 mmol, 2.0 eq.; HFIP: 0.07 mL, 0.619 mmol, 2.1 eq.) were reacted following the general procedure to give **Q10D3** (CH₂Cl₂: 297 mg; HFIP: 85 mg).

Aspect: pale yellow oil

Yield: CH₂Cl₂: quantitative; HFIP: quantitative

TLC: R_f ≈ 0.75 (cyclohex./AcOEt: 7/3), visualised by UV and KMnO₄

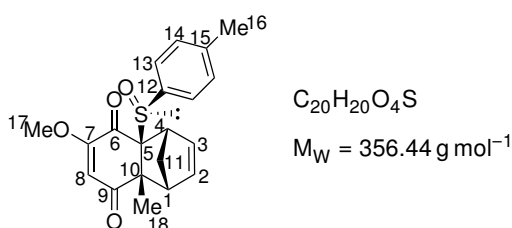
¹H NMR (500 MHz, CDCl₃): δ (ppm) **8.10-8.00** (m, 2H, C⁸H + C¹¹H), **7.80-7.70** (m, 2H, C⁹H + C¹⁰H), **3.69** (s, 4H, C⁴H + C¹⁸H₃), **2.70** (d, 1H, *J* = 18.2 Hz, 1/2 × C⁴H₂), **2.47-2.35** (m, 2H, 1/2 × C¹H₂ + C⁴H₂), **2.23-2.09** (m, 1H, 1/2 × C¹H₂), **1.66** (ddt, 3H, *J* = 2.8; 1.9; 0.9 Hz, C¹⁶H₃), **1.61** (ddt, 3H, *J* = 2.8; 1.9; 0.9 Hz, C¹⁶H₃)

¹³C NMR (126 MHz, CDCl₃): δ (ppm) **196.35** (C_q⁶), **193.67** (C_q¹³), **171.01** (C_q¹⁷), **134.88** (C⁹H or C¹⁰H), **134.46** (C¹⁰H or C⁹H), **133.73** (C_q⁷ or C_q¹²), **133.19** (C_q¹² or C_q⁷), **127.43** (C⁸H or C¹¹H), **127.16** (C¹¹H or C⁸H), **123.18** (C_q² or C_q³), **123.05** (C_q³ or C_q²), **61.01** (C_q⁵), **53.22** (C¹⁸H₃), **49.37** (C¹⁴H), **34.22** (C⁴H₂), **30.66** (C¹H₂), **18.90** (C¹⁵H₃ or C¹⁶H₃), **18.82** (C¹⁶H₃ or C¹⁵H₃)

IR: ν̄ (cm⁻¹) 2915, 1735, 1694, 1593, 1434, 1278, 1230, 1159, 1128, 1105, 1067, 1026, 978, 845, 796

HRMS (ESI+): for [M+H]⁺ calc.: 299.1283, found: 299.1278

(-)-(1*R*,4*S*,4*aS*,8*aR*)-6-Methoxy-8*a*-methyl-4*a*-((*S*)-*p*-tolylsulfinyl)-1,4,4*a*,8*a*-tetrahydro-1,4-methanonaphthalene-5,8-dione (α-SQ1D1/α-319)



Quinone **SQ1/318a** (CH₂Cl₂: 257 mg, 0.885 mmol, 1.0 eq.; HFIP: 260 mg, 0.896 mmol, 1.0 eq.) and diene **D1** (CH₂Cl₂: 0.15 mL, 1.78 mmol, 2.0 eq.; HFIP: 0.15 mL, 1.78 mmol, 2.0 eq.) were reacted following the general procedure.^a The crude product was purified by flash chromatography on demetallated silica gel (CH₂Cl₂/AcOEt/acetone: 40/1/0.2) to isolate α-**SQ1D1/α-319** (CH₂Cl₂: 103 mg; HFIP: 186 mg).

Aspect: brown powder

Yield: CH₂Cl₂: 33%; HFIP: 58%

^aThe use of other solvents for the study of the Diels-Alder reaction of sulfinylquinone **318a** and cyclopentadiene (**151**) followed the same procedure with the same proportions and concentrations. The times, yields and ratios of the reactions are reported in Table 5.3 in Chapter 5.

TLC: $R_f \approx 0.61$ ($\text{CH}_2\text{Cl}_2/\text{AcOEt}/\text{acetone}$: 40/5/1), visualised by UV and *p*-anisaldehyde

m_p : 124-126 °C (degradation)

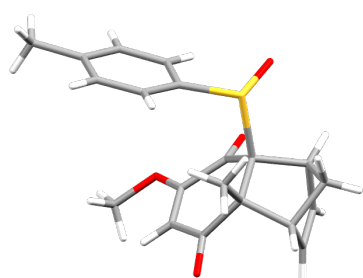
$[\alpha]_D^{20}$: -249.6° ($c = 1.0$; CHCl_3)

$^1\text{H NMR}$ (500 MHz, CDCl_3): δ (ppm) **7.50** (d, 2H, $J = 8.2$ Hz, $2 \times \text{C}^{13}\text{H}$), **7.27** (d, 2H, $J = 8.2$ Hz, $2 \times \text{C}^{14}\text{H}$), **6.24** (dd, 1H, $J = 5.5, 2.9$ Hz, C^2H or C^3H), **5.48** (s, 1H, C^8H), **4.07** (s (br), 1H, C^4H), **3.32** (s, 3H, C^{17}H_3), **3.24** (s (br), 1H, C^1H), **2.39** (s, 3H, C^{16}H_3), **1.98** (dd, 2H, AB, $J_{AB} = 10.0$ Hz, $\Delta\nu_{AB} = 286.2$ Hz, C^{11}H_2), **1.85** (s, 3H, C^{18}H_3)

$^{13}\text{C NMR}$ (126 MHz, CDCl_3): δ (ppm) **199.87** (C_q^9), **187.01** (C_q^6), **163.99** (C_q^7), **142.70** (C_q^{15}), **140.39** (C^2H or C^3H), **136.82** ($\text{C}_q^{12} + \text{C}^2\text{H}$ or C^3H), **129.79** ($2 \times \text{C}^{14}\text{H}$), **126.46** ($2 \times \text{C}^{13}\text{H}$), **111.58** (C^8H), **81.12** (C_q^5), **58.19** (C_q^{10}), **56.04** (C^{17}H_3), **54.47** (C^1H), **49.99** (C^4H), **43.47** (C^{11}H_2), **25.78** (C^{18}H_3), **21.56** (C^{16}H_3)

IR: $\bar{\nu}$ (cm^{-1}) 2923, 2853, 1661, 1604, 1443, 1362, 1244, 1187, 1075, 1056, 807

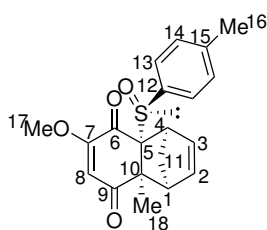
The experimental data were in agreement with those reported in the literature.⁴⁰



Orthorhombic	$P2_12_12_1$
$a = 7.9696(4)$ Å	$\alpha = 90^\circ$
$b = 10.2226(4)$ Å	$\beta = 90^\circ$
$c = 21.4477(8)$ Å	$\gamma = 90^\circ$
$V = 1747.34(13)$ Å ³	$Z = 4$
$R = 4.92\%$	$F = -0.01(4)$

Figure 8.33: X-ray structure of α -**SQ1D1**/ α -**319** and parameters of the crystal. Crystallisation by slow evaporation from dichloromethane.

(+)-(1*S*,4*R*,4*aR*,8*aS*)-6-Methoxy-8*a*-methyl-4*a*-((*S*)-*p*-tolylsulfinyl)-1,4,4*a*,8*a*-tetrahydro-1,4-methanonaphthalene-5,8-dione (β -SQ1D1**/ β -**319**)**



$\text{C}_{20}\text{H}_{20}\text{O}_4\text{S}$

$M_W = 356.44$ g mol⁻¹

The same procedure as α -**SQ1D1**/ α -**319** was followed to isolate β -**SQ1D1**/ β -**319** (CH_2Cl_2 : 189 mg; HFIP: 25 mg) in the second fraction.

Aspect: brown powder

Yield: CH_2Cl_2 : 60%; HFIP: 7.9%

TLC: $R_f \approx 0.37$ ($\text{CH}_2\text{Cl}_2/\text{AcOEt}/\text{acetone}$: 40/5/1), visualised by UV and *p*-anisaldehyde

m_p : 130-132 °C (degradation)

$[\alpha]_D^{20}$: $+525.1^\circ$ ($c = 1.0$; CHCl_3)

$^1\text{H NMR}$ (500 MHz, CDCl_3): δ (ppm) **7.43** (d, 2H, $J = 8.2$ Hz, $2 \times \text{C}^{13}\text{H}$), **7.39** (d, 2H, $J = 8.2$ Hz, $2 \times \text{C}^{14}\text{H}$), **6.26** (dd, 1H, $J = 5.5, 2.9$ Hz, C^2H or C^3H), **5.83** (s, 1H, C^8H), **5.80** (dd, 1H, $J = 5.5; 3.1$ Hz,

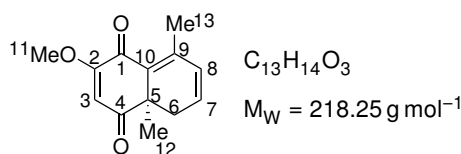
C^3H or C^2H), **3.77** (s, 3H, $C^{17}H_3$), **3.27** (s (br), 1H, C^1H), **2.87** (s (br), 1H, C^4H), **2.48** (s, 3H, $C^{16}H_3$), **2.17** (s, 3H, $C^{18}H_3$), **1.83** (dd, 2H, AB, $J_{AB} = 9.5$ Hz, $\Delta\nu_{AB} = 243.1$ Hz, $C^{11}H_2$)

^{13}C NMR (126 MHz, $CDCl_3$): δ (ppm) **200.76** (C_q^9), **190.62** (C_q^6), **164.91** (C_q^7), **143.59** (C_q^{15}), **141.15** (C^2H or C^3H), **136.66** (C_q^{12}), **135.67** (C^3H or C^2H), **129.59** ($2 \times C^{14}H$), **126.90** ($2 \times C^{13}H$), **112.00** (C^8H), **79.32** (C_q^5), **59.59** (C_q^{10}), **56.74** ($C^{17}H_3$), **53.30** (C^1H), **51.01** (C^4H), **43.40** ($C^{11}H_2$), **24.98** ($C^{18}H_3$), **21.87** ($C^{16}H_3$)

IR: $\bar{\nu}$ (cm^{-1}) 2922, 2852, 1691, 1655, 1611, 1448, 1364, 1239, 1181, 1162, 1081, 1034, 818, 734

The experimental data were in agreement with those reported in the literature.⁴⁰

(-)-(R)-2-Methoxy-4a,8-dimethyl-4a,5-dihydronaphthalene-1,4-dione (β -SQ1D2P1)



Quinone **SQ1** (HFIP: 187 mg, 0.645 mmol, 1.0 eq.) and diene **D2** (HFIP: 0.13 mL, 1.30 mmol, 2.0 eq.) were reacted following the general procedure. Once the reaction was over, the HFIP was removed *in vacuo* and replaced by the same volume of dichloromethane to let the adduct pyrolyse overnight. The solvent was evaporated and the crude product was purified by flash chromatography on demetallated silica gel (cyclohex./AcOEt: 9/1 to 8/2) to give β -**SQ1D2P1** (HFIP: 111 mg).

Aspect: yellow oil that crystallises in the fridge

Yield: 79%

TLC: $R_f \approx 0.31$ (cyclohex./AcOEt: 2/1), visualised by UV and $KMnO_4$

m_p: 129-131 °C

$[\alpha]_D^{20}$: -109.2° ($c = 0.40$; $CHCl_3$)

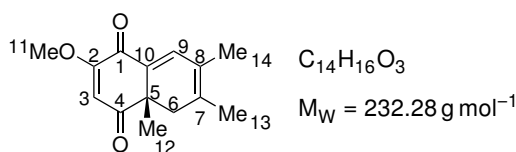
1H NMR (500 MHz, $CDCl_3$): δ (ppm) **6.28** (ddd, 1H, ABXY, $J_{XY} = 9.4$ Hz, $J_{AX} = 6.4$ Hz, $J_{BX} = 2.8$ Hz, C^7H), **6.10** (dd, 1H, ABXY, $J_{XY} = 9.4$ Hz, $J_{BY} = 2.8$ Hz, C^8H), **5.90** (s, 1H, C^3H), **3.83** (s, 3H, $C^{11}H_3$), **2.57** (dd + ddd, 2H, ABXY, $J_{AB} = 18.9$ Hz, $J_{AX} = 6.4$ Hz, $J_{BX} = J_{BY} = 2.8$ Hz, $\Delta\nu_{AB} = 92.8$ Hz, C^6H_2), **2.35** (s, 3H, $C^{13}H_3$), **1.26** (s, 3H, $C^{12}H_3$)

^{13}C NMR (126 MHz, $CDCl_3$): δ (ppm) **201.25** (C_q^4), **181.42** (C_q^1), **164.09** (C_q^2), **147.56** (C_q^9), **134.07** (C^8H), **131.16** (C^7H), **128.32** (C_q^{10}), **107.71** (C_q^3), **53.51** ($C^{11}H_3$), **45.51** (C_q^5), **32.48** (C^6H_2), **26.44** ($C^{12}H_3$), **22.28** ($C^{13}H_3$)

IR: $\bar{\nu}$ (cm^{-1}) 2968, 1655, 1605, 1529, 1453, 1356, 1240, 1219, 1167, 1025, 853

The experimental data were in agreement with those reported in the literature.⁴⁰

(±)-(S)-2-Methoxy-4a,6,7-trimethyl-4a,5-dihydro-naphthalene-1,4-dione (α -SQ1D3P1)



Quinone **SQ1** (HFIP: 198 mg, 0.682 mmol, 1.0 eq.) and diene **D3** (HFIP: 0.16 mL, 1.41 mmol, 2.1 eq.) were reacted following the general procedure. The crude was purified by flash chromatogra-

phy on demetallated silica gel (cyclohex./AcOEt: 9/1 to 8/2) to give α -**SQ1D3P1** (HFIP: 15 mg) in the first fraction.

Aspect: yellow oil

Yield: 9.7%

TLC: $R_f \approx 0.56$ (cyclohex./AcOEt: 5/5), visualised by UV and *p*-anisaldehyde

$[\alpha]_D^{20}$: +12.8° (c = 0.40; CHCl₃)

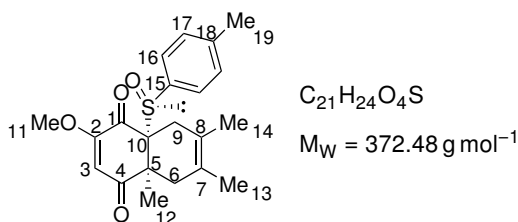
¹H NMR (500 MHz, CDCl₃): δ (ppm) **7.16** (s, 1H, C⁹H), **5.94** (s, 1H, C³H), **3.84** (s, 3H, C¹¹H₃), **2.56-2.43** (m, 2H, C⁶H₂), **1.92** (s (br), 3H, C¹³H₃), **1.89** (s (br), 3H, C¹⁴H₃), **1.21** (s, 3H, C¹²H₃)

¹³C NMR (126 MHz, CDCl₃): δ (ppm) **201.14** (C_q⁴), **179.79** (C_q¹), **163.67** (C_q²), **140.45** (C_q⁷ or C_q⁸), **138.82** (C⁹H), **131.49** (C_q¹⁰), **125.18** (C⁸H or C⁷H), **109.48** (C³H), **56.52** (C¹¹H₃), **44.78** (C_q⁵), **39.42** (C⁶H₂), **26.06** (C¹²H₃), **20.86** (C¹³H₃), **17.16** (C¹⁴H₃)

IR: $\bar{\nu}$ (cm⁻¹) 2925, 2854, 1664, 1597, 1549, 1453, 1365, 1238, 1213, 1166, 1097, 1022, 856

The experimental data were in agreement with those reported in the literature.⁴⁰

(-)-(4a*S*,8a*R*)-2-Methoxy-4a,6,7-trimethyl-8a-((*S*)-*p*-tolylsulfinyl)-4a,5,8,8a-tetrahydronaphthalene-1,4-dione (β -SQ1D3)



The same procedure as α -**SQ1D3P1** was followed to give β -**SQ1D3** (HFIP: 181 mg) in the second fraction.

Aspect: yellow solid

Yield: 71%

TLC: $R_f \approx 0.49$ (cyclohex./AcOEt: 5/5), visualised by UV and *p*-anisaldehyde

m_p: 125-126 °C

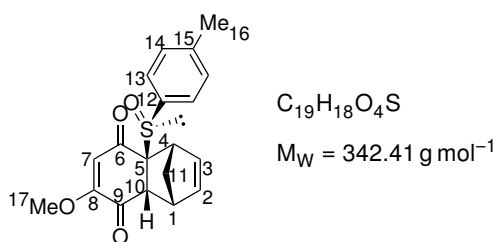
$[\alpha]_D^{20}$: -207.0° (c = 1.0; CH₂Cl₂)

¹H NMR (500 MHz, C₆D₆): δ (ppm) **7.21** (d, 2H, $J = 7.7$ Hz, 2 × C¹⁶H), **6.87** (d, 2H, $J = 7.7$ Hz, 2 × C¹⁷H), **6.10** (s, 1H, C³H), **2.97** (s, 3H, C¹¹H₃), **2.64** (d, 1H, $J = 17.4$ Hz, 1/2 × C⁹H₂), **2.20** (d, 1H, $J = 17.4$ Hz, 1/2 × C⁶H₂), **2.07** (d, 1H, $J = 17.4$ Hz, 1/2 × C⁹H₂), **1.89** (s, 3H, C¹⁹H₃), **1.82** (d, 1H, $J = 17.4$ Hz, 1/2 × C⁶H₂), **1.78** (s, 3H, C¹²H₃), **1.44** (s, 3H, C¹⁴H₃), **1.22** (s, 3H, C¹³H₃)

¹³C NMR (126 MHz, C₆D₆): δ (ppm) **197.42** (C_q⁴), **186.31** (C_q¹), **161.67** (C_q²), **142.50** (C_q¹⁸), **136.42** (C_q¹⁵), **129.94** (2 × C¹⁷H), **125.56** (2 × C¹⁶H), **122.81** (C_q⁷ or C_q⁸), **121.93** (C_q⁸ or C_q⁷), **113.32** (C³H), **79.11** (C_q¹⁰), **55.27** (C¹¹H₃), **49.77** (C_q⁵), **45.21** (C⁶H₂), **30.10** (C⁹H₂), **21.19** (C¹⁹H₃), **18.58** (C¹³H₃ or C¹⁴H₃), **18.50** (C¹⁴H₃ or C¹³H₃), **16.94** (C¹²H₃)

IR: $\bar{\nu}$ (cm⁻¹) 1668, 1605, 1453, 1360, 1242, 1195, 1045, 810

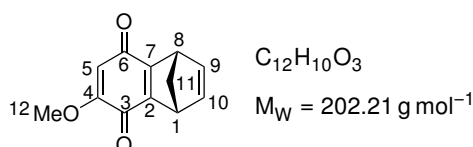
The experimental data were in agreement with those reported in the literature.⁴⁰

(1R,4S,4aS,8aR)-7-Methoxy-4a-(S)-p-tolylsulfinyl)-1,4,4a,8a-tetrahydro-1,4-methanonaphthalene-5,8-dione (α -SQ3D1)

Quinone **SQ3** (HFIP: 66 mg, 0.238 mmol, 1.0 eq.) and diene **D1** (HFIP: 0.04 mL, 0.476 mmol, 2.0 eq.) were reacted following the general procedure to give the crude product α -**SQ3D1**.

TLC: $R_f \approx 0.68$ (PhMe/AcOEt: 8/2), visualised by UV and *p*-anisaldehyde

1H NMR (500 MHz, $CDCl_3$): δ (ppm) **7.35** (2H, d, $J = 8.4$ Hz, $2 \times C^{13}H$ or $2 \times C^{14}H$), **7.20** (2H, d, $J = 8.4$ Hz, $2 \times C^{14}H$ or $2 \times C^{13}H$), **6.24** (dd, 1H, $J = 5.5, 3.0$ Hz, C^2H or C^3H), **6.18** (dd, 1H, $J = 5.5, 2.8$ Hz, C^3H or C^2H), **5.33** (s, 1H, C^7H), **3.84-3.81** (m, 1H, C^1H or C^4H), **3.75** (s, 1H, $C^{10}H$), **3.56-3.53** (m, 1H, C^4H or C^1H), **3.39** (s, 3H, $C^{17}H_3$), **2.34** (s, 3H, $C^{16}H_3$), **2.30-2.27** (m, 1H, $1/2 \times C^{11}H_2$), **1.51-1.40** (m, 1H, $1/2 \times C^{11}H_2$)

(+)-(1S,4R)-6-Methoxy-1,4-dihydro-1,4-methanonaphthalene-5,8-dione (α -SQ3D1P2)

HFIP was removed *in vacuo* and replaced by the same volume of dichloromethane and the adduct α -**SQ3D1** was allowed to pyrolyse overnight. The crude product was purified by flash chromatography on demetallated silica gel (cyclohex./AcOEt: 9/1) to give α -**SQ3D1P2** (22 mg).

Aspect: pale yellow powder

Yield: 46%

TLC: $R_f \approx 0.12$ (cyclohex./AcOEt: 6/4), visualised by UV and $KMnO_4$

m_p : 110-113 °C (degradation)

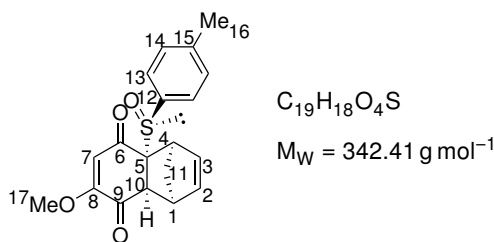
$[\alpha]_D^{20}$: +3.1 ° (c = 0.50; $CHCl_3$)

1H NMR (500 MHz, $CDCl_3$): δ (ppm) **6.89-6.85** (m, 1H, C^9H), **6.85-6.80** (m, 1H, $C^{10}H$), **5.69** (s, 1H, C^5H), **4.11** (s (br), 1H, C^8H), **4.08** (s (br), 1H, C^1H), **3.78** (s, 3H, $C^{12}H_3$), **2.36-2.21** (m, 2H, $C^{11}H_2$)

^{13}C NMR (126 MHz, $CDCl_3$): δ (ppm) **184.26** (C_q^3), **178.31** (C_q^6), **162.61** (C_q^7), **159.31** (C_q^4), **158.37** (C_q^2), **142.74** (C^9H or $C^{10}H$), **142.53** ($C^{10}H$ or C^9H), **106.03** (C^5H), **73.83** ($C^{11}H_2$), **56.67** ($C^{12}H_2$), **48.65** (C^1H), **48.34** (C^8H)

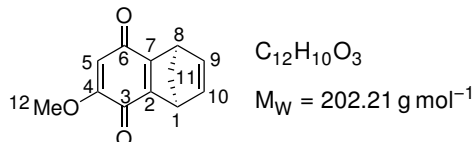
IR: $\bar{\nu}$ (cm^{-1}) 2924, 1717, 1666, 1636, 1582, 1217, 1010, 808

HRMS (ESI+): for $[M+H]^+$ calc.: 203.0708, found: 203.0703

(1*S*,4*R*,4*aR*,8*aS*)-7-Methoxy-4*a*-(*S*)-*p*-tolylsulfinyl)-1,4,4*a*,8*a*-tetrahydro-1,4-methanonaphthalene-5,8-dione (β -SQ3D1)

Quinone **SQ3** (CH_2Cl_2 : 154 mg, 0.558 mmol, 1.0 eq.) and diene **D1** (CH_2Cl_2 : 0.10 mL, 1.19 mmol, 2.1 eq.) were reacted following the general procedure to give the crude product β -**SQ3D1**.

TLC: $R_f \approx 0.27$ (CH_2Cl_2 /cyclohex./AcOEt/acetone: 3/7/0.2), visualised by UV and *p*-anisaldehyde
 1H NMR (500 MHz, $CDCl_3$): δ (ppm) **7.35** (2H, d, $J = 8.4$ Hz, $2 \times C^{13}H$ or $2 \times C^{14}H$), **7.20** (2H, d, $J = 8.4$ Hz, $2 \times C^{14}H$ or $2 \times C^{13}H$), **6.23** (dd, 1H, $J = 5.3, 3.1$ Hz, C^2H or C^3H), **6.17** (dd, 1H, $J = 5.3, 3.2$ Hz, C^3H or C^2H), **5.33** (s, 1H, C^7H), **3.84-3.82** (m, 1H, C^1H or C^4H), **3.77** (s, 1H, $C^{10}H$), **3.56-3.53** (m, 1H, C^4H or C^1H), **3.38** (s, 3H, $C^{17}H_3$), **2.33** (s, 3H, $C^{16}H_3$), **2.32-2.29** (m, 1H, $1/2 \times C^{11}H_2$), **1.49-1.45** (m, 1H, $1/2 \times C^{11}H_2$)

(-)-(1*S*,4*R*)-6-Methoxy-1,4-dihydro-1,4-methanonaphthalene-5,8-dione (β -SQ3D1P2)

Once the cycloaddition was over, the adduct β -**SQ3D1** was allowed to pyrolyse overnight. The crude product was purified by flash chromatography on demetallated silica gel (cyclohex./AcOEt: 9/1) to give β -**SQ3D1P2** (41 mg).

Aspect: pale yellow powder

Yield: 36%

TLC: $R_f \approx 0.12$ (cyclohex./AcOEt: 6/4), visualised by UV and $KMnO_4$

m_p : 110-113 °C (degradation)

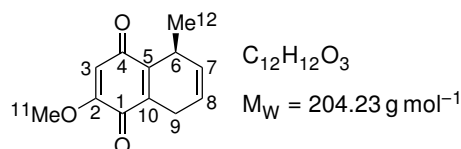
$[\alpha]_D^{20}$: -3.0° ($c = 0.50$; $CHCl_3$)

1H NMR (500 MHz, $CDCl_3$): δ (ppm) **6.89-6.85** (m, 1H, C^9H), **6.85-6.80** (m, 1H, $C^{10}H$), **5.69** (s, 1H, C^5H), **4.11** (s (br), 1H, C^8H), **4.08** (s (br), 1H, C^1H), **3.78** (s, 3H, $C^{12}H_3$), **2.36-2.21** (m, 2H, $C^{11}H_2$)

^{13}C NMR (126 MHz, $CDCl_3$): δ (ppm) **184.26** (C_q^3), **178.31** (C_q^6), **162.61** (C_q^7), **159.31** (C_q^4), **158.37** (C_q^2), **142.74** (C^9H or $C^{10}H$), **142.53** ($C^{10}H$ or C^9H), **106.03** (C^5H), **73.83** ($C^{11}H_2$), **56.67** ($C^{12}H_2$), **48.65** (C^1H), **48.34** (C^8H)

IR: $\bar{\nu}$ (cm^{-1}) 2924, 1717, 1666, 1636, 1582, 1217, 1010, 808

HRMS (ESI+): for $[M+H]^+$ calc.: 203.0708, found: 203.0712

(±)-(5S)-2-Methoxy-5-methyl-5,8-dihydronaphthalene-1,4-dione (β-SQ3D2P2)

Quinone **SQ3** (CH₂Cl₂: 84 mg, 0.304 mmol, 1.0 eq.; HFIP: 90 mg, 0.326 mmol, 1.0 eq.) and diene **D2** (CH₂Cl₂: 0.06 mL, 0.602 mmol, 2.0 eq.; HFIP: 0.06 mL, 0.602 mmol, 1.8 eq.) were reacted following the general procedure. The crude product was purified by flash chromatography on demetallated silica gel (cyclohex./AcOEt: 95/5) to give **SQ3D2P2** (CH₂Cl₂: 33 mg; HFIP: 42 mg).

Aspect: orange powder

Yield: CH₂Cl₂: 53%; HFIP: 63%

TLC: R_f ≈ 0.57 (cyclohex./AcOEt: 7/3), visualised by UV and KMnO₄

m_p: 84–87 °C (degradation)

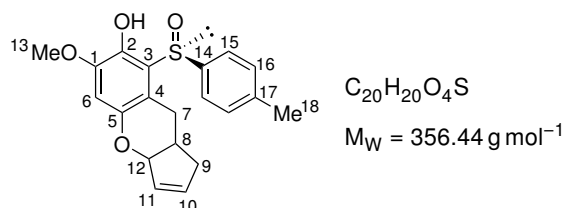
[α]_D²⁰ (c = 0.50, CHCl₃): +100.9° from CH₂Cl₂; +85.1° from HFIP

¹H NMR (500 MHz, CDCl₃): δ (ppm) **5.88** (s, 1H, C³H), **5.83–5.72** (m, 2H, C⁷H + C⁸H), **3.80** (s, 3H, C¹¹H₃), **3.43** (qdd, 1H, J = 7.0; 3.7; 1.3 Hz, C⁶H), **3.21–2.89** (m, 2H, C⁹H₂), **1.18** (d, 3H, J = 7.0 Hz, C¹²H₃)

¹³C NMR (126 MHz, CDCl₃): δ (ppm) **186.84** (C_q¹ or C_q⁴), **182.14** (C_q⁴ or C_q¹), **158.45** (C_q²), **144.76** (C_q⁵), **137.47** (C_q¹⁰), **130.02** (C⁷H), **121.29** (C⁸H), **107.63** (C³H), **56.26** (C¹¹H₃), **29.13** (C⁶H), **24.07** (C⁹H₂), **22.29** (C¹²H₃)

IR: ν̄ (cm⁻¹) 2931, 1737, 1667, 1634, 1602, 1456, 1444, 1352, 1301, 1218, 1178, 1138, 1059, 1046, 1018, 976, 942, 870, 850, 716

HRMS (ESI⁺): for [M+H]⁺ calc.: 205.0865, found: 205.0860

8.6.2 Solvent study: unexpected products**6-Methoxy-8-((S)-p-tolylsulfinyl)-1,3a,9,9a-tetrahydrocyclopenta[*b*]chromen-7-ol (501)**

This compounds was prepared following the general procedure with cyclopentadiene (**151**). For the times, yields and ratios of the reaction, see Table 5.3 in Chapter 5. In the case of DMSO and DMF, at the end of the reaction, the solution was diluted with 20 mmol of dichloromethane per mmol of sulfinylquinone **318a**. The organic phase was washed several times with water and then dried over MgSO₄. The solvent was then evaporated and the crude mixture was purified by flash chromatography on demetallated silica gel (CH₂Cl₂/AcOEt/acetone: 40/1/0.2). The product was obtained as an inseparable mixture of two diastereoisomers and the analyses were done with on mixture.

Aspect: orange oil

TLC: $R_f \approx 0.71$ ($\text{CH}_2\text{Cl}_2/\text{AcOEt}$: 8/2), visualised by UV and *p*-anisaldehyde

IR: $\bar{\nu}$ (cm^{-1}) 1594, 1441, 1265, 1121, 1017, 988, 809, 729

HRMS (ESI+): for $[\text{M}+\text{H}]^+$ calc.: 357.1161, found: 357.1168

Product 501a

^1H NMR (400 MHz, CDCl_3): δ (ppm) **7.58** (d, 2H, $J = 7.6$ Hz, $2 \times \text{C}^{15}\text{H}$), **7.27** (d, 2H, $J = 7.6$ Hz, $2 \times \text{C}^{16}\text{H}$), **6.54** (s, 1H, C^6H), **5.90** (dd, 1H, $J = 6.0$; 2.0 Hz, C^{10}H or C^{11}H), **5.78** **5.90** (dd, 1H, $J = 6.0$; 2.0 Hz, C^{10}H or C^{11}H), **5.18** (d, 1H, $J = 8.4$ Hz, C^{12}H), **3.80** (s, 3H, C^{13}H_3), **2.91** (dd, 1H, $J = 9.6$; 4.4 Hz, $\frac{1}{2} \times \text{C}^7\text{H}_2$), **2.80** (m, 1H, C^8H), **2.59** (dd, 1H, $J = 14.4$, 5.6 Hz, $\frac{1}{2} \times \text{C}^9\text{H}_2$), **2.34** (s, 3H, C^{18}H_3), **2.13** **2.13** (m, 1H, $\frac{1}{2} \times \text{C}^7\text{H}_2$), **1.86** (m, 1H, $\frac{1}{2} \times \text{C}^9\text{H}_2$)

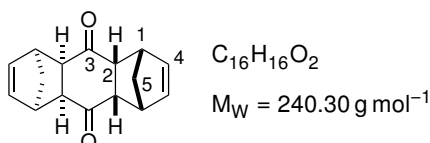
^{13}C NMR (100 MHz, CDCl_3): δ (ppm) **148.09** (C_q^5), **147.81** (C_q^1), **144.58** (C_q^2), **142.47** (C_q^{17}), **140.17** (C_q^{14}), **136.92** ($\text{C}^{10}\text{H} + \text{C}^{11}\text{H}$), **130.36** ($2 \times \text{C}^{16}\text{H}$), **125.66** ($2 \times \text{C}^{15}\text{H}$), **120.93** (C_q^3), **115.40** (C_q^4), **106.37** (C^6H), **82.25** (C^{12}H), **56.17** ($\text{C}^{56,17}\text{H}_{13}$), **38.69** (C^9H_2), **36.30** (C^8H), **24.91** (C^7H_2), **21.14** (C^{18}H_3)

Product 501b

^1H NMR (400 MHz, CDCl_3): δ (ppm) **7.59** (d, 2H, $J = 8.2$ Hz, $2 \times \text{C}^{15}\text{H}$), **7.28** (d, 2H, $J = 8.2$ Hz, $2 \times \text{C}^{16}\text{H}$), **6.59** (s, 1H, C^6H), **5.90** (dd, 1H, $J = 6.4$; 3.2 Hz, C^{10}H), **5.78** (dd, 1H, $J = 6.0$; 3.0 Hz, C^{11}H), **5.11** (d, 1H, $J = 7.6$ Hz, C^{12}H), **3.82** (s, 3H, C^{13}H_3), **2.96** (dd, 1H, $J = 14.8$; 6.4 Hz, $\frac{1}{2} \times \text{C}^7\text{H}_2$), **2.77** (m, 1H, C^8H), **2.48** (dd, 1H, $J = 18.0$; 9.2 Hz, $\frac{1}{2} \times \text{C}^9\text{H}_2$), **2.38** (s, 3H, C^{18}H_3), **2.25** (dd, 1H, $J = 14.4$; 8.0 Hz, C^7H_2), **1.86** (m, 1H, $\frac{1}{2} \times \text{C}^9\text{H}_2$)

^{13}C NMR (100 MHz, CDCl_3): δ (ppm) **148.40** (C_q^5), **144.46** (C_q^1), **144.46** (C_q^2), **142.69** (C_q^{17}), **140.17** (C_q^{14}), **135.44** ($\text{C}^{10}\text{H} + \text{C}^{11}\text{H}$), **130.36** ($2 \times \text{C}^{16}\text{H}$), **126.10** ($2 \times \text{C}^{15}\text{H}$), **120.17** (C_q^3), **116.05** (C_q^4), **105.84** (C^6H), **85.41** (C^{12}H), **56.21** (C^{13}H_3), **36.70** (C^8H), **25.44** (C^7H_2), **21.55** (C^{18}H_3)

(1*R*,4*S*,4*aR*,5*S*,8*R*,8*aS*,9*aS*,10*aR*)-1,4,4*a*,5,8,8*a*,9*a*,10*a*-Octahydro-1,4:5,8-dimethanoanthracene-9,10-dione (153**)**



Quinone **Q1** (HFIP: 57 mg, 0.525 mmol, 1.0 eq.) and diene **D1** (HFIP: 0.09 mL, 1.07 mmol, 2.0 eq.) were reacted following general procedure to give **153** (HFIP: 118 mg).

Aspect: white powder

Yield: 93%

TLC: $R_f \approx 0.33$ (cHex/AcOEt: 8/2), visualised by UV and *p*-anisaldehyde

m_p : 156-158 °C (degradation)

^1H NMR (500 MHz, CDCl_3): δ (ppm) **6.18** (dd, 4H, ABXYZ, $J_{AX} = J_{XY} = 1.8$ Hz, $4 \times \text{C}^4\text{H}$), **3.35-3.32** (m, ABXYZ, 4H, $4 \times \text{C}^1\text{H}$), **2.88-2.83** (m, ABXYZ, 4H, $4 \times \text{C}^2\text{H}$), **1.39** (dddd, 4H, ABXYZ, $J_{AX} = J_{AY} = 1.8$ Hz, $J_{BY} = J_{BZ} = 1.4$ Hz, $J_{AB} = 8.6$ Hz, $\Delta\nu_{AB} = 84.6$ Hz, $2 \times \text{C}^5\text{H}_2$)

^{13}C NMR (126 MHz, CDCl_3): δ (ppm) **212.85** ($2 \times \text{C}_q^3$), **136.49** ($4 \times \text{C}^4\text{H}$), **53.34** ($4 \times \text{C}^2\text{H}$), **49.71** ($2 \times \text{C}^5\text{H}_2$), **48.37** ($4 \times \text{C}^1\text{H}$)

IR: $\bar{\nu}$ (cm⁻¹) 1684, 1304, 1244, 1194, 1032, 807, 707, 517

The experimental data were in agreement with those reported in the literature.⁶⁹

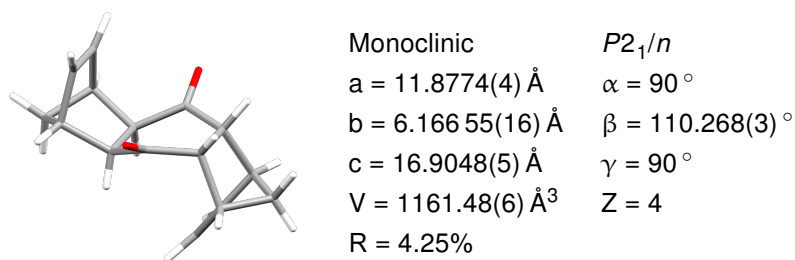
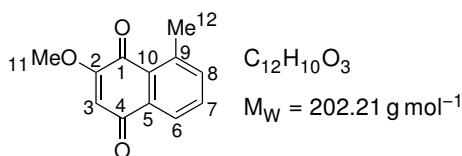


Figure 8.34: X-ray structure of **153** and parameters of the crystal. Recrystallisation from boiling hexane.

2-Methoxy-8-methylnaphthalene-1,4-dione (**503**)



Quinone **Q5** (CH₂Cl₂: 116 mg, 0.535 mmol, 1.0 eq.; HFIP: 50 mg, 0.229 mmol, 1.0 eq.) and diene **D2** (CH₂Cl₂: 0.11 mL, 1.10 mmol, 2.1 eq.; HFIP: 0.05 mL, 0.501 mmol, 2.2 eq.) were reacted following the general procedure. Once the cycloaddition was over (remove HFIP *in vacuo* and replace it by the same volume of dichloromethane), Et₃N (CH₂Cl₂: 0.15 mL, 1.08 mmol, 2.0 eq.; HFIP: 0.07 mL, 0.504 mmol, 2.3 eq.) was added to the solution and the mixture was stirred overnight at room temperature. The solution was washed with a saturated solution of NH₄Cl and brine, successively, and dried over Na₂SO₄. The solution was filtered and the solvent evaporated. The crude product was purified by filtration over silica gel (eluent: CH₂Cl₂) to give **503** (CH₂Cl₂: 80 mg; HFIP: 33 mg).

Aspect: pale yellow powder

Yield: CH₂Cl₂: 74%; HFIP: 71%

TLC: R_f ≈ 0.54 (cyclohex./AcOEt: 7/3), visualised by UV and KMnO₄

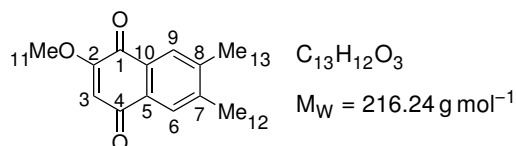
m_p: 133-135 °C

¹H NMR (500 MHz, CDCl₃): δ (ppm) **8.04-7.98** (m, 1H, C⁶H), **7.58** (dd, 1H, $J = 7.7; 7.6$ Hz, C⁷H), **7.50-7.47** (m, 1H, C⁸H), **6.12** (s, 1H, C³H), **3.89** (s, 3H, C¹¹H₃), **2.75** (s, 3H, C¹²H₃)

¹³C NMR (126 MHz, CDCl₃): δ (ppm) **185.21** (C_q⁴), **181.68** (C_q¹), **160.99** (C_q²), **142.01** (C_q⁹), **137.45** (C⁸H), **133.67** (C_q⁵), **133.54** (C⁷H), **128.79** (C_q¹⁰), **125.16** (C⁶H), **108.62** (C³H), **56.56** (C¹¹H₃), **23.00** (C¹²H₃)

IR: $\bar{\nu}$ (cm⁻¹) 2930, 1732, 1675, 1646, 1613, 1586, 1461, 1439, 1422, 1377, 1359, 1339, 1302, 1277, 1251, 1213, 1195, 1170, 1153, 1111, 1089, 1033, 1006, 867, 817, 795, 777, 731, 715, 702, 692

The experimental data were in agreement with literature.⁷⁰

2-Methoxy-6,7-dimethylnaphthalene-1,4-dione (504)

From quinone Q5 : Quinone **Q5** (CH_2Cl_2 : 102 mg, 0.470 mmol, 1.0 eq.; HFIP: 62 mg, 0.288 mmol, 1.0 eq.) and diene **D3** (CH_2Cl_2 : 0.11 mL, 0.972 mmol, 2.1 eq.; HFIP: 0.07 mL, 0.619 mmol, 2.1 eq.) were reacted following the general procedure. Once the cycloaddition was over (HFIP was removed *in vacuo* and replaced by the same volume of dichloromethane), Et_3N (CH_2Cl_2 : 0.13 mL, 0.935 mmol, 2.0 eq.; HFIP: 0.08 mL, 0.576 mmol, 2.0 eq.) was added and the reaction mixture was stirred overnight at room temperature. The solution was washed with a saturated solution of NH_4Cl and brine, successively, and dried over Na_2SO_4 . The solution was filtered and the solvent evaporated. The crude product was purified by filtration over silica gel (eluent: CH_2Cl_2) to give **504** (CH_2Cl_2 : 76 mg; HFIP: 45 mg).

From quinone SQ3 : Quinone **SQ3** (CH_2Cl_2 : 91 mg, 0.328 mmol, 1.0 eq.; HFIP: 90 mg, 0.326 mmol, 1.0 eq.) and diene **D3** (CH_2Cl_2 : 0.07 mL, 0.619 mmol, 1.9 eq.; HFIP: 0.07 mL, 0.619 mmol, 1.9 eq.) were reacted following the general procedure. The crude product was purified by flash chromatography on demetallated silica gel (cyclohex./AcOEt: 9/1) to give **504** (CH_2Cl_2 : 38 mg; HFIP: 39 mg).

Aspect: pale yellow powder

Yield: CH_2Cl_2 : 75%; HFIP: 72% (from quinone **Q5**)

Yield: CH_2Cl_2 : 53%; HFIP: 56% (from quinone **SQ3**)

TLC: $R_f \approx 0.38$ (cyclohex./AcOEt: 7/3), visualised by UV and $KMnO_4$

m_p : 168-169 °C

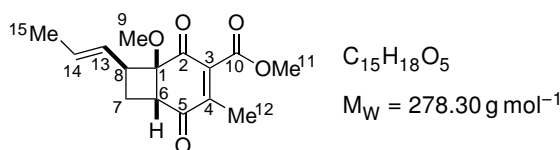
1H NMR (500 MHz, $CDCl_3$): δ (ppm) **7.88** (s, 1H, C^6H), **7.82** (s, 1H, C^9H), **6.10** (s, 1H, C^3H), **3.89** (s, 3H, $C^{11}H_3$), **2.39(3)** (s, 3H, $C^{13}H_3$), **2.38(6)** (s, 3H, $C^{12}H_3$)

^{13}C NMR (126 MHz, $CDCl_3$): δ (ppm) **185.45** (C_q^1), **180.49** (C_q^4), **160.53** (C_q^2), **144.51** (C_q^7), **143.22** (C_q^8), **130.16** (C_q^5), **129.14** (C_q^{11}), **127.92** (C^6H), **127.42** (C^9H), **56.50** ($C^{11}H_3$), **20.44** ($C^{13}H_3$), **20.20** ($C^{12}H_3$)

IR: $\bar{\nu}$ (cm^{-1}) 2948, 1685, 1651, 1598, 1566, 1451, 1359, 1325, 1302, 1250, 1195, 1184, 1154, 1077, 1013, 996, 872, 803, 741

The experimental data were in agreement with those reported in the literature.⁷¹

Methyl (\pm)-*rel*-(1*R*,6*R*,8*S*)-1-methoxy-4-methyl-2,5-dioxo-8-((*E*)-prop-1-en-1-yl)bicyclo[4.2.0]oct-3-ene-3-carboxylate (505)



Quinone **Q8** (CH_2Cl_2 : 80 mg, 0.381 mmol, 1.0 eq.) and diene **D2** (CH_2Cl_2 : 0.08 mL, 0.802 mmol, 2.1 eq.) were reacted following the general procedure. After fifteen days, the solvent was evaporated and the crude mixture was purified by flash chromatography on silica gel (cHex/AcOEt: 9/1) to give 53 mg of the title compound **505**.

Aspect: yellow oil

Yield: 50%

TLC: $R_f \approx 0.54$ (cHex/AcOEt: 7/3), visualised by UV and *p*-anisaldehyde

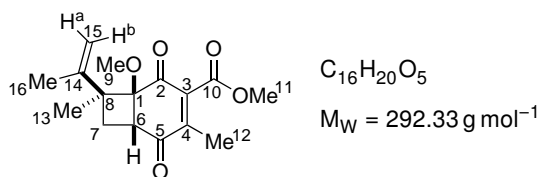
1H NMR (500 MHz, $CDCl_3$): δ (ppm) **5.74-5.53** (m, 2H, $C^{13}H$ + $C^{14}H$), **3.91** (s, 3H, $C^{11}H_3$), **3.40** (dd, 1H, $J = 10.9$; 6.5 Hz, C^6H), **3.21** (s, 3H, C^9H_3), **3.21-3.17** (m, 1H, C^8H), **2.39** (td, 1H, $J = 11.6$; 6.1 hertz, $1/2 \times C^7H_2$), **2.16** (ddd, 1H, $J = 11.6$; 8.6, 6.5 Hz), **2.04** (s, 3H, $C^{12}H_3$), **1.71** (d, 3H, $J = 5.2$ Hz, $C^{15}H_3$)

^{13}C NMR (126 MHz, $CDCl_3$): δ (ppm) **197.74** (C_q^5), **193.13** (C_q^2), **165.02** (C_q^{10}), **147.24** (C_q^4), **142.11** (C_q^3), **129.76** ($C^{14}H$), **126.61** ($C^{13}H$), **81.80** (C_q^1), **52.97** (C^9H_3 or $C^{11}H_3$), **52.95** (C^9H_3 or $C^{11}H_3$), **46.36** (C^6H), **44.00** (C^8H), **27.88** (C^7H_2), **18.32** ($C^{15}H_3$), **14.43** ($C^{12}H_3$)

IR: $\bar{\nu}$ (cm^{-1}) 2955, 2855, 1739, 1679, 1436, 1240, 1058, 964

HRMS (ESI⁺): for $[M+Na]^+$ calc.: 301.1046, found: 301.1033

Methyl (\pm)-*rel*-(1*R*,6*S*,8*R*)-1-methoxy-4,8-dimethyl-2,5-dioxo-8-(prop-1-en-2-yl)bicyclo[4.2.0]oct-3-ene-3-carboxylate (506)



Quinone **Q8** (CH_2Cl_2 : 76 mg, 0.362 mmol, 1.0 eq.) and diene **D3** (CH_2Cl_2 : 0.08 mL, 0.707 mmol, 2.0 eq.) were reacted following the general method. After fifteen days, the solvent was evaporated and the crude mixture was purified by flash chromatography on silica gel (cHex/AcOEt: 9/1) to give 25 mg of the title compound **506**.

Aspect: yellow oil

Yield: 24%

TLC: $R_f \approx 0.62$ (cHex/AcOEt: 7/3), visualised by UV and *p*-anisaldehyde

1H NMR (500 MHz, $CDCl_3$): δ (ppm) **4.96** (s, 1H, $C^{15}H^a$), **4.79** (s, 1H, $C^{15}H^b$), **3.92** (s, 3H, $C^{11}H_3$), **3.24** (dd, 1H, $J = 11.1$; 5.1 Hz, C^6H), **3.16** (s, 3H, C^9H_3), **2.96** (t, 1H, $J = 11.6$ Hz, $1/2 \times C^7H_2$), **2.07** (s, 3H, $C^{12}H_3$), **2.06-2.03** (m, 1H, $1/2 \times C^7H_2$), **1.82** (s, 3H, $C^{16}H_3$), **1.14** (s, 3H, $C^{13}H_3$)

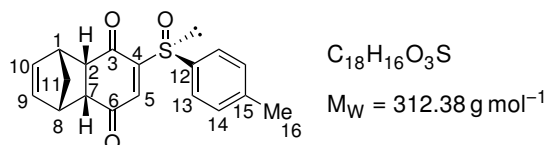
^{13}C NMR (126 MHz, $CDCl_3$): δ (ppm) **199.19** (C_q^5), **193.80** (C_q^2), **165.04** (C_q^{10}), **147.74** (C_q^3 or C_q^4 or C_q^{14}), **147.66** (C_q^3 or C_q^4 or C_q^{14}), **143.97** (C_q^3 or C_q^4), **110.99** ($C^{15}H_2$), **85.90** (C_q^1), **52.97** (C_q^9 or C_q^{11})

C_q^{11}), **52.76** (C_q^9 or C_q^{11}), **51.37** (C_q^8), **43.90** (C^6H), **34.09** (C^7H_2), **24.32** ($C^{13}H_3$), **20.46** ($C^{16}H_3$), **14.63** ($C^{12}H_3$)

IR: $\bar{\nu}$ (cm^{-1}) 2926, 2854, 1743, 1681, 1437, 1378, 1260, 1234, 1061, 964, 892

HRMS (ESI+): for $[M+Na]^+$ calc.: 315.1203, found: 315.1189

(+)-(1*S*,4*R*,4*aS*,8*aR*)-6-((*S*)-*p*-Tolylsulfinyl)-1,4,4*a*,8*a*-tetrahydro-1,4-methanonaphthalene-5,8-dione (α -306)



Quinone **SQ2** (CH_2Cl_2 : 151 mg, 0.611 mmol, 1.0 eq.; HFIP: 158 mg, 0.640 mmol, 1.0 eq.) and diene **D1** (CH_2Cl_2 : 0.06 mL, 0.713 mmol, 1.2 eq.; HFIP: 0.06 mL, 0.713 mmol, 1.1 eq.) were reacted following the general procedure. The crude product was purified by flash chromatography on demetallated silica gel (CH_2Cl_2 /acetone: 100/0 to 100/5) to give α -**306** (CH_2Cl_2 : 116 mg; HFIP: 120 mg) in the second fraction.

Aspect: yellow oil

Yield: CH_2Cl_2 : 61%; HFIP: 60%

TLC: $R_f \approx 0.48$ (CH_2Cl_2 /acetone: 10/1), visualised by UV and *p*-anisaldehyde

$[\alpha]_D^{20}$: +273.2° ($c = 1.0$; CHCl_3)

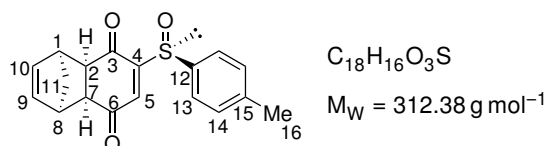
$^1\text{H NMR}$ (500 MHz, CDCl_3): δ (ppm) **7.53** (d, 2H, $J = 8.7 \text{ Hz}$, $2 \times C^{13}H$), **7.27** (d, 2H, $J = 8.7 \text{ Hz}$, $2 \times C^{14}H$), **7.16** (s, 1H, C^5H), **5.83** (dd, 1H, $J = 6.2$; 3.1 Hz , C^9H), **4.81** (dd, 1H, $J = 6.2$; 2.7 Hz , $C^{10}H$), **3.47** (s (br), 1H, C^8H), **3.28-3.18** (m, 3H, $C^1H + C^2H + C^7H$), **2.38** (s, 3H, $C^{16}H_3$), **1.49-1.23** (m, 2H, $C^{11}H_2$)

$^{13}\text{C NMR}$ (126 MHz, CDCl_3): δ (ppm) **196.74** (C_q^3 or C_q^6), **196.16** (C_q^6 or C_q^3), **161.16** (C_q^4), **142.81** (C_q^{15}), **139.07** (C_q^{12}), **136.58** (C^5), **135.34** (C^9H), **134.13** ($C^{10}H$), **130.00** ($2 \times C^{14}H$), **126.10** ($2 \times C^{13}H$), **50.26** (C^1H or C^2H or C^7H or C^8H), **49.85** (C^1H or C^2H or C^7H or C^8H), **49.74** (C^1H or C^2H or C^7H or C^8H), **49.68** (C^1H or C^2H or C^7H or C^8H), **49.42** ($C^{11}H_2$), **21.60** ($C^{16}H_3$)

IR: $\bar{\nu}$ (cm^{-1}) 2921, 2869, 1667, 1335, 1244, 1081, 1047, 917, 810, 723

The experimental data were in agreement with those reported in the literature.⁷²

(+)-(1*R*,4*S*,4*aR*,8*aS*)-6-((*S*)-*p*-Tolylsulfinyl)-1,4,4*a*,8*a*-tetrahydro-1,4-methanonaphthalene-5,8-dione (β -306)



The same procedure as α -**306** was followed to give β -**306** (CH_2Cl_2 : 54 mg; HFIP: 36 mg) in the first fraction.

Aspect: yellow solid

Yield: CH_2Cl_2 : 28%; HFIP: 18%

TLC: $R_f \approx 0.61$ (CH_2Cl_2 /acetone: 10/1), visualised by UV and *p*-anisaldehyde

m_p : 160-162 °C

$[\alpha]_D^{20}$: +471.6° (c = 1.0; CHCl₃)

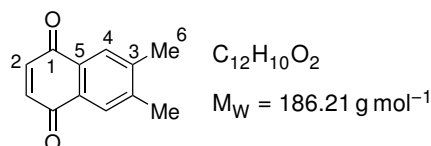
¹H NMR (500 MHz, CDCl₃): δ (ppm) **7.60** (d, *J* = 8.3 Hz, 2 × C¹³H), **7.27** (d, *J* = 8.3 Hz, 2 × C¹⁴H), **7.21** (s, 1H, C⁵H), **6.19-6.14** (m, 2H, C⁹H + C¹⁰H), **3.59-3.48** (m, 2H, C¹H + C⁸H), **3.17** (ddd, 2H, ABXY, *J*_{AB} = 8.5 Hz, *J*_{AX} = *J*_{BY} = 4.0 Hz, Δ*v*_{AB} = 49.0 Hz, C²H + C⁷H), **2.38** (s, 3H, C¹⁶H₃), **1.63-1.42** (m, 2H, C¹¹H₂)

¹³C NMR (126 MHz, CDCl₃): δ (ppm) **196.94** (C_q³ or C_q⁶), **196.03** (C_q⁶ or C_q³), **160.95** (C_q⁴), **142.85** (C_q¹⁵), **142.65** (C_q¹²), **137.29** (C⁵H), **135.83** (C⁹H or C¹⁰H), **135.43** (C¹⁰H or C⁹H), **130.28** (2 × C¹⁴H), **125.92** (2 × C¹³H), **50.45** (C²H or C⁷H), **49.65** (C⁷H or C²H), **49.07** (C¹¹H₂), **48.87** (C¹H or C⁸H), **48.86** (C⁸H or C¹H), **21.67** (C¹⁶H₃)

IR: $\bar{\nu}$ (cm⁻¹) 2922, 2854, 1666, 1602, 1490, 1245, 1078, 1059, 804, 771, 715

The experimental data were in agreement with those reported in the literature.⁷²

6,7-Dimethylnaphthalene-1,4-dione (305)



Quinone **SQ2** (CH₂Cl₂: 100 mg, 0.406 mmol, 1.0 eq.; HFIP: 152 mg, 0.615 mmol, 1.0 eq.) and diene **D3** (CH₂Cl₂: 0.05 mL, 0.442 mmol, 1.1 eq.; HFIP: 0.07 mL, 0.619 mmol, 1.0 eq.) were reacted following the general procedure. In the case of HFIP, the solvent was evaporated *in vacuo* after the completion of the cycloaddition and replaced by the same volume of dichloromethane and the adduct was allowed to pyrolyse overnight. The crude product was purified by flash chromatography on demetallated silica gel (cyclohex./CH₂Cl₂: 7/3) to give **305** (CH₂Cl₂: 8 mg; HFIP: 17 mg).

Aspect: brown powder

Yield: CH₂Cl₂: 11%; HFIP: 15%

TLC: R_f ≈ 0.54 (cyclohex./CH₂Cl₂/acetone: 6/4/0.5), visualised by UV and KMnO₄

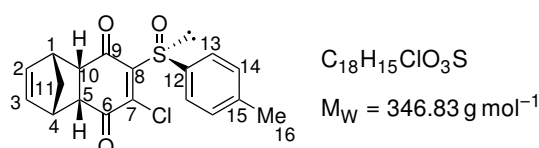
¹H NMR (500 MHz, CDCl₃): δ (ppm) **7.82** (s, 2H, 2 × C⁴H), **6.90** (s, 2H, 2 × C²H), **2.40** (s, 6H, 2 × C⁶H₃)

¹³C NMR (126 MHz, CDCl₃): δ (ppm) **185.50** (2 × C_q¹), **143.95** (2 × C_q³), **138.69** (2 × C²H), **130.05** (2 × C_q⁵), **127.57** (2 × C⁴H), **20.36** (2 × C₆H₃)

IR: $\bar{\nu}$ (cm⁻¹) 3057, 1644, 1590, 1306, 1083, 942, 888

The experimental data were in agreement with those reported in the literature.⁷³

(+)-(1*R*,4*S*,4*aR*,8*aS*)-6-Chloro-7-((*S*)-*p*-tolylsulfinyl)-1,4,4*a*,8*a*-tetrahydro-1,4-methano-naphthalene-5,8-dione (α-507)



Quinone **SQ4** (CH₂Cl₂: 106 mg, 0.377 mmol, 1.0 eq.; HFIP: 104 mg, 0.370 mmol, 1.0 eq.) and diene **D1** (CH₂Cl₂: 0.06 mL, 0.713 mmol, 1.9 eq.; HFIP: 0.06 mL, 0.713 mmol, 1.9 eq.) were reacted

following the general procedure. The crude product was purified by flash chromatography on demetallated silica gel (CH₂Cl₂: 100%) to give α -**507** (CH₂Cl₂: 55 mg; HFIP: 72 mg) in the first fraction.

Aspect: yellow oil

Yield: CH₂Cl₂: 42%; HFIP: 55%

TLC: R_f \approx 0.62 (CH₂Cl₂/acetone: 20/1), visualised by UV and KMnO₄

$[\alpha]_D^{20}$: +132° (c = 0.75; CHCl₃)

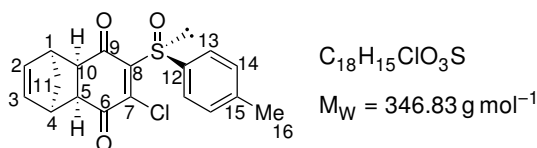
¹H NMR (500 MHz, CDCl₃): δ (ppm) **7.67** (d, 2H, $J = 8.2$ Hz, $2 \times C^{13}H$), **7.30** (d, 2H, $J = 8.2$ Hz, $2 \times C^{14}H$), **5.93** (ddd, 2H, ABXY, $J_{AB} = 5.6$ Hz, $J_{AX} = J_{BY} = 2.8$ Hz, $\Delta\nu_{AB} = 69.7$ Hz, $C^2H + C^3H$), **3.53** (s (br), 1H, C^1H), **3.50** (s (br), 1H, C^4H), **3.34** (ddd, 2H, A'B'XY, $J_{A'B'} = 8.5$ Hz, $J_{A'X} = J_{B'X} = 3.9$ Hz, $C^5H + C^{10}H$), **2.39** (s, 3H, $C^{16}H_3$), **1.48** (dddd, 2H, A''B''XY, $J_{A''B''} = 9.0$ Hz, $J_{A''X} = J_{A''Y} = 1.7$ Hz, $J_{B''X} = J_{B''Y} = 1.5$ Hz, $C^{11}H_2$)

¹³C NMR (126 MHz, CDCl₃): δ (ppm) **192.44** (C_q^6 or C_q^9), **190.05** (C_q^9 or C_q^6), **152.24** (C_q^7 or C_q^8), **148.35** (C_q^8 or C_q^7), **142.33** (C_q^{15}), **138.19** (C_q^{12}), **135.83** (C^2H or C^3H), **135.08** (C^3H or C^2H), **130.09** ($2 \times C^{14}H$), **125.29** ($2 \times C^{13}H$), **50.37** (C^1H or $C^4H + C^5H$ or $C^{10}H$), **49.79** (C^1H or C^4H), **49.41** ($C^{11}H_2$), **48.52** (C^5H or $C^{10}H$), **21.61** ($C^{16}H_3$)

IR: $\bar{\nu}$ (cm⁻¹) 2943, 2870, 1694, 1556, 1491, 1335, 1215, 1087, 1057, 910, 808, 729, 690

The experimental data were in agreement with those reported in the literature.⁴²

(+)-(1*S*,4*R*,4*aS*,8*aR*)-6-Chloro-7-((*S*)-*p*-tolylsulfinyl)-1,4,4*a*,8*a*-tetrahydro-1,4-methanonaphthalene-5,8-dione (β -507**)**



The same procedure as α -**507** was followed to give β -**507** (CH₂Cl₂: 43 mg; HFIP: 21 mg) in the second fraction.

Aspect: yellow oil

Yield: CH₂Cl₂: 33%; HFIP: 17%

TLC: R_f \approx 0.53 (CH₂Cl₂/acetone: 20/1), visualised by UV and KMnO₄

$[\alpha]_D^{20}$: +89.9° (c = 0.5; CHCl₃)

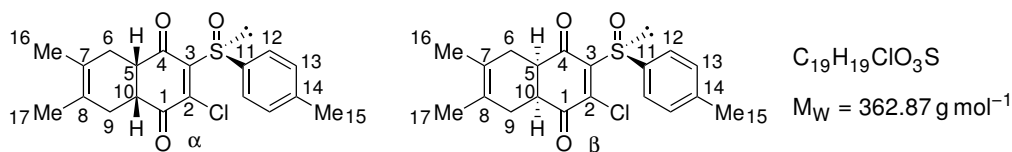
¹H NMR (500 MHz, CDCl₃): δ (ppm) **7.68** (d, 2H, $J = 8.1$ Hz, $2 \times C^{13}H$), **7.30** (d, 2H, $J = 8.1$ Hz, $2 \times C^{14}H$), **5.99** (ddd, 2H, ABXY, $J_{AB} = 5.6$ Hz, $J_{AX} = J_{BY} = 2.9$ Hz, $\Delta\nu_{AB} = 55.3$ Hz, $C^2H + C^3H$), **3.60-3.46** (m, 2H, $C^1H + C^4H$), **3.35** (ddd, 2H, A'B'XY, $J_{A'B'} = 8.8$ Hz, $J_{A'X} = J_{B'X} = 3.7$ Hz, $\Delta\nu_{A'B'} = 13.7$ Hz, $C^5H + C^{10}H$), **2.40** (s, 3H, $C^{16}H_3$), **1.49** (dddd, 2H, A''B''XY, $J_{A''B''} = 9.0$ Hz, $J_{A''X} = J_{A''Y} = 1.8$ Hz, $J_{B''X} = J_{B''Y} = 1.4$ Hz, $\Delta\nu_{A''B''} = 59.2$ Hz, $C^{11}H_2$)

¹³C NMR (126 MHz, CDCl₃): δ (ppm) **192.31** (C_q^6 or C_q^9), **189.86** (C_q^9 or C_q^6), **152.26** (C_q^7 or C_q^8), **148.53** (C_q^8 or C_q^7), **142.37** (C_q^{15}), **138.22** (C_q^{12}), **136.09** (C^2H or C^3H), **135.53** (C^3H or C^2H), **130.13** ($2 \times C^{14}H$), **125.35** ($2 \times C^{13}H$), **50.47** (C^5H or $C^{10}H$), **49.21** (C^1H or C^4H), **49.03** ($C^{11}H_2$), **48.93** ($C^{10}H$ or C^5H), **48.89** (C^4H or C^1H), **21.62** ($C^{16}H_3$)

IR: $\bar{\nu}$ (cm⁻¹) 2922, 1702, 1669, 1562, 1217, 1081, 1023, 809, 693

The experimental data were in agreement with those reported in the literature.⁴²

(4a*S*,8a*R*)-2-Chloro-6,7-dimethyl-3-((*S*)-*p*-tolylsulfinyl)-4a,5,8,8a-tetrahydronaphthalene-1,4-dione (α -308a) and (4a*R*,8a*S*)-2-chloro-6,7-dimethyl-3-((*S*)-*p*-tolylsulfinyl)-4a,5,8,8a-tetrahydronaphthalene-1,4-dione (β -308a)



Quinone **SQ4** (CH_2Cl_2 : 97 mg, 0.344 mmol, 1.0 eq.; HFIP: 30 mg, 0.107 mmol, 1.0 eq.) and **D3** (CH_2Cl_2 : 0.09 mL, 0.795 mmol, 2.3 eq.; HFIP: 0.02 mL, 0.177 mmol, 1.7 eq.) were reacted following the general procedure to give a mixture of α -**308a** and β -**308a** (CH_2Cl_2 : 112 mg; HFIP: 32 mg).

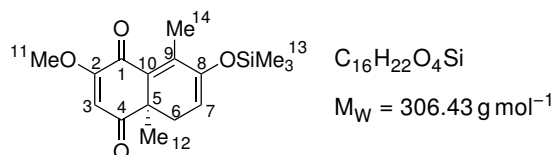
Aspect: pale orange solid foam

Yield: CH_2Cl_2 : 90%, α/β : 79/21; HFIP: 82%, α/β : 39/61

1H NMR (400 MHz, C_6D_6) on the α/β mixture from dichloromethane: δ (ppm): **7.90-7.79** (m, 2H, $2 \times C^{12}H$), **6.90-6.80** (m, 2H, $2 \times C^{13}H$), **2.40-1.95** (m, 2H, $C^5H + C^{10}H$), **1.90** (s (br), 0.63H, $C^{15}H_3$ (β)), **1.88** (s (br), 2.37H, $C^{15}H_3$ (α)), **1.85-1.33** (m, 4H, $C^6H_2 + C^9H_2$), **1.29** (s (br), 2.37H, $C^{16}H_3$ or $C^{17}H_3$ (α)), **1.27** (s (br), 0.67H, $C^{16}H_3$ or $C^{17}H_3$ (β)), **1.18** (s (br), 0.63H, $C^{17}H_3$ or $C^{16}H_3$ (β)), **1.15** (s (br), 2.37H, $C^{17}H_3$ or $C^{16}H_3$ (α))

8.6.3 Diels-Alder reactions for the synthesis of momilactones

(*R*)-2-Methoxy-4a,8-dimethyl-7-((trimethylsilyl)oxy)-4a,5-dihydronaphthalene-1,4-dione (519**)**



In a 25 mL round bottom flask under argon atmosphere, a solution of sulfinylquinone **318a** (1.000 g, 3.44 mmol, 1.0 eq.) in 15 mL of dichloromethane was cooled down to $-20^\circ C$. Diene **373a** (948 mg, 6.07 mmol, 1.8 eq.) was added and the flask was placed in the fridge at $-20^\circ C$ for ten days. The solvent was then evaporated and the crude was vacuum dried. The crude was purified by flash chromatography on demetallated silica gel (cHex/AcOEt: 9/1 \rightarrow 8/2) to give 896 mg of **519**.

Aspect: bright yellow powder

Yield: 85%

TLC: $R_f \approx 0.39$ (cHex/AcOEt: 7/3), visualised by UV and $KMnO_4$

m_p : 115-117 $^\circ C$

$[\alpha]_D^{20}$: -159.3° ($c = 0.5$; CH_2Cl_2)

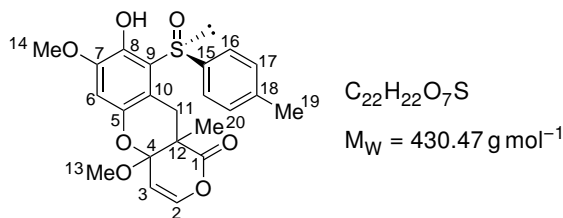
1H NMR (500 MHz, $CDCl_3$): δ (ppm) **5.90** (s, 1H, C^3H), **5.37** (dd, 1H, ABX, $J_{AX} = 6.9 \text{ Hz}$, $J_{BX} = 3.1 \text{ Hz}$, C^7H), **3.83** (s, 3H, $C^{11}H_3$), **2.54** (ddd, 2H, ABX, $J_{AB} = 18.4 \text{ Hz}$, $J_{AX} = 6.9 \text{ Hz}$, $J_{BX} = 3.1 \text{ Hz}$, $\Delta\nu_{AB} = 38.8 \text{ Hz}$, C^6H_2), **2.29** (s, 3H, $C^{14}H_3$), **1.28** (s, 3H, $C^{12}H_3$), **0.24** (s, 9H, $3 \times C^{13}H_3$)

^{13}C NMR (126 MHz, $CDCl_3$): δ (ppm) **200.95** (C_q^4), **181.162** (C_q^1), **164.28** (C_q^2), **149.33** (C_q^3), **147.97** (C_q^9), **130.77** (C_q^{10}), **109.65** (C^7H), **107.84** (C^3H), **56.60** ($C^{11}H_3$), **45.75** (C^5), **31.22** (C^6H_2), **26.00** ($C^{12}H_3$), **16.02** ($C^{14}H_3$), **0.24** ($3 \times C^{13}H_3$)

IR: $\bar{\nu}$ (cm⁻¹) 2961, 1654, 1605, 1535, 1359, 1240, 1216, 1156, 1020, 920, 853

The experimental data were in agreement with those reported in the literature.^{8,40}

8-Hydroxy-4a,7-dimethoxy-10a-methyl-9-((S)-p-tolylsulfinyl)-4a,10a-dihydro-1H,10H-pyrano [4,3-b]chromen-1-one (525)



In a 25 mL round bottom flask equipped with a condenser, a solution of sulfinylquinone **318a** (216 mg, 0.745 mmol, 1.0 eq.) and pyrone **373e** (106 mg, 0.745 mmol, 1.0 eq.) in 5 mL of chloroform was refluxed for three days. The solvent was then evaporated and the crude was purified by flash chromatography on demetallated silica gel (cHex/CH₂Cl₂/acetone: 7/3/0.1 → 7/3/0.5) to give 125 mg of **525b** (major) in the first fraction and 75 mg of **525a** (minor) in the second one.

Product 525a (minor)

Aspect: orange mushy solid

Yield: 23%

TLC: R_f ≈ 0.57 (cHex/AcOEt: 5/5), visualised by UV and *p*-anisaldehyde

¹H NMR (500 MHz, CDCl₃): δ (ppm) **10.76** (s (br), 0.80H, OH), **7.62** (d, 2H, *J* = 8.2 Hz, 2 × C¹⁶H), **7.31** (d, 2H, *J* = 8.2 Hz, 2 × C¹⁷H), **6.67** (d, 1H, *J* = 6.2 Hz, C²H), **6.49** (s, 1H, C⁶H), **5.74** (d, 1H, *J* = 6.2 Hz, C³H), **3.81** (s, 3H, C¹⁴H₃), **3.50** (d, 1H, *J* = 16.1 Hz, 1/2 × C¹¹H₂), **3.33** (s, 3H, C¹³H₃), **2.40** (s, 3H, C¹⁹H₃), **2.30** (d, 1H, *J* = 16.1 Hz, 1/2 × C¹¹H₂), **1.25** (s, 3H, C²⁰H₃)

¹³C NMR (126 MHz, CDCl₃): δ (ppm) **170.22** (C_q¹), **149.07** (C_q⁷), **145.65** (C_q⁸), **143.01** (C²H), **142.94** (C_q¹⁸), **142.27** (C_q⁵), **139.72** (C_q¹⁵), **130.59** (2 × C¹⁷H), **126.34** (2 × C¹⁶H), **119.95** (C_q⁹), **108.66** (C_q¹⁰), **104.96** (C⁶H), **104.58** (C³H), **97.21** (C_q⁴), **56.28** (C¹⁴H₃), **50.13** (C¹³H₃), **44.81** (C_q¹²), **27.13** (C¹¹H₂), **21.63** (C¹⁹H₃), **20.31** (C²⁰H₃)

IR: $\bar{\nu}$ (cm⁻¹) 3400-3000, 1668, 1615, 1589, 1359, 1300, 1289, 1202, 1039, 987, 837

HRMS (ESI+): for [M+H]⁺ calc.: 431.1164, found: 431.1158

Product 525b (major)

Aspect: white mushy solid

Yield: 39%

TLC: R_f ≈ 0.68 (cHex/AcOEt: 5/5), visualised by UV and *p*-anisaldehyde

¹H NMR (500 MHz, CDCl₃): δ (ppm) **10.37** (s (br), 0.75H, OH), **7.68** (d, 2H, *J* = 8.3 Hz, 2 × C¹⁶H), **7.32** (d, 2H, *J* = 8.3 Hz, 2 × C¹⁷H), **6.65** (d, 1H, *J* = 6.2 Hz, C²H), **6.49** (s, 1H, C⁶H), **5.77** (d, 1H, *J* = 6.2 Hz, C³H), **3.78** (s, 3H, C¹⁴H₃), **3.39** (s, 3H, C¹³H₃), **3.10** (dd, 2H, AB, *J*_{AB} = 16.3 Hz, Δ*v*_{AB} = 157.1 Hz, C¹¹H₂), **2.38** (s, 3H, C¹⁹H₃), **1.41** (s, 3H, C²⁰H₃)

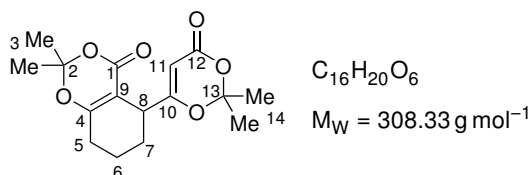
¹³C NMR (126 MHz, CDCl₃): δ (ppm) **170.70** (C_q¹), **149.15** (C_q⁷), **145.60** (C_q⁸), **142.91** (C²H), **142.24** (C_q⁵ or C_q¹⁸), **138.98** (C_q¹⁵), **130.39** (2 × C¹⁷H), **125.60** (2 × C¹⁶H), **120.66** (C_q⁹), **108.98** (C_q¹⁰), **104.85** (C⁶H), **104.79** (C³H), **97.38** (C_q⁴), **56.22** (C¹⁴H₃), **50.10** (C¹³H₃), **44.85** (C_q¹²), **27.32** (C¹¹H₂), **21.54**

($C^{19}H_3$), **20.72** ($C^{20}H_3$)

IR: $\bar{\nu}$ (cm^{-1}) 3500-3100, 1671, 1619, 1578, 1456, 1352, 1311, 1284, 1210, 1154, 1026, 968

HRMS (ESI+): for $[M+H]^+$ calc.: 431.1164, found: 431.1159

5-(2,2-Dimethyl-4-oxo-4H-1,3-dioxin-6-yl)-2,2-dimethyl-5,6,7,8-tetrahydro-4H-benzo[d][1,3]dioxin-4-one (529)



This product was obtained during the attempt of a Diels-Alder reaction between sulfinylquinone **318a** and diene **373c** under high pressure. In a vial, a solution of sulfinylquinone **318a** (107 mg, 0.370 mmol, 1.0 eq.) and diene **373c** (114 mg, 0.741 mmol, 2.0 eq.) in 2 mL of dichloromethane was submitted to a pressure of 9 kbar for 48 h. The solvent was then evaporated and the crude was purified by flash chromatography on demetallated silica gel ($\text{CH}_2\text{Cl}_2/\text{AcOEt}$: 98/2) to obtain 45 mg of the dimer **529**.

Aspect: yellow oil

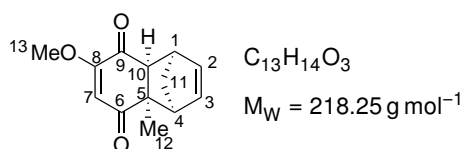
Yield: 39% from the amount of diene **373c** introduced in the reaction.

TLC: $R_f \approx 0.58$ ($\text{CH}_2\text{Cl}_2/\text{AcOEt}$: 8/1), visualised by UV and KMnO_4

^1H NMR (400 MHz, CDCl_3): δ (ppm) **5.22** (s, 1H, $C^{11}H$), **3.41** (t, 1H, $J = 5.8 \text{ Hz}$, C^8H), **2.26-2.22** (m, 2H, C^5H_2), **1.89-1.71** (m, 4H, $C^6H_2 + C^7H_2$), **1.70** (s, 3H, C^3H_3 or $C^{14}H_3$), **1.68** (s, 3H, C^3H_3 or $C^{14}H_3$), **1.66** (s, 3H, C^3H_3 or $C^{14}H_3$), **1.63** (s, 3H, C^3H_3 or $C^{14}H_3$)

^{13}C NMR (100 MHz, CDCl_3): δ (ppm) **172.94** (C_q^{12}), **167.82** (C_q^1), **161.48** (C_q^{10}), **160.69** (C_q^4), **106.85** (C_q^2 or C_q^{13}), **105.90** (C_q^2 or C_q^{13}), **100.70** (C_q^9), **93.80** ($C^{11}H$), **37.11** (C^8H), **27.41** (C^5H_2 or C^7H_2), **26.88** (C^5H_2 or C^7H_2), **26.23** (C^3H_3 or $C^{14}H_3$), **25.50** (C^3H_3 or $C^{14}H_3$), **24.73** (C^3H_3 or $C^{14}H_3$), **24.30** (C^3H_3 or $C^{14}H_3$), **18.78** (C^6H_2)

(-)-(1R,4S,4aR,8aS)-7-Methoxy-4a-methyl-1,4,4a,8a-tetrahydro-1,4-methanonaphthalene-5,8-dione (532)



This product was synthesised by following the procedure described by Corey *et al.*^{74,75}

Preparation of the oxazaborolidine pre-catalyst. In a 100 mL two-neck flask under argon atmosphere, equipped with a condenser and a dropping funnel filled with 20 g of 4 Å molecular sieve, a solution of *S*-(-)- α,α -diphenyl-2-pyrrolidinemethanol (165 mg, 0.651 mmol, 1.0 eq.) and tri(*o*-tolyl)boroxine (74 mg, 0.209 mmol, 0.32 eq.) in 25 mL of toluene was refluxed for three hours. The reaction was cooled down to 60 °C and toluene was distilled. When the volume was reduced to ca. 5 mL, 5 mL of

toluene were added the solution was redistilled. That operation was repeated a second time. The obtained oil was vacuum dried for one hour and dissolved in 8 mL of dry dichloromethane under argon atmosphere. That solution (ca. 0.078 M of oxazaborolidine) can be used for several catalytic tests.

Asymmetric Diels-Alder reaction. In a dry 25 mL round bottom flask under argon atmosphere, a 0.078 M solution of oxazaborolidine (2.0 mL, 0.156 mmol, 0.24 eq.) was cooled down to $-20\text{ }^{\circ}\text{C}$. A 0.205 M of trifluoromethanesulfonimide (0.65 mL, 0.133 mmol, 0.20 eq.) in dichloromethane was added dropwise to the oxazaborolidine solution. After ten minutes, a solution of quinone **369a** (100 mg, 0.657 mmol, 1.0 eq.) in 2 mL of dichloromethane was added dropwise and the mixture was stirred ten minutes at $-20\text{ }^{\circ}\text{C}$. Cyclopentadiene (**151**) (0.07 mL, 0.832 mmol, 1.3 eq.). When the reaction was over (40 min), 10 mL of water was added, and the phases were separated. Then, the aqueous phase was extracted with dichloromethane. The organic phases were gathered, dried over Na_2SO_4 and the solvent was evaporated. The crude product was purified by flash chromatography on silica gel (cHex/AcOEt: 7/3) to give 133 mg of **532**.

Aspect: white powder

Yield: 93%

TLC: $R_f \approx 0.24$ (cHex/AcOEt: 7/3), visualised by UV and *p*-anisaldehyde

ee: 96%; $t_r^{\text{major}} = 40.8$ min, $t_r^{\text{minor}} = 49.8$ min

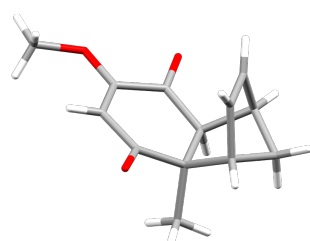
$[\alpha]_D^{20}$: -37.6° ($c = 1.0$; CHCl_3)

$^1\text{H NMR}$ (400 MHz, CDCl_3): δ (ppm) **6.16** (dd, 1H, $J = 5.7$; 2.9 Hz, C^{10}H), **5.98** (dd, 1H, $J = 5.7$; 2.8 Hz, C^9H), **5.85** (s, 1H, C^4H), **3.72** (s, 3H, C^{13}H_3), **3.45** (s (br), 1H, C^8H), **3.07** (s (br), 1H, C^1H), **2.88** (d, 1H, $J = 3.9$ Hz, C^7H), **1.60** (ddt, 2H, ABX, $J_{\text{AB}} = 9.2$ Hz, $J_{\text{AX}} = 1.4$ Hz, $J_{\text{BX}} = 1.7$ Hz, $\Delta\nu_{\text{AB}} = 56.8$ Hz, C^{11}H_2), **1.47** (s, 3H, C^{12}H_3)

$^{13}\text{C NMR}$ (126 MHz, CDCl_3): δ (ppm) **202.46** (C_q^3), **194.56** (C_q^6), **162.60** (C_q^5), **138.70** (C^{10}H), **134.09** (C^9H), **114.13** (C^4H), **57.20** (C^7H), **56.46** (C^{13}H_3), **53.50** (C_q^2), **53.48** (C^1H), **49.65** (C^8H), **46.58** (C^{11}H_2), **26.68** (C^{12}H_3)

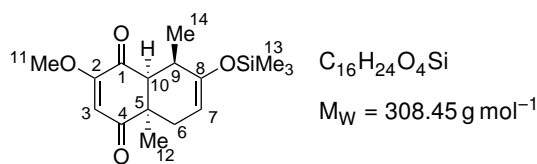
IR: $\bar{\nu}$ (cm^{-1}) 2992, 2960, 1754, 1734, 1690, 1641, 1602, 1451, 1362, 1319, 1233, 1147, 990, 867, 733

The experimental data were in agreement with the racemic **Q3D1**.



Orthorombic	$P2_12_12_1$
$a = 8.12720(10)$ Å	$\alpha = 90^{\circ}$
$b = 10.50660(10)$ Å	$\beta = 90^{\circ}$
$c = 12.91920(10)$ Å	$\gamma = 90^{\circ}$
$V = 1103.161(19)$ Å ³	$Z = 4$
$R = 2.88\%$	Flack = 0.02(5)

Figure 8.35: X-ray structure of **532** and parameters of the crystal. Crystallisation by slow evaporation from dichloromethane.

(4a*R*,8*R*,8a*S*)-2-Methoxy-4a,8-dimethyl-7-((trimethylsilyl)oxy)-4a,5,8,8a-tetrahydronaphthalene-1,4-dione (ent-370aa)

In a dry 25 mL round bottom flask under argon atmosphere, a 0.078 M solution of oxazaborolidine (2.0 mL, 0.156 mmol, 0.23 eq.) was cooled down to $-20\text{ }^{\circ}\text{C}$. A 0.205 M of trifluoromethanesulfonimide (0.65 mL, 0.133 mmol, 0.20 eq.) in dichloromethane was added dropwise to the oxazaborolidine solution. After ten minutes, a solution of quinone **369a** (103 mg, 0.680 mmol, 1.0 eq.) in 2 mL of dichloromethane was added dropwise and the mixture was stirred ten minutes at $-20\text{ }^{\circ}\text{C}$. After ten minutes, diene **373a** (131 mg, 840 μmol , 1.2 eq.). After 17 h, the reaction was diluted with hexane and the organic phase was washed with water and brine. It was then dried over Na₂SO₄ and the solvent was evaporated to give 46 mg of a crude oil. The attempt of purification led to degradation of the product and the analyses were done on the crude product.

Aspect: yellow oil

Yield: 22% (unclean)

TLC: R_f \approx 0.45 (cHex/AcOEt: 7/3), visualised by UV and *p*-anisaldehyde

¹H NMR (400 MHz, CDCl₃): δ (ppm) **5.83** (s, 1H, C³H), **4.69** (td, 1H, $J = 4.0; 1.7$ Hz, C⁷H), **3.78** (s, 3H, C¹¹H₃), **3.08** (d, 1H, $J = 5.8$ Hz, C¹⁰H), **2.73** (ddd, 1H, $J = 17.3; 3.7; 2.4$ Hz, 2 \times C⁷H₂), **2.60-2.49** (m, 1H, C⁹H), **1.85** (ddd, 1H, $J = 17.3; 3.9; 1.9$ Hz, 2 \times C⁷H₂), **1.34** (s, 3H, C¹²H₃), **1.09** (d, 3H, $J = 7.4$ Hz, C¹⁴H₃), **0.19** (s, 9H, 3 \times C¹³H₃)

References

- [1] Merck (previously Sigma-Aldrich), <https://www.sigmaaldrich.com/>, Accessed: 14 September 2021.
- [2] fluorochem, <http://www.fluorochem.co.uk/>, Accessed: 14 September 2021.
- [3] Tokyo Chemical Industry, <https://www.tcichemicals.com/>, Accessed: 14 September 2021.
- [4] Biosynth Carbosynth, <https://www.carbosynth.com/>, Accessed: 14 September 2021.
- [5] Fisher Scientific, <https://www.fishersci.be/>, Accessed: 14 September 2021.
- [6] J&K Scientific, <https://www.jk-scientific.com/>, Accessed: 14 September 2021.
- [7] Armarego, W. L. F.; Chai, C. L. L. *Purification of Laboratory Chemicals*, 7th ed.; Butterworth-Heinemann: Boston, 2013.
- [8] Lanfranchi, D. A. Vers la synthèse totale de la salvinorine A et d'analogues structuraux. Ph.D. thesis, Université Louis Pasteur, Strasbourg, France, 2006.
- [9] Suffert, J. Simple Direct Titration of Organolithium Reagents Using *N*-Pivaloyl-*o*-toluidine and/or *N*-pivaloyl-*o*-benzylaniline. *J. Org. Chem.* **1989**, *54*, 509–510.
- [10] Eurisotop, <https://www.eurisotop.com/>, Accessed: 15 September 2021.
- [11] Hubbard, J. S.; Harris, T. M. Condensations at the 6 Position of the Methyl Ester and the Dimethylamide of 3,5-Dioxohexanoic Acid via 2,4,6-Tri-anions. *J. Org. Chem.* **1981**, *46*, 2566–2570.
- [12] Pirrung, M. C. Purification of products. In *The Synthetic organic chemist's companion*; John Wiley & Sons, Inc., 2007; Chapter 13, pp 131–139.
- [13] Gottlieb, H. E.; Kotlyar, V.; Nudelman, A. NMR Chemical Shifts of Common Laboratory Solvents as Trace Impurities. *J. Org. Chem.* **1997**, *62*, 7512–7515.
- [14] Rigaku Oxford Diffraction. *CrysAlis PRO*. Rigaku Oxford Diffraction: Oxford, UK 2020.
- [15] Dolomanov, O. V.; Bourhis, L. J.; Gildea, R. J.; Howard, J. A. K.; Puschmann, H. *OLEX2: A Complete Structure Solution, Refinement and Analysis Program*. *J. Appl. Crystallogr.* **2009**, *42*, 339–341.
- [16] Hübschle, C. B.; Sheldrick, G. M.; Dittrich, B. *ShelXle: A Qt Graphical User Interface for SHELXL*. *J. Appl. Crystallogr.* **2011**, *44*, 1281–1284.
- [17] Sheldrick, G. M. *SHELXT – Integrated Space-Group and Crystal-Structure Determination*. *Acta Crystallogr. Sect. A: Found. Adv.* **2015**, *71*, 3–8.
- [18] Sheldrick, G. M. Crystal Structure Refinement with *SHELXL*. *Acta Crystallogr., Sect. C: Struct. Chem.* **2015**, *71*, 3–8.
- [19] Ackland, D. J.; Pinhey, J. T. The Chemistry of Aryl-lead(IV) Tricarboxylates. Reaction with Vinylogous β -Keto Esters. *J. Chem. Soc., Perkin Trans. 1* **1987**, 2689–2694.
- [20] Schrof, R.; Altmann, K.-H. Studies toward the Total Synthesis of the Marine Macrolide Salarin C. *Org. Lett.* **2018**, *20*, 7679–7683.
- [21] Gupta, P.; Kumar, P. An Efficient Total Synthesis of Decarestrictine D. *Eur. J. Org. Chem.* **2008**, 1195–1202.
- [22] Padhi, B.; Reddy, D. S.; Mohapatra, D. K. Gold-catalyzed diastereoselective synthesis of 2,6-*trans*-disubstituted tetrahydropyran derivatives: application for the synthesis of the C1–C13 fragment of bis-tramide A and B. *RSC Adv.* **2015**, *5*, 96758–96768.
- [23] Hayashi, Y.; Yamaguchi, H.; Toyoshima, M.; Okado, K.; Toyo, T.; Shoji, M. Formal Total Synthesis of Fostriecin by 1,4-Asymmetric Induction with an Alkyne–Cobalt Complex. *Chem. Eur. J.* **2010**, *16*, 10150–10159.
- [24] Sudina, P. R.; Motati, D. R.; Seema, A. Stereocontrolled Total Synthesis of Nonenolide. *J. Nat. Prod.* **2018**, *81*, 1399–1404.
- [25] Matsubara, R.; Jamison, T. F. Nickel-Catalyzed Allylic Substitution of Simple Alkenes. *J. Am. Chem. Soc.* **2010**, *132*, 6880–6881.
- [26] Fache, F.; Batt, F. Towards the Synthesis of the 4,19-Diol Derivative of (–)-Mycothiazole: Synthesis of a Potential Key Intermediate. *Eur. J. Org. Chem.* **2011**, 6039–6055.
- [27] Xie, L.; Saunder, W. H., Jr. Unusual induced isotope effects in the reaction of 2-pentanone with dialkylamide bases. Evidence on the nature of the reactive base species. *J. Am. Chem. Soc.* **1991**, *113*, 3123–3130.
- [28] Ohta, S.; Shimabayashi, A.; Hatano, S.; Okamoto, M. Preparation of *t*-Butyl 3-Oxopent-4-enoate and its Use as a Nazarov Reagent. *Synthesis* **1983**, 715–716.
- [29] Hoffman, R. V.; Kim, H.-O.; Wilson, A. L. 2-(((*p*-Nitrophenyl)sulfonyl)oxy)-3-keto Esters: Versatile Intermediates for the Preparation of 1,2,3-Tricarbonyl Compounds. *J. Org. Chem.* **1990**, *55*, 2820–2822.
- [30] Gebauer, J.; Blechert, S. Synthesis of γ,δ -Unsaturated- β -keto Lactones via Sequential Cross Metathesis-Lactonization: A Facile Entry to Macrolide Antibiotic (–)-A26771B. *J. Org. Chem.* **2006**, *71*, 2021–2025.
- [31] Rabe, P.; Klapschinski, T. A.; Brock, N. L.; Citron, C. A.; D'Alvise, P.; Gram, L.; Dickschat, J. S. Synthesis and bioactivity of analogues of the marine antibiotic tropodithietic acid. *Beilstein J. Org. Chem.* **2014**, *10*, 1796–1801.
- [32] Ng, K.-M. E.; McMorris, T. C. An efficient synthesis of pteroin C and other pterosins. *Can. J. Chem.* **1984**,

- 62, 1945–1953.
- [33] Körner, M.; Hiersemann, M. Enantioselective Synthesis of the C8–C20 Segment of Curvicolide C. *Org. Lett.* **2007**, *9*, 4979–4982.
- [34] Minich, M. L.; Watson, I. D.; Filipski, K. J.; Pfefferkorn, J. A. Novel and efficient synthesis of 4-sulfonyl-2-pyridones. *Tetrahedron Lett.* **2009**, *50*, 2094–2096.
- [35] Effenberger, F.; Ziegler, T.; Schönwälder, K.-H. Enoether, XVI. Synthese von 4-Hydroxy-2H-pyran-2-onen. *Chem. Ber.* **1985**, *118*, 741–752.
- [36] Effenberger, F.; Ziegler, T. Diels-Alder-Reaktionen mit 2H-Pyran-2-onen: Reaktivität und Selektivität. *Chem. Ber.* **1987**, *120*, 1339–1346.
- [37] Fujiki, K.; Tanifuji, N.; Sasaki, Y.; Yokoyama, T. New and Facile Synthesis of Thiosulfonates from Sulfinate/Disulfide/I₂ System. *Synthesis* **2002**, 343–348.
- [38] Okumura, S.; Takeda, Y.; Kiyokawa, K.; Minakata, S. Hypervalent Iodine(III)-Induced Oxidative [4+2] Annulation of *o*-Phenylenediamines and Electron-Deficient Alkynes: Direct Synthesis of Quinoxalines from Alkyne Substrates under Metal-Free Conditions. *Chem. Commun.* **2013**, *49*, 9266–9268.
- [39] Solladié, G.; Hutt, J.; Girardin, A. Improved Preparation of Optically Active Methyl *p*-Tolyl Sulfoxide. *Synthesis* **1987**, 173.
- [40] Lanfranchi, D. A.; Hanquet, G. Asymmetric Diels-Alder Reactions of a New Enantiomerically Pure Sulfinylquinone: A Straightforward Access to Functionalized Wieland-Miescher Ketone Analogues with (*R*) Absolute Configuration. *J. Org. Chem.* **2006**, *71*, 4854–4861.
- [41] Carreño, M. C.; García Ruano, J. L.; Urbano, A. Synthesis of Optically Active *p*-Tolylsulfinylquinones. *Synthesis* **1992**, 651–653.
- [42] Carreño, M. C.; García Ruano, J. L.; Toledo, M. A.; Urbano, A. Synthesis and Diels-Alder reactions of (*S*)-3-Chloro and (*S*)-3-Ethyl-2-*p*-tolylsulfinyl-1,4-benzoquinones. *Tetrahedron Lett.* **1994**, *35*, 9759–9762.
- [43] Ferreira, A. J.; Nel, J. W.; Brandt, E. V.; Bezuidenhout, B. C. B.; Ferreira, D. Oligomeric isoflavonoids. Part 3. Daljanelins A–D, the first pterocarpan- and isoflavanoid-neoflavanoid analogues. *J. Chem. Soc., Perkin Trans. 1* **1995**, 1049–1056.
- [44] Guzikowski, A. P.; Cai, S. X.; Espitia, S. A.; Hawkinson, J. E.; Huettner, J. E.; Nogales, D. F.; Tran, M.; Woodward, R. M.; Weber, E.; Keana, J. F. W. Analogs of 3-Hydroxy-1*H*-1-benzazepine-2,5-dione: Structure-Activity Relationship at *N*-Methyl-D-aspartate Receptor Glycine Sites. *J. Med. Chem.* **1996**, *39*, 4643–4653.
- [45] García Ruano, J. L.; Alemán, J.; Aranda, M. T.; Arévalo, M. J.; Padwa, A. Highly Stereoselective Vinylogous Pummerer Rearrangement. *Phosphorus, Sulfur Silicon Relat. Elem.* **2005**, *180*, 1497–1498.
- [46] García Ruano, J. L.; Alemán, J.; Aranda, M. T.; Arévalo, M. J.; Padwa, A. Highly Stereoselective Vinylogous Pummerer Reaction Mediated by Me₃SiX. *Org. Lett.* **2005**, *7*, 19–22.
- [47] Miyawaki, A.; Kikuchi, D.; Niki, M.; Manabe, Y.; Kanematsu, M.; Yokoe, H.; Yoshida, M.; Shishido, K. Total Synthesis of Natural Enantiomers of Heliespirones A and C via the Diastereoselective Intramolecular Hosomi-Sakurai Reaction. *J. Org. Chem.* **2012**, *77*, 8231–8243.
- [48] McDonald, J. W.; Miller, J. E.; Kim, M.; Velu, S. E. An expedient synthesis of murrayaquinone A via a novel oxidative free radical reaction. *Tetrahedron Lett.* **2018**, *59*, 550–553.
- [49] Möller, K.; Wienhöfer, G.; Schröder, K.; Join, B.; Junger, K.; Beller, M. Selective Iron-Catalyzed Oxidation of Phenols and Arenes with Hydrogen Peroxide: Synthesis of Vitamin E Intermediates and Vitamin K₃. *Chem. Eur. J.* **2010**, *16*, 10300–10303.
- [50] Lu, L.; Chen, F. A Novel Convenient Synthesis of Coenzyme Q₁. *Synth. Commun.* **2004**, *34*, 4049–4053.
- [51] Nilchan, N.; Phetsang, W.; Nowwarat, T.; Chaturongakul, S.; Jiarpinitnun, C. Halogenated trimethoprim derivatives as multidrug-resistant *Staphylococcus aureus* therapeutics. *Bioorg. Med. Chem.* **2018**, *26*, 5343–5348.
- [52] Cross, B. E.; Zamitt, L. J. Pigments of *Gnomonia erythrostoma* — IV. The synthesis of 5,8-dibenzoyloxy-3-hydroxy-6-methoxy-1,4-naphthoquinone. *Tetrahedron* **1976**, 1587–1590.
- [53] Inman, M.; Moddy, C. J. Synthesis of Indolequinones from Bromoquinones and Enamines Mediated by Cu(OAc)₂·H₂O. *J. Org. Chem.* **2010**, *75*, 6023–6026.
- [54] Mazzini, F.; Alpi, E.; Salvadori, P.; Netscher, T. First Synthesis of (8-²H₃)-(all-*rac*)- δ -Tocopherol. *Eur. J. Org. Chem.* **2003**, 2840–2844.
- [55] Brimble, M. A.; Burgess, C.; Halim, R.; Petersson, M.; Ray, J. Synthesis of pyrrolo[3,2-*b*]benzofurans and pyrrolo[3,2-*b*]naphthofurans via addition of a silyloxy pyrrole to activated quinones. *Tetrahedron* **2004**, *60*, 5751–5758.
- [56] Yamamoto, Y.; Itonaga, K. Synthesis of Chromans via [3 + 3] Cyclocoupling of Phenols with Allylic Alcohols Using a Moo-Chloranil Catalyst System. *Synthesis* **2009**, *11*, 717–720.
- [57] Alves, A. P. L.; Júnior, J. A. B. C.; Slana, G. B. A.; Cardoso, J. N.; Wang, Q.; Lopes, R. S. C.; Lopes, C. C. Synthesis of 1,2,4-Trimethoxybenzene and Its Selective Functionalization at C-3 by Directed Metalation. *Synth. Commun.* **2009**, *39*, 3693–3709.
- [58] Park, C. H.; Kim, K. H.; Lee, I. K.; Lee, S. Y.; Choi, S. U.; Lee, J. H.; Lee, K. R. Phenolic Constituents of

- Acorus gramineus*. *Arch. Pharm. Res.* **2011**, *34*, 1289–1296.
- [59] Witiak, D. T.; Loper, J. T.; Ananthan, S.; Almerico, A. M.; Verhoef, V. L.; Filppi, J. A. Mono and Bis(bioreductive) Alkylating Agents: Synthesis and Antitumor Activities in a B16 Melanoma Model. *J. Med. Chem.* **1989**, *32*, 1636–1642.
- [60] Crowther, G. P.; Sundberg, R. J.; Sarpeshkar, A. M. Dilithiation of Aromatic Ethers. *J. Org. Chem.* **1984**, *49*, 4657–4663.
- [61] Mal, D.; Ray, S. First Synthesis of 9,10-Dimethoxy-2-methyl-1,4-anthraquinone: A Naturally Occurring Unusual Anthraquinone. *Eur. J. Org. Chem.* **2008**, 3014–3020.
- [62] Wright, M. W.; Smalley, T. L., Jr.; Welker, M. E.; Rheingold, A. L. Synthesis of Cobalt-Substituted 1,3-Diene Complexes with Unusual Structures and Their Exo-Selective Diels-Alder Reactions. *J. Am. Chem. Soc.* **1994**, *116*, 6777–6791.
- [63] Seymour, C. P.; Tohda, R.; Tsubaki, M.; Hayashi, M.; Matsubara, R. Photosensitization of Fluorofuroxans and Its Application to the Development of Visible Light-Triggered Nitric Oxide Donor. *J. Org. Chem.* **2017**, *82*, 9647–9654.
- [64] Yoshida, N.; Konno, H.; Kamikubo, T.; Takahashi, M.; Ogasawara, K. Preparation of a synthetic equivalent of chiral methyl 2,5-dihydroxycyclohexane-1,4-dienecarboxylate. *Tetrahedron: Asymmetry* **1999**, *10*, 3849–3857.
- [65] Evans, D. A.; Wu, J. Enantioselective Rare-Earth Catalyzed Quinone Diels-Alder Reactions. *J. Am. Chem. Soc.* **2003**, *125*, 10162–10163.
- [66] Nishimoto, K.; Okada, Y.; Kim, S.; Chiba, K. Rate acceleration of Diels–Alder reactions utilizing a fluoros micellar system in water. *Electrochim. Acta* **2011**, *56*, 10626–10631.
- [67] Katoh, T.; Monma, H.; Wakasugi, J.; Koichi, N.; Katoh, T. Synthesis of β -Lapachone, a Potential Anti-cancer Agent from the Lapacho Tree. *Eur. J. Org. Chem.* **2014**, 7099–7103.
- [68] Martí-Centelles, V.; Lawrence, A. L.; Lusby, P. J. High Activity and Efficient Turnover by a Simple Self-Assembled “Artificial Diels-Alderase”. *J. Am. Chem. Soc.* **2018**, *140*, 2862–2868.
- [69] Halterman, R. L.; Jan, S. T. Catalytic asymmetric epoxidation of unfunctionalized alkenes using the first D_4 -symmetric metallotetraphenylporphyrin. *J. Org. Chem.* **1991**, *56*, 5253–5254.
- [70] Bohlmann, F.; Mathar, W.; Schwarz, H. Über die Regioselektivität von Diensynthesen substituierter Chinone. *Chem. Ber.* **1977**, *110*, 2028–2045.
- [71] Hayakawa, K.; Ueyama, K.; Kanematsu, K. A Useful Synthone Approach to Bicyclic Enols: Acid-Catalyzed and Base-Catalyzed Rearrangements of Diels-Alder Adducts of 2-Methoxy-5-methyl-1,4-benzoquinone. *J. Org. Chem.* **1985**, *50*, 1963–1969.
- [72] Carreño, M. C.; García Ruano, J. L.; Urbano, A. Synthesis and asymmetric Diels-Alder reactions of (S)-2-*p*-tolylsulfinyl-1,4-benzoquinone. *Tetrahedron Lett.* **1989**, *30*, 4003–4006.
- [73] Catir, M.; Hamdullah, K. Bis(trifluoroacetoxyiodo)benzene-Induced Activation of *tert*-butyl Hydroperoxide for the Direct Oxyfunctionalization of Arenes to Quinones. *Synlett* **2004**, 2151–2154.
- [74] Ryu, D. H.; Corey, E. J. Triflimide Activation of a Chiral Oxazaborolidine Leads to a More General Catalytic System for Enantioselective Diels-Alder Addition. *J. Am. Chem. Soc.* **2003**, *125*, 6388–6390.
- [75] Ryu, D. H.; Zhou, G.; Corey, E. J. Enantioselective and Structure-Selective Diels-Alder Reactions of Unsymmetrical Quinones Catalyzed by a Chiral Oxazaborolidine Cation. Predictive Selection Rules. *J. Am. Chem. Soc.* **2004**, *126*, 4800–4802.